Copy
RM E55G28

C2

NACA

RESEARCH MEMORANDUM

ADAPTATION OF COMBUSTION PRINCIPLES TO AIRCRAFT PROPULSION

VOLUME II - COMBUSTION IN AIR-BREATHING JET ENGINES

By Fuels and Combustion Research Division

Lewis Flight Propulsion Laboratory
Cleveland, Ohio

NATIONAL ADVISORY COMMITTEE
FOR AERONAUTICS

WASHINGTON

May 2, 1956

NACA RM E55G28

ADAPTATION OF COMBUSTION PRINCIPLES TO AIRCRAFT PROPULSION

Vol. II - COMBUSTION IN AIR-BREATHING JET ENGINES

By Fuels and Combustion Research Division

Lewis Flight Propulsion Laboratory
Cleveland, Ohio

Edited by

Henry C. Barnett
Robert R. Hibbard

FOREWORD

The chapters in this volume continue the NACA study of combustion principles for aircraft propulsion. Information on the various aspects of combustion pertinent to jet engines is organized and interpreted in this study. The sources of information are quite extensive, particularly for basic, or fundamental, subject matter.

The report concerns air-breathing engines and hydrocarbon fuels, and not rocket engines and high-energy fuels. Another limitation is that the references have been selected to illustrate important points; thus the bibliographies, while thorough, are not complete.

The previous chapters (Volume I - Basic Considerations in the Combustion of Hydrocarbon Fuels with Air, NACA RM E54I07) review such fundamental processes as atomization and evaporation of fuel, flow and mixing of gases, ignition and flammability, laminar and turbulent flames, flame stabilization, diffusion flames, oscillations in combustors, and smoke and coke. The practical significance of each of these processes to combustor design is briefly discussed therein.

The present chapters describe the observed performance and design problems of engine combustors of the principal types. Included in the discussion are combustor-inlet conditions; starting, acceleration, combustion limits, combustion efficiency, coke deposits, and smoke formation in turbojets; ram-jet performance; and afterburner performance and design. An attempt is made to interpret performance in terms of the fundamental processes and theories reviewed in volume I.

Volumes I and II provide the basis for future efforts to define combustor design principles. Accordingly the studies in these volumes will be further interpreted in order to develop specific guide lines for the design of high-speed combustion systems. At the same time an attempt will be made to extend the existing information to meet the conditions imposed by future flight requirements.

W. T. Olson
Chief, Fuels and Combustion Research Division

[redacted]

TABLE OF CONTENTS

[redacted]

Chapter Page

Chapter Page

Chapter Page

CHAPTER X

EFFECT OF ENGINE OPERATING VARIABLES ON COMBUSTOR-INLET PARAMETERS

By Wilfred E. Scull and Anthony W. Jones

INTRODUCTION

Studies of the fundamental processes of combustion are usually concerned with wide ranges of investigation of individual processes. In general, each fundamental combustion process may be studied in an environment that is most suited to its evaluation and possibly unrelated basically to any practical application. The majority of the data presented in volume I of this series concern the fundamental aspects of combustion as functions of the individual occurrence of various contributing processes.

In a jet engine, however, the various fundamental combustion processes may occur simultaneously and may interact. Furthermore, the engine environment usually does not permit independent variation of single combustion parameters, since specified operating conditions impose specific values on the parameters. In volume II, data are presented to show the effect of operating conditions on the over-all combustion process in different combustion components. To show the effect of operating conditions, it is necessary to specify the range of these conditions within which combustion components may operate.

Therefore, this chapter presents only the operating conditions that might be required in the primary combustors and afterburners of typical current turbojet engines. (Corresponding information on ram-jet engines is presented in ch. XIV.) This chapter is not intended to serve as an explanation of engine operation. The operating conditions of the combustion components are presented in terms of total pressures and temperatures at the primary-combustor and afterburner inlets, reference velocities and outlet total temperatures of the primary combustors, and velocities at the plane of the flameholder in the afterburners. The data are presented to relate the operating regions of typical current turbojet combustion components to flight altitudes, Mach numbers, and modes of engine operation. Specifically, data are presented for the combustion parameters of the primary combustor and afterburner of three turbojet engines having rated compressor total-pressure ratios of 5, 8, and 12 under full-throttle conditions. Operational data for the primary combustor also include part-throttle operation at 70, 80, and 90 percent of rated engine speed and windmilling operation. The range of flight conditions includes altitudes from sea level to 65,000 feet and flight Mach numbers from zero to 1.6.

SYMBOLS

A	cross-sectional area
f	fuel-air ratio
N	engine rotational speed
p	absolute pressure
T	absolute temperature
V	velocity

w	weight-flow rate
δ	ratio of total pressure to NACA standard sea-level pressure
θ	ratio of total temperature to NACA standard sea-level temperature
ρ	density

Subscripts:

A,B,C	engine A, B, or C
a	air
ab	afterburner
c	primary combustor
g	gas
r	reference
sls	rated, sea-level static
t	total
X	engine X
2	compressor inlet
3	combustor inlet
4	turbine inlet
6	flameholder plane

GENERAL ENGINE DATA

Engine Descriptions

All operating conditions presented herein are theoretical. However, the conditions are for three turbojet-engine designs chosen to cover representative current combustion components and their operation. Basic descriptive data for the three engines are presented in table I.

Three engines having sea-level rated compressor total-pressure ratios of 5, 8, and 12 were considered. The combustor reference areas, that is, the maximum cross-sectional area of the combustor housing and the area of the afterburner housing at the plane of the flameholders, correspond to the actual areas of current turbojet engines having approximately the same rated compressor total-pressure ratios. The sea-level rated air flows of each engine were chosen so that the reference velocities of the primary combustors at rated conditions approximated the reference velocities in a current engine of the type specified. Compressor operational characteristics were extrapolated from the compressor map of a current engine for engine A. For engines B and C, the compressor operational characteristics were extrapolated from the performance map of a high-performance NACA compressor. The compressor maps of engines A, B, and C are presented in figure 1. Maximum turbine-inlet total temperatures were specified to be 2060° R, a value which conforms closely to those used for current

engines. Turbine adiabatic efficiencies and combustor total-pressure-loss ratios were actual values for current turbojet engines approximated by the design specifications. Full-throttle operation was specified to be at a constant mechanical engine speed. Part-throttle operation was determined at three percentages of rated engine speed. The engines were considered to have variable-area exhaust nozzles.

Engine Operation

Although the engines discussed herein were primarily intended for subsonic operation, some data are presented for the transonic and supersonic regions to show the ranges and trends of operating conditions at high Mach numbers.

A schematic diagram of a typical turbojet engine together with the over-all trends of pressures, temperatures, and velocities of air and gases as they pass through the engine is shown in figure 2. At subsonic flight speeds, ambient air entering the engine is compressed adiabatically in the inlet diffuser with a small loss in total pressure. Further compression occurs as the air passes through the engine compressor. Fuel is added to the compressed air and combustion occurs in the primary combustor, with an accompanying rise in total and static temperatures and gas velocities. A decrease in total and static pressure occurs because of the momentum change imparted to the gases by the addition of heat. The hot combustion gases expand through the turbine to lower pressures and temperatures. The turbine removes only enough energy from the gases to operate the compressor and overcome any mechanical inefficiencies. The somewhat cooler, lower-pressure gases are expanded to ambient pressure through the exhaust nozzle. The high-velocity gases leaving the exhaust nozzle produce a jet thrust to propel the unit. At supersonic flight speeds, shock waves attend the compression process at or ahead of the engine inlet and increase the total-pressure loss of the inlet diffuser. Otherwise, the process is the same as for subsonic flight speeds.

In engines with afterburners, additional fuel is added to and burned with the gases leaving the turbine. The temperature of the gases in the afterburner is raised to a much higher average temperature than would be allowable in the primary combustor, which must operate at temperatures limited by the stress requirements of the turbine. The additional momentum imparted to the gases in the afterburner by the addition of heat increases the velocity of the gases expanding through the jet nozzle and thus augments the thrust that a nonafterburning engine might develop. An afterburner is usually operated only under full-throttle engine operating conditions.

Primary-combustor operating conditions are defined as the combustor-inlet total pressure and temperature, reference velocity, and combustor-outlet total temperature. From the preceding paragraphs, combustor-inlet total pressures and temperatures are seen to depend primarily on the flight altitude and Mach number and on the operational characteristics of the diffuser and the compressor-turbine combination. Combustor reference velocity is defined as

$$V_{c,r} = \frac{w_{a,c}}{A_{c,r}\rho_{a,t,3}}$$

where

$A_{c,r}$ reference (maximum cross-sectional) area of primary-combustor housing

$V_{c,r}$ reference velocity of primary combustor

$w_{a,c}$ weight-flow rate of air through primary combustor

$\rho_{a,t,3}$ combustor-inlet total air density

This parameter is a function of these same variables and the combustor-housing maximum cross-sectional area. The maximum combustor-outlet total temperature (or turbine-inlet total temperature) depends primarily on the design and material of the turbine. Afterburner-inlet total pressures and temperatures are functions of the same variables as the combustor-inlet conditions, with additional dependence on the design and operating characteristics of the combustor, turbine, and afterburner-inlet diffuser. Afterburner gas velocity is defined as

$$V_{ab,g} = \frac{w_{a,c}(1 + f_c + f_{ab})}{A_{ab,6}\rho_{g,6}}$$

where

$A_{ab,6}$ cross-sectional area enclosed by afterburner housing at flameholder plane

f_{ab} fuel-air ratio in afterburner

f_c fuel-air ratio in primary combustor

$V_{ab,g}$ afterburner gas velocity

$\rho_{g,6}$ weight per unit volume of gases at plane of flameholder in afterburner

This parameter is a function of the same variables together with the cross-sectional area enclosed by the afterburner housing at the plane of the flameholders.

In this chapter, the primary-combustor operating parameters were determined for full-throttle, part-throttle, and engine windmilling operation. Idling operation of the engine was not considered. Afterburner operating conditions were determined for full-throttle engine operation and are discussed separately.

OPERATING CONDITIONS

Primary Combustor

Full throttle. - The calculations of full-throttle operation of all engines were based on a constant mechanical engine speed, maximum turbine-inlet total temperature (combustor-outlet total temperature) of 2060° R, and use of variable-area exhaust nozzles to maintain choked flow through the turbine nozzles (ref. 1).

Combustor-inlet total pressure and total temperature and reference velocity for engine A over a range of flight altitudes and Mach numbers are presented in figure 3. All parameters increase as the Mach number increases at any flight altitude, the increase becoming greater as the flight Mach number increases. Combustor-inlet total pressures decrease with increases in altitude at any flight Mach number.

At any flight Mach number, combustor-inlet total temperatures and reference velocities decrease as the altitude increases to the tropopause (36,089 ft) and remain constant at higher altitudes if Reynolds number effects are neglected. High-altitude operation at low Reynolds numbers generally results in decreased component

efficiencies in a turbojet engine. The air flow is generally reduced, whereas the temperature ratio across the compressor is usually increased. The trend of the pressure ratio across the compressor cannot be predicted accurately, and therefore, the effect of this type of operation on the reference velocity cannot be predicted with certainty either.

Shown in figure 4 are combustor-inlet total pressure and total temperature and reference velocity for engine B over a range of altitudes and flight speeds. The trends of the combustion parameters are similar to those of engine A; however, the absolute values at any Mach number and altitude are quite different. Since engine B is a higher-pressure-ratio engine than A, the inlet total pressures of engine B (fig. 4(a)) are higher than those of engine A (fig. 3(a)). For the same reason, the inlet total temperatures of engine B (fig. 4(b)) are higher than those of engine A (fig. 3(b)) at any specific operating point. The combustor reference velocities of engine B (fig. 4(c)), however, are less than those of engine A (fig. 3(c)), primarily because the increase in pressure is greater than the increase in temperature at any particular operating condition.

The combustor parameters inlet total pressure, inlet total temperature, and reference velocity for engine C over a range of flight altitudes and Mach numbers are shown in figure 5. The trends of the combustion parameters for engine C are similar to those of engines A and B. Since engine C has the highest compressor total-pressure ratio, both the combustor-inlet total pressure (fig. 5(a)) and total temperature (fig. 5(b)) at any operating point are higher than the same parameters for either engine A or B. The combustor reference velocity for engine C is lower than that of either A or B at any flight speed and altitude operating condition.

With the assumptions that the maximum combustor-outlet total temperature and combustor air loading (lb of air/(sec)(sq ft of combustor reference area)) do not vary greatly, that the Reynolds number effect is neglected, and that the engine is operated at a constant mechanical speed, the following generalizations are made:

(1) Combustor-inlet total pressure and total temperature and combustor reference velocity increase with flight Mach number at any altitude.

(2) Combustor-inlet total pressure decreases with increasing altitude, whereas inlet total temperature and velocity decrease with increasing altitude to the tropopause and then remain constant in the stratosphere at a given flight Mach number.

(3) The absolute values of combustor-inlet total pressure and total temperature increase as the compressor total-pressure ratio increases at any flight speed and altitude.

(4) The absolute values of combustor reference velocity decrease as the compressor total-pressure ratio is increased at any flight speed and altitude.

Part throttle. - In general, part-throttle operation of a turbojet engine is desirable in order that the engine may operate with either minimum specific fuel consumption or maximum thrust. In a turbojet engine having a fixed-area exhaust nozzle, part-throttle operation is controlled by varying the fuel flow and thus the engine speed. At a given flight Mach number, only one operating point is possible for a given engine speed.

Operation at this point may not result in the minimum specific fuel consumption that might be obtained if turbine-inlet total temperature could be varied. For an engine having a variable-area exhaust nozzle, operation is theoretically possible at an infinite number of points for a given engine speed and flight Mach number, by

variation in turbine-inlet total temperature and also in exhaust-nozzle area. Operation at various engine speeds at a given flight Mach number and altitude thus results in a family of curves for specific fuel consumption that are functions of engine thrust and turbine-inlet temperature. Each of these curves has a point of minimum specific fuel consumption. In general, it is usual to construct a curve tangent to this family of curves. The tangent curve represents a controlled operational curve, which will result in minimum specific fuel consumption for a given engine thrust at any engine mechanical speed.

The part-throttle data included in this discussion are calculated for engines having variable-area exhaust nozzles. The data are presented for engine mechanical speeds that are 70, 80, and 90 percent of rated mechanical speed and for operation at flight Mach numbers from 0.6 to 1.0 in the stratosphere. Not much value should be assigned to operation at 70 percent of rated engine speed. In all the engines, the most efficient operation at this speed occurred near the compressor-surge region, and it is doubtful whether operation would be desirable or possible for long periods of time under such conditions. In addition, engine thrusts were so low that the net effect would probably be little more than that of engine idling. Data for operation at 100 percent of rated speed included on some of the figures are for operation at the limiting turbine-inlet total temperature of 2060° R. Operation is possible at 100 percent of rated speed and lower turbine-inlet temperatures by varying exhaust-nozzle area. However, such operation usually results in lower engine thrusts. The data are presented in terms of combustor-inlet total pressures and temperatures, combustor-outlet total temperatures, and combustor reference velocities.

Combustor-inlet total pressures for part-throttle operation of engines A, B, and C are presented in figure 6. For each engine, inlet total pressures increased with increasing flight Mach number and decreased with increasing flight altitudes and decreasing percentages of rated engine speed. Among the three engines considered, at any flight Mach number, flight altitude, and percent of rated engine speed, inlet total pressures varied in the order of the compressor total-pressure ratios.

Combustor-inlet total temperatures are presented in figure 7(a). At all altitudes above the tropopause, combustor-inlet total temperatures are a function only of flight Mach number and compressor operating characteristics. Thus, data of figure 7(a) apply at all altitudes above the tropopause. Combustor-inlet total temperatures increase with increasing flight Mach number and increasing percentages of rated engine speed; combustor-inlet total temperatures vary in the same order as do the rated compressor total-pressure ratios.

Combustor-outlet total temperatures or turbine-inlet total temperatures required for operation at three part-throttle conditions are presented in figure 7(b). Part-throttle turbine-inlet total temperatures more than any other combustor parameter are a function of the particular engine under consideration and its particular compressor, combustor, and turbine operating characteristics. For this reason, the turbine-inlet total temperatures of figure 7(b) exhibit no definite trends due to flight Mach number or compressor total-pressure ratio. However, for a particular engine, turbine-inlet total temperatures do increase with increasing percentages of rated engine speed.

Combustor reference velocities for engines A, B, and C during stratospheric part-throttle operation are presented in figure 7(c). In part-throttle operation as in full-throttle operation, reference velocities increase with increasing flight Mach number, and at a given flight Mach number, decrease with increasing compressor pressure ratio. For all engines, the reference velocities at 100 percent rated speed were less than or equal to the velocities at 80 or 90 percent of rated engine speed. This effect is due to operation at 100 percent rated speed at the limiting turbine-inlet total temperature, which is not the point of minimum specific fuel consumption but is the maximum-thrust condition. Operation at the point of minimum specific fuel

consumption corresponding to 100 percent rated engine speed at any flight Mach number would result in a lower temperature ratio between the turbine inlet and compressor inlet than would be required at the maximum-thrust condition. The lower temperature ratio would result in a reduced compressor pressure ratio with accompanying decreased combustor-inlet total pressures and temperatures. Since the air flow remains practically constant and the change in pressure across the compressor is greater than the change in temperature, the combustor reference velocity would increase.

Windmilling. - The windmilling characteristics of turbojet engines are important in the study of turbojet primary combustors because the ignition or relighting of combustors at any flight condition depends on the combustor parameters of inlet total pressure and temperature and reference velocity (ref. 2). Few data exist to establish combustor operating conditions during engine windmilling. A simple method of determination is to assume that the combustor-inlet total pressure is equal to the ambient pressure at altitude plus any isentropic ram-pressure rise and minus any engine-inlet-diffuser total-pressure losses. Combustor-inlet total temperatures are assumed equal to ambient temperature at altitude plus any isentropic ram-temperature rise. A better method for determining engine windmilling characteristics is reported in reference 3. Corrected windmilling engine speeds, equivalent air flows through the engines, and corrected total-pressure losses from the compressor inlet to the turbine exit were each generalized for a series of several engines into single curves that were functions of flight Mach number. The total-pressure loss through the engine was equal to the sum of the total-pressure changes through the compressor, combustor, and turbine. Thus, although the total-pressure losses for several different engines generalized into a single curve as a function of flight Mach number, the component pressure changes for individual engines were quite different. The windmilling total-pressure losses for the combustors and turbines of the various engines increased with increasing flight Mach number. Total-pressure losses through the compressor increased to a maximum with flight Mach number and then decreased, until at a given flight speed, the windmilling pressure change through the compressor became positive. That is, the pressure began to rise through the compressor. This rise is explained by the fact that the engine windmilling speed increases with increasing flight Mach number, and the turbine operates closer to its design speed. Eventually, at a particular engine windmilling speed, the turbine work becomes greater than necessary to offset compressor losses, with a resultant rise in total pressure through the compressor. For the particular engines discussed in reference 3, enough data are presented to calculate combustor-inlet total pressures.

No data are reported in reference 3 on temperature variation during windmilling. However, reference 4 includes some data for variation of pressures, temperatures, and velocities in a windmilling 4.7-pressure-ratio engine at simulated Mach numbers of 0.25 to 0.85 and at altitudes of 20,000 to 40,000 feet. The total-temperature change across the compressor at low flight Mach numbers was practically zero, and in some cases, a slight total-temperature decrease was shown.

For engines A, B, and C, the corrected windmilling air flow, the total-pressure drop across the engine, and the corrected windmilling engine speed were determined from reference 3. Windmilling total-pressure losses through the combustors and turbines of engines A, B, and C were calculated by determining the total-pressure losses at sea-level rated conditions and assuming that the windmilling total-pressure losses varied in the same manner with flight speed as the pressure losses of the engine components of reference 3. However, it was necessary to correct the turbine total-pressure losses because of differences in turbine-blade lengths and tip diameters, in windmilling speeds, and in the number of stages with quantities similar to those of the engines of reference 3. These corrections were made as shown in reference 5. From these data, the compressor total-pressure changes during windmilling of engines

A, B, and C were calculated at various flight speeds. Combustor-inlet total pressures were then determined by correcting the ambient pressure at altitude for the effects of flight Mach number and engine-inlet diffuser and for the total-pressure change through the compressor.

Combustor-inlet total temperatures during windmilling of engines A, B, and C were calculated by assuming that the inlet total temperatures varied in the same manner with altitude and flight Mach number at all windmilling speeds at which a compressor total-pressure drop existed as did the combustor-inlet total temperatures of reference 4. At all flight Mach numbers at which a windmilling total-pressure rise occurred in the compressor, the combustor-inlet total temperature was calculated from the isentropic pressure-temperature relation. These values of inlet total temperature thus represent minimum values.

Windmilling combustor parameters of engine A are presented in figure 8. Combustor-inlet total pressures increase with increasing flight Mach number and decrease with increasing altitude. Combustor-inlet total temperatures and reference velocities increase with flight Mach number and decrease with increasing altitude up to the tropopause, above which the temperatures and velocities remain constant at a given flight Mach number. Windmilling combustor reference velocities become quite large at high flight Mach numbers. This effect reflects the relatively large windmilling air flows and small compressor pressure changes.

Combustor operational parameters for engines B and C are presented in figures 9 and 10. These figures show the same effect of flight speed and altitude on the combustor parameters as does figure 8. A comparison of combustor operational parameters of engines A, B, and C at a given flight Mach number and altitude shows, in general, that highest and lowest combustor-inlet total pressures and temperatures were found with engines C and B, respectively, while reference velocities were highest and lowest with engines A and B, respectively. These effects are essentially due to the windmilling pressure-change characteristics of the compressor and the ratios of combustor reference and compressor frontal areas of the individual engines.

Afterburner

As stated previously, the afterburner on a turbojet engine ordinarily operates only during full-throttle engine operation. The data on afterburners discussed herein were calculated for the same full-throttle flight conditions as those for the previously discussed primary combustors. The afterburner operating conditions that are primarily of interest are the afterburner-inlet total pressure, temperature, and velocity. The afterburner-inlet total pressures were calculated by assuming that a 5-percent total-pressure loss occurred in the afterburner-inlet diffuser between the turbine exit and the afterburner flameholder. Afterburner-inlet total temperatures were equal to turbine-outlet total temperatures. The afterburner velocities were calculated from the gas flow through the afterburner, the gas density, and the maximum cross-sectional area of the afterburner housing at the plane of the flameholders.

Afterburner-inlet total pressures, temperatures, and velocities for engine A are presented in figure 11. The general shape of the afterburner-inlet total-pressure curves is much the same as that of the primary-combustor-inlet total pressures. Afterburner-inlet total pressures increase with increasing flight Mach number and decreasing altitudes. Afterburner-inlet total temperatures increase with increasing altitudes up to the tropopause, above which the inlet total temperatures remain constant. Afterburner-inlet total temperatures in general decrease with increasing Mach number. Afterburner velocities in general decrease with increasing altitude up to the tropopause, above which the velocities remain constant for a given flight speed. At high flight Mach numbers, however, the effect of operating characteristics of the compressor, combustor, and turbine become apparent in the variation of afterburner-inlet total temperature and velocity.

[redacted]

Similar data for engines B and C are presented in figures 12 and 13. In a comparison among the three engines, highest and lowest afterburner-inlet total pressures at a given flight condition were obtained with engines B and A, respectively. The difference in the effects of compressor total-pressure ratio on the primary combustor and afterburner of the three engines at any flight speed, altitude, and turbine-inlet temperature is quite marked. An increase in rated compressor total-pressure ratio results in more favorable operating conditions (higher pressures and temperatures and lower reference velocities) for the primary combustor. In the afterburners, the increase in compressor total-pressure ratios results in an increase in afterburner-inlet pressure up to some maximum value. Further increase in compressor total-pressure ratio results in a decrease in afterburner-inlet pressure. This comparison of the afterburner-inlet total pressures demonstrates the dependency of the afterburner-inlet conditions on the component operating characteristics of the individual engines.

At a given flight condition, highest afterburner-inlet total temperatures occur in engine A and lowest temperatures in engine C. This trend agrees with the increased amounts of power required to operate compressors with increasing compressor total-pressure ratios. No significant trend is apparent in a comparison of the afterburner velocities in the three engines. This fact is attributed to the component operating characteristics and afterburner areas of the individual engines.

APPLICATIONS TO OTHER ENGINES

The foregoing material applies specifically to engines A, B, and C. However, in many cases, it may be necessary to extrapolate or interpolate the data for an engine differing somewhat in compressor and combustor configurations. In addition, other engines may differ in maximum turbine-inlet total temperature or may have various materials injected into the compressor or the combustor.

Improvements in compressor design may permit a compressor of the same frontal area, pressure ratio, and efficiency as those specified in table I to handle greater weight flows of air. For the same combustor geometry, the increase in air flow would increase the reference velocity through the primary combustor by the ratio of the air weight flows. For other combustor geometries and rated air flows, the reference velocity may be expressed by

$$(V_{c,r,sls})_X = (V_{c,r,sls})_{A,B,C} \frac{\left(\frac{w_{a,c,sls}}{A_{c,r}}\right)_X}{\left(\frac{w_{a,c,sls}}{A_{c,r}}\right)_{A,B,C}}$$

where

$(V_{c,r,sls})_X$ reference velocity through combustor of engine X at rated sea-level static conditions

$(V_{c,r,sls})_{A,B,C}$ reference velocity through combustors of engine A, B, or C at rated sea-level static conditions

$\left(\frac{w_{a,c,sls}}{A_{c,r}}\right)_X$ rated sea-level static weight-flow rate of air per unit combustor reference area of engine X

$\left(\frac{w_{a,c,sls}}{A_{c,r}}\right)_{A,B,C}$ rated sea-level static weight-flow rate of air per unit combustor reference area of engine A, B, or C

[redacted]

New and improved turbine materials, cooled turbines, or combinations of new materials and cooling will permit higher allowable turbine-inlet total temperatures than the values specified in this chapter. Operation at higher turbine-inlet total temperatures at the same engine speed would result in approximately the same weight flows of air but higher compressor total-pressure ratios. Higher pressure ratios would benefit the primary combustor. That is, the effect of the higher turbine-inlet total temperature at the same engine speed would be an increase in combustor-inlet total pressure and a decrease in combustor reference velocity.

The addition of water, water and alcohol, hydrogen peroxide, or other liquids into the primary combustor of an engine effectively increases the weight flow through the combustor and at the same time decreases the turbine-inlet total temperature. The subsequent addition of more fuel to restore the turbine-inlet temperature introduces additional mass into the combustor. Since choked turbine nozzles are specified, the compressor total-pressure ratio must be increased to force the total weight flow through the turbine nozzles. Thus, the effect of additives is beneficial to the primary combustor. That is, the net result is increased combustor-inlet total pressures and probably reduced reference velocities.

In general, the results of this chapter may be used to approximate closely the combustor operating conditions in engines whose combustor air loadings and turbine-inlet total temperatures are similar to those presented. The approximation becomes less accurate with changes in maximum turbine-inlet total temperatures, liquid injection into the combustor, compressor air bleed, appreciable Reynolds number effects, and high inlet-diffuser losses.

Lewis Flight Propulsion Laboratory
National Advisory Committee for Aeronautics
Cleveland, Ohio, November 28, 1955

REFERENCES

1. Pinkel, Benjamin, and Karp, Irving M.: A Thermodynamic Study of the Turbojet Engine. NACA Rep. 891, 1947. (Supersedes NACA WR E-241.)

2. Foster, Hampton H., and Straight, David M.: Effect of Fuel Volatility Characteristics on Igniton-Energy Requirements in a Turbojet Combustor. NACA RM E52J21, 1953.

3. Wallner, Lewis E., and Welna, Henry J.: Generalization of Turbojet and Turbine-Propeller Engine Performance in Windmilling Condition. NACA RM E51J23, 1951.

4. Wilsted, H. D., and Armstrong, J. C.: Effect of Fuel Volatility on Altitude Starting Limits of a Turbojet Engine. NACA RM E50G10, 1950.

5. Kearton, William J.: Steam Turbine Theory and Practice. Fourth ed., Pitman Pub. Corp., 1947, pp. 169-173.

TABLE I. - DESCRIPTIVE ENGINE DATA

Engine	Type compressor	Rated compressor total-pressure ratio, $\left(\frac{P_{t,3}}{P_{t,2}}\right)_{sls}$	Rated air flow, $(w_a)_{sls}$, lb/sec	Compressor frontal area, A_2, sq ft	Combustor reference area, $A_{c,r}$, sq ft	Afterburner area at flameholder, A_{ab}, sq ft	Rated air flow per unit combustor reference area, $\frac{(w_a)_{sls}}{A_{c,r}}$, lb/(sec)(sq ft)	Maximum turbine-inlet total temperature, T_4, $^{\circ}R$	Rated combustor reference velocity, $(V_{c,r})_{sls}$, ft/sec
A	Axial-flow	5	94.8	4.55	3.84	5.79	24.69	2060	109
B	Axial-flow	8	140	4.75	5.63	5.55	24.87	2060	78
C	Axial-flow	12	175	7.08	6.95	7.02	25.18	2060	59

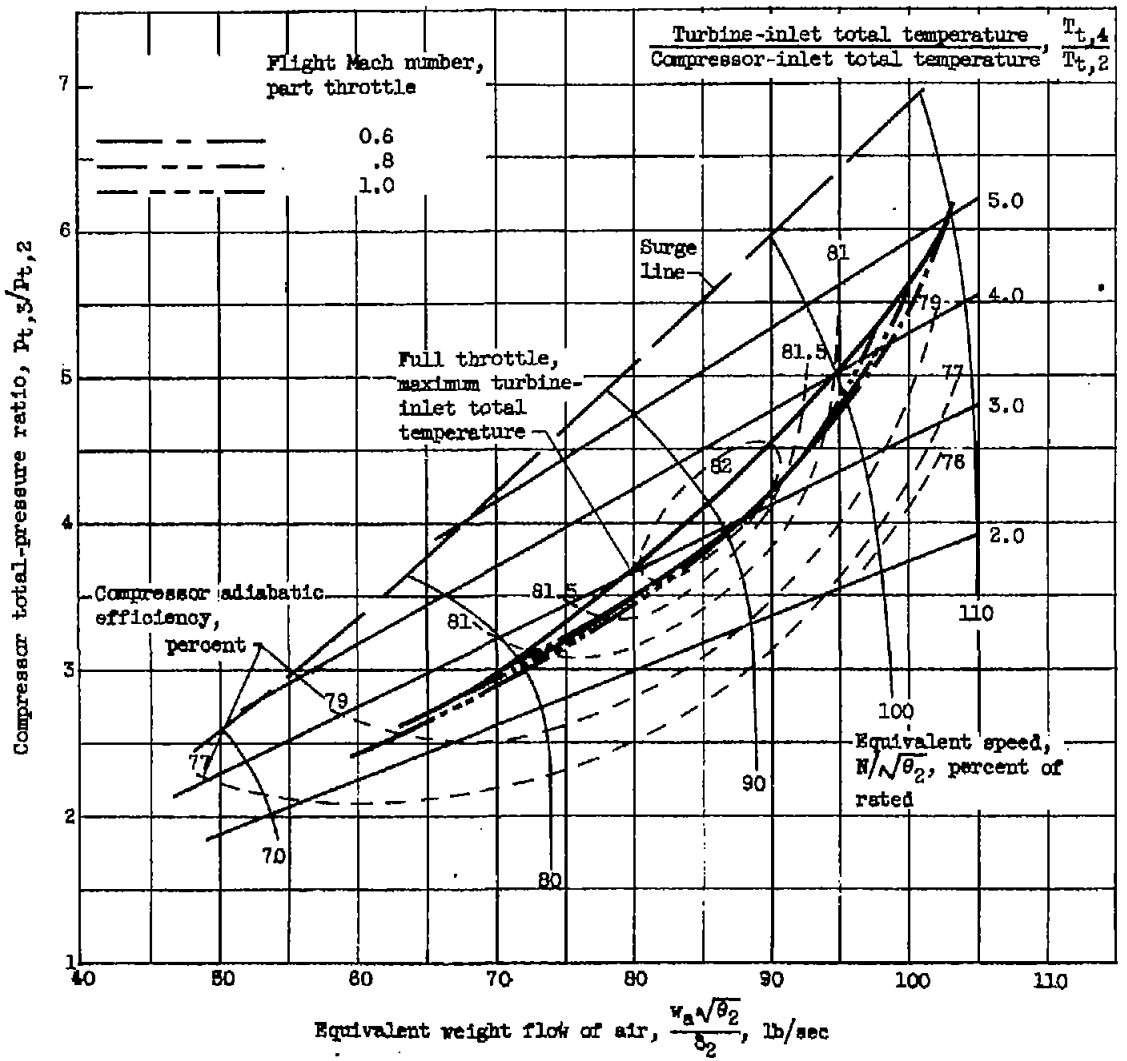

(a) Engine A.

Figure 1. - Engine compressor operational map.

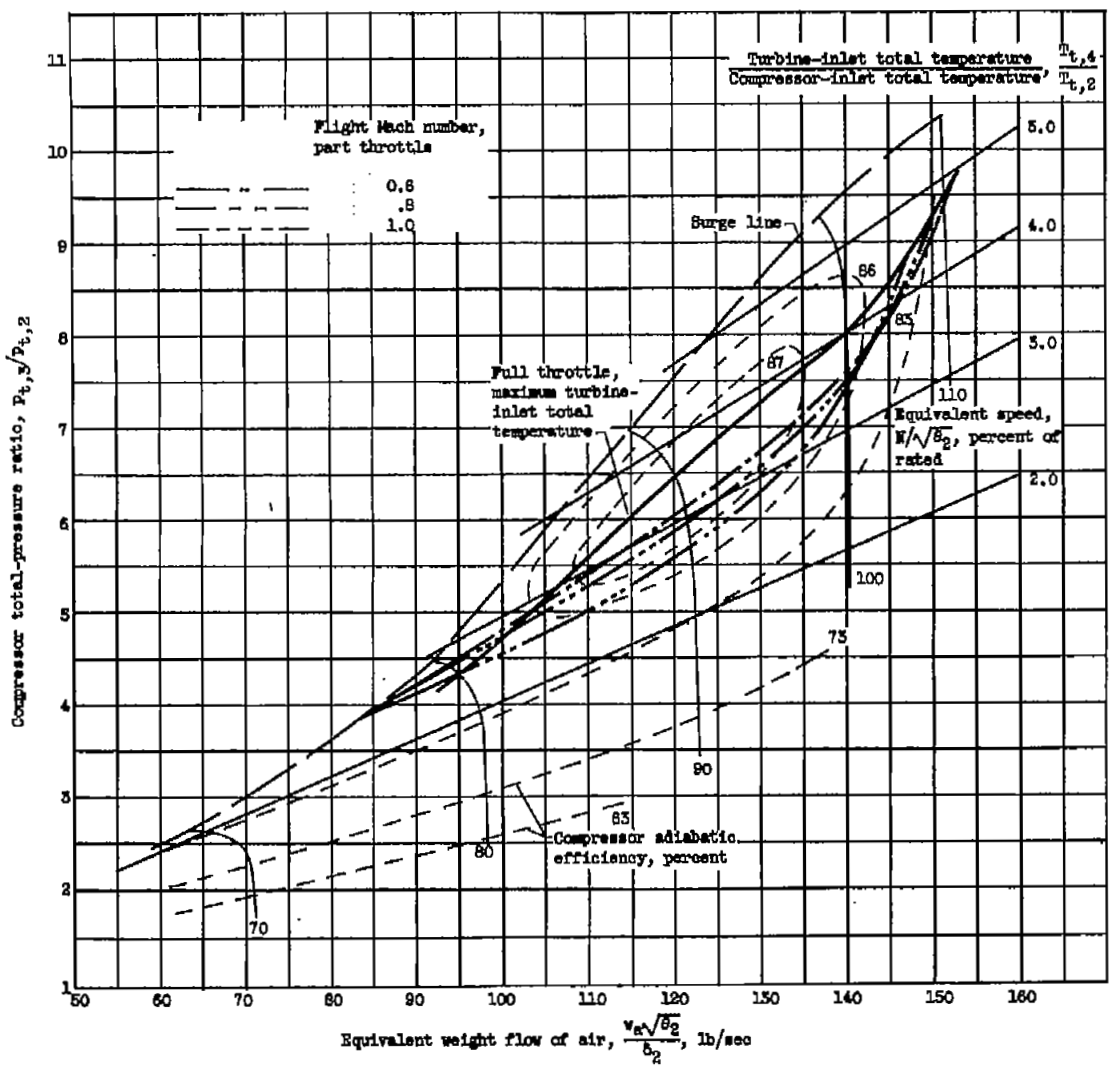

(b) Engine B.

Figure 1. - Continued. Engine compressor operational map.

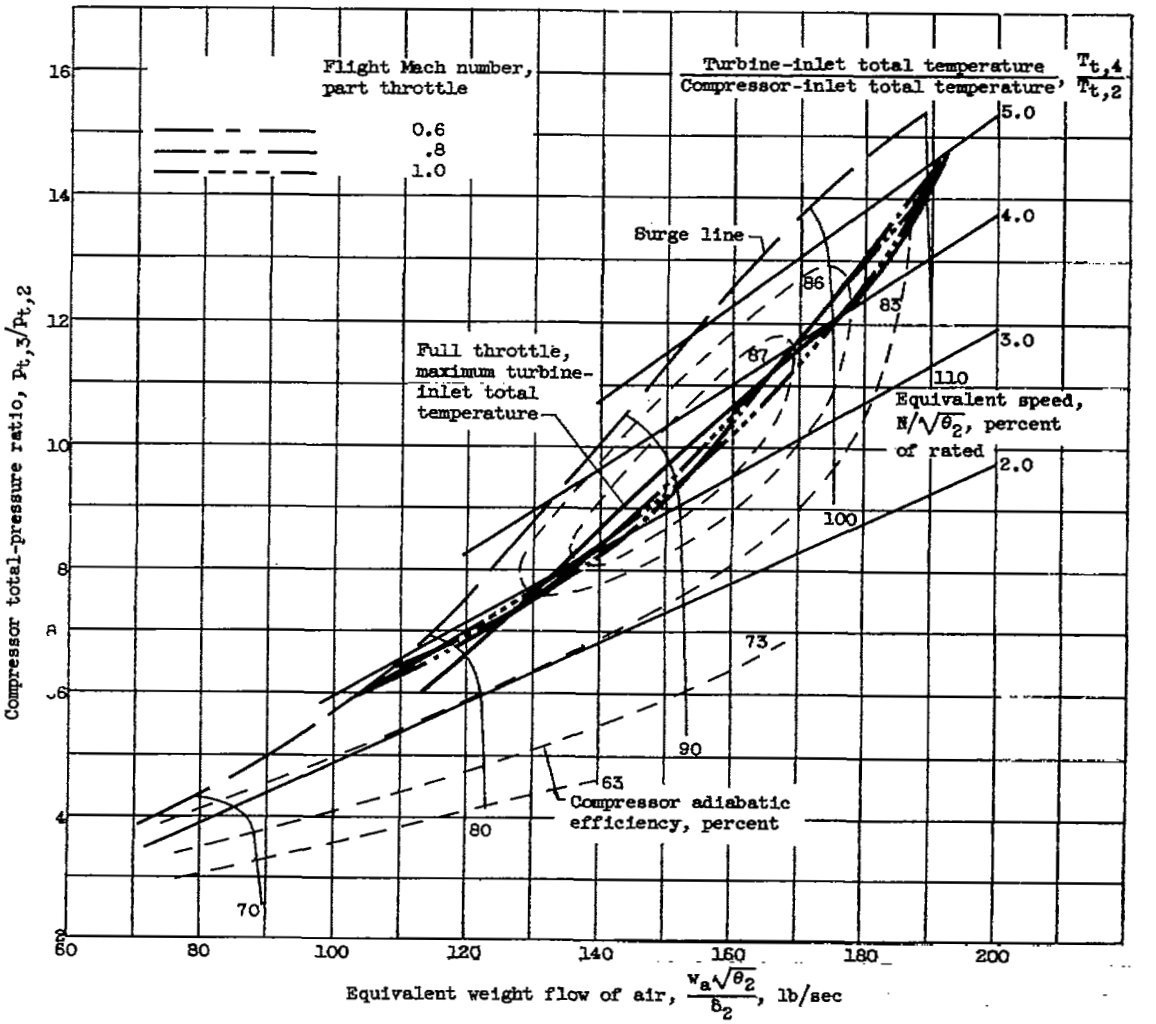

(c) Engine C.

Figure 1. - Concluded. Engine compressor operational map.

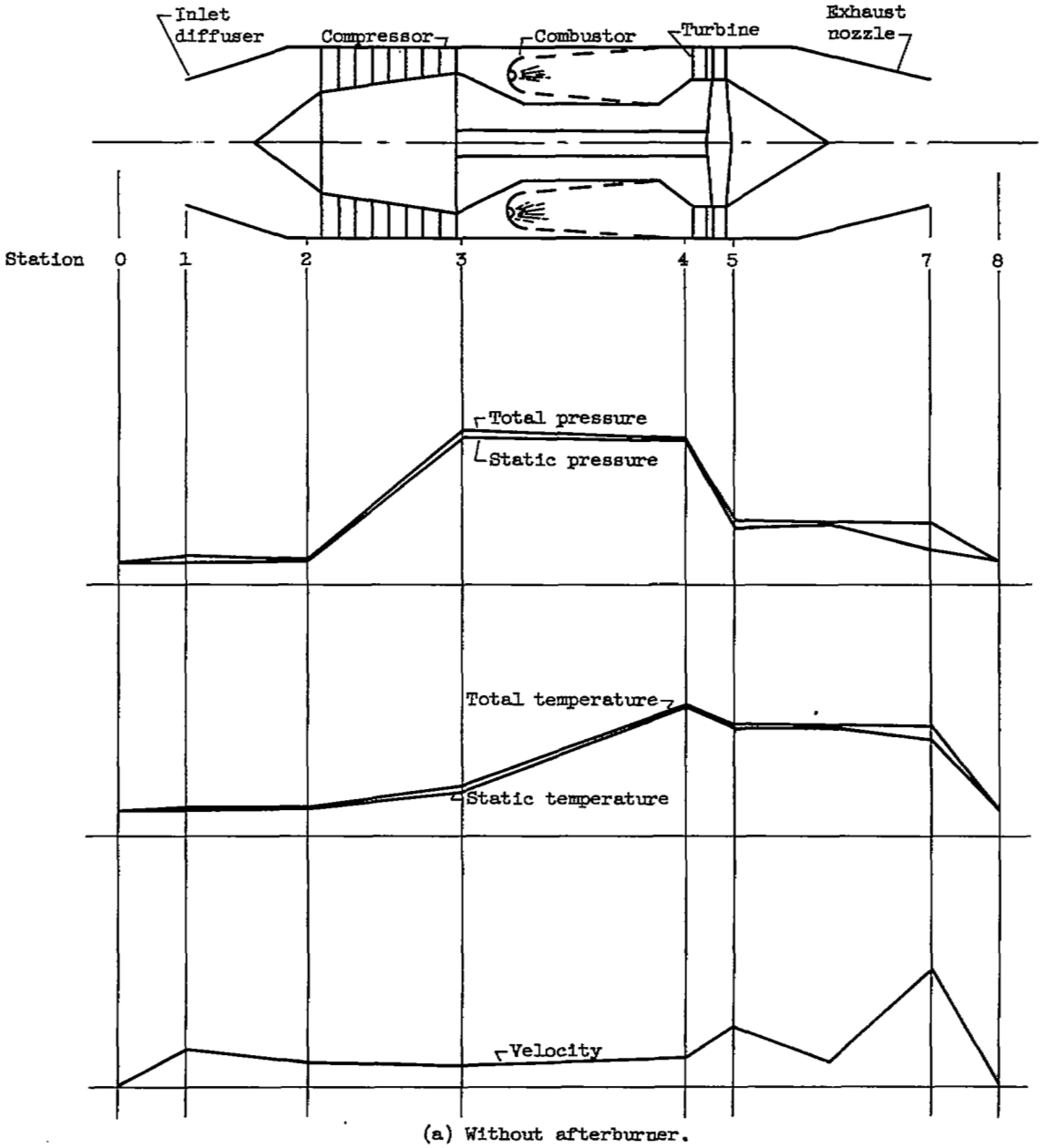

(a) Without afterburner.

Figure 2. - Pressure, temperature, and velocity trends in turbojet engine.

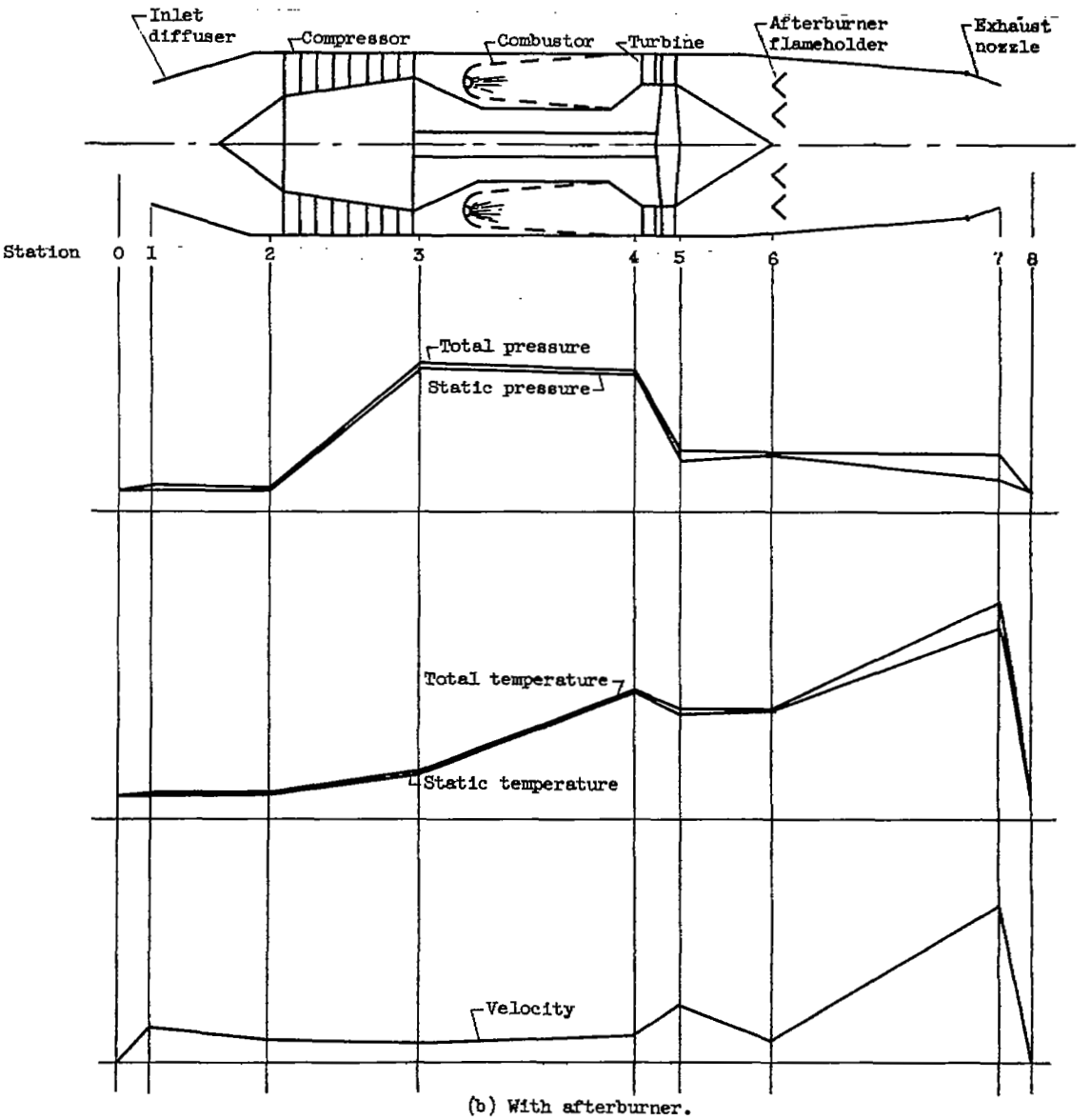

(b) With afterburner.

Figure 2. - Concluded. Pressure, temperature, and velocity trends in turbojet engine.

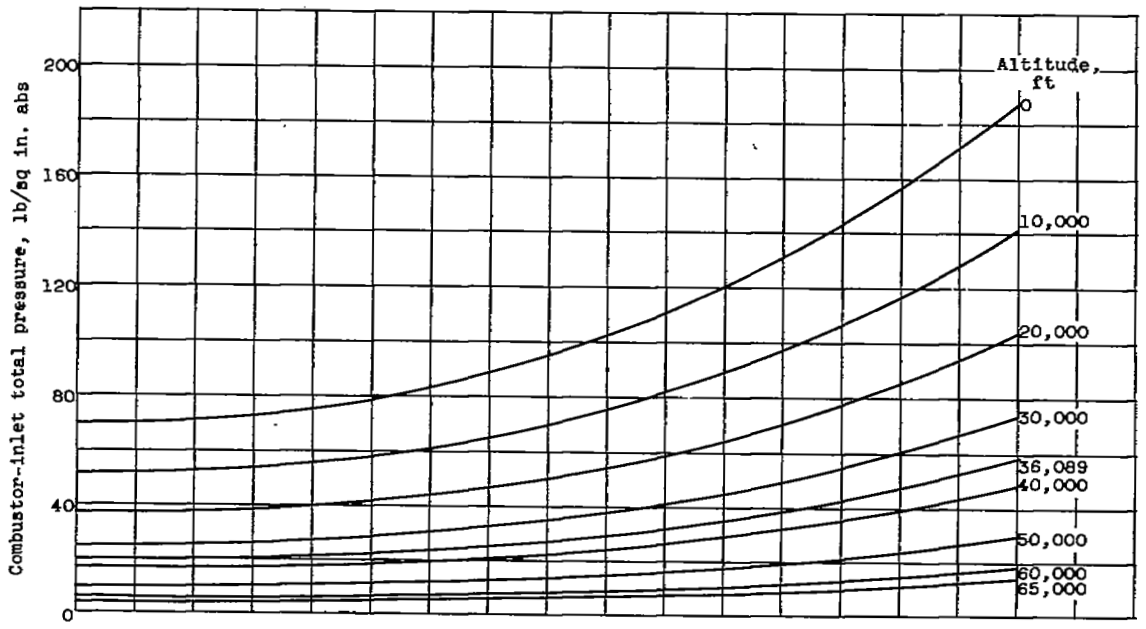

(a) Inlet total pressure.

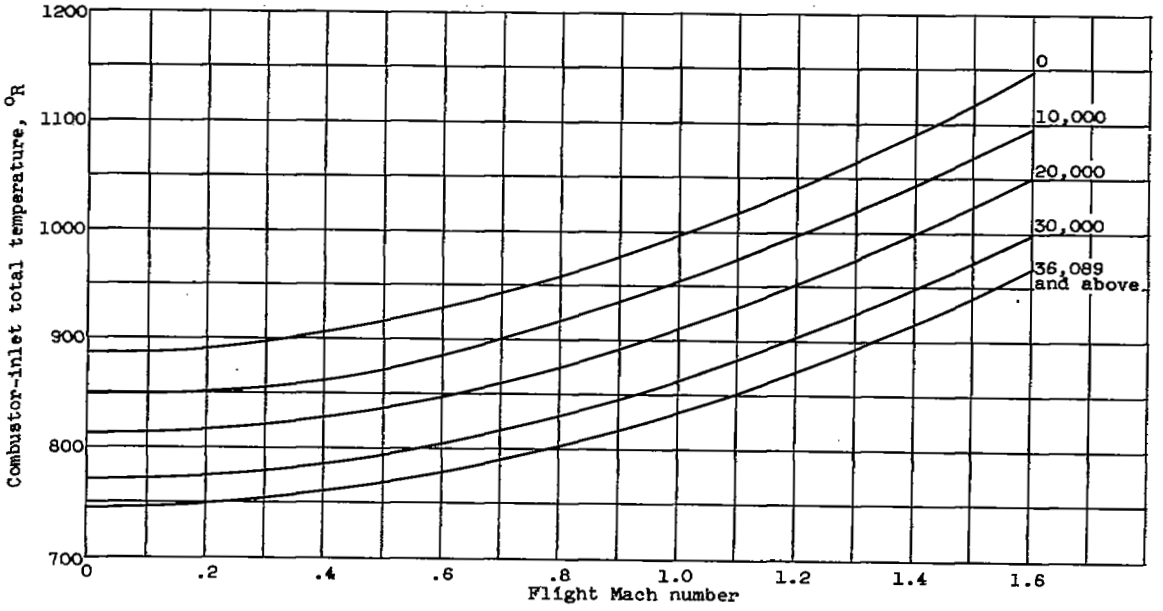

(b) Inlet total temperature.

Figure 3. - Variation of combustor parameters with flight operating conditions for full-throttle operation of engine A.

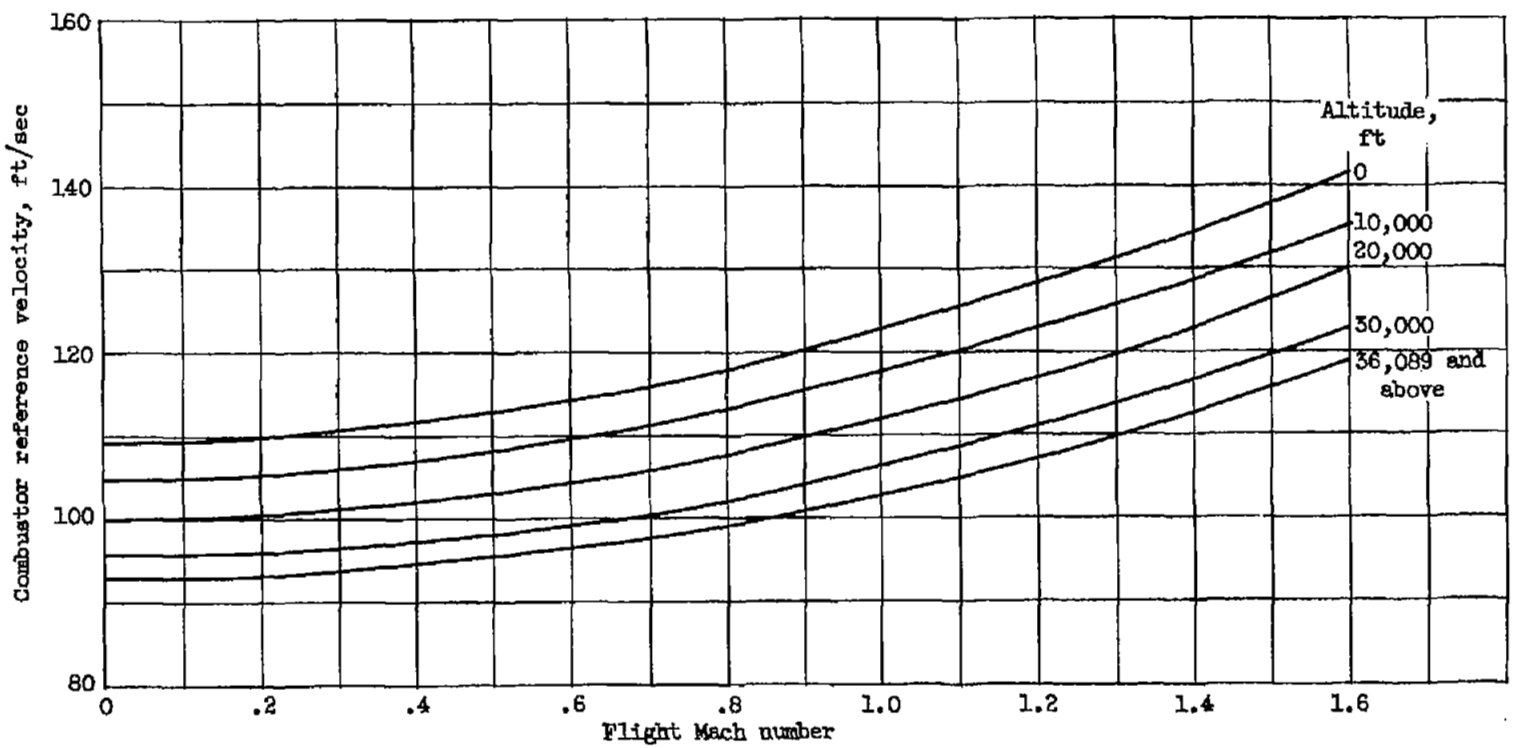

(c) Reference velocity.

Figure 3. - Concluded. Variation of combustor parameters with flight operating conditions for full-throttle operation of engine A.

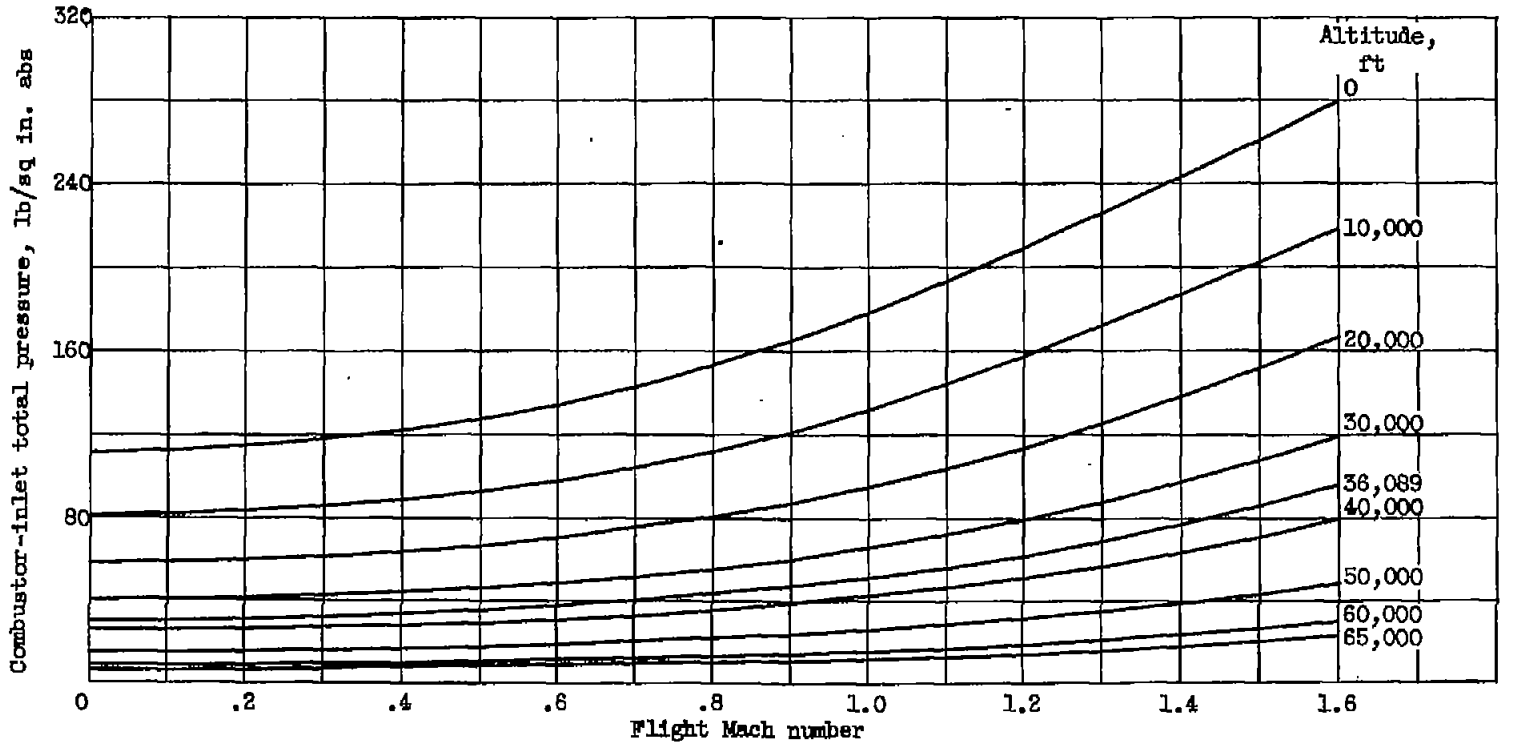

(a) Inlet total pressure.

Figure 4. - Variation of combustor parameters with flight operating conditions for full-throttle operation of engine B.

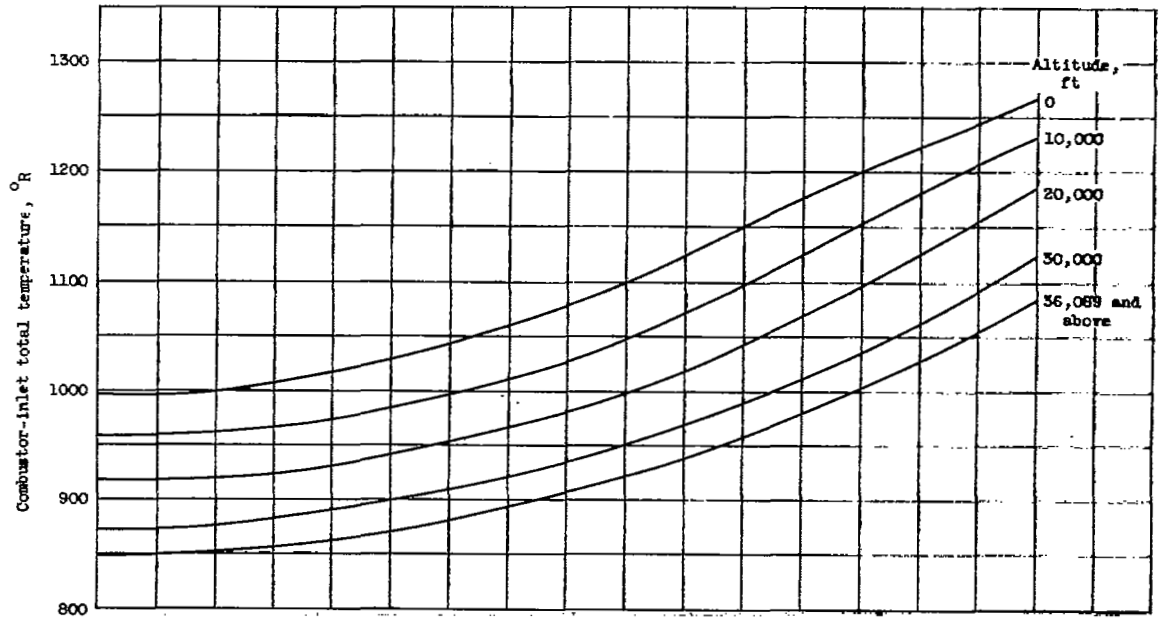

(b) Inlet total temperature.

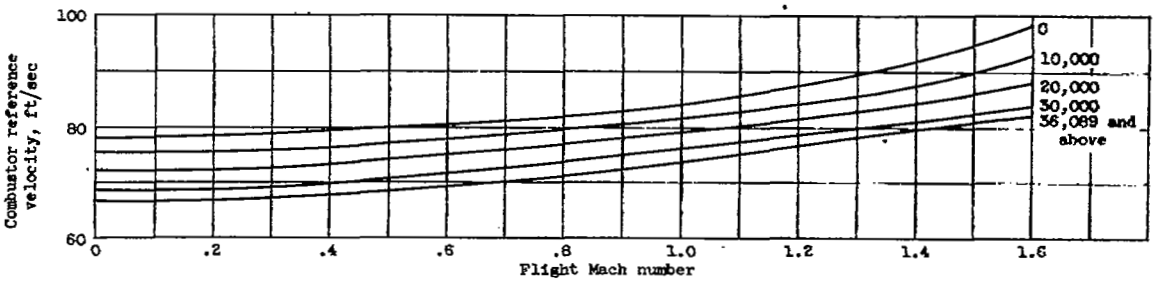

(c) Reference velocity.

Figure 4. - Concluded. Variation of combustor parameters with flight operating conditions for full-throttle operation of engine B.

[redacted]

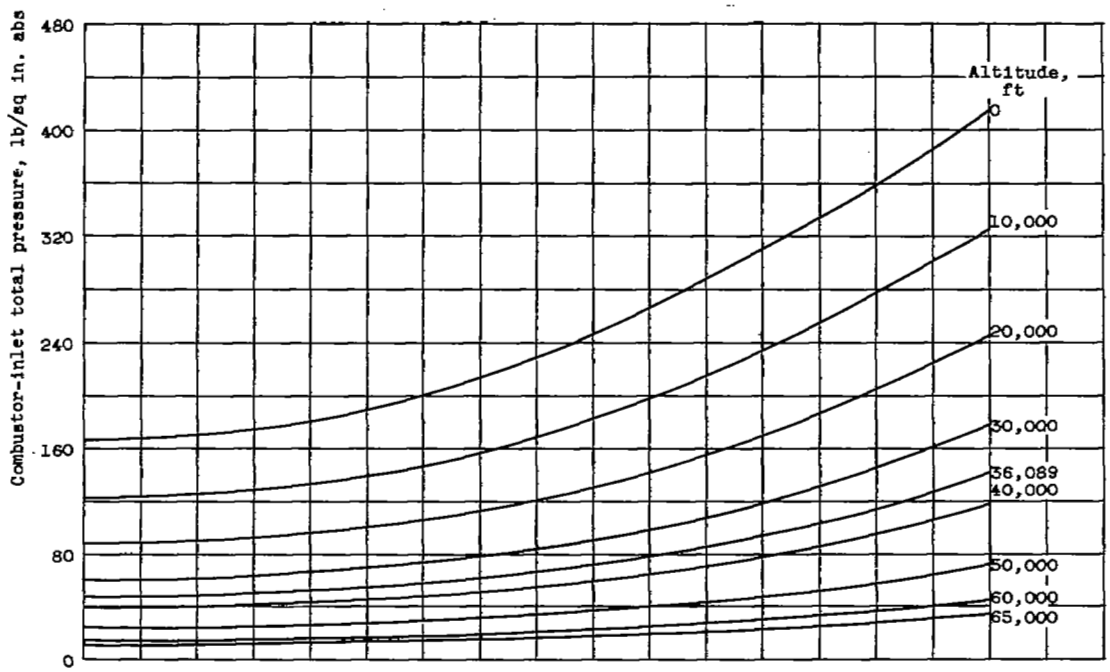

(a) Inlet total pressure.

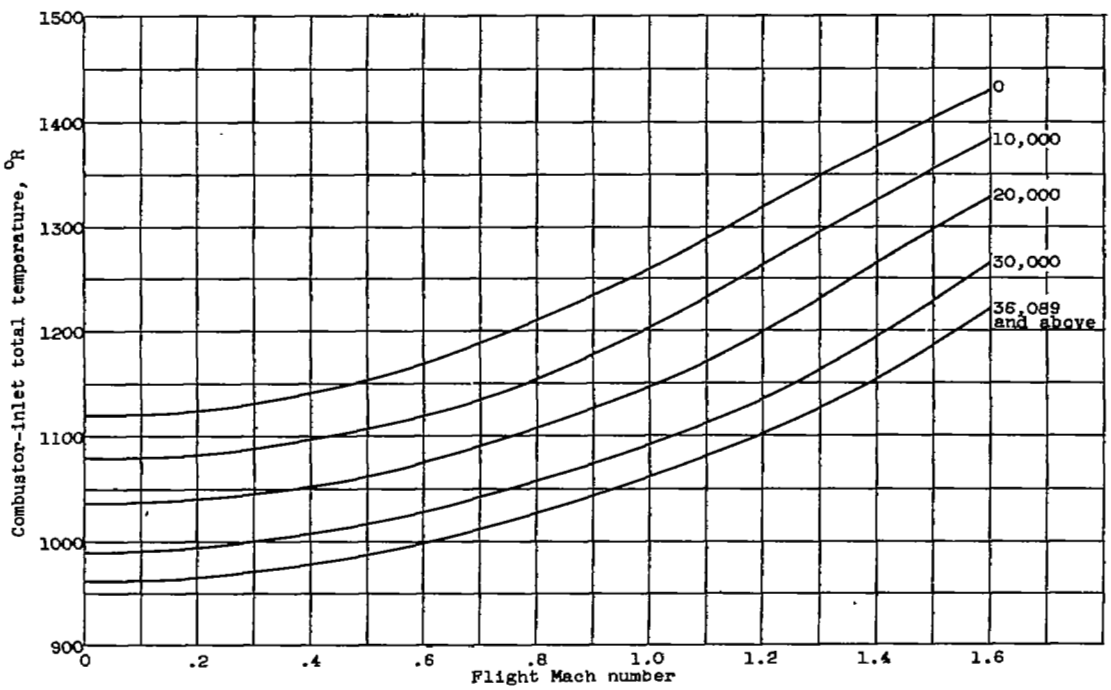

(b) Inlet total temperature.

Figure 5. - Variation of combustor parameters with flight operating conditions for full-throttle operation of engine C.

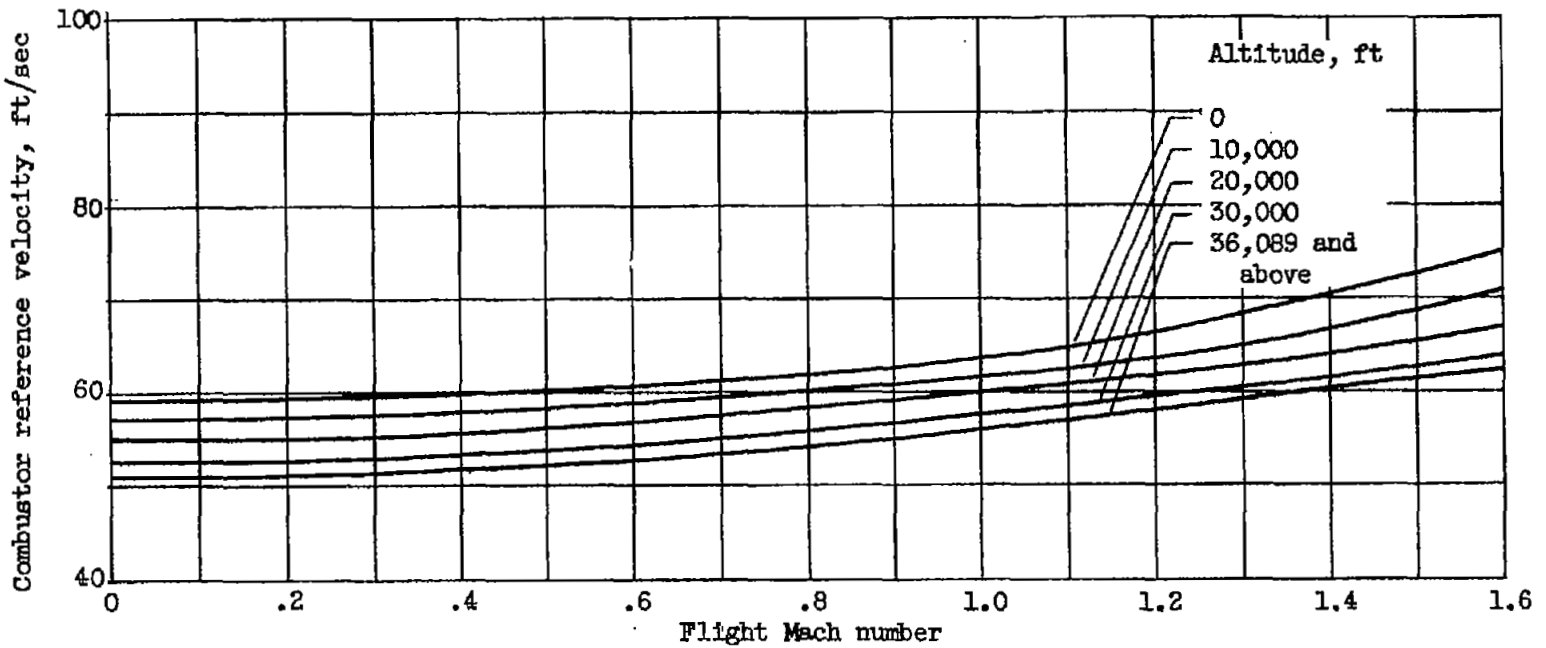

(c) Reference velocity.

Figure 5. - Concluded. Variation of combustor parameters with flight operating conditions for full-throttle operation of engine C.

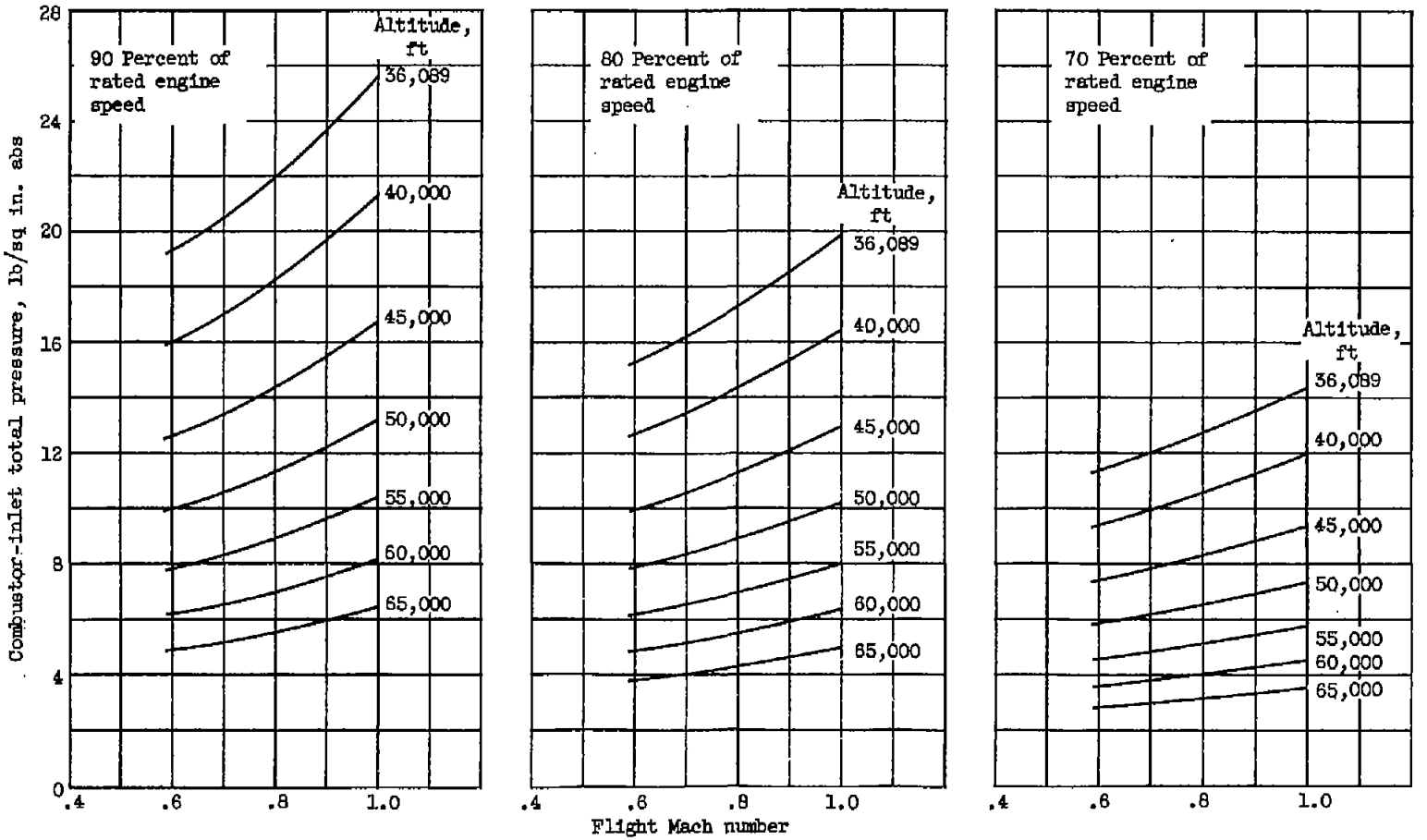

(a) Engine A.

Figure 6. - Variation of combustor-inlet total pressure with flight operating conditions for part-throttle operation.

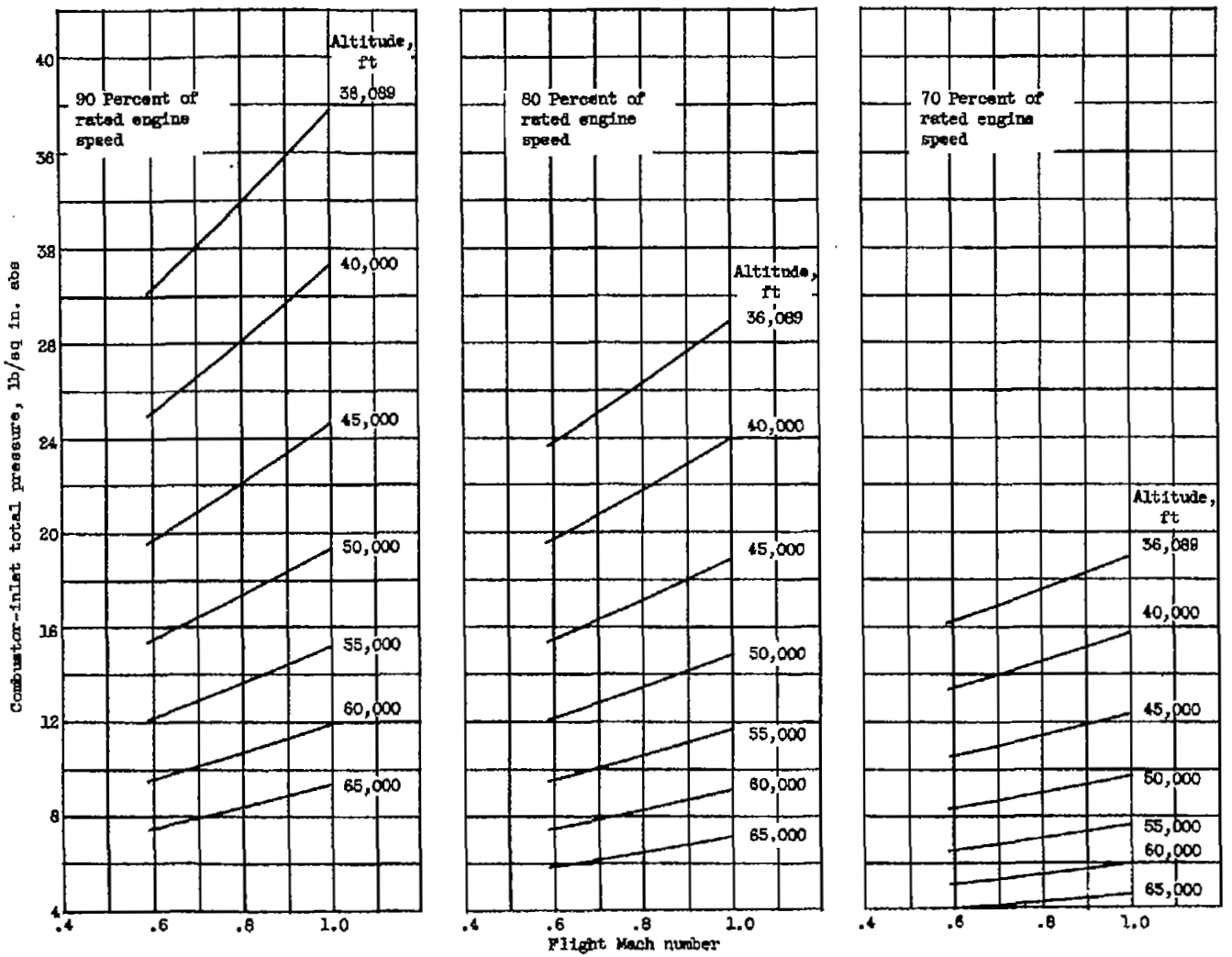

(b) Engine B.

Figure 6. - Continued. Variation of combustor-inlet total pressure with flight operating conditions for part-throttle operation.

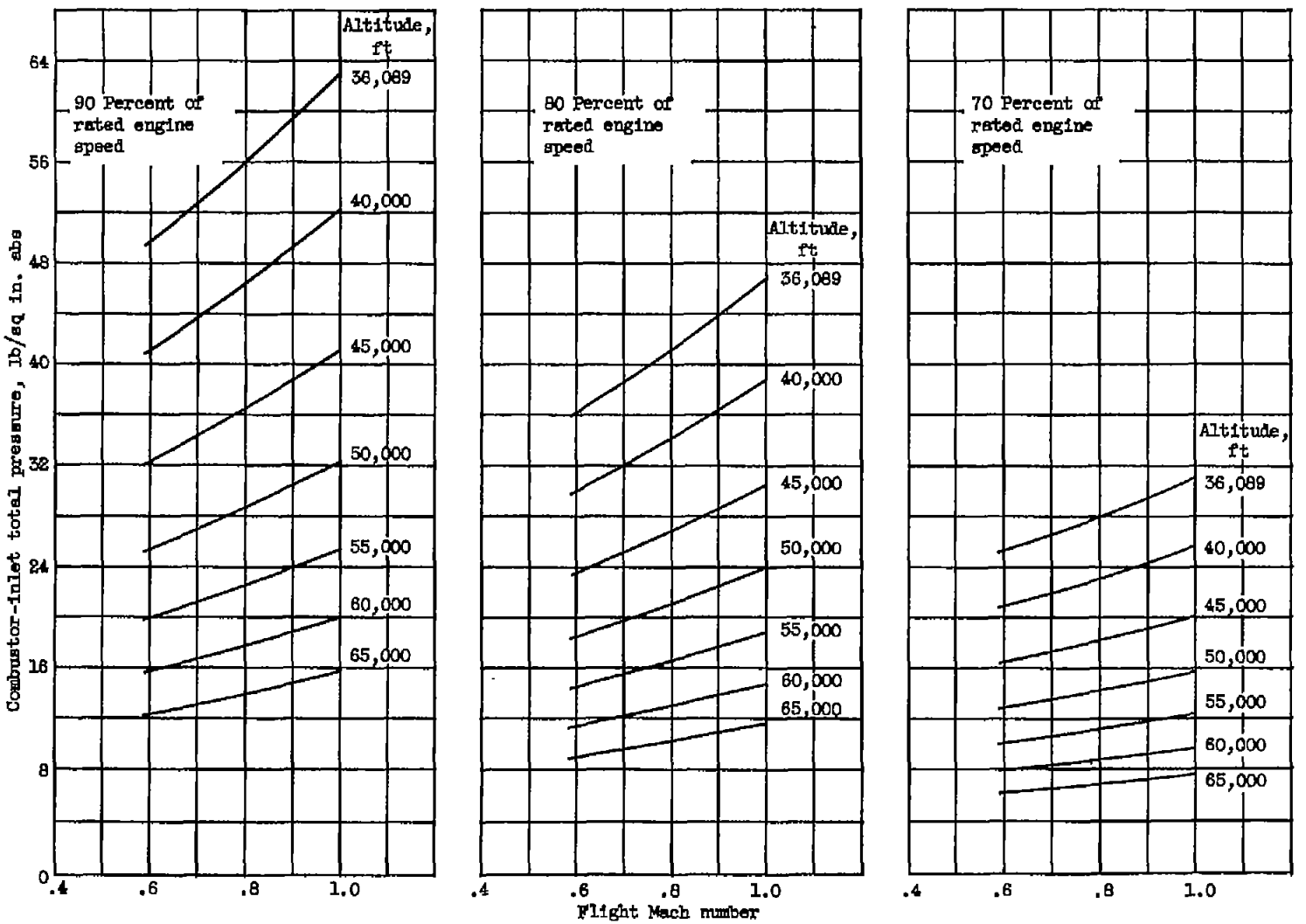

(c) Engine C.

Figure 6. - Concluded. Variation of combustor-inlet total pressure with flight operating conditions for part-throttle operation.

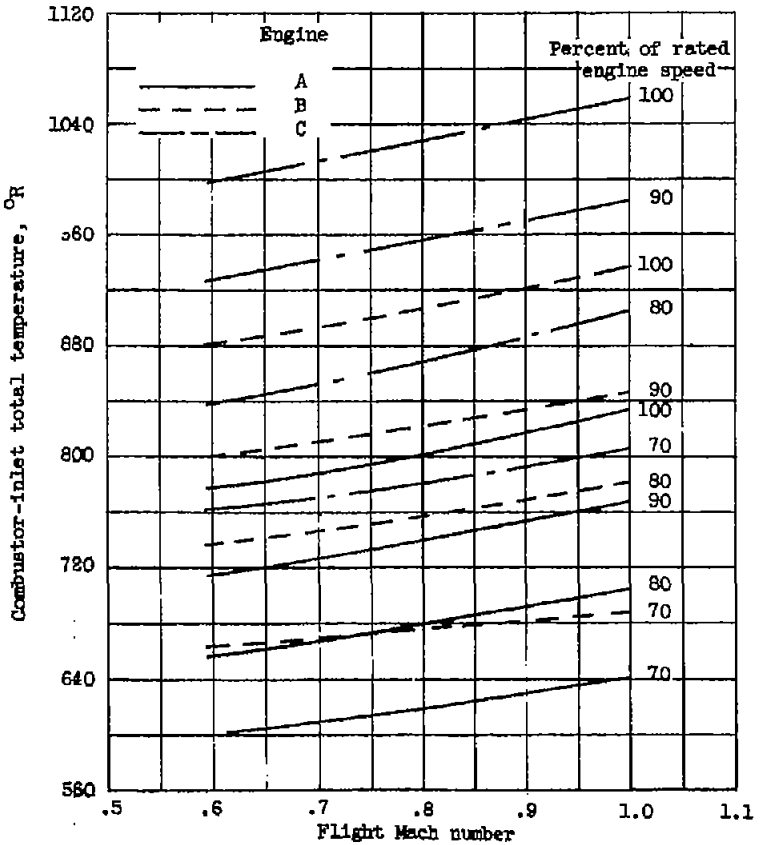

(a) Inlet total temperature.

Figure 7. - Variation of combustor parameters with flight operating conditions in stratosphere for part-throttle operation of engines A, B, and C.

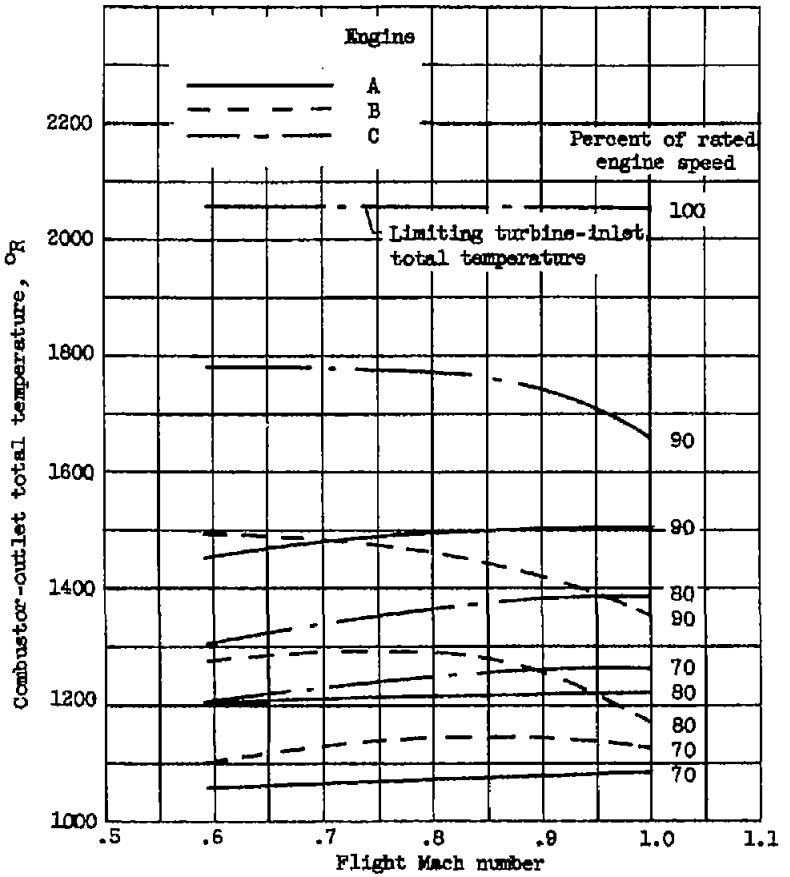

(b) Outlet total temperature.

Figure 7. - Continued. Variation of combustor parameters with flight operating conditions in stratosphere for part-throttle operation of engines A, B, and C.

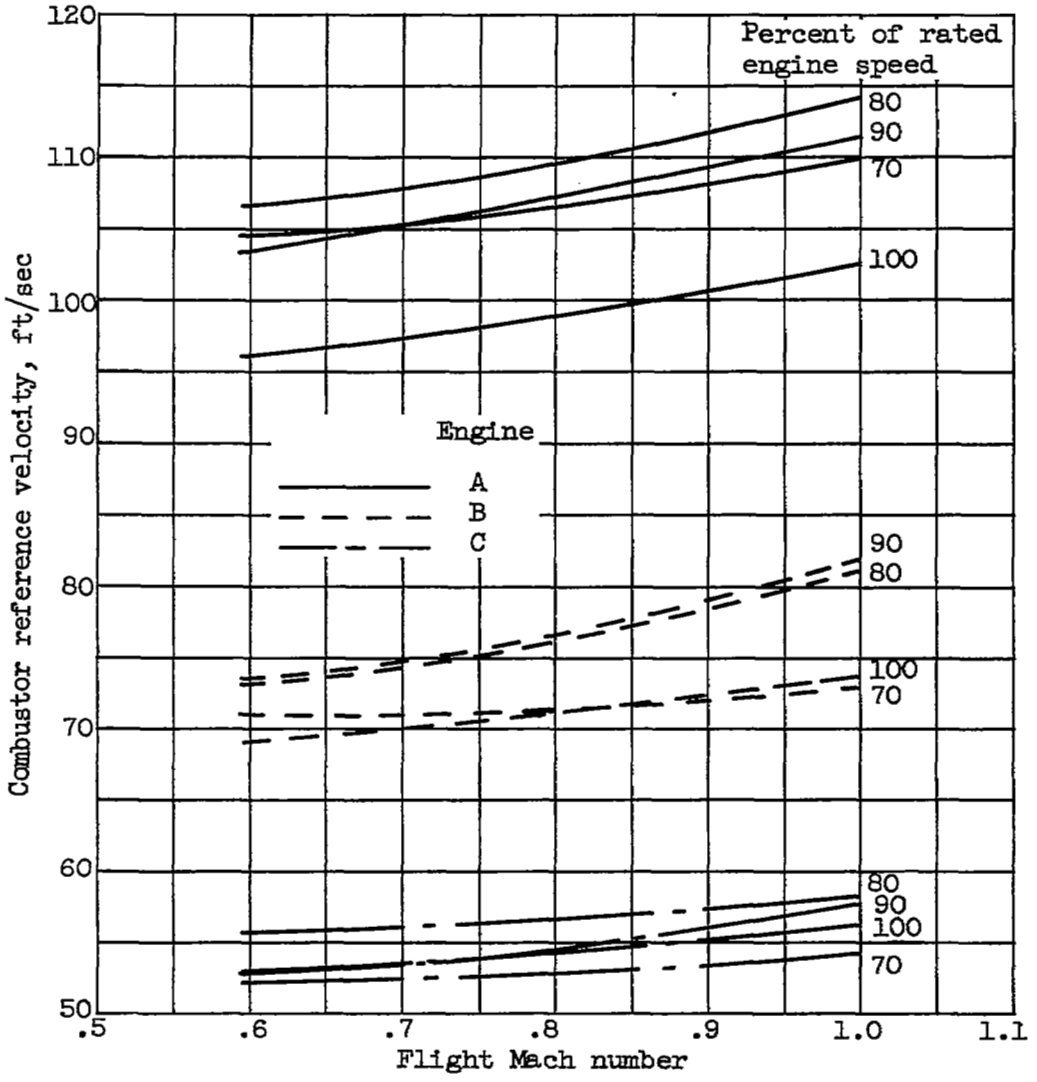

(c) Reference velocity.

Figure 7. - Concluded. Variation of combustor parameters with flight operating conditions in stratosphere for part-throttle operation of engines A, B, and C.

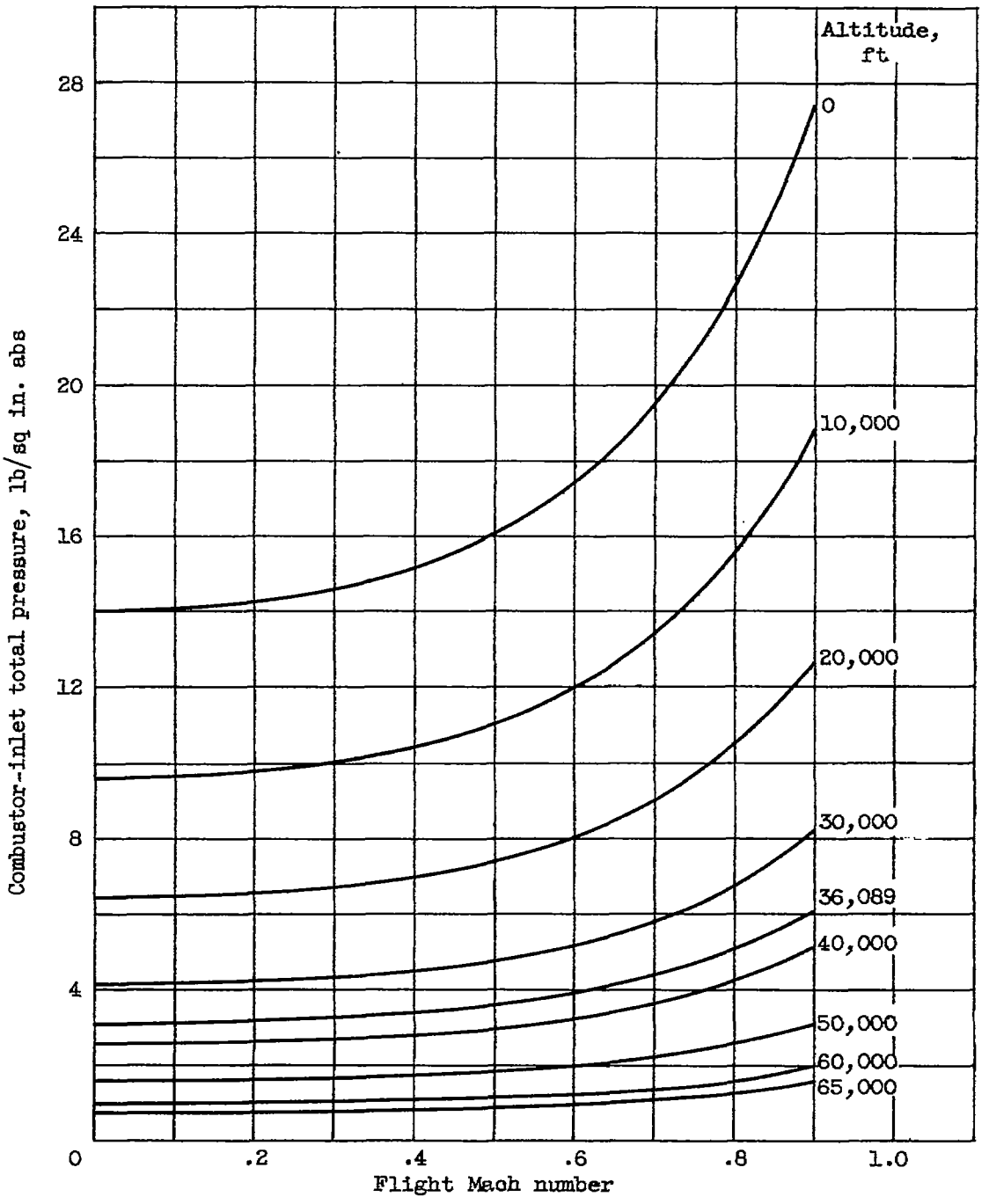

(a) Inlet total pressure.

Figure 8. - Variation of combustor parameters with flight operating conditions for windmilling operation of engine A.

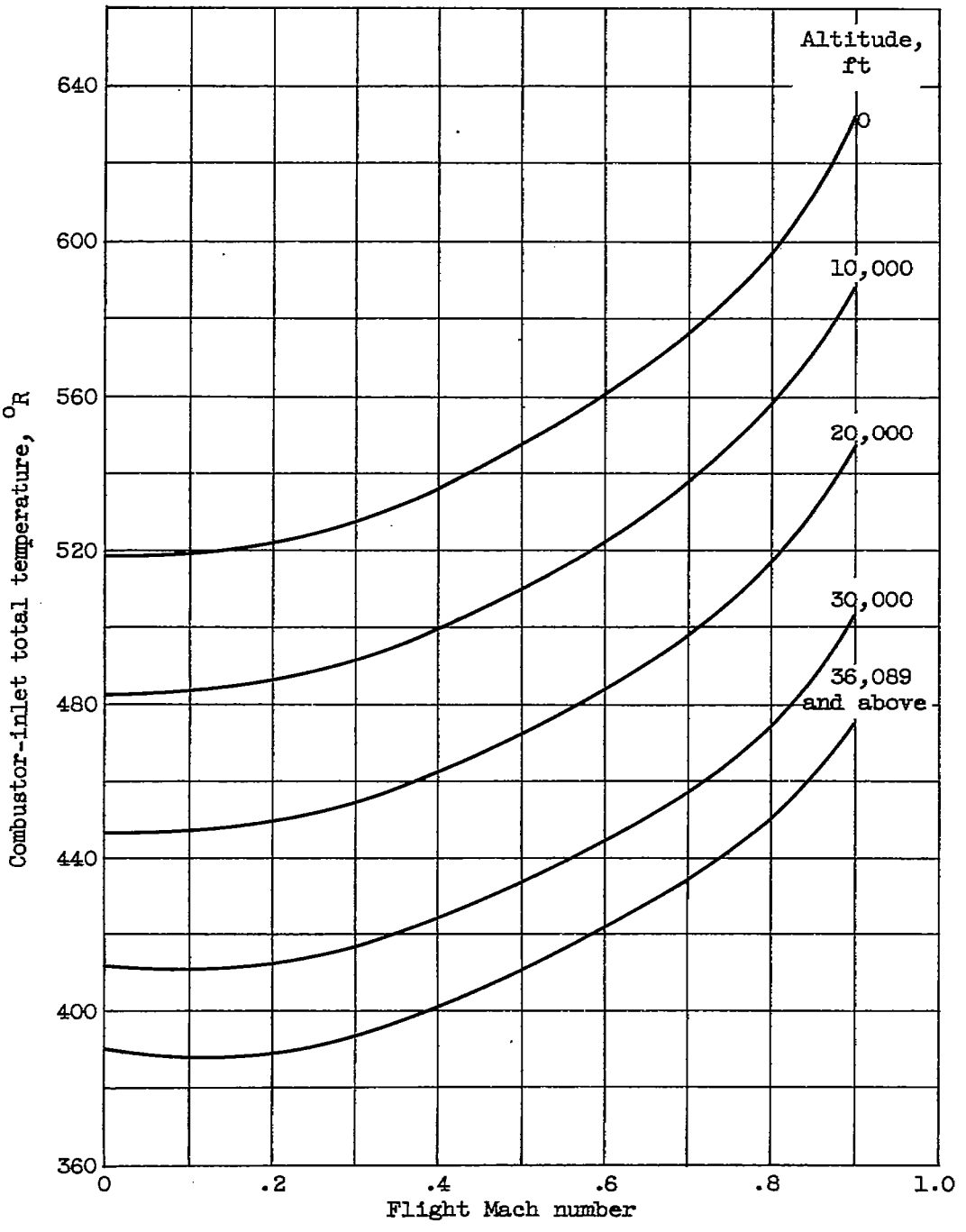

(b) Inlet total temperature.

Figure 8. - Continued. Variation of combustor parameters with flight operating conditions for windmilling operation of engine A.

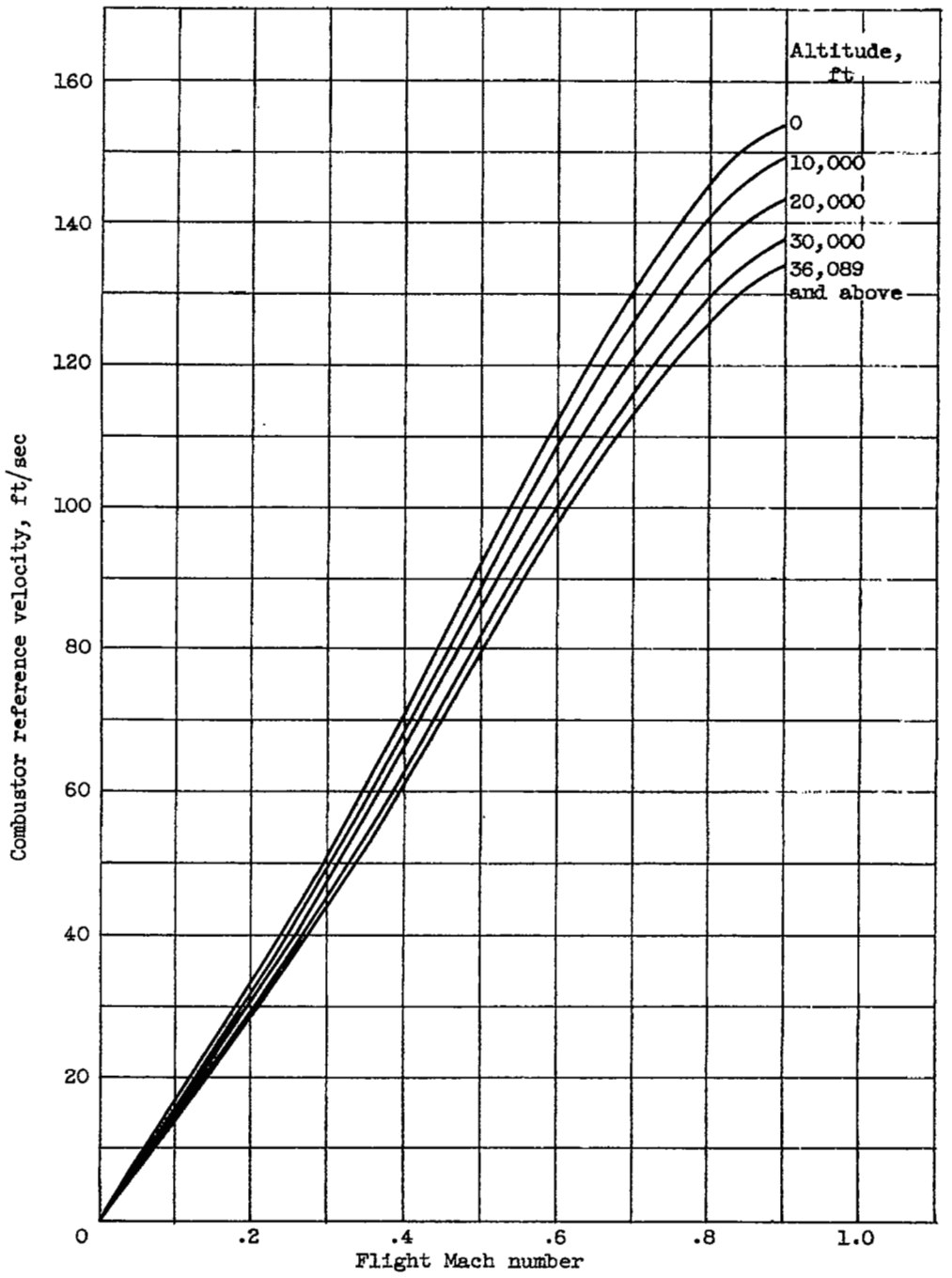

(c) Reference velocity.

Figure 8. - Concluded. Variation of combustor parameters with flight operating conditions for windmilling operation of engine A.

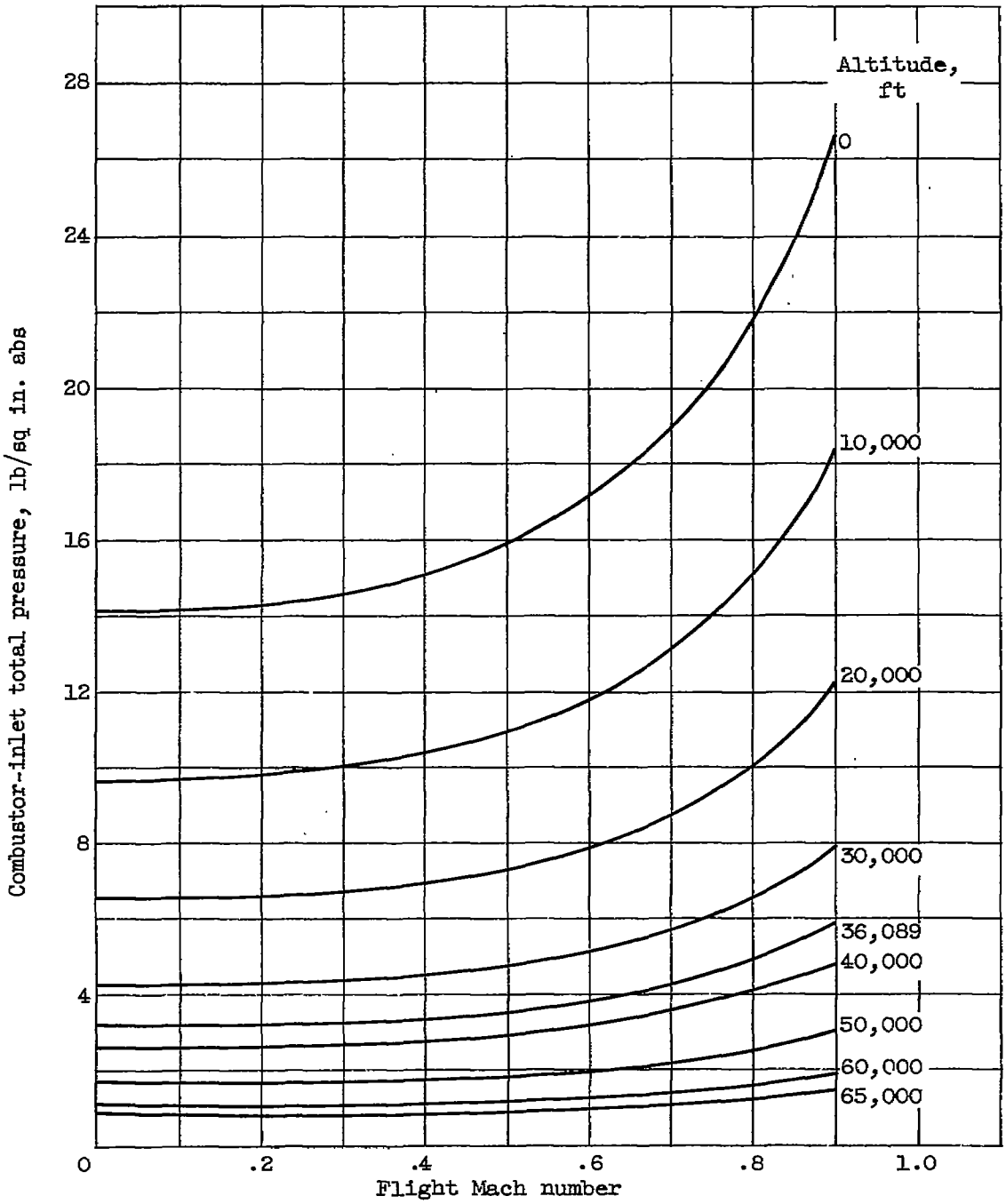

(a) Inlet total pressure.

Figure 9. - Variation of combustor parameters with flight operating conditions for windmilling operation of engine B.

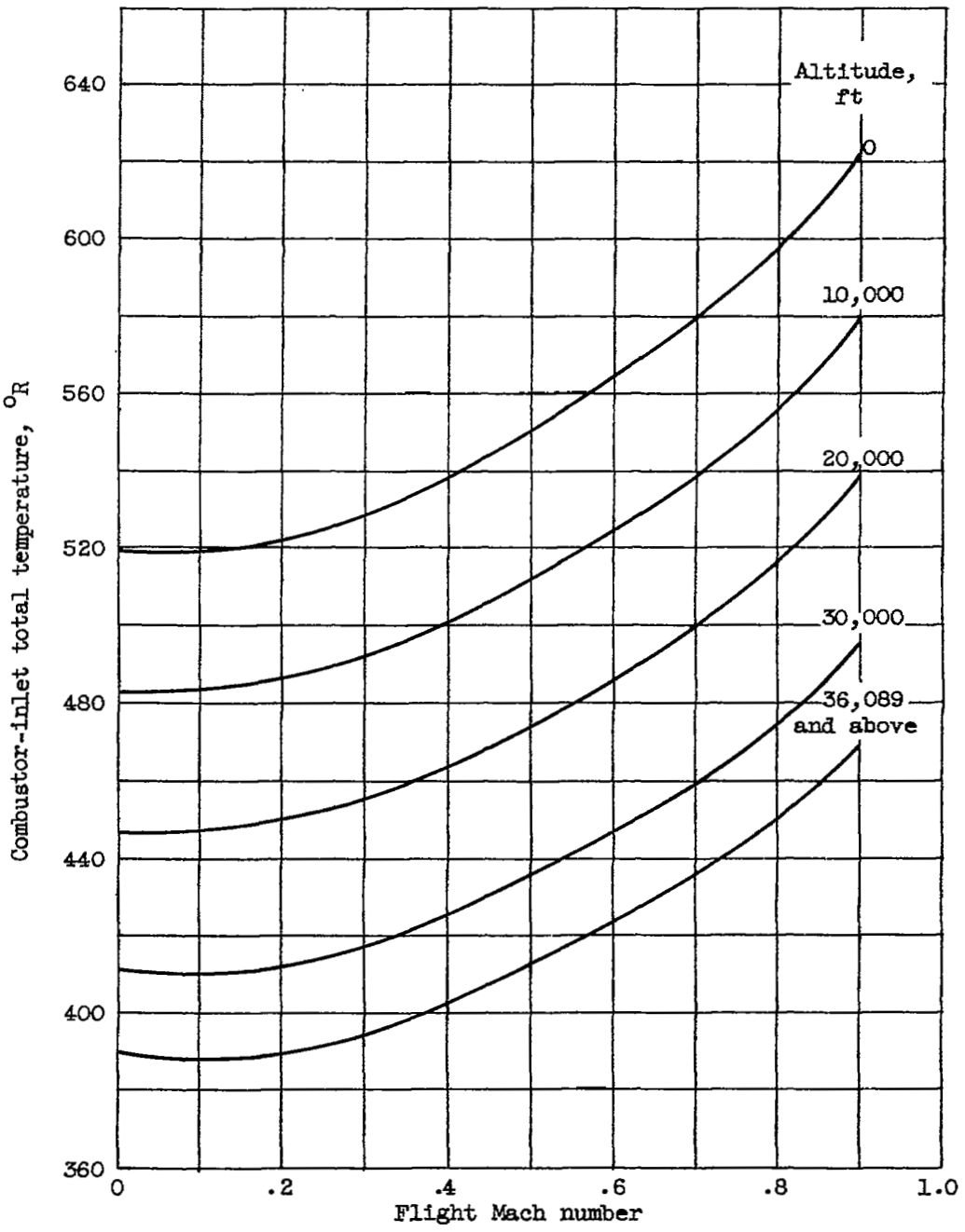

(b) Inlet total temperature.

Figure 9. - Continued. Variation of combustor parameters with flight operating conditions for windmilling operation of engine B.

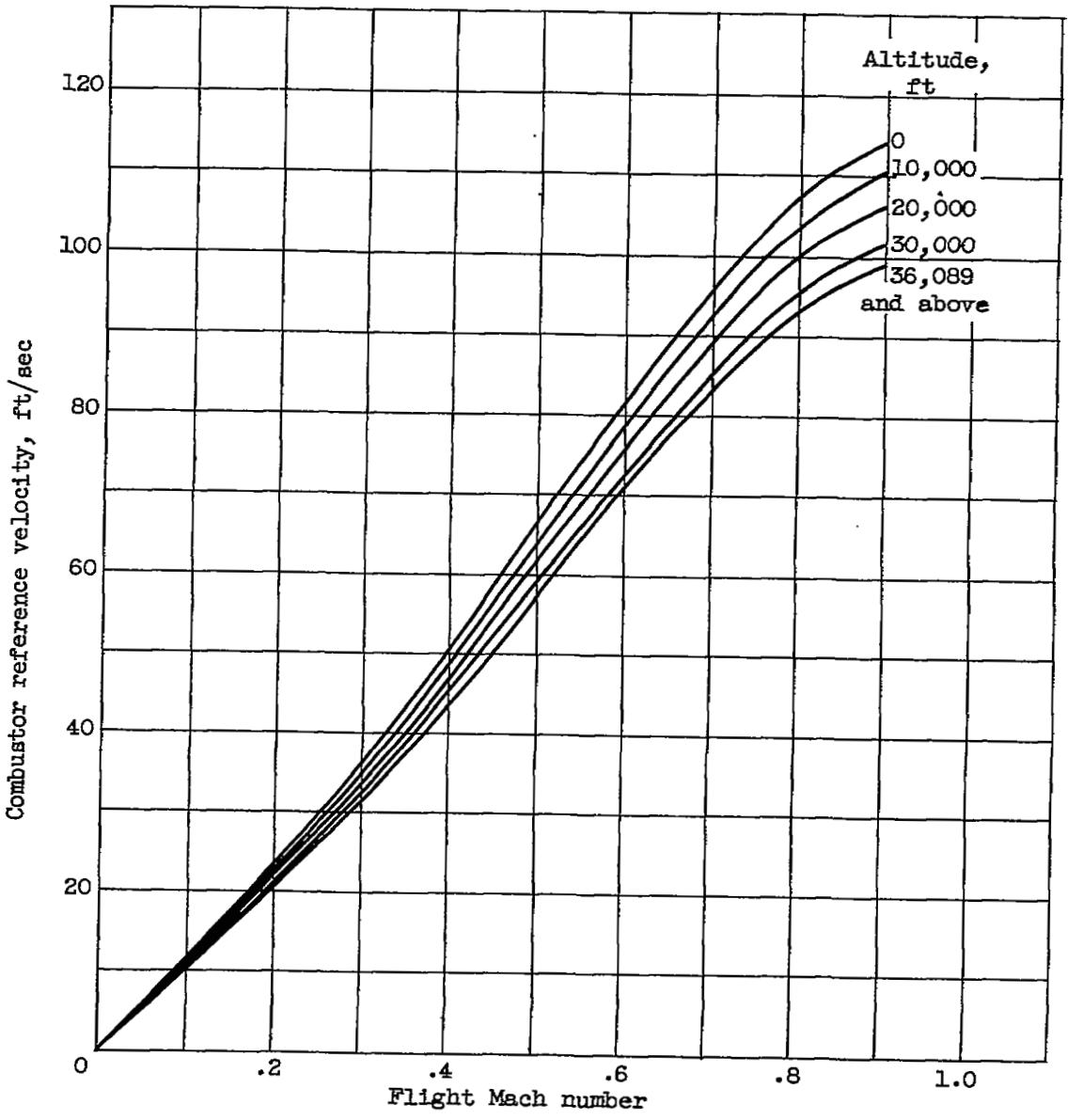

(c) Reference velocity.

Figure 9. - Concluded. Variation of combustor parameters with flight operating conditions for windmilling operation of engine B.

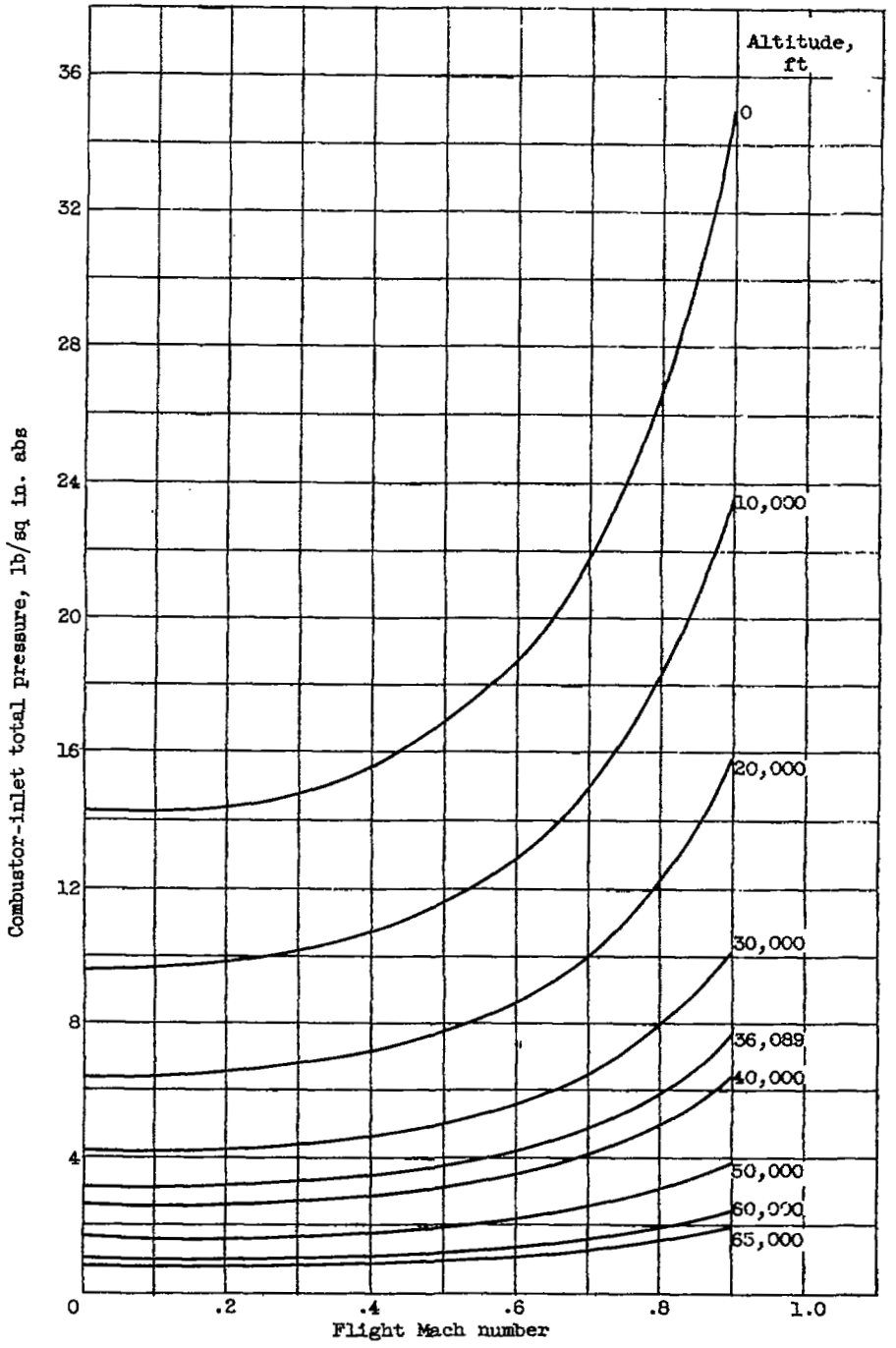

(a) Inlet total pressure.

Figure 10. - Variation of combustor parameters with flight operating conditions for windmilling operation of engine C.

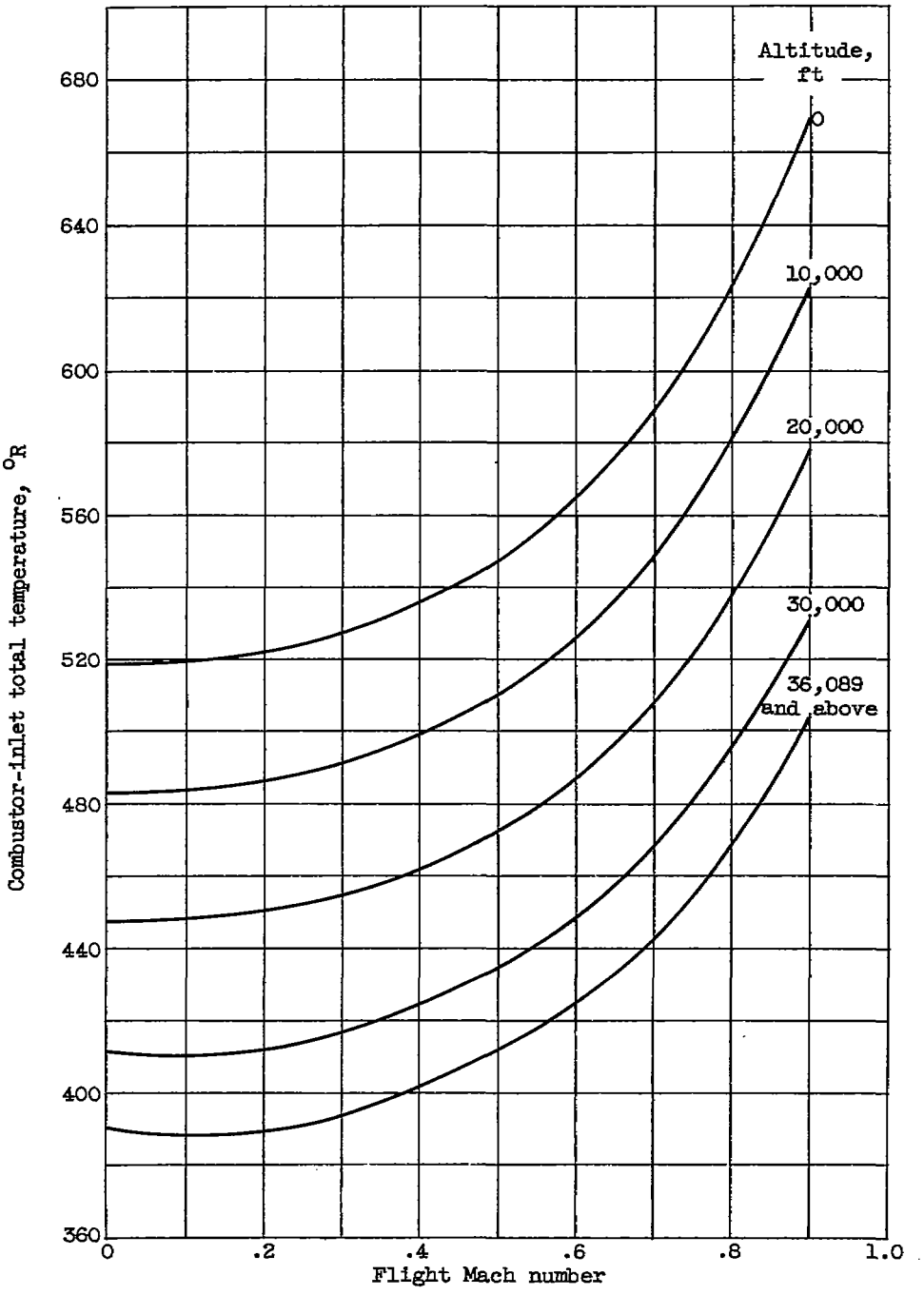

(b) Inlet total temperature.

Figure 10. - Continued. Variation of combustor parameters with operating conditions for windmilling operation of engine C.

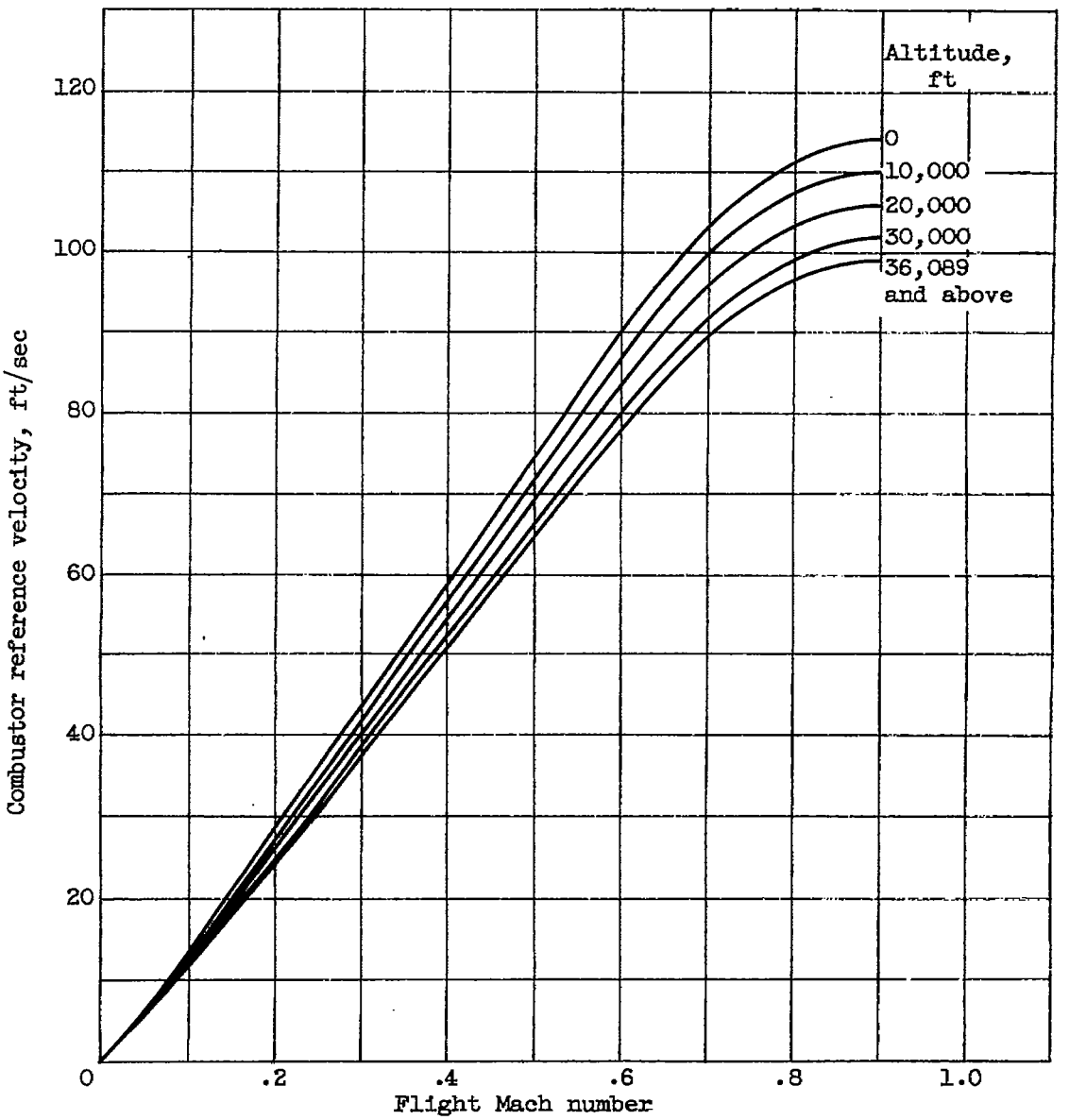

(c) Reference velocity.

Figure 10. - Concluded. Variation of combustor parameters with operating conditions for windmilling operation of engine C.

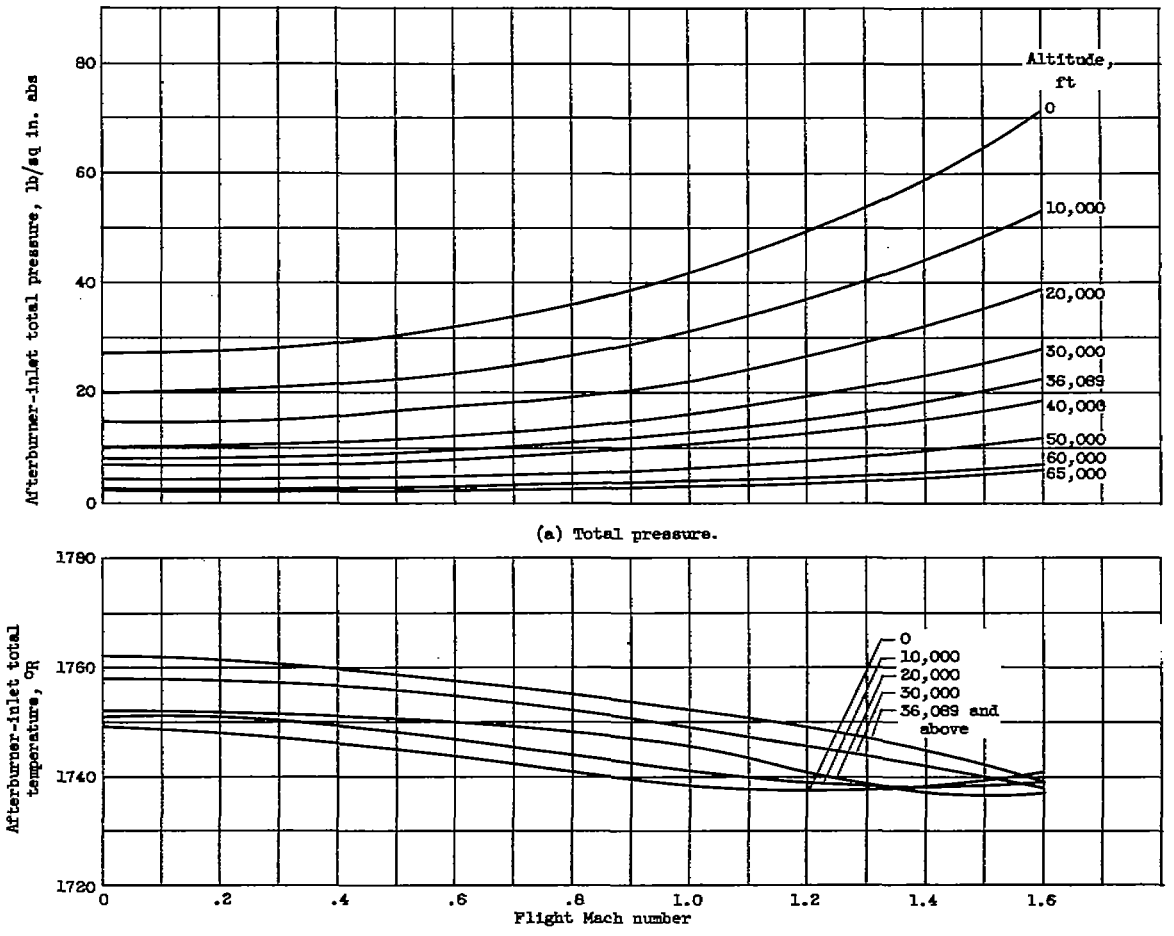

(a) Total pressure.

(b) Total temperature.

Figure 11. - Variation of afterburner-inlet parameters with flight operating conditions for full-throttle operation of engine A.

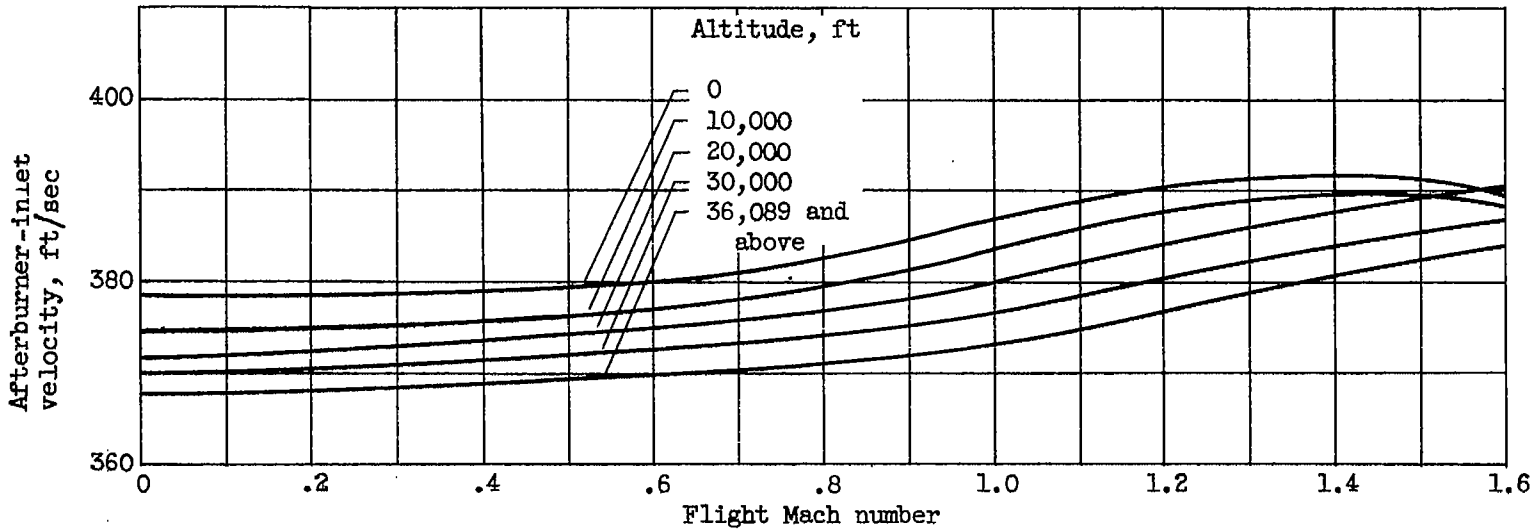

(c) Velocity.

Figure 11. - Concluded. Variation of afterburner-inlet parameters with flight operating conditions for full-throttle operation of engine A.

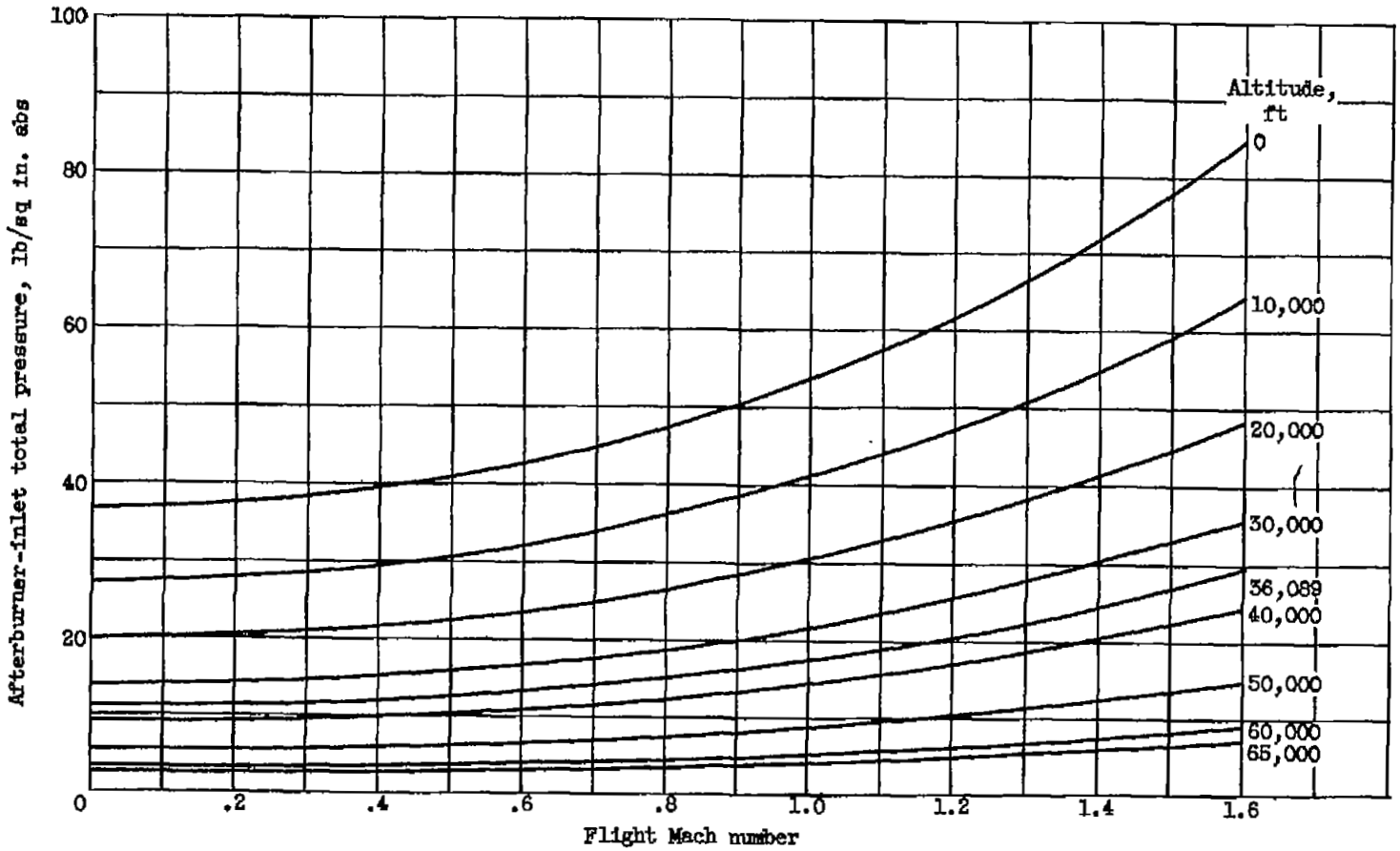

(a) Total pressure.

Figure 12. - Variation of afterburner-inlet parameters with flight operating conditions for full-throttle operation of engine B.

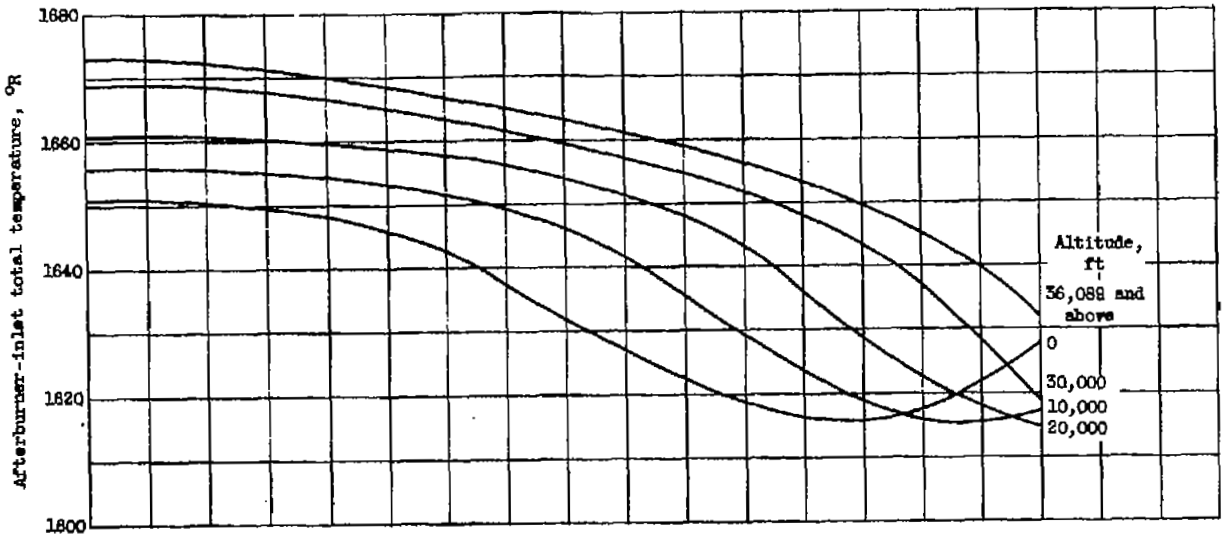

(b) Total temperature.

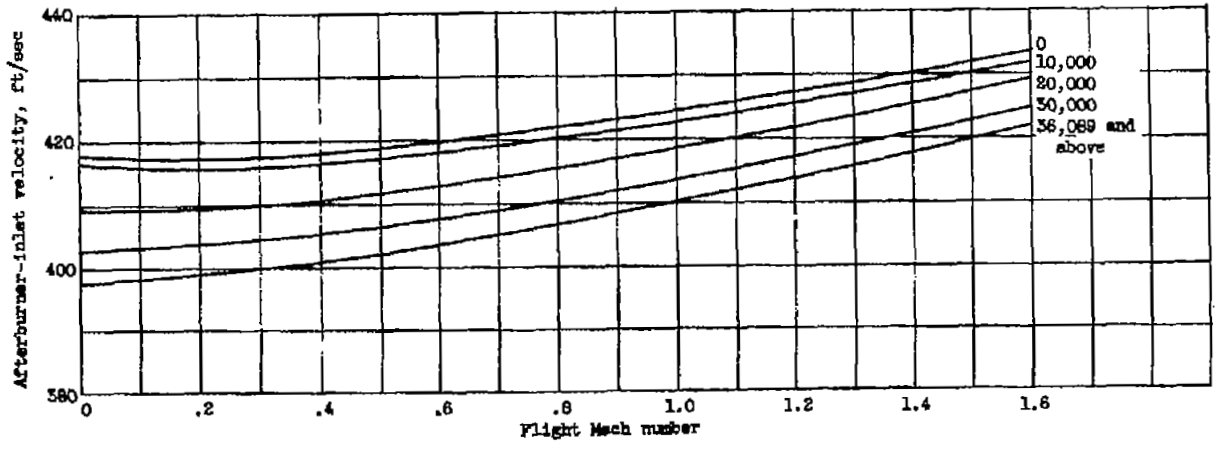

(c) Velocity.

Figure 12. - Concluded. Variation of afterburner-inlet parameter with flight operating conditions for full-throttle operation of engine B.

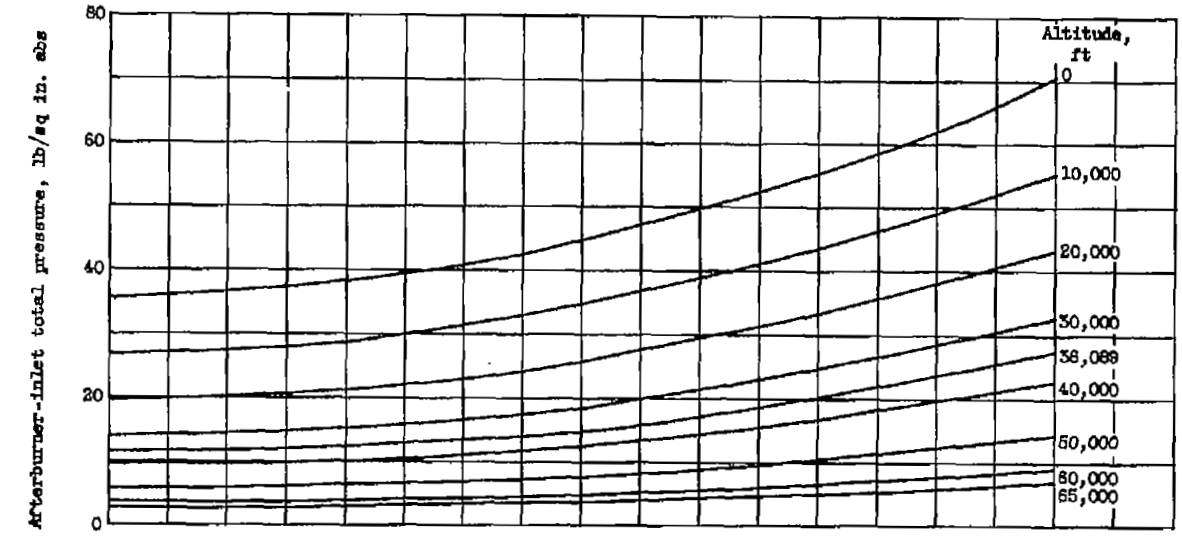

(a) Total pressure.

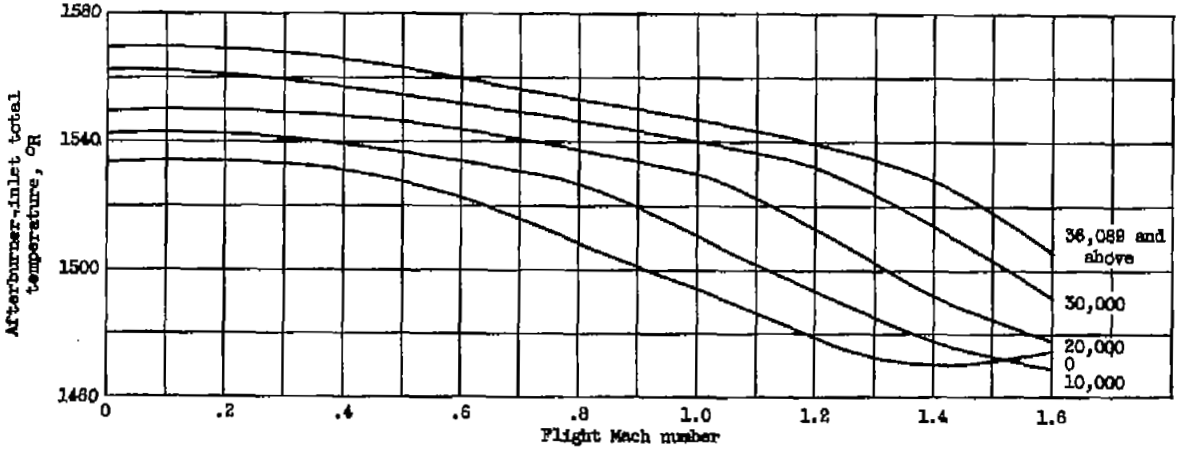

(b) Total temperature.

Figure 13. - Variation of afterburner-inlet parameters with flight operating conditions for full-throttle operation of engine C.

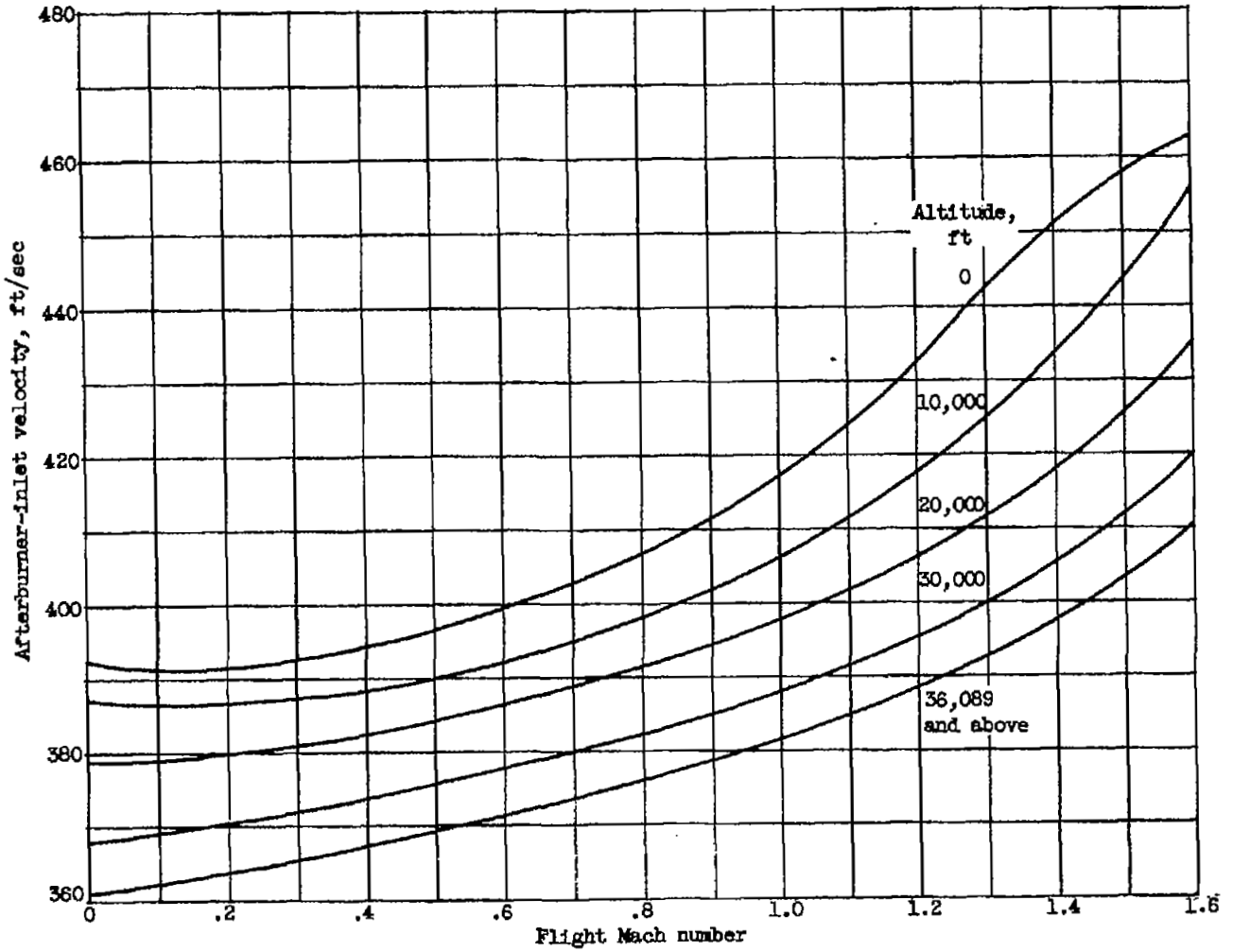

(c) Velocity.

Figure 13. - Concluded. Variation of afterburner-inlet parameters with flight operating conditions for full-throttle operation of engine C.

CHAPTER XI

TURBOJET-ENGINE STARTING AND ACCELERATION

By David M. Straight and Richard J. McCafferty

INTRODUCTION

From considerations of safety and reliability in performance of gas-turbine aircraft, it is clear that engine starting and acceleration are of utmost importance. For this reason extensive efforts have been devoted to the investigation of the factors involved in the starting and acceleration of engines.

In chapter III it is shown that certain basic combustion requirements must be met before ignition can occur; consequently, the design and operation of an engine must be tailored to provide these basic requirements in the combustion zone of the engine, particularly in the vicinity of the ignition source. It is pointed out in chapter III that ignition by electrical discharges is aided by high pressure, high temperature, low gas velocity and turbulence, gaseous fuel-air mixture, proper mixture strength, and an optimum spark duration. The simultaneous achievement of all these requirements in an actual turbojet-engine combustor is obviously impossible, yet any attempt to satisfy as many requirements as possible will result in lower ignition energies, lower-weight ignition systems, and greater reliability. These factors together with size and cost considerations determine the acceptability of the final ignition system.

CG-6 back

It is further shown in chapter III that the problem of wall quenching affects engine starting. For example, the dimensions of the volume to be burned must be larger than the quenching distance at the lowest pressure and the most adverse fuel-air ratio encountered. This fact affects the design of cross-fire tubes between adjacent combustion chambers in a tubular-combustor turbojet engine. Only two chambers in these engines contain spark plugs; therefore, the flame must propagate through small connecting tubes between the chambers. The quenching studies indicate that if the cross-fire tubes are too narrow the flame will not propagate from one chamber to another.

In order to better understand the role of the basic factors in actual engine operation, many investigations have been conducted in single combustors from gas-turbine engines and in full-scale engines in altitude tanks and in flight. The purpose of the present chapter is to discuss the results of such studies and, where possible, to interpret these results qualitatively in terms of the basic requirements reported in chapter III. The discussion parallels the three phases of turbojet engine starting:

(1) Ignition of the fuel-air mixture

(2) Propagation of flame throughout the combustion zone

(3) Acceleration of the engine to operating speed

EFFECT OF VARIABLES ON IGNITION IN TURBOJET ENGINES

Turbojet engines are usually started by

(1) Cranking or windmilling the compressor and turbine to provide air flow

(2) Turning on an ignition source

(3) Spraying fuel into the combustor

After the engine is started, the rotating speed of the compressor and turbine is increased from cranking or windmilling speed to an idle speed by increasing the fuel flow. Following this initial acceleration, acceleration to higher engine speeds is necessary to provide thrust for take-off and altitude flight conditions.

The most difficult starting conditions are those encountered on the ground at low ambient temperatures and those found at high altitude. The need for easy starting on the ground at all temperatures is obvious. Starts at altitude are also required after flame-outs, or occasionally, in the operation of multiengine aircraft, where all engines are not operated at all times. The following sections review the various factors involved in the starting of turbojet engines.

Engine Operating Variables

Both flight and tunnel tests on full-scale engines have shown that the ease of starting is controlled by altitude, flight speed, and engine speed. These engine operating variables can be related to combustor-inlet temperatures, pressures, and velocities; such relations are given in chapter X. This relation permits the study of ignition in single turbojet combustors operated in connected-duct facilities where these inlet variables plus fuel flows and temperatures can be controlled to simulate engine operating conditions. Successful ignition is defined as continued burning after the ignition source has been shut off. A maximum time of 30 seconds is often the limit allowed for ignition attempts. Typical apparatus and procedure for single-combustor ignition studies are described in references 1 to 3.

Full-scale engine altitude tests are conducted in large altitude chambers or wind tunnels and by flight tests. In altitude test facilities, flight operating conditions are simulated by controlling engine inlet and outlet pressures, and fuel and air inlet temperatures. Instrumentation is provided to indicate engine inlet and outlet pressures (simulating altitude and flight Mach number), engine speed, air flow, fuel flow, and pressures and temperatures at various stations in the engine including combustor-inlet conditions. The ignition procedure consists in setting the altitude and flight-speed pressure and temperature conditions and allowing the engine windmilling speed to stabilize. The ignitor is then turned on and the fuel throttle opened slowly until ignition is obtained. If ignition does not occur, the throttle is manipulated to vary fuel flow over a wide range in further attempts to obtain ignition. A maximum time limit (usually 20 to 45 sec) is allowed for ignition. Another method of feeding fuel is to allow only a fixed flow rate to exist upon opening the throttle. The value of this flow rate is varied for different ignition attempts for these automatic starts.

Operational and design requirements of full-scale turbojet engines necessarily influence the selection of parameters for presenting single-combustor ignition limits. Full-scale engines must be started without exceeding the maximum allowable turbine temperature; thus, minimum fuel flow for ignition is a useful parameter for indicating ignition limits. It is desirable to design engine accessory systems with minimum weight, size, and cost. Hence, the ignition-energy supply system should be light weight, which, in turn, means use of low ignition energies. Therefore, minimum ignition energy is also used as a parameter for indicating the altitude and flight-speed ignition limits of these engines. In addition, the minimum combustor-inlet pressure for ignition is a useful parameter for establishing the altitude ignition limit of single combustors when the ignition energy is constant.

Fuel and air temperature. - The effect of sea-level ambient temperature on minimum starting fuel flow for three engine speeds is presented in figure 14. A decrease in ambient temperature or an increase in engine speed resulted in large increases in the minimum fuel flow required for starting. The effect of engine speed on starting fuel requirements is primarily an effect of combustor-inlet velocity; at 60° F, for example, increasing engine speed from 1600 to 4000 rpm increased combustor-inlet absolute pressure and temperature only 10 to 20 percent but increased inlet velocities about 150 percent. Inspection of figure 14 shows that decreases in ambient temperature increase the starting fuel-flow requirements at all engine speeds (or combustor-inlet velocities) but that the effect is most marked at the higher-speed or higher-velocity condition.

The effect of temperature on starting fuel flows can best be explained in terms of fuel volatility. As the temperature is lowered, the evolution of vapor from fuel spray droplets is retarded; therefore, more liquid fuel is required to produce a flammable mixture of vapor in the immediate vicinity of the spark plug. This explanation is substantiated by laboratory studies discussed in chapter I. Further discussion of volatility effects is contained in a later section of the present chapter. Properties of the fuels used for the investigations reported in this chapter are presented in table II.

Whether the ignition limits are defined in terms of minimum spark energy or minimum required fuel flow, the explanation based on the volatility consideration still applies. For example, figure 15 indicates that more spark energy is necessary for ignition at low temperatures. (The spark energies presented in this chapter are the stored energy in condenser-discharge-type ignition systems except where otherwise noted.) The minimum spark energy increased by a factor of approximately 3 as temperature was decreased from 80° to -40° F. Figure 15 further indicates that, for a given temperature, the less volatile fuels (high 15-percent-evaporated temperature) require greater spark energy for ignition.

The effects of temperature on starting of full-scale engines are qualitatively the same as those obtained in single-combustor studies. As either fuel or air temperature was decreased (fig. 16), the altitude ignition limit decreased. A decrease in fuel temperature from 30° to -2° F changed the altitude ignition limit generally less than 5000 feet; but when the fuel temperature was reduced to -30° F, a very abrupt lowering of the altitude limit occurred with engine inlet-air temperature lower than 0° F.

Pressure and velocity. - Fundamental studies of the ignition of premixed vapor fuel and air in a flowing system (ch. III) show that minimum spark energy for ignition increases at low pressures and high velocities. The minimum fuel flow required for starting varies with the rate of evaporation of the fuel spray. Tests described in chapter I showed that the evaporation rate is greater at low pressures and high velocities as well as at high temperatures. The effects of pressure on ignition in a single combustor are illustrated in figure 17, where the variation of minimum starting fuel flow with altitude indicates that the effect of altitude is significant at high engine speed. At low-speed conditions, the effect is not serious at altitudes below 20,000 feet. As altitude is increased at constant speed the combustor-inlet temperature and pressure decrease substantially; therefore, the effect shown is actually the combined effect of temperature and pressure. Velocity in this case is nearly constant.

The results shown in figure 17 may also be explained in terms of volatility in that greater quantities of liquid fuel are required at high altitude to produce the fuel-air vapor mixture necessary at the spark plug. This requirement is also apparent from the flammability studies illustrated in figure III-15 of chapter III. In that figure it may be seen that as the pressure is decreased, richer fuel-air mixtures are required to establish a flammable condition.

In order to evaluate the energies required for ignition at various pressures, single-combustor studies with several fuels have been made (ref. 2). These studies are illustrated in figure 18 where the effects of pressure on minimum ignition energy for several air flows are shown. For the conditions covered by these tests, the spark energy required varied between 0.02 and 12 joules. These energies are greater by a factor of 100 or more than the energies required to ignite flowing, premixed gaseous fuel and air (ch. III).

A cross plot of the data of figure 18 is presented in figure 19 to show the minimum pressure ignition limits for various constant ignition energies (an engine ignition system usually provides constant energy) over a wide range of air-flow rates. The minimum pressure burning limits for this combustor (ref. 2) are included for comparison. Ignition is possible near the burning limits with a spark energy of 10 joules at the lower air-flow rates.

Each curve of figure 18 was obtained at constant air flow; thus, as pressure was decreased, reference velocity increased. (The term reference velocity indicates the mean air velocity at the maximum cross-sectional area of the combustor, and is computed from the maximum cross-sectional area, the air flow, and the combustor-inlet density.) An empirical relation is developed in reference 4 to determine the separate effects of pressure and velocity on the ignition-energy requirements. This relation $V/\sqrt{P}$ (where V is the reference velocity in ft/sec, and P is the combustor-inlet total pressure in in. Hg abs) correlated the data of figure 18 as shown in figure 20. Although considerable scatter of the data exists, this parameter best correlated the data obtained with most fuels (ref. 4). The parameter $V/\sqrt{P}$ indicates that reference velocity has a greater effect on minimum energy than does combustor-inlet pressure.

The results found in single-combustor studies of the effect of pressure and velocity on ignition are reflected by full-scale-engine studies (refs. 5 and 6). The effect of engine windmilling speed, which varies linearly with flight Mach number, and altitude on the ignition fuel flow is presented in figure 21. As flight speed increases, the fuel flow required for ignition increases markedly. For example, at an altitude of 45,000 feet, an increase in flight Mach number from 0.3 to 0.75 resulted in a four-fold increase in ignition fuel flow. The ignition fuel flow increased, in general, with increase in altitude, the increase being greater at the higher flight speeds. At 50,000 feet, the engine could not be started at flight speeds higher than a Mach number of 0.53 because of limited maximum fuel flow.

A full-scale engine was ignited at higher altitudes by increasing the spark energy supplied to the ignitors (ref. 5). Typical results are presented in figure 22 for the engine windmilling at a flight Mach number of 0.6. The altitude ignition limit increased rapidly from 35,000 feet at 0.25 joule per spark to 45,000 feet at 0.5 joule per spark. (These energies were measured at the spark gap.) Approximately 1.4 joules per spark were necessary to obtain ignition at an altitude of 50,000 feet. Any further increase in altitude starting seemed difficult to realize, for it was impossible to obtain ignition at 55,000 feet with the highest available spark energy (about 3.7 joules).

Similar large increases in altitude ignition limit were observed at other flight speeds. In figure 23 the altitude ignition limits with a spark energy of 3.7 joules per spark (measured at spark gap) are indicated for a range of flight Mach numbers from 0.4 to 1.2. At a flight Mach number of 0.8 with a low-energy ignition system (0.02 joule/spark), the altitude ignition limit was generally less than 10,000 feet (ref. 5).

Fuel Variables

Under normal or imposed conditions of temperature and pressure the volatility of a fuel is not always sufficiently great to produce the desired mixtures of vapor

fuel and air for ignition and combustion. However, by producing a fine spray of liquid droplets under a given condition of temperature and pressure, the rate of evaporation is greatly increased. The basic considerations involved in atomization and evaporation are described in chapter I. It has been shown that the rate of evaporation of a fuel spray varies with drop size or degree of atomization. The vaporized fuel concentration available for ignition will thus vary with atomization.

This section discusses results of studies which attempt to evaluate the influence of atomization and fuel volatility on the ignition process in jet engines.

Spray characteristics. - The variation of atomization with fuel flow in a fixed-area fuel nozzle spraying into quiescent air is shown in figure 24. It is apparent that as fuel flow increases the spray tends to spread into a more nearly conical shape with greater dispersion of droplets. The droplets at the high flows are smaller and thus the rate of evaporation is improved. Data in figures 14 and 17 were determined in the fuel-flow range represented by figure 24; however, direct comparison cannot be made since one system is quiescent and the other dynamic.

An investigation reported in reference 7 indicated that combustor-inlet pressure (14 to 37 in. Hg abs) had a negligible effect on spray formation, but increases in air velocity (35 to 80 ft/sec) improved atomization. It should be noted, however, that insofar as ignition is concerned, the improved atomization due to velocity increase may be offset by the decreased residence time of the fuel-air mixture and the increased turbulence in the vicinity of the spark gap.

Great improvements in engine starting characteristics can be obtained by changes in the fuel atomizer (ref. 8). This is also shown in figure 25 where the minimum ignition energies required for starting over a range of combustor-inlet pressures are shown for two fixed-area and one variable-area nozzle. Also listed on this figure are the starting fuel flows for each nozzle. It can be seen that the smaller capacity fixed-area nozzle requires both lower spark energies and lower fuel flows for starting at all combustor-inlet pressures than does the larger-capacity fixed-area nozzle. The variable-area nozzle has spark-energy and fuel-flow requirements that are much the same as those for the smaller-capacity fixed-area nozzle. The improvements in ignition characteristics of the variable-area and smaller-capacity fixed-area nozzles may be attributed to finer atomization and the accompanying increase in the rate of evaporation of the fuel (ref. 9). Drop sizes and evaporation rates may be calculated from relations given in chapter I. The variable-area nozzle has the added advantage of being capable of handling much higher fuel rates, permitting engine operation over wide ranges of conditions without requiring excessive fuel pressures (ref. 8).

No complete systematic study of the effect of fuel-spray characteristics on the altitude ignition limits of a full-scale turbojet engine has been reported. Engine data reported in reference 5 for a low-volatility fuel indicated that the engine could not be started at sea level at a flight Mach number of 0.2. A similar engine could be ignited at 40,000 feet at the same flight speed, as reported in reference 10. The difference in the ignition limits of these two engines is probably due to the difference in fuel-spray characteristics, since in the engine of reference 5 duplex nozzles were used, whereas the engine of reference 10 was equipped with variable-area nozzles. Duplex and variable-area nozzles differ in fuel drop size, cone angle, and penetration produced. Any one or all of these spray variables could produce the performance differences observed in the engines.

Sea-level starting tests were made with a full-scale engine using three different sets of fuel nozzles having different degrees of atomization (ref. 11). A much larger fuel flow (50 lb/hr) was required for ignition with large 40-gallon-per-hour (rated pressure of 100 lb/sq in.) nozzles than for ignition with small 10.5-gallon-per-hour nozzles (20 lb/hr). In reference 8, engine starting data with variable-area nozzles

show that a constant fuel flow can be set automatically to obtain ignition and accelerate the engine to idle speed without exceeding the safe-temperature limitation during starting. These data indicate that a large reduction in starting fuel flow can be achieved by providing finer atomization at starting conditions.

Volatility. - The preceding discussions show that easier starting is obtained by providing vaporized fuel in the vicinity of the ignition source. Higher inlet fuel and air temperatures as well as improved atomization help provide this vaporized fuel. A more direct method for providing vaporized fuel is by use of fuels of higher volatility.

It is shown in chapter I that the rate of evaporation of a fuel spray increases with increase in fuel volatility. Hence, it would be expected that lower starting fuel flows and ignition energies would be required for fuels of high volatility. On the other hand, the volatility of a multicomponent fuel of the type used commercially is not easily defined; consequently, the fuel properties most frequently used to define volatility have not produced completely satisfactory correlations of engine starting data. For example, the order of the curves in figure 15 and the scatter of points in figure 26 indicate that neither Reid vapor pressure nor the A.S.T.M. 15-percent-evaporation points adequately describe fuel volatility. From these data it may then be assumed that either the volatility of fuels as it affects starting has not been properly defined or that other properties of the fuels are producing significant effects in the ignition process.

Of the fuel properties examined to date, the A.S.T.M. 15-percent-evaporation point offers the greatest promise of correlation of starting data. However, in order to compensate for variations in altitude operating conditions, the additional pressure-velocity parameter $V/\sqrt{P}$ (ref. 4) may be introduced. Figure 27 illustrates the relation between A.S.T.M. 15-percent-evaporation point and required ignition energy for several values of $V/\sqrt{P}$. These data taken at altitude conditions indicate about a 2:1 increase in minimum spark energy at a low value of $V/\sqrt{P}$ and an 8:1 increase at the highest value of the parameter for the same range of 15-percent-evaporation fuel temperature. Thus, the effect of fuel volatility on minimum spark energy is greater at more severe operating conditions.

Data to confirm the effect of fuel volatility on ignition at sea level are reported in reference 1. A decrease in fuel volatility resulted in a large increase in the fuel flow required for starting, the increase being larger at low ambient temperature. The same effect occurred under altitude conditions with the effect being greater at high altitudes where temperatures and pressures are lower. Under altitude conditions the data (ref. 1) indicate that the increase in evaporation rate due to low pressure is apparently offset by the low temperature.

It is perhaps misleading to attribute the effects of low temperature solely to the influence of temperature on volatility, for decreases in temperature are also accompanied by increases in viscosity. These increases in viscosity may have detrimental effects on atomization (ch. I) and thereby retard the rate of evaporation. A study of photographs presented in reference 1 indicates that the spray produced by the fuel nozzle varied with the different fuels used as well as with the fuel temperatures. The viscosity of the three fuels varied as much as did volatility.

The minimum fuel-air ratios required for ignition in a small (2-in.-diam. liner) laboratory combustor have been determined for several experimental fuels of varying volatility (ref. 12). Increased volatility permitted ignition at lower fuel-air

ratios; however, the change in fuel-air ratio over a range of combustor-inlet temperatures from -40° to 40° F was less than that reported in reference 1. The fuel nozzle chosen for the investigation of reference 12 resulted in nozzle pressure drops of the order of 10 to 25 pounds per square inch; hence, effects of fuel viscosity would be lower than those found in the investigation of reference 1.

The results of single-combustor studies discussed in the preceding paragraphs have been substantiated by limited tests in full-scale engines. Data presented in figure 28 show that lower fuel flows are required for starting with the more volatile fuel (Reid vapor pressure of 5.4 lb/sq in.). Similar results were also obtained in full-scale engine studies reported in references 5, 10, and 13. Data are presented in figure 29. For both the axial-type compressor (fig. 29(a)) and the centrifugal type (fig. 29(c)), gains in altitude ignition limits up to 15,000 feet were obtained when fuel volatility was increased from a low (0 to 1.0) to a high (5.4 to 6.2) value of Reid vapor pressure.

Results of full-scale-engine tests reported in reference 14 also substantiate qualitatively the results of the single-combustor studies on fuel volatility. The amount of fuel evaporated according to A.S.T.M. distillation curves at the conditions of the test predicted the altitude ignition limits more accurately than did Reid vapor pressure.

Spark-Ignition Design Variables

As previously stated, ignition at a spark gap is aided by high pressure, high temperature, low gas velocity and turbulence, gaseous fuel-air mixture, proper mixture strength, and an optimum spark duration. Some of these variables are fixed by the particular engine, operating conditions, and fuels involved. Others can be altered by design changes.

Reliability of ignition can be improved by two different methods. First, supply enough spark energy to ignite the fuel-air mixture in spite of poor environmental conditions; second, design the ignition system, ignitor, and combustor to reduce the spark energy required. A size and weight limit (and thus a maximum energy limit) exists, however, for practical spark ignition systems.

It is the purpose of this section to discuss results of studies in which the ignition system and the environment at the spark gap were changed.

Ignition system design. - Induction-type ignition systems were used in most early turbojet engines. In general, these systems had high spark repetition rates but low energy per spark. The energy for a typical early ignition system (ref. 5) was 0.02 joule at 800 sparks per second. It was previously shown that increase in spark energy increased the altitude ignition limits (fig. 22). Condenser discharge ignition systems have been developed which permit higher spark energy with lower equipment weight (ref. 15); however, the spark repetition rates are lower.

Several design variables in condenser discharge systems affect the spark-energy requirements of a combustor. One of these variables, spark-repetition rate, affects the ignition pressure limit of a single combustor (ref. 16), as illustrated in figure 30. At a low air flow (1.87 lb/(sec)(sq ft)), the minimum pressure ignition limit was decreased from 14 to 10 inches of mercury absolute as the spark-repetition rate was increased from 3 to 140 sparks per second. At a high air flow (3.75 lb/(sec)(sq ft)), the effect was greater and the pressure limit was reduced from 28 to 18 inches of mercury absolute. Although improved ignition limits are possible by increasing the spark rate, the total power required and weight of equipment is increased.

[redacted]

Spark-repetition-rate studies in a full-scale engine (ref. 5) show the same trends as the single-combustor results. The effect of spark-repetition rate on the spark energy and power requirements for ignition in the engine at an altitude of 50,000 feet and a flight Mach number of 0.6 is presented in figure 31. The spark energy required for ignition at this condition decreased from 1.4 joules per spark (measured at spark gap) at 1 spark per second to 0.34 joule per spark at 188 sparks per second (fig. 31(a)). Low spark-repetition rates, however, are more desirable since the power required for ignition is lower, as shown in figure 31(b). Thus, battery drain is less even though the energy per spark is greater. For example, ignition was obtained at the same altitude windmilling condition with 62 watts of power at 188 sparks per second as compared with only 1.4 watts at 1 spark per second.

3196

The size and weight of a capacitance-discharge-type ignition system will vary with the circuit of the systems. A high-resistance system, for example, needs a larger storage condenser than does a low-resistance system to achieve equal energy at the spark gap.

The basic circuits of three typical low-voltage (300 to 3000 volts) high-energy condenser-discharge ignition systems are presented in figure 32. The first of these systems (fig. 32(a)) is a low-loss system designed with a high-voltage (10,000 volts) trigger to fire air-gap ignitors. A separate low-energy supply of electric current is fed intermittantly through the primary of a pulse transformer. The high-voltage, low-energy pulse of current induced in the secondary of the transformer (located in the main ignition lead) ionizes the ignitor air gap and allows the low-voltage, high-energy spark to follow. The secondary of the transformer was of special design to minimize losses (low resistance) resulting from flow of the low-voltage current from the storage condenser to the spark gap.

The second of the high-energy systems (fig. 32(b)) is a triggered system and was designed to fire either air-gap or surface-discharge ignitors. Surface-discharge ignitors are constructed with a semiconductive material or coating between the electrodes to permit flow of low-voltage current without high-voltage ionization (these are discussed in a later section). Since surface-discharge gap materials are semiconductive, a barrier gap is used to prevent discharge of the storage condenser until the break-down voltage of the barrier gap is reached. In figure 32(b) is shown a small trigger condenser that discharges through the barrier gap and then through the primary of a pulse transformer. The induced low-energy high-voltage (20,000 volts) ionization spark that occurs at the ignitor electrodes allows the high-energy, low-voltage spark to follow. This system will also fire air-gap ignitors that are badly fouled with carbon or other deposits. Figure 32(c) shows the basic circuit of a high-energy, low-voltage nontriggered ignition system that will fire only surface-discharge ignitors since no high-voltage trigger is provided. The flow of energy stored in the condenser to the semiconductive spark gap is controlled by a mechanical switch or barrier gap in the main ignition lead.

Losses occur in capacitance discharge ignition systems between the storage condenser and the spark gap; for example, energy is dissipated in barrier gaps that have a relatively high resistance. Reference 5 reports that the energy at the spark gap could be quadrupled by decreasing the resistance of an ignition cable from 1.2 to 0.007 ohm. Other data (unpublished) have shown that only 10 to 40 percent of the stored energy is available at the spark gap as determined by a calorimeter method. The relative performances of two of the three ignition systems having the basic circuits of figure 32 are presented in figure 33. The minimum spark-energy ignition limits were determined at two air-flow rates in a single tubular combustor for the low-loss and the triggered system both firing the same air-gap ignitor. The spark energy (stored energy) required for ignition with the triggered system is greater by a factor of about 10 than that for the low-loss system. Most of this large loss probably occurs in the barrier gap in the triggered system. Since the nontriggered system will not fire an air-gap ignitor, the performance is not shown for this system in figure 33.

[redacted]

Fundamental studies (ch. III) indicate that an optimum spark duration exists where the spark energy required for ignition of a vapor fuel-air mixture is at a minimum. The spark duration of the capacitance-discharge systems herein described depends on the circuit and spark-energy level involved, and is believed to be near the optimum for minimum ignition energy, although the energy level is much higher than the fundamental studies show.

Ignitor design. - Some of the variables that aid ignition such as low gas velocity and turbulence, gaseous fuel-air mixture, and proper mixture strength can be altered or controlled locally to some extent by the design of the ignitor itself. Normally, a very random fuel and air environment exists in the vicinity of the spark electrodes (ref. 7). The ignition performances of several ignitors designed to have better local environment and thus reduce spark energy are reported in reference 9. Other spark-gap variables such as gap width and surface-discharge sparks are also included. Figures 34 and 35 show some of the ignitor designs and the results obtained with them.

The effect of gap width on spark energy is shown in figure 34(a) for two ignitor designs. Increasing the gap width of the wire electrode ignitor from 0.03 to 0.24 inch had practically no effect on the energy required for ignition. The effect of quenching (ch. III) is shown for the ignitor having the heavier disk electrodes; the energy required is higher at all spark gaps up to the limit of the tests at 0.20 inch.

In reference 7 it is reported that the spark electrodes were wet with liquid fuel and that excess ignition energy may be required to vaporize some of the fuel to form a flammable mixture for ignition. The ignitor shown in figure 34(b) was fabricated with a Nichrome heating element near the spark gap, which was heated separately by an electric current. The results of combustor tests show that the spark energy required for ignition was reduced; however, the total energy required (sum of spark and heating energy) was much greater than that for the reference ignitor. At very severe ignition conditions near the limiting pressure where spark energy increases very rapidly, heating elements may aid ignition since the curves (fig. 34(b)) show a lower pressure ignition limit with the heating element in use.

Several ignitor designs were fabricated that incorporated various types of shields to lower velocity and turbulence in the vicinity of the spark electrodes (ref. 9). The largest improvement in ignition-energy requirements resulted from blocking the annular clearance around the ignitor where it passed through the combustor liner and by blanking off all cooling air passing through the plug body (fig. 34(c)). Blocking the annular clearance reduced the spark energy required by a factor of as much as 5. Blocking the cooling-air hole further reduced the spark energy.

A series of surface-discharge ignitors was also investigated (ref. 9) and included both triggered and nontriggered designs. The conducting surface of the triggered ignitors was a thin coating of semiconductive material glazed onto the insulator. These ignitors, in general, had poor contact between the electrodes and semiconductive material; thus, triggering was necessary. In other designs, semiconductive sintered ceramic materials were used for the spark-gap material. With these materials, good contact could be made with the electrodes and, thus, no triggering was required. Drawings of the triggered ignitor and the nontriggered ignitor that performed best are presented in figure 35. The performances of these two ignitors were compared with the performance of a reference ignitor when fired by the triggered ignition system (fig. 32(b)). The best triggered ignitor gave better performance than the best nontriggered ignitor when fired by their respective ignition systems.

The results of ignitor design studies in a single combustor are summarized in figure 36. The dashed curves show the spark energy required for ignition with the reference ignitor (standard installation in the single combustor used). Reductions in spark energy were observed for many ignitor design changes, but the greatest improvement was obtained by reducing local air velocity and turbulence. The best surface-discharge ignitor was about equally effective for ignition as the reference air-gap ignitors when fired by the low-loss system.

Although no complete systematic study of ignitor-design variables has been made in a full-scale engine, several investigations have included changes in ignitor design in attempts to improve the altitude ignition limits.

The results of flight investigations reported in reference 17 indicate that surface-discharge ignitors were about equally effective as air-gap ignitors. Nonshielded (flush-gap type) ignitors were better than shielded ignitors. Carbon formation on the shielded ignitors prevented the fuel-air mixture from coming into close contact with the spark, thus preventing ignition although the plugs continued to fire even when badly fouled. Brief tests were also made with a standard air-gap ignitor with a larger cooling-air hole. Lower altitude ignition limits resulted from the greater cooling air, as was also shown by the single-combustor ignitor-design studies.

Large increases in altitude ignition limit were obtained by blanking off a gap around the ignitor where it went through the liner of an annular combustor (unavailable NACA publication). The altitude ignition limit was increased from about 5000 feet to a maximum of 50,000 feet at a flight Mach number of 0.9.

Fuel prevaporizing combustion chambers such as the Python (ref. 18) require a torch-type ignitor for ignition. These, in general, consist of a small separate fuel nozzle in combination with a spark gap. The ignition spark ignites the spray from the nozzle, and the resulting torch vaporizes and ignites the main fuel feed, which is injected into the vaporizing tubes of the combustor.

Spark-gap location. - In different combustor designs the air-flow patterns and fuel-air-ratio distribution may vary. Thus, it is necessary to locate the spark gap in the most favorable position where gas velocity and turbulence are low and where the fuel-air mixture is most apt to be near the ideal conditions.

In one single-combustor study (ref. 7), the air-flow patterns at nonburning conditions and the manner of initial flame spreading indicated that a more favorable mixture for ignition may exist in the center of the combustor where reverse flow occurs. In reference 9, the spark-gap emersion depth was varied in this same combustor (J33). The spark energy required for ignition is presented in figure 37. Immersion depth had a negligible effect on the spark-energy requirements except very close to the liner where the required energy was greater.

Flight tests with a J33 full-scale engine (ref. 17) indicated that an optimum immersion depth of about 0.85 inch existed for a surface-discharge ignitor. This position is relatively near the combustor liner wall. In a J35 combustor (ref. 5), moving the spark gap to the center of the combustor increased the altitude ignition limit by 20,000 feet at a Mach number of 0.8 (fig. 38) but had less effect at lower flight speeds.

Apparently the optimum spark-gap location in a combustor is best found by experimentation since there appears to be no consistent optimum position in different combustor designs. Spark-gap location may become of lesser importance when other ignition design features such as shielding against high local velocities are incorporated.

Combustor design. - Since the spark energy required for ignition is sensitive to the local environment at the spark gap, it is logical that the combustor liner itself may be designed to provide low velocity and turbulence in the ignition zone. For example, a flame could be maintained by the ignition spark in an experimental combustor (ref. 19) at pressures below the stable burning pressure limit. Burning was maintained in this combustor at pressures of 3.8 and 5.0 inches of mercury absolute at air-flow rates of 0.93 and 1.47 pounds per second per square foot, respectively, by an ignition spark having an estimated spark energy of 0.025 joule per spark. Comparison of these data with figure 19 shows that large gains in reducing spark energy can be achieved through combustor design.

Summary of Spark-Ignition Variables

The variables that aid ignition in fundamental studies also aid ignition in turbojet combustors in both single combustors and full-scale engines. Improved ignition was indicated by lower starting fuel flows and ignition spark energy. The spark energy level, however, was much higher than that required in the fundamental studies.

As predicted by fundamental studies, ignition in turbojet combustors was easier as pressure and temperature increased and as velocity decreased. These variables are, in general, fixed by the particular engine and operating conditions involved, except where the local velocity and turbulence at a spark gap can be altered by design. Indeed, ignitors and combustors designed for low local velocity and turbulence may greatly reduce the required spark energy.

Starting tests with fuels of different volatility showed that the more volatile fuels ignited at lower fuel flows and with less spark energy. This reflects the fundamental requirements that a gaseous fuel-air mixture with a proper mixture strength is desirable. The more volatile fuels evaporate more readily to produce the proper mixtures at lower fuel flows. Spray nozzles designed to produce finer atomization also aid ignition by allowing fuel to evaporate more readily.

Other design variables such as the circuit of the ignition system also have a large effect on the spark energy required for ignition.

Since both fuel flow and spark energy indicated ease of ignition, there probably is an empirical relation between the two. When sufficient data are available, the parameter $V/\sqrt{P}$ can probably be expanded to include all the operational and fuel variables.

Special Techniques

Chemical ignition. - Very limited data have been obtained on igniting turbojet-engine combustors by chemical means. Chemicals that are spontaneously flammable in air and have a high rate of energy release may offer a relatively simple source of ignition for turbojet combustors. In reference 3, the possibilities of using aluminum borohydride as an ignition source are discussed. This chemical is one of the most highly flammable substances known and has a heating value equivalent to 32,000 joules per cubic centimeter.

Special injectors were developed to inject the chemical into the combustion chamber; however, difficulties were encountered because of oxides formed by the burning liquid and a polymer that formed in the chemical storage space in the injector.

Ignition with aluminum borohydride (approximately 2 cc) was obtained down to the pressures indicated in figure 39. It is believed that lower ignition limits

can be obtained by improved methods of injecting the chemical. The comparison in figure 39 of aluminum borohydride ignition limits with those for spark ignition systems indicates the chemical to be a more effective ignition source than the 10-joule spark system.

The spark ignition data of figure 39 (also data from ref. 4) are replotted in figure 40 as a function of the empirical parameter $V/\sqrt{P}$. With the curve through the data extrapolated to values of $V/\sqrt{P}$ corresponding to the aluminum borohydride ignition limits, a spark energy of approximately 100 joules per spark would be required to achieve ignition, if the extrapolation is assumed valid. The amount of energy in the chemical, however, is approximately 60,000 joules (2 cc).

Additional tests of mixtures of aluminum borohydride in n-pentane indicated that mixtures of as little as 20 mole percent aluminum borohydride were spontaneously flammable in a static test chamber filled with relatively dry air at room temperature at an absolute pressure of 1 inch of mercury. This pressure condition is more severe than any current turbojet operating condition.

Although these data show that aluminum borohydride is potentially an excellent source of ignition for turbojet combustors, practical means of storing, transporting, and injecting the chemical must be devised before it can be used in aircraft. Other spontaneously flammable substances may also warrant study.

Further work on chemical ignition was recently published in reference 20. Aluminum borohydride was diluted with hydrocarbons as a possible means for easing the storage and injection problems. A mixture of 40 percent aluminum borohydride in JP-4 fuel ignited a turbojet combustor almost as well as the undiluted chemical. Ignition was improved by using longer injection durations, which were obtained by using small capillary injection tubes or by diluting with a viscous material such as mineral oil. At -40° F, a 40-percent mixture of aluminum borohydride in mineral oil had a much better ignition limit than a 40-percent mixture in JP-4 fuel.

Oxygen enrichment. - Brief full-scale-engine investigations are reported in reference 21 and another (unavailable) NACA publication of the effect of feeding oxygen into the primary zone of the combustors equipped with ignition sources. Although this oxygen enrichment resulted in ignition and flame propagation in a shorter time at an altitude approximately 20,000 feet higher, its use in a flight installation might be impractical because of the extra weight of injection equipment.

FLAME CROSSOVER IN TURBOJET ENGINES

In engines equipped with individual tubular combustors, after ignition of the fuel-air mixture is accomplished in the combustors containing ignition sources, the flames must spread to the combustors without ignition sources. Hollow cross-fire tubes interconnecting the inner-liner chambers are utilized in this propagation process. Flame crossover in engines equipped with annular combustion chambers is not a serious problem, since the flame must propagate only from one fuel spray to another around the engine.

The mechanism of flame propagation through cross-fire tubes has been shown to be a result of a pressure differential between ignited and unignited combustors (ref. 5). The two cross-fire tubes attached to a combustor equipped with a spark ignitor were instrumented with velocity pressure probes facing both directions. A flow velocity away from the ignited combustor was noted in both tubes simultaneously with occurrence of temperature rise in the combustor, the velocity increasing as the temperature rise increased. After the combustors containing no ignition sources indicated a temperature rise, the velocity through the tubes decreased. Thus, the pressure differential between combustors results in the transference of ignited gases through the cross-fire tubes to ignite adjacent combustors.

[redacted]

Effect of Cross-Fire-Tube Diameter

The degree of success of flame propagation is dependent on the ability of the flowing gases to support combustion and is therefore subject to the mixing and quenching variables previously discussed in connection with ignition. Inflammability limits of propane-air mixtures in terms of pressure for various tube diameters are presented in chapter III (fig. III-8). With an optimum propane-air mixture, the pressure limit at which propagation could occur decreased from 4.0 to 0.8 inch of mercury absolute when the tube diameter was enlarged from 0.63 to 2.6 inches.

Investigations with various full-scale engines in both altitude research facilities and flight tests show a similar effect of tube diameter on flame propagation limits. The results of a representative investigation with a typical turbojet engine in an altitude chamber are shown in figure 41. The altitude flame propagation limits are shown for a range of flight Mach number for three cross-fire-tube diameters. An increase in diameter from $\frac{7}{8}$ to $1\frac{3}{8}$ inches increased the altitude limits at flight Mach numbers of 0.4 to 0.8 from 30,000 to 45,000 feet. Increasing the diameter to 2 inches resulted in successful propagation to the maximum altitude at which ignition was obtainable, 55,000 feet. However, these high-altitude propagation limits were obtained only with considerable manual throttle manipulation.

Effect of Cross-Fire-Tube Location

The location of cross-fire tubes with respect to fuel-spray pattern and combustion flame front is important. The investigation concerning cross-fire-tube diameter also included data on tube location (ref. 5). The propagation limits for three axial locations of the 2-inch-diameter cross-fire tube is shown in figure 42. As the tube was moved from the standard location of 5 inches downstream of the fuel-nozzle tip to 7.5 and 10 inches downstream, there was a progressive drop in propagation limits from an average altitude of about 55,000 to 45,000 feet. These results suggest that for any particular combination of combustor and fuel-nozzle design there is an optimum location of the cross-fire tubes.

Effect of Fuel Atomization and Volatility

The requirement of a proper vapor fuel-air mixture concentration for optimum flame propagation velocities, as discussed in chapters IV and V, indicates the importance of fuel atomization and volatility as influencing factors in flame propagation. The effect of fuel atomization on propagation at sea-level starting conditions is demonstrated in reference 11. The time required for full flame conditions to be established in all 14 combustors of the J33 turbojet engine was cut in half by decreasing fuel-nozzle size from 40 to 10.5 gallons per hour (100 lb/sq. in. pressure differential) using AN-F-32 fuel (MIL-F-5616, grade JP-1). The effect of fuel atomization at altitude conditions over a range of flight Mach numbers was qualitatively investigated by comparing propagation limits with three different types of fuel nozzle in a typical turbojet engine (ref. 5). The data obtained are plotted in figure 43. The cross-fire tubes used were $1\frac{3}{8}$-inches in diameter (larger than the standard 7/8-in.-diam. size for this engine). The difference in propagation limits was small, but the nozzles producing the finest atomization (simplex, 5-gal/hr) provided the maximum limits over the entire range of flight speeds investigated.

The effect of fuel volatility was obtained in the same engine using standard cross-fire tubes and variable-area fuel nozzles. Figure 44 shows the propagation limit increased about 5000 feet for an increase in Reid vapor pressure from 1.0 to 6.2 pounds per square inch. Results reported in reference 14 show that the fuel-air ratios required for propagation to occur in a full-scale engine varied with fuel volatility, as best indicated by the distillation curves of the fuels rather than by Reid vapor pressure.

[redacted]

It is also reported in reference 14 that the minimum time for propagation increased from less than 2 seconds to 14 seconds as the fuel volatility increased, as indicated by the distillation curves. This phenomenon is explained by the mechanism of flame crossover previously discussed. High-volatility fuels ignite at lower fuel-air ratios. Thus, the pressure difference to propagate flame through the crossover tubes is less, and longer propagation times result. The time for propagation was also greater at high altitudes (above 45,000 ft).

The data available concerning flame propagation through cross-fire tubes indicate that proper concentration of vaporized fuel-air mixtures and large-diameter cross-fire tubes, short as possible to keep quenching effects to a minimum, properly located in the combustor liner are primary factors in providing maximum altitude propagation limits.

ACCELERATION

The third phase of a successful engine start is the acceleration of the compressor-turbine combination to steady-state operating levels. This acceleration is accomplished by increasing the fuel rate, thus raising the turbine-inlet-air temperature and pressure and providing the necessary power. The acceleration problem can be separated into two phases: acceleration from the low speeds at which flame propagation was accomplished to normal operating speeds and acceleration from one steady-state speed to a higher value. The time required for acceleration from starting rotor speed is apt to be several times longer than acceleration from 50-percent rotor speed to maximum rotor speed; however, both phases of acceleration are influenced by the same variables. The discussion of acceleration in this chapter does not differentiate between these two phases.

The three main factors controlling the rate of acceleration are compressor surge and stall, combustion blow-out, and the maximum allowable turbine-inlet temperature. Successful acceleration is accomplished by adding fuel in such a manner that the compressor-turbine combination speeds up in a minimum time without exceeding the maximum allowable turbine temperature. Compressor surge is characterized by a sudden reduction and severe fluctuation of pressure throughout the engine, a decrease of air flow, and excessively high turbine-outlet temperatures. During acceleration, the compressor-outlet pressure increases to a value above the steady-state value because of high turbine-inlet temperatures and, without occurrence of surge, remains higher throughout most of the transient. The pressure ratio that is tolerated by the compressor without flow breakdown is limited, and as a result, the rate of acceleration is limited by the surge characteristics of the compressor. Also, inasmuch as fuel can be added rapidly enough to reach the rich-limit fuel-air ratio, combustion blow-out can limit acceleration.

The discussion of acceleration is divided into two categories, full-scale-engine results and single-combustor results. The effects of operating variables and engine components, including control systems, are assessed. The single-combustor results are discussed with regard to their application to engine acceleration problems.

Engine Investigations

The hypothesis is made in reference 22 that the dynamics of a turbojet engine during acceleration might be considered as a series of equilibrium states. Equations are developed that foretell the transient behavior of the engine variables as a function of engine rotor speed and fuel flow. However, deviations between observed and predicted performance were found, especially for rapid acceleration rates, that indicate the assumption of quasi-static processes is not rigid.

In the experimental engine investigations covered in the discussion presented herein, the transient behavior of engine variables such as compressor-turbine rotor speed, compressor-outlet pressure, fuel flow, turbine-outlet temperature and pressure, and exhaust-nozzle area were measured by means of oscillographs, which continuously recorded the change of each variable during acceleration. Analysis of the data obtained in this manner shows that good correlation exists between steady-state surge and surge obtained by means of transients.

A steady-state operating line, compressor surge characteristics, and typical variation of compressor pressure ratio with corrected rotor speed for two transients for a J40 turbojet engine are presented in figure 45. This plot shows the relation existing among the various engine operating lines. Successful acceleration with no surge encountered is shown as run 1, where the rotor speed before acceleration was 6300 rpm. During the initial part of the transient, the pressure ratio increased very rapidly with little change in engine speed. Then the engine speed began increasing at a normal rate and the surge line was approached but not reached. Since the recovery line is below the steady-state line (in terms of pressure ratio for a given engine speed), the compressor can recover from surge only when the pressure ratio is reduced below the steady-state value at a given engine speed. Recovery can be accomplished by reducing fuel flow, or by increasing rotor speed without increasing pressure ratio by permitting the engine to accelerate through surge, if possible. An example of recovery by accelerating through surge is run 2, where surge was encountered during the initial part of the fuel transient because the steady-state line and surge line are close together at this low speed. After surge was encountered, the fuel flow remained constant and the engine speed increased slowly with little increase in pressure ratio until the recovery line was met; then the engine accelerated in a normal manner with pressure ratio increasing rapidly until full speed was attained. This method of acceleration required substantially more time for the transient to take place than would acceleration with no surge. Of course, if blow-out had occurred during surge, acceleration would cease and deceleration to windmilling speed would have followed.

The fact that all engines do not have the same sensitivity to compressor surge is shown by an investigation of a similar engine, a J34 engine, in which acceleration was accomplished in the shortest time at an altitude of 40,000 feet by passing through surge rather than avoiding it (unpublished data). This method of acceleration was successful with this engine because the surge encountered was not severe enough to cause a complete flow breakdown at these operating conditions. However, this method is not recommended, because vibrations and temperature pulses accompanying surge could result in shortening the structural life of the engine.

Typical accelerations have been described and the relation existing among the various engine operating parameters has been discussed. The many factors influencing acceleration and their effects on acceleration are discussed in the following paragraphs:

Compressor-turbine speed. - The effect of rotor speed on acceleration can be seen by referring to figure 45. The excess power available for acceleration, indicated by the distance between the steady-state operating line and the surge line, was considerably lessened as rotor speed was reduced. Thus, the amount of power available for acceleration decreased with decreasing rotor speed. It is noted that pressure-ratio margin is only an approximate index of engine acceleration capability, at least with some engines. One investigation of an axial-flow engine with inlet guide vanes closed showed little or no change in maximum acceleration rate with an increase in engine speed and pressure-ratio margin (ref. 23).

[redacted]

Operating altitude. - The rate of engine acceleration is dependent upon the inertia and friction of the rotating parts, the ram energy of the engine-inlet air, the internal aerodynamic friction of the engine, and the excess power available. As altitude is increased, the air flow, the ram energy of the air, the internal aerodynamic friction, and the excess power developed by the turbine all decrease, but the inertia and mechanical friction of the rotating parts remain constant. In addition, as altitude is increased the steady-state pressure ratio increases (for a constant exhaust-nozzle area), while the surge line remains unaffected or does not change as much as the steady-state line. As a general rule, the pressure-ratio margin between steady-state and surge narrows, resulting in a decrease in available power and fuel-input margin for acceleration.

The time required to accelerate a J47 engine at various altitudes is shown in figure 46 where time is plotted against percent of rated rotor speed for several altitudes at constant initial flight Mach number (unpublished data). At an altitude of 15,000 feet, an acceleration from 76 percent rated speed to 100 percent rated speed required 6 seconds; whereas, at 45,000 feet, the time required for the same acceleration was 40 seconds. Above an altitude of about 30,000 feet, manual control of the acceleration was necessary, since the engine control system advanced the throttle too fast, causing compressor surge.

Above 35,000 feet, very rapid throttle advances usually resulted in combustion blow-out. Blow-out became more severe as altitude was increased. More severe surges may also be encountered at higher altitudes since, with less fuel margin between steady state and surge available, a throttle burst may force the pressure-ratio farther into the surge region than at low altitudes. Other aspects of the combustion process are presented in the discussion of the results obtained with single-combustor apparatus.

Flight Mach number. - A reduction in time required for acceleration can be accomplished by increasing the air flow through the engine and by increasing the pressure ratio across the turbine. The maximum pressure ratio obtainable across the turbine is a measure of maximum power available for acceleration. Increasing flight Mach number adds air flow because of ram effects and also allows a greater turbine pressure ratio for a given exhaust-nozzle area. Hence, increasing flight Mach number has a widening effect on the distance between the steady-state and surge lines similar to the effect of decreasing altitude. The effect of flight Mach number on the acceleration of a J47 engine is shown in figure 47 for three Mach numbers at a constant altitude of 40,000 feet (unpublished data). At a Mach number of 0.37 acceleration from 76 to 97 percent of rated speed required 22 seconds, while at a Mach number of 0.62 only 9 seconds were required.

Exhaust-nozzle area. - The primary purpose of a variable-area exhaust nozzle is to modulate thrust with constant engine speed. A variable-area exhaust nozzle also allows more power for acceleration by decreasing the turbine-outlet pressure. The effect of exhaust-nozzle area on acceleration time is presented in figure 48 for a J47 engine (ref. 24) at two altitudes and at a flight Mach number of 0.19. At an altitude of 15,000 feet, acceleration time was 13.5 seconds for the variable-area nozzle as compared with 18 seconds for the constant-area nozzle. At 45,000 feet, the acceleration times for the two nozzles were 22 and 35 seconds, respectively. Another investigation (unpublished data) of a J47 engine reported that when the exhaust-nozzle area was increased by 50 percent, the acceleration times at 35,000 and 45,000 feet were reduced 50 and 35 percent, respectively. Thus, use of maximum exhaust-nozzle area greatly reduces acceleration time, but acceleration times at high-altitude operation are still long. Maximum altitude ignition limits are obtained with a minimum exhaust-nozzle area (condition of highest combustor pressure); therefore, the variable-area nozzle is closed during starting and opened wide during acceleration.

Inlet guide vanes. - The use of variable inlet guide vanes ahead of the compressor for the purpose of improving acceleration characteristics is suggested by analysis in reference 25. Experimental data demonstrating the effectiveness of vanes were obtained with an axial-flow turbojet engine in reference 23. Results obtained are shown in figure 49 where maximum acceleration rate is plotted as a function of engine rotor speed for three inlet-vane positions. Maximum acceleration rate increased considerably as the vanes were closed, especially in the low-speed range. For any vane setting, larger fuel steps result in higher maximum acceleration rates, and since much larger fuel steps are permitted (before surge occurs) with the vanes closed, faster accelerations were attained. As a general rule, surge characteristics of virtually all engines are improved in the low-rotor-speed range by use of inlet guide vanes, but not necessarily in the high-rotor-speed range. However, the vanes may not always allow increased acceleration rates, since fuel-step size may be limiting at high altitudes because of combustion blow-out.

The effects of inlet-air pressure distortion on the operational characteristics of the engine were also observed. Either radial or circumferential distortions with the guide vanes open reduced both surge-fuel-flow and compression-ratio lines, and thus resulted in a decrease in the maximum acceleration rate of about 17 percent at a rotor speed of 7000 rpm. However, all engines do not behave in this manner; acceleration characteristics of some have been improved by radial distortions.

Control systems. - The function of an engine control system is to ensure engine operation at optimum settings of all engine variables at any given operating condition, considering operational, performance, and safety factors. The values of the various engine parameters are used to control fuel input and exhaust-nozzle position. Several investigations with different engines have shown that, in general, maximum acceleration was obtained near surge (refs. 26 to 28). The investigation of an early J47 engine reported in reference 24 showed that combustion blow-out data correlated with compressor surge. This relation can then be used to obtain optimum acceleration characteristics with protection from surge and blow-out. A number of engine-parameter combinations might be used as control schedules; the choice would depend on the characteristics of the particular engine considered and the range of operating conditions desired.

An example of acceleration using the relation between fuel flow and compressor-outlet total pressure (altitude compensated) for the J47D engine is shown in figure 50. A steady-state operating line, the highest permissible setting of the maximum fuel limit, and the path of a typical throttle-burst acceleration as governed by the electronic control are also shown. The fuel flow increased from point A at the beginning of the throttle burst to the limit curve BCD, followed it as the compressor-outlet pressure increased with rotor speed until at point D the turbine-outlet temperature limit was reached, reducing the flow to the steady-state value. The loop in the curve near the steady-state line was caused by the control seeking equilibrium conditions. In this manner engine controls can be scheduled to provide fast accelerations with a minimum chance of encountering surge or blow-out.

An aspect of engine behavior that complicates the job of this type of control is reproducibility. Acceleration data obtained with three engines are compared in reference 23. Two different engines of the same model and the same engine before and after dismantling and rebuilding were used. The maximum acceleration rate varied through a two-fold range among these engines at a given rotor speed and an altitude of 35,000 feet. The variation in ability to accelerate was due to shifting surge lines; the pressure-ratio margin was different with each engine. The acceleration characteristics of axial-flow engines are apparently quite sensitive to accumulation of tolerance errors or assembly clearances.

Another type of engine control based on a detectable signal from pressure transient or blade-stress phenomena that would warn of impending stall or surge is discussed in reference 27. For the engine investigated, the only stall warning observed was in a limited speed range. Engine controls of this type would be feasible if a reliable warning signal could be found.

The minimum fuel-flow setting must be considered for proper control design, as discussed in reference 29. A minimum fuel flow must be set on the control to prevent lean combustion blow-out and allow sufficient fuel flow for engine starting. Performance penalties at high altitude can be incurred, however. A fixed minimum fuel flow could result in an altitude ceiling below that desired since this fixed flow might be slightly above the flow required for steady-state operation. Overtemperature of the turbine or overspeeding of the engine might result. These difficulties can be overcome by varying the minimum fuel-flow setting with total inlet pressure to avoid lean-limit blow-out without restricting performance at high altitudes.

3196

Single-Combustor Investigations

The data discussed in this section resulted from six investigations. Combustion chambers from the 19XB-2 and early J47 turbojet engines were used to show the amount of temperature rise available for acceleration at high-altitude steady-state operation (unavailable NACA publications). Reference 30 presents data obtained in small-scale laboratory burners with a number of fuels in an effort to determine the behavior of the combustion process during fuel acceleration. Transient combustion characteristics were also studied in a series of three investigations (refs. 31, 32, and 33) with both J35 and J47 production combustors.

Turbojet engines have steady-state altitude ceilings that are imposed by the ability of the combustion process to supply sufficient heat to operate the turbine. This maximum altitude is usually referred to as the altitude operational limit and varies for different engines. An example of such an altitude operational limit for an early engine, the 19XB-1 engine, is shown in figure 51. Included on the figure are lines of excess temperature rise available for acceleration, that is, the maximum temperature rise produced by the combustor minus the temperature rise required to operate the turbine at the particular rotor-speed - altitude condition. It is apparent that the amount of temperature rise available for acceleration decreases as the altitude operational limit is approached, which means that acceleration of the engine would become progressively more sluggish until little or no acceleration would occur.

Data obtained in the J47 combustion rig indicate that, at a 30,000-foot altitude, acceleration was limited at low rotor speeds by the ability of the combustor to produce temperature rise, whereas, at high rotor speeds, the maximum allowable turbine-inlet temperature was restricting. This effect is due to the combustor-inlet conditions at low rotor speeds being more severe toward the combustion process. As rotor speed is increased at a constant altitude, the inlet conditions become less severe, as indicated by the shape of the altitude-operational-limit curve shown in figure 51. A discussion of altitude operational limits and the combustor-inlet-parameter effects on combustion performance is presented in reference 34. This inability of the combustion process to supply sufficient heat at low rotor speeds and at conditions near the altitude operational limits coupled with the smaller margin between steady-state and compressor surge lines, as pointed out previously in this chapter, indicates the difficulty of obtaining acceleration at high altitude and low rotor speeds.

The small-scale laboratory burners (ref. 30) were 2- and 3-inch-diameter combustors of varying design. The data were obtained for the following combustor-inlet air and fuel conditions: pressures varying from 16 to 49 inches of mercury absolute, air

flows from 0.04 to 0.10 pound per second, fuel accelerations up to fuel-air ratio changes per second of 0.6, constant inlet conditions, and conditions of increasing pressure as supplied by the temperature rise. The fuel types studied included normal paraffin, isoparaffin, olefin, production jet fuels, propylene oxide, isopropyl chloride, isopropyl alcohol, and various blends. Data obtained showed that unsteady-state blow-out and maximum temperature rise, though not reproducible, were as high as or higher than steady-state blow-out temperatures for all burner operating conditions and fuels used.

The production combustor data were obtained with MIL-F-5624A, grade JP-4, fuel at part-throttle altitude conditions. A motor-driven fuel valve that produced fuel input changes (with time) of varying slope and magnitude was employed. The combustor fuel flows, temperatures, and pressures were recorded by fast-response instrumentation that provided a continuous recording of these variables with time during the fuel transients. The system was similar to recording procedures for the full-scale-engine data. Oscillograph records typical of those obtained with the production combustors are presented in figure 52.

The first investigation in the series used a J35 combustor with a dual-entry duplex fuel nozzle (ref. 31). Data were obtained at the two simulated-altitude - rotor-speed conditions of a 25,000-foot altitude with 70-percent rated rotor speed and a 50,000-foot altitude with 70-percent rated rotor speed. The second in the series studied the effect of axial position of the combustor liner with respect to the nozzle using the same combustor and fuel nozzle operated at the same altitude - rotor-speed conditions (ref. 32). In the third investigation, a J47 combustion chamber and four different fuel nozzles were used (ref. 33). Data were taken at conditions simulating 35,000- and 45,000-foot altitudes at 58-percent rated rotor speed.

Results observed with the J35 engine and the dual-entry duplex nozzle showed that combustion may follow one of three transient response paths as a result of increase in fuel-flow rate: (1) successful acceleration with sustained burning at higher levels of temperature, pressure, and fuel-air ratio; (2) momentarily successful acceleration to higher temperatures, pressure, and fuel-air ratio followed by combustion blow-out; and (3) immediate cessation of burning without any temperature or pressure rise.

In paths (1) and (2), the inlet-air pressure and outlet temperature first decreased and then increased with an increase in fuel-flow rate. This initial dip in temperature, or the time necessary for the temperature to recover to its initial value at the start of the acceleration, averaged about 2.0 seconds at an altitude of 50,000 feet and 0.2 second at an altitude of 25,000 feet at comparable engine rotor speeds. A temperature and pressure dip of such short duration as this would probably have little effect on the engine speed, but if the engine control used turbine-inlet conditions as an indication of the amount of fuel required during acceleration, too much fuel input might possibly be supplied, forcing the combustion farther toward rich-limit blow-out. Even at sea-level static conditions, delay times of about 0.03 second were observed in acceleration tests of an engine; these delays consisted of time for fuel transport and the combustion process (ref. 27). The delay was listed as one of the factors making proper engine control difficult.

Typical data from oscillograph records obtained at the simulated-35,000-foot-altitude test condition for the J47 combustor are presented in figure 53. The variations of fuel flow, combustor-outlet temperature (as indicated by a single compensated thermocouple), and combustor-inlet static pressure during accelerations with each of the four nozzles are shown. Similar response paths were obtained in both the J47 and J35 combustors with the dual-entry duplex nozzle. In figure 53(a), the two runs correspond to response paths (1) and (3) previously listed. The response

characteristics with the other three nozzles, a single-entry duplex and two simplex, were different. Combustor-outlet temperatures and inlet-static pressures did not follow the dip and rise pattern in response to added fuel; during successful accelerations they increased immediately. However, response lag was still present, since the temperature and pressure did not respond as rapidly as the fuel could be added without blow-out. At a 35,000-foot simulated altitude with the fuel added in 0.12 second, the time required to reach the final temperature varied with the individual nozzle. The shortest time was 2 seconds, and the longest about 10 seconds. These response lags could account for an appreciable portion of the time required to accelerate an engine at altitude and probably interfere with the operation of control systems.

Acceleration rate, calculated as the change in fuel-air ratio per unit time, is plotted against fuel-air ratio at the end of acceleration in figure 54 for the simulated 45,000-foot-altitude - part-throttle condition. These data were obtained in the J47 combustor operated with four fuel nozzles (ref. 33). The range of steady-state rich-blow-out fuel-air ratios is included on the figure. Unsuccessful accelerations were observed with the dual-entry duplex nozzle. (A line is faired through the data to represent limits of successful acceleration.) Acceleration limits were found with the dual-entry duplex nozzle in both the J35 and J47 combustors. However, no limits were observed in the J35 combustor when the nozzle was retracted until the nozzle tip was flush with the contour of the liner inner dome wall (ref. 32).

No unsuccessful accelerations were found with the other three nozzles in the range of conditions investigated, except when the final fuel-air ratios were within the steady-state rich-blow-out range (fig. 54). For successful acceleration, then, the final fuel-air ratio after acceleration must always be below the steady-state rich-blow-out limits.

Photographic evidence was presented that showed the dual-entry duplex nozzle ceased flow output for about 0.03 to 0.04 second immediately after the start of the acceleration; the other nozzles had no such interruption (ref. 33). The unsuccessful accelerations and "dead time" response observed with this nozzle were attributed to this flow interruption. The fact that no unsuccessful accelerations were found when the nozzle was retracted was attributed to increasing fuel wash on the liner walls. The larger amount of fuel wash acted as a reservoir during acceleration which counteracted the fuel interruption effects. It was suggested that combustion failures during high-altitude acceleration cannot be attributed to transient flow effects on the ability of the combustion process to produce temperature rise, but are due to rich-blow-out limitation or discontinuity in fuel delivery, which is a function of the fuel nozzle used. This conclusion is supported by the laboratory burner data discussed previously (ref. 30).

Steady-state combustion-efficiency performance before acceleration was shown to be no reliable criterion for judging transient performance, because the best efficiencies were obtained with the dual-entry nozzle which gave the unsuccessful acceleration data.

In summary, then, combustion failures during acceleration are not due to transient fuel-input effects on combustion, but are caused by fuel-air ratios attaining the steady-state rich-blow-out limits or malfunctioning of the fuel injector system. However, during acceleration, combustor-outlet temperatures and pressures do not respond as rapidly as fuel can be added, an aspect of combustion behavior that makes control of engine acceleration difficult and affects the rate of engine acceleration at high altitude.

[redacted]

ANALYSIS

According to the previously discussed single-combustor investigations, combustion blow-out during acceleration is not a transient combustion phenomenon induced by the fuel change, but a steady-state limitation. It should then be possible to predict (with certain assumptions) the acceleration performance of a combustion and engine system with a knowledge of the steady-state fuel-air-ratio operating limits of the combustor and the characteristics of the compressor in the engine.

The operating limits for a J47 combustor in terms of combustor inlet-air variables and fuel-air ratio are shown in figure 55. These blow-out data are reported in reference 35. The combustion parameter used as the ordinate scale in figure 55 is presented in reference 36, and it provides a common basis to evaluate combustion performance of any combustion system in terms of inlet-air variables. The value of this parameter is given by temperature ($^{\circ}$R) multiplied by pressure (lb/sq ft abs) divided by reference velocity (ft/sec). The velocity is based on maximum cross-sectional combustor area and inlet-air density.

3196

A compressor performance map for an early version of the J47 engine is shown in figure 56. Included on the figure are turbine-inlet to compressor-inlet temperature-ratio lines; also, a part-throttle operating line for the engine at an altitude of 36,000 feet (or higher) at a flight Mach number of 0.6. By assuming that acceleration from any point along this part-throttle operating line would follow a constant-rotor-speed line until either surge, excessive turbine-inlet temperatures, or combustor blow-out limited the increase in compression ratio, it is possible to establish the location of a limiting turbine-temperature line and a blow-out line. The limiting turbine line is determined by the temperature-ratio lines, since the compressor-inlet temperature is constant and calculable for stratosphere operation at a steady flight speed. The turbine limiting temperature was assumed to be 1600° F. By calculating the combustion-parameter value for a given altitude and rotor speed existing on the part-throttle line, the operating fuel-air-ratio range can be determined from figure 55. With a constant combustion efficiency assumed for the particular combustion-parameter value, the temperature rise through the combustor at the fuel-air ratio causing blow-out can be located by interpolation among the temperature-ratio lines. This method demands that an appropriate combustion-efficiency value be assumed and that the increase in compression ratio does not take place until the added fuel necessary for the acceleration is injected. Because the combustion-parameter value would increase as compression ratio increased, the latter assumption might show the combustion environment to be more severe than it is.

The results are presented in figure 57 where compression ratio is plotted against corrected rotor speed. The surge line, part-throttle operating line, turbine-inlet temperature-limit line, and blow-out-limit lines for altitudes of 30,000, 40,000, and 50,000 feet are shown. The 30,000-foot-altitude condition is not exactly on the part-throttle line, because this altitude is below the tropopause, but this divergence would not significantly influence the trends observed. The barred regions on the plot show the range of engine rotor speed for the three altitudes where blow-out would limit acceleration; that is, the added fuel would reach the steady-state fuel-air-ratio limits before surge or a temperature of 1600° F at the turbine inlet would be attained. For each altitude, acceleration at higher rotor speeds than covered by the barred region along the part-throttle line would be limited by surge or turbine temperature.

The analysis of this particular engine operating at Mach 0.6 shows that combustion blow-out would not be encountered during acceleration at rotor speeds of 4000 rpm or greater until an altitude of at least 30,000 feet would be reached. The analysis also shows that combustion blow-out occurs near the surge line. Investigation of the acceleration characteristics of a similar J47 engine presented in reference 24 showed that blow-out was prevalent above an altitude of 35,000 feet and that blow-out and surge occurred at the same values of compression ratio. Some blow-outs were

observed at rotor speeds greater than figure 57 would predict, an effect which might be explained if the turbine-inlet temperature was allowed to go above 1600° F. Since the blow-out lines are between the turbine temperature limitation and surge line at rotor speeds above 6500 rpm, blow-out would occur before surge. From this analysis of one engine, this method of predicting acceleration characteristics would appear to be accurate enough to provide a general idea of the performance of a particular compressor-combustor system.

SIGNIFICANCE OF RESULTS IN RELATION TO DESIGN

The results obtained from both the single-combustor and full-scale-turbojet-engine investigations of the effect of many variables on starting and acceleration characteristics reveal information which is useful to the engine designer.

Fuel spray nozzles designed to provide finer atomization, particularly at the low fuel flows encountered at engine starting conditions, are desirable. It was shown that finer atomization reduced minimum starting fuel flows, ignition spark energies, ignition pressure limits, and time to spread the flame around an engine. Fine atomization is particularly desirable for engine starting conditions where pressures and temperatures are low and combustor reference velocities are high. Low-volatility fuels should be even more finely atomized than high-volatility fuels for ease of ignition.

The spark energy required for ignition increased with decrease in pressure, temperature, and fuel volatility and with increase in reference velocity. Reductions in the spark energy required were accomplished by shielding the spark gap from local high air velocity and turbulence. Differences in the spark energy required were found for different ignition supply systems and different combustor designs. It was better to trade high spark-repetition rates at low energy per spark for low repetition rate at high energy per spark in order to obtain lower power input. Size and weight of an ignition system limit the maximum spark energy that can be obtained practically (approximately 10 joules).

The use of chemicals for ignition appears attractive since a large quantity of energy can be provided by a small quantity of chemical. Tests with aluminum borohydride illustrated that excellent ignition limits are attainable; however, many injector-design and logistic problems have not been studied.

The altitude limits of flame propagation through cross-fire tubes on engines requiring them increased with increase in tube diameter, fineness of fuel atomization, and fuel volatility. In addition, there was an optimum axial position of the cross-fire tube in the combustor.

The function of a turbojet-engine control system is to assure engine operation at optimum settings of all engine variables during steady-state and transient conditions. Fuel input and engine variable components are controlled with consideration for engine performance and safety factors. The three main factors limiting the acceleration rate of an engine are compressor instability, combustion blow-out, and maximum allowable turbine-inlet temperature. Several relations have been established in full-scale-engine transient studies. Transient compressor surge correlated with steady-state surge and also with transient combustor blow-out for one particular engine. Acceleration (as limited by surge and blow-out) is more critical at low rotor speeds and high altitudes. The time required for acceleration is less at high flight speeds and can be decreased by employing variable-area exhaust nozzle.

Several combustion characteristics influence engine acceleration. The amount of temperature rise available for acceleration will be limited at high altitudes

near the steady-state operational limits of the engine. Combustor temperature and pressure decreases observed at the beginning of fuel acceleration with one fuel-nozzle-combustor combination may result in excessive fuel input by the engine control. With all the nozzle-combustor combinations investigated, lag in temperature and pressure responses were observed which would hamper engine control operation. These lag times were sufficient to account for an appreciable portion of the total time required to accelerate an engine at high altitude. Combustion failures during acceleration were caused by fuel-air ratios attaining steady-state rich-blow-out values or by discontinuities in fuel flow from the nozzles. Any change in engine component performance or operating conditions that would be detrimental to the combustion environment would be reflected, therefore, in poorer acceleration performance of the combustor.

REFERENCES

1. Rayle, Warren D., and Douglass, Howard W.: Investigation of Ignition Characteristics of an AN-F-32 and Two AN-F-58a Fuels in Single Can-Type Turbojet Combustor. NACA RM E50H16a, 1950.

2. Foster, Hampton H.: Ignition-Energy Requirements in a Single Tubular Combustor. NACA RM E51A24, 1951.

3. Straight, David M., Fletcher, Edward A., and Foster, Hampton H.: Aluminum Borohydride as an Ignition Source for Turbojet Combustors. NACA RM E53G15, 1953.

4. Foster, Hampton H., and Straight, David M.: Effect of Fuel Volatility Characteristics on Ignition - Energy Requirements in a Turbojet Combustor. NACA RM E52J21, 1953.

5. Armstrong, John C., and Wilsted, H. D.: Investigation of Several Techniques for Improving Altitude-Starting Limits of Turbojet Engines. NACA RM E52I03, 1952.

6. Sobolewski, Adam E., and Lubick, Robert J.: Altitude Operational Characteristics of Prototype J40-WE-8 Turbojet Engine. NACA RM E52L29, 1953.

7. Straight, David M., and Gernon, J. Dean: Photographic Studies of Preignition Environment and Flame Initiation in Turbojet-Engine Combustors. NACA RM E52I11, 1953.

8. Gold, Harold, and Straight, David M.: Gas-Turbine-Engine Operation with Variable-Area Fuel Nozzles. NACA RM E8D14, 1948.

9. Foster, Hampton H., and Straight, David M.: Effect of Ignitor Design and Ignitor Spark-Gap Environment on Ignition in a Turbojet Combustor. NACA RM E54A14, 1954.

10. Wilsted, H. D., and Armstrong, J. C.: Effect of Fuel Volatility on Altitude Starting Limits of a Turbojet Engine. NACA RM E50G10, 1950.

11. Koenig, Robert J., and Dandois, Marcel: Control During Starting of Gas-Turbine Engines. NACA RM E7L17, 1948.

12. Marshall, E. F.: Jet Propulsion Fuels - Seventh Annual Summary Report, May 1, 1951 to Apr. 30, 1952. Rep. No. 7, Automotive Lab., Res. and Dev. Dept., Sun Oil Co., Sept. 10, 1952. (USAF Contract No. W 33-038-ac-9086.)

13. Wilsted, H. D., and Armstrong, J. C.: Comparison of Performance of AN-F-58 and AN-F-32 Fuels in J33-A-23 Turbojet Engine. NACA RM E8K24, 1948.

[redacted]

14. Braithwaite, Willis M., and Sivo, Joseph N.: Evaluation of Altitude-Ignition Characteristics of Three Fuels of Different Volatility in a Turbojet Engine. NACA RM E53L11, 1954.

15. Anon.: Development of Bendix Ignition Systems for Jet Engines. Scintilla Magneto Div., Bendix Aviation Corp., Sidney (N.Y.), 1951.

16. Foster, Hampton H.: Effect of Spark Repetition Rate on the Ignition Limits of a Single Tubular Combustor. NACA RM E51J18, 1951.

17. Coapman, A. Lincoln: Flight Test, Scintilla Low Voltage - High Energy Ignition System. Memo. Rep. No. FTD-51-15, Air Force Flight Test Center, Air Res. and Dev. Command, Edwards Air Force Base, Edwards (Calif.), Oct. 24, 1951.

18. Meyer, Carl L., and Johnson, LaVern A.: Performance and Operational Characteristics of a Python Turbine-Propeller Engine at Simulated Altitude Conditions. NACA RM E51I14, 1952.

19. Dittrich, Ralph T.: Investigation of Low-Pressure Performance of Experimental Tubular Combustors Differing in Air-Entry-Hole Geometry. NACA RM E53G01, 1953.

20. Foster, Hampton H., Fletcher, Edward A., and Straight, David M.: Aluminum Borohydride - Hydrocarbon Mixtures as a Source of Ignition for a Turbojet Combustor. NACA RM E54K12, 1955.

21. Golladay, Richard L., and Bloomer, Harry E.: Investigation of Altitude Starting and Acceleration Characteristics of J47 Turbojet Engine. NACA RM E50G07, 1951.

22. Otto, Edward W., and Taylor, Burt L., III: Dynamics of a Turbojet Engine Considered as a Quasi-Static System. NACA Rep. 1011, 1951. (Supersedes NACA TN 2091.)

23. Dobson, W. F., and Wallner, Lewis E.: Acceleration Characteristics of a Turbojet Engine with Variable-Position Inlet Guide Vanes. NACA RM E54I30, 1955.

24. Conrad, E. William, Bloomer, Harry E., and Sobolewski, Adam E.: Altitude Operational Characteristics of J47D (RX1-1 and RX1-3) Turbojet Engines with Integrated Electronic Control. NACA RM E51E08, 1952.

25. Benser, William A.: Analysis of Part-Speed Operation for High-Pressure-Ratio Multistage Axial-Flow Compressors. NACA RM E53I15, 1953.

26. Oppenheimer, Frank L., and Pack, George J.: Investigation of Acceleration Characteristics of a Single-Spool Turbojet Engine. NACA RM E53H26, 1953.

27. Delio, G. J., and Stiglic, P. M.: Experimental Investigation of Control Signals and the Nature of Stall and Surge Behavior in a Turbojet Engine. NACA RM E54I15, 1954.

28. Stiglic, Paul M., Schmidt, Ross D., and Delio, Gene J.: Experimental Investigation of Acceleration Characteristics of a Turbojet Engine Including Regions of Surge and Stall for Control Applications. NACA RM E54H24, 1954.

29. Vasu, George, and Hinde, William L.: Effect of Engine and Control Limits on Steady-State and Transient Performance of Turbojet Engine with Variable-Area Exhaust Nozzle. NACA RM E52E23, 1953.

[redacted]

30. Schirmer, R. M., et al.: A Study of Methods of Evaluation of Combustion Performance of Aircraft Thermojet Engine Fuels. Rep. No. 403-9-51R, Res. Div., Phillips Petroleum Co., Bartlesville (Okla.), Aug. 1951. (Final Rep. for Navy Contract NOa(s) 10652.)

31. Donlon, Richard H., McCafferty, Richard J., and Straight, David M.: Investigation of Transient Combustion Characteristics in a Single Tubular Combustor. NACA RM E53L10, 1954.

32. McCafferty, Richard J., and Donlon, Richard H.: Effect of Fuel Nozzle Protrusion on Transient and Steady-State Turbojet Combustor Performance. NACA RM E54K08, 1955.

33. McCafferty, Richard J., and Donlon, Richard H.: Transient and Steady-State Performance of a Single Turbojet Combustor with Four Different Fuel Nozzles. NACA RM E55H03a, 1955.

34. Childs, J. Howard, McCafferty, Richard J., and Surine, Oakley W.: Effect of Combustor-Inlet Conditions on Performance of an Annular Turbojet Combustor. NACA Rep. 881, 1947. (Supersedes NACA TN 1357.)

35. Friedman, Robert, and Zettle, Eugene V.: Performance of a Pair of Tubular Combustors with an External Pilot Chamber. NACA RM E54E11, 1954.

36. Childs, J. Howard: Preliminary Correlation of Efficiency of Aircraft Gas-Turbine Combustors for Different Operating Conditions. NACA RM E50F15, 1950.

[redacted]

TABLE II. - FUEL INSPECTION DATA

Property	NACA fuel											
	JP-1	49-162	50-174	51-196	51-194	51-192	51-190	50-197	52-53	51-38	JP-3	JP-4
A.S.T.M. distillation - D86-46, °F												
Initial boiling point	340	109	114	109	94	128	129	181	136	113	117	139
Percentage evaporated												
5	350	135	128	138	122	292	192	242	183	146	155	201
10	355	158	138	250	144	337	241	271	200	169	187	224
20	360	210	149	343	204	350	329	300	225	198	234	250
30	364	270	160	356	325	355	355	319	244	218	266	269
40	367	323	174	364	392	360	368	332	263	236	291	286
50	375	360	188	372	426	365	375	351	278	254	312	303
60	380	398	204	381	454	370	384	365	301	270	333	322
70	384	432	231	393	473	377	396	381	321	293	358	344
80	391	460	330	412	488	386	417	403	347	325	394	375
90	402	500	439	452	517	402	455	441	400	388	449	421
Final boiling point	440	584	533	530	565	443	523	508	498	473	523	486
Residue, percent	1.0	1.0	1.0							1.0	1.3	1.2
Loss, percent	1.0	1.0	1.0							1.2	1.3	0.3
Freezing point, °F	<-76	<-76	-72							<-76		
Accelerated gum, mg/100 ml	0	16										
Air-jet residue, mg/100 ml	1	8										
Sulfer, percent by weight	<0.02	<0.50										
Aromatics, percent by volume												
D875-46T	15	25										
Silica gel	15	31	5.7									
Specific gravity	0.831	0.801	0.725	0.749	0.749	0.754	0.752	0.780	0.757	0.742	0.765	0.760
Viscosity, centistokes at -40° F/100° F	9.2	4.1	1.65	8.01 1.305	8.04 1.299	8.58 1.324	8.02 1.293	1.06	0.762			
Bromine number	0	12	0.9									
Reid vapor pressure, lb/sq in.	(a)	4.5	6.5	6.8	6.5	2.9	2.7	1.0	2.9	6.2	5.4	2.8
Hydrogen-carbonratio	0.154	0.150	0.172							0.172	0.170	0.171
Net heat of combustion Btu/lb	18,530	18,500								18,763	18,700	18,730

[a]Not measurable.

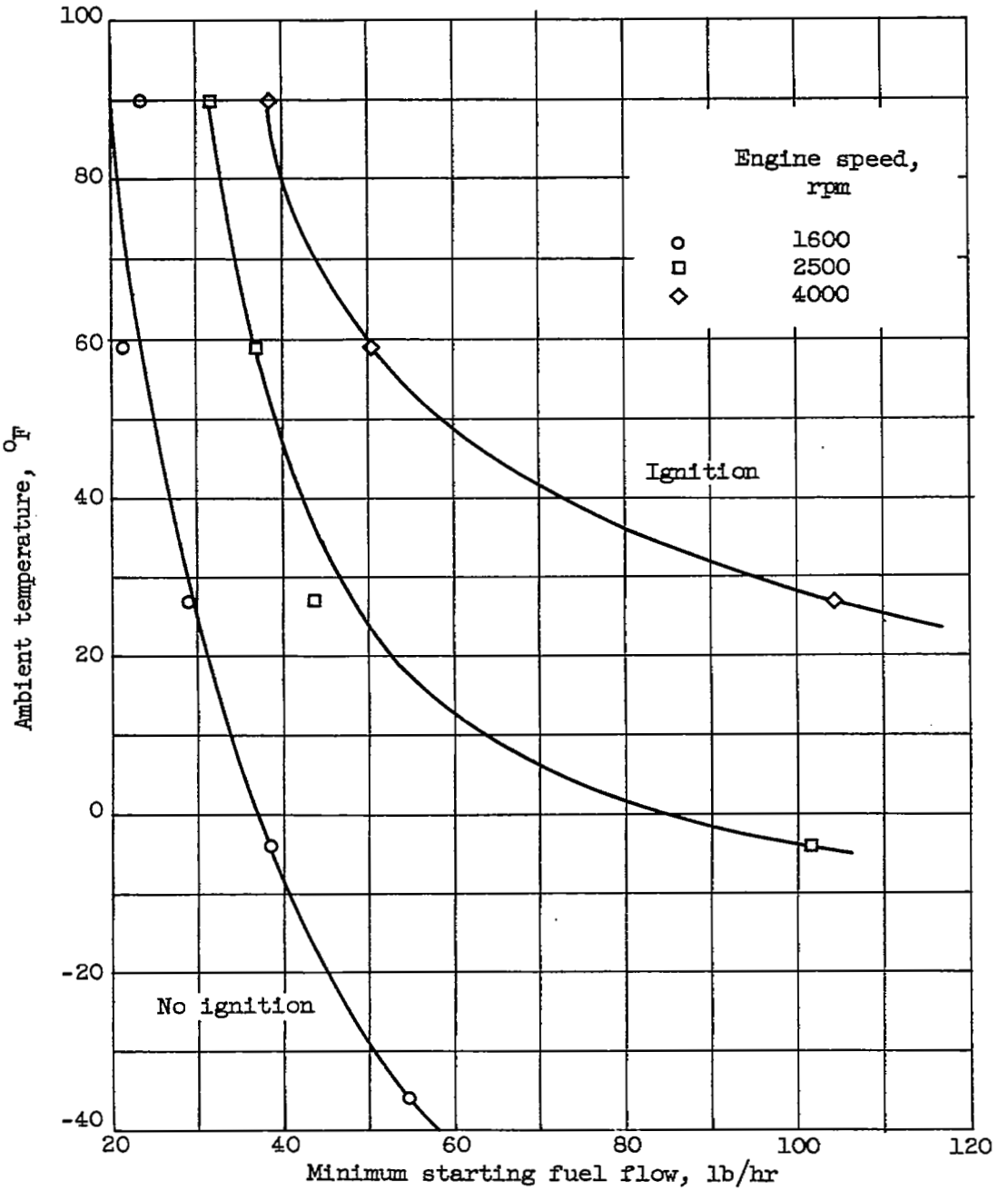

Figure 14. - Effect of ambient temperature on minimum starting fuel flow in single J33 combustor at three engine speeds. Sea level; flight Mach number, 0; NACA fuel 49-162, fixed-area fuel nozzle; spark energy, constant (data from ref. 1).

[redacted]

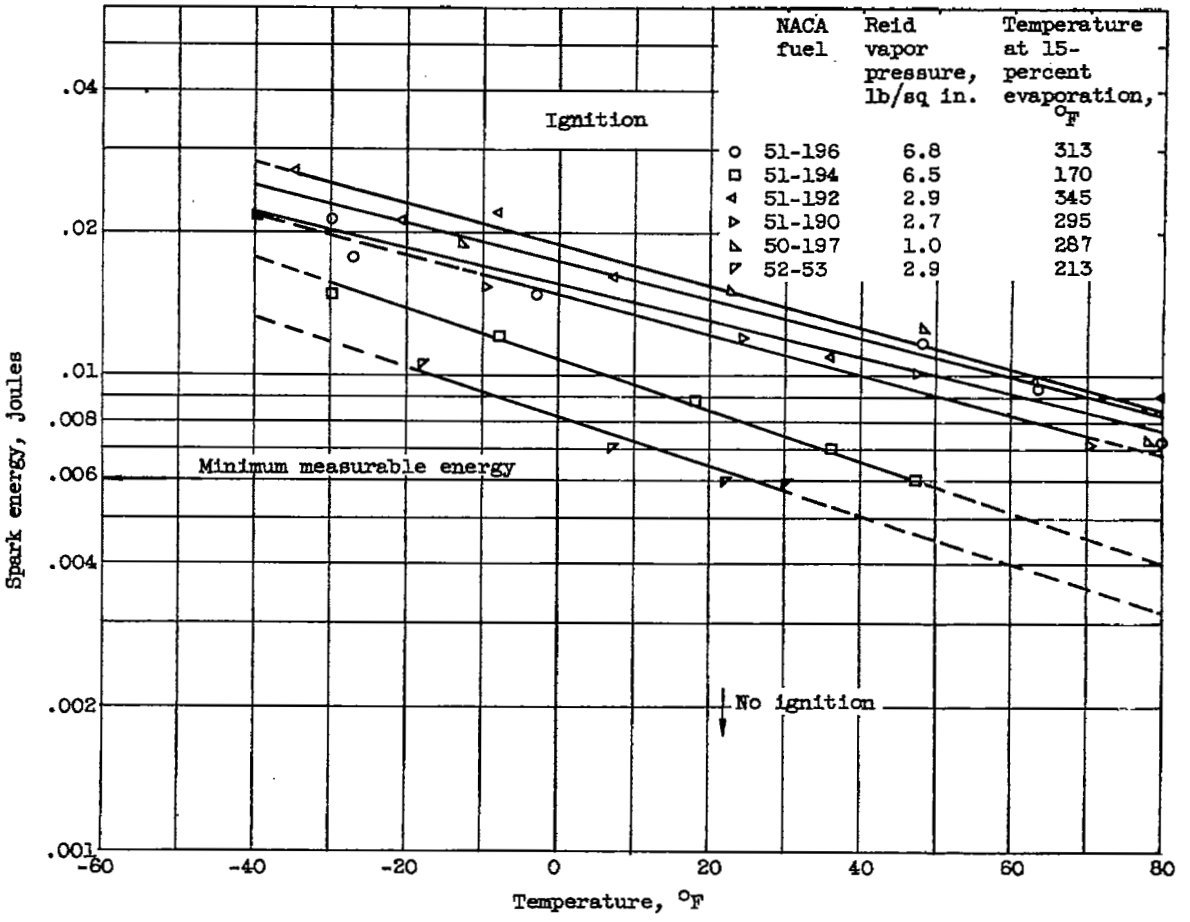

Figure 15. - Effect of combustor-inlet air and fuel temperature on minimum spark energy required for ignition of six fuels of different volatility characteristics. Simulated J33 engine cranking speed, 9 percent of normal rated speed; static sea-level conditions; air flow, 1.38 to 1.68 pounds per second per square foot; combustor-inlet total pressure, 31.3 to 31.6 inches of mercury absolute; 10.5-gallon-per-hour, fixed-area fuel nozzle; sparking rate, 8 sparks per second (ref. 4).

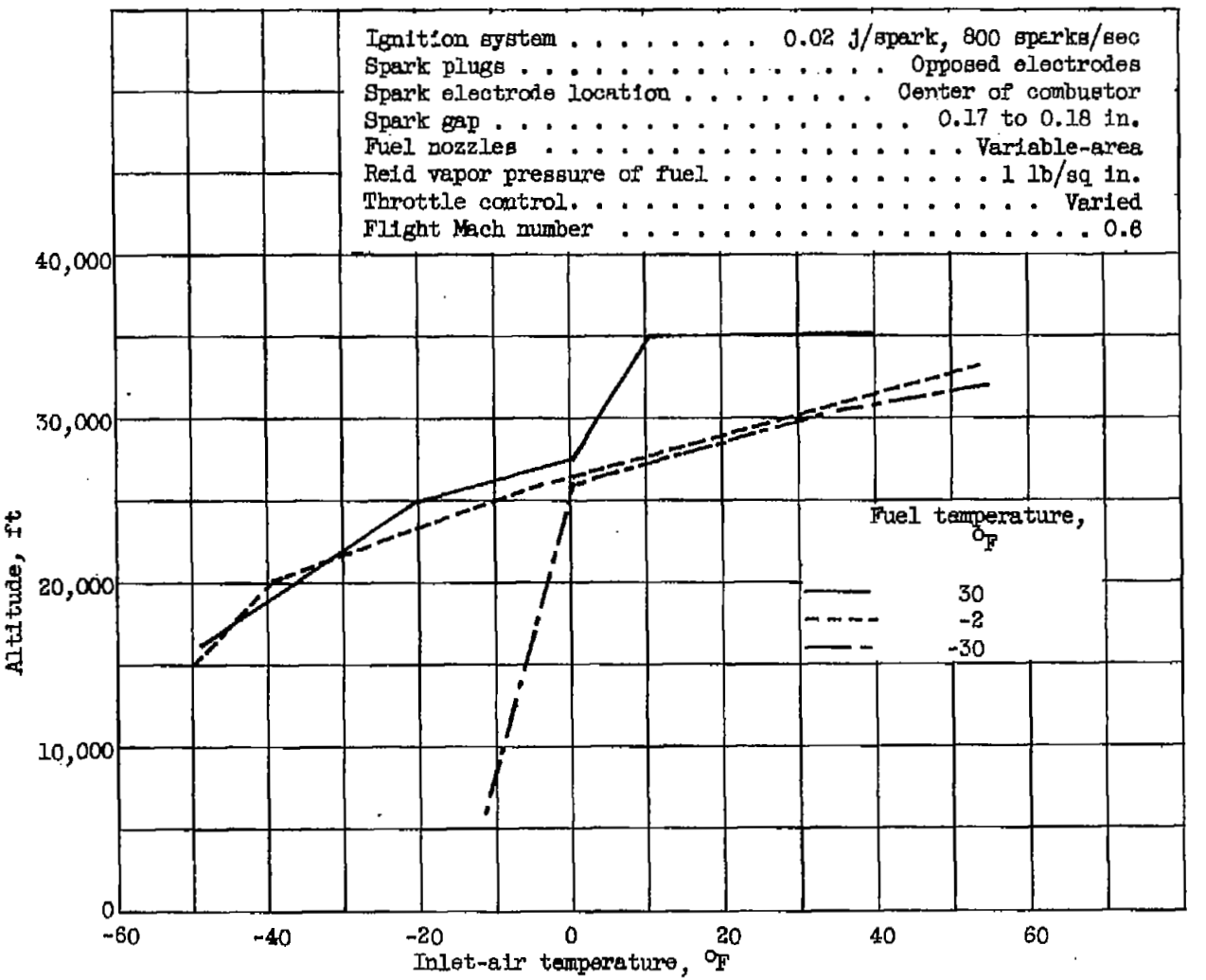

Figure 16. - Effect of engine inlet-air and fuel temperatures on altitude ignition limits of turbojet engine (ref. 5).

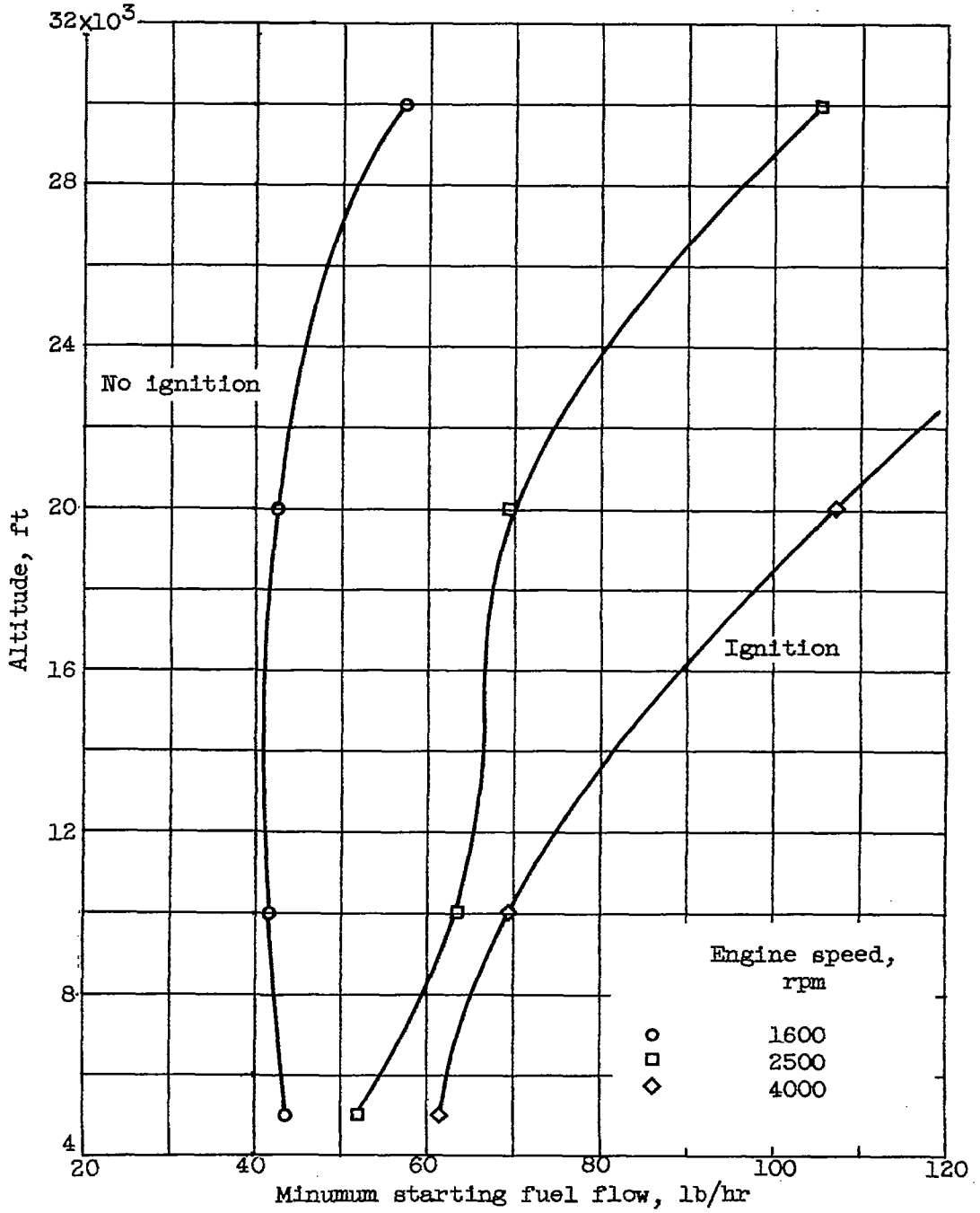

Figure 17. - Effect of altitude on minimum starting fuel flow in single J33 combustor at three engine speeds. Flight Mach number, 0.6; NACA fuel 49-162; fixed-area fuel nozzle; spark energy, constant (data from ref. 1).

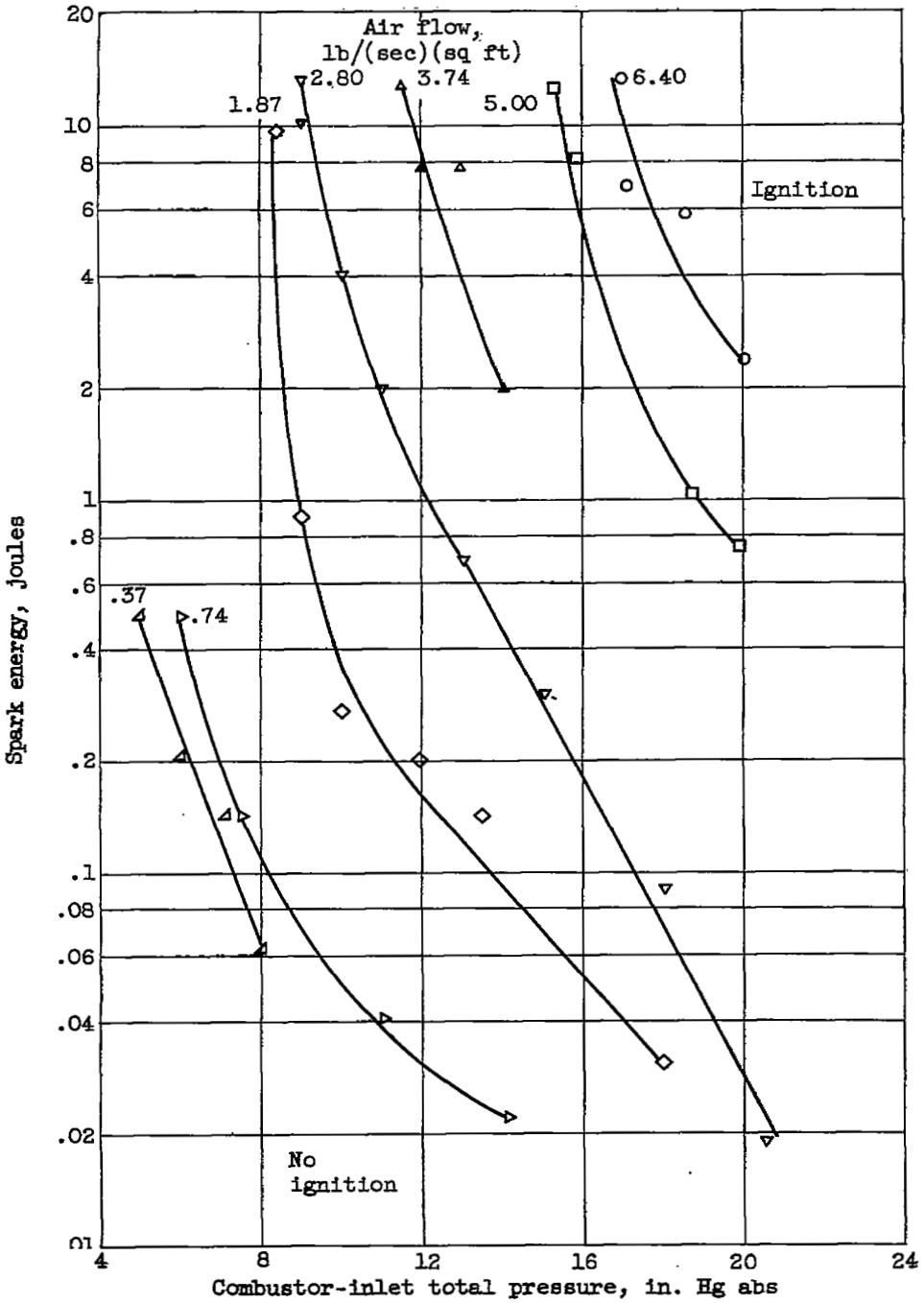

Figure 18. - Effect of air-flow rate and pressure on spark energy required for ignition in single tubular J33 combustor. Inlet-air temperature, -10° F; inlet-fuel temperature, -40° F; grade JP-3 fuel (NACA fuel 50-174); variable-area fuel nozzle; sparking rate, 8 sparks per second (ref. 2).

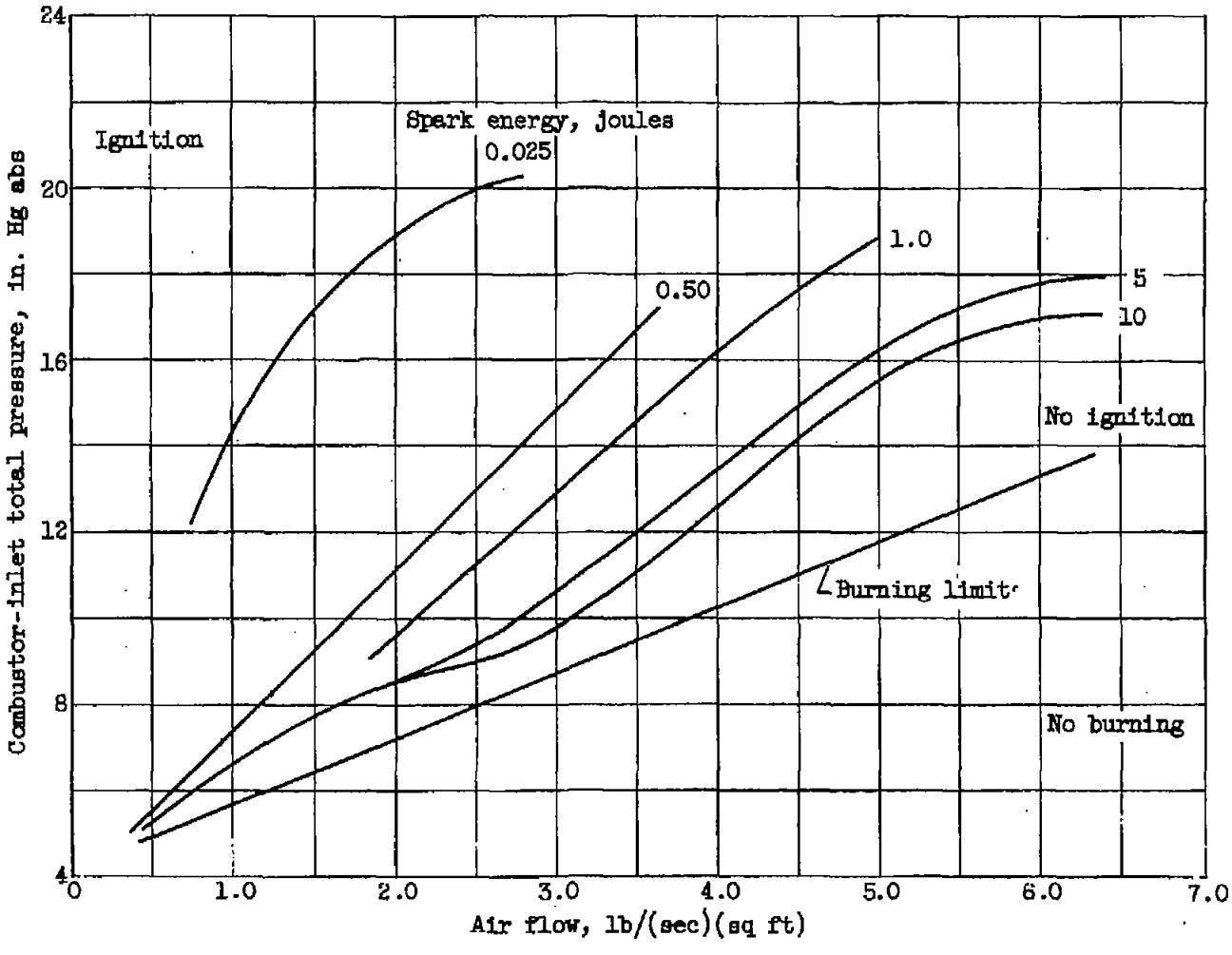

Figure 19. - Comparison of boundaries of ignition and burning limits of single tubular J33 combustor. Inlet-air temperature, -10° F; inlet-fuel temperature, -40° F; grade JP-3 fuel (NACA fuel 50-174); variable-area fuel nozzle; sparking rate, 8 sparks per second (ref. 2).

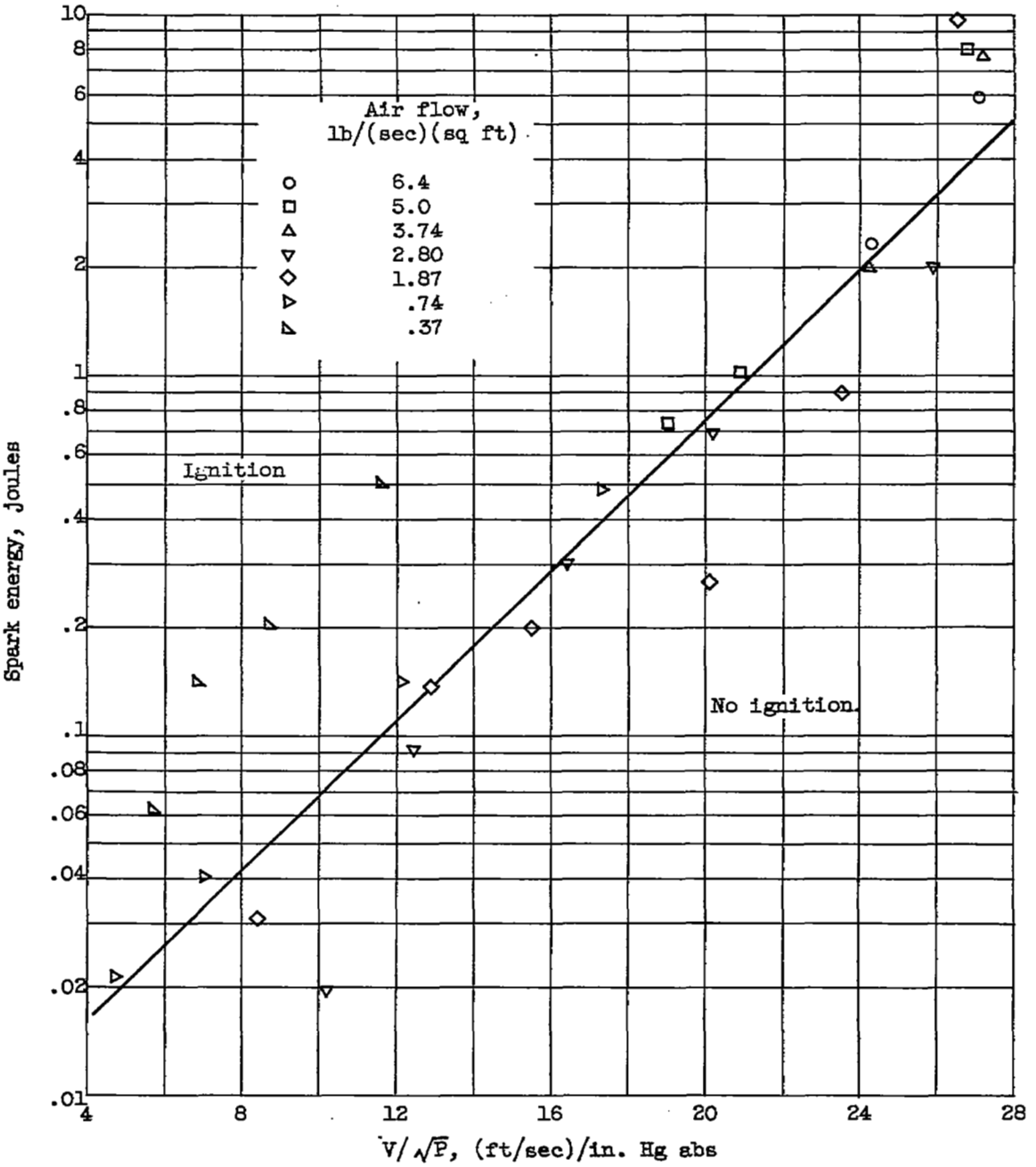

Figure 20. - Minimum spark energy required for ignition as function of combustor-inlet pressure and velocity. Combustor-inlet air temperature, -10° F; combustor-inlet fuel temperature, -40° F; grade JP-3 fuel (NACA fuel 50-174); variable-area fuel nozzle; sparking rate, 8 sparks per second (ref. 4).

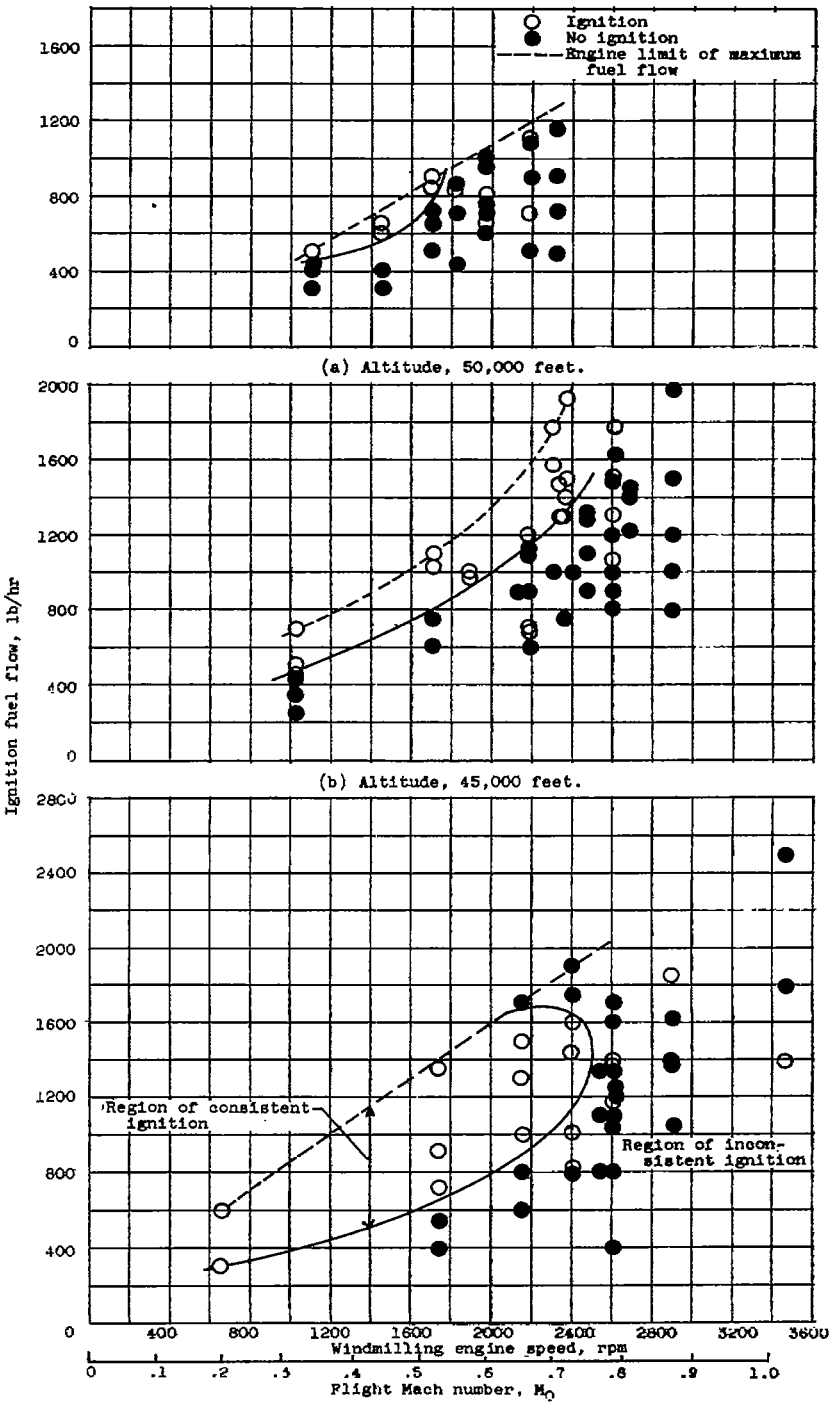

Figure 21. - Effect of fuel flow on aititude ignition characteristics with MIL-F-5624A, grade JP-4 fuel. Fuel temperature, approximately 50° F; engine-inlet air temperature, approximately 0° F (ref. 6).

[redacted]

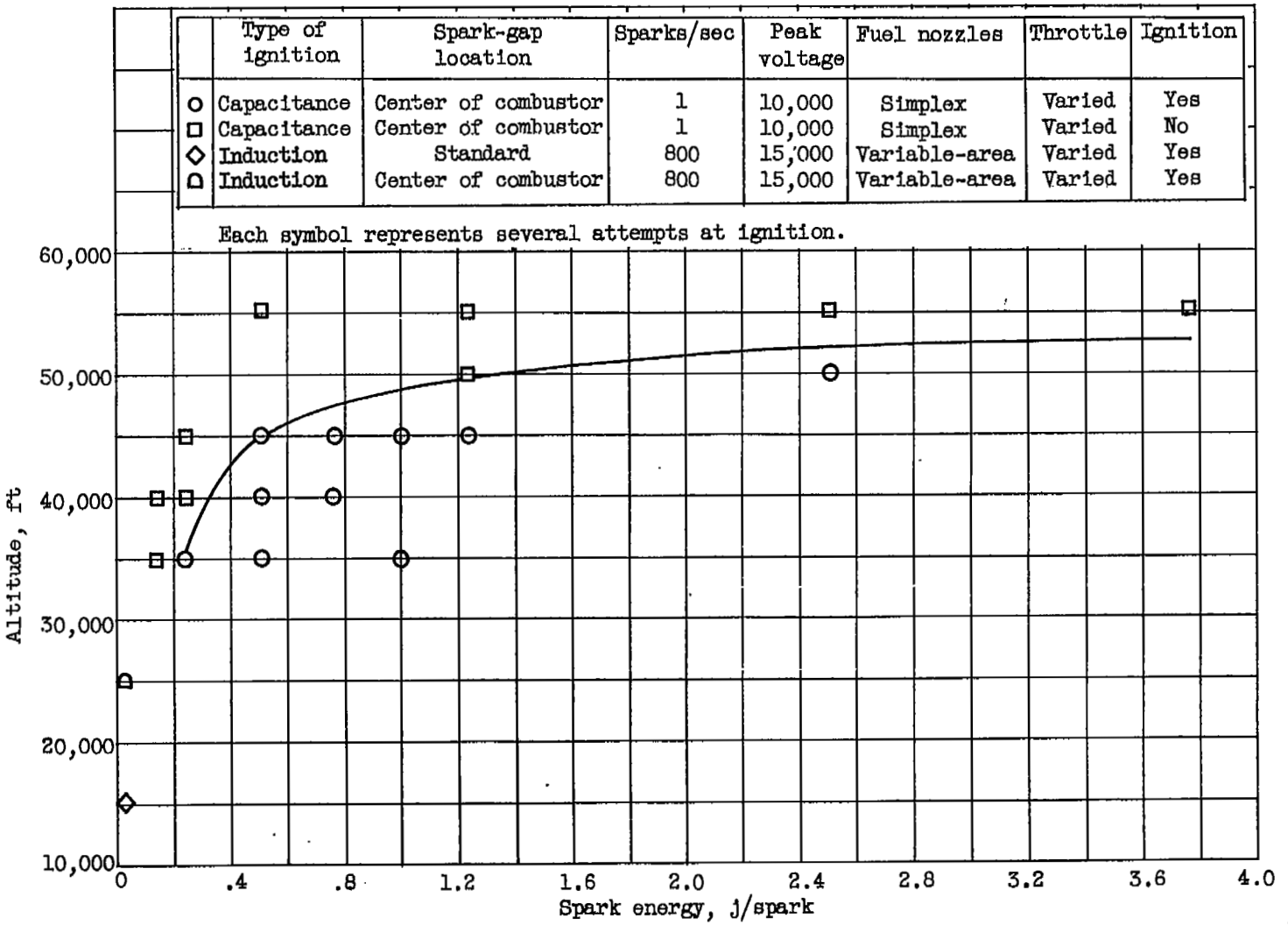

Figure 22. - Effect of spark energy on altitude ignition limits of full-scale engine at flight Mach number of 0.6 (ref. 5).

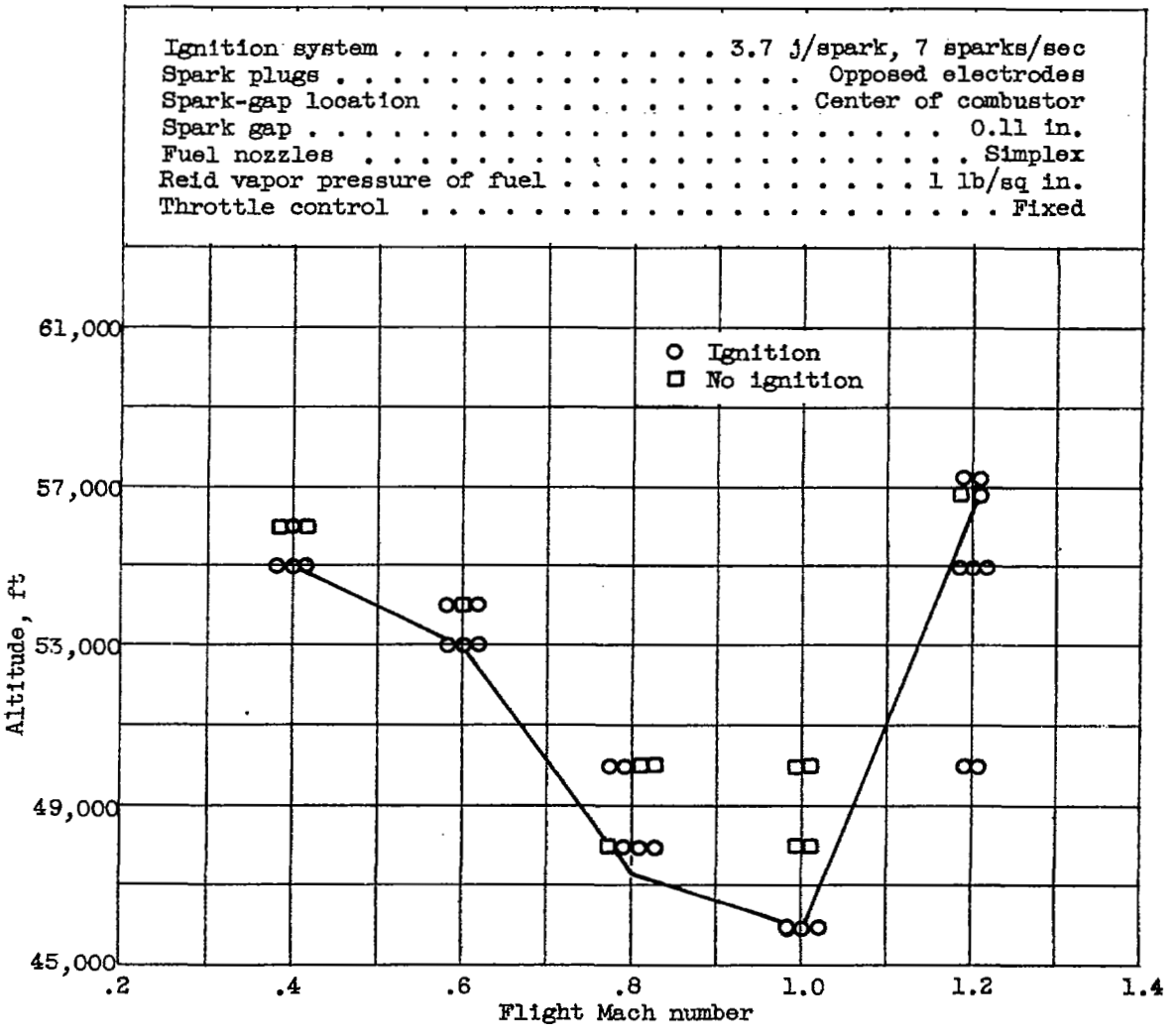

Figure 23. - Effect of flight Mach number on altitude ignition limit of turbojet engine using 10,000-volt capacitance ignition unit (ref. 5).

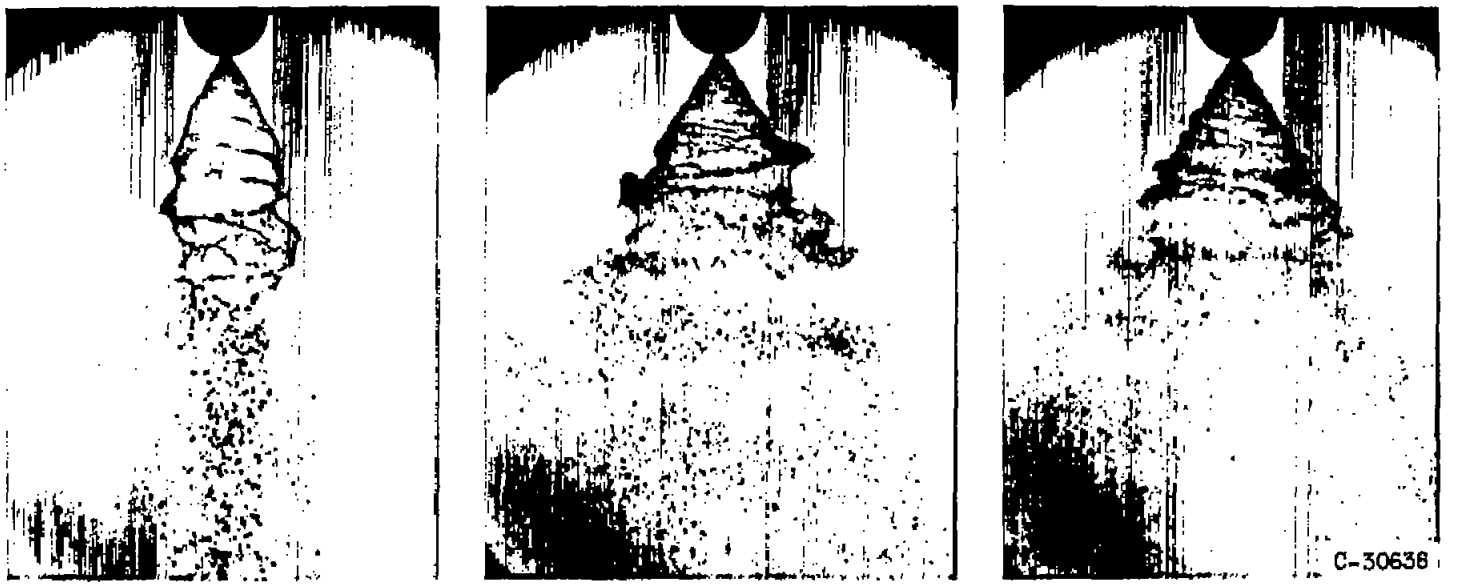

(a) Fuel flow. 40 pounds per hour. (b) Fuel flow. 65 pounds per hour. (c) Fuel flow. 80 pounds per hour.

Figure 24. - Fixed-area fuel nozzle spraying into quiescent air. Nozzle rated at 40 gallons per hour at pressure drop of 100 pounds per square inch (ref. 7).

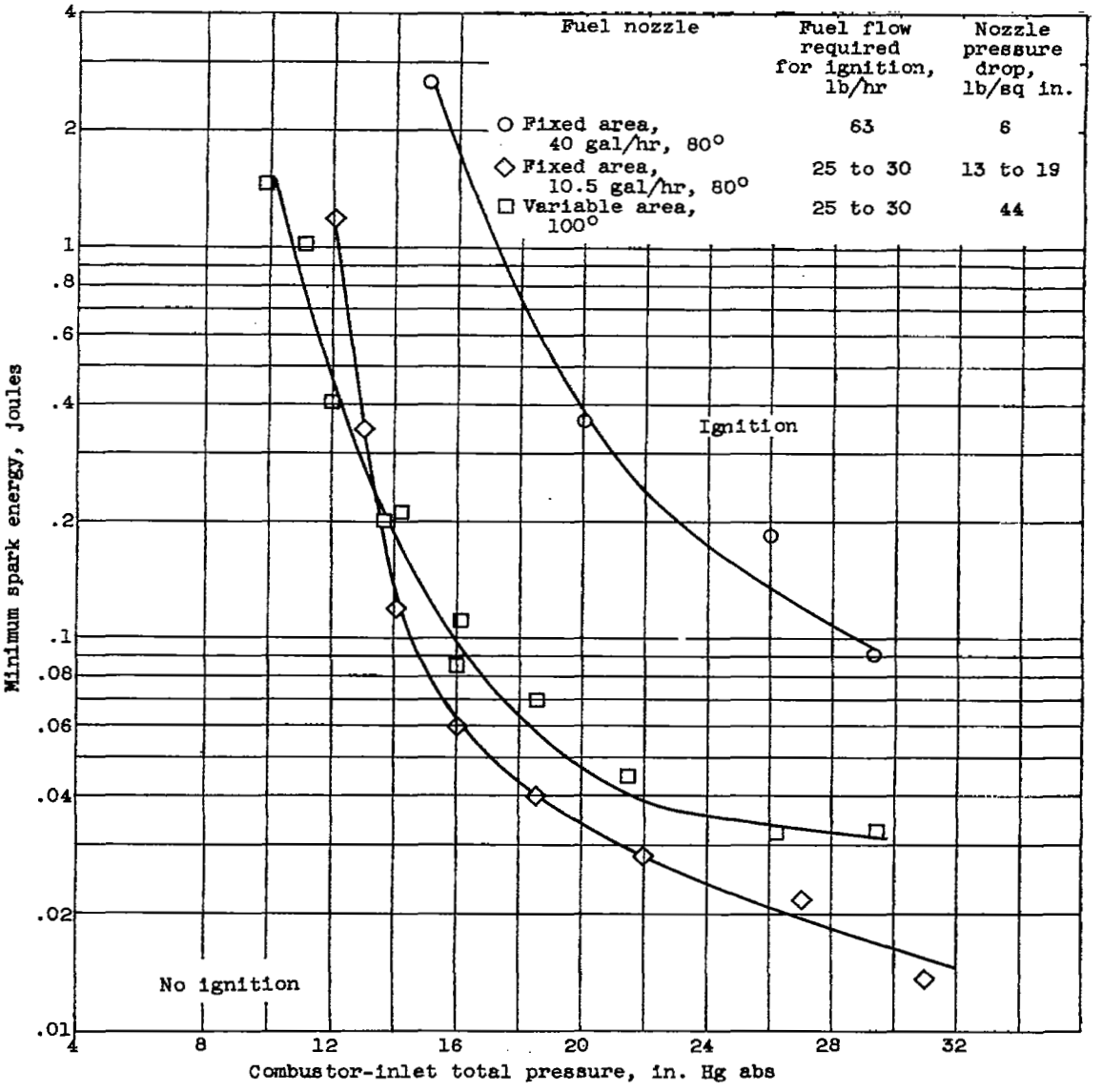

Figure 25. - Effect of fuel spray nozzle on spark energy required for ignition in single tubular combustor. Air flow, 1.87 pounds per second per square foot; inlet-air and fuel temperature, 10° F; NACA fuel 51-192; sparking rate, 8 sparks per second (ref. 9).

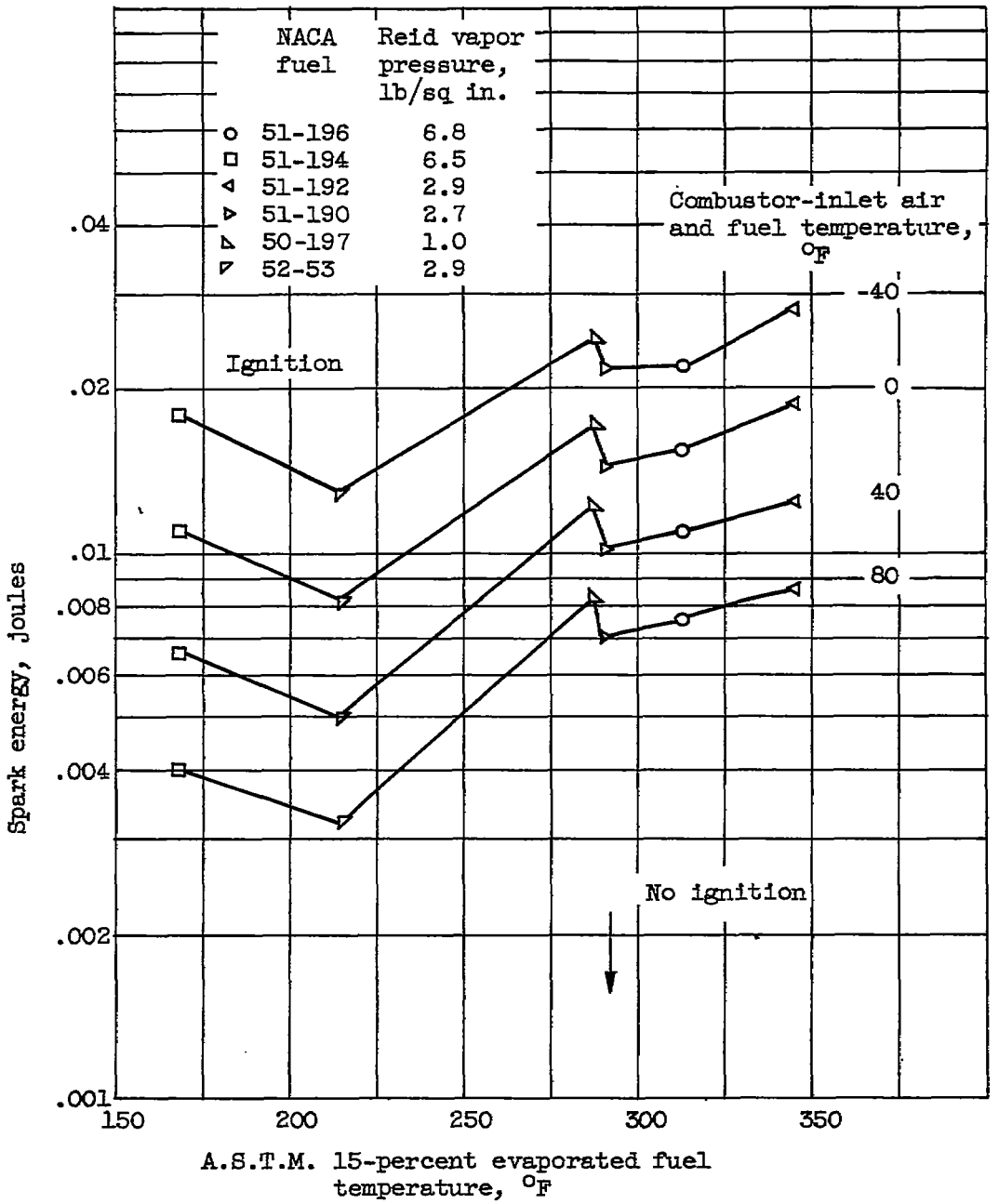

Figure 26. - Minimum spark energy required in single J33 combustor for ignition of six fuels as function of 15-percent evaporated fuel temperature at several combustor-inlet air and fuel temperatures. Simulated engine cranking speed, 9 percent of normal rated speed; static sea-level conditions; 10.5-gallon-per-hour, fixed-area fuel nozzle; sparking rate, 8 sparks per second (ref. 4).

[redacted]

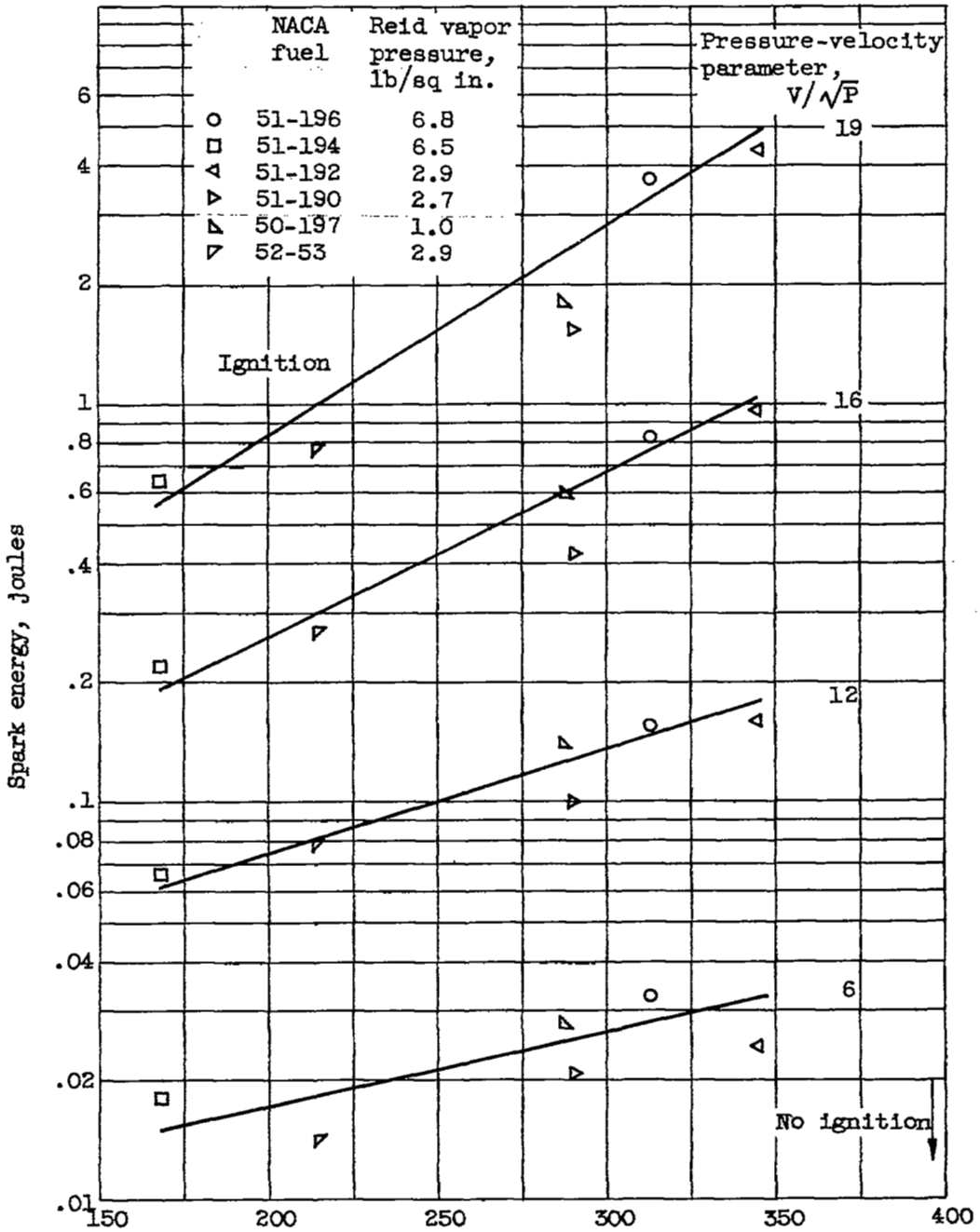

Figure 27. - Minimum spark energy required in J33 single combustor for ignition of six fuels as function of 15-percent evaporated fuel temperature at several values of $V/\sqrt{P}$. Combustor-inlet air and fuel temperature, 10° F (ref. 4).

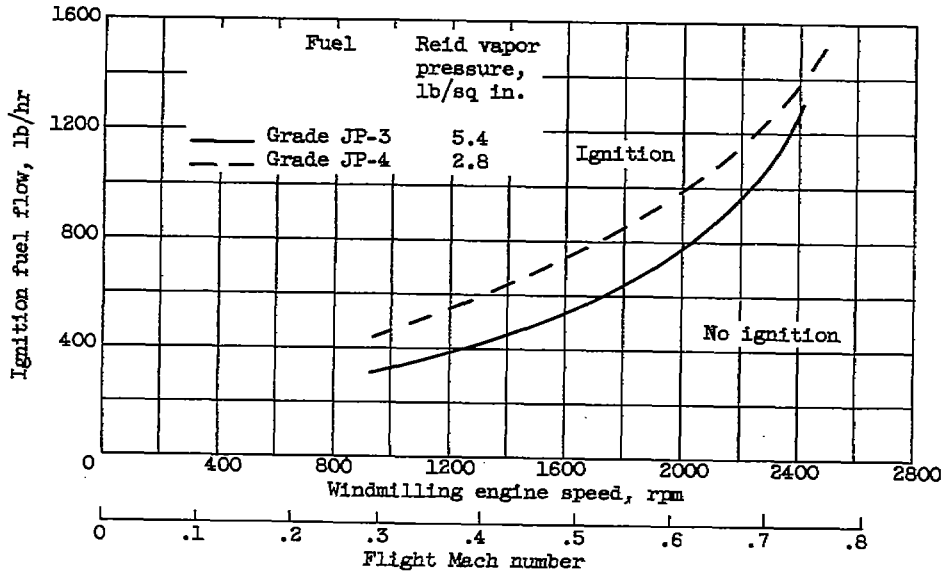

Figure 28. - Effect of two grades of fuel on altitude ignition characteristics. Fuel temperature, approximately 50° F; engine-inlet air temperature, approximately 0° F; altitude, 45,000 feet (data from ref. 6).

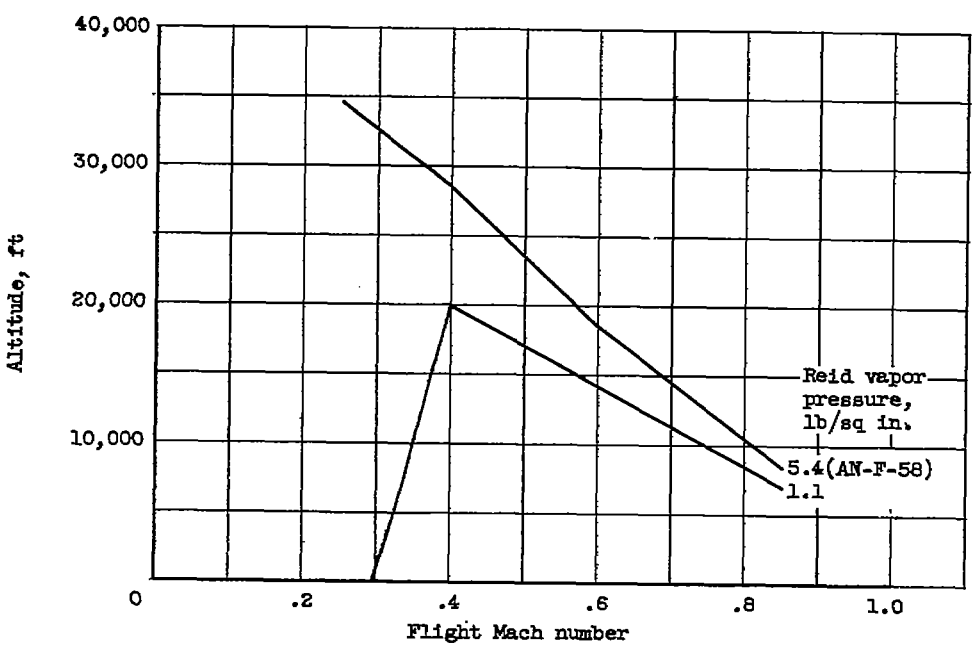

(a) Engine with axial-flow compressor and duplex fuel nozzles (ref. 10).

Figure 29. - Effect of fuel volatility on altitude ignition limits of turbojet engine.

[redacted]

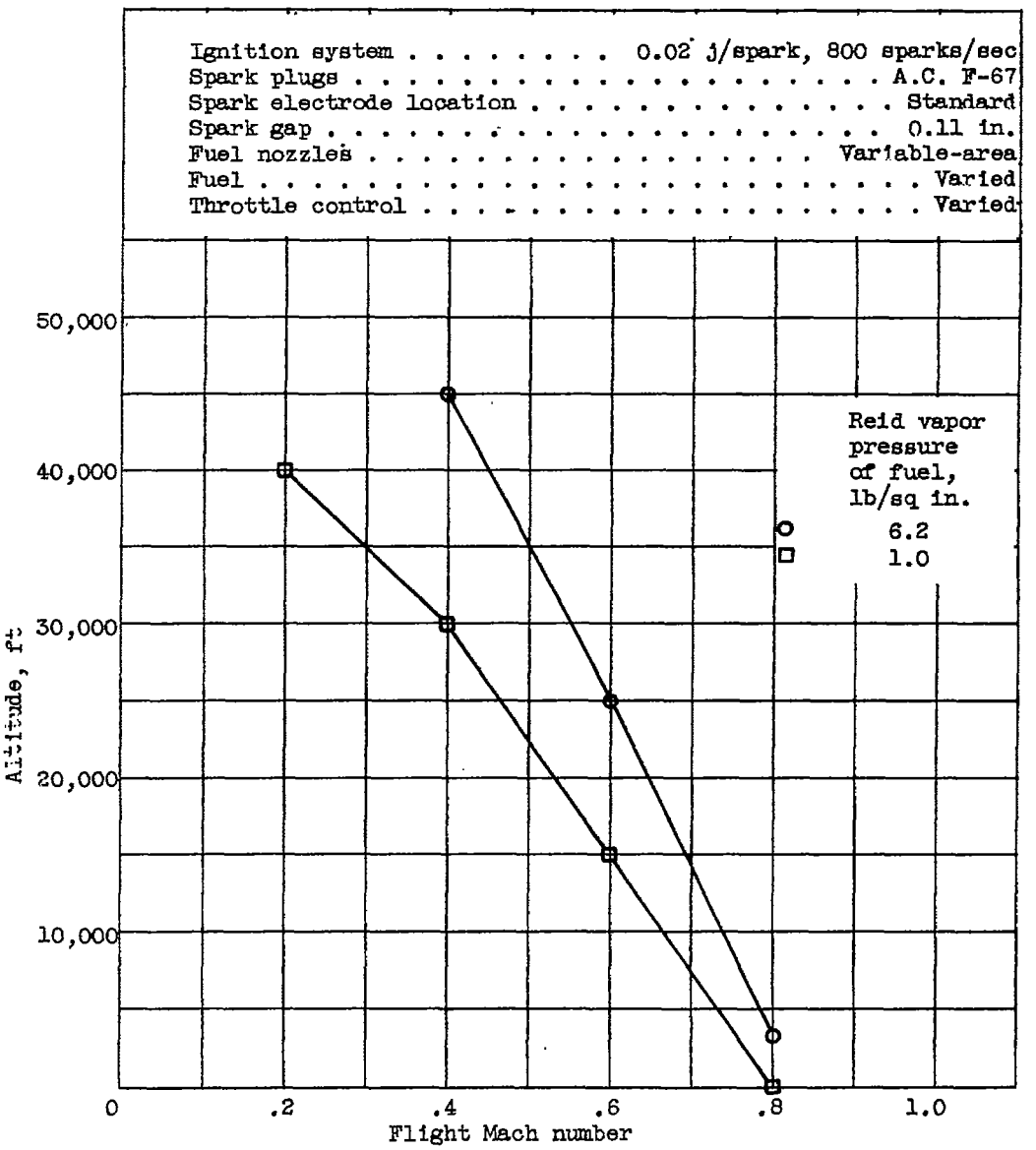

(b) Engine with axial-flow compressor and variable-area fuel nozzles (ref. 5).

Figure 29. - Continued. Effect of fuel volatility on altitude ignition limits of turbojet engine.

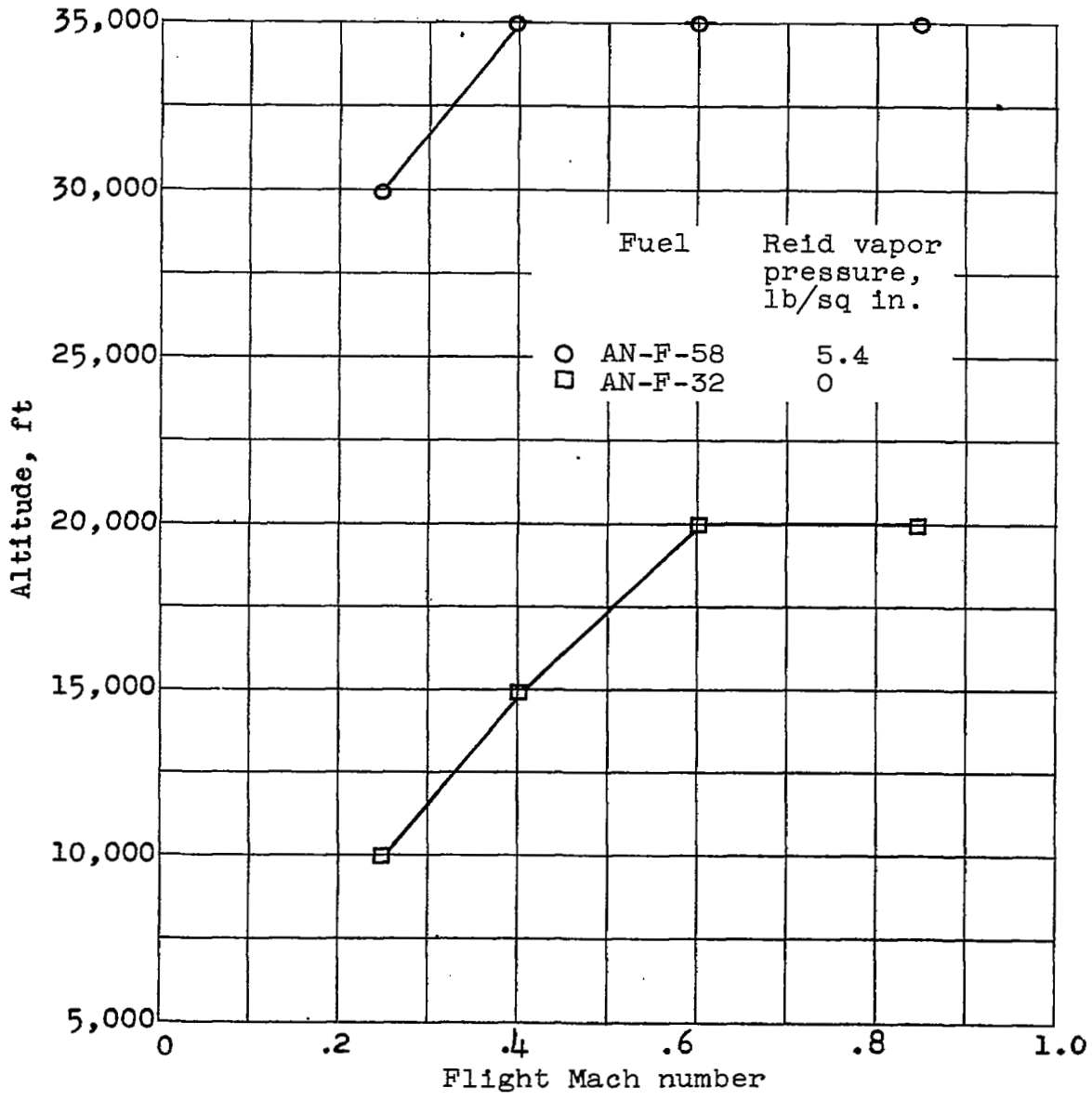

(c) Engine with centrifugal-flow compressor (ref. 13).

Figure 29. - Concluded. Effect of fuel volatility on altitude ignition limits of turbojet engine.

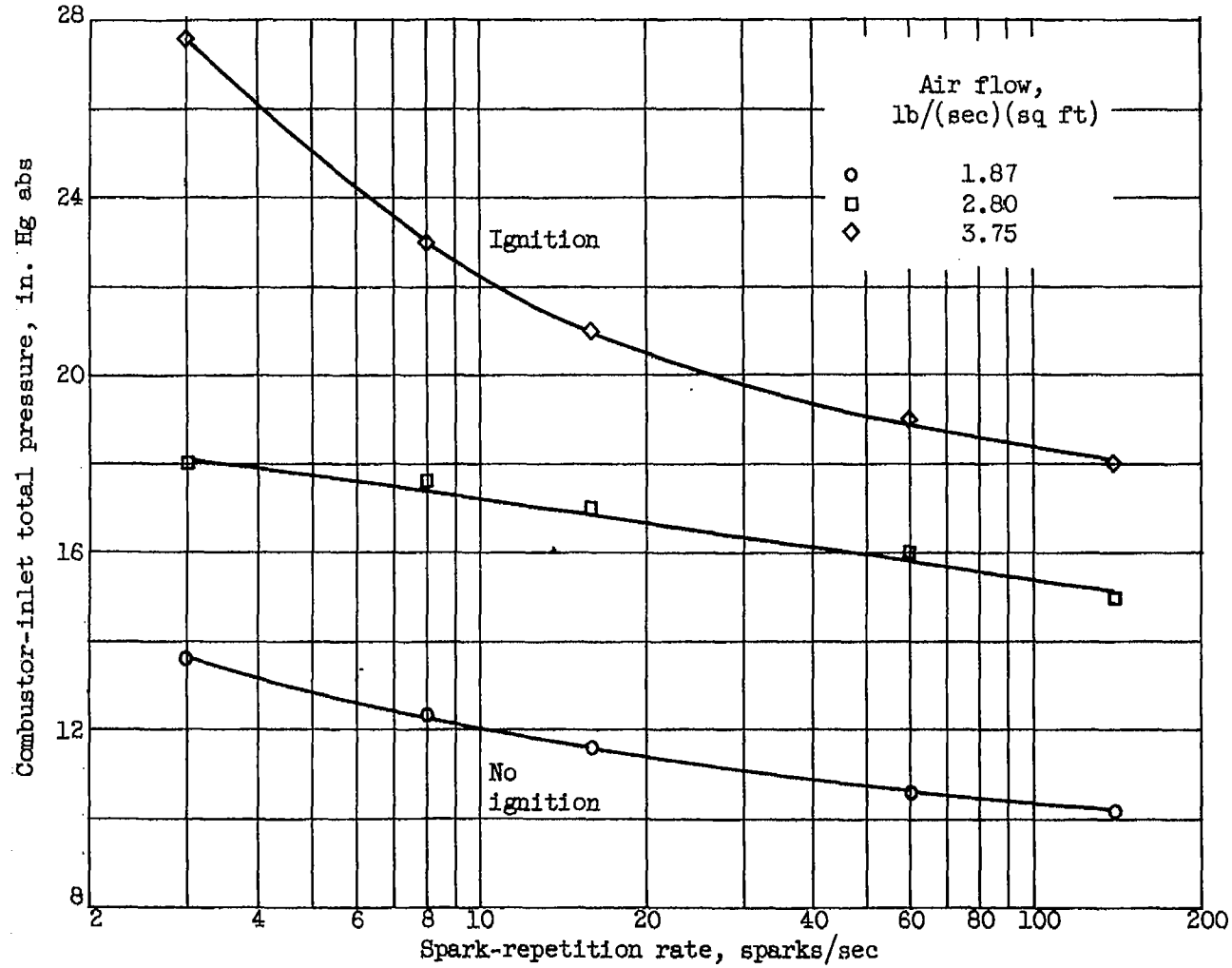

Figure 30. - Effect of spark-repetition rate on minimum combustor-inlet pressure for ignition in single J33 combustor at three air-flow rates. Air and fuel temperature, -10° F; NACA fuel 51-38; variable-area fuel nozzle; spark energy, constant (data from ref. 16).

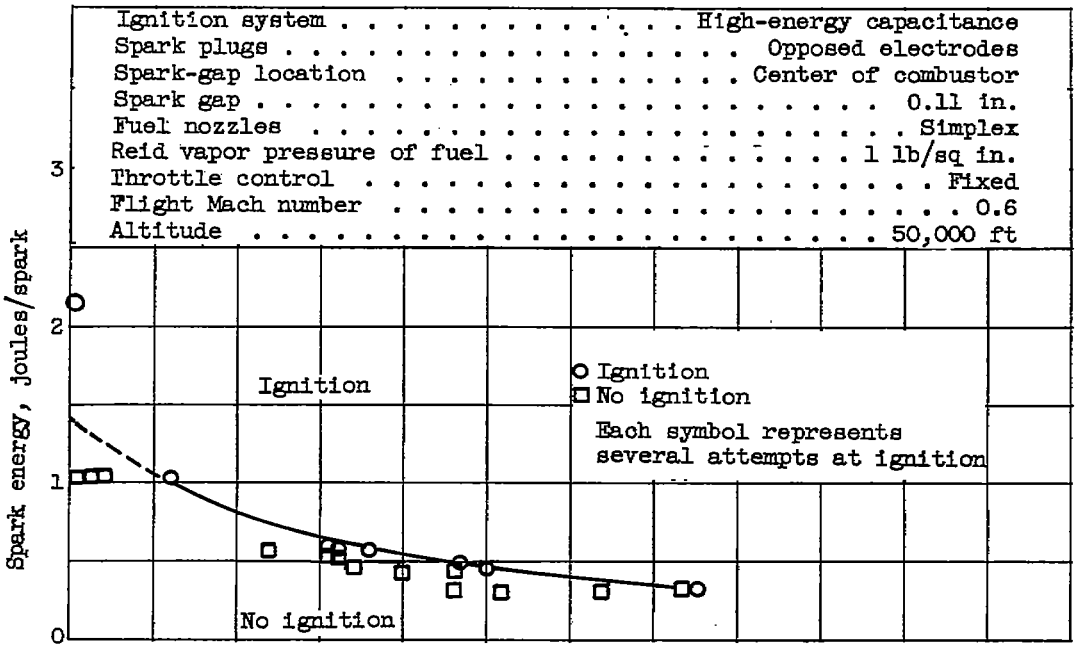

(a) Effect of spark-repetition rate on spark energy requirements.

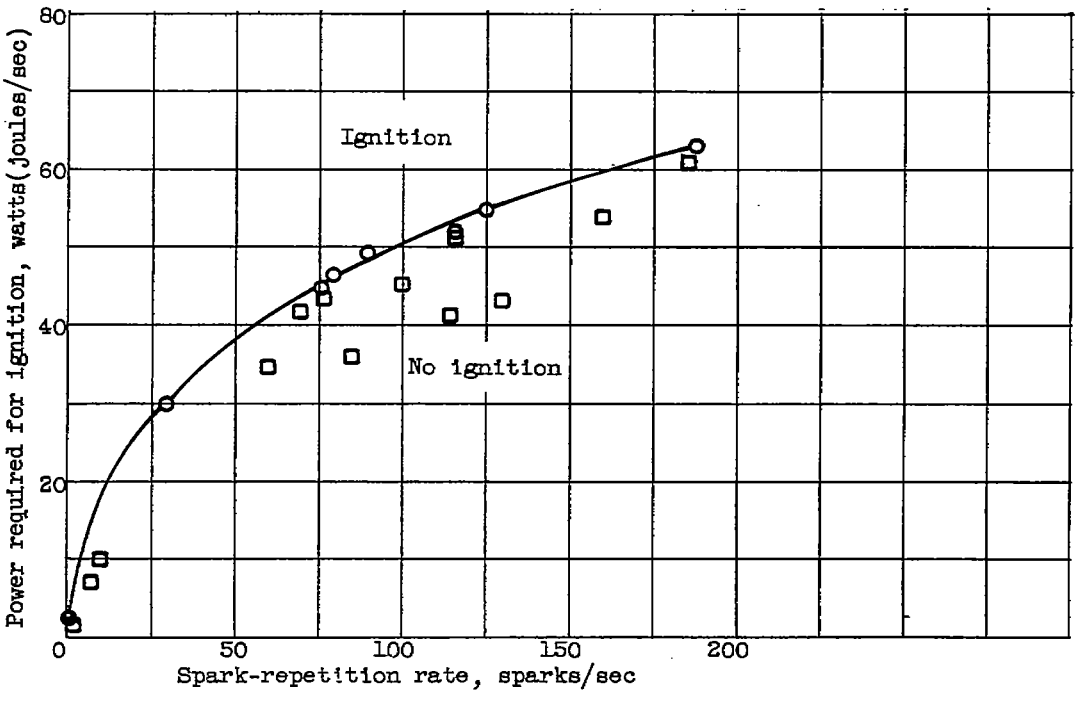

(b) Power required for ignition at various spark energies.

Figure 31. - Spark energy and power required for ignition in full-scale engine at various spark-repetition rates (ref. 5).

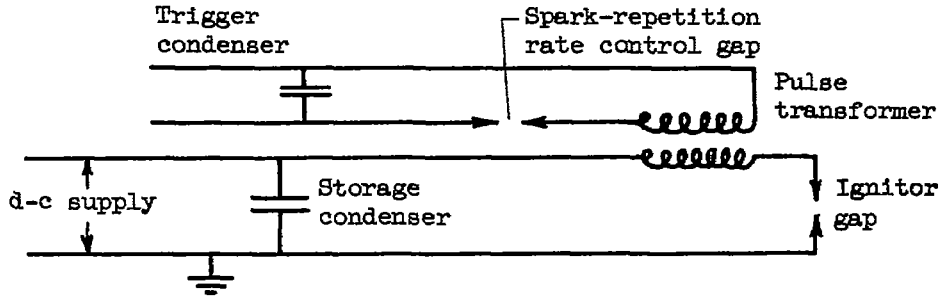

(a) Triggered low-loss system; for air-gap ignitors only.

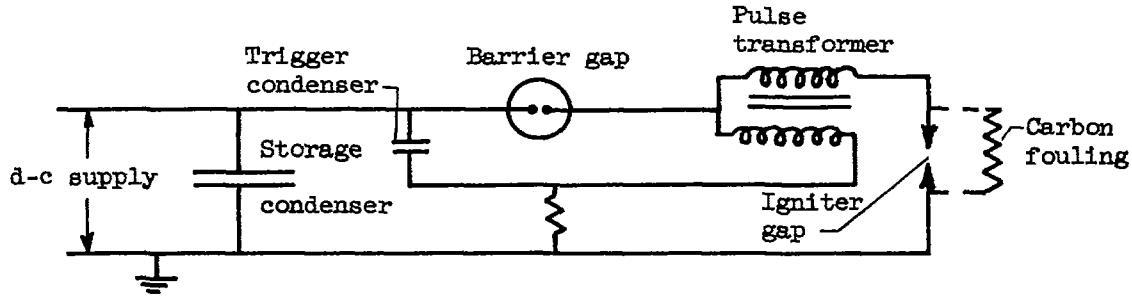

(b) Triggered system with barrier gap; for air-gap or surface-discharge ignitors.

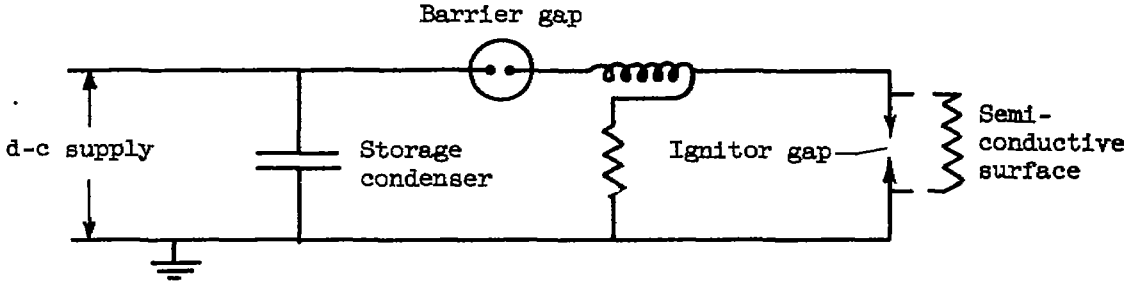

(c) Nontriggered system; for surface-discharge ignitors only.

Figure 32. - Basic circuits of low-voltage high-energy spark ignition systems.

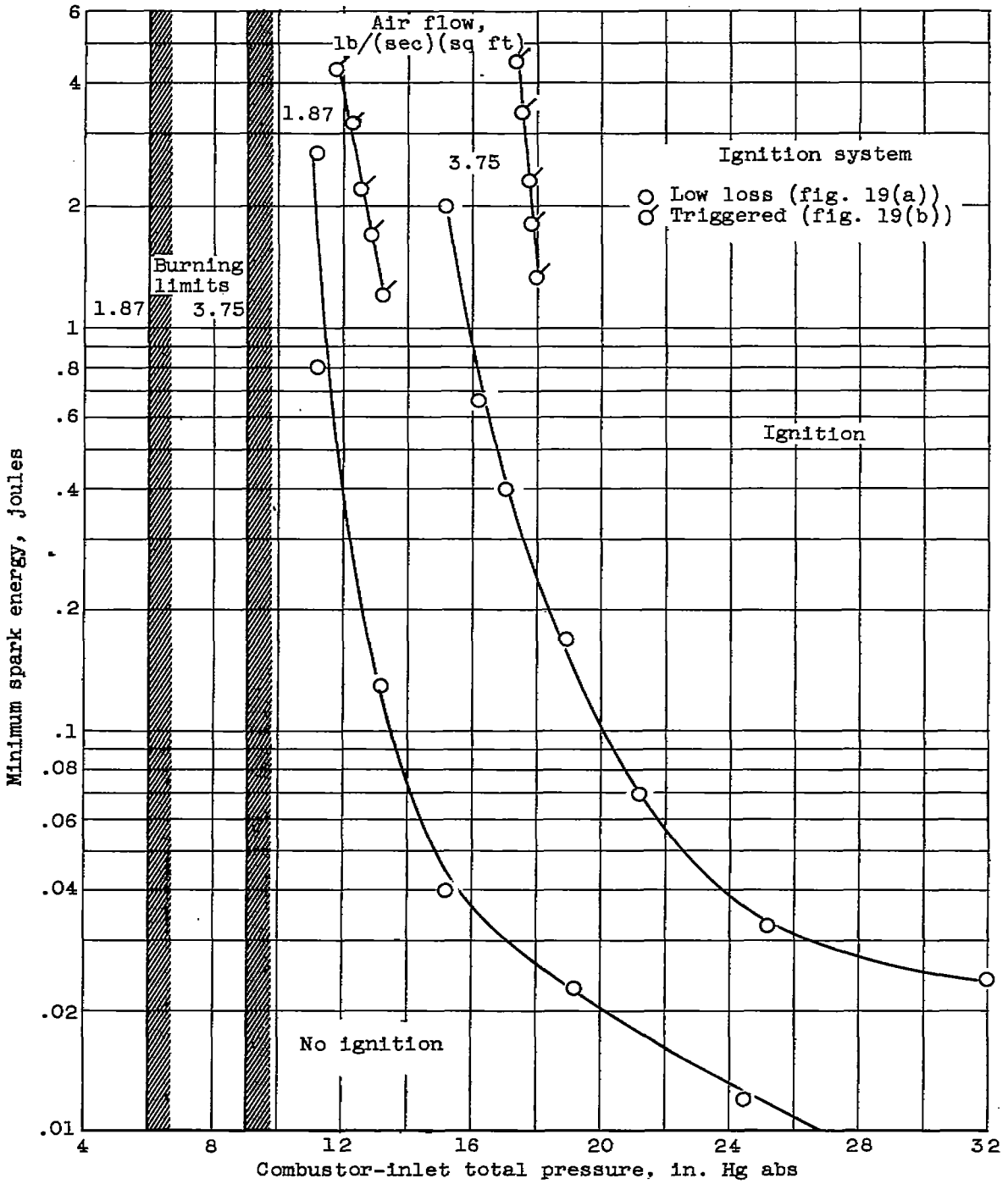

Figure 33. - Comparison of combustor ignition energy requirements in single tubular J33 combustor with two ignition systems. Air-gap ignitor; inlet-air and fuel temperature, 10° F; NACA fuel 50-197; 10.5-gallon-per-hour, fixed-area fuel nozzle (ref. 9).

[redacted]

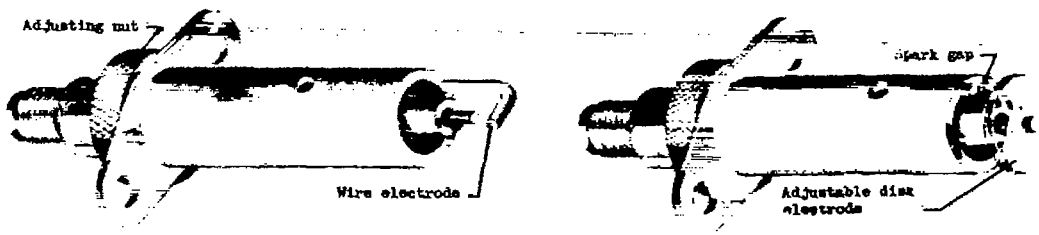

3196

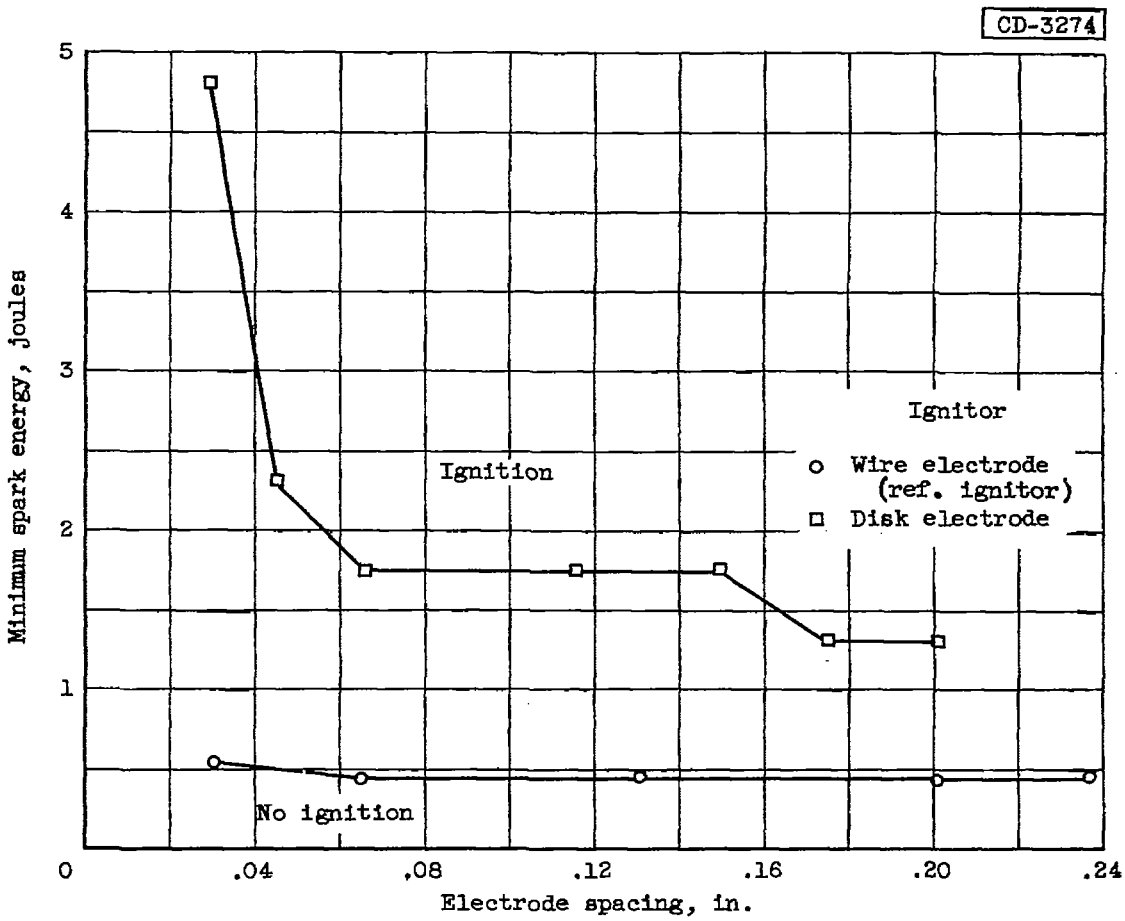

(a) Effect of electrode spacing. Air flow, 1.87 pounds per square foot; inlet-air pressure, 12 inches of mercury absolute; 10.5-gallon-per-hour, fixed-area fuel nozzle.

Figure 34. - Ignition energy requirements of single tubular J33 combustor. Low-loss ignition system; inlet-air and fuel temperature, 10° F; NACA fuel 50-197; sparking rate, 8 sparks per second (ref. 9).

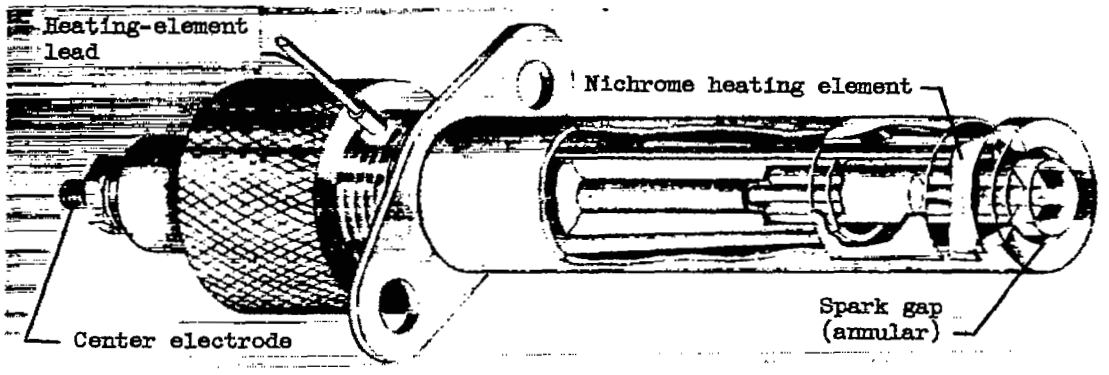

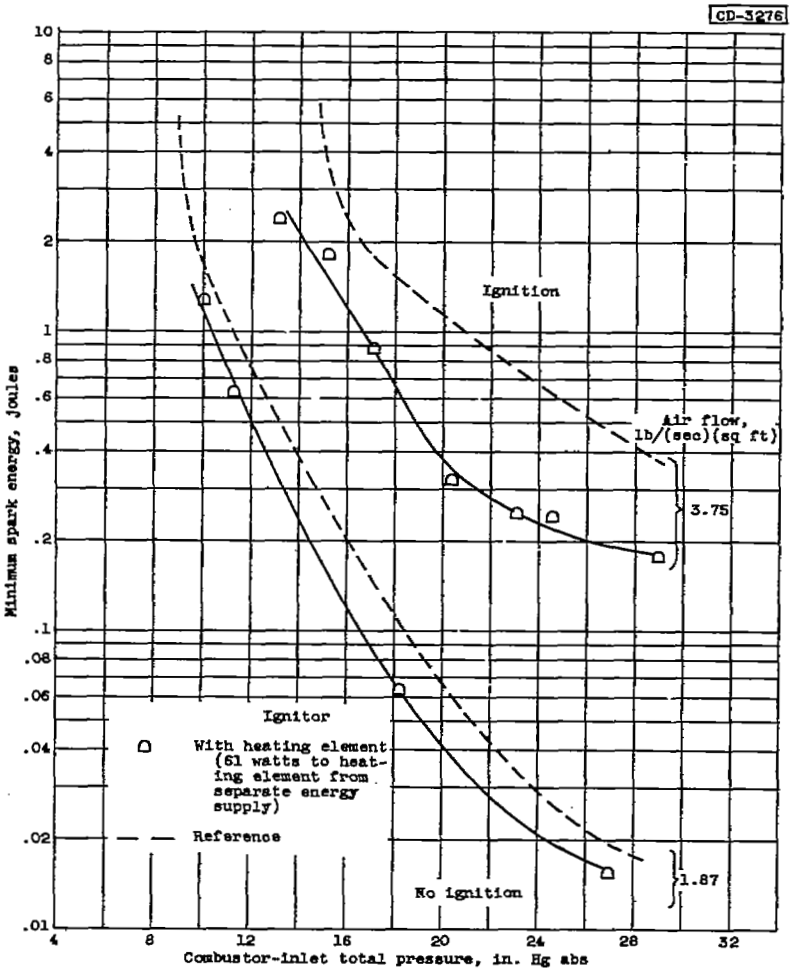

(b) Effect of fuel heating at spark electrodes. Variable-area fuel nozzle.

Figure 34. - Continued. Ignition energy requirements of single tubular J33 combustor. Low-loss ignition system; inlet-air and fuel temperature, 100° F; NACA fuel 50-197; sparking rate, 8 sparks per second (ref. 9).

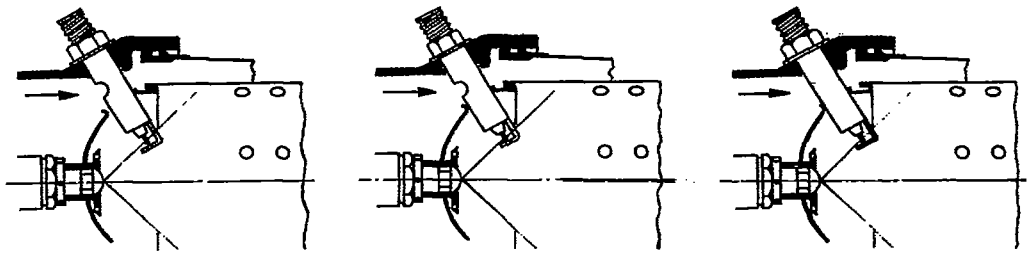

Standard installation; $\frac{1}{16}$-inch diametral clearance between ignitor and combustor; cooling-air hole open.

Cooling air reduced; diametral clearance reduced to zero.

No cooling air; no diametral clearance or cooling-air hole.

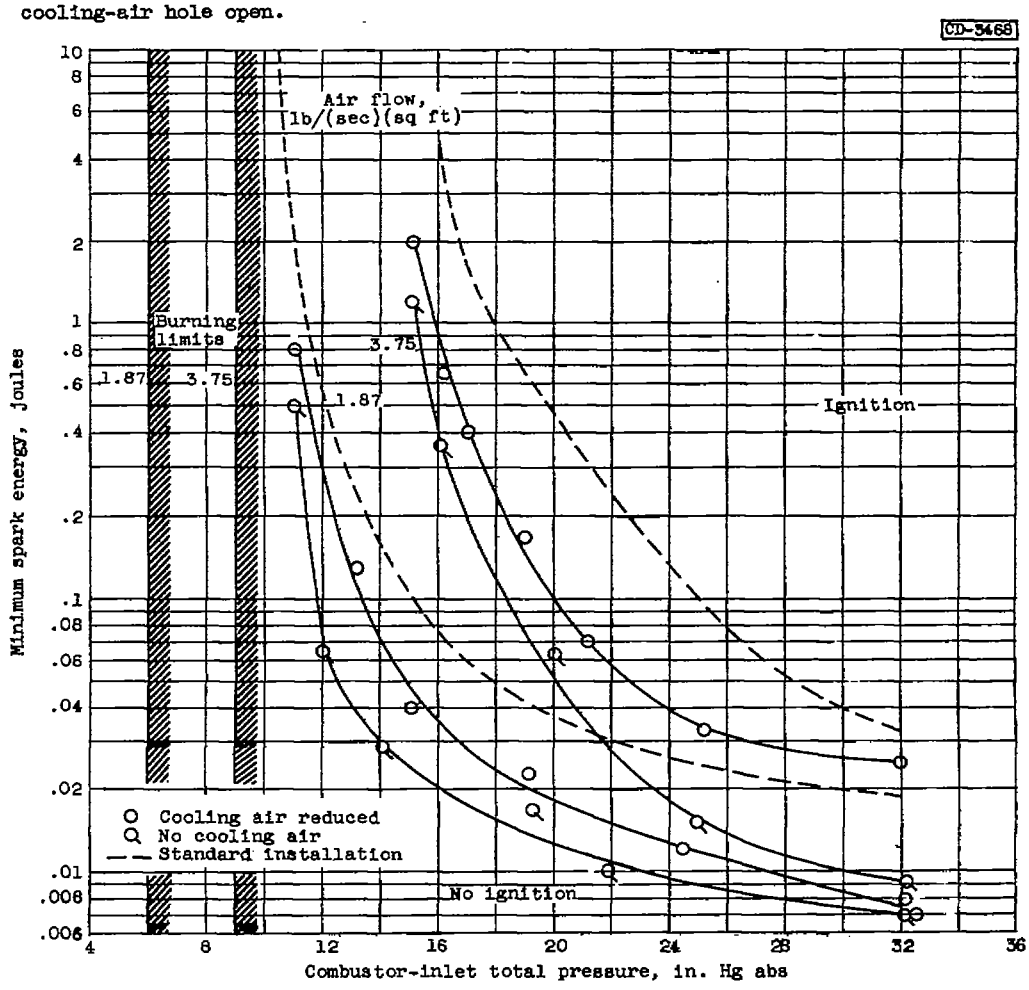

(c) Effect of air flow at spark gap. 10.5-Gallon-per-hour, fixed-area fuel nozzle.

Figure 34. - Concluded. Ignition energy requirements of single tubular J33 combustor. Low-loss ignition system; inlet-air and fuel temperature, 10° F; NACA fuel 50-197; sparking rate, 8 sparks per second (ref. 9).

[redacted]

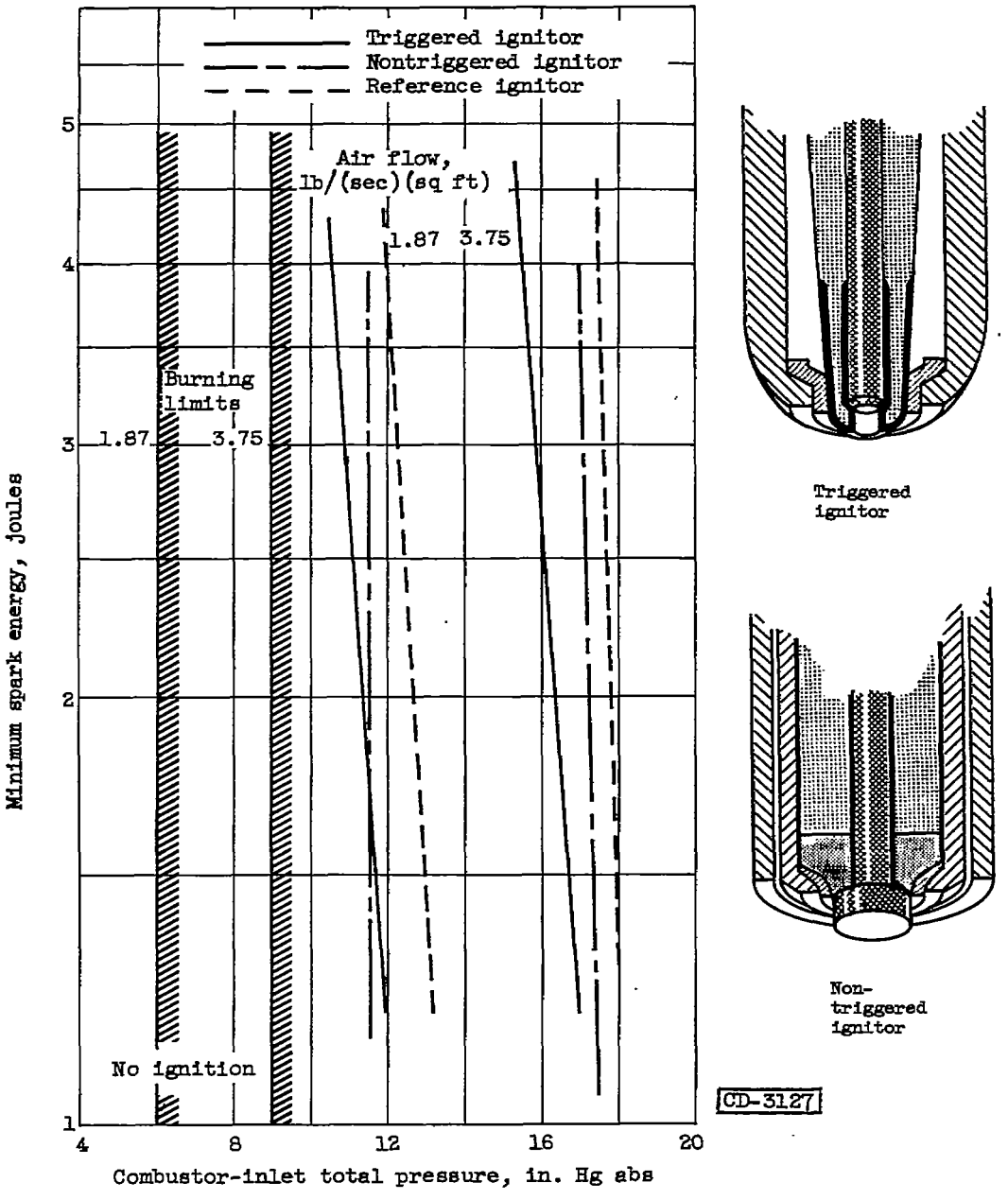

Figure 35. - Comparison of ignition limits of single tubular J33 combustor with nontriggered and triggered surface-discharge ignitors and with reference air-gap ignitor. Triggered ignition system with barrier gap; inlet-air and fuel temperature, 10° F; NACA fuel 50-197; 10.5-gallon-per-hour, fixed-area fuel nozzle (ref. 9).

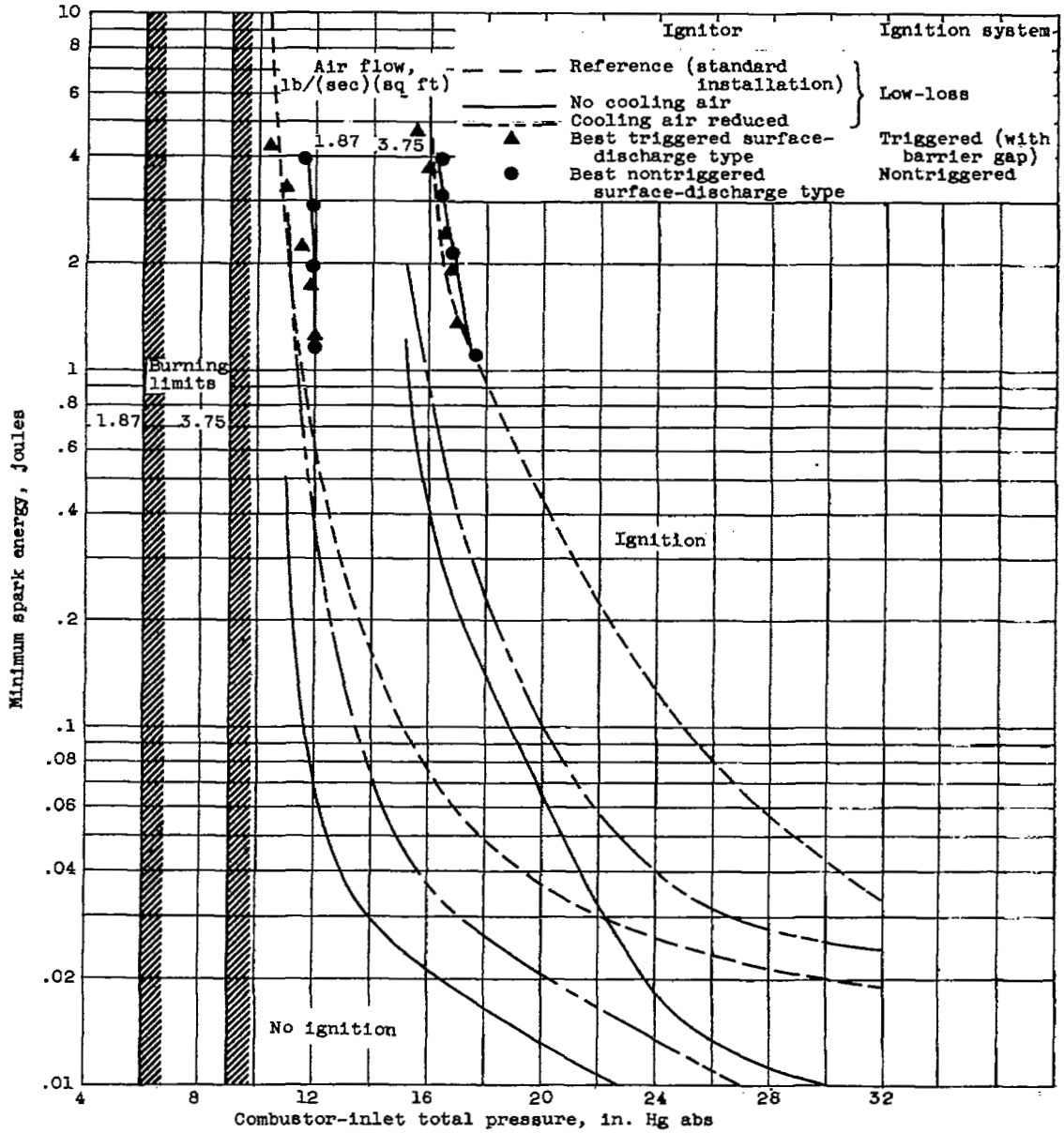

Figure 36. - Comparison of combustor ignition energy requirements for several experimental ignitors. Inlet-air and fuel temperature, 10° F; NACA fuel 50-197; 10.5-gallon-per-hour, fixed-area fuel nozzle (data from ref. 9).

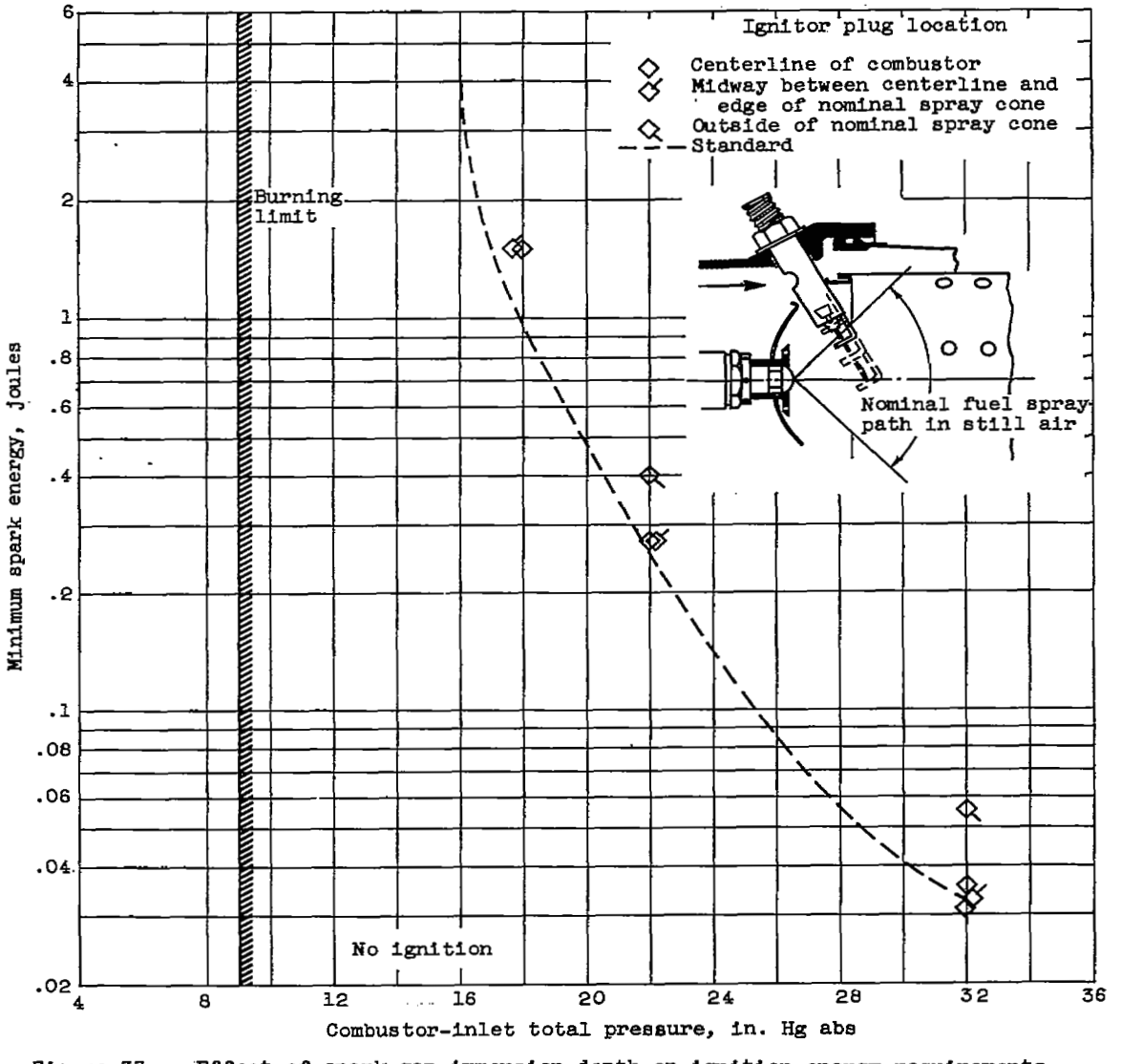

Figure 37. - Effect of spark-gap immersion depth on ignition energy requirements of single tubular J33 combustor. Low-loss ignition system; air flow, 3.75 pounds per second per square foot; inlet-air and fuel temperature, 10° F; NACA fuel 50-197; 10.5-gallon-per-hour, fixed-area fuel nozzle; sparking rate, 8 sparks per second (ref. 9).

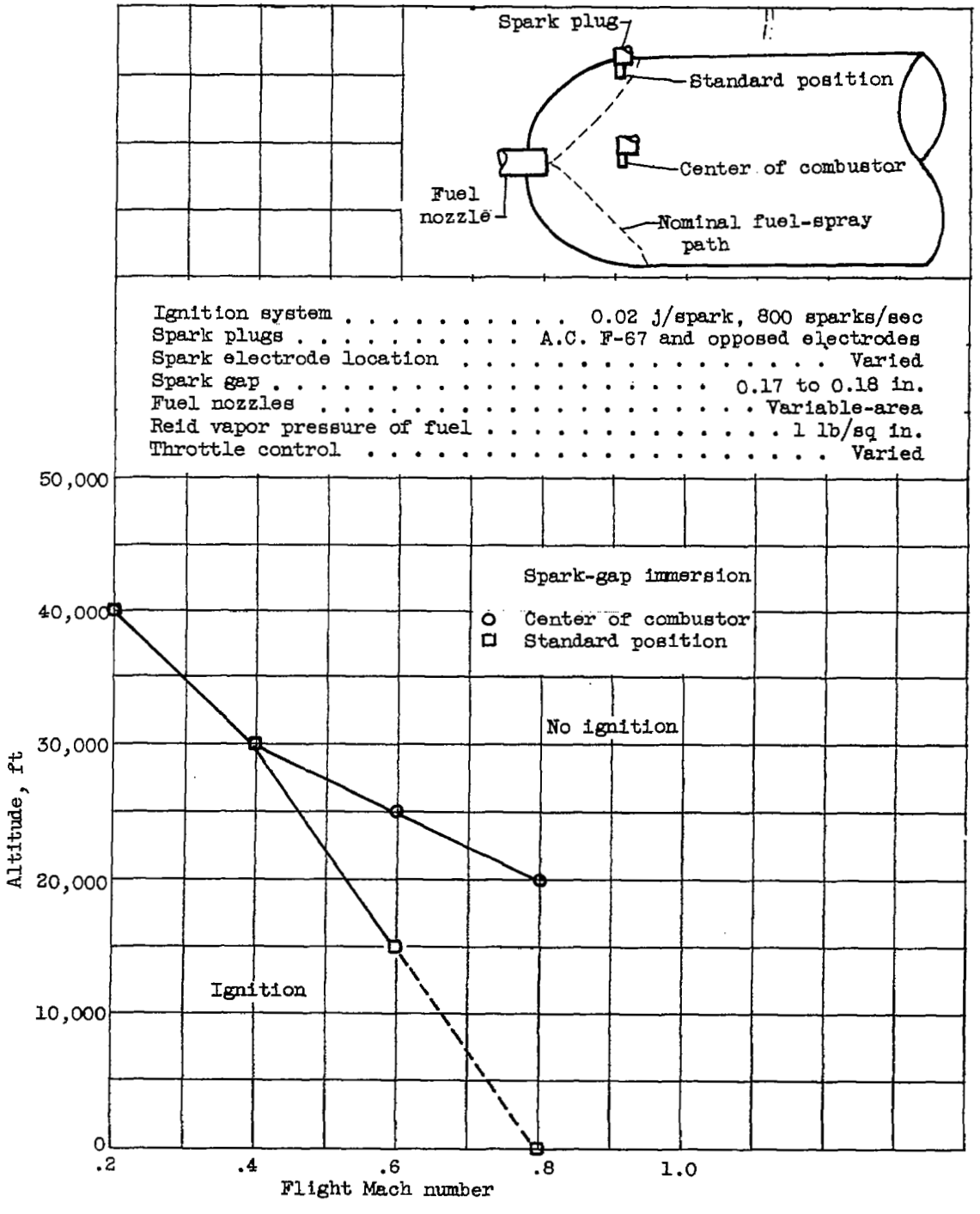

Figure 38. - Effect of spark-gap immersion on altitude ignition limits of turbojet engine (ref. 5).

[redacted]

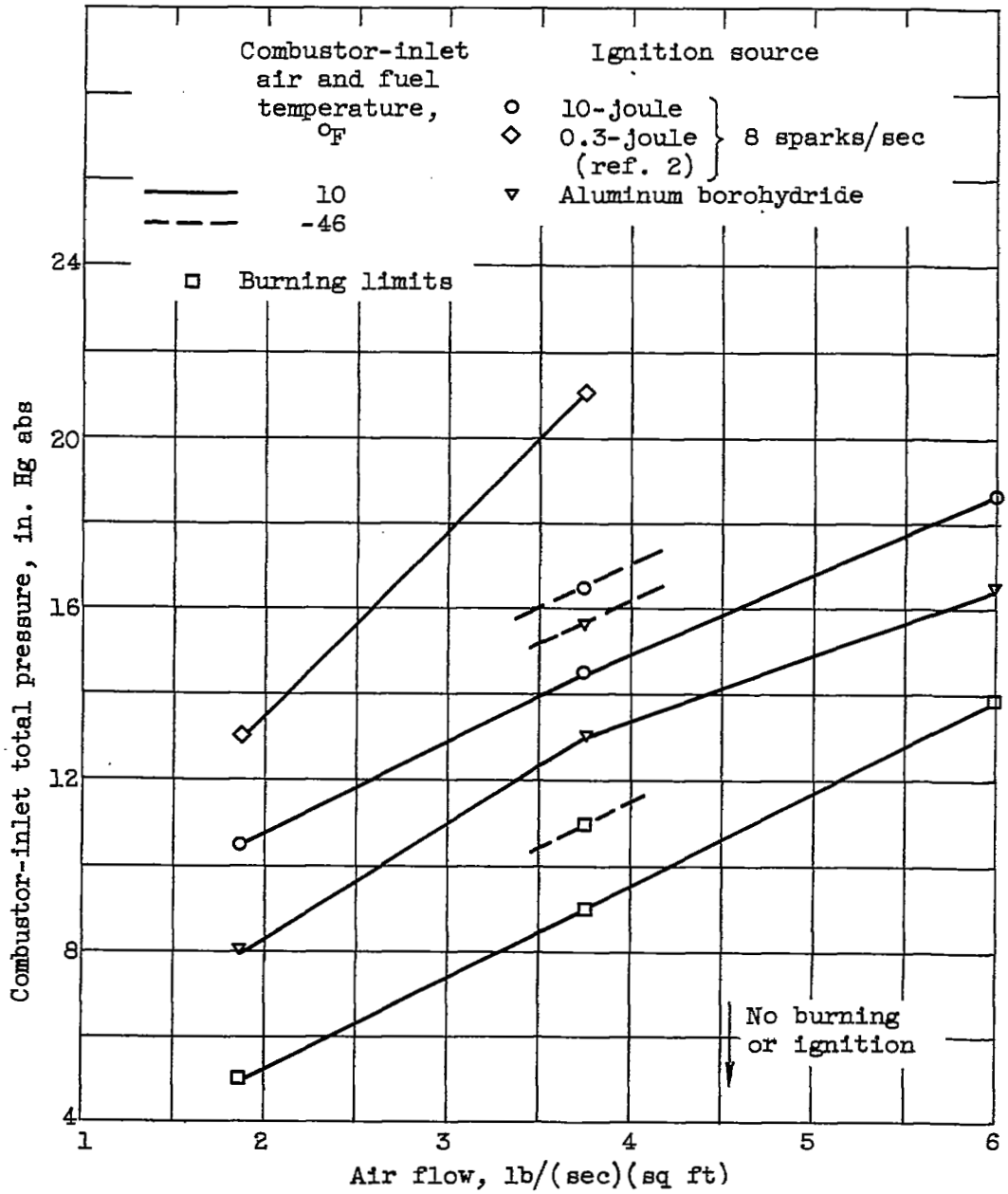

Figure 39. - Comparison of burning limits with ignition limits obtained with electric spark and with aluminum borohydride as sources of ignition in J33 single combustor. NACA fuel 50-197; Reid vapor pressure of fuel, 1 pound per square inch; 10.5-gallon-per-hour, fixed-area fuel nozzle; spray-cone angle, 80° (ref. 3).

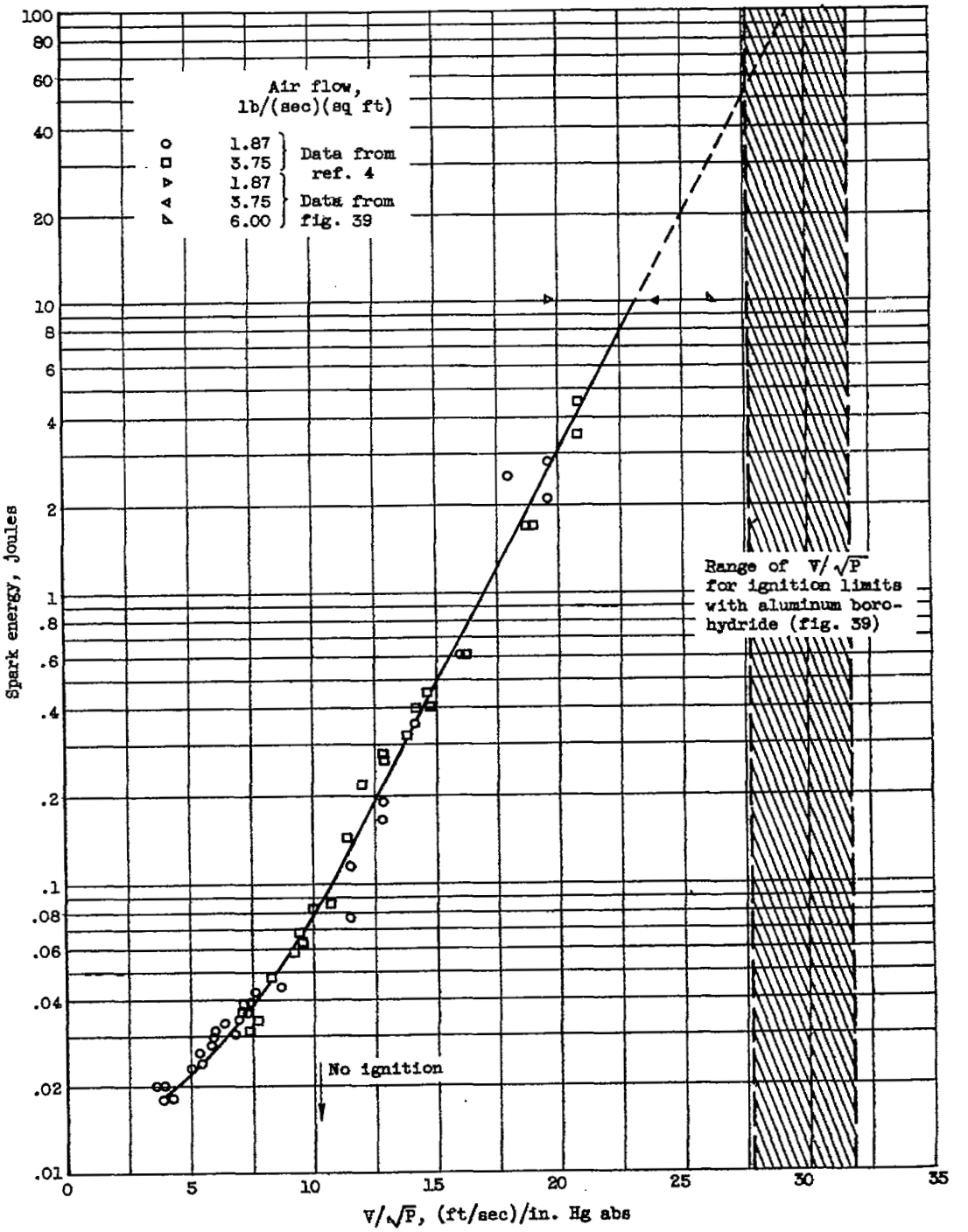

Figure 40. - Minimum spark energy required for ignition as a function of combustor-inlet air pressure and velocity. Combustor-inlet air and fuel temperature, 10° F; NACA fuel 50-197 (ref. 3).

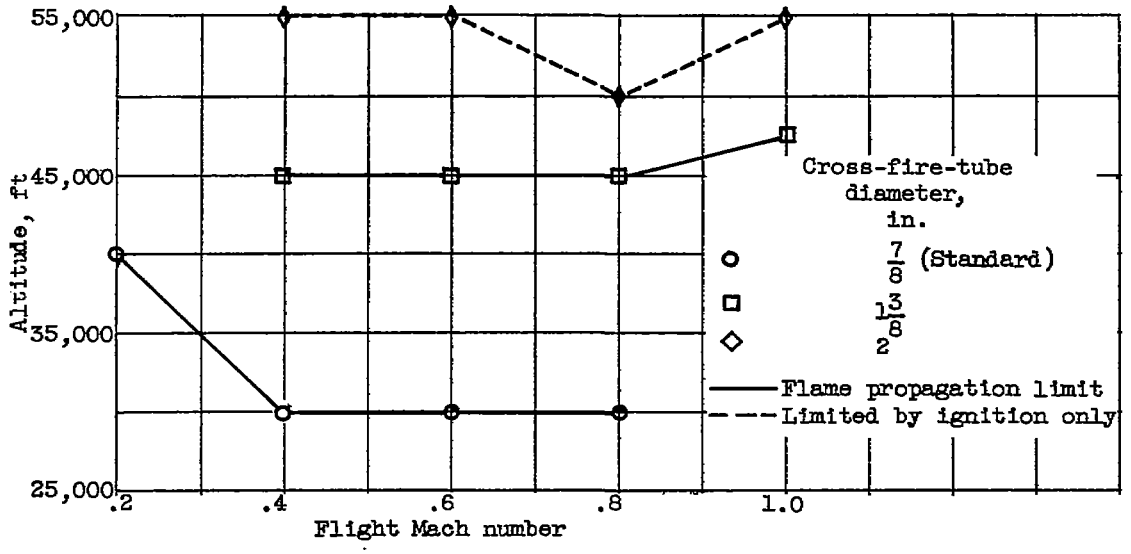

Figure 41. - Effect of cross-fire-tube diameter on flame propagation limits of turbojet engine with variable-area fuel nozzles and standard cross-fire-tube location (ref. 5).

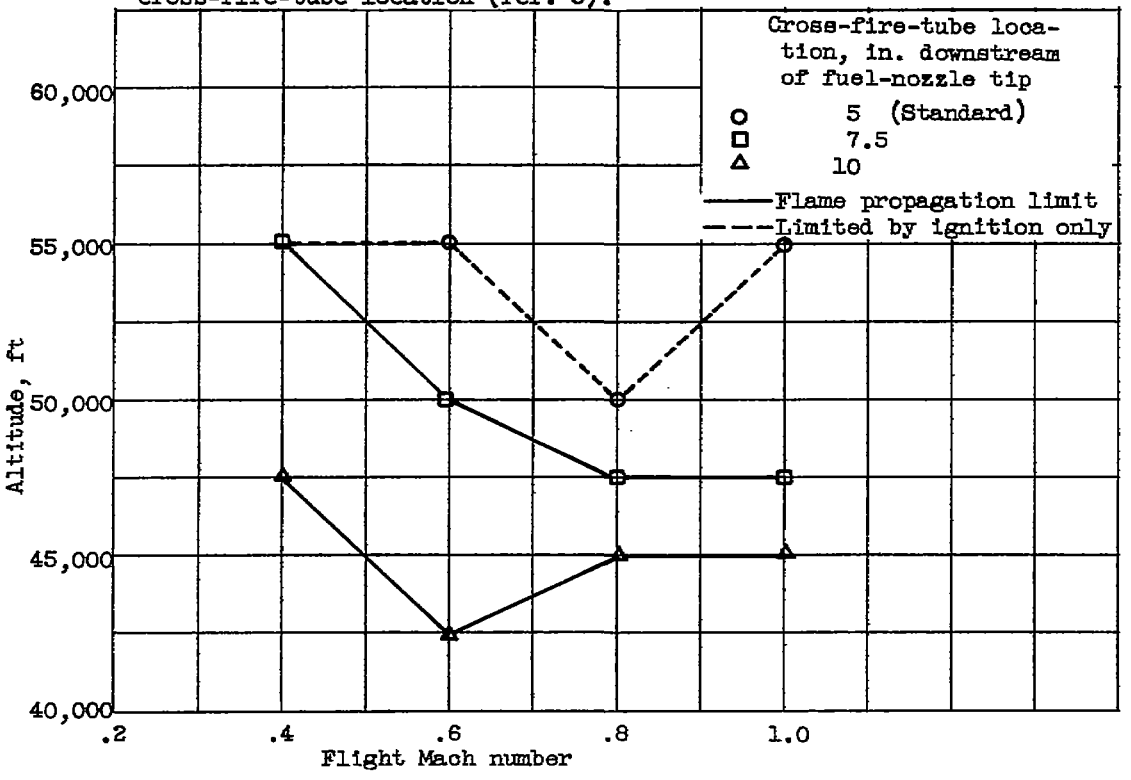

Figure 42. - Effect of cross-fire-tube location on flame propagation limits of turbojet engine with 2-inch-diameter cross-fire tubes and variable-area fuel nozzles (ref. 5).

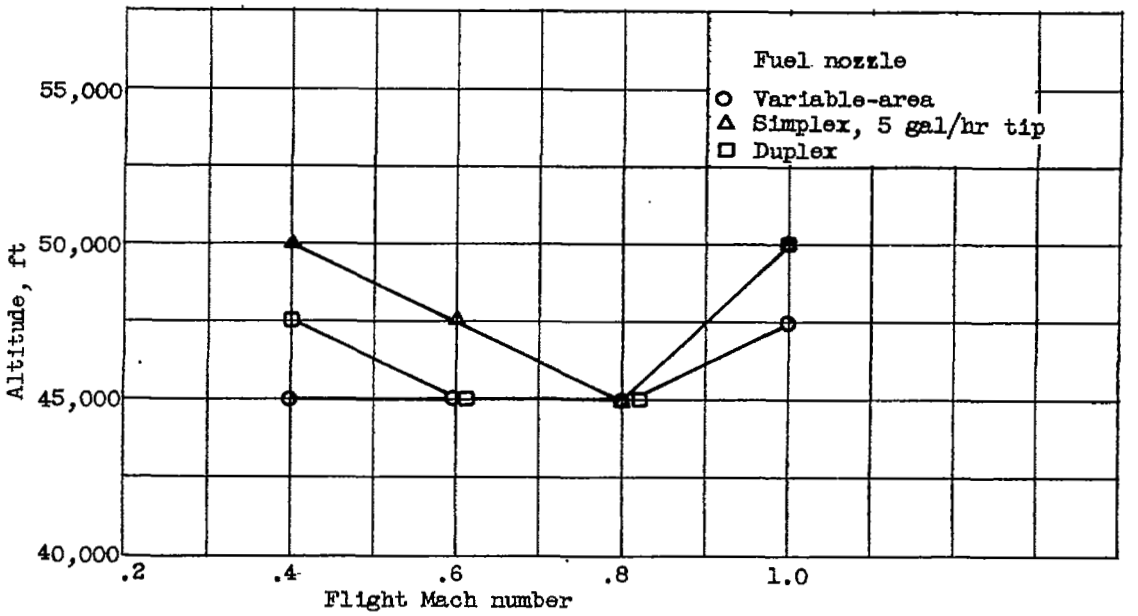

Figure 43. - Effect of three types of fuel nozzle on flame propagation limits of turbojet engine with $1\frac{3}{8}$-inch-diameter cross-fire tubes in standard location (ref. 5).

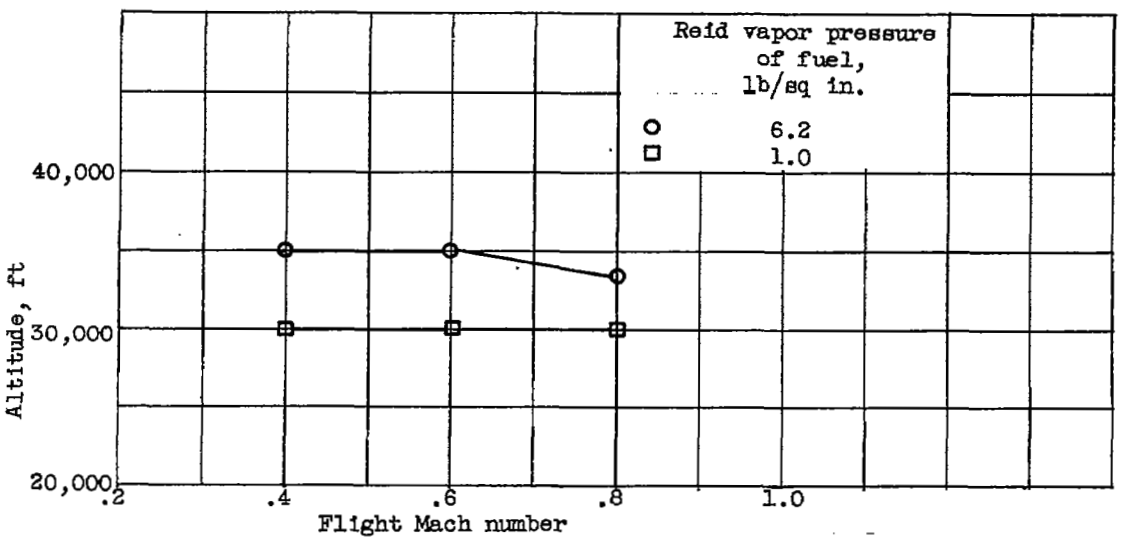

Figure 44. - Effect of fuel volatility on flame propagation limits of turbojet engine. Cross-fire-tube diameter, 7/8 inch; standard engine location; variable-area fuel nozzle (ref. 5).

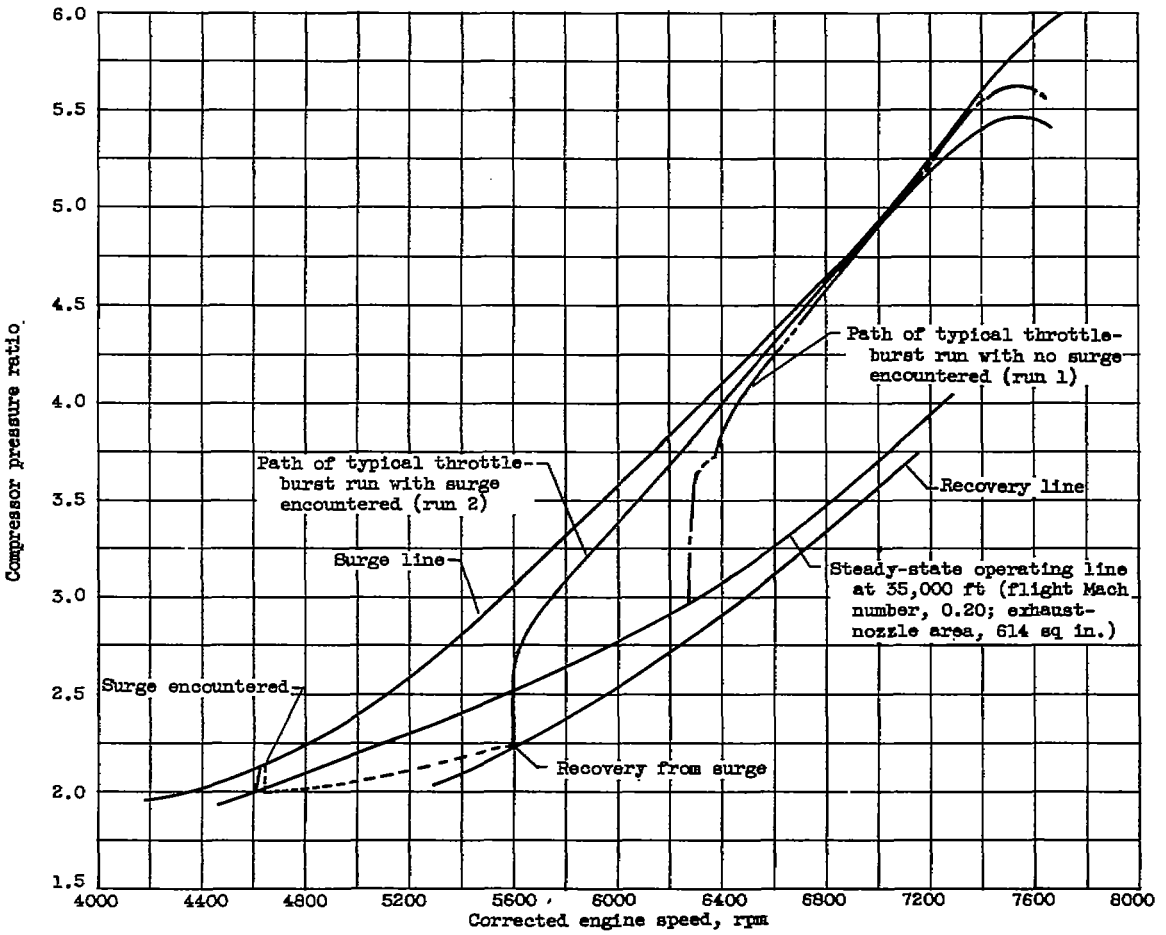

Figure 45. - Relation of compressor steady-state operating line to surge and recovery limits (ref. 6).

[redacted]

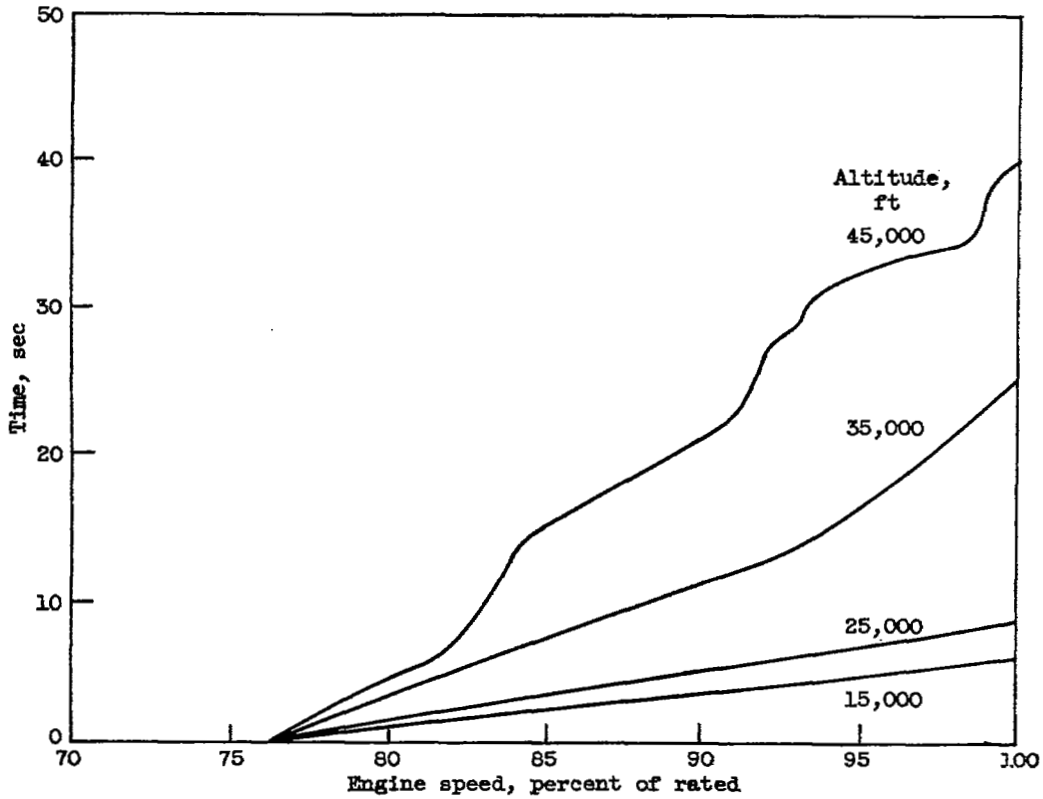

Figure 46. - Typical altitude acceleration in J47 engine. Grade JP-1 fuel.

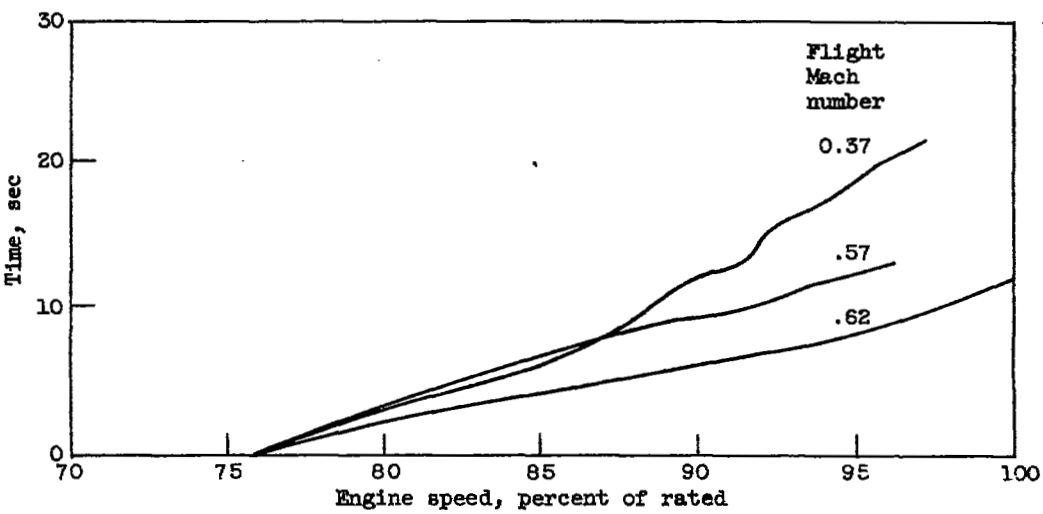

Figure 47. - Effect of flight Mach number on acceleration in J47 engine. Altitude, 40,000 feet; grade JP-1 fuel.

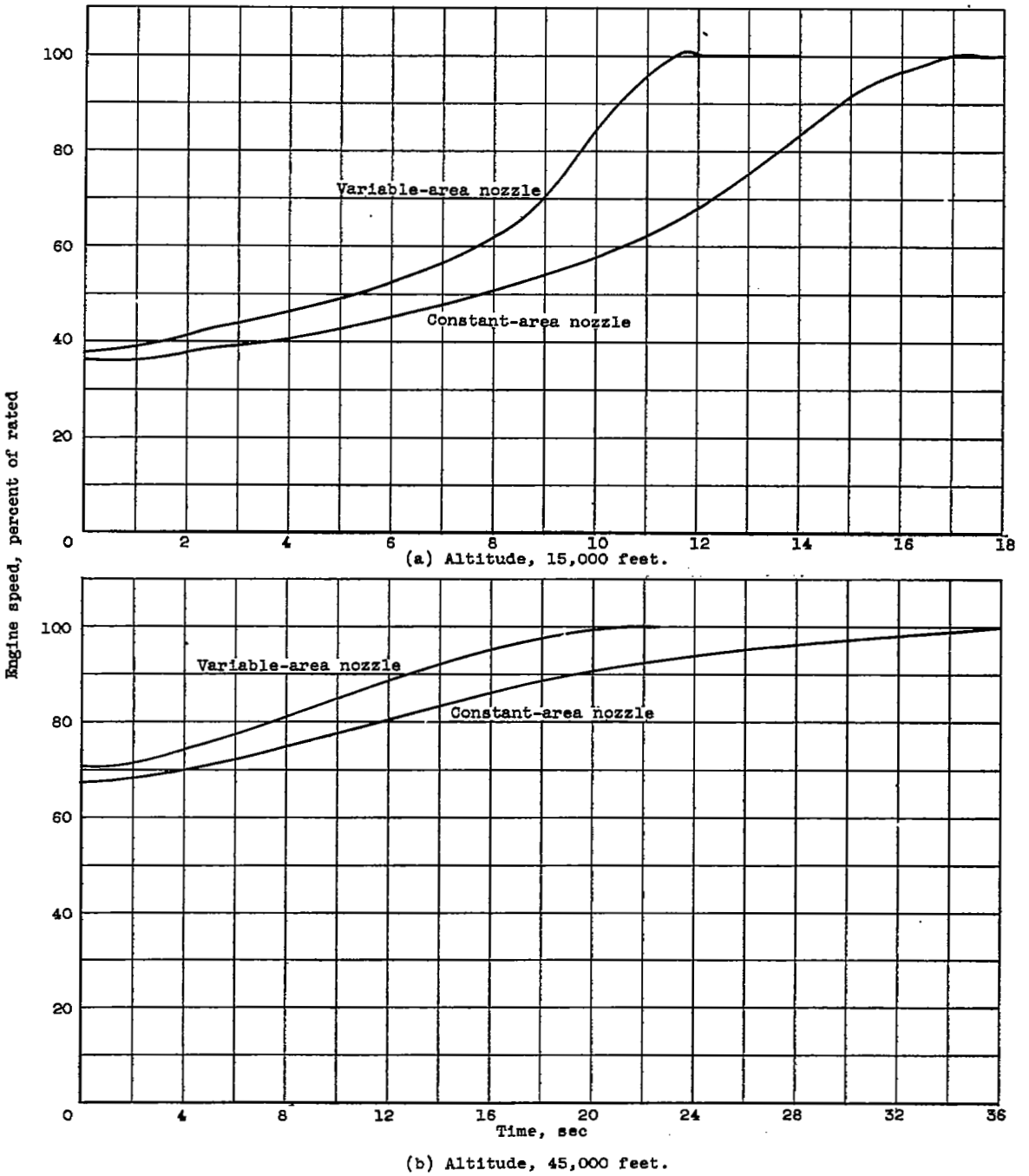

Figure 48. - Comparison of acceleration times with variable-area nozzle and constant-area nozzle for thrust-selector bursts from 10 to 90 degrees. Flight Mach number, 0.19 (ref. 24).

[redacted]

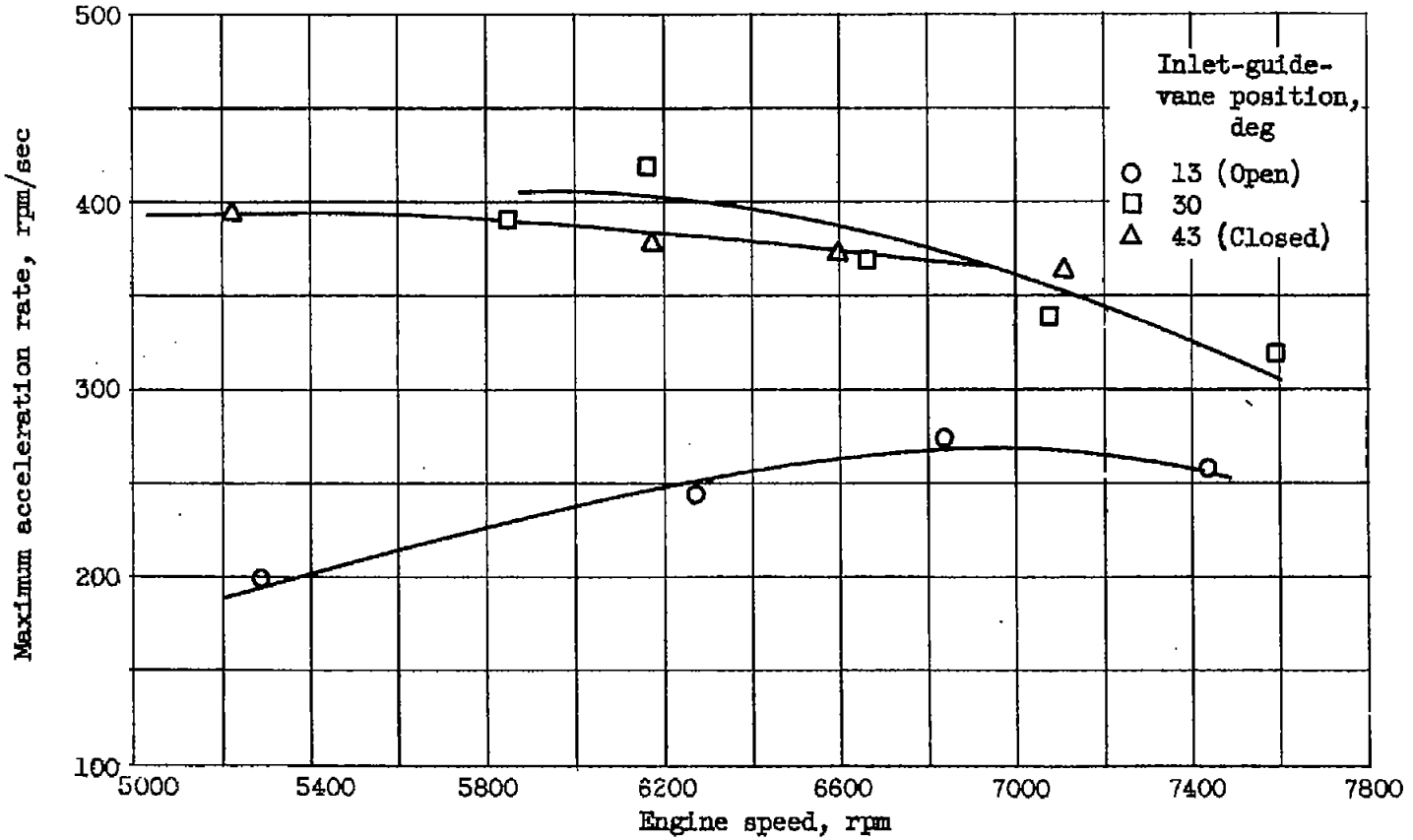

Figure 49. - Effect of inlet-guide-vane position on maximum acceleration. (Surge limited fuel steps.) Altitude, 35,000 ft; flight Mach number, 0.8 (ref. 23).

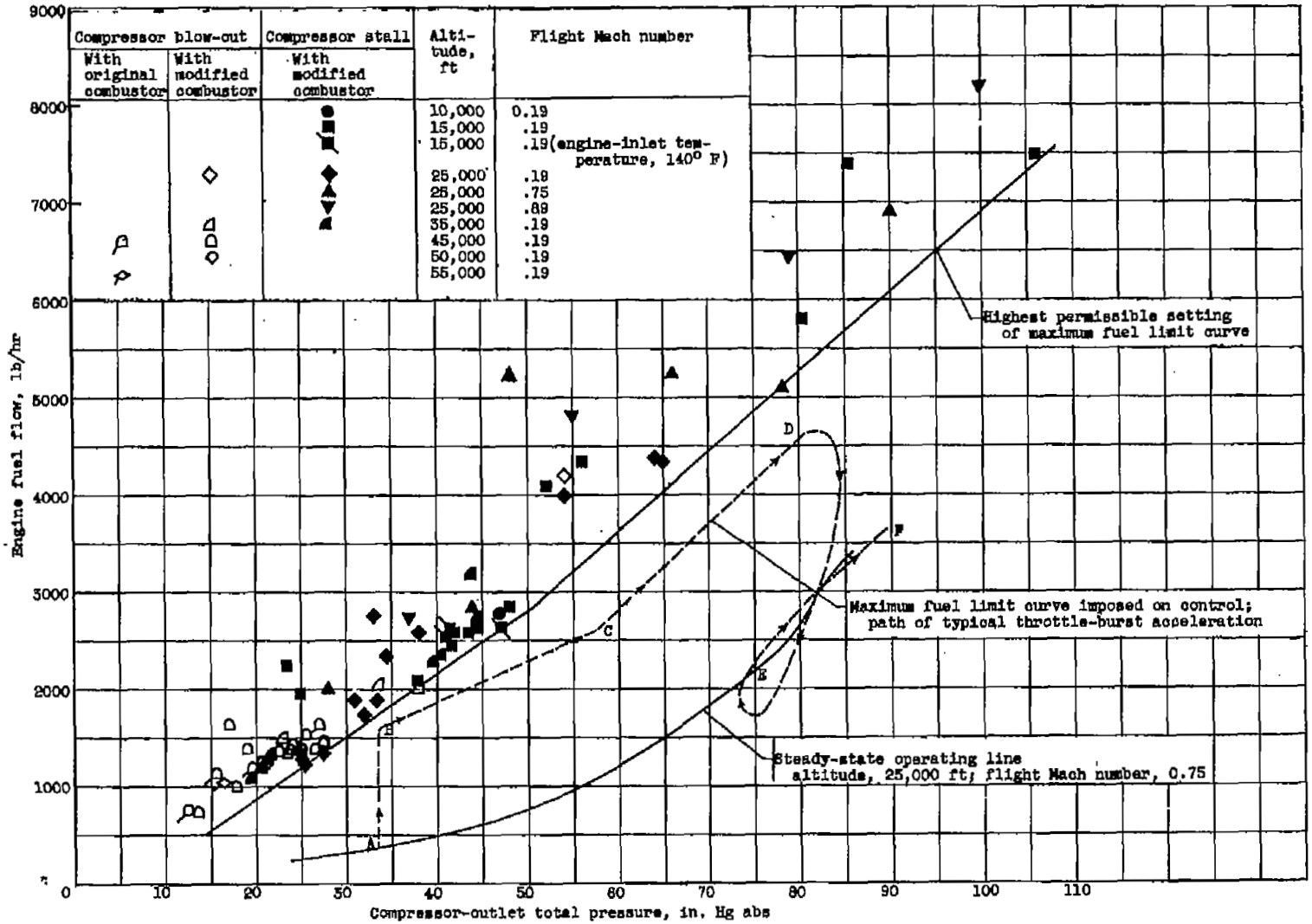

Figure 50. - Correlation of compressor stall and combustor blow-out with engine fuel flow and compressor-outlet pressure (ref. 24).

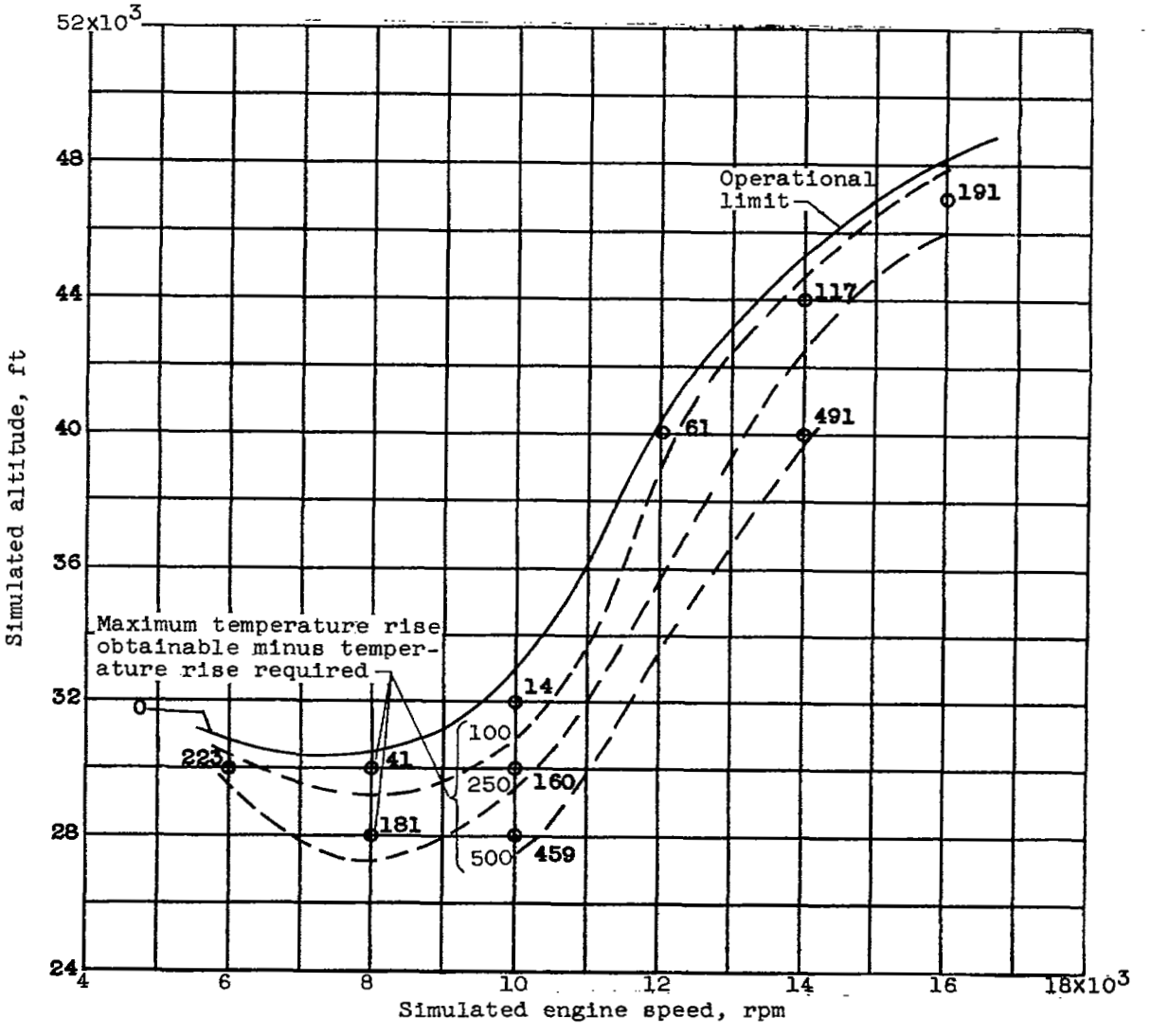

Figure 51. - Available acceleration of 19XB-1 turbojet engine as indicated by difference between maximum temperature rise obtainable in investigation of combustor and temperature rise required for nonaccelerating engine operation.

(a) Compensated outlet temperature.

(b) Fuel flow.

(c) Average uncompensated outlet temperature.

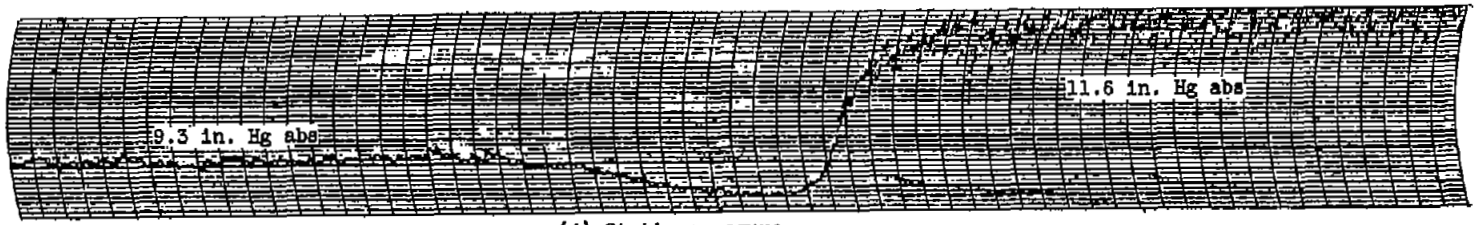

(d) Static pressure.

Figure 52. - Typical oscillograph trace of combustor variables during successful fuel acceleration. Chart speed, 5 divisions per second. Altitude, 50,000 feet; rated rotor speed, 70 percent (ref. 31).

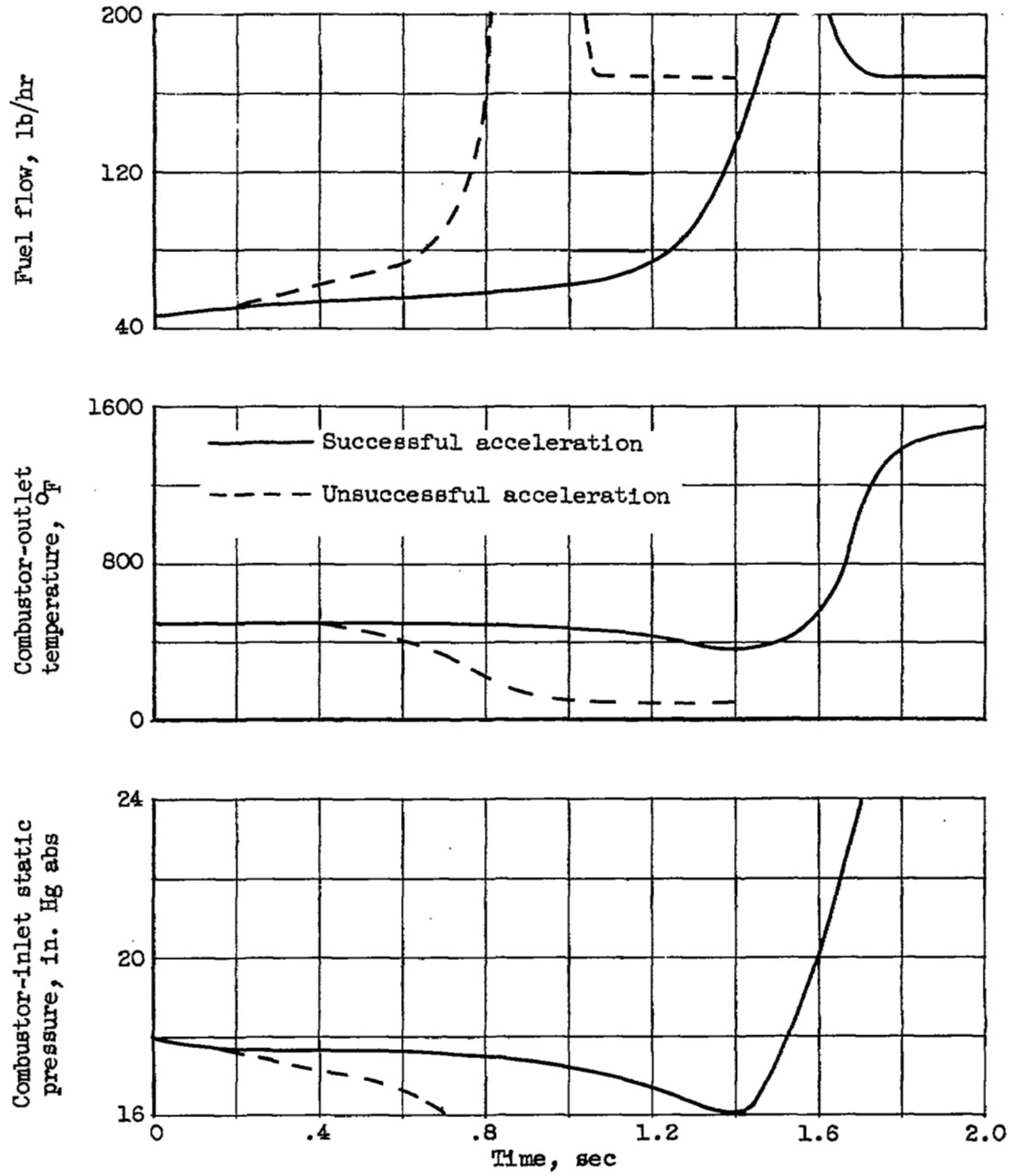

(a) Dual-entry duplex nozzle.

Figure 53. - Comparison of combustor-outlet temperature and combustor-inlet static-pressure responses to fuel acceleration with four fuel nozzles. Simulated altitude, 35,000 feet; rotor speed, 58 percent of rated; J47 combustor (data from ref. 33).

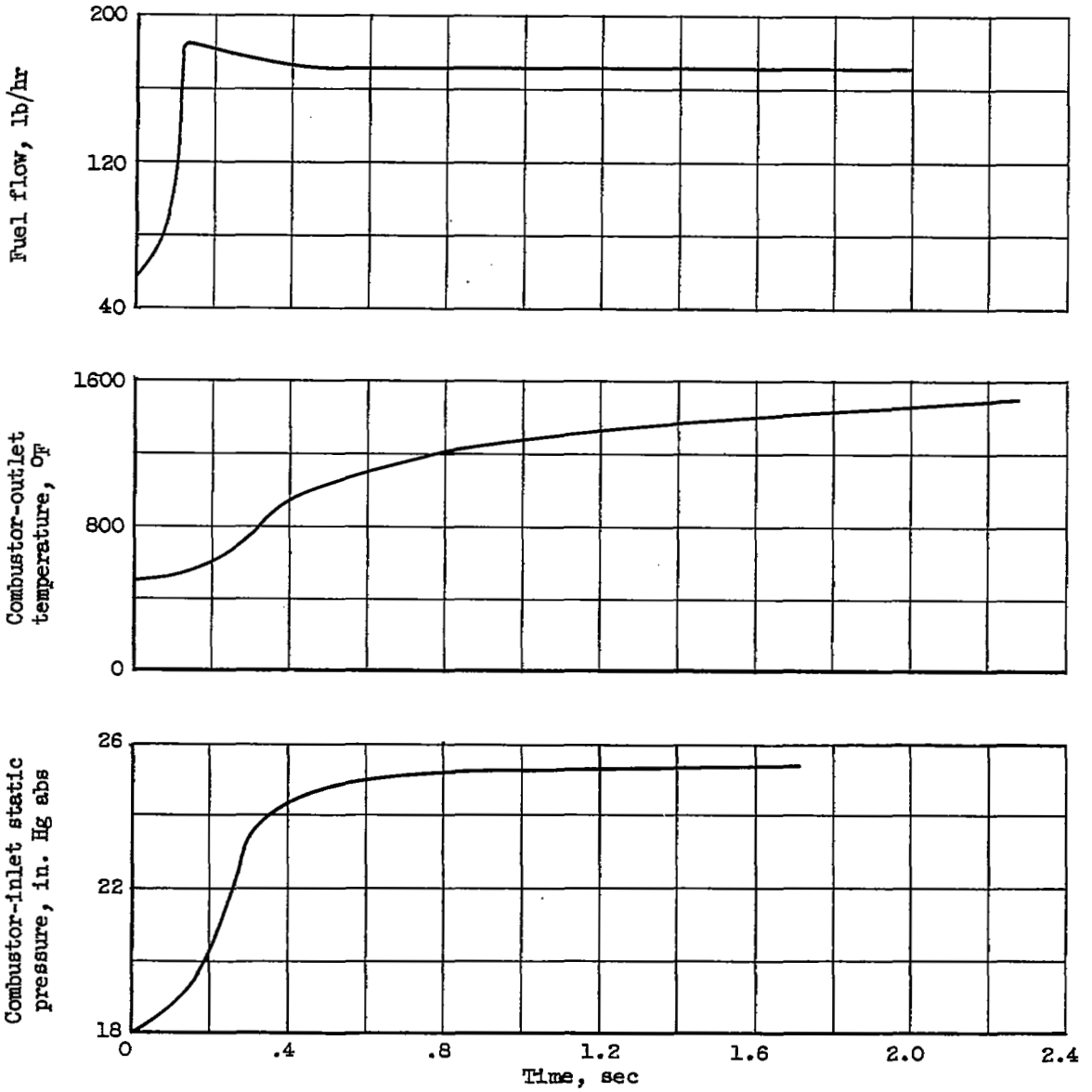

(b) Single-entry duplex nozzle.

Figure 53. - Continued. Comparison of combustor-outlet temperature and combustor-inlet static-pressure responses to fuel acceleration with four fuel nozzles. Simulated altitude, 35,000 feet; rotor speed, 58 percent of rated; J47 combustor (data from ref. 33).

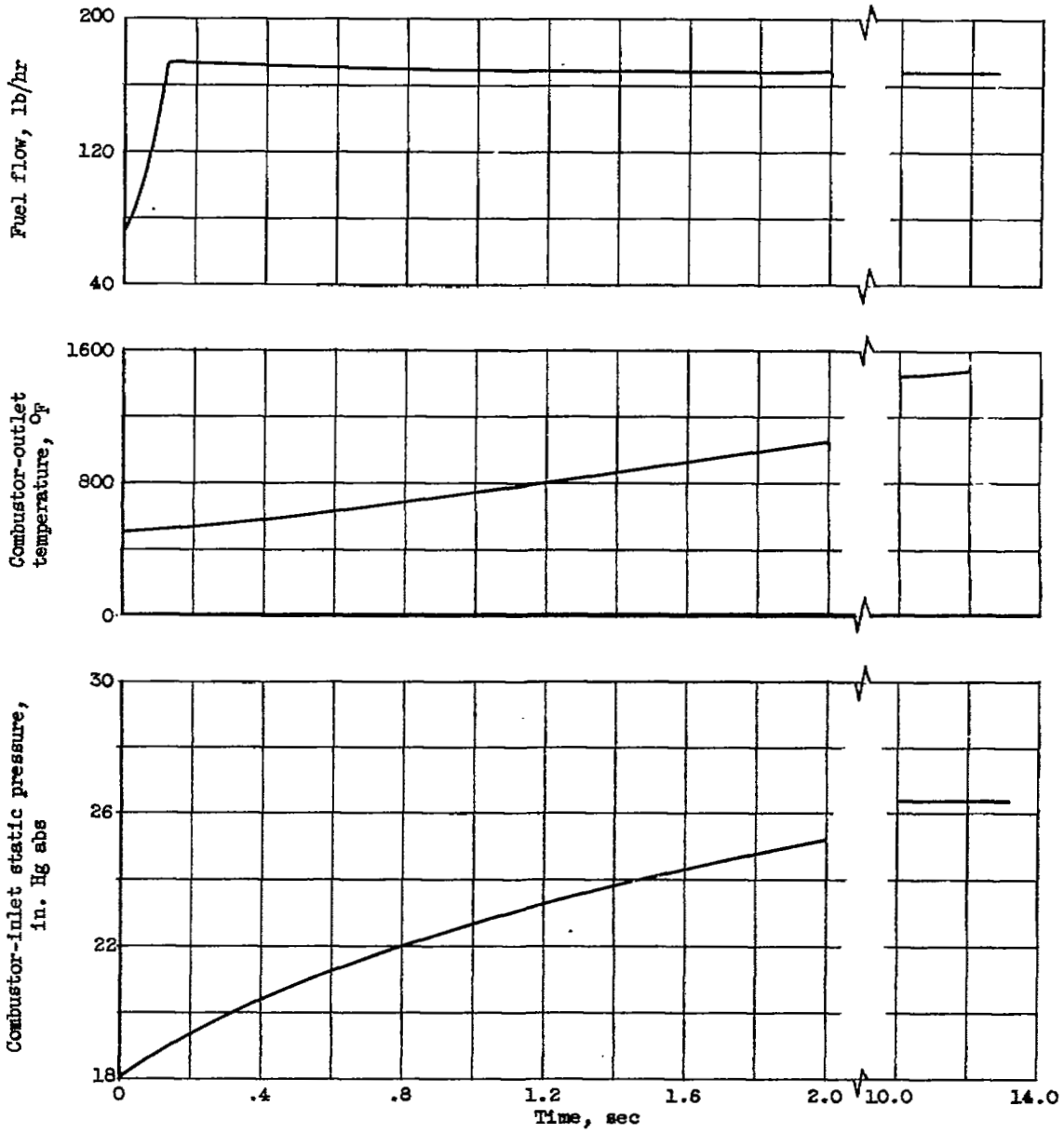

(c) 60.0-Gallon-per-hour simplex nozzle.

Figure 53. - Continued. Comparison of combustor-outlet temperature and combustor-inlet static-pressure responses to fuel acceleration with four fuel nozzles. Simulated altitude, 35,000 feet; rotor speed, 58 percent of rated; J47 combustor (data from ref. 33).

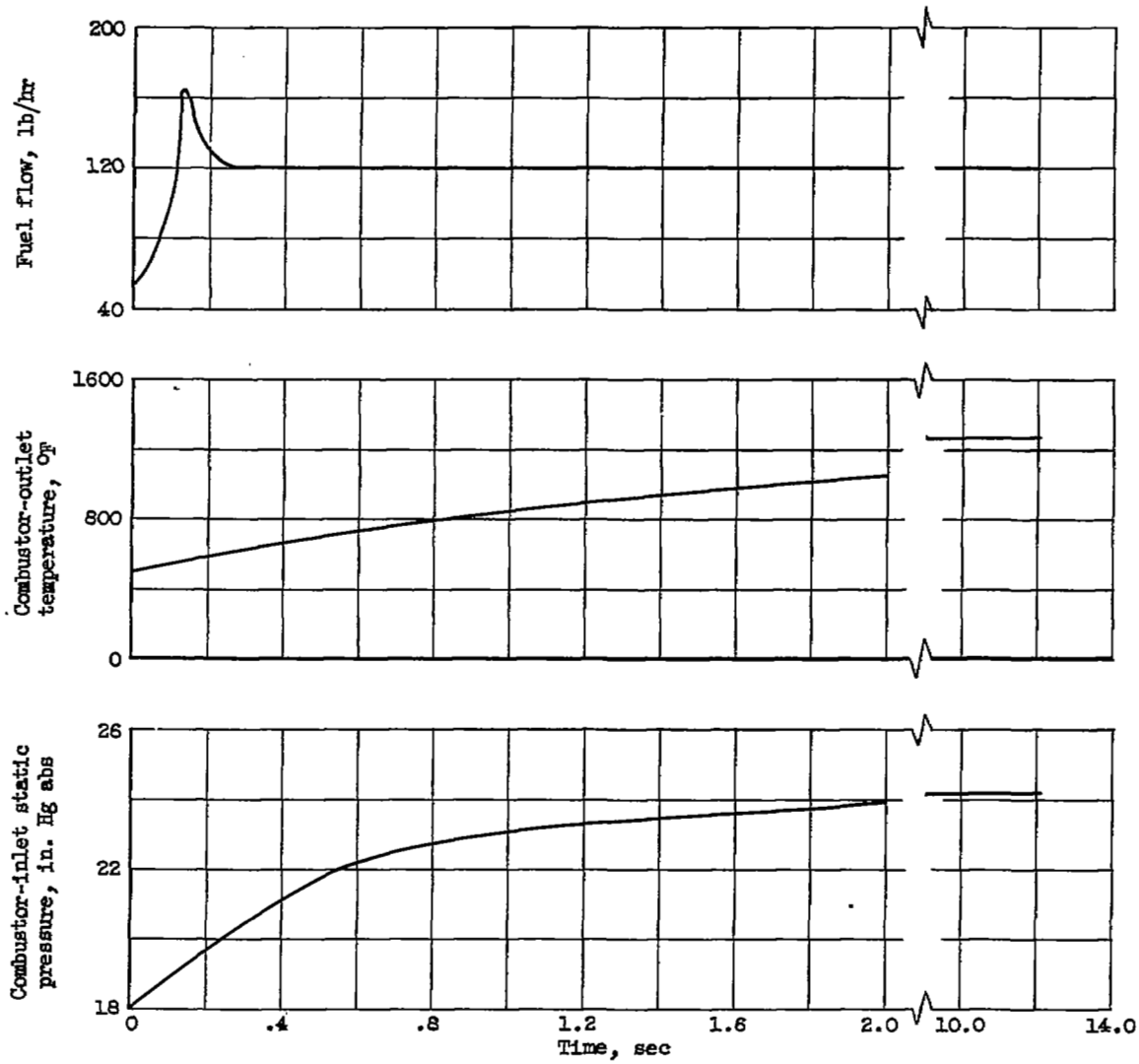

(d) 15.3-Gallon-per-hour simplex nozzle.

Figure 53. - Concluded. Comparison of combustor-outlet temperature and combustor-inlet static-pressure responses to fuel acceleration with four fuel nozzles. Simulated altitude, 35,000 feet; rotor speed, 58 percent of rated; J47 combustor (data from ref. 33).

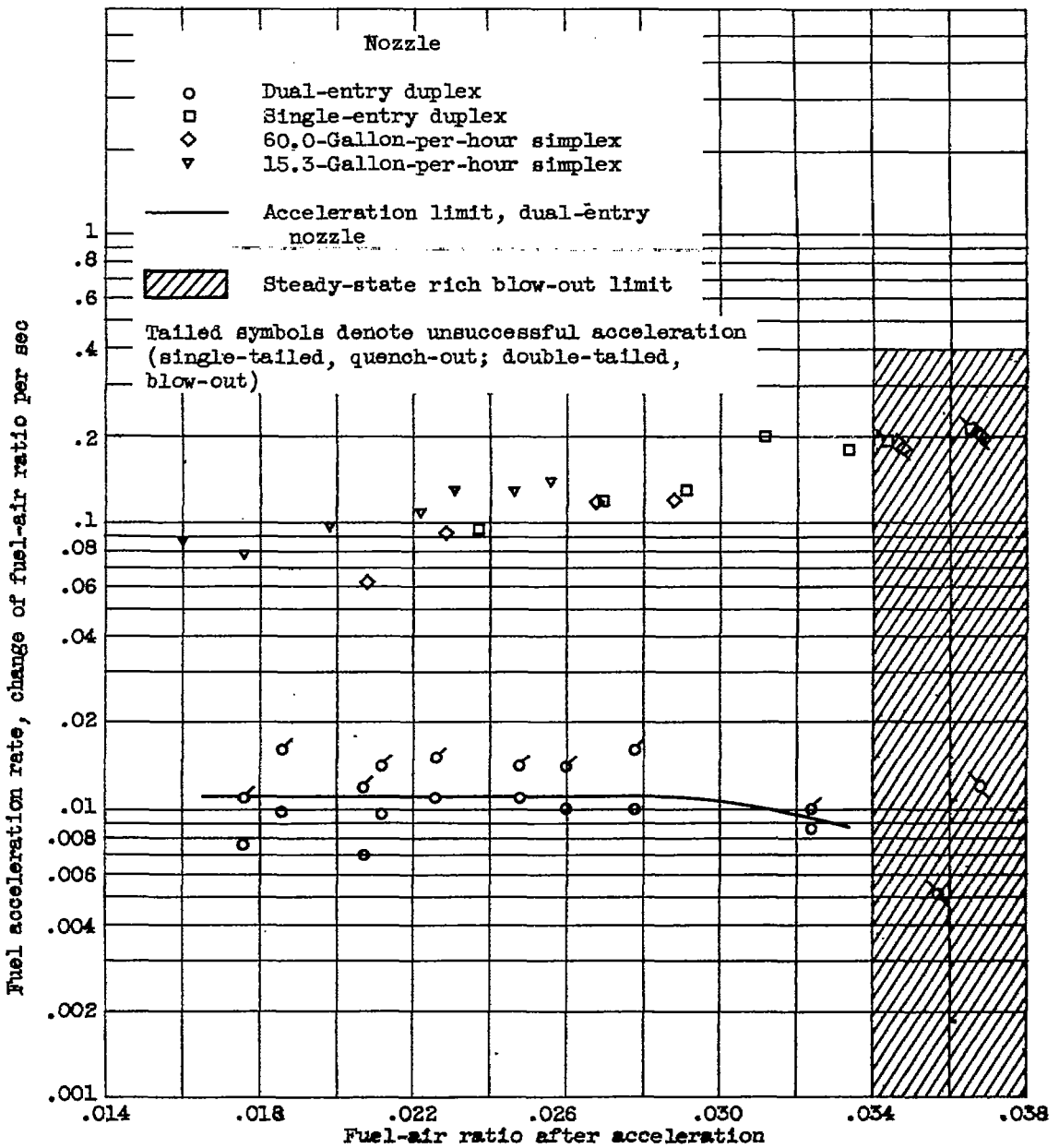

Figure 54. - Combustor fuel acceleration data obtained with four nozzles. Simulated altitude, 45,000 feet; rotor speed, 58 percent of rated; J47 combustor (ref. 33).

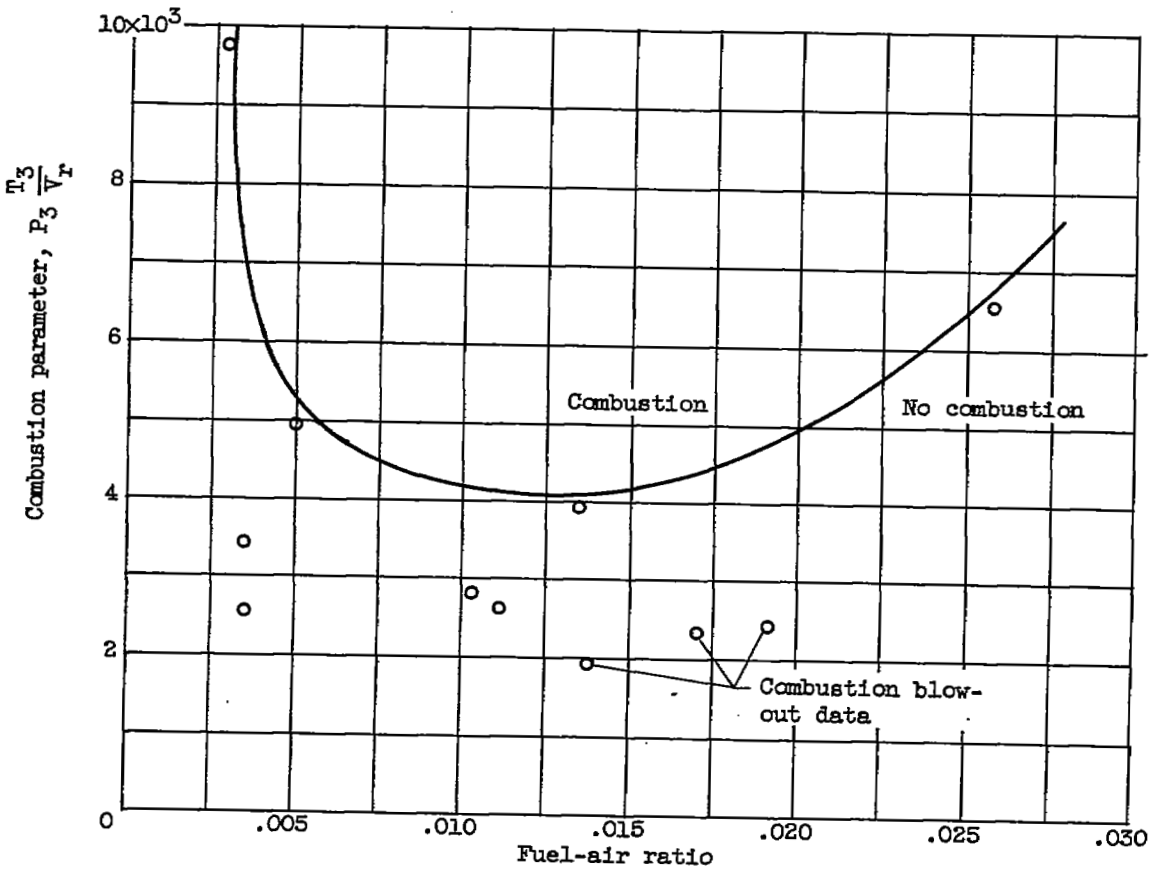

Figure 55. - Experimental combustion blow-out data with J47 tubular combustor (data from ref. 35).

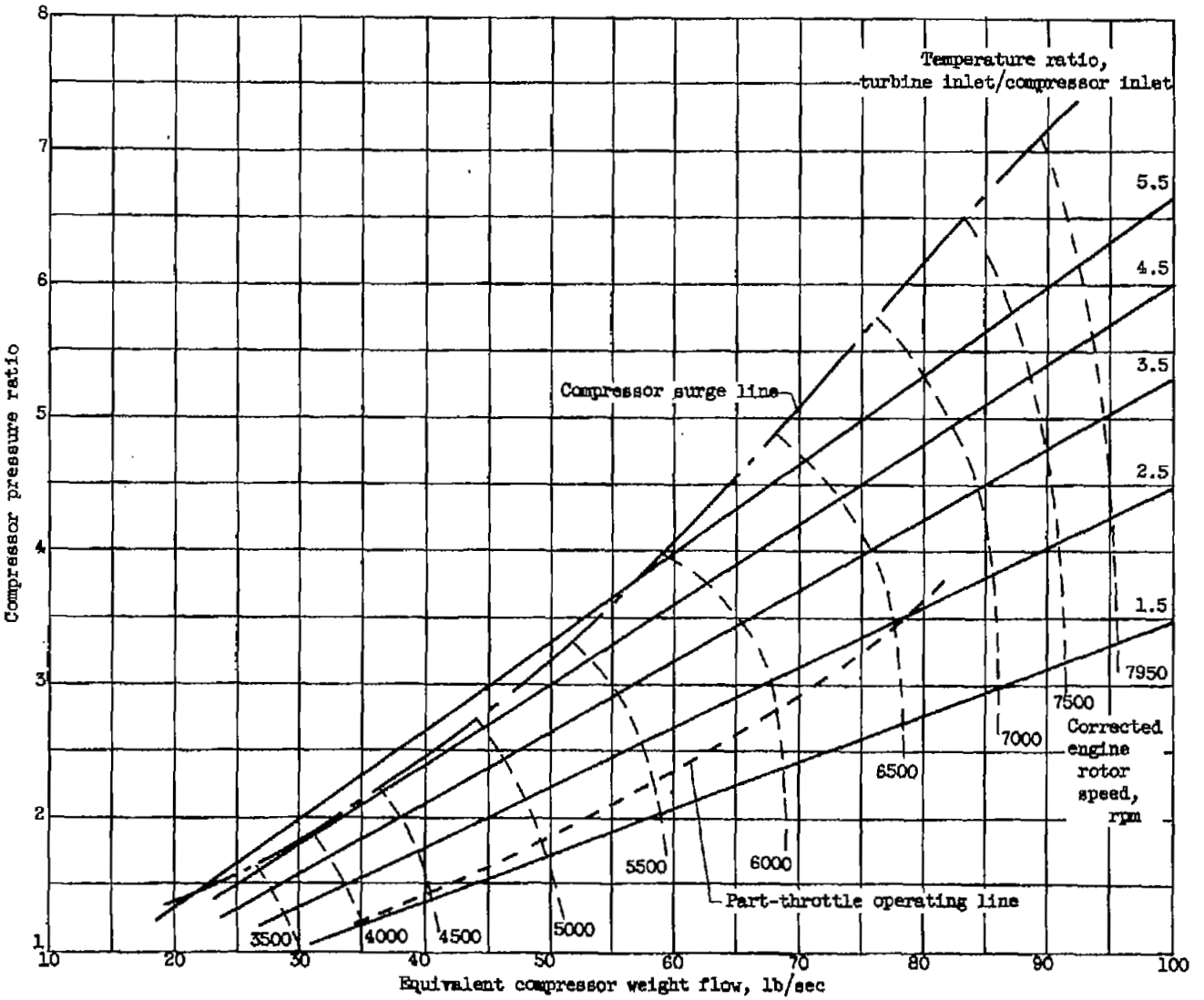

Figure 56. - Compressor performance characteristics for early J47 turbojet engine. Part-throttle operating line for Mach number of 0.6 in stratosphere.

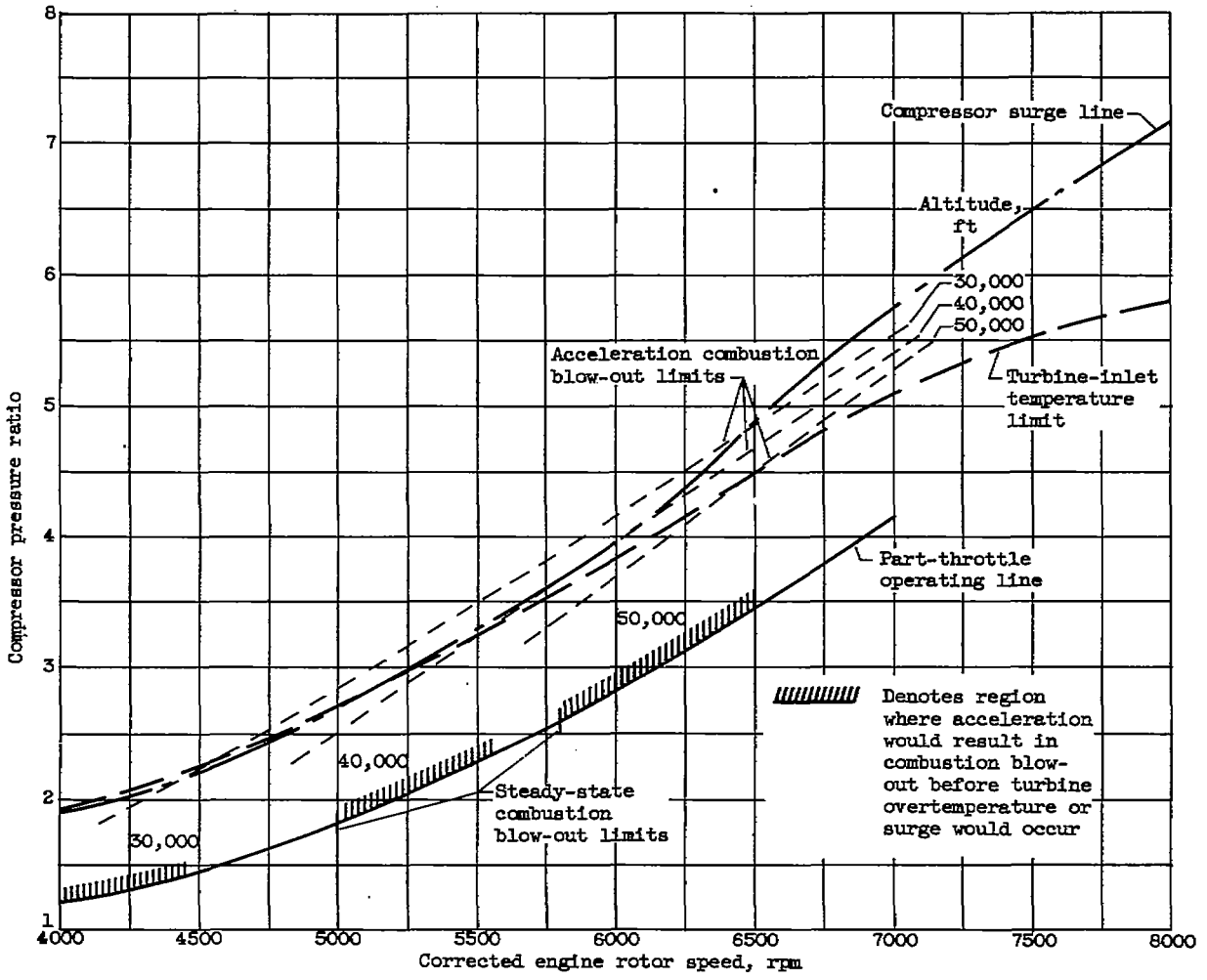

Figure 57. - Comparison of combustor acceleration blow-out limits with compressor surge and turbine temperature limits for early J47 turbojet engine. Mach number, 0.6; combustion efficiency range assumed, 75 to 95 percent.

CHAPTER XII

COMBUSTION LIMITS AND EFFICIENCY OF TURBOJET ENGINES

By Edmund R. Jonash and Henry C. Barnett

INTRODUCTION

Combustion must be maintained in the turbojet-engine combustor over a wide range of operating conditions resulting from variations in required engine thrust, flight altitude, and flight speed. Furthermore, combustion must be efficient in order to provide the maximum aircraft range. Thus, two major performance criteria of the turbojet-engine combustor are (1) operatable range, or combustion limits, and (2) combustion efficiency.

Several fundamental requirements for efficient, high-speed combustion are evident from the discussions presented in chapters III to V. The fuel-air ratio and pressure in the burning zone must lie within specific limits of flammability (fig. III-16(b)) in order to have the mixture ignite and burn satisfactorily. Increases in mixture temperature will favor the flammability characteristics (ch. III). A second requirement in maintaining a stable flame is that low local flow velocities exist in the combustion zone (ch. VI). Finally, even with these requirements satisfied, a flame needs a certain minimum space in which to release a desired amount of heat, the necessary space increasing with a decrease in pressure (ref. 1). It is apparent, then, that combustor design and operation must provide for (1) proper control of vapor fuel-air ratios in the combustion zone at or near stoichiometric, (2) mixture pressures above the minimum flammability pressures, (3) low flow velocities in the combustion zone, and (4) adequate space for the flame.

It is desirable to consider how the operation and the design of current turbojet combustors match these fundamental combustion requirements. Because of turbine-blade temperature limitations, over-all fuel-air ratios considerably leaner than stoichiometric must be maintained in the turbojet combustor; because of the high propulsive thrust per unit frontal area required, combustion-chamber velocities of 100 feet per second or greater must be tolerated; and because of availability and handling considerations, liquid hydrocarbon fuels that require vaporization and mixing with the air prior to combustion must be used. Combustor design alleviates the first two problems, velocity and fuel-air ratio, by allowing approximately 80 percent of the air to bypass the combustion zone, thus providing for lower velocities and higher fuel-air ratios within the combustion zone. In addition, considerable turbulence, which increases the flame surface area and hence the effective flame velocity (ch. V), is generated in the combustion zone by means of swirling-air entry ports and penetrating air jets. Heating the fuel-air mixture to its ignition temperature is aided by recirculating high-temperature exhaust gases into the fresh charge. Vaporization of the liquid fuel is aided by pressure atomizing nozzles or by any of a number of fuel prevaporization methods that are currently being used.

The design of current turbojet combustors has not completely satisfied the fundamental requirements for complete combustion at all conditions of operation. Moreover, attempts to answer the ever-pressing need for greater heat-release rates from smaller combustors in shorter lengths and over wider ranges of operating conditions result in incomplete combustion or flame blow-out under certain conditions. Performance trends typical of those observed in current turbojet engines are shown in figure 58. Combustion efficiency is plotted against the engine speed corrected to standard sea-level conditions $N/\sqrt{\theta}$, where N is the engine rotational speed and θ is the ratio of engine-inlet total temperature to NACA standard sea-level

static temperature. Since the value of $\sqrt{\theta}$ does not vary greatly from unity for the range of conditions shown the abscissa scale is a close representation of the actual engine rotational speed. These data, which were obtained in full-scale engine tests at simulated altitude conditions (ref. 2), show that combustion efficiencies decrease with a decrease in engine rotational speed, with an increase in altitude, and with a decrease in flight Mach number. At high-altitude conditions, efficiencies as low as 50 percent were encountered, representing a very considerable loss in aircraft range.

The problem of combustion limits encountered in some engines at high altitude is illustrated in figure 59 (ref. 3). The curve represents an altitude operational limit imposed on the engine by the inability of the combustor to release sufficient heat to drive the engine at the required conditions. Altitude operation of the engine is severely limited, particularly at low engine speeds.

Two major tasks confronting designers of turbojet combustors are (1) optimizing the design for a particular engine and flight application and (2) predicting the flight performance of the design. The solutions to both problems require an understanding of the effects of the individual operating and design variables on performance. This chapter treats these variables in some detail. The effects of inlet-air conditions, fuel and air admission characteristics, and fundamental combustion characteristics on performance are considered. Although these variables have been recognized for some time, their interrelated effects on performance cannot yet be expressed quantitatively. As a result, combustor design remains, to a large extent, an art. Approximate methods that have been developed to relate effects of operating variables and to estimate the performance characteristics of a given combustor are described in this chapter.

EFFECT OF ENGINE OPERATING VARIABLES ON COMBUSTION EFFICIENCY AND LIMITS

Among the primary engine operating variables affecting combustion efficiency and stability are combustor inlet-air pressure, inlet-air temperature, inlet-air velocity, and fuel-air ratio. The degree to which these variables influence performance in different turbojet engines may vary, but the trends observed are reasonably uniform for most engines. From the large amount of data accumulated during the past several years, representative results are presented here to illustrate the effects of these variables on combustion efficiency and stability. This section is concerned only with performance data obtained with liquid fuels in atomizing-type annular and tubular combustors. Combustor performance characteristics with vaporized fuel are treated in a later section that considers the effects of fuel variables on engine performance.

Combustor Inlet-Air Pressure

The effect of combustor inlet-air pressure on combustion efficiency is shown in figure 60(a) for data obtained in two different combustors (refs. 3 and 4) at constant values of inlet-air temperature, reference velocity[1], and fuel-air ratio. These and other data show conclusively that decreases in combustor pressure cause significant decreases in efficiency. For different combustors the shape of the curves is reasonably consistent, but the pressure at which significant losses in efficiency occur will vary, as illustrated by the two curves in figure 60(a).

[1]Mean combustor air velocity based on density and flow rate of inlet air and maximum combustor cross section.

Also, with more or less favorable conditions of inlet temperature, reference velocity, and fuel-air ratio than those used for the data in the figure, the curves may be displaced to higher or lower values of combustion efficiency and to lower or higher values of pressure. The decrease in efficiency with decreased pressure may be attributed to any of several fundamental factors involved. For example, the volume required for the flame increases (ref. 1) and the flammability mixture limits decrease as pressure is reduced (ch. III). These and other factors are discussed further in a later section of this chapter.

Studies reported in chapter III and cited earlier in this chapter show the existence of pressure flammability limits that define pressures below which combustion cannot be sustained. In turbojet combustors, a decrease in combustor pressure causes decreases in efficiency, as shown in figure 60(a); as lower and lower pressures are imposed, the combustion process passes through a phase of instability, and eventually the flame is completely extinguished. Although the particular range of operating conditions represented by the curves of figure 60(a) did not result in flame blow-out, it can be assumed that blow-out would occur at pressures not far below the lower limits of the curves shown. In any case, the lower pressure limit of a turbojet combustor always occurs at a pressure considerably higher than the flammability pressure limits (about 1.0 lb/sq in. abs) presented in figure III-16. This fact may be attributed to the very great difference between the static, homogeneous fuel-air-mixture conditions represented by the data of figure III-16 and the dynamic, heterogeneous situation existing in a turbojet combustor.

Combustor Inlet-Air Temperature

In general, the effect of a decrease in combustor-inlet temperature on combustion efficiency is similar to the effect of a decrease in pressure. Representative trends are illustrated in figure 60(b) for the same combustors used to obtain the data of figure 60(a). These data, which were obtained at constant values of inlet-air pressure, velocity, and fuel-air ratio, show that combustion efficiency decreases at an increasing rate as the inlet temperature is decreased, particularly in combustor A.

The effect of combustor inlet-air temperature on combustion efficiency is in part associated with the problem of evaporating the fuel in the combustion chamber. Chapter I shows that the rate of evaporation of a liquid fuel spray increases with approximately the fourth power of the air temperature (fig. I-22). In addition, increased temperature favors fundamental combustion reactions, as evidenced by increased flame speed (ch. IV).

Combustor Inlet-Air Velocity

Typical variations of combustion efficiency with reference velocity are illustrated by the data in figure 60(c), which were obtained at constant values of inlet-air pressure, temperature, and fuel-air ratio. Combustion efficiency decreases rapidly with an increase in velocity in combustor A; increases in velocity beyond about 105 feet per second would probably result in flame blow-out. In the range of velocities investigated, combustion efficiency of combustor B was less sensitive to variations in velocity than was that of combustor A. For combustor B, increases in velocity first increased and then decreased combustion efficiency. The decreased combustion efficiency encountered at low velocities in combustor B occurs in many combustors and is attributed, in many cases, to impaired fuel-spray characteristics obtained with some fuel-injection nozzles at the low fuel flows attending low air velocities. Generally, this phenomenon is encountered at "off-design" conditions

only, that is, at velocities considerably below those encountered in actual engine operation. The decrease in combustion efficiency at high velocity encountered with combustors A and B may be associated with the decrease in residence time of the fuel-air mixture in the combustion zone. However, other factors can be involved; for example, variations of the fuel-air mixing characteristics with velocity.

The effect of velocity on combustion efficiency may be assumed to be generally represented by the curve of combustor B. Thus, there is an optimum value of velocity for all combustors. The normal operating ranges of different combustors may, however, be limited to different parts of this general curve, depending upon combustor design and other operating parameters.

Fuel-Air Ratio

The effects of fuel-air ratio on combustion efficiencies obtained in combustors A and B are shown in figure 60(d). Each combustor was operated at conditions of constant combustor inlet-air pressure, temperature, and velocity. Combustion efficiency in combustor A first increased and then decreased with increased fuel-air ratio. Combustion efficiency in combustor B increased with fuel-air ratio throughout the range of fuel-air ratio investigated. The fuel-air-ratio curves of figure 60(d) eventually terminate in the "lean" and "rich" blow-out limits of the combustor. Additional examples of the effects of fuel-air ratio on combustion efficiency may be found in references 5 and 6.

The decrease in combustion efficiency at low fuel-air ratios (fig. 60(d)) is normally associated with insufficient fuel vaporization resulting from poor fuel atomization at low flow rates; thus, liquid fuel might be permitted to flow through the combustor without burning. Actual observation and sampling of exhaust gases from combustors has, in fact, indicated the presence of liquid fuel droplets. In addition, of course, low over-all fuel-air ratios may result in pockets of fuel-air mixtures in the primary zone that are too lean to burn. The decrease in efficiency at high fuel-air ratios is frequently associated with overenrichment of the combustion zone resulting from high fuel-flow rates and improved atomization and vaporization of the fuel. Depending on the combustor and, particularly, on injector design characteristics and operating conditions, combustion efficiency may be more or less sensitive to fuel-air ratio than the curves of figure 60(d) indicate. Furthermore, in operating a particular combustor in a particular engine, only certain parts of the more general curve (combustor A) may apply.

Analysis of Engine Performance Characteristics

It was noted in connection with figure 58 that combustion efficiency in a full-scale turbojet engine decreases with (1) an increase in altitude, (2) a decrease in engine speed, and (3) a decrease in flight Mach number. The variations in combustor-inlet parameters (pressure, temperature, and velocity) that occur with these changes in engine conditions are discussed in chapter X. Figures 3(a), 3(b), 6, and 7(a) indicate that both combustor inlet-air pressure and temperature always decrease with the variations in engine operating conditions noted previously that cause a decrease in combustion efficiency. These trends are consistent with the data presented in figures 60(a) and (b). Further examination of the data of figures 3(c) and 7(c) indicates that the variations in combustor velocity (1) are relatively small and (2) do not exhibit any well-defined trends with the observed combustion efficiency (fig. 58). Figure 60(c) shows that combustion efficiency can either decrease or increase with an increase in velocity. These comparisons do, of course, neglect what can be very important effects of fuel-air ratio on combustion efficiency. Particularly large variations in fuel-air ratio occur with variations in engine speed.

As altitude is increased, a turbojet engine may approach an altitude operational limit (fig. 59). At any engine operating condition, the combustor must furnish a certain required temperature rise (ch. X). The ability of a combustor to supply high values of temperature rise is limited either by rapidly decreasing combustion efficiencies at high fuel-air ratios (fig. 60(d)) or by flame blow-out. As might be expected, then, the maximum temperature rise obtainable with a combustor usually varies in much the same manner as does combustion efficiency. The data of reference 3 show a decrease in maximum temperature rise with a decrease in temperature or pressure and, generally, with an increase in velocity. Figure 61 shows the relation between the maximum temperature rise and that required for operation over a range of altitude at a constant engine rotational speed. Although the temperature rise required does not vary appreciably with altitude for this particular engine, the available temperature rise decreased rapidly with an increase in altitude. The altitude at which the two curves cross (about 32,000 ft) represents the operational limit of the engine.

As the operating altitude of a turbojet combustor is increased, the character of the flame changes noticeably. At low-altitude, high-pressure operating conditions, most turbojet combustor flames are a brilliant orange-yellow. This luminosity is due to incandescent carbon particles suspended in the hot gas stream. The emissivity of such a flame can be of the order of 0.8 (ref. 7). As the operating altitude is increased, a gradual transition to a relatively nonluminous blue flame occurs. Finally, at conditions near the operational limits of the combustor, varying degrees and types of flame instability appear, frequently in the form of low-frequency pulsations. These pulsations are often accompanied by movement of the flame-seating zone along the length of the combustor. Flame fluctuations are discussed further in a later section.

EFFECT OF FUEL AND AIR ADMISSION CHARACTERISTICS ON COMBUSTION EFFICIENCY AND LIMITS

The foregoing discussion, indicating the general effects of operational variables on the limits and efficiency of combustion in turbojet combustors using liquid fuels, suggested that the effects of some of these variables are due, in part, to the influence of the variables on preparation of flammable fuel-air mixtures. A number of fuel and combustor design variables that influence the preparation of this mixture are considered in this section.

In a liquid-atomizing combustor the flammable mixture is prepared by atomizing the liquid fuel, vaporizing the resulting fuel droplets, and admitting the proper quantity of air. Although these individual processes are discussed separately, they are by no means independent of one another, nor does each occur in a distinct zone of the combustor.

Fuel-Atomization Factors

The fuel-atomization characteristics that would be expected to influence mixture preparation in the turbojet combustor are drop size and spray pattern. The data of chapter I show that the rate of evaporation of a liquid drop is directly proportional to its diameter. Since the number of drops in a given mass of spray is inversely proportional to the cube of the average drop diameter, the evaporation rate of the spray is inversely proportional to the square of the average drop diameter. More direct evidence of the importance of drop size is shown in figure 62 (ref. 8). The time required to burn a single drop of kerosene fuel increased by a factor of 13 when drop

size was increased three-fold. The second atomization factor, spray pattern, will influence the distribution of the drops and, hence, local fuel-air ratios in the combustion zone.

Atomization characteristics. - Atomization characteristics are not only influenced by design of the nozzle and by properties of the fuel (viscosity, surface tension), but also vary with operating condition. Figure 63 shows the variation in flow rate, drop diameter, and cone angle with nozzle pressure differential for two simple swirl-type nozzles. The mean drop diameter (Sauter mean diameter) was calculated from equation (34) of chapter I. Mean drop diameter decreases with an increase in pressure and, hence, with an increase in flow rate. For a given pressure differential, the use of the smaller nozzle also results in somewhat smaller drops. For a given flow rate, it is apparent that considerably smaller drops will be obtained with nozzles of smaller size. Comparison of the data of figures 62 and 63 indicates that the mean drop sizes obtained from these nozzles would have a burning time of less than 0.01 second for the conditions represented.

The cone angle of the spray (fig. 63) first increases and then decreases as the flow rate is increased. At values of flow rate (and pressure) below those shown, the cone angle decreases very rapidly until a "bulb" type spray results. Since the operation of a turbojet engine requires a very wide range of flow rate, it is evident that, with a simple pressure-atomizing nozzle, atomization characteristics will vary considerably with operating conditions.

Effects of atomization. - A typical example of the effect of fuel atomization on the combustion efficiency of a full-scale turbojet engine (ref. 9) is presented in figure 64. At the high-altitude cruising conditions investigated, combustion efficiency was reduced as much as 25 percent as a result of increasing the fuel-nozzle capacity from 3 to 7 gallons per hour (nominal ratings of 100 lb/sq in.). This marked decrease in combustion efficiency may be attributed to the poorer atomization resulting from the decrease in nozzle pressure drop encountered with the use of larger fuel nozzles.

More detailed studies of the effects of fuel atomization characteristics on combustion performance have been conducted in direct-connect-duct investigations with tubular and annular combustors. Results of one of these studies (ref. 10) are illustrated in figure 65. The variation of combustion efficiency with combustor temperature rise for aviation gasoline is shown in figure 65(a) for three fuel-nozzle sizes and at fixed inlet-air conditions. At low values of temperature rise corresponding to low fuel-flow rates, the smallest nozzle gave the highest efficiency; at high values of temperature rise, the largest nozzle gave the highest combustion efficiency. With all three nozzles, maximum-temperature-rise conditions were encountered, indicating conditions of overrich fuel-air mixtures. The values of maximum temperature rise increased with increase in fuel-nozzle size.

These data, in addition to data obtained with other nozzle sizes, are further analyzed in figure 65(b) to indicate the fuel-nozzle pressure differential required at the various operating conditions. At low values of temperature rise, high pressure differentials gave the best performance. As temperature rise was increased, however, use of the higher pressure differential resulted in maximum-temperature-rise conditions and in rapid decreases in combustion efficiency; whereas, with the lower pressure differential, temperature rise continued to increase with increased combustion efficiency. Thus, a certain minimum quality of atomization, or a maximum drop size, is required at all conditions of operation, but it is possible to atomize a fuel too well and thereby produce primary-zone mixtures that are too rich to burn. The use of larger nozzles at high fuel flows increases drop size (fig. 63), the increase in turn reducing the rate of evaporation and extending the zone of

[redacted]

evaporation farther downstream where additional air is being introduced. These results cannot be assumed to apply to all combustor designs, operating conditions, and fuels. With a particular combination of these variables, only a part of the over-all trends may be observed.

The thrust range required of a turbojet engine results in a wide range of fuel-flow rate (about 12 to 1 in current engines). The use of a single pressure-atomizing nozzle of the type used in the studies described necessitates large variations in fuel pressure and in spray characteristics, as shown in figure 63. The data of figure 65 show that these variations in spray characteristics can markedly affect the combustor performance. A single fuel nozzle may provide insufficient atomization at low flow rates and excessive atomization at high flow rates. It appears desirable, then, to consider the use of multiple nozzles, of different sizes, in the combustor to ensure more nearly constant atomization characteristics and to avoid excessive fuel-system pressures.

Duplex nozzles, combining the principal components of two individual nozzles of different size, have been developed for use in many current turbojet engines. A further development of the duplex nozzle is the variable-area nozzle (ref. 11), which produces a finely atomized spray over a flow range from about 30 to 500 pounds per hour with a corresponding range of pressure differential from about 50 to 70 pounds per square inch. The nozzle was tested in a full-scale engine at sea-level conditions (ref. 11) and at high-altitude conditions (ref. 12). Figure 66 presents combustion-efficiency data obtained with a conventional fixed-area nozzle and with a variable-area nozzle in a full-scale engine operating at an altitude of 40,000 feet and a ram pressure ratio of 1.00. Use of the variable-area nozzle resulted in an increase in combustion efficiency of approximately 5 percent at this particular operating condition. By combining the data obtained over a range of altitudes from sea level to 40,000 feet and a range of ram pressure ratios, the curve shown in figure 67 was obtained. These data show that reductions in fuel consumption as large as 16 percent were obtained with the variable-area fuel nozzle, the largest reductions occurring at low fuel-flow rates where the fixed-area nozzle did not provide sufficient fuel atomization.

Effects of spray pattern. - Combustion efficiencies for a 40-gallon-per-hour, 80°-cone-angle nozzle are compared in figure 68 with those for a 15.3-gallon-per-hour, 30°-cone-angle nozzle in a tubular combustor operating at severe conditions. The combustion efficiencies for the smaller, narrow-cone-angle nozzle decreased more rapidly with a decrease in fuel-air ratio than did those obtained with the larger, wide-cone-angle nozzle. This trend indicates that leaner fuel-air ratios were present in the combustion zone with a narrow-cone-angle nozzle in spite of the finer atomization resulting from the higher attendant pressure differentials. Reducing the angle of the spray cone and increasing the pressure differential increased spray penetration through the center of the combustor without effecting sufficient spreading in the upstream, primary-combustion region. The accompanying reduction in fuel residence time and the poor mixing served to reduce combustion efficiency.

The data of figure 68 indicate that wide-cone-angle nozzles should be used to attain high combustion efficiency. The investigation reported in reference 13 shows, however, that wide-angle fuel sprays, such as those produced by the 80°-cone-nozzle, can result in appreciable wetting of combustion-chamber walls with fuel. Illustrative data in figure 69 indicate that installation of fuel "dams" to collect and return fuel films from the wall of the combustor to the combustion zone improved combustion efficiencies significantly. The most pronounced effects were noted at low fuel-air ratios, probably because the power atomization at these conditions induced greater wall wetting. This evidence indicates that fuel depositing on the walls of the combustion chambers may pass through the combustor without

entering into the combustion process and cause a loss in efficiency. In addition, wetting of the wall with fuel has been found to be conducive to another deleterious combustor characteristic, carbon deposition (ch. XIII). A certain amount of wall-wetting occurs in most combustors. Depending upon the design of the combustor, varying quantities of the liquid fuel deposited may be reatomized by the incoming jets of air.

The effect of distribution of atomized fuel in the primary zone of a tubular combustor on combustion performance was investigated in reference 4. Figure 70 presents data of reference 4 obtained with several liquid injectors using liquid MIL-F-5624A, grade JP-3 fuel. Comparison of the two atomizing nozzles (simplex and duplex) shows that the duplex nozzle gave considerably higher combustion efficiencies at low values of temperature rise and somewhat lower combustion efficiencies at high values of temperature rise. From preceding discussions of fuel atomization effects, it may be concluded that the simplex nozzle did not provide sufficient atomization at the low fuel-air ratios, while the duplex nozzle provided excessive atomization at high fuel-air ratios and resulted in fuel-rich mixture conditions.

The other four injectors shown in figure 70 are considered "solid-stream" injectors, since no provisions for fuel swirl are incorporated; all use simple orifices. Among the solid-stream injectors, the highest combustion efficiencies were obtained with a tube injector (tube B) that distributed fuel along the length of the combustor. From a comparison of the performance of the three different tube injectors, a noticeable effect of the distribution of injection holes along the axis may also be observed. An explanation for the poor performance of the radial injector with liquid fuel may be the fact that with this injector solid streams of unatomized fuel were injected in the downstream direction with too much penetration and too short a residence time for the fuel drops.

The preceding discussion shows the important effects of fuel-spray characteristics on the combustion performance of liquid fuels. Fuel-spray characteristics are affected not only by injector design but also by properties of the fuel and by the design of the combustor. Mean drop size is proportional to surface tension of the fuel to powers from 0.6 to 0.7 or less, and to viscosity of the fuel to the 0.25 power (ch. I). Very substantial effects of the air-flow currents on liquid fuel sprays also were observed in investigations reported in reference 14. Figure 71 (from ref. 14) indicates that air flow in a tubular combustor increased fuel atomization considerably over that observed with the spray in quiescent air. Other photographic evidence presented in reference 14 shows that increased air velocity resulted in increased fuel atomization and distribution. Thus, it is generally not possible to predict, from photographs or measurements made in quiescent atmospheres, the spray characteristics that will be obtained with a particular injector installed in a combustor. Furthermore, satisfactory methods of measurement of fuel-spray characteristics, drop size and distribution, are generally too complex to be readily adaptable to the actual turbojet combustor.

Because the end result of fuel atomization, distribution, and evaporation is the formation of flammable fuel-air mixtures in the combustion zone, the fuel-spray characteristics required for optimum performance depend on operating conditions and combustor design. Some combustor designs have been evolved that minimize, to a large extent, the effects of fuel-spray variables on combustor performance. An example of data obtained with such a design is shown in figure 72 (ref. 9). In an experimental annular combustor, two fuel nozzles (capacities, 10.5 and 6 gal/hr) were tested at a simulated flight altitude of 30,000 feet, and three fuel nozzles (capacities, 10.5, 6.0, and 3.0 gal/hr) were tested at 40,000 feet. The data indicate only minor effects of fuel-injector size on combustion efficiency. Near the rated speed of the engine, the larger nozzles gave slightly higher combustion

efficiencies. This trend is in agreement with data presented in preceding sections; that is, at the high fuel-air ratios required at rated speed, the finer atomization produced by the smaller nozzles resulted in over-rich mixtures in the combustion zone. The experimental combustor represented by these data was of the same general over-all dimensions and was tested in the same engine as the combustor represented by the data of figure 64, which shows very significant effects of fuel-nozzle size on the performance of that combustor.

Fuel Vaporization Factors

The rate of vaporization of a fuel spray is a function of the degree of atomization and of the volatility characteristics of the fuel. It is also a function of operating conditions - temperature, pressure, and velocity of the fluid surrounding the fuel drops (ch. I). Effects of atomization characteristics on combustion performance are discussed in the preceding section of this chapter. Data show that there is an optimum degree of atomization associated with a particular combustor and particular operating conditions. Fuel sprays that are either finer or coarser than this optimum can result in too-rich or too-lean fuel-air-ratio conditions and, hence, in decreased combustion performance. Fuel volatility characteristics would be expected to influence combustion performance in a similar manner. That is, optimum fuel volatility characteristics may depend upon the choice of operating conditions and combustor design.

Fuel volatility. - Typical effects of fuel volatility on combustor performance are illustrated in figures 73 and 74. Combustion efficiency of an annular combustor is plotted against altitude in figure 73 for three types of fuel varying from highly volatile aviation gasoline to low-volatility Diesel fuel (ref. 10). These data illustrate the same trend of combustion efficiency with simulated flight altitude that was observed in figure 58. The combustion efficiencies of the fuels tend to converge near 100 percent at a low altitude, indicating that at sea level the differences among fuels may not be great. At high altitude, however, the more volatile fuel, aviation gasoline, produces considerably higher efficiencies.

The effect of fuel volatility on the altitude operational limits of an annular combustor is illustrated in figure 74 (ref. 10). At engine speeds in excess of 60-percent rated engine rotor speed, Diesel fuel produces the highest altitude limit; at lower speeds the more volatile gasoline gives higher limits. This result is consistent with the studies discussed previously in this chapter, where it is pointed out that a too-rapid vaporization rate may, at some conditions of operation, produce a mixture too rich to burn. Very fine atomization and rapid vaporization occur at the higher engine speeds that correspond to higher fuel flows in the engine; at these conditions gasoline vaporizes too rapidly, and Diesel fuel, because of its lower volatility, vaporizes more slowly and at a more nearly optimum rate. At low engine speeds the reverse is true; that is, the fuel flows are low, and the vaporization required is more nearly fulfilled by the more volatile aviation gasoline.

The interrelation between fuel volatility and fuel-spray characteristics is further illustrated in figure 75. The combustion efficiencies obtained with Diesel fuel and aviation gasoline using two nozzles of widely different spray characteristics are shown. With the larger nozzles giving coarser atomization at the same flow rate, the more volatile gasoline produced the higher combustion efficiencies. With the smaller nozzles giving finer atomization, overenrichment of the primary combustion zone occurred and the lower volatility fuel, Diesel fuel, gave higher combustion efficiencies.

The results of tests in a 7-inch-diameter tubular combustor with a larger number of fuels of varying volatility are presented in figure 76. The fuels represented in figure 76(a) were relatively pure materials that vary only slightly in their fundamental combustion characteristics (discussed in a later section of this chapter). As the average boiling temperature, represented by the A.S.T.M. 50-percent distillation temperature, was increased, combustion efficiency first increased and then decreased, indicating an optimum distillation temperature of about 200° F for these particular operating conditions. The distillation (or boiling) temperature of a fuel is only one of several fuel factors that may affect vaporization rate. For example, the evaporation rate of single drops into high-temperature surroundings can be correlated with the total heat required to evaporate a unit mass of fuel (ref. 15). This quantity of heat is a function of the initial temperature, the boiling temperature, and the latent heat of vaporization of the fuel. Plotting the combustion-efficiency data of figure 76(a) against the heat required for evaporation would result in curves of the same form as those shown in the figure because of observed relations between boiling temperature and latent heat of vaporization of hydrocarbon fuels.

The general trend in combustion efficiency with boiling temperature shown in figure 76(a) is not usually encountered in turbojet combustors. In most cases, the range of fuel volatility, operating range, and combustor design used results in a continuous decrease in efficiency with an increase in boiling temperature, as shown in figure 76(b). These data (ref. 16) were obtained with mixed hydrocarbon fuels of the general type that may be supplied for turbojet-engine use.

Fuel and air temperature. - Since the effects of fuel volatility on combustion performance are intimately related to the design of the combustion chamber and to the fuel-injection technique, it is possible to design a combustion system around either a low- or a high-volatility fuel to provide both high efficiency and satisfactory stability. The difficulty of achieving this design, however, may be considerably greater with very-low-volatility fuels. If, for economic or other reasons, it is desirable to use low-volatility fuels, the effects of volatility can be reduced by preheating or prevaporizing the fuel. In figure 77, a comparison is made of the combustion efficiencies obtained at two fuel temperature conditions in an experimental annular combustor using MIL-F-5624A, grade JP-4 fuel. Preheating the fuel to 300° F appreciably improved the combustion efficiency at the low combustor-inlet pressure of 2.5 pounds per square inch absolute (ref. 17). This trend is also apparent in figure 78, which shows the effects of air and fuel temperature on combustion efficiency of a tubular combustor for JP-1 fuel and for monomethylnaphthalene, two fuels that differ considerably in both volatility and composition. Increases in fuel and air temperature caused an increase in combustion efficiency for both fuels. Comparison of the two parts of figure 78 shows that variations in inlet-air temperature had a more pronounced effect on combustion efficiency than did variations in fuel temperature. Increasing the temperature of monomethylnaphthalene to 300° F did not increase performance sufficiently to equal the performance with unheated (100° F) JP-1 fuel. For unheated monomethylnaphthalene, increasing the air temperature to 200° F increased efficiency to a value just slightly below that obtained with unheated JP-1 fuel at an air temperature of 100° F.

The pronounced effect of inlet-air temperature on combustion efficiency shown in figure 78 may be expected from spray evaporation studies. Experimental studies of the evaporation of gasoline-type fuel sprays cited in chapter I show that the rate of evaporation is proportional to the 4.4 power of the air temperature. Data of reference 18 show that evaporation of a fuel boiling between 317° and 346° F increased 1 percent for each 4° F increase in air temperature and for each 7.5° increase in fuel temperature. Furthermore, it should be recognized that increases in inlet-air temperature will increase the rate of chemical reaction as well as the rate of evaporation.

Fuel prevaporization. - From the results presented in figures 77 and 78, it may be concluded that methods of increasing the rate of evaporation of the liquid fuel spray can improve combustion efficiency. Other investigations (e.g., refs. 4 and 19) have also shown that the use of a completely vaporized fuel will increase combustion efficiencies in current liquid-atomizing combustors. A number of turbojet combustion systems have been designed with fuel "prevaporizers," which generally incorporate flame-bathed fuel-vaporizing tubes. With a fuel prevaporizer, the effects of fuel volatility on combustion efficiency would be expected to disappear. The combustion efficiencies obtained in a commercial vaporizing combustor with eight fuels of varying volatility are reported in reference 20. The least-volatile fuel tested was a kerosene. Over the range of fuel-air ratios investigated, all the fuels gave about the same combustion efficiencies. The inlet-air operating conditions were not given in reference 20; however, they were presumably severe enough to cause significant differences in the performance of the fuels in a liquid-atomizing combustor.

Investigations of the combustion performance of monomethylnaphthalene and JP-3 fuel in a different vaporizing combustor are reported in reference 21. Combustion efficiencies were determined for a range of combustor inlet-air temperature, inlet-air pressure, and air velocity. Representative results are presented in figure 79, which shows that in all cases the performance of the more volatile JP-3 fuel exceeded the performance of the high-boiling hydrocarbon monomethylnaphthalene. With regard to stability, the data show that the more volatile JP-3 fuel sustained combustion at lower inlet pressures and at higher velocities. Thus, the use of the fuel prevaporizer in this case did not eliminate the effect of fuel volatility on combustion performance. It should be noted that the compositions of JP-3 fuel and monomethylnaphthalene are considerably different. Variations in composition may also affect combustion performance. The data of figure 79 are compared in reference 21 with similar data obtained with the same fuels in a liquid-atomizing combustor. The trends indicated that the vaporizing combustor did diminish the effect of fuel properties on combustion efficiency. The fact that the differences were not entirely eliminated may be attributed to inadequate vaporizing capacity of the combustor for the high-boiling monomethylnaphthalene, and to differences in fuel composition.

It was suggested that increased inlet-air temperature improves combustion efficiency in one way by causing more rapid vaporization of liquid fuel sprays. The use of a fuel prevaporizer, then, should diminish the effect of inlet-air temperature on combustion efficiency. Figure 79 shows that, in the prevaporizing combustor tested, combustor inlet-air temperature had some effect on the efficiencies obtained with monomethylnaphthalene and essentially no effect on those obtained with the JP-3 fuel. These trends again indicate that, since the prevaporizer was not designed to handle fuels such as monomethylnaphthalene, prevaporization of this fuel was probably not very complete.

Vapor fuel distribution. - Even if the combustor design is such that complete fuel prevaporization occurs, performance difficulties may still result from improper distribution of the vaporized fuel. The effect of vapor fuel distribution on the combustion efficiency of a tubular combustor is studied in reference 22; results obtained with four different fuel injectors are presented in figure 80. The injectors were similar to several of those discussed in the section of this chapter entitled Fuel Atomization Factors (fig. 70). Even with the fuel vaporization step completely eliminated, combustion efficiency was markedly affected by the design of the vapor fuel injector. A comparison of the two injectors having single orifices indicates that the larger orifice provided a higher combustion efficiency. It may be considered that the lower-velocity jet issuing from the larger nozzle was mixed more uniformly with the air, while the higher-velocity jet from the smaller nozzle maintained a fuel-rich region in the center of the combustor. Also, the smaller-orifice injector may have increased fuel penetration sufficiently to reduce residence time

of the fuel in the combustion zone, resulting in decreased combustion efficiencies. The radial spoke-type injector distributed the fuel more uniformly over the cross section of the combustion zone, thereby affording greater mixing rates and, hence, higher combustion efficiency. The best performance was obtained with the tube injector, which distributed the fuel axially along the length of the primary zone, mixing the fuel with the incoming air jets and, also, possibly mixing with reverse air-flow currents within the combustor. Additional studies of the effect of vapor fuel distribution on the performance of an annular combustor are described in reference 23.

Air Admission Factors

The effects of the fuel atomization and vaporization steps on the performance of turbojet combustors are discussed in the preceding sections of this chapter. The data presented emphasize the need for maintaining optimum fuel-air-mixture conditions in the combustion zone. Two ways of accomplishing this (at least partially) were described (1) control of fuel properties and (2) proper design of the fuel-injection system. The third factor that influences the fuel-air mixture is the design of the air admission ports.

The design of the air admission system in the turbojet combustor is based not only on the requirements of high combustion efficiency and wide limits of operation but also on factors such as outlet-temperature distribution, carbon deposition, ignition, and durability of the combustor. The present discussion is limited to a brief review of the trends in limits and efficiency of combustion that have been observed with variations in air admission geometry of the primary combustion zone.

The primary-air-admission ports are designed (1) to provide adequate quantities of air for combustion and (2) to promote a high rate of mixing of the fuel with the air. It is apparent that the air admission characteristics must be matched to the design of the fuel injectors and to the fuel properties in order to achieve optimum fuel-air-mixture conditions in the primary combustion zone. Current turbojet combustor configurations do not provide completely separated, well-defined primary combustion zones. For discussion purposes, however, the primary zone is generally assumed to occupy the first one-third to one-half of the total combustor length. The amount of air introduced into this region is not independently controlled but rather is a function of the air-admission-port design over the entire length of the combustor, combustor cross-sectional geometry, and pressure loss (ch. II).

Effects of primary-air admission. - Some laboratory studies have been conducted with combustors incorporating separated and controlled primary-air admission. Figure 81 presents results of one such study in a tubular combustor operating at over-all fuel-air ratios from 0.0057 to 0.0145 (ref. 24). For a given over-all fuel-air ratio, increasing the percentage of primary air above a critical value resulted in a decrease in temperature rise, and hence in combustion efficiency. This decrease in efficiency may be attributed to over-lean primary-zone mixtures. The trends may also be explained on the basis of primary-zone velocity; as primary-air flow is increased, velocity is also increased, and residence time of the fuel-air mixture is decreased. These and other data reported in reference 24 indicate, however, that mixture fuel-air ratio in the primary zone was the principal factor influencing the performance of this tubular combustor. The data also show that smaller percentages of primary air are required at low over-all fuel-air ratios to maintain high efficiency. The parametric curves of constant primary fuel-air ratio indicate that a minimum primary fuel-air ratio of about 0.05 is required to assure best performance.

The data of figure 81 indicate that, so long as the percentage of primary air is less than about 10 percent, maximum efficiency is obtained. The data presented in this figure are limited to a relatively narrow range of operating conditions; data presented previously in this chapter indicate that overenrichment of the primary zone can also cause decreases in efficiency. One example of the more general trend that can be expected is presented in figure 82 (ref. 25). These and all subsequent data presented in this section were obtained in combustors not incorporating separately controlled primary air. The amount of air entering the primary zone is assumed to be proportional to the open area of the air admission ports in that region. While this assumption is reasonably satisfactory for observing general performance trends, it is accurate for high-pressure-loss combustors only (ch. II, fig. II-13). More precise methods for estimating air distribution in turbojet combustors are noted in chapter II. Figure 82 shows that at fuel-air ratios less than about 0.014 a decrease in open area at the front end of the combustor (a decrease in primary-air flow) increased combustion efficiency, a trend similar to that shown in figure 81. At high fuel-air ratios, however, overenrichment of the primary zone occurred, and a decrease in open area in the primary zone decreased combustion efficiency. Similar trends are illustrated in figure 83 by data obtained in a 9.5-inch-diameter combustor (ref. 26). The air-entry-hole area of a 5.8-inch-diameter primary zone (pilot chamber) was varied over a range from about 25 to 10.9 square inches. At low fuel-air ratios, intermediate open areas gave the best performance; at fuel-air ratios greater than about 0.012, there is a regular trend of increasing efficiencies with increasing open area.

Optimum air admission design. - As is apparent from the data of figures 82 and 83, a single, fixed, air admission geometry will be optimum for specific operating conditions only. Unless variable air admission controls are incorporated into a combustor design, compromises are required to achieve the best over-all combustion characteristics of the combustor. Research studies have been conducted in many laboratories to determine the air admission design criteria for optimum combustion performance. Illustrative results obtained at the Lewis laboratory are presented in the following discussion. These results were obtained primarily in direct-connect-duct facilities, utilizing both annular and tubular combustors.

While most current liquid-atomizing combustors use longitudinal rows of circular holes for introducing air (e.g., fig. 71(b)), the experimental combustors described here incorporate a variety of hole shapes and locations. For example, the experimental annular combustors used in reference 27 incorporated long rectangular slots for admission of primary combustion air, while those of reference 17 had small circular holes. Figure 84 presents one-quarter cutaway views of these particular experimental combustors. Figure 85 illustrates a variety of air admission techniques investigated in a tubular combustor (ref. 25), each of the configurations shown tending to produce a different air-flow pattern within the combustion zone.

The altitude operational limits obtained with two circular-hole designs in an early annular combustor are presented in figure 86. Near-optimum design increased altitude operational limits about 12,000 feet; combustion efficiency was also increased considerably. The air-admission-hole designs of the two combustors are represented in figure 87 by the plot of percentage of open area against axial distance from the upstream end of the combustor liner. The design giving the higher performance had substantially reduced open area in the first portion of the combustor, approximately 16 percent of the total open area being located in the first half of the combustor length. The total-pressure losses through the two combustor designs were approximately the same. The reduction in open area in the upstream region may be considered to have increased local fuel-air ratios and to have reduced local flow velocities.

[redacted]

The extent to which air admission design affects performance depends very markedly on operating conditions. The axial distributions of air-entry-hole area for three experimental annular combustors designed for high combustion performance (ref. 28) at high-altitude (low-pressure) operating conditions are presented in figure 88. The combustors used very similar patterns of circular holes for admitting air into the primary zone and, as shown in figure 88, also had very similar axial distributions of open area. Even these small differences in primary-air-admission design produced the large differences in performance shown in figure 89. Figure 90 presents the axial distribution of open area for each of two widely different combustor designs investigated in reference 29. Combustor A utilized circular holes for admitting primary air; combustor B, slots and louvers. The combustion efficiencies obtained with these combustors over a range of inlet-air-pressure conditions are presented in figure 91. At low-pressure conditions simulating high-altitude, low-speed flight, large differences in performance were observed. At inlet-air pressures above about 1 atmosphere simulating higher-speed flight, higher-pressure-ratio engines, or lower-altitude conditions, the large differences in open-area distribution did not markedly affect combustion efficiency.

It is apparent from the data presented herein that the best axial distribution of open area of a combustor will depend, partially, on the required operating conditions. It will also depend on the fuel-injection and fuel-volatility characteristics, since these factors will affect the amount of vapor fuel present at any location. Finally, it will depend on the combustor design itself, the pressure-loss characteristics and the shape of the air-entry ports. Examples of near-optimum air-entry-hole-area distributions for a number of experimental combustor designs varying in all the above factors are presented in figure 92, where the principal features of the various combustors are noted. Combustors C and E injected prevaporized fuel, and D and F injected atomized liquid fuel into the combustion zone. Primary air was admitted through circular holes, longitudinal slots, or both. The various designs represented had from about 20 to about 50 percent of the total liner open area located in the first half of the combustor.

It has been shown that in the turbojet combustor air admission design influences the limits and efficiency of combustion to a very great extent. Its effects are related to the fundamental combustion requirements of a low-velocity combustion zone containing flammable fuel-air mixtures. If these proper burning conditions at any particular combustor operating condition are to be obtained, the air admission design must be matched with the fuel-injection and vaporization characteristics. Because of the desirability of fixed combustor geometries with a minimum of moving parts, the fuel-air mixture will be optimum over only a part of the entire combustor operating range, and compromises in performance must be expected at some conditions. The effects of adverse fuel-air-mixture conditions are most pronounced at low-pressure and low-temperature (high-altitude) conditions. As would be expected, then, in engines having higher pressure ratios and operating at high flight speeds, the conditions for combustion are less severe, and more freedom in the design of the combustor components is allowable.

CORRELATION OF OPERATING VARIABLES WITH COMBUSTION EFFICIENCY

One of the principal objectives in conducting engine studies is the development of methods that will enable the engine designer to estimate or predict the performance of new engines. A logical approach to this problem is the development of correlations of engine performance characteristics with the engine operating variables. In the case of the turbojet combustor, one performance characteristic of interest to the designer is combustion efficiency; the operating variables of interest are inlet-air pressure, inlet-air temperature, air velocity, and temperature rise. A preceding portion of

this chapter is devoted to a discussion of these variables and their relation to combustion efficiency. This section concerns existing methods of combining these operating variables into suitable parameters for correlation with combustion efficiency.

Losses in combustion efficiency occur because the conversion processes that take place in the turbojet combustor are too slow. These processes include vaporization of liquid fuel, mixing of the fuel and air to form flammable mixtures, ignition, and oxidation. Combustion can be visualized as a competition between these processes and the quenching that occurs when the reacting mixture is swept out of the burning zone and diluted with cold air and when the mixture contacts the relatively cool walls of the combustor liner. Because of the obvious complexity of the combustion process, no exact theoretical treatment of combustion efficiency is currently possible. Nevertheless, correlations have been developed, both empirically and theoretically, by making simplifying assumptions regarding the combustion mechanism.

Correlation with a Simplified Reaction-Kinetics Equation

The effects of the inlet-air variables on combustion efficiency have been considered to be the result of their effects on the rate of chemical reaction. Second-order reaction equations have been used to explain flame stability phenomena observed in ram-jet combustion chambers (ref. 30). In addition, it has been suggested that chemical-reaction kinetics control the performance of jet-engine combustors (ref. 31).

A theoretical analysis (ref. 32) based on the kinetics of a bimolecular chemical reaction yielded the following relation between combustion efficiency and the combustor-inlet variables:

$$\ln\left(\frac{1 - \frac{N_A}{N_B}\eta_b}{1 - \eta_b}\right) + K_5 = K_3 \frac{(\sigma_A + \sigma_B)^2 (N_B - N_A)\, e^{-\frac{E}{RT_b}}}{R^{1/2} T_b^{3/2}} \frac{LK_7^2}{K_8 K_9} \frac{p_i T_i}{V_r} \qquad (1)$$

where

E	apparent energy of activation
K_5, K_3, K_7, K_8, K_9	constants
L	length of reaction zone
N_A, N_B	concentration of two reactants in burning zone
p_i	combustor-inlet static pressure
R	gas constant
T_b	static temperature in burning zone
T_i	combustor-inlet static temperature
V_r	combustor reference velocity
η_b	combustion efficiency
σ_A, σ_B	effective molecular diameter

For a given combustor, fuel, and fuel-air ratio, and if the burning-zone temperature T_b is considered independent of changes in inlet conditions and other simplifying assumptions noted in reference 32 are made, then

$$\eta_b = f\left(\frac{p_i T_i}{V_r}\right) \tag{2}$$

Equation (2) is applied, in reference 32, to data obtained in 14 different turbojet engines and combustors. The reference velocity V_r is based on the mass-flow rate, the combustor inlet-air density, and the maximum cross-sectional area of the combustor flow passage. Illustrations of the relation between the parameter $p_i T_i/V_r$ and combustion efficiency η_b are shown in figure 93. Experimental points are shown on this plot to illustrate the extent of scatter in the data. The precision of correlations such as these is not good. Some scatter may be expected since it is difficult, at identical test conditions, to reproduce values of combustion efficiency accurately in day-to-day operation. Studies of this reproducibility show that values of combustion efficiency differing by 4 percent are common with most combustors, but at severe operating conditions the differences may be as great as 10 percent.

The parameter $p_i T_i/V_r$ obviously does not include possible effects of fuel-air ratio on combustion efficiency. Data presented in figure 60(d) indicate that the effect of fuel-air ratio on efficiency varies with combustor design; it may also vary with operating conditions. Many combustors give substantially constant efficiency for a range of fuel-air ratios; when this occurs, the correlation of $p_i T_i/V_r$ with combustion efficiency is generally improved. Thus, some of the scatter of data noted in the correlations of figure 93 may be attributed to the effect of fuel-air ratio.

The data for the 14 combustors investigated (ref. 32) all produce curves of the same general shape. The examples shown in figure 93 indicate that at higher values of the parameter the efficiencies of the combustor are good, but combustion efficiency may decrease rapidly at low values. This general characteristic of the curves led to the suggestion (ref. 32) that a concept of a critical value of the parameter might be developed to distinguish between satisfactory and unsatisfactory ranges of operating conditions. Combustors could then be rated according to these critical values of the parameter. In other words, an examination could be made of the relative ratings of combustors and engines at a selected value of combustion efficiency, and the rating values would be expressed in terms of the parameter $p_i T_i/V_r$. On such a scale, the best combustors would have low values of critical $p_i T_i/V_r$.

In order to obtain a more critical test of the assumption that the rate of chemical reaction controls turbojet combustion efficiency, combustor tests were conducted with a variable concentration of oxygen in the inlet oxygen-nitrogen mixture. Investigations show marked effects of oxygen concentration on combustion properties such as minimum spark-ignition energy, quenching distance, and burning velocity (ref. 33, pp. 303, 304, 405-407, and 460-467). Oxygen concentration is, therefore, a means of varying the combustion characteristics without appreciably changing such factors as inlet velocity, turbulent mixing as associated with inlet conditions, and fuel-spray characteristics.

The effects of oxygen concentration on combustion efficiencies obtained with both liquid fuel (isooctane) and gaseous fuel (propane) were determined in a 7-inch tubular turbojet combustor (refs. 19 and 34). Typical data are presented in

figure 94. Even though such flow parameters as velocity and Reynolds number were constant, the combustion efficiency increased with oxygen concentration, the rate of increase being greater at lower values of oxygen concentration. This observation establishes the importance of molecular processes in the combustion process. As would be expected, combustion efficiency also increased with an increase in inlet-air pressure and was higher with the vapor fuel. These results indicate that, when grosser physical processes associated with combustor-inlet conditions are held constant, variations in the molecular-scale processes will affect the performance of a turbojet combustor.

3080

In the application of the variable-oxygen-concentration data of references 19 and 34 to the basic kinetics equation (1), the burning-zone temperature T_b could no longer be considered independent of inlet conditions, since variations in oxygen concentration result in appreciable changes in the flame temperature of stoichiometric or richer fuel-oxygen-nitrogen mixtures. The burning zone temperature T_b was therefore arbitrarily taken as the stoichiometric adiabatic equilibrium temperature. For these conditions, the ratio of the reactants (fuel and oxygen) $N_A N_B$ is assumed constant in the combustion zone, and equation (1) can be expressed as

$$\eta_b = f\left[\alpha \frac{p_i T_i}{V_r}\left(\frac{e^{\frac{-E}{RT}}_{eq}}{T_{eq}^{3/2}}\right)\right] \tag{3}$$

where T_{eq} is the stoichiometric adiabatic equilibrium temperature, and α is the oxygen concentration.

The application of equation (3) to experimental data of references 19 and 34 is shown in figure 95 for a fuel-air ratio of 0.012. The equilibrium temperatures were computed by methods described in reference 35. An activation energy E of 37,000 calories per gram-mole satisfactorily correlated the data obtained with liquid isooctane. This value is in reasonable agreement with the apparent activation energy of 32,000 calories per gram-mole obtained from adiabatic-compression-ignition data (ref. 33, p. 188). For the correlation of the data obtained with gaseous propane (fig. 95(b)), a value of E of 27,818 calories per gram-mole was used. However, because of the sensitivity of the correlation parameter to oxygen-concentration measurements in the low-combustion-efficiency range, any value of E between about 27,000 and about 33,000 calories per gram-mole would be satisfactory. A value of 38,000 calories per gram-mole is cited in reference 36.

The scatter of data from the mean correlation curves of figure 95 is considerably less than that of figure 93. Perhaps a major reason for the improvement in the correlation was the removal, in the data of figure 95, of the variable fuel-air ratio. A comparison of data obtained with the liquid fuel at four fuel-air ratios is presented in figure 96. The correlation curve varies considerably with fuel-air ratio, combustion efficiency increasing with an increase in fuel-air ratio. With gaseous propane fuel (ref. 19), fuel-air ratio had a relatively small effect on combustion efficiencies, except at low values of oxygen concentration.

Correlation with Fundamental Combustion Properties

The data presented in the preceding section of this chapter indicate that the combustion reaction step can be a rate-controlling step in the turbojet combustion process. An analysis based on this fact provided a possible means of predicting the effects of operating variables on combustion efficiency. Other attempts to define

the rate-controlling step have considered fundamental combustion properties of fuels, such as burning velocity, minimum ignition energy, inflammability limit, or quenching distance. The data required to develop possible relations between these factors and combustion efficiency have been obtained (1) with fuels having different fundamental combustion properties (refs. 5, 37, and 38) and (2) with various inlet oxygen-nitrogen mixtures (refs. 19 and 34).

Minimum spark-ignition energy. - A comparison of the effect of pressure and oxygen concentration on minimum spark-ignition energy and combustion efficiency of isooctane fuel was made (ref. 34) using values of minimum spark-ignition energy arbitrarily taken at the equivalence ratios giving the lowest values of energy. The following approximate relation for combustion efficiency η_b, combustor-inlet pressure p_i, and minimum spark-ignition energy E_m was developed for data obtained in the single tubular combustor at constant inlet-air temperature, air flow rate, and fuel-air ratio:

$$\eta_b = f\left(\frac{p_i^2}{E_m}\right) \tag{4}$$

The correlation at one fuel-air ratio with liquid isooctane fuel is shown in figure 97. Similar correlations were obtained at other fuel-air ratios.

Attempts were made in the same manner to correlate data obtained with gaseous propane (ref. 19), but there was no consistent relation between combustion efficiency and minimum spark-ignition energy. The inability to obtain a satisfactory correlation was attributed to large errors arising in the required extrapolation of the ignition-energy data. Results obtained in turbojet combustor tests with wide varieties of fuels (refs. 5, 37, and 38) indicate no consistent relation between minimum spark-ignition energy and turbojet combustion efficiency.

Quenching distance. - It has been found (ch. III) that, over wide ranges of pressure and oxygen concentration, quenching distance d and minimum spark-ignition energy E_m are approximately related by the expression

$$E_m = kd^2$$

where k is a constant. Quenching distance would, therefore, be expected to correlate satisfactorily the combustion efficiency data obtained with isooctane in reference 34 but not to correlate the date of references 5, 19, 37, and 38. Attempts to correlate the combustion-efficiency data obtained with gaseous propane (ref. 19) with quenching-distance data for propane (ref. 39) have not been successful.

Burning velocity. - Another combustion characteristic of interest in the evaluation of combustor performance is burning velocity. Basic investigations of burning velocity are discussed extensively in chapter IV, and certain relations are developed to show the effect of variables on burning velocity. An effort is made in reference 34 to relate basic burning-velocity considerations to combustor performance data obtained with varying inlet oxygen concentration. The equation developed in reference 34 relates combustion efficiency and maximum laminar-flame speed u_f by the expression

$$\eta_b = f\left(p_i^{1/3}\frac{u_f}{V_r}\right) \tag{5}$$

This equation assumes constant inlet-air temperature and constant flow rate of fuel and oxygen-nitrogen mixture. For constant inlet temperature and for flame speed assumed independent of pressure and Reynolds number (ref. 36), the maximum flame

speed of at least some fuel oxygen-nitrogen mixtures has been found to be proportional to the term $(\alpha - K)$ (ch. IV), where K is a constant dependent on fuel type, and α is the oxygen concentration by percent. Substitution of this term in equation (5) gives

$$\eta_b = f\left[\frac{p_i^{1/3}\ (\alpha - K)}{V_r}\right] \tag{6}$$

As shown in figure 98(a), the flame-speed parameter of equation (6) satisfactorily correlates combustion-efficiency data obtained with liquid isooctane (K = 12) at one fuel-air ratio and over a range of combustor-inlet pressure and oxygen concentration. Equally satisfactory correlations were obtained at other fuel-air ratios. Equation (6) was also found to be suitable for correlation of gaseous-propane (K = 11.5) data (ref. 19), as shown in figure 98(b).

Investigations conducted with five different hydrocarbon fuels in a turbojet combustor (ref. 5) indicated that the most consistent performance trends were obtained with maximum fundamental burning velocity. Combustion efficiency generally increased with an increase in burning velocity. Exceptions to this trend occurred, particularly at very low air-flow rates, indicating the presence of other controlling factors not considered. Other fundamental combustion properties that were considered in reference 5 included minimum ignition energy, spontaneous-ignition temperature, and flammability range. The fuels that were chosen have minimum variations in physical properties. With this restriction the possible range in combustion properties was necessarily quite small.

Investigations of 13 hydrocarbon and nonhydrocarbon fuels having considerably greater variation in combustion properties are reported in reference 37. Tests were conducted in the same combustor and at the same operating conditions as those used in reference 5. Figure 99 shows the variation in combustion efficiency with maximum burning velocity for the data of references 5 and 37 at one of the two inlet-air temperatures investigated. Included in the figure are comparable combustion-efficiency data obtained with isooctane and varying mixtures of oxygen and nitrogen (ref. 34). There is a definite trend towards an increase in combustion efficiency with an increase in maximum burning velocity. Nevertheless, wide deviations from the single curve are apparent. Less distinct trends were obtained with the other fundamental combustion properties.

The 18 fuels represented in figure 99 vary markedly not only in composition, including hydrocarbons, oxygenated hydrocarbons, and fuels containing nitrogen, sulfur, and silicon, but also in physical properties, particularly those reflecting vaporization rate. Consequently, the fundamental burning velocity u_f was combined, empirically, with the latent heat of vaporization H into the correlating parameter $u_f/H^{0.33}$. Figure 100, which shows the relation between this empirical parameter and combustion efficiency using data of figure 99, indicates some degree of correlation; however, several fuels, notably carbon disulfide, deviate considerably from the faired curve.

The range of combustion properties represented by the data of references 5 and 37 was considerably greater than would be encountered in conventional, readily available turbojet fuels; therefore, insofar as combustion efficiency is concerned, fuel composition is not regarded as an important factor in the selection of fuels for general operational use. Evidence that the rate of combustion reactions may influence the performance of the combustor at some conditions of operation has led many investigators to study the effectiveness of fuel additives. A large number of additives have been examined, including oxygenated materials and organo-metallic

compounds, but in general, no significant improvements in combustion efficiency have been noted. These observations are consistent with results of fundamental studies described in chapter IV.

Significance of Combustion-Efficiency Correlations

Satisfactory correlations between combustion efficiency and operating variables have resulted from assumptions that the efficiency was limited by either (1) the rate of oxidation of the fuel or (2) the rate of spreading of the flame into unburned mixture. These assumptions yielded two distinct correlating parameters, $p_i T_i / V_r$ from the reaction-kinetics analysis and $p_i^{1/3} u_f / V_r$ from the flame-spreading analysis. The parameter $p_i^{1/3} u_f / V_r$ is applicable only for conditions of constant combustor inlet-air temperature. For a given fuel, a more general form of this parameter that includes the inlet-air temperature as a variable but neglects the effect of pressure and Reynolds number on flame speed is $p_i^{1/3} T_i^{1.1} / V_r$ (ref. 40). The similarities between the two parameters derived by different methods of analysis are now apparent. Since the exponents of the pressure and temperature variables are not the same in the two cases, it is also apparent that both parameters will not adequately correlate combustion-efficiency data obtained over wide ranges of inlet-air conditions.

The chemical reaction parameter $p_i T_i / V_r$ is equal to a dimensional constant times the parameter p_i^2 / w_a, where w_a is air-flow rate. The flame-spreading parameter $p_i^{1/3} T^{1.1} / V_r$ is, similarly, equivalent to a dimensional constant times $p^{1.3} T_i^{0.1} / w_a$. The ratio of exponents on the pressure and air-flow terms in the two cases are 2 and 1.3, respectively.

Tests were conducted in a turbojet combustor operating on gaseous propane fuel over a wide range of pressure and air flow in order to determine experimental values of the exponents (ref. 40). Representative results at one fuel-air ratio are shown in figure 101. The slope of a line indicates the ratio of exponents of the correlating parameter that best fits the experimental data. At low values of pressure and weight flow, the slope is about 2, which corresponds to that predicted by the reaction-kinetics parameter. At high values of air flow and pressure, the slope is about 1.3, a value corresponding to that of the flame-spreading parameter. These data indicate a shift from one rate-controlling process to another as combustor operating conditions are varied through wide ranges. The fact that the reaction-kinetics parameter appears to control combustion only at very low-pressure conditions might be attributed to the dependence of the chemical reaction on the square of the pressure. At the higher pressures, the reaction is very rapid and is no longer the rate-controlling step.

The correlations of combustion efficiency with the reaction-kinetics and the flame-spreading parameters are based on very limited data obtained over a relatively narrow range of operating and design variables. Hence, the conclusions drawn from the correlations must be considered very tentative.

The conversion processes just discussed are not, of course, the only ones that might be considered to limit combustion efficiency. Theoretical analyses have been made at the Lewis laboratory assuming one of the following as the rate-determining step: (1) fuel vaporization, (2) fuel-air turbulent mixing, and (3) fuel droplet burning (ref. 41). With each of these assumptions, however, the theoretical predicted effects of operating variables on combustion efficiency differed markedly from the effects observed experimentally. Nevertheless, empirical correlations have

been developed that illustrate a very important effect of at least one of these steps, fuel vaporization. In figure 100, for example, combustion efficiency was correlated with the parameter $u_r/H^{0.33}$. Data presented in figure 102 (ref. 42) indicate a relation between combustion efficiency and the Sauter mean diameter of the fuel spray, combustion efficiency increasing as the mean fuel drop size decreases. This relation and that shown in figure 100 both predict an increase in efficiency with an increase in the rate of fuel vaporization. The data presented in figure 65(b) indicate that reduced efficiencies can result from either too fine or too coarse a degree of atomization, depending upon the operating conditions. Thus, although fuel atomization and vaporization factors have marked influences on combustor performance, they may not be used successfully to correlate combustion-efficiency data over a wide range of conditions.

The preceding discussion indicates that either of at least two of the conversion processes that occur in the turbojet combustor, fuel vaporization, or combustion, may be rate-controlling, depending upon the choice of operating conditions and combustor design. Furthermore, the ways in which each step limit the conversion process may vary with operating conditions. It is reasonable to expect, then, that the combustion-efficiency trends of the turbojet combustor will be completely described only by a complex parameter that accounts for changes in the rate-controlling steps with changes in operating conditions.

Methods of Estimating Combustion Efficiency of Turbojet Combustor

The preceding discussions have illustrated several methods by which combustion efficiency has been correlated with combustor operating variables. The simplified form p_1T_1/V_r of the reaction-kinetics parameter (eq. (2)) was chosen in further investigations (ref. 43) to develop a convenient method for estimating combustion efficiency at altitude flight conditions from a minimum quantity of combustor test data.

The method developed is illustrated in figure 103. Sections I, II, and III of the figure convert the effects of pressure ratio, flight Mach number, air-flow rate per unit cross-sectional area, and flight altitude on combustor-inlet variables into the parameter V_r/p_1T_1. In section IV of the chart, V_r/p_1T_1 is plotted against combustion efficiency for three combustors to give typical correlation curves. The combustion parameter is inverted from the form presented in preceding figures, because the reciprocal form V_r/p_1T_1 was found, in reference 17, to give very nearly straight line relations on linear coordinates.

Use of figure 103 requires that the following data be available for the particular combustor and engine under consideration: (1) sufficient combustor data for establishing the V_r/p_1T_1 correlation and (2) the sea-level static performance of the engine (for establishing air-flow rate, pressure ratio, and turbine-inlet temperature at various engine speeds). With these data, it is possible to select, in order, the pressure ratio and the flight Mach number (sec. I), the air-flow rate (sec. II), and the altitude (sec. III), and to predict the combustion efficiency that would be obtained with any combustor for which the correlation curve is plotted in section IV. The values of pressure ratio and air-flow rate at the desired altitude conditions are determined from plots of these variables against the corrected engine speed $N/\sqrt{\theta}$.

The chart is based on the assumption that the operating characteristics of engine components other than the combustor do not vary with changes in altitude; that is,

corrected air-flow rates, pressures, and temperatures of these components are assumed to be unique functions of corrected engine speed. It must also be recognized, of course, that the accuracy of prediction is no greater than the accuracy of the relation between V_r/p_iT_i and combustion efficiency. As discussed previously in this chapter, some combustors may give very poor correlations, particularly if combustion efficiency varies appreciably with fuel-air ratio.

CORRELATION OF OPERATING VARIABLES WITH COMBUSTION LIMITS

At high-altitude operating conditions turbojet engines may encounter an altitude operational limit (figs. 59 and 74). As in the case of combustion efficiency, attempts have been made to correlate these limits with operating variables. In addition to facilitating prediction of full-scale engine operating characteristics from limited laboratory tests, such correlations indicate the relative importance of the various operating variables concerned.

Altitude operational limits occur when the combustor is unable to supply the temperature rise required to operate the engine at the desired altitude and engine-speed conditions (fig. 61). Although the lean fuel-air-ratio limit may, in some engines, restrict the idling speed of the engine, the rich limit (maximum temperature rise) will usually establish the altitude ceiling in the normal operating speed range. For this reason, the maximum-temperature-rise characteristics of combustors have been emphasized in most combustion studies, and the correlations discussed herein consider only these characteristics.

The combustor inlet-air variables that affect the maximum combustor temperature rise include inlet-air pressure, temperature, and velocity. The effects of these variables on stability are, in many cases, similar to their effects on combustion efficiency; thus, as pressure and temperature are decreased, and as velocity is increased, the maximum combustor temperature rise is generally reduced. As a result of these trends, correlations of similar form have been developed for both combustion stability and combustion efficiency. The maximum combustor temperature rise obtainable at selected flow conditions is correlated with a modification of the combustion-efficiency parameter p_iT_i/V_r in reference 44. Typical data are presented in figure 104, with the ratio of maximum temperature rise to combustor inlet temperature plotted against the factor $p_i^{1.46}/w_a$ for two laboratory-scale and three full-scale combustors. For a given combustor inlet temperature, higher combustor temperature rises are obtainable at higher pressures and lower velocities (lower air flows).

Additional data obtained in laboratory-scale and full-scale prevaporizer combustors are correlated with a slightly modified parameter ($\sqrt{p_iT_i}/V_r$), which is proportional to $p_i^{1.5}/w_a$, in references 45 and 46. Stability-limit data obtained at the Lewis laboratory in two full-scale combustors (refs. 3 and 5) are plotted against the modified parameter $\sqrt{p_iT_i}/V_r$ of reference 45 in figure 105. A fair correlation was obtained. For comparison purposes the stability data of figure 105 are replotted against the combustion-efficiency parameter p_iT_i/V_r in figure 106. Some increase in scatter of data points is noted in figure 106.

Correlating parameters of the form $p_i^nT_i/V_r$ can be used in conjunction with charts similar to that shown in figure 103 to predict altitude operational limits of a turbojet engine. For example, maximum-temperature-rise values could be plotted against p_iT_i/V_r in section IV of figure 103. Comparisons of the maximum temperature rise obtainable with the combustor and the temperature rise required by the

[redacted]

engine at various operating conditions would establish the altitude operational limits of the engine. A chart similar to the one shown in figure 103 could also be constructed by using the parameter $\sqrt{p_i T_i}/V_r$.

Fuel variables, as well as operating variables, affect maximum obtainable temperature rise. With very limited data, a relation is established in reference 5 between maximum temperature rise and the maximum burning velocity of the fuel. This relation is shown in figure 107, where maximum temperature rise generally increased with an increase in burning velocity. However, at some conditions the results obtained with n-heptane deviate from the general trend. Other fundamental combustion characteristics examined in the investigation of reference 5 did not indicate consistent trends.

From the data presented herein it may be concluded that some degree of correlation has been obtained between maximum temperature rise and parameters of the form $p_i{}^n T_i/V_r$. The correlations indicate the relative effect of operating variables on stability; however, only approximate estimates of engine performance can be obtained at the present time by use of the correlations. Research also indicates some relation between temperature-rise limits and the fundamental flame speed of the fuel. The degree of correlation obtained in these investigations may be influenced significantly by the accuracy of the combustion data considered; data obtained at or near blow-out conditions are frequently difficult to reproduce.

EFFECT OF COOLANT INJECTION ON COMBUSTOR PERFORMANCE

The maximum thrust output of a turbojet engine may be increased, particularly for short periods of operation as in take-off and combat maneuvering, by the injection of a liquid coolant into the airstream. Coolants such as water, water-alcohol mixtures, and ammonia have been injected into the engine inlet, the compressor, and the combustion chambers (refs. 47 to 49) to provide thrust increases of 20 to 25 percent. The quantity of coolant injected, and, hence, the thrust increase, is limited by combustion performance of both the primary combustor and the afterburner (refs. 48 and 49).

The ratios of augmented to normal combustion efficiencies obtained in a turbojet engine equipped with water-alcohol injection ports in tubular combustors (fig. 108) are presented in figure 109 (ref. 47). At altitudes of 30,000 to 50,000 feet combustion efficiency decreased only slightly as the liquid-air ratio was increased to approximately 0.10 (liquid: 30 percent alcohol, 70 percent water). Analysis of the data indicates that at least a part of the alcohol that was introduced burned within the combustion chambers. The effect of coolant injection on combustion efficiency appears to be most significant at the lower altitudes; at sea-level, with a variable exhaust nozzle, combustion efficiency decreased rapidly with an increase in liquid-air ratio above about 0.06. The loss in efficiency at low altitudes was attributed to the greater penetration of the coolant at the higher liquid flow rates (hence, higher pressure drops) required. It may be assumed that the penetrating coolant jet quenched volumes of fuel-air mixture that had not yet burned.

In another investigation (ref. 48) the effect of alcohol-water injection on the combustion efficiency of a tail-pipe burner was determined. Combustion efficiency was reduced as much as 35 percent at some fuel-air-ratio conditions; a reduction of 25 percent was observed at the optimum tail-pipe fuel-air ratio. Unstable operation of the tail-pipe burner accompanied the rapid decrease in combustion efficiency. A similar investigation (ref. 49) using anhydrous liquid ammonia injected at the compressor inlet indicated no loss in combustion efficiency at stoichiometric mixture

conditions (including the ammonia as a combustible). Operation at leaner or richer than stoichiometric mixtures resulted in significant decreases in combustion efficiency. Calculations made in reference 50 indicate that approximately 35 percent of the ammonia burned in the engine combustion chambers at high weight flows of ammonia, permitting a decrease in fuel-flow rate.

An investigation (ref. 51) was conducted in a direct-connect-duct installation to determine the effect of water injection on the maximum obtainable combustor temperature rise in a combustor similar to those used in the engine of reference 48. Water was injected from spray nozzles located (1) ahead of the combustor-inlet station, (2) in the upstream end of the combustor liner, (3) halfway along the length of the combustor liner, and (4) in the downstream end of the combustor. With water injection at the first two stations, no indications of liquid water at the combustor outlet were present. With water injection at the last two stations, liquid water in the exhaust was observed at high liquid-air ratios. Figure 110 presents results of this investigation in terms of the variation in maximum total liquid-air ratio with altitude for each of the four injection stations. The maximum liquid-air ratio was limited by either flame blow-out or inability of the combustor to attain the required temperature rise at the rated-engine-speed conditions investigated. The total liquid-air ratio was most severely limited at the lowest and the highest altitudes investigated. Higher liquid-air ratios could be tolerated when the coolant was injected farther downstream in the combustion chamber (stations 3 and 4).

The effect of water injection on combustion is also of significance in considering flight of turbojet-powered aircraft through heavy precipitation. Figure 111 shows the maximum atmospheric water-air ratios that might be expected, based on a precipitation rate of 33.5 inches per hour measured over a 10-minute period and over an area of 1.0 square mile (ref. 52). The curve representing the limiting water-air ratios that could be tolerated, at rated engine speed, by the combustor of reference 51 is included in figure 111. This curve was obtained with water injection 62 inches upstream of the combustor (station 1). Comparison of the curves of figure 111 indicates that no combustion problems should result from ingestion of water by a turbojet engine operating in heavy rainfall. The data were obtained for only one turbojet combustor design, however, and other designs could conceivably be more sensitive to water ingestion.

EFFECT OF AIR-FLOW FLUCTUATIONS ON COMBUSTOR PERFORMANCE

Chapter XI discusses the phenomenon of compressor surge and associated unsteady-state flow conditions existing in turbojet engines during engine acceleration or deceleration. It is pointed out that during transient operation unfavorable mixture conditions may exist in the combustor, resulting in flame blow-out. The discussion (ch. XI) considers primarily the effects of fuel-flow-rate changes on combustor blow-out. It would be expected that rapid changes in air-flow rates resulting from pressure surging may also affect mixture conditions and, hence, flame blow-out characteristics. Another phenomenon that may be considered to cause flow fluctuations is combustion resonance, which has been observed in both single-burner and full-scale-engine test units. The following discussion describes typical effects of flow oscillations, caused by either air-supply fluctuations or burner resonance, on the performance of turbojet combustors.

The variation of combustor temperature rise with fuel-air ratio obtained in an annular combustor operating over a range of air-flow rate and inlet-air temperature is shown in figure 112(a) (ref. 3). Regions of resonating combustion observed in the tests are denoted in the figure by dashed curves. The faired curve representing an air-flow rate of 11.2 pounds per second has been modified somewhat from that

presented in reference 3 in order to show more clearly the effect of combustion resonance on performance. Resonant combustion occurred at the higher fuel-air ratios and was accompanied by a decrease in combustor temperature rise and in combustion efficiency based on theoretical temperature rise. Reductions in efficiency that accompanied combustion resonance were more pronounced and were evident over wider ranges of fuel-air ratio as the air-flow rate was increased and the inlet-air temperature was decreased. The resonance encountered in the regions of the dashed curves was described in reference 3 as "temperature fluctuations at combustor outlet" accompanied by either "rapid flickering at base of flame" or "noisy vibration of combustor and adjacent ducting." In general, the resonant combustion was encountered at conditions that approached the operational limits of the combustor.

3080

Similar data were obtained in a single tubular combustor operating over a range of fuel-air ratio and air-flow rate at constant inlet-air pressure and inlet-air temperature; typical results are presented in figure 112(b). In the tubular combustor, resonance was observed only at the lower air-flow rates. Combustor temperature rise and, hence, combustion efficiency increased when resonance occurred in the tubular combustor, whereas in the annular combustor, efficiency decreased (fig. 112(a)). This difference in trend may be attributed to differences in combustor design, operating conditions, fuel characteristics, or to differences in the characteristics of the resonance encountered. A variable-area fuel nozzle operating at a constant pressure differential of 25 pounds per square inch was used to obtain the data shown in figure 112(b). Since it was considered possible for the spring-loaded mechanism in this nozzle to incite the observed resonance, tests were repeated with a fixed-area nozzle. Similar trends were observed, but resonance generally occurred at lower fuel-air ratios with the smaller, fixed-area nozzle.

Data obtained in the same tubular combustor with three fuels varying both in hydrocarbon type and in volatility are presented in figure 113. At these conditions, resonant combustion, accompanied by an increase in performance, occurred with all three fuels. However, the fuel-air ratio and the temperature rise at which resonance first occurred varied with the fuel used. Other data obtained with a number of fuels at various operating conditions in a similar tubular combustor (table II, ref. 5) indicate that combustion resonance was encountered at certain operating conditions; however, no significant effects of the resonance on performance were observed. No explanation for variations in the observed effects of resonance on performance is apparent from the limited data available.

The investigation reported in reference 53 was an attempt to study more thoroughly the effect of inlet-air flow fluctuations on the performance of a 2-inch-diameter turbojet-type combustor. By varying the rotative speed of an inlet-air butterfly valve, an oscillating flow of controllable frequency could be supplied to the small-scale combustor. Figure 114 shows the effect of oscillation frequency on combustion efficiency of two fuels at two operating conditions in the small-scale combustor. At the higher pressure and air-flow rate (fig. 114(a)), an increase in oscillation frequency increased combustion efficiency slightly; at the lower pressure and air-flow rate (fig. 114(b)), an increase in oscillation frequency decreased combustion efficiency. A maximum reduction in combustion efficiency of 15 percent was observed with isooctane fuel with an oscillatory frequency of about 180 cycles per second.

The effect of the oscillation frequency on the maximum stable temperature rise of the combustor is shown in figure 115. As frequency was increased, the maximum temperature rise decreased rapidly, reached a minimum value, and then increased. Similar trends were observed with the two fuels investigated, n-heptane and isooctane. The greatest effect of the induced oscillations on the maximum temperature rise was observed at a frequency of about 80 cycles per second. Data obtained in the same combustor at a lower pressure and a lower air flow (ref. 53) showed that the maximum reduction in temperature-rise limit occurred at a lower frequency of about 40 cycles per second.

[redacted]

From the data presented herein it is concluded that air-flow fluctuations may affect the performance of turbojet combustors. The nature and the degree of the effects are apparently functions of combustor operating conditions, combustor design, fuel characteristics, and possibly combustor accessory ducting. The frequency and perhaps the amplitude of the fluctuations influence the results obtained. Basic considerations of combustion suggest that flow fluctuations probably affect combustion performance by (1) varying the degree of turbulence in the flame zone, (2) altering air-distribution characteristics, (3) altering fuel-spray characteristics, and (4) rapidly shifting the flame front in and out of favorable combustion zones. A more complete discussion of the causes and characteristics of combustion resonance may be found in chapter VIII.

SIGNIFICANCE OF COMBUSTION EFFICIENCY AND STABILITY DATA IN COMBUSTOR DESIGN

Reduced combustion efficiency and stability of turbojet combustors at high-altitude operating conditions seriously limit the usefulness of the turbojet engine. Examination of the basic factors affecting these performance characteristics indicates that decreased combustor inlet-air temperature and pressure and increased air velocities result in decreased efficiencies and stability. The effects of these combustor inlet-air variables on combustion efficiency are correlated by several parameters derived from theoretical considerations of (1) flame velocity, (2) minimum ignition energy, and (3) reaction kinetics. A simplified form of a reaction-kinetics parameter $V_r/p_i T_i$ appears generally satisfactory for much of the combustion data considered. Its application to the problem of predicting combustion efficiencies of a given combustor in full-scale engines at flight conditions has been described. Parameters of the same general form may also be used to correlate combustion-limit data, allowing estimates to be made of the altitude operational limits of a turbojet engine.

In addition to the inlet-air variables, the over-all fuel-air ratio has very important effects on combustor performance; overlean or overrich fuel-air mixtures in the combustion zone result in decreased efficiencies and in flame blow-out. The fuel-air-mixture conditions are influenced by three factors: (1) fuel atomization and distribution characteristics, (2) fuel vaporization rate, and (3) air admission patterns. Optimum performance of the combustor is obtained only if all these factors are tailored to one another.

The magnitude of the effects of fuel-air-mixture variables on combustor performance depends upon the severity of the inlet-air conditions. More accurate control of these variables is required as inlet-air pressure or temperature is reduced or as air velocity is increased. Thus, the problem of designing high-performance combustors becomes more difficult as the operating altitudes of aircraft are increased and as the air-handling capacities of engines and, hence, combustor flow rates are increased.

REFERENCES

1. Hibbard, Robert R., Drell, Isadore L., Metzler, Allen J., and Spakowski, Adolph E.: Combustion Efficiencies in Hydrocarbon-Air Systems at Reduced Pressures. NACA RM E50G14, 1950.

2. Sobolewski, Adam E., Miller, Robert R., and McAulay, John E.: Altitude Performance Investigation of Two Single-Annular Type Combustors and the Prototype J40-WE-8 Turbojet Engine Combustor with Various Combustor-Inlet Air Pressure Profiles. NACA RM E52J07, 1953.

3. Childs, J. Howard, McCafferty, Richard J., and Surine, Oakley W.: Effect of Combustor-Inlet Conditions on Performance of an Annular Turbojet Combustor. NACA Rep. 881, 1947. (Supersedes NACA TN 1357.)

4. McCafferty, Richard J.: Liquid-Fuel-Distribution and Fuel-State Effects on Combustion Performance of a Single Tubular Combustor. NACA RM E51B21, 1951.

5. Wear, Jerrold D., and Dittrich, Ralph T.: Performance of Pure Fuels in a Single J33 Combustor. I - Five Liquid Hydrocarbon Fuels. NACA RM E52J03, 1952.

6. Wear, Jerrold D., and Jonash, Edmund R.: Combustion-Efficiency and Altitude-Limit Investigations of Five Fuels in an Annular Turbojet Combustor. NACA RM E7L30, 1948.

7. Topper, Leonard: Radiant Heat Transfer from Flames in a Single Tubular Turbojet Combustor. NACA RM E52F23, 1952.

8. Hall, A. R., and Diederichsen, J.: An Experimental Study of the Burning of Single Drops of Fuel in Air at Pressures up to Twenty Atmospheres. Fourth Symposium (International) on Combustion, The Williams & Wilkins Co. (Baltimore), 1953, pp. 837-846.

9. Harp, James L., Jr., and Vincent, Kenneth R.: Altitude Performance Investigation of Single- and Double-Annular Turbojet-Engine Combustors with Various Size Fuel Nozzles. NACA RM E51L14, 1952.

10. McCafferty, Richard J.: Effect of Fuels and Fuel-Nozzle Characteristics on Performance of an Annular Combustor at Simulated Altitude Conditions. NACA RM E8C02a, 1948.

11. Gold, Harold, and Straight, David M.: Gas-Turbine-Engine Operation with Variable-Area Fuel Nozzles. NACA RM E8D14, 1948.

12. Gold, H., and Rosenzweig, S.: Altitude Operation of Gas-Turbine Engine with Variable-Area Fuel-Nozzle System. NACA RM E51A04, 1951.

13. Butze, Helmut F., and Jonash, Edmund R.: Turbojet Combustor Efficiency with Ceramic-Coated Liners and with Mechanical Control of Fuel Wash on Walls. NACA RM E52I25, 1952.

14. Straight, David M., and Gernon, J. Dean: Photographic Studies of Preignition Environment and Flame Initiation in Turbojet-Engine Combustors. NACA RM E52I11, 1953.

15. Godsave, G. A. E.: The Burning of Single Drops of Fuel. Pt. III. Comparison of Experimental and Theoretical Burning Rates and Discussion of the Mechanism of the Combustion Process. Rep. R.88, British N.G.T.E., Aug. 1952.

16. Dittrich, Ralph T.: Combustion-Efficiency Investigation of Special Fuels in Single Tubular-Type Combustor at Simulated Altitude Conditions. NACA RM E7F11, 1947.

17. Norgren, Carl T., and Childs, J. Howard: Effect of Liner Air-Entry Holes, Fuel State, and Combustor Size on Performance of an Annular Turbojet Combustor at Low Pressures and High Air-Flow Rates. NACA RM E52J09, 1953.

[redacted]

18. Longwell, J. P., Van Sweringen, R. A., Jr., Weiss, M. A., and Hatt, F. G.: Preparation of Air-Fuel Mixtures for Ramjet Combustors. Bumblebee Ser. Rep. No. 168, Esso Labs., Standard Oil Dev. Co., Nov. 1951. (Contract NOrd 9233 with Bur. Ord., U.S. Navy.)

19. Graves, Charles C.: Effect of Inlet Oxygen Concentration on Combustion Efficiency of J33 Single Combustor Operating with Gaseous Propane. NACA RM E53A27, 1953.

20. Sharp, J. G.: Fuels for Gas-Turbine Aero-Engines. Aircraft Eng., vol. XXIII, no. 263, Jan. 1951, pp. 2-8.

21. Jones, Anthony W., and Cook, William P.: Combustion Efficiency Performance of a MIL-F-5624 Type Fuel and Monomethylnaphthalene in a Single Vaporizing-Type Combustor. NACA RM E51K30, 1952.

22. McCafferty, Richard J.: Vapor-Fuel-Distribution Effects on Combustion Performance of a Single Tubular Combustor. NACA RM E50J03, 1950.

23. Norgren, Carl T., and Childs, J. Howard: Effect of Fuel Injectors and Liner Design on Performance of an Annular Turbojet Combustor with Vapor Fuel. NACA RM E53B04, 1953.

24. Pavia, R. E.: The Derwent V Combustor with Separated Air Supplies. (ii) The Effects of Primary and Dilution Air Flows. Engines Note 157, Aero. Res. Labs., Dept. Supply, Commonwealth of Australia, Nov. 1951.

25. Dittrich, Ralph T.: Investigation of Low-Pressure Performance of Experimental Tubular Combustors Differing in Air-Entry-Hole Geometry. NACA RM E53G01, 1953.

26. Scull, Wilfred E.: High-Altitude Performance of 9.5-Inch-Diameter Tubular Experimental Combustor with Fuel Staging. NACA RM E54A06, 1954.

27. Mark, Herman, and Zettle, Eugene V.: Axial-Slot Air Admission for Controlling Performance of a One-Quarter-Annulus Turbojet Combustor and Comparison with Complete Engine. NACA RM E52A21, 1952.

28. Norgren, Carl T., and Childs, J. Howard: Performance of an Annular Turbojet Combustor Having Reduced Pressure Losses and Using Propane Fuel. NACA RM E53G24, 1953.

29. Zettle, Eugene V., Norgren, Carl T., and Mark, Herman: Combustion Performance of Two Experimental Turbojet Annular Combustors at Conditions Simulating High-Altitude Supersonic Flight. NACA RM E54A15, 1954.

30. Longwell, John P., Frost, Edward E., and Weiss, Malcolm A.: Flame Stability in Bluff Body Recirculation Zones. Ind. and Eng. Chem., vol. 45, no. 8, Aug. 1953, pp. 1629-1633.

31. Avery, W. H., and Hart, R. W.: Combustor Performance with Instantaneous Mixing. Ind. and Eng. Chem., vol. 45, no. 8, Aug. 1953, pp. 1634-1637.

32. Childs, J. Howard: Preliminary Correlation of Efficiency of Aircraft Gas-Turbine Combustors for Different Operating Conditions. NACA RM E50F15, 1950.

33. Lewis, Bernard, and von Elbe, Guenther: Combustion, Flames and Explosions of Gases. Academic Press, Inc. (New York), 1951, pp. 303-304; 405-407; 460-467.

[redacted]

34. Graves, Charles C.: Effect of Oxygen Concentration of the Inlet Oxygen-Nitrogen Mixture on the Combustion Efficiency of a Single J33 Turbojet Combustor. NACA RM E52F13, 1952.

35. Hottel, H. C., Williams, G. C., and Satterfield, C. H.: Thermodynamic Charts for Combustion Processes. Pts. I and II. John Wiley & Sons, Inc., 1949.

36. Jost, Wilhelm: Explosion and Combustion Processes in Gases. McGraw-Hill Book Co., Inc., 1946, p. 437.

37. Smith, Arthur L., and Wear, Jerrold D.: Performance of Pure Fuels in a Single J33 Combustor. II - Hydrocarbon and Nonhydrocarbon Fuels. NACA RM E55B02, 1955.

38. Calcote, H. F., et al.: Minimum Spark Energy Correlation with Ramjet and Turbojet Burner Performance. TP-36, Experiment, Inc., Richmond (Va.), Mar. 1950. (Final Rep. No. 1 to Bur. Aero. under Contract NOa(s) 10115.)

39. Berlad, Abraham L.: Flame Quenching by a Variable-Width Rectangular-Slot Burner as a Function of Pressure for Various Propane-Oxygen-Nitrogen Mixtures. NACA RM E53K30, 1954. (See also Jour. Phys. Chem., vol. 58, no. 11, Nov. 1954, pp. 1023-1026.)

40. Childs, J. Howard, and Graves, Charles C.: Relation of Turbine-Engine Combustion Efficiency to Second-Order Reaction Kinetics and Fundamental Flame Speed. NACA RM E54G23, 1954.

41. Graves, Charles C.: Burning Rates of Single Fuel Drops and Their Application to Turbojet Combustion Process. NACA RM E53E22, 1953.

42. Nicholson, H. M.: The Correlation of Combustion Efficiency and Burner Characteristics under Simulated Altitude Idling Conditions. Memo. No. M.113, British N.G.T.E., Apr. 1951.

43. Olson, Walter T., Childs, J. Howard, and Scull, Wilfred E.: Method for Estimating Combustion Efficiency at Altitude Flight Conditions from Combustion Efficiency at Altitude Flight Conditions from Combustor Tests at Low Pressures. NACA RM E53F17, 1953.

44. Britton, S. C., Schirmer, R. M., and Fox, H. M.: A Design Study for Equipment to Evaluate Performance of Aircraft Gas Turbine Fuels. Rep. No. 763-49R, Res. Dept., Phillips Petroleum Co., Oct. 12, 1949. (Final Rep. for Navy Contract NOa(s) 9596.)

45. Kittredge, G. D., and Fromm, E. H.: Evaluation of Fuel Characteristics in Thermojet Engine Combustion Processes. Prog. Rep. No. 6, Rep. No. 403-17-52R, Res. Div., Phillips Petroleum Co., 1952. (Navy Contract NOas 52-132-C.)

46. Schirmer, R. M., Kittredge, G. D., and Fromm, E. H.: Evaluation of Fuel Characteristics in Thermojet Engine Combustion Processes. Rep. No. 403-19-52R, Summary Rep., Phillips Petroleum Co., Jan. 1953. (Navy Contract NOas 52-132-C.)

47. Jansen, E. T., and Renas, P. E.: Altitude Investigation of Thrust Augmentation Using Water-Alcohol Injection into the Combustion Chambers of an Axial-Flow Turbojet Engine. NACA RM E52L12, 1953.

48. Useller, James W., and Povolny, John H.: Experimental Investigation of Turbojet-Engine Thrust Augmentation by Combined Compressor Coolant Injection and Tail-Pipe Burning. NACA RM E51H16, 1951.

[redacted]

49. Useller, James W., Harp, James L., Jr., and Fenn, David B.: Turbojet-Engine Thrust Augmentation at Altitude by Combined Ammonia Injection into the Compressor Inlet and Afterburning. NACA RM E52L19, 1953.

50. Harp, James L., Jr., Useller, James W., and Auble, Carmon M.: Thrust Augmentation of a Turbojet Engine by the Introduction of Liquid Ammonia into the Compressor Inlet. NACA RM E52F18, 1952.

51. Cook, William P., and Zettle, Eugene V.: Performance Investigation of Can-Type Combustor. II - Water Injection at Various Stations in Combustor. NACA RM E8F28, 1948.

52. Useller, James W., Lewis, William, and Zettle, Eugene V.: Effect of Heavy Rainfall on Turbojet Aircraft Operation. Aero. Eng. Rev., vol. 14, no. 2, Feb. 1955, pp. 40-42.

53. Schirmer, R. M., Fromm, E. H., and Kittredge, G. D.: Fuel Characteristics in Thermojet Engine Combustion Processes. Prog. Rep. No. 3, Res. Div., Phillips Petroleum Co., Apr. 15, 1953. (Navy Contract NOas 52-132-C.)

54. Hibbard, Robert R., Metzler, Allen J., and Scull, Wilfred E.: Low-Pressure Performance of Experimental Prevaporizing Tubular Combustor Using Approximately Stoichiometric Admission of Fuel-Air Mixture into the Primary Zone. NACA RM E54F25a, 1954.

55. Norgren, Carl T.: Performance of a Vaporizing Annular Turbojet Combustor at Simulated High Altitudes. NACA RM E54G21, 1954.

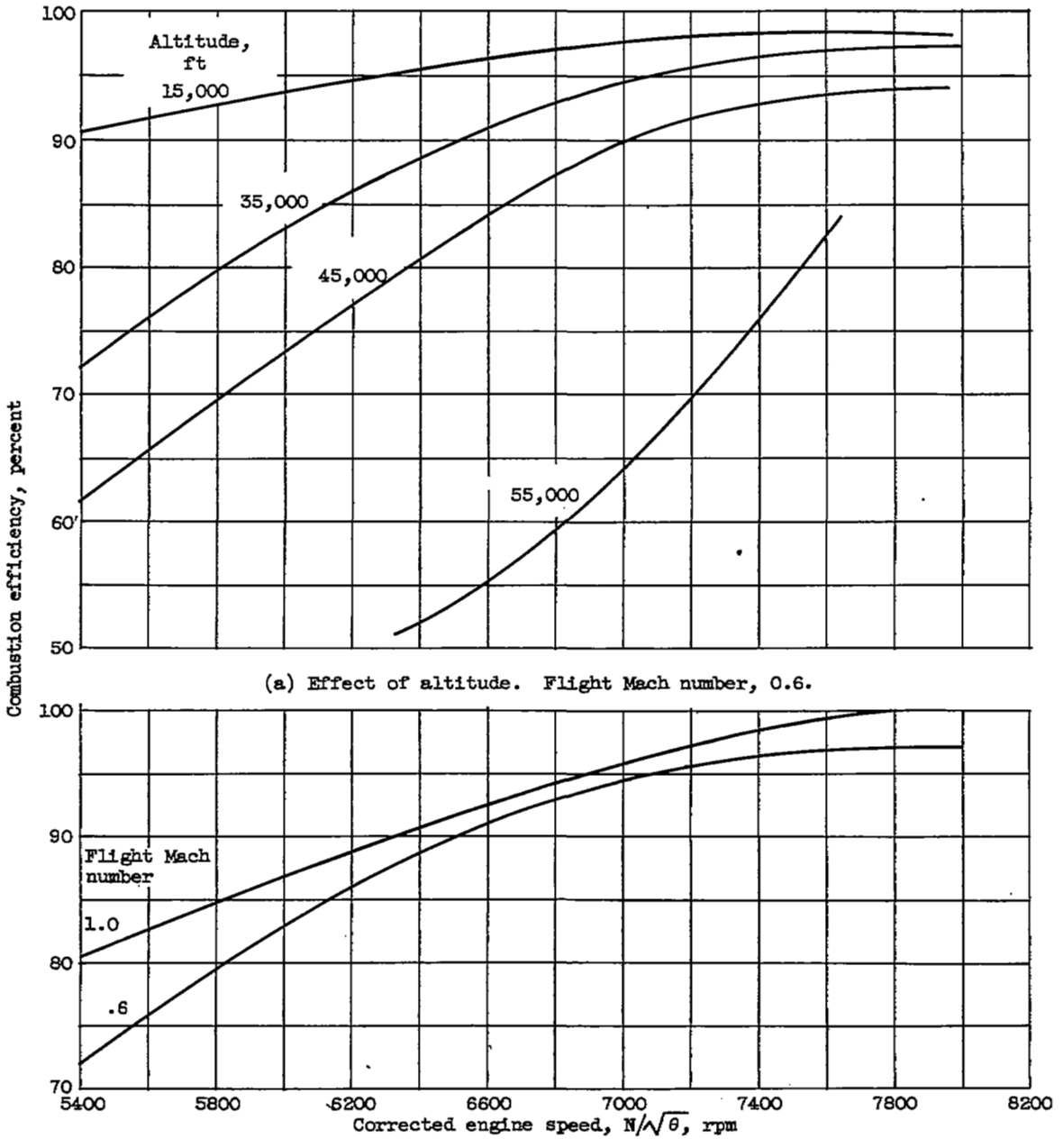

(a) Effect of altitude. Flight Mach number, 0.6.

(b) Effect of flight Mach number. Altitude, 35,000 feet.

Figure 58. - Effect of flight conditions on combustion efficiency of turbojet engine over range of engine rotational speed. Engine sea-level pressure ratio, 5; exhaust-nozzle area, 534 square inches (ref. 2).

[redacted]

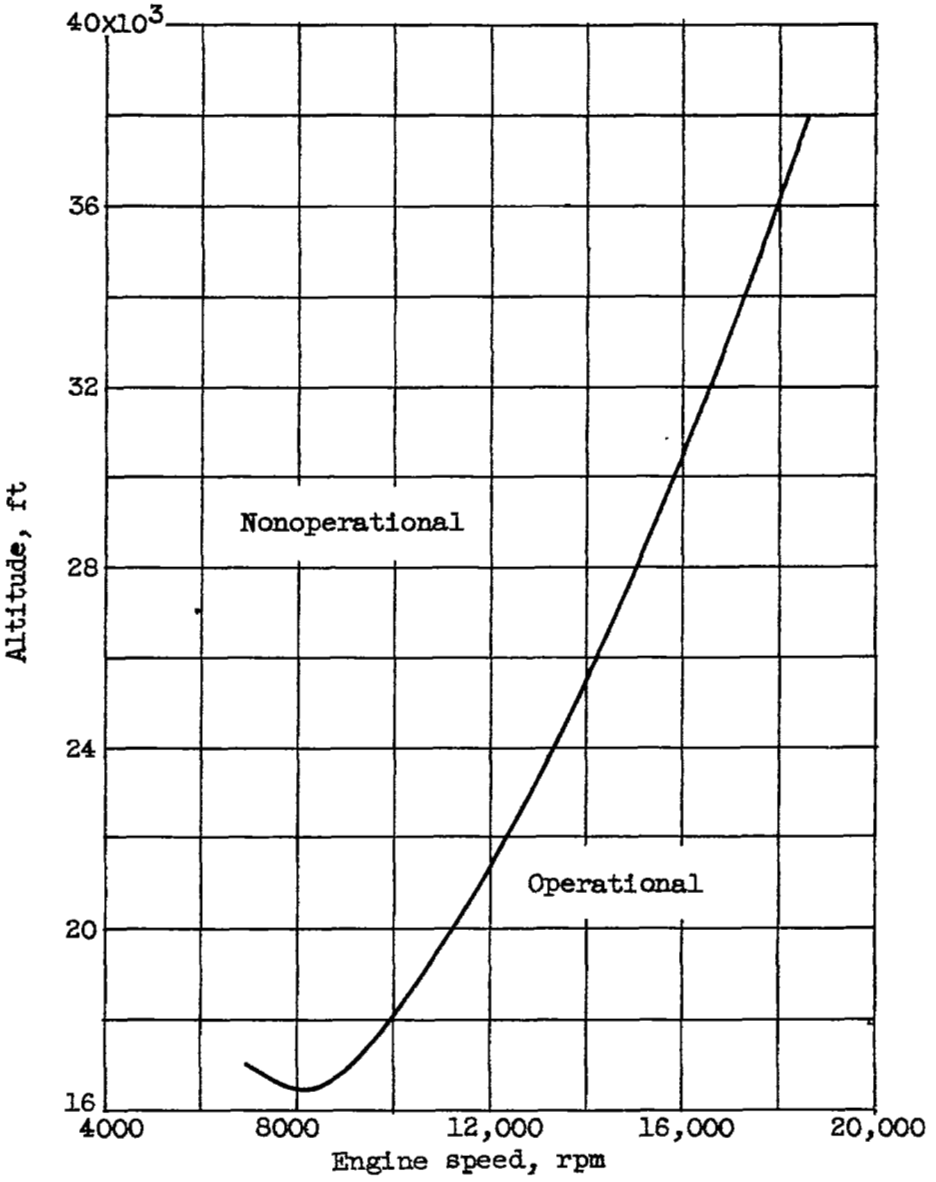

Figure 59. - Altitude operational limits of combustor at conditions simulating static operation. Engine sea-level pressure ratio, 3 (ref. 3).

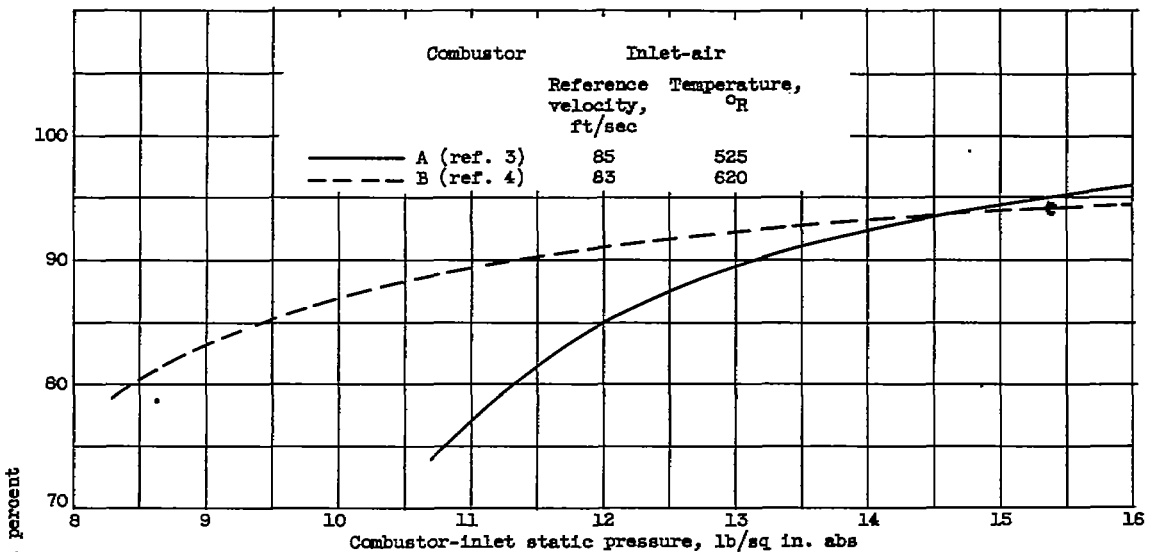

(a) Combustor inlet-air pressure. Fuel-air ratio, 0.014.

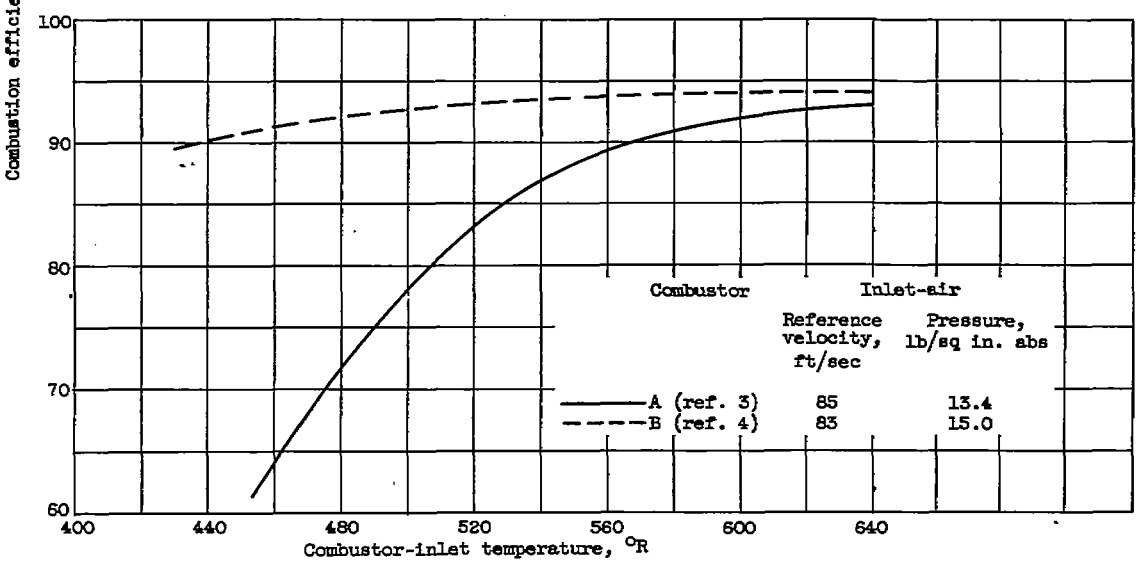

(b) Combustor inlet-air temperature. Fuel-air ratio, 0.014.

Figure 60. - Effect of operating variables on combustion efficiency of two different turbojet combustors.

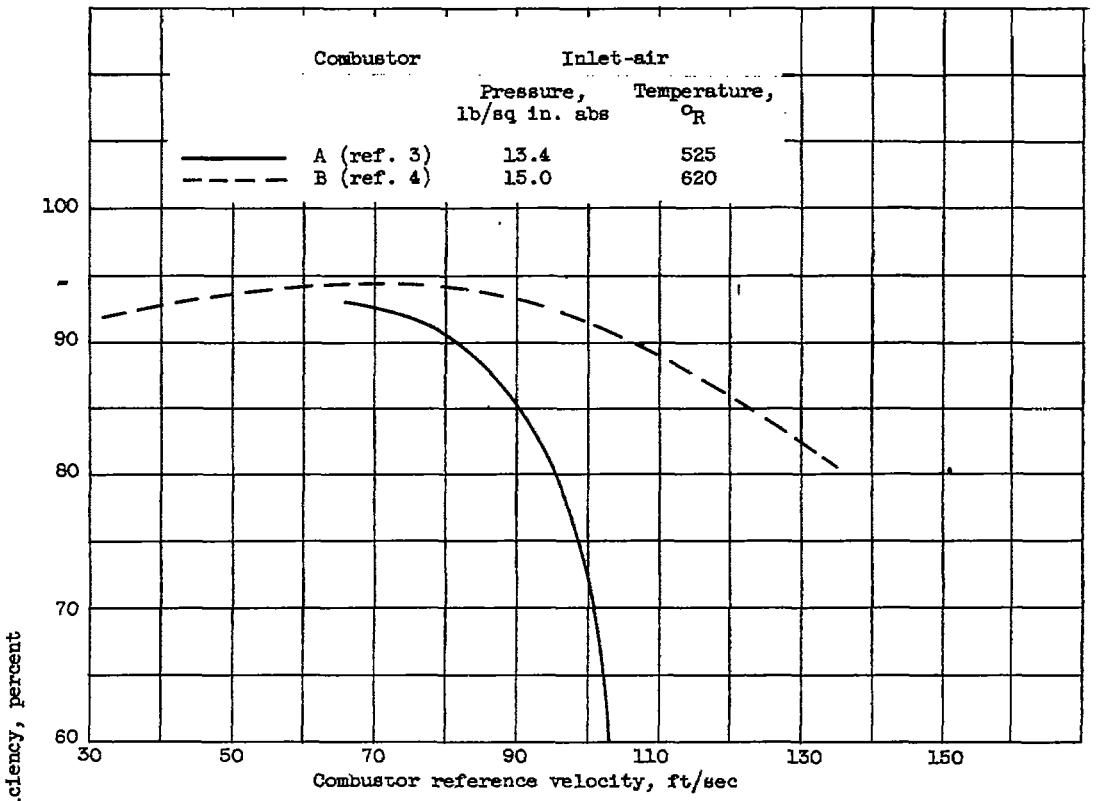

(c) Combustor reference velocity. Fuel-air ratio, 0.014.

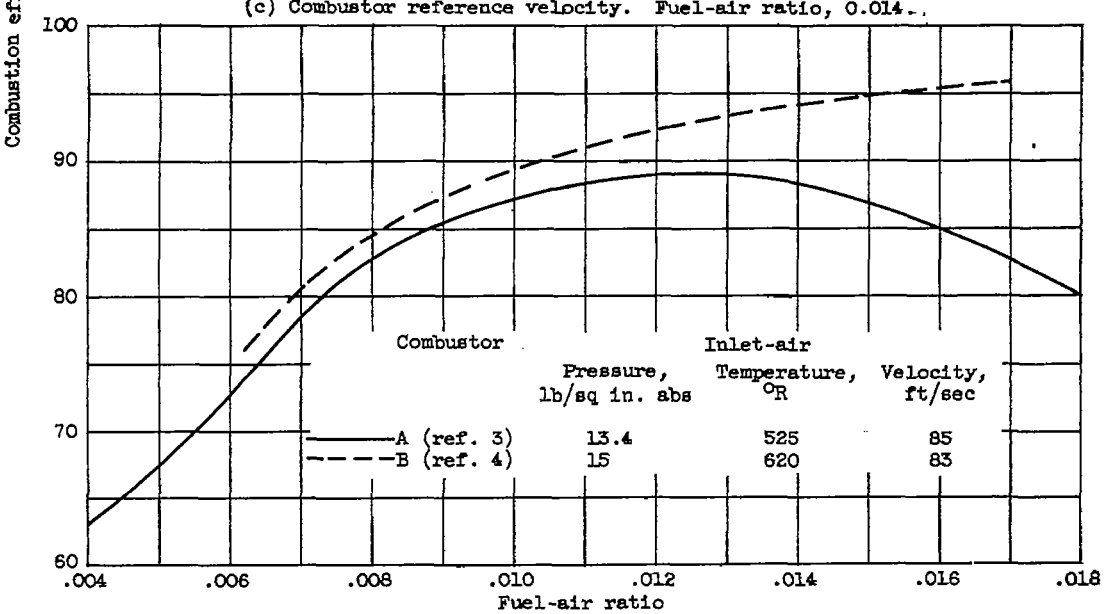

(d) Combustor fuel-air ratio.

Figure 60. - Concluded. Effect of operating variables on combustion efficiency of two different turbojet combustors.

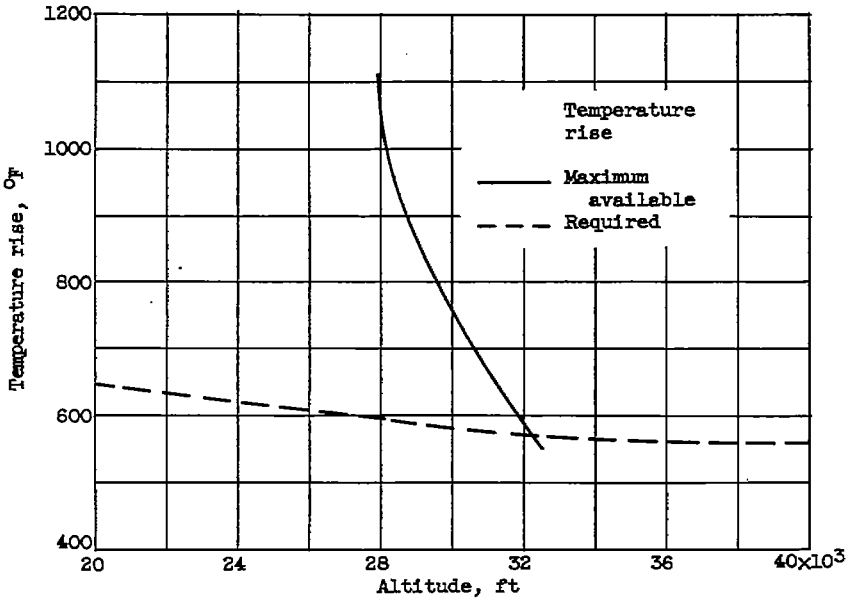

Figure 61. - Effect of altitude on required and available temperature rise of turbojet combustor. Engine rated sea-level pressure ratio, 4; engine rotational speed, 10,000 rpm; fuel, aviation gasoline (AN-F-28).

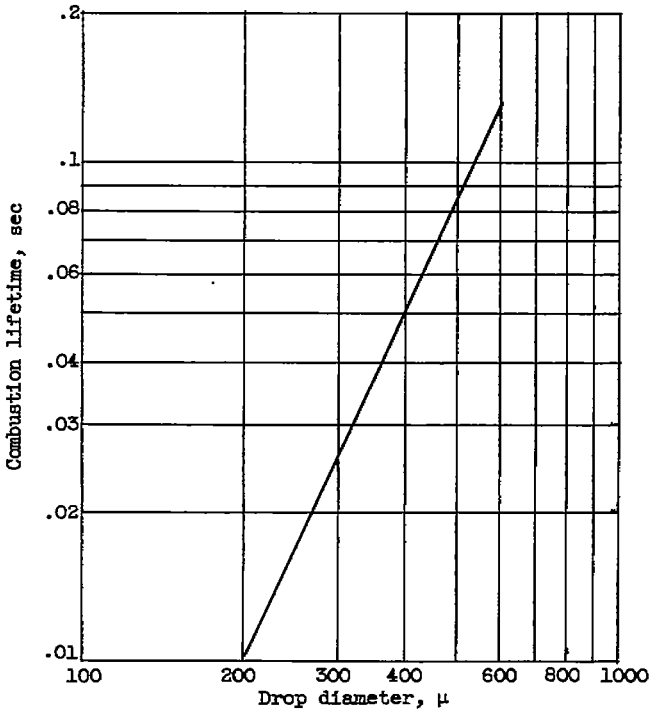

Figure 62. - Combustion lifetime of liquid kerosene drops of varying size. Pressure, 1 atmosphere (ref. 8).

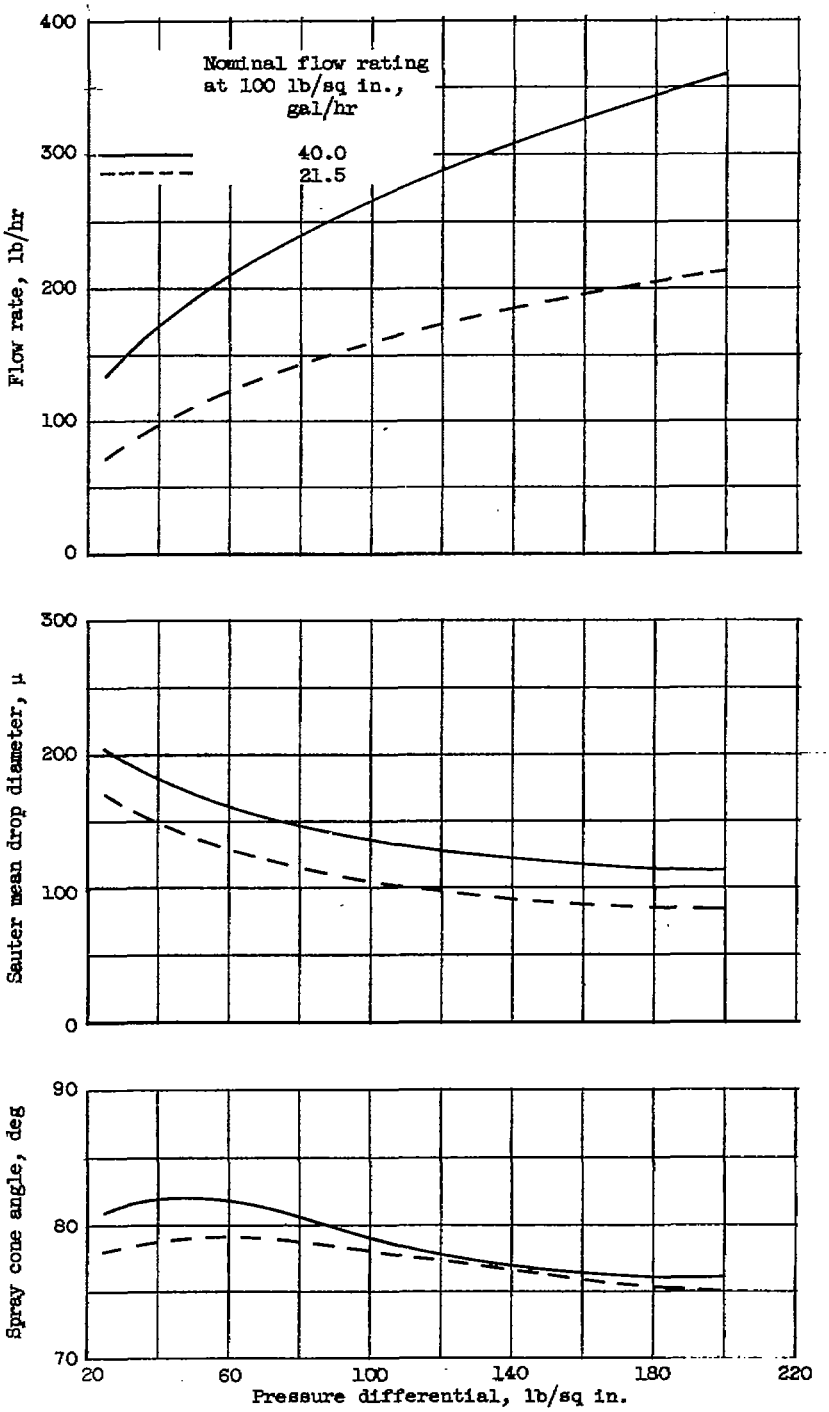

Figure 63. - Spray characteristics of two swirl-type pressure-atomizing nozzles. Nominal cone angle, 80°; fuel, Diesel fuel oil at 111° F (specific gravity 0.802).

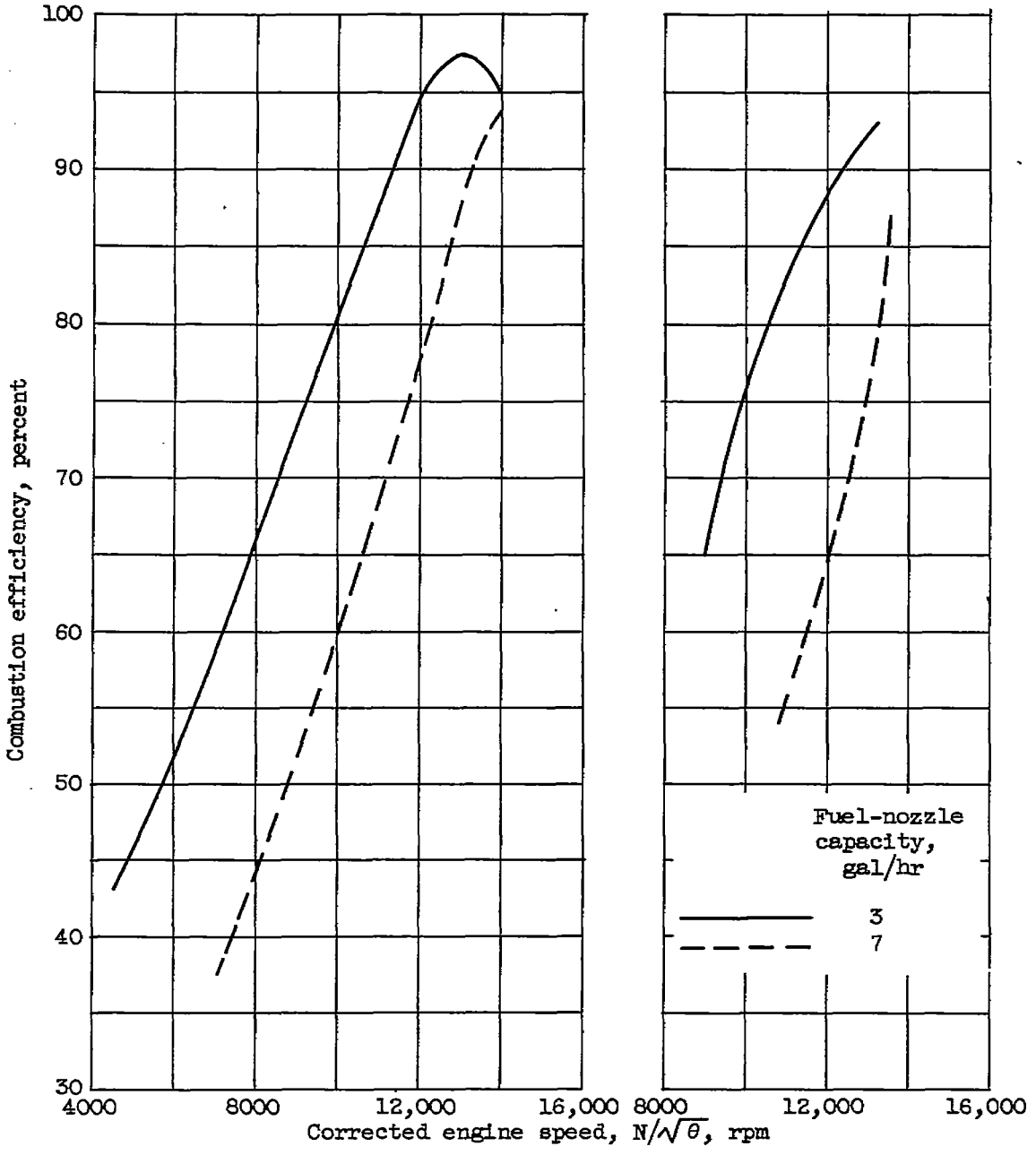

(a) Altitude, 30,000 feet. (b) Altitude, 40,000 feet.

Figure 64. - Effect of fuel-nozzle capacity on combustion efficiency of turbojet engine at two altitude conditions. Flight Mach number, 0.3 (ref. 9).

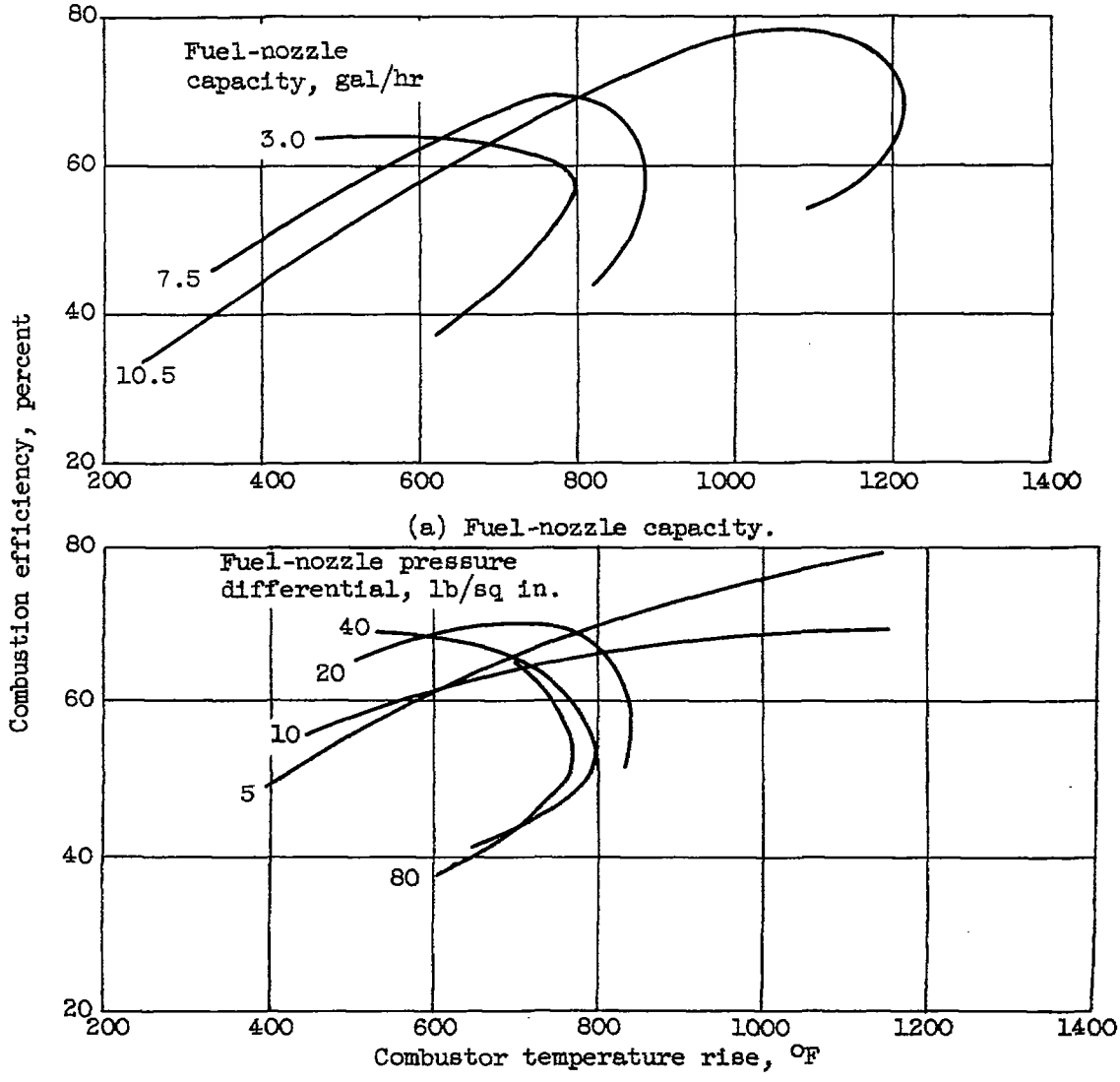

Figure 65. - Effect of fuel-nozzle capacity and injection pressure on combustion efficiency of an annular turbojet combustor using aviation gasoline. Inlet-air pressure, 7.7 pounds per square inch absolute; inlet-air temperature, 530° R; reference velocity, 64 feet per second (ref. 10).

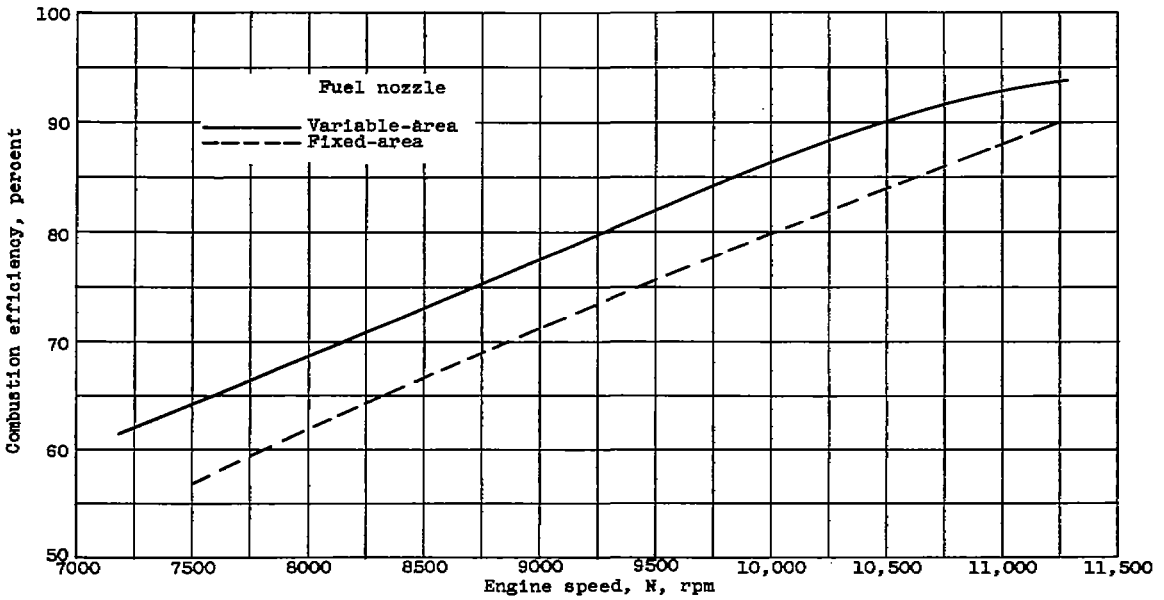

Figure 66. - Combustion efficiency of turbojet engine operating with variable-area or with fixed-area fuel nozzle. Ram pressure ratio, 1.00; altitude, 40,000 feet (ref. 12).

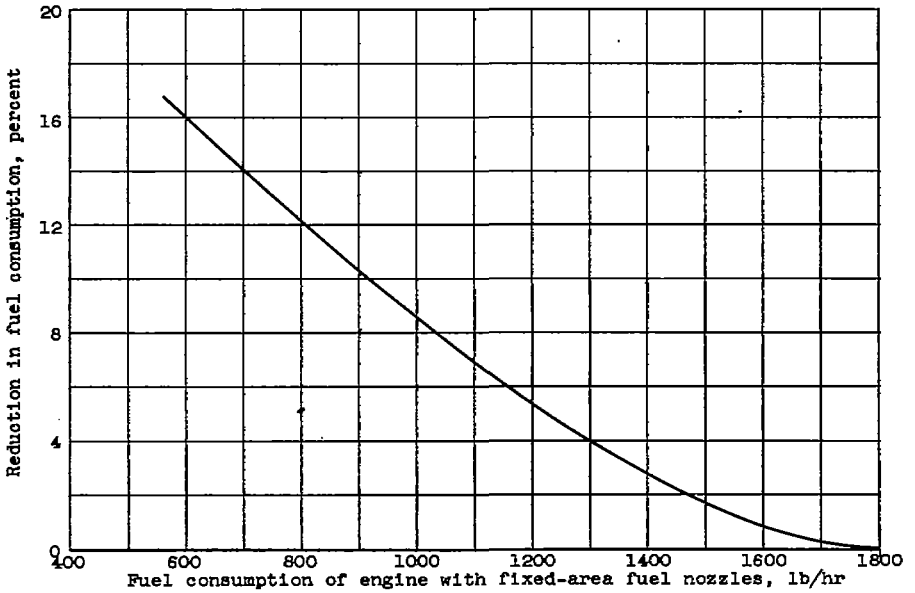

Figure 67. - Reduction in fuel consumption resulting from use of variable-area fuel nozzles in turbojet engine operating over range of altitudes, engine speeds and ram pressure ratios (ref. 12).

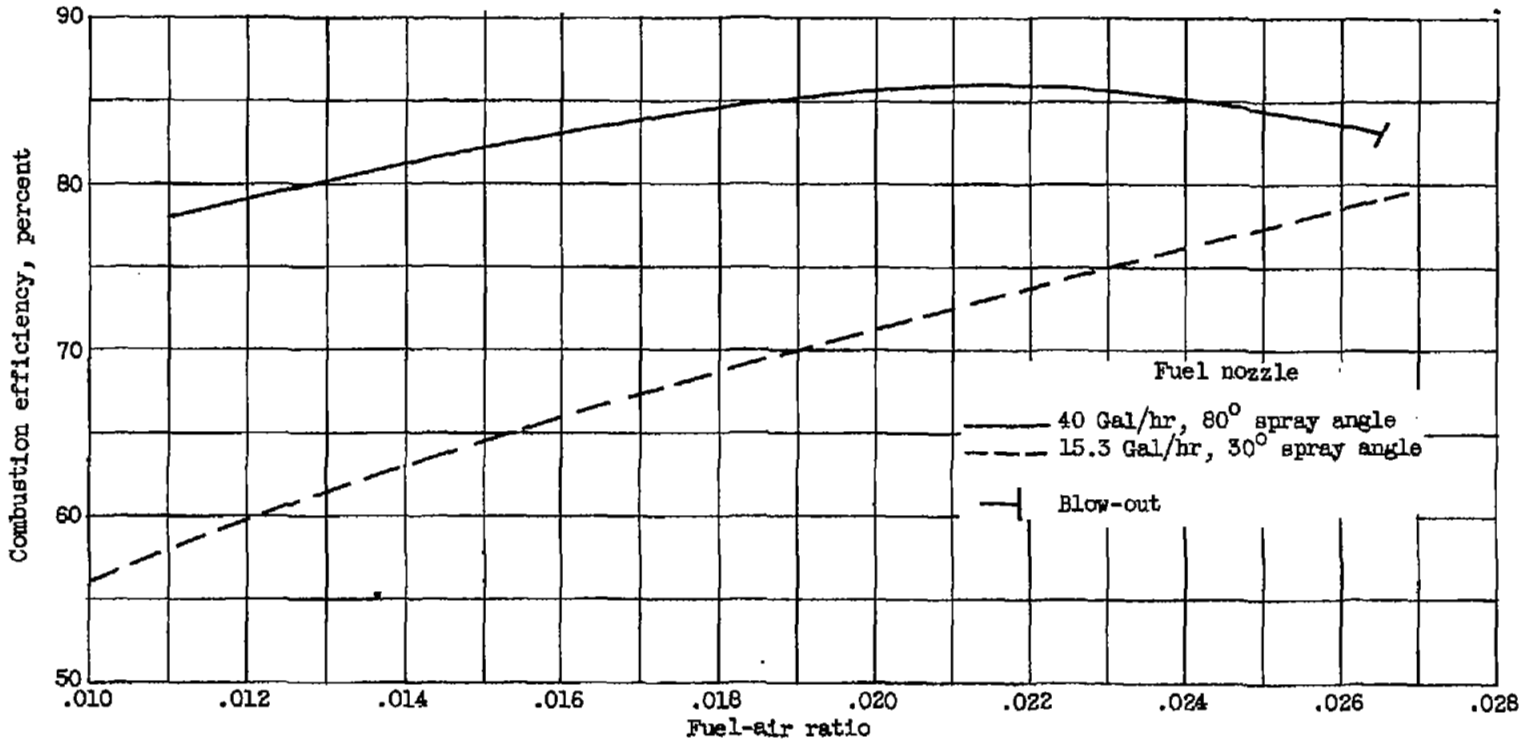

Figure 68. - Effect of fuel injector on combustion efficiency of single J33 combustor. Inlet-air pressure, 7.4 pounds per square inch absolute; inlet-air temperature, 728° R; reference velocity, 130 feet per second; fuel, MIL-F-5624A grade JP-4 (ref. 13).

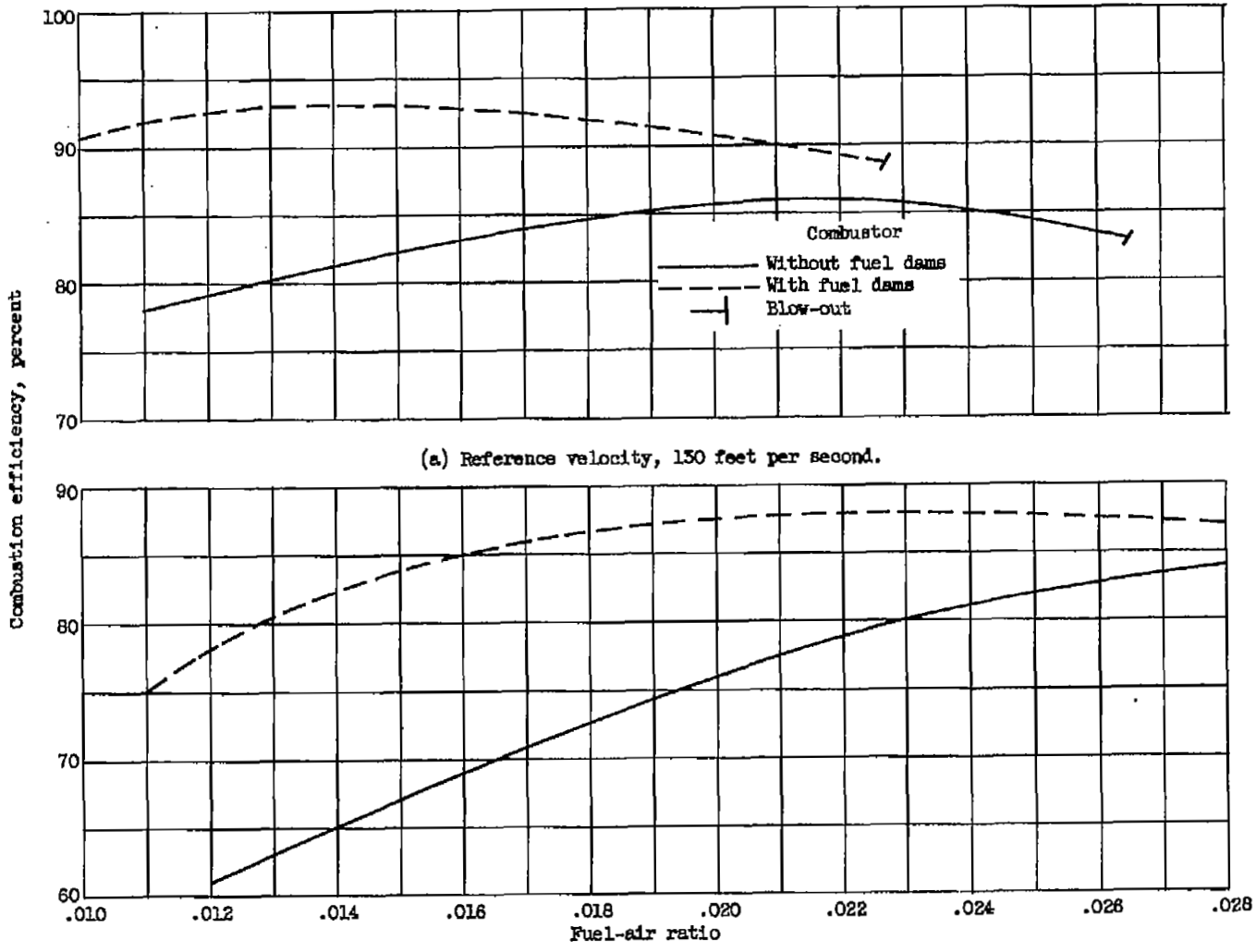

(a) Reference velocity, 130 feet per second.

(b) Reference velocity, 78 feet per second.

Figure 69. - Effect of fuel dams on combustion efficiency of single J33 combustor using 40-gallon-per-hour, 80°-spray-angle nozzle. Inlet-air pressure, 7.4 pounds per square inch absolute; inlet-air temperature, 728° R; fuel, MIL-F-5624A grade JP-4 (ref. 13).

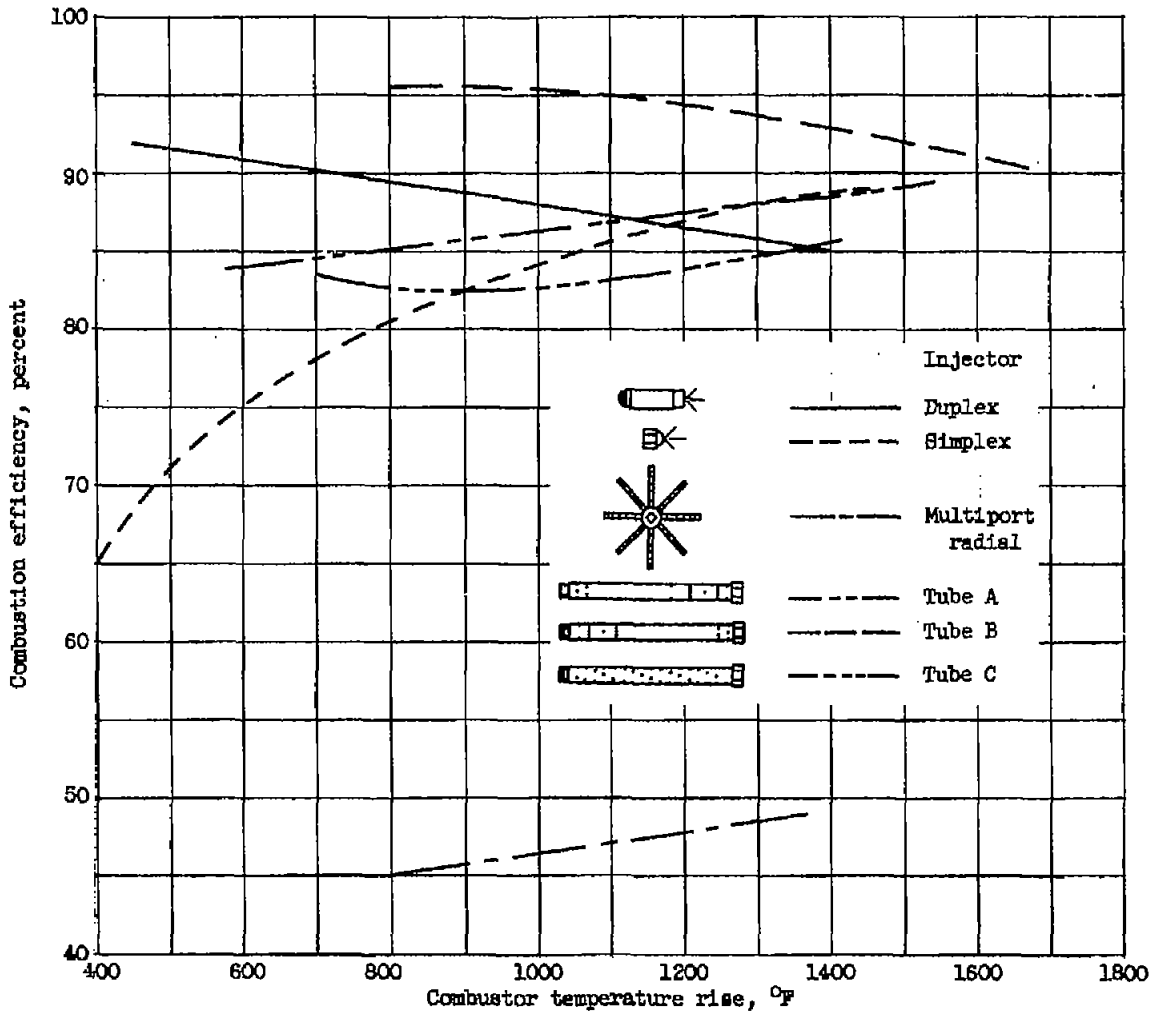

Figure 70. - Variation of combustion efficiency with combustor temperature rise obtained in single tubular combustor using different injectors. Inlet-air pressure, 8.3 pounds per square inch absolute; inlet-air temperature, 620° R; inlet-air velocity, 80 feet per second; fuel, MIL-F-5624A grade JP-3 (ref. 4).

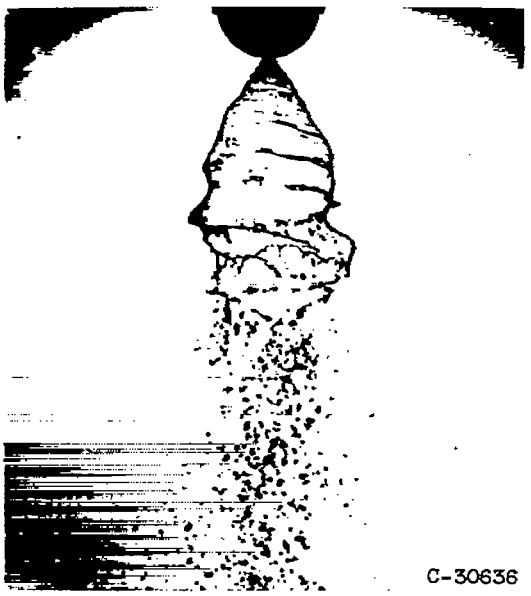

(a) Spray photograph in quiescent air. Fuel-flow rate, 40 pounds per hour.

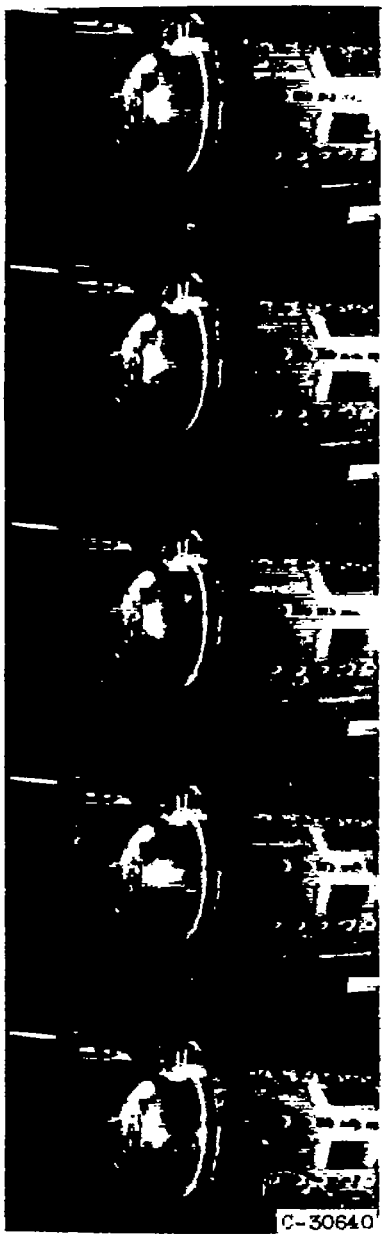

(b) Spray photograph in turbojet combustor. Fuel-flow rate, 47 pounds per hour; air velocity, 80 feet per second.

Figure 71. - Photographs of fuel sprays in quiescent air and in nonburning tubular turbojet combustor. Inlet-air pressure, 12.8 pounds per square inch absolute; inlet-air temperature, 510° R; 40-gallon-per-hour, 80°-spray cone; fixed-area nozzle (ref. 14).

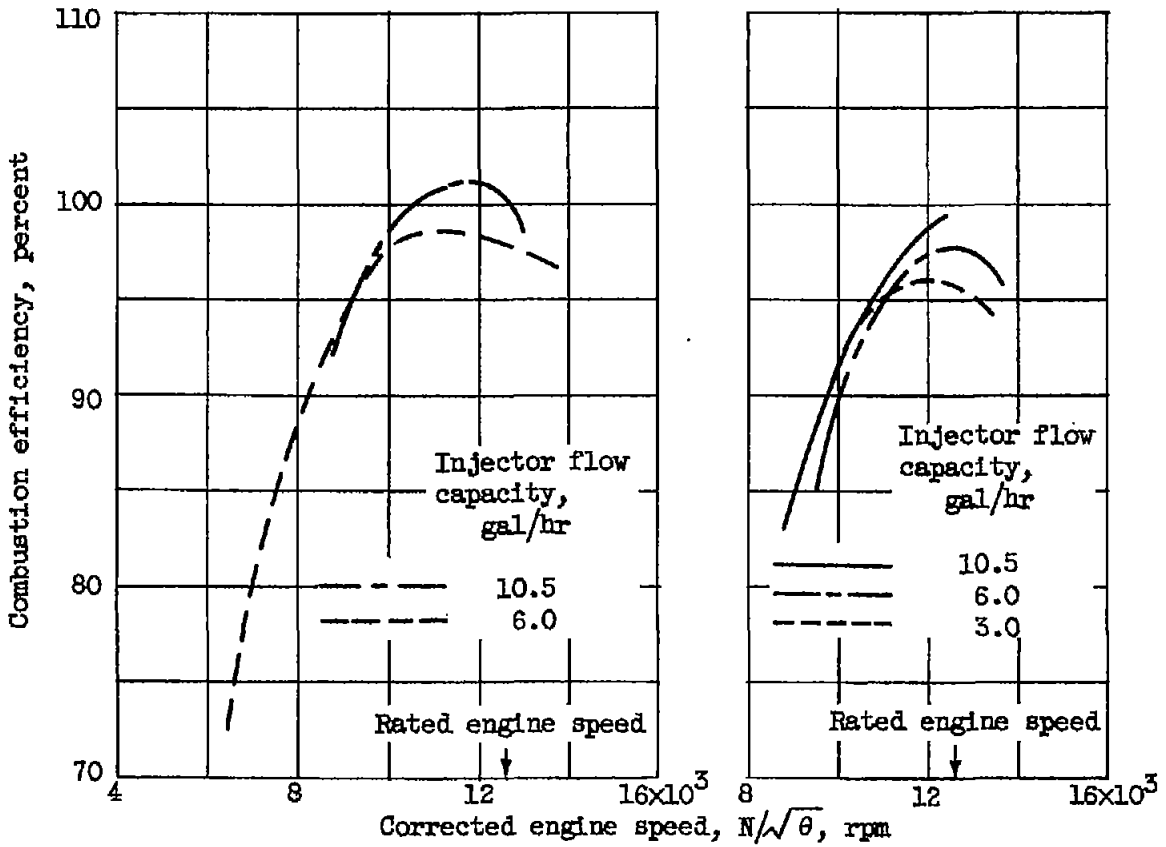

(a) Altitude, 30,000 feet. (b) Altitude, 40,000 feet.

Figure 72. - Effect of fuel-nozzle size on combustion efficiency of experimental single-annular combustor. Flight Mach number, 0.60 (ref. 9).

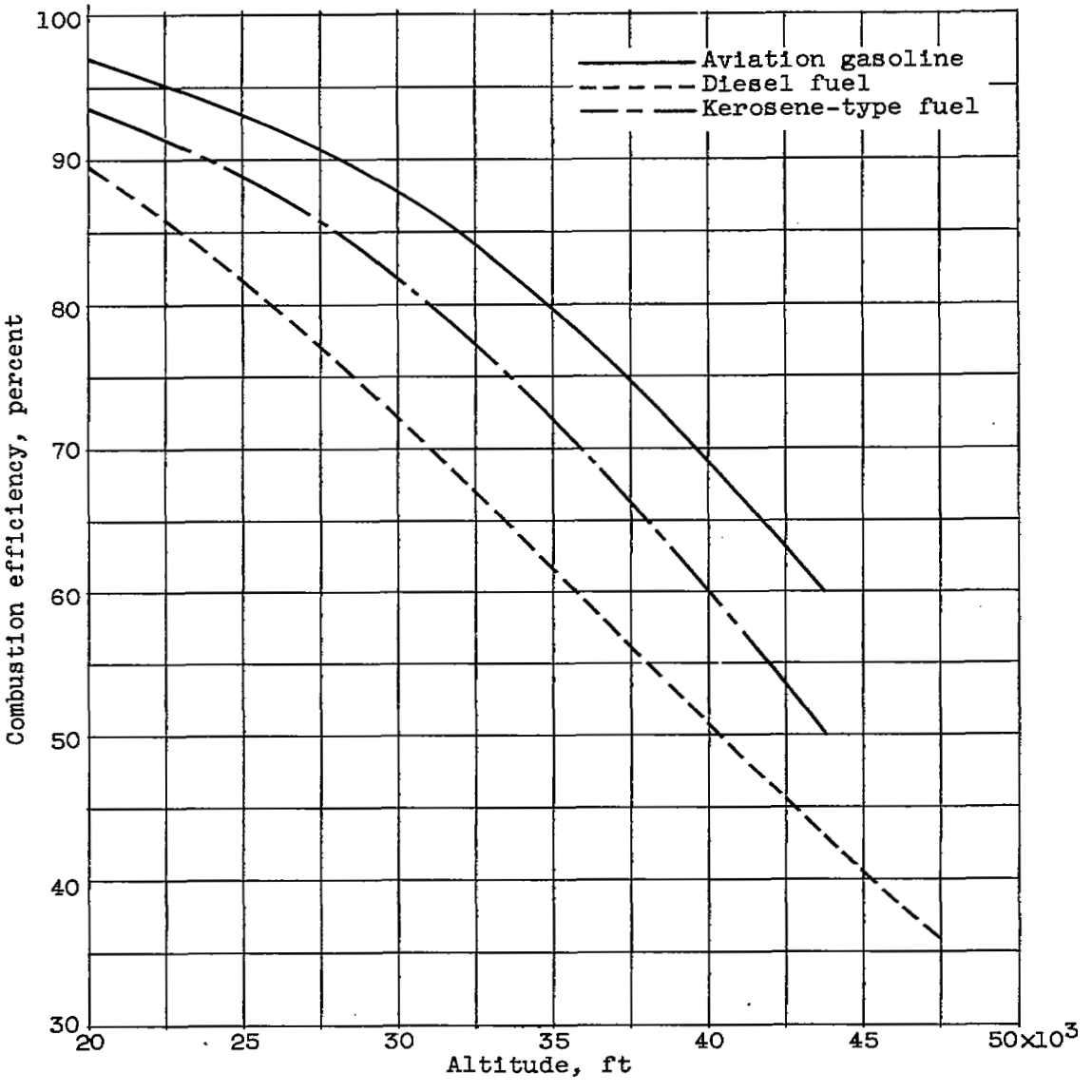

Figure 73. - Variation of combustion efficiency with altitude for three fuels of different volatility in annular combustor. Simulated compressor pressure ratio, 4; engine speed, 80 percent of rated; flight Mach number, 0.0 (ref. 10).

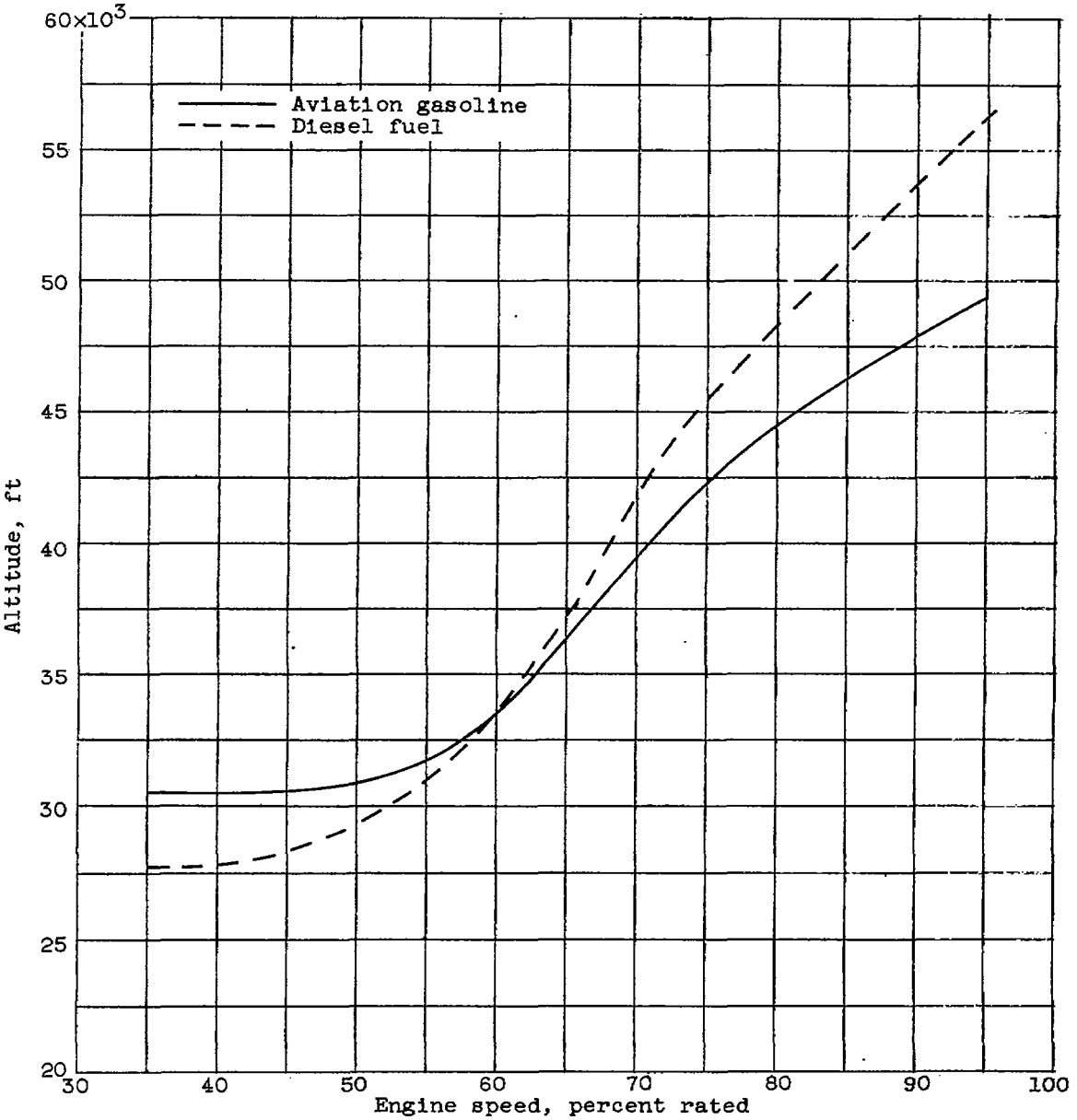

Figure 74. - Comparison of altitude operational limits for two fuels in annular turbojet combustor. Simulated compressor pressure ratio, 4; flight Mach number, 0.0 (ref. 10).

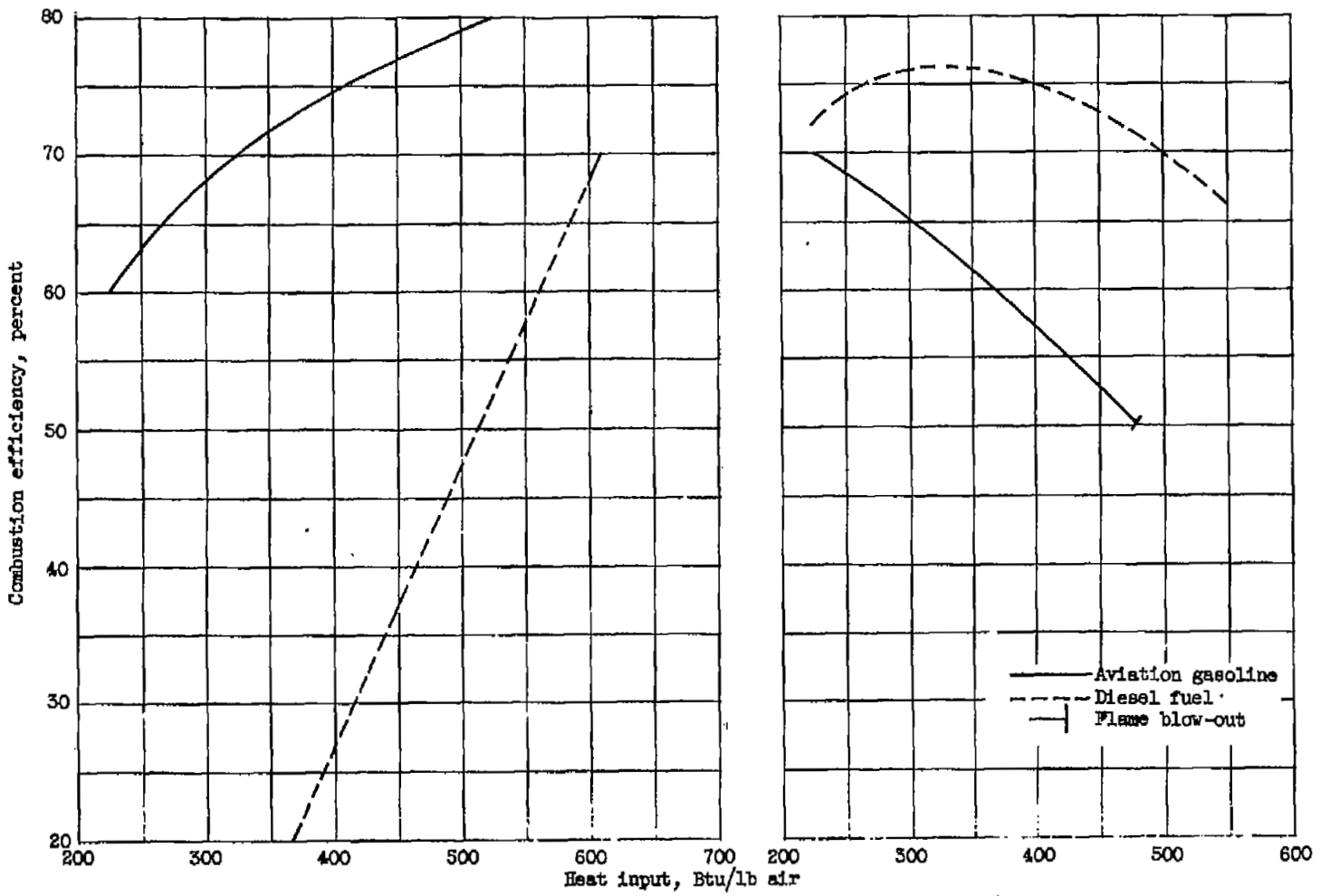

(a) 17.5-Gallon-per-hour nozzle.

(b) 3.0-Gallon-per-hour nozzle.

Figure 75. - Effect of fuel volatility characteristics of two fuels on combustion efficiency. Inlet-air pressure, 9.2 pounds per square inch absolute; inlet-air temperature, 700° R; reference velocity, 80 feet per second (ref. 10).

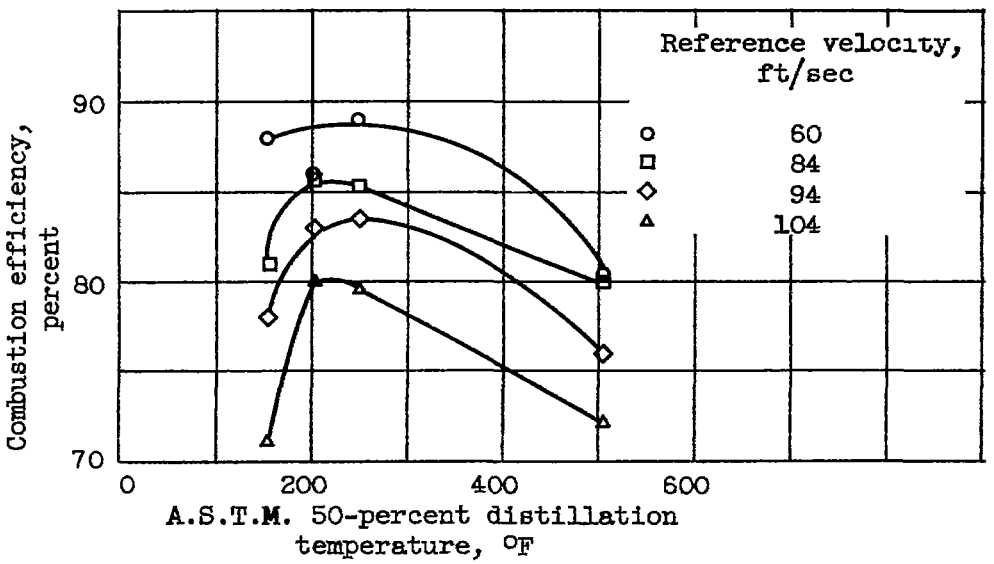

(a) Relatively pure straight-chain hydrocarbon fuels. Inlet-air pressure, 7 pounds per square inch absolute; inlet-air temperature, 500° R.

Figure 76. - Effect of fuel volatility on combustion efficiency in tubular turbojet combustor.

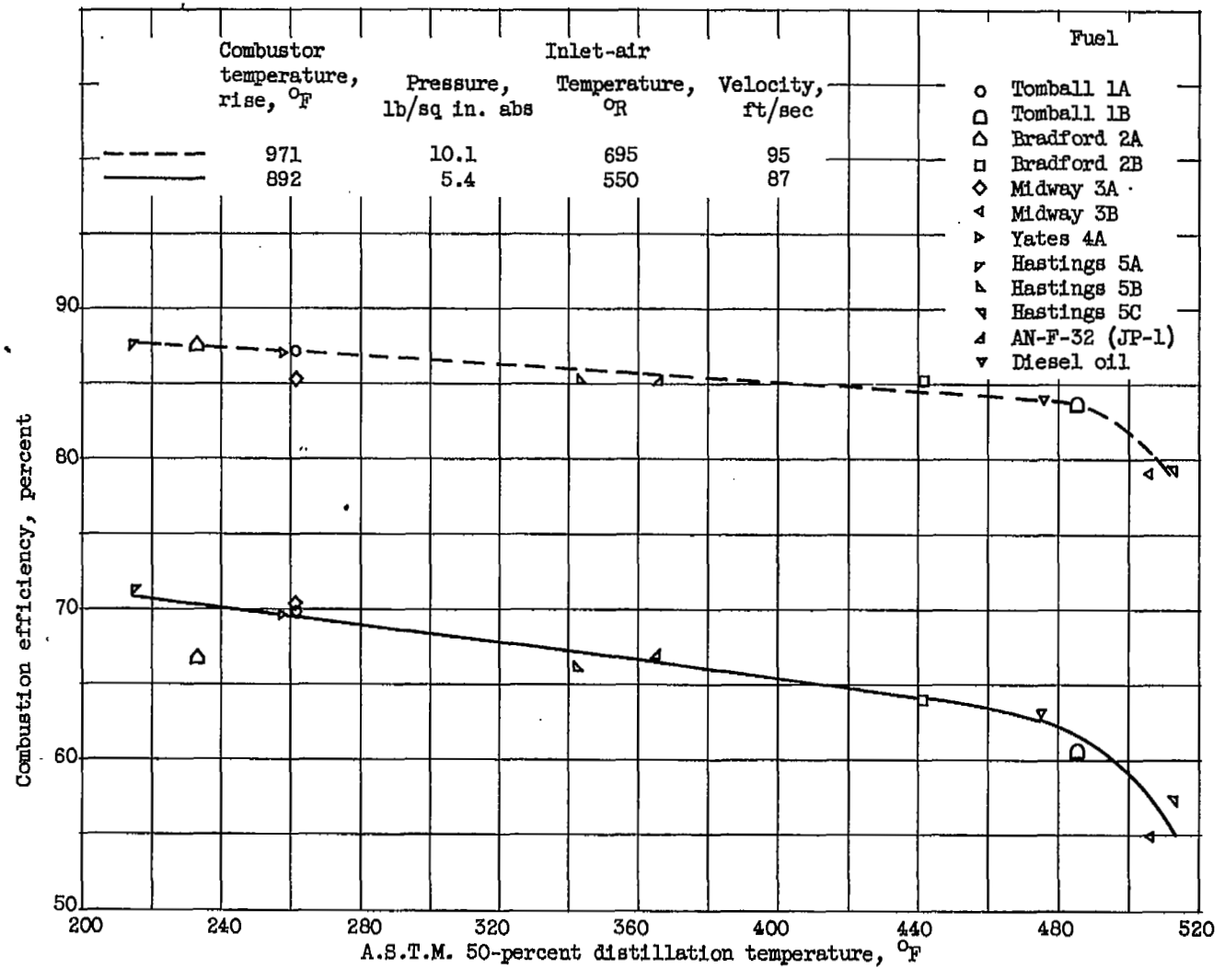

(b) Mixed hydrocarbon fuels (ref. 16).

Figure 76. - Concluded. Effect of fuel volatility on combustion efficiency in tubular turbojet combustor.

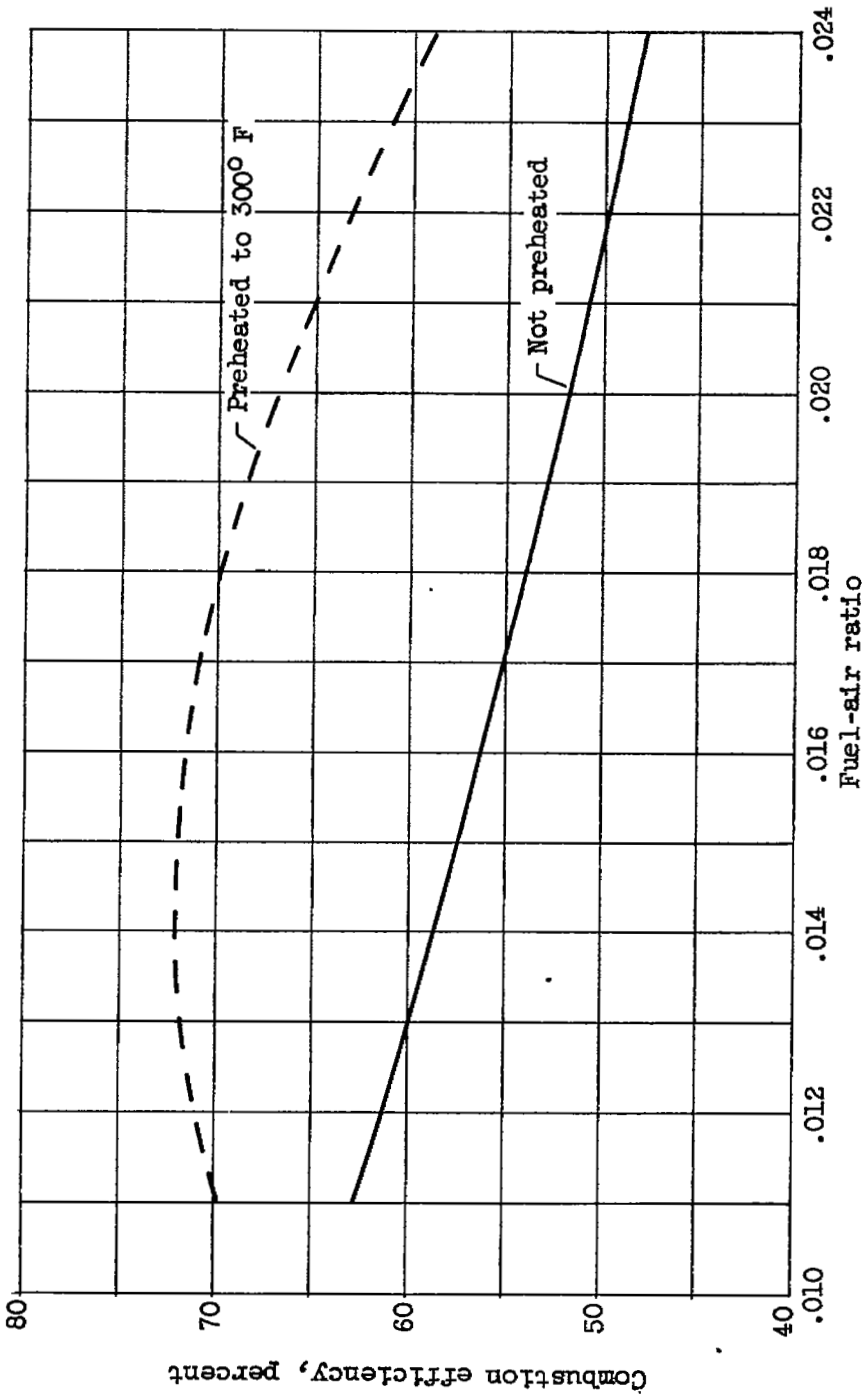

Figure 77. - Effect of preheating JP-4 fuel on combustion efficiency in experimental turbojet combustor. Combustor-inlet total pressure, 2.5 pounds per square inch absolute; combustor-inlet total temperature, 728° R; reference velocity, 103 feet per second (ref. 17).

3080

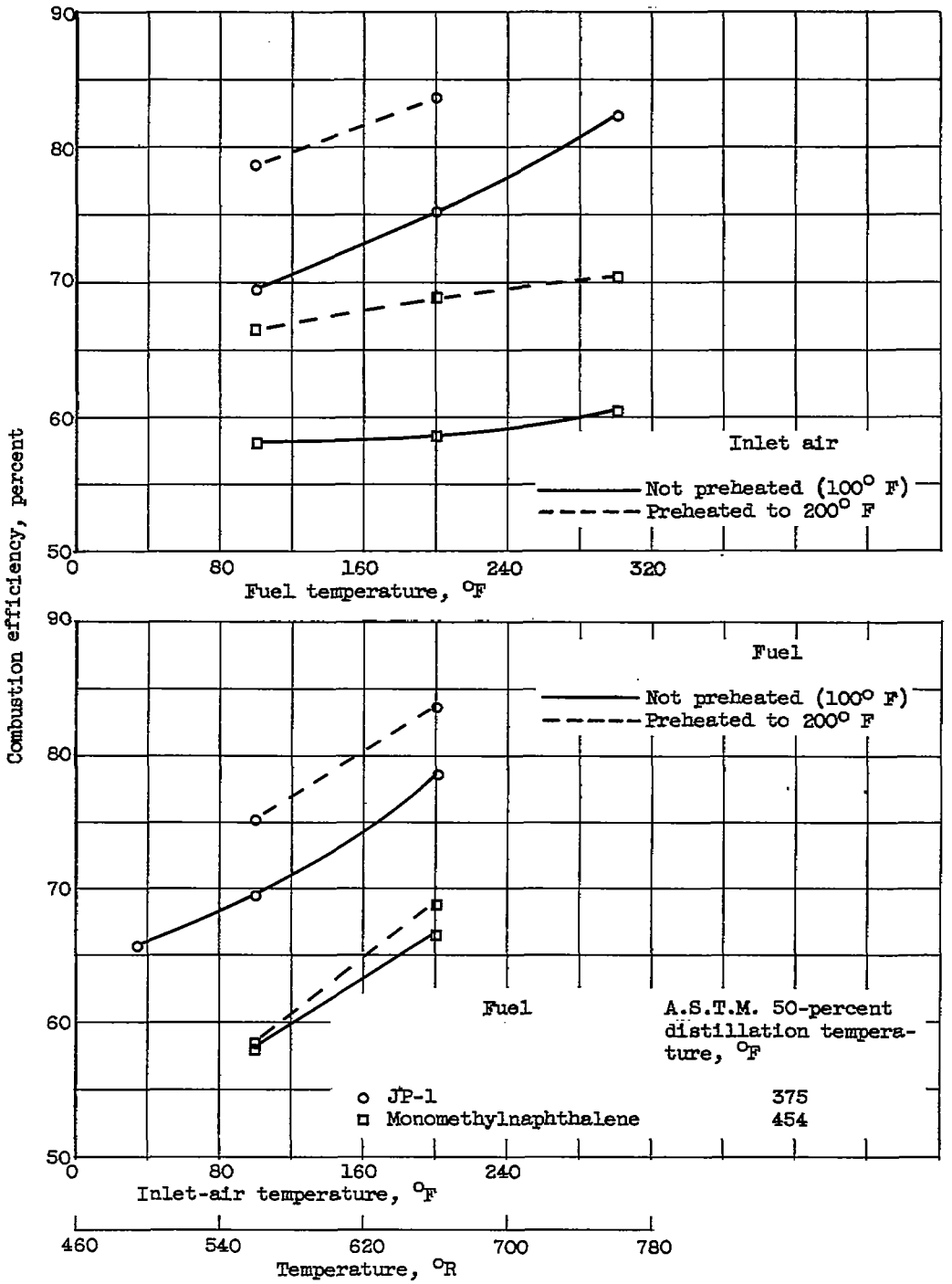

Figure 78. - Effect of fuel and inlet-air temperatures on combustion efficiency of two fuels in tubular turbojet combustor. Combustor inlet-air pressure, 10 pounds per square inch absolute; air-flow rate, 4000 pounds per hour; heat-input rate, 240 Btu per pound of air.

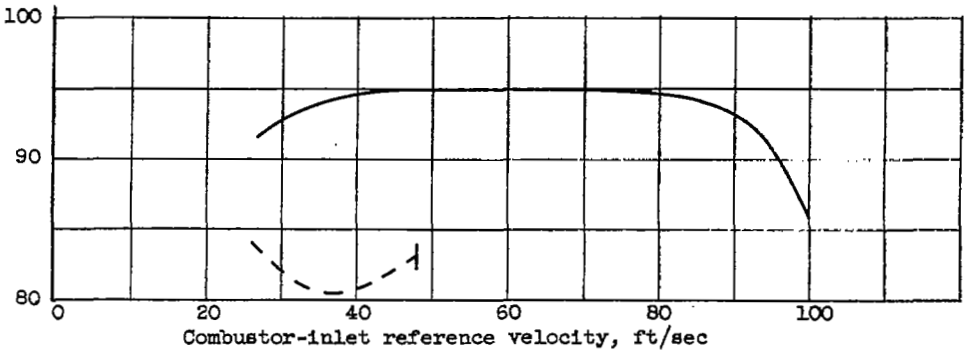

(a) Effect of combustor-inlet reference velocity. Inlet-air pressure, 15 pounds per square inch absolute; inlet-air temperature, 620° R.

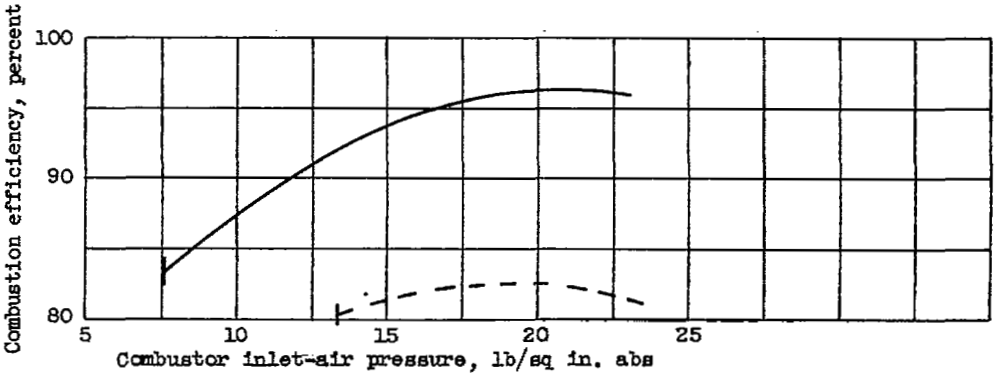

(b) Effect of combustor inlet-air pressure. Inlet-air temperature, 620° R; reference velocity, 45 feet per second.

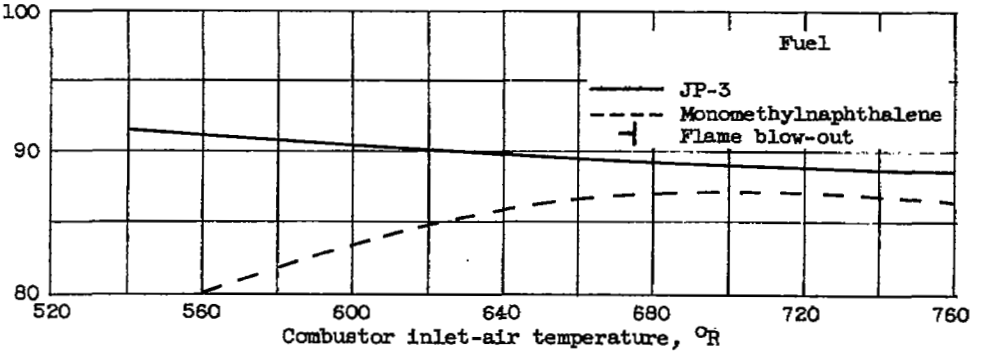

(c) Effect of combustor inlet-air temperature. Inlet-air pressure, 15 pounds per square inch absolute; reference velocity, 45 feet per second.

Figure 79. - Effect of operating variables on combustion efficiency of two fuels in tubular vaporizing combustor. Heat input, 366 Btu per pound of air (ref. 21).

[redacted]

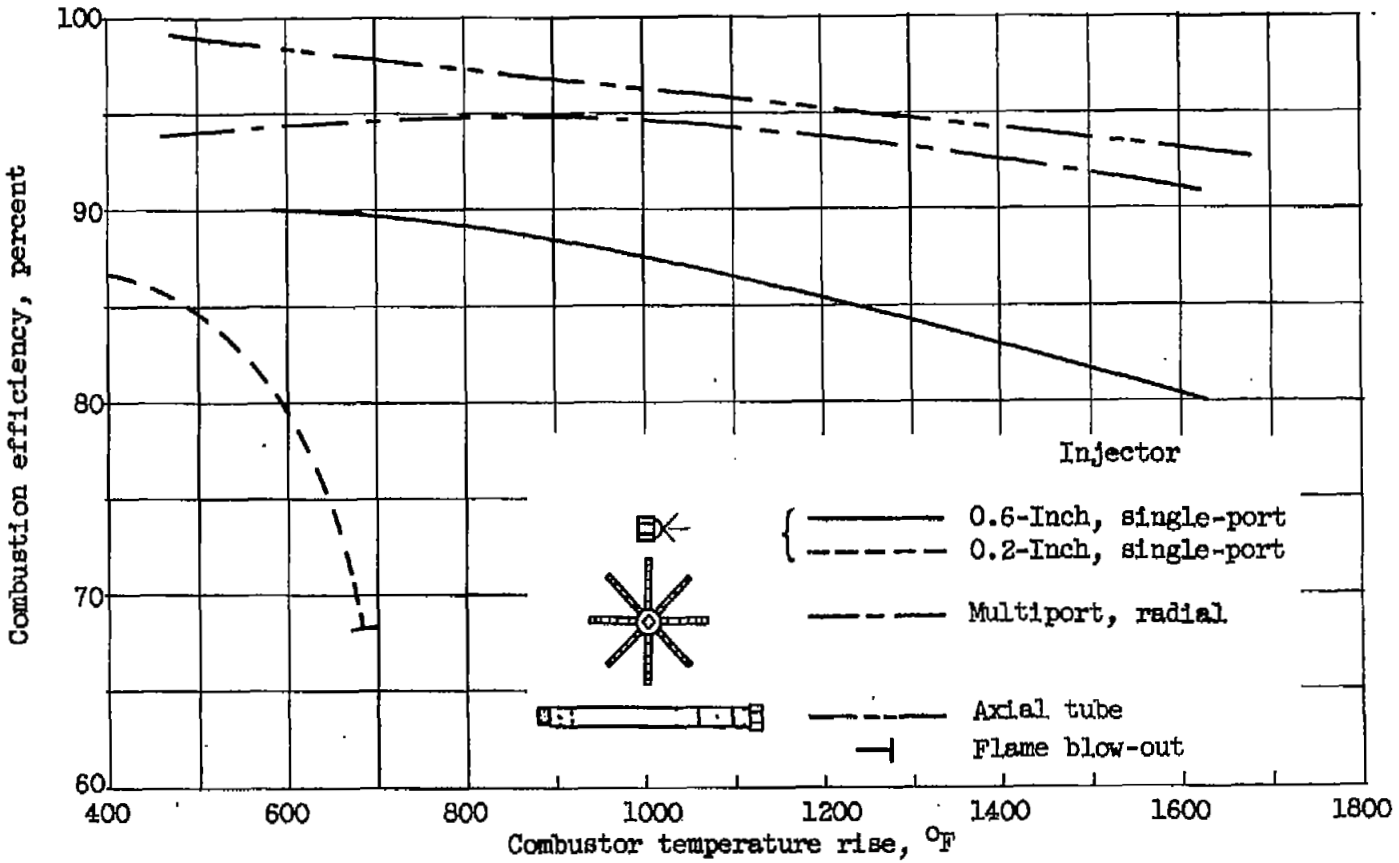

Figure 80. - Variation of combustion efficiency with combustor temperature rise obtained in single tubular combustor. Inlet-air pressure, 8.3 pounds per square inch absolute; inlet-air temperature, 620° R; inlet-air velocity, 80 feet per second; fuel, propane vapor (ref. 22).

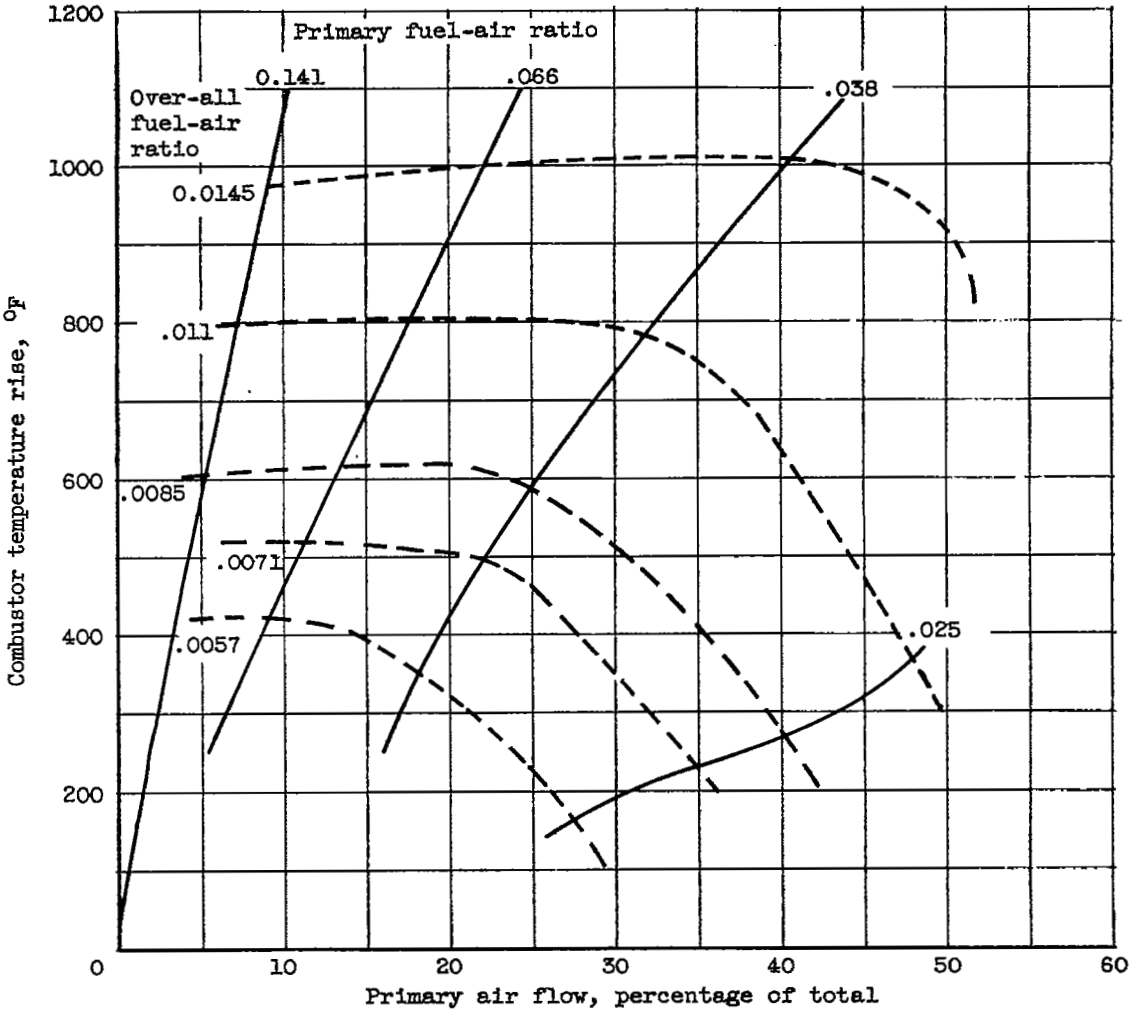

Figure 81. - Effect of varied air distribution on temperature rise obtained in single tubular combustor. Total air-flow rate, 2.36 pounds per second (ref. 24).

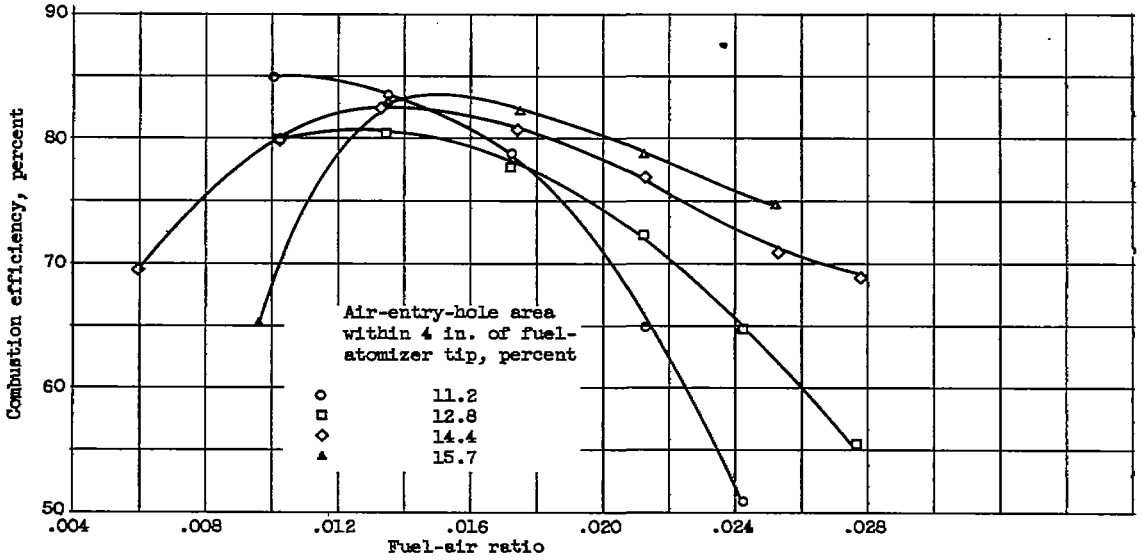

Figure 82. - Effect of variation in percent of total area of air-entry holes within 4 inches of plane of fuel-atomizer tip on combustion efficiency of 6.25-inch-diameter tubular combustor. Inlet-air pressure, 3.9 pounds per square inch absolute; inlet-air temperature, 728° R; reference velocity, 102 feet per second (ref. 25).

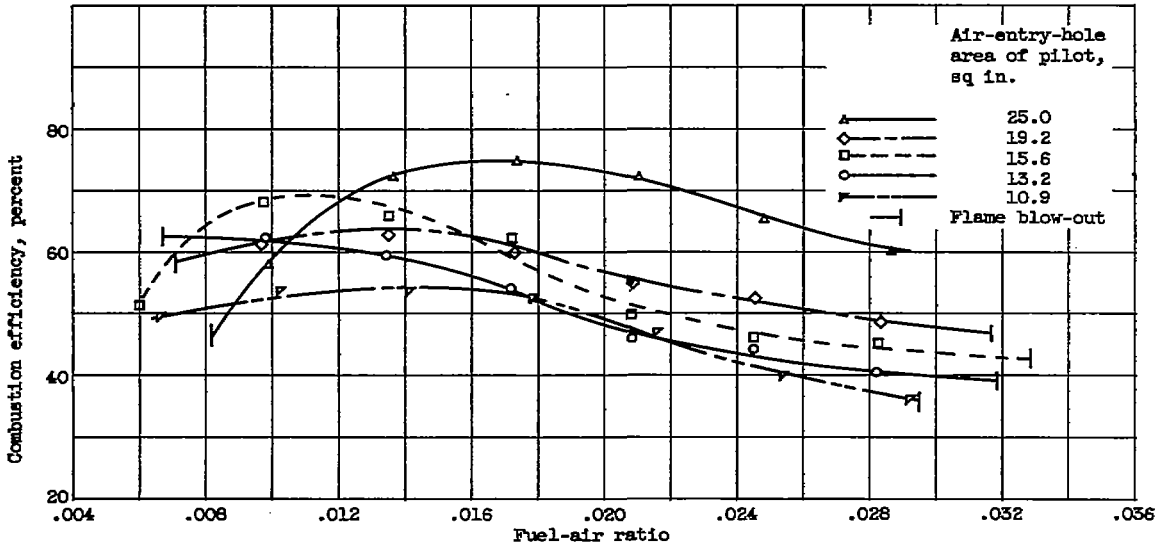

Figure 83. - Effect of pilot air-entry-hole area on combustion efficiency of 9.5-inch-diameter tubular combustor. Combustor inlet-air pressure, 3.9 pounds per square inch absolute; temperature, 695° R; reference velocity, about 100 feet per second (ref. 26).

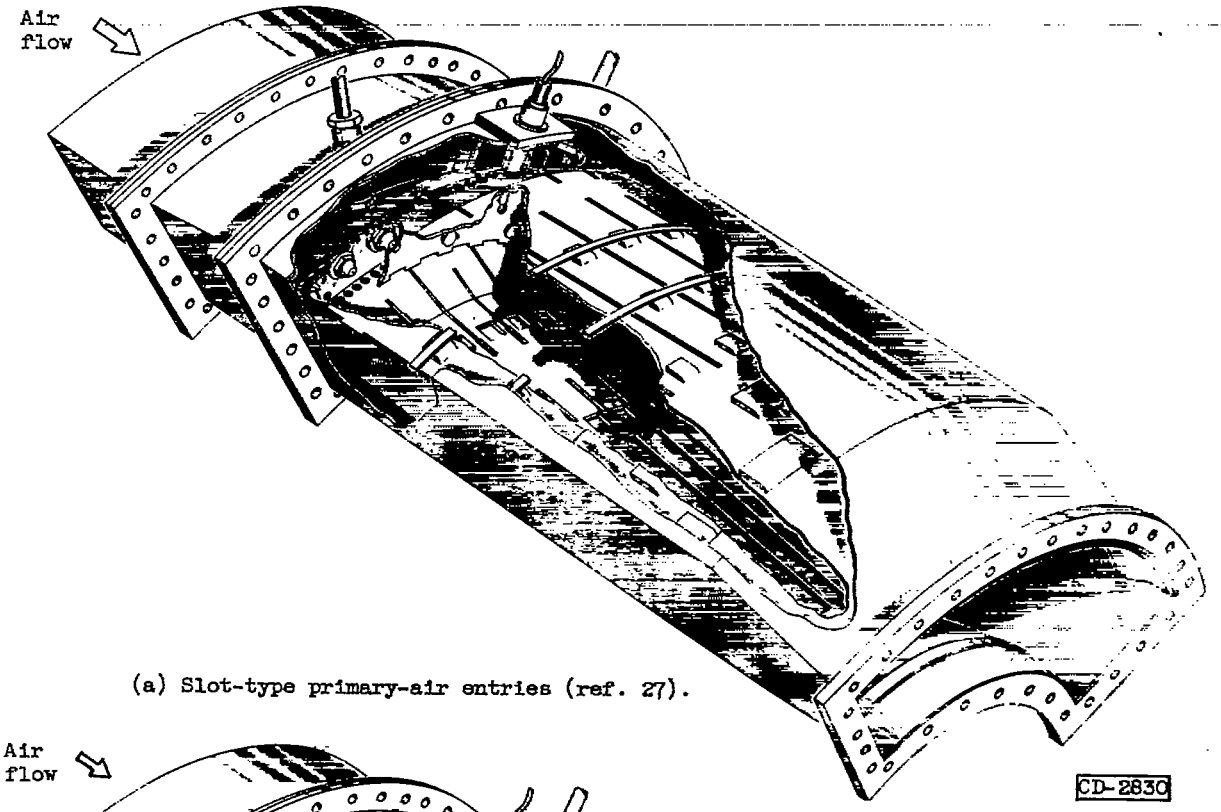

(a) Slot-type primary-air entries (ref. 27).

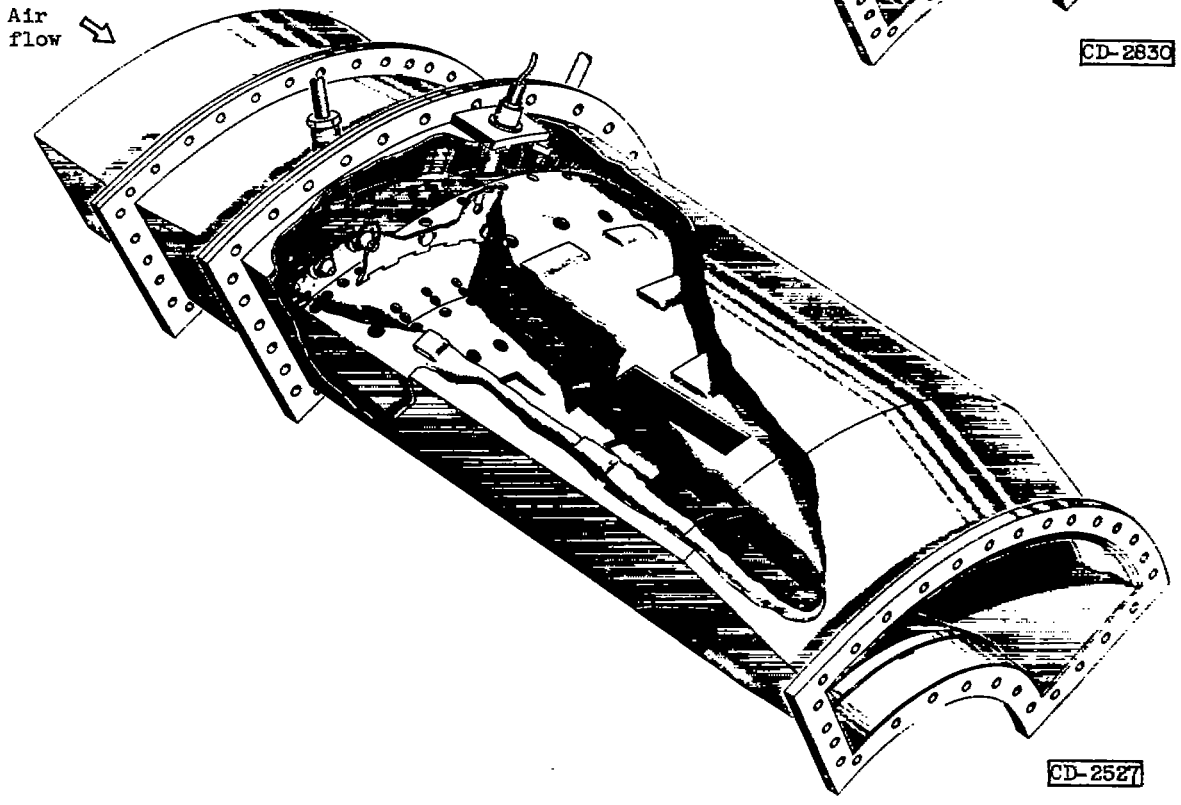

(b) Circular primary-air entries (ref. 17).

Figure 84. - One-quarter views of experimental annular combustors.

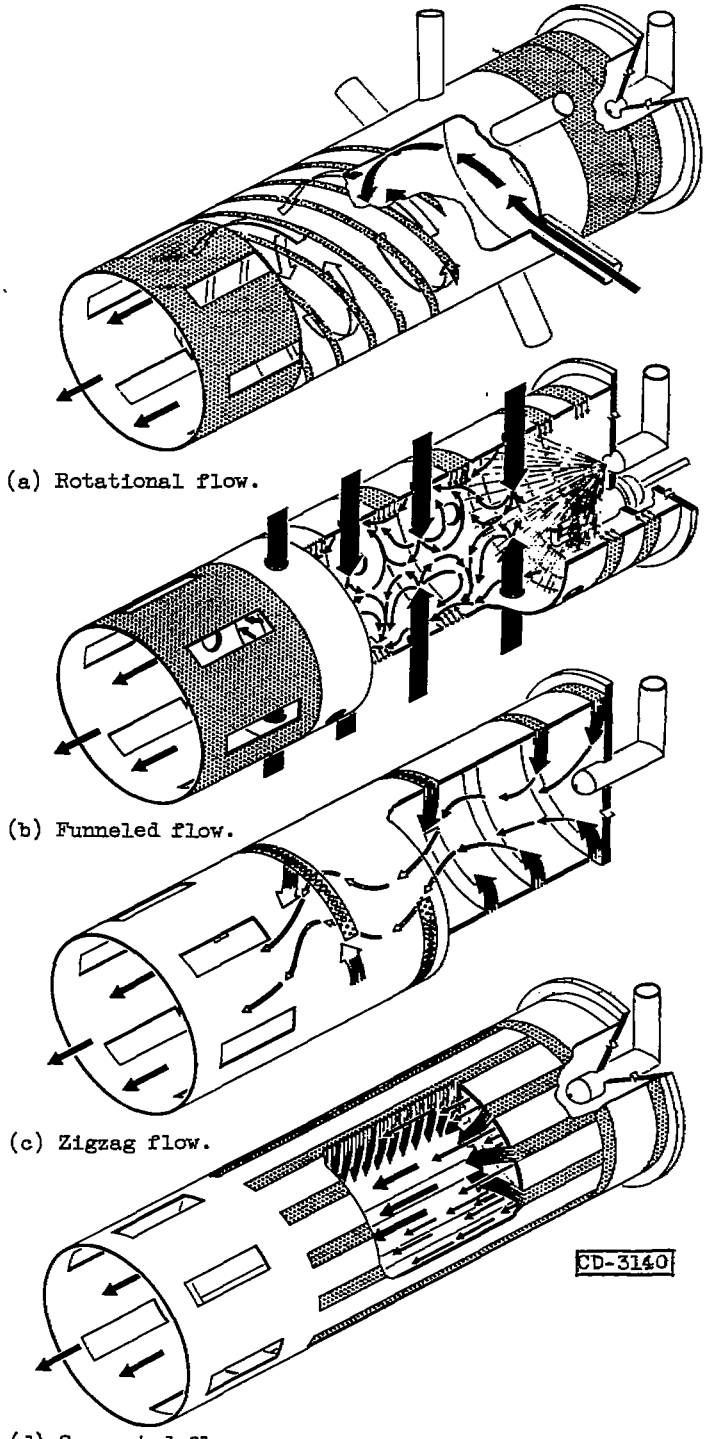

(a) Rotational flow.

(b) Funneled flow.

(c) Zigzag flow.

(d) Segmented flow.

Figure 85. - Sketches of experimental tubular-combustor configurations showing internal air-flow patterns (ref. 25).

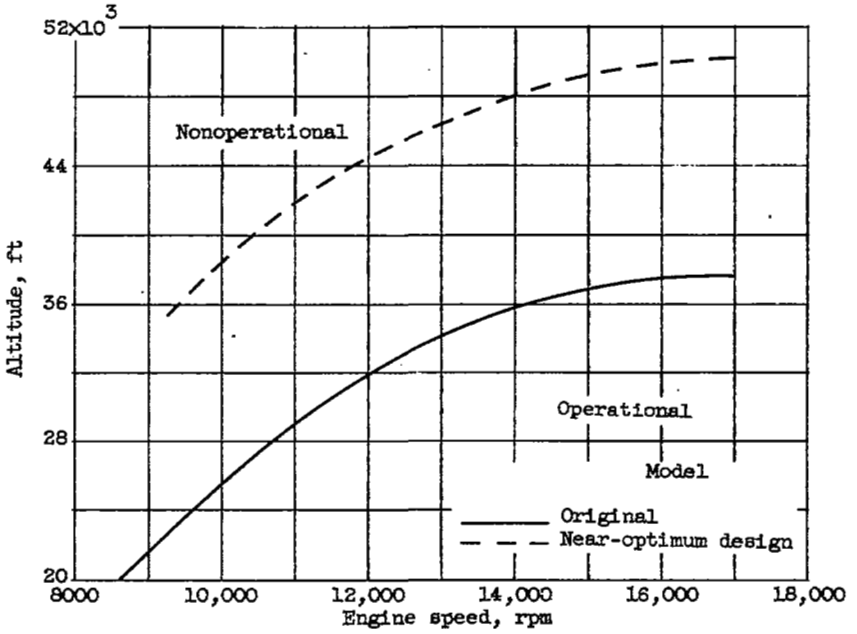

Figure 86. - Altitude operational limits obtained with two different circular-hole air admission designs in annular turbojet combustor. Engine pressure ratio, 4.

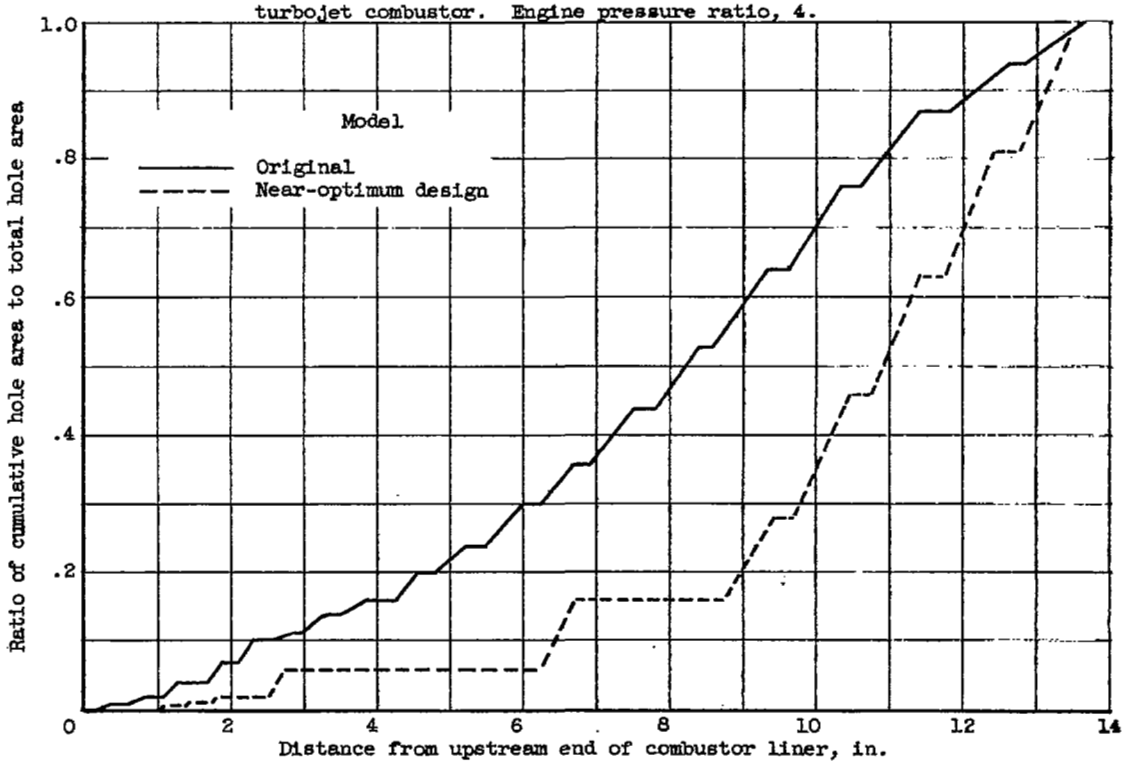

Figure 87. - Axial distribution of hole area in liners of two experimental annular turbojet combustors of figure 86.

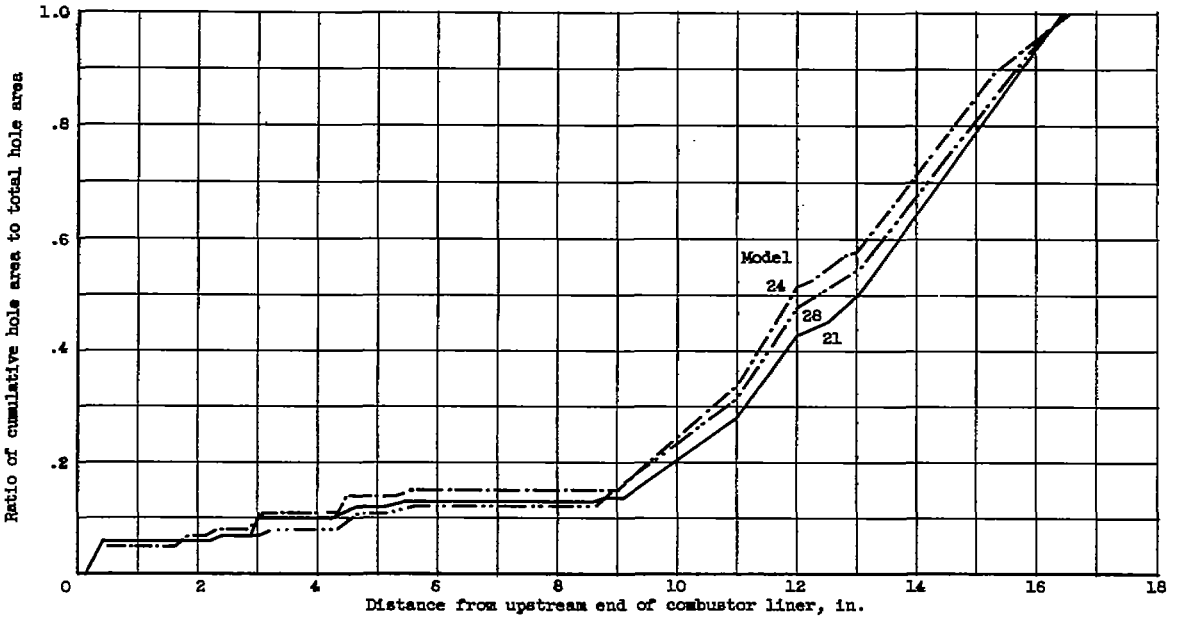

Figure 88. - Axial distribution of hole area in liners of three experimental annular turbojet combustors having similar patterns of circular holes for admission of primary air (ref. 28).

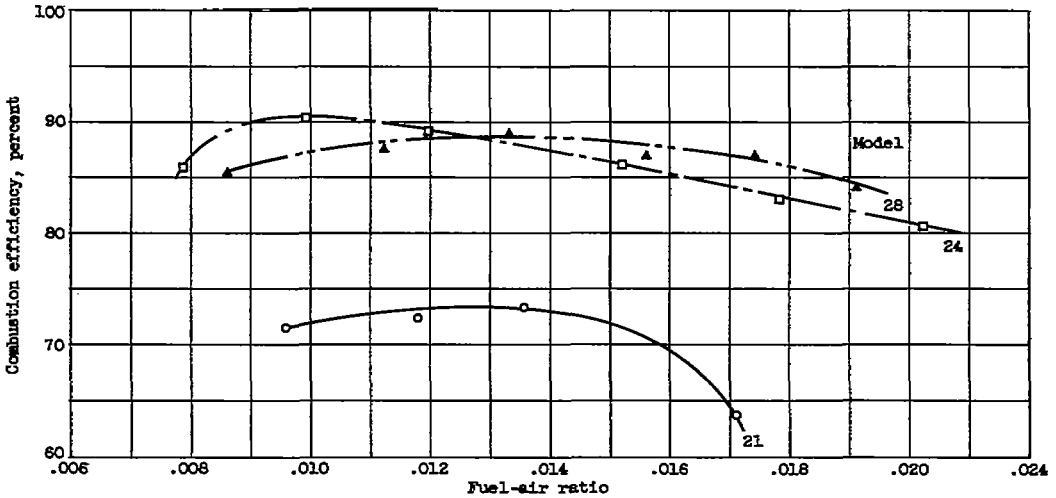

Figure 89. - Combustion efficiencies obtained with three annular turbojet combustor configurations of figure 88. Combustor inlet-air pressure, 2.5 pounds per square inch absolute; inlet-air temperature, 728° R; reference velocity, 80 feet per second (ref. 28).

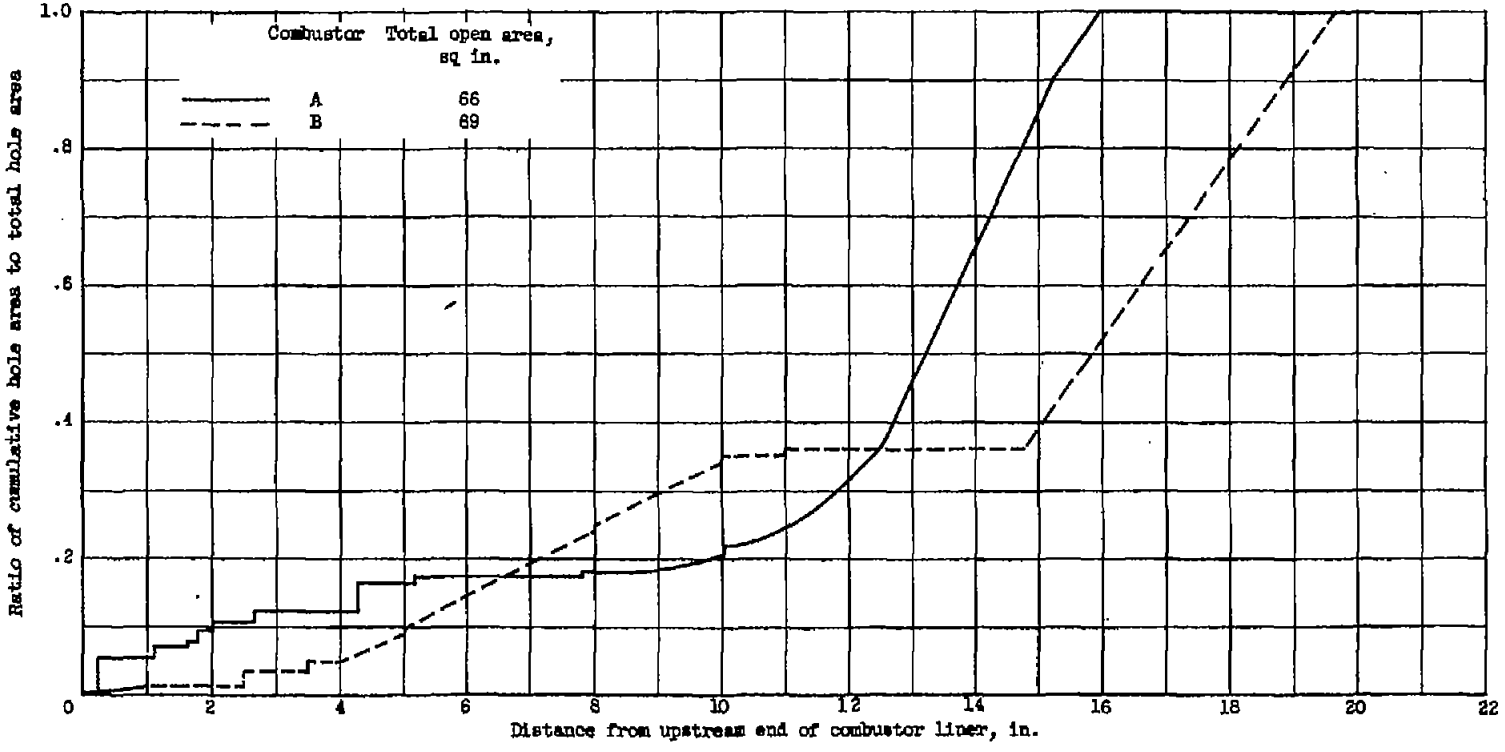

Figure 90. - Axial distribution of hole area in liners of two experimental annular turbojet combustors having dissimilar primary-air-admission designs (ref. 29).

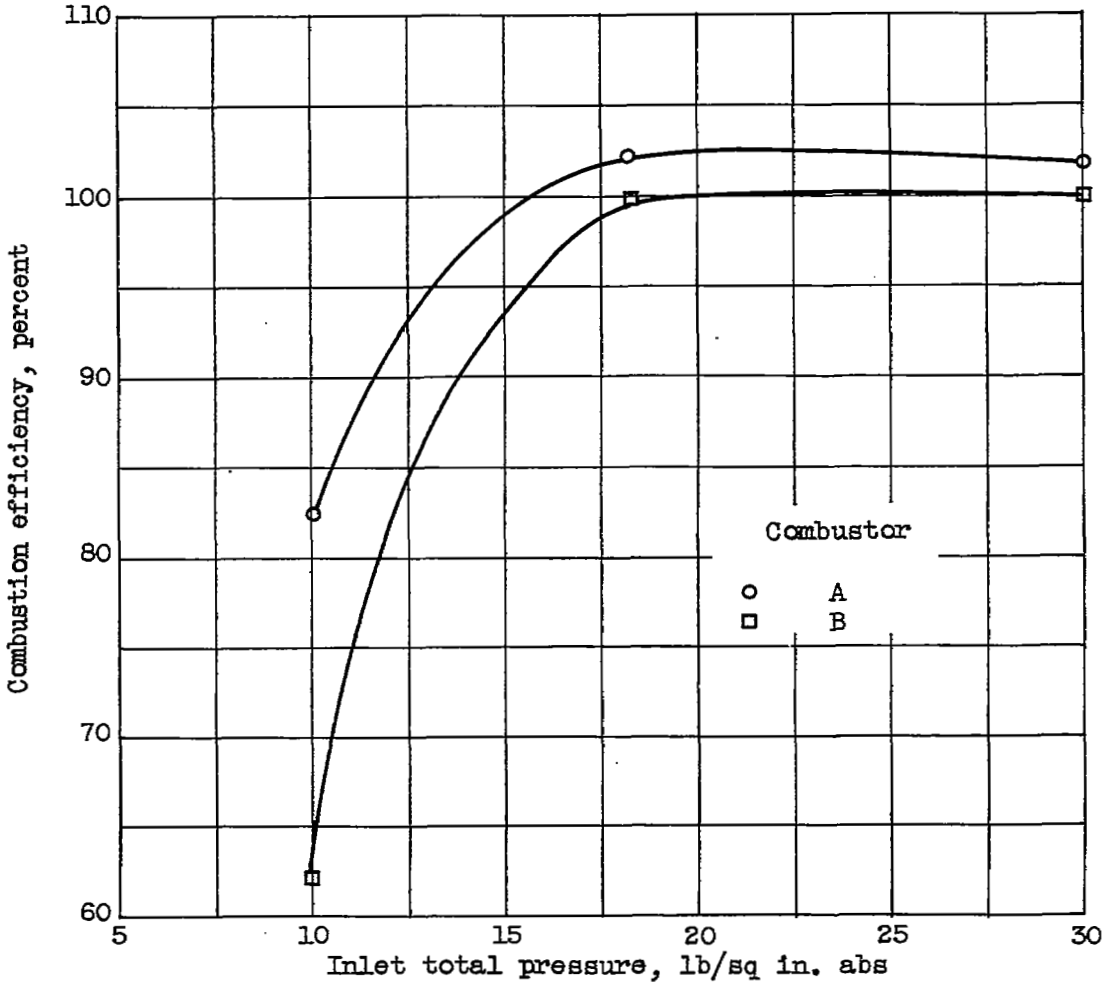

Figure 91. - Effect of pressure on combustion efficiency of two experimental annular turbojet combustors of figure 90. Inlet-air temperature, 1330° R; average outlet temperature, 2260° R; reference velocity, 165 feet per second (ref. 29).

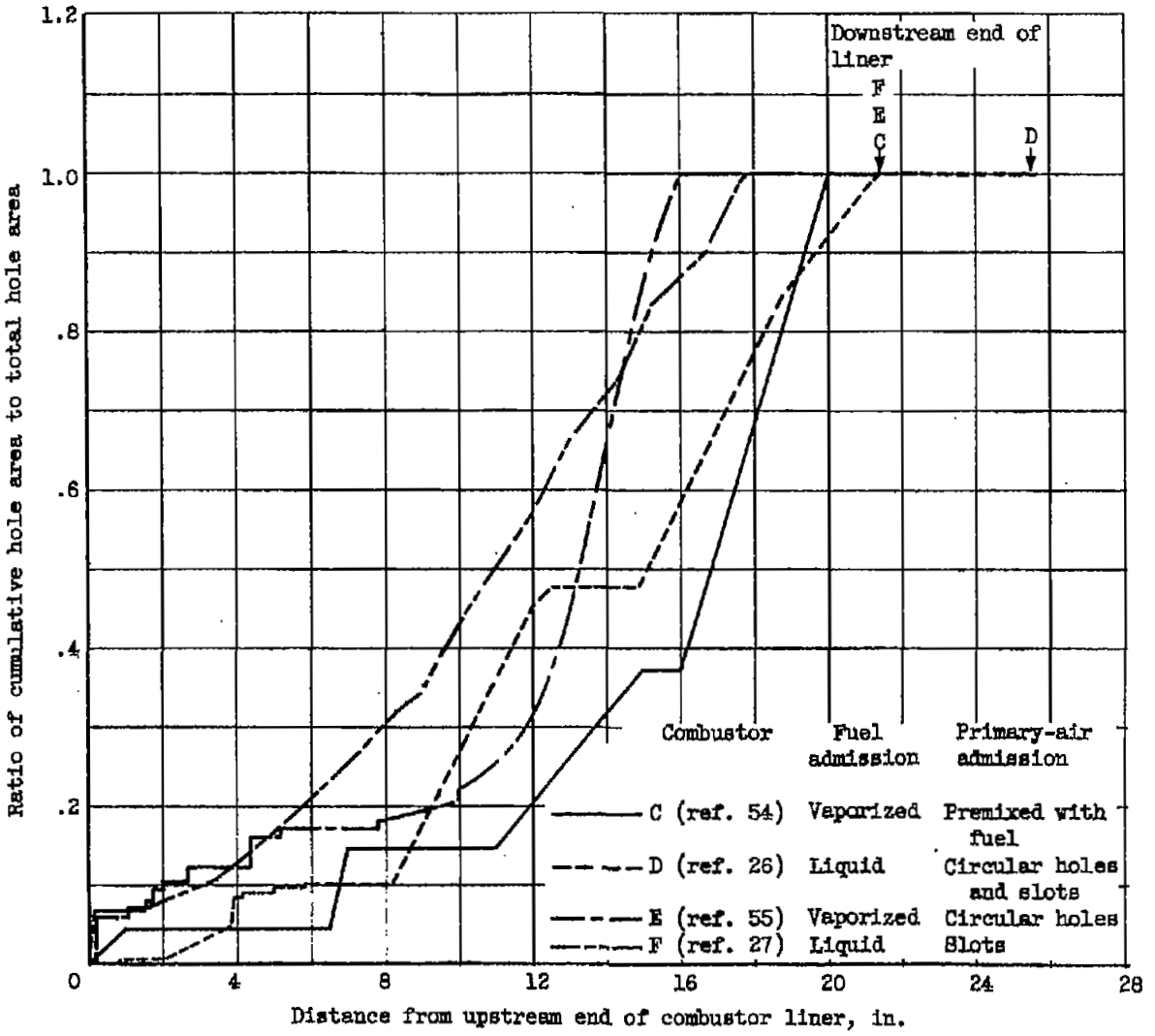

Figure 92. - Axial distribution of hole area of several turbojet combustor configurations designed for high efficiency at low-pressure conditions.

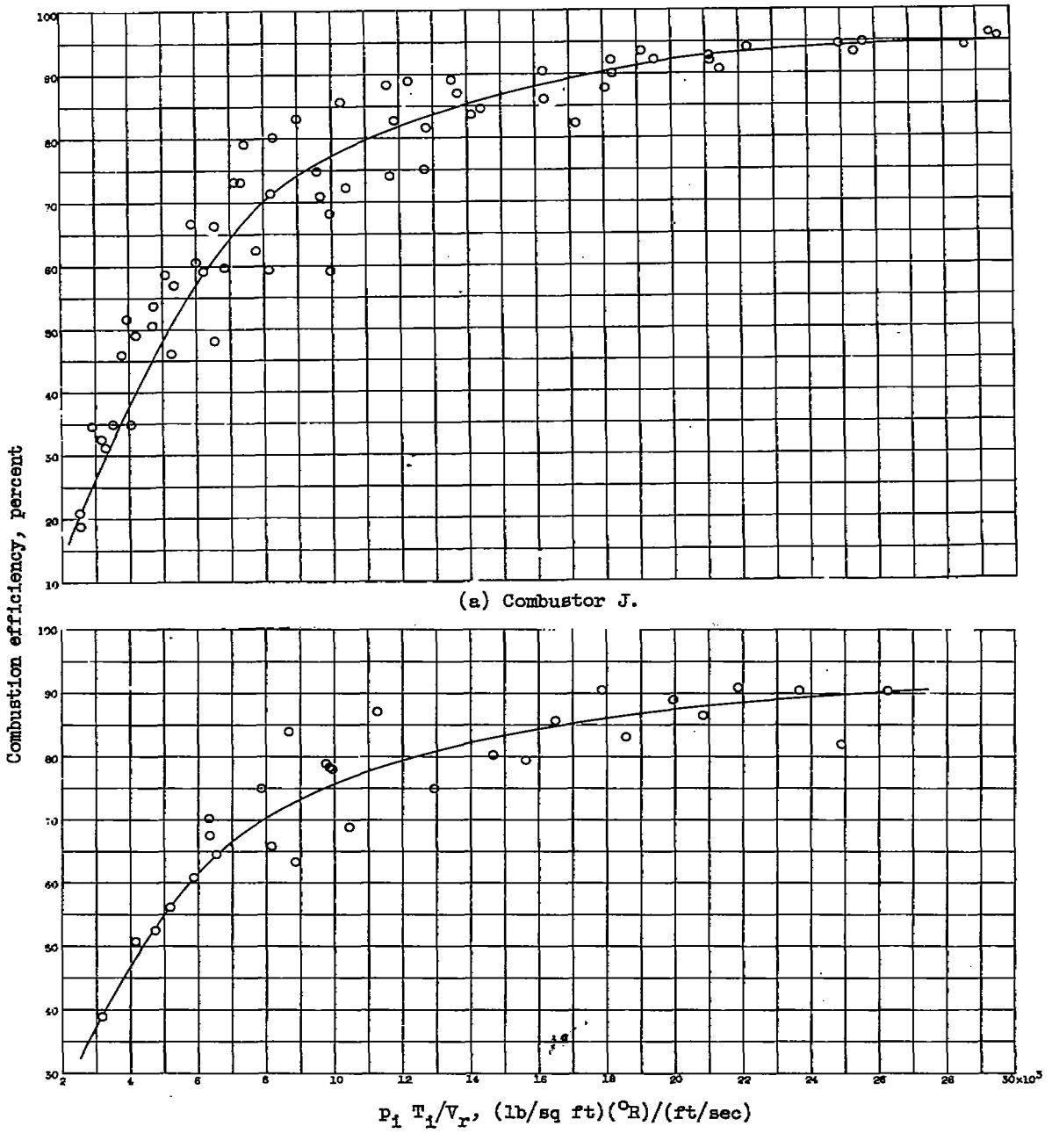

(a) Combustor J.

(b) Combustor M.

Figure 93. - Correlation between combustion efficiency and $p_i T_i/V_r$ for data obtained in two turbojet combustors (ref. 32).

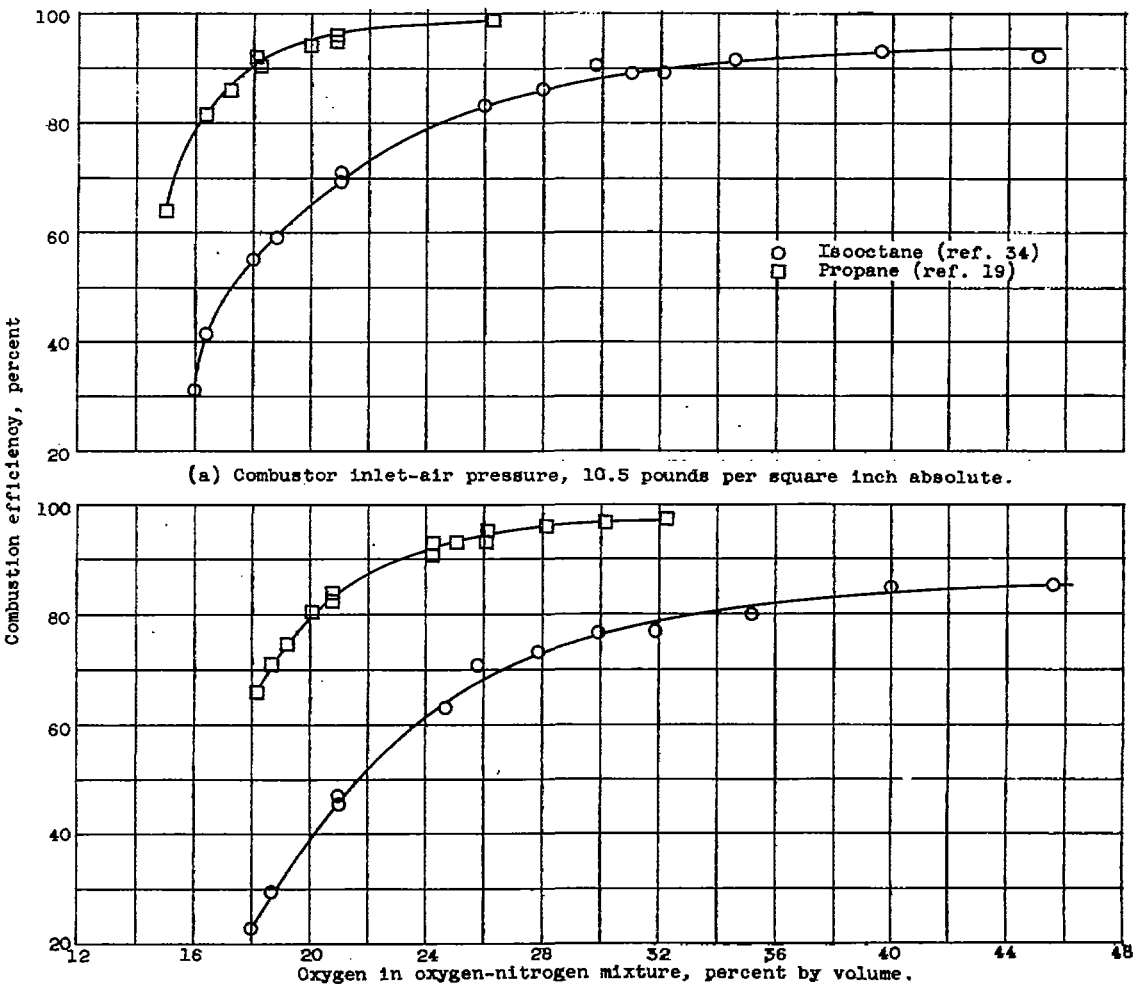

(a) Combustor inlet-air pressure, 10.5 pounds per square inch absolute.

(b) Combustor inlet-air pressure, 7 pounds per square inch absolute.

Figure 94. - Effect of oxygen concentration on combustion efficiencies obtained with liquid and gaseous fuels in 7-inch-diameter tubular combustor operating at two different combustor-inlet pressures. Combustor inlet-air temperature, 500° R; oxygen-nitrogen flow rate, 3600 pounds per hour; fuel-air ratio, 0.012.

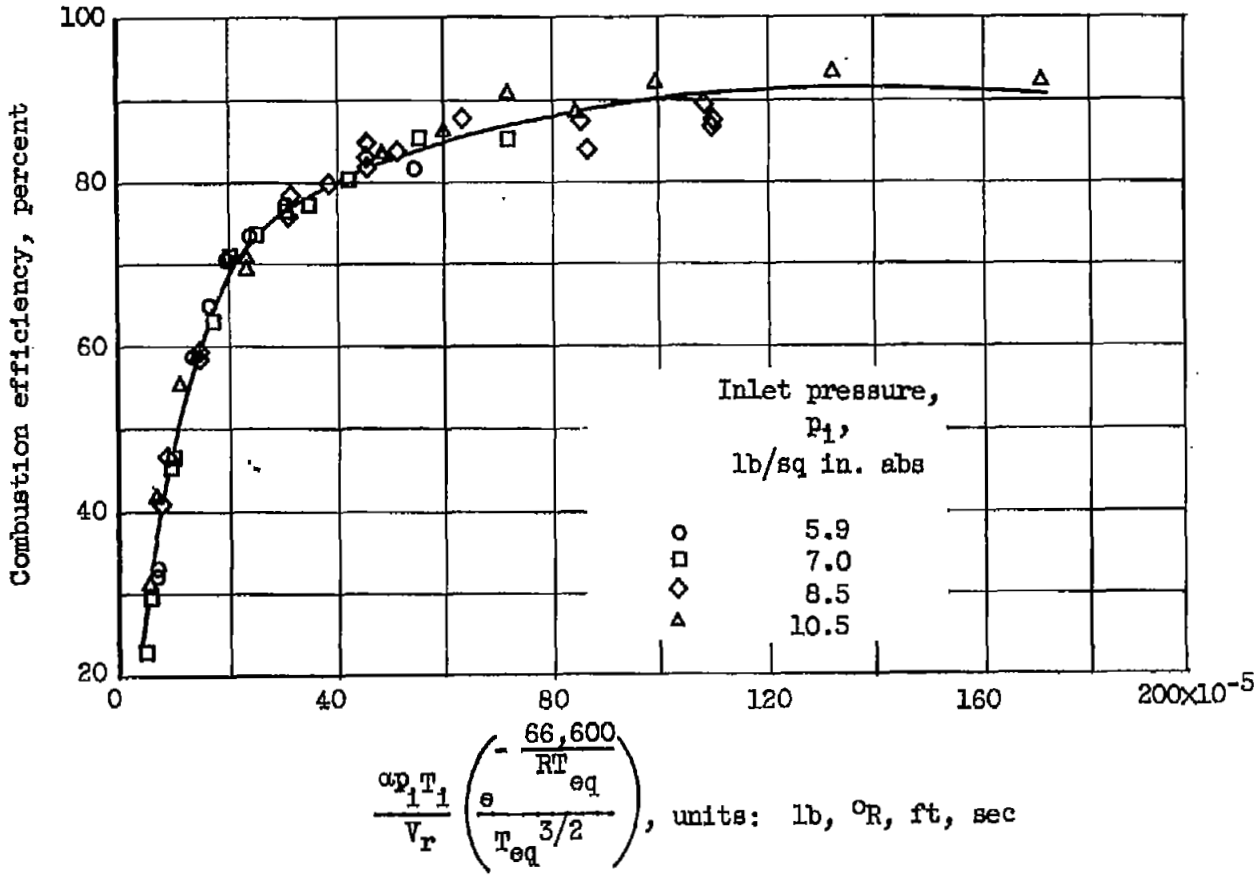

(a) Isooctane fuel (ref. 34).

Figure 95. - Correlation of combustion efficiency of single tubular combustor with parameter from second-order-reaction equation. Inlet-air temperature, 500° R; oxygen-nitrogen flow rate, 3600 pounds per hour; fuel-air ratio, 0.012.

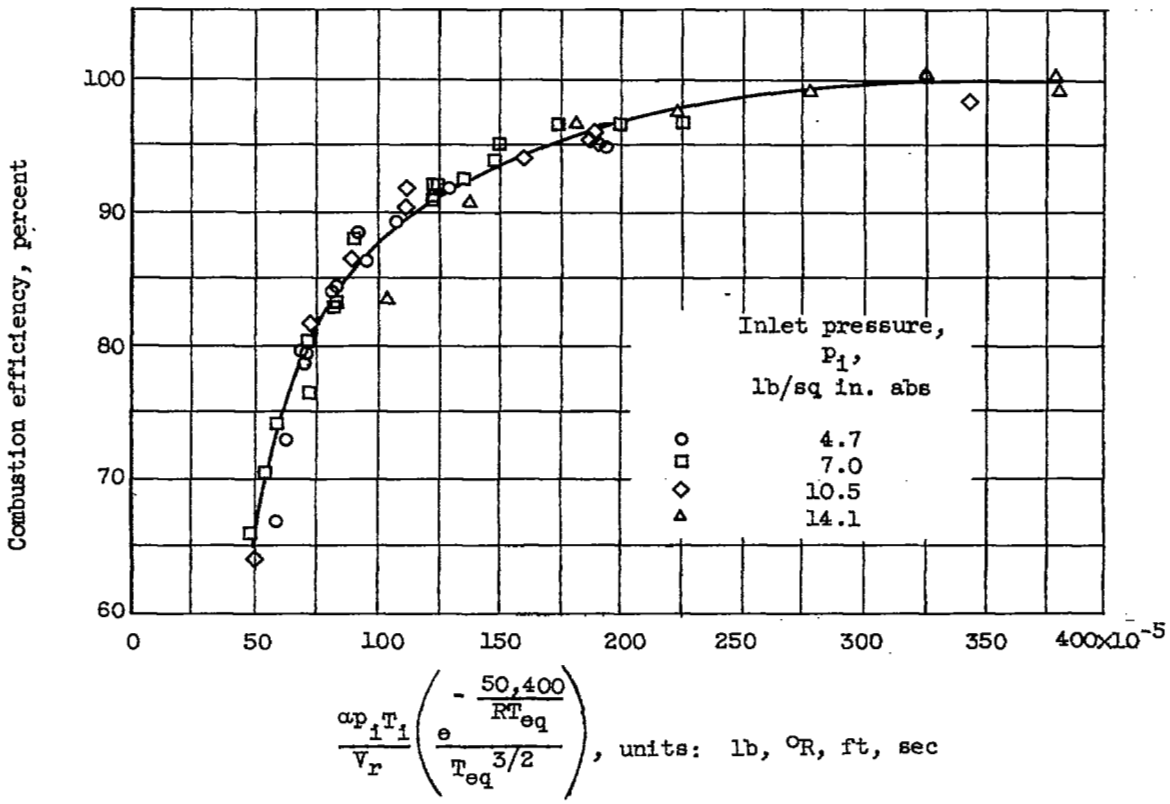

(b) Propane fuel (ref. 19).

Figure 95. - Concluded. Correlation of combustion efficiency of single tubular combustor with parameter from second-order-reaction equation. Inlet-air temperature, 500° R; oxygen-nitrogen flow rate, 3600 pounds per hour; fuel-air ratio, 0.012.

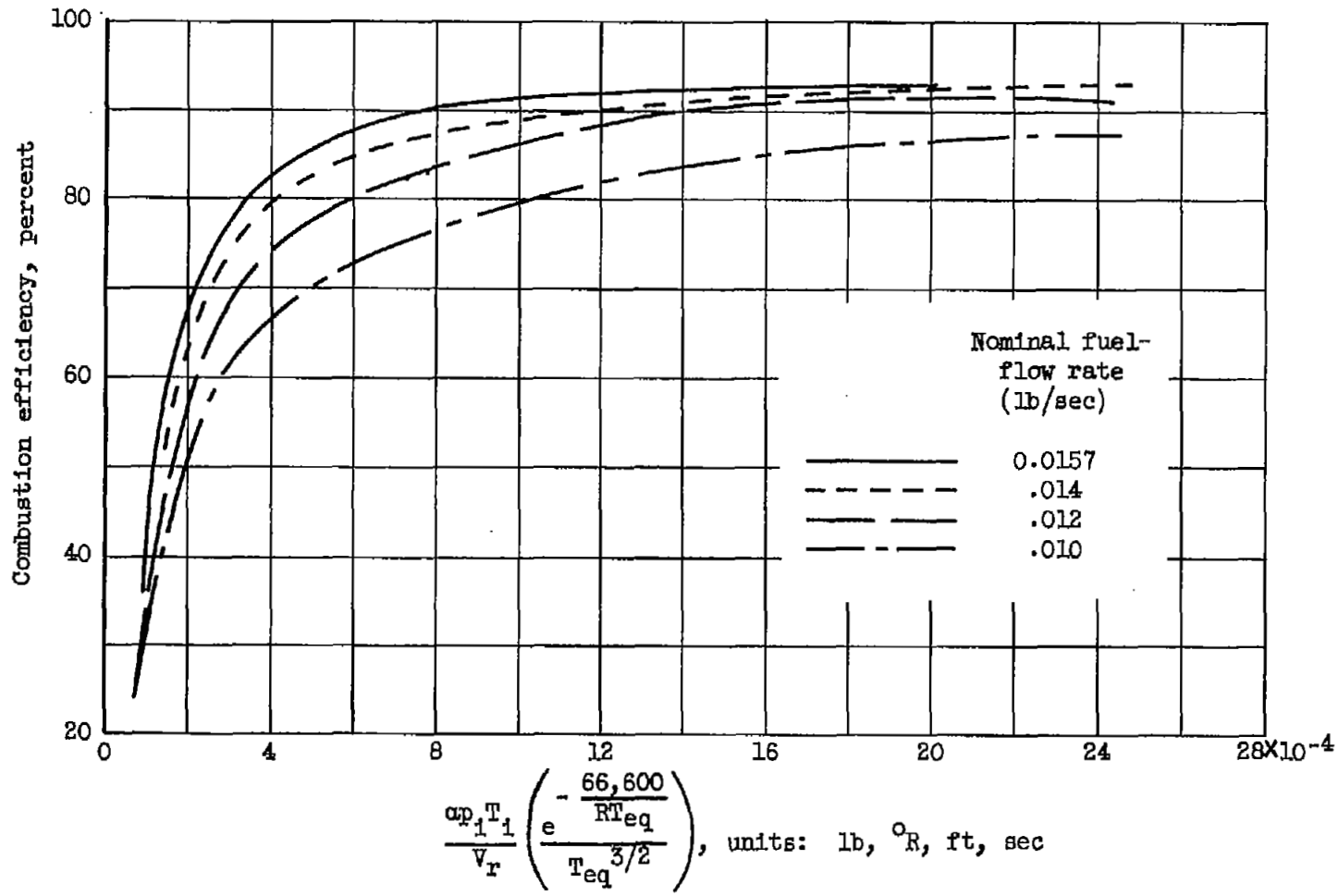

Figure 96. - Effect of fuel-air ratio on correlation of combustion efficiency with parameter from second-order-reaction equation for single tubular combustor operating with isooctane fuel. Inlet-air temperature, 500° R:, oxygen-nitrogen flow rate, 3600 pounds per hour; (ref. 34).

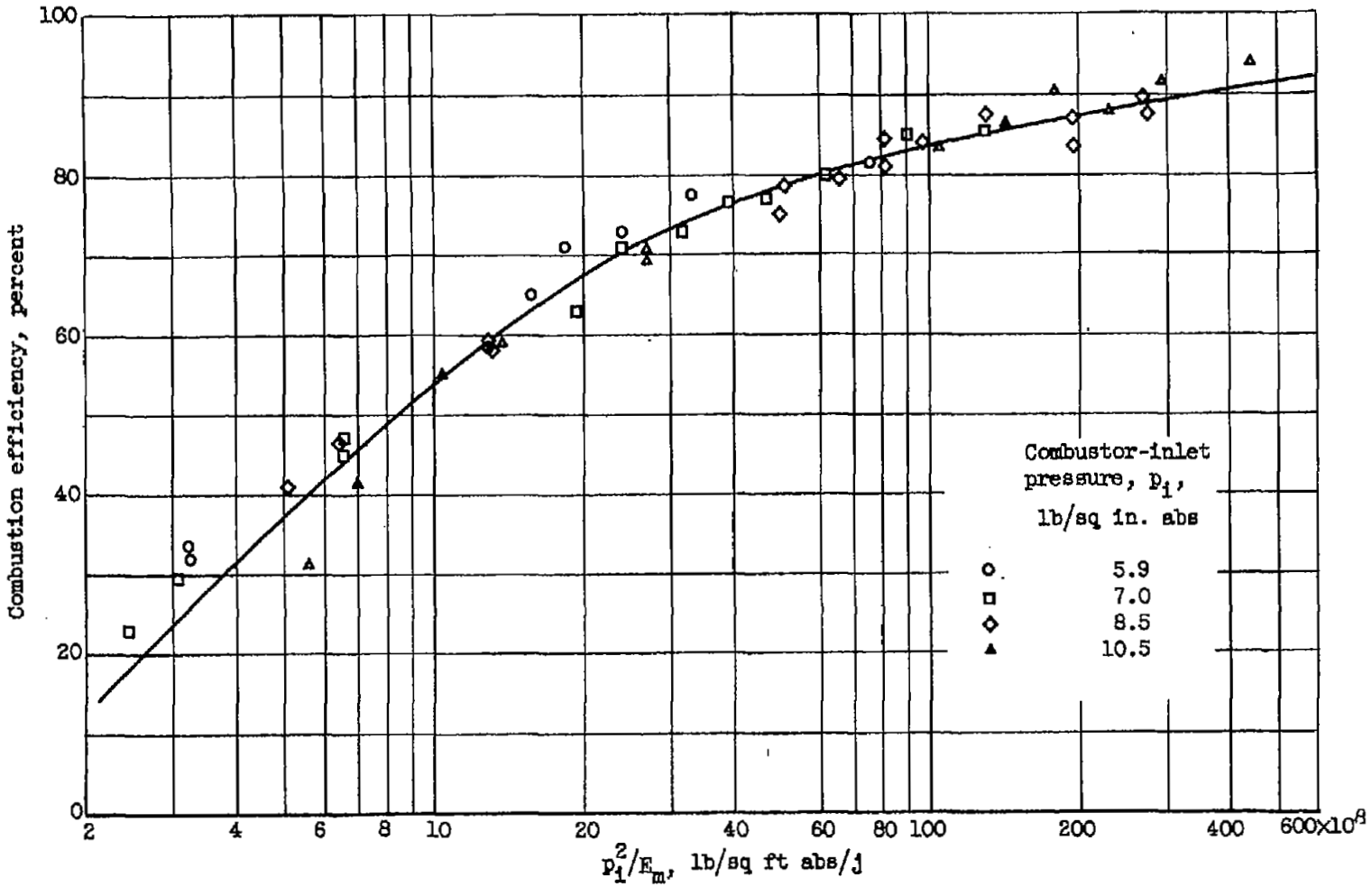

Figure 97. - Correlation of combustion efficiency of isooctane fuel in single tubular combustor with function of minimum spark-ignition energy and combustor-inlet pressure. Inlet-air temperature, 500° R; oxygen-nitrogen flow rate, 3600 pounds per hour; fuel-air ratio, 0.012 (ref. 34).

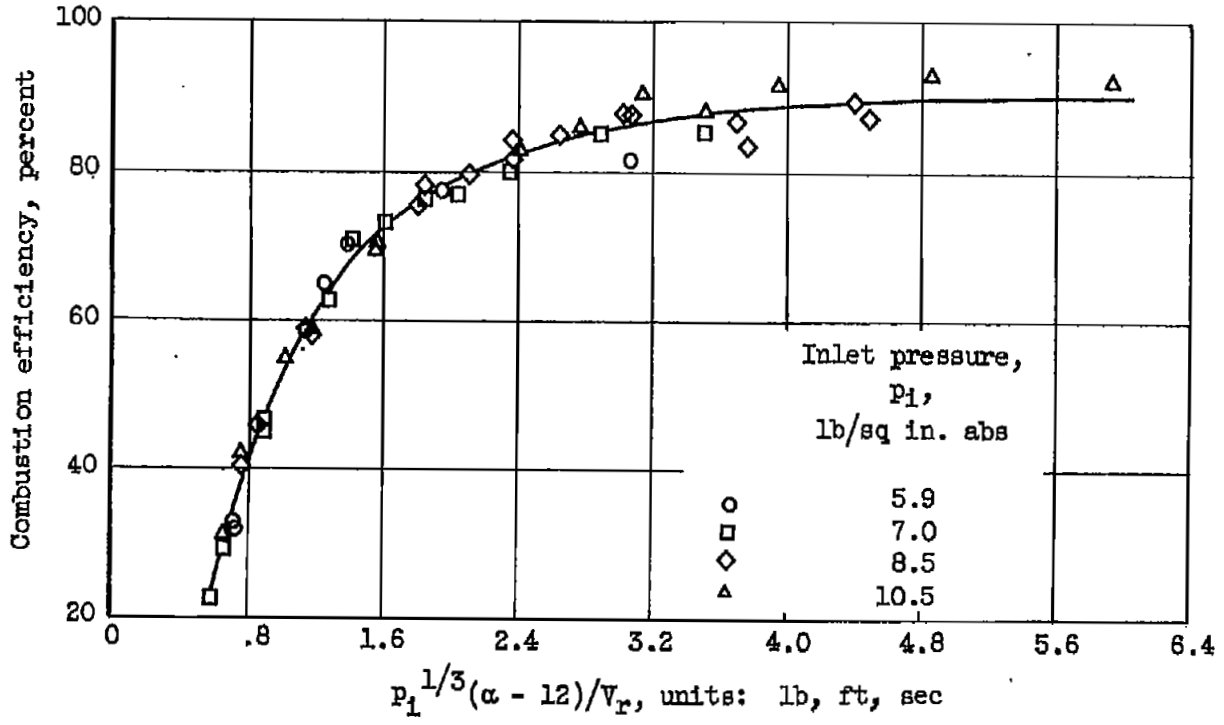

(a) Isooctane fuel (ref. 34).

Figure 98. - Correlation of combustion efficiency in single tubular combustor with flame-speed parameter. Inlet-air temperature, 500° R; oxygen-nitrogen flow rate, 3600 pounds per hour; fuel-air ratio, 0.012.

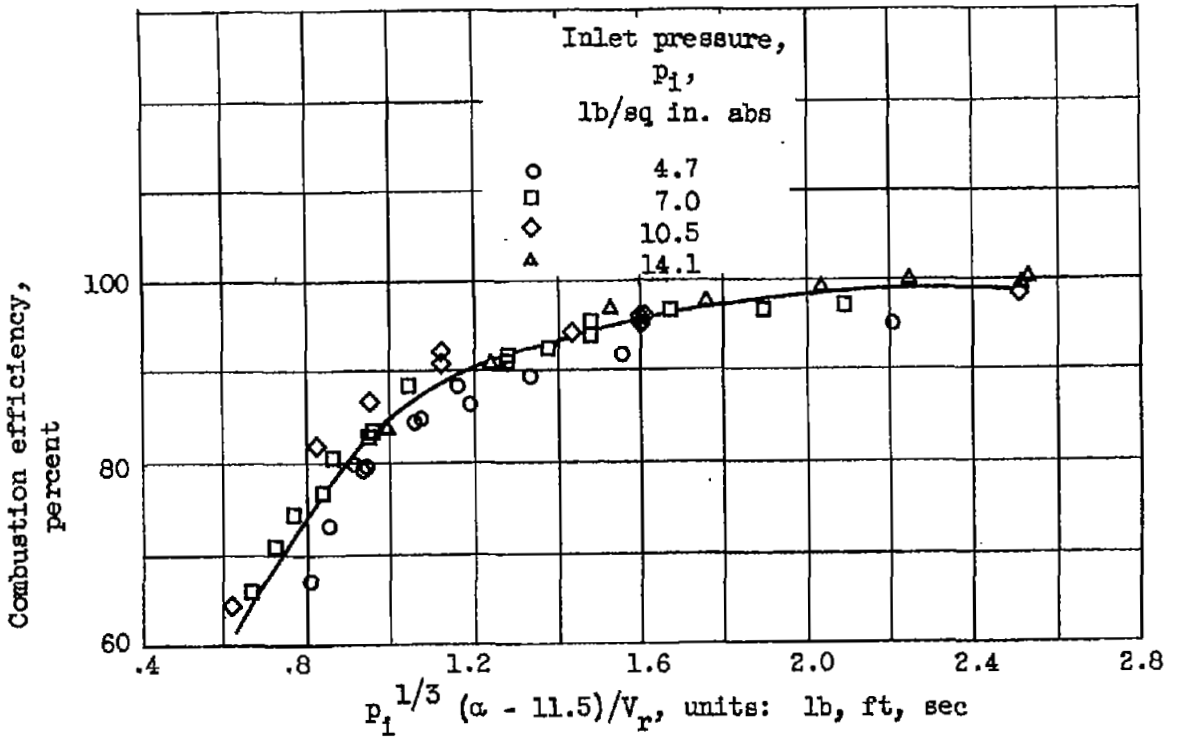

(b) Propane fuel (ref. 19).

Figure 98. - Concluded. Correlation of combustion efficiency in single tubular combustor with flame-speed parameter. Inlet-air temperature, 500° R; oxygen-nitrogen flow rate, 3600 pounds per hour; fuel-air ratio, 0.012.

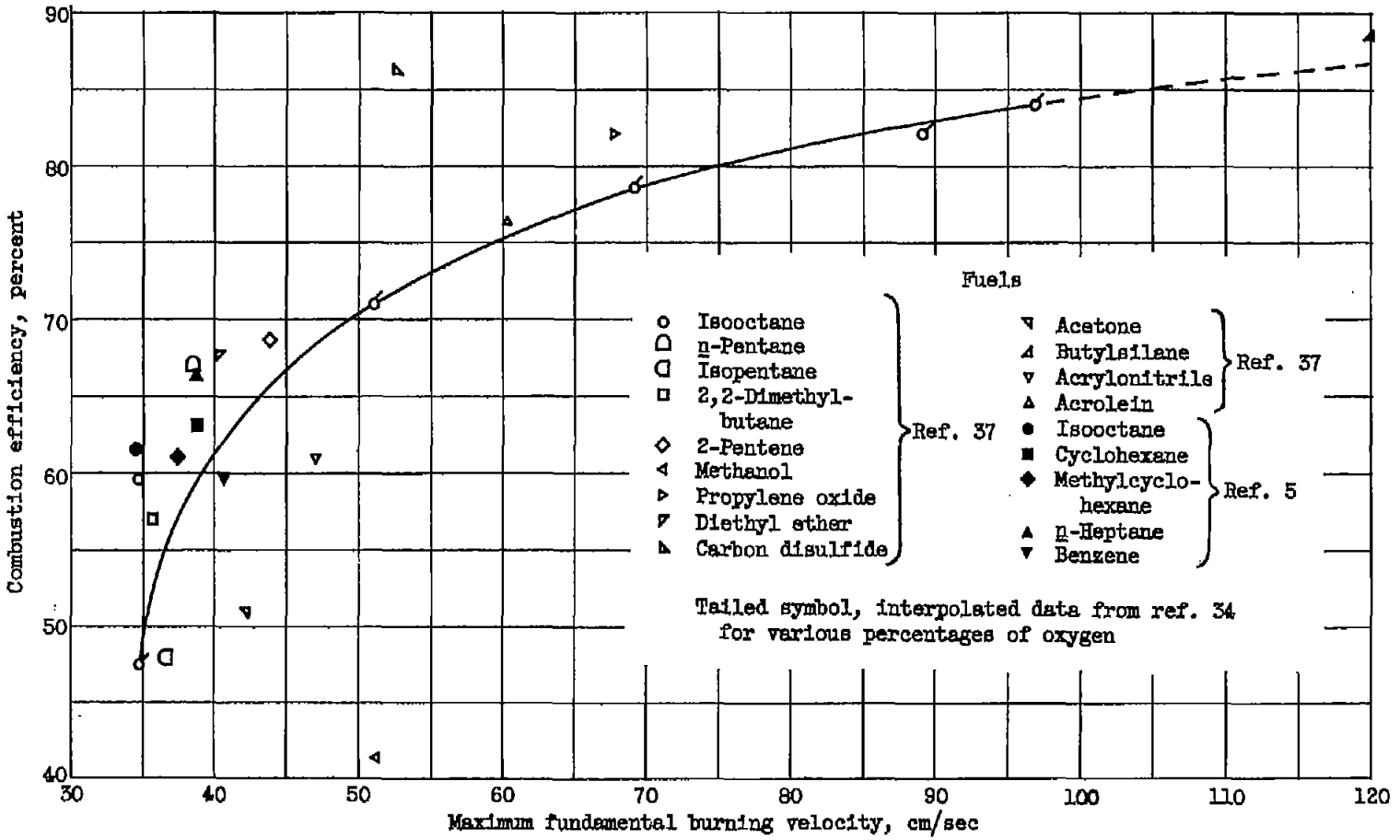

Figure 99. - Correlation of combustion efficiency with maximum fundamental burning velocity. Single tubular combustor; inlet-air pressure, 7 pounds per square inch absolute; inlet-air temperature, 500° R; heat input, 250 Btu per pound of air; air-flow rate, 1.0 pound per second.

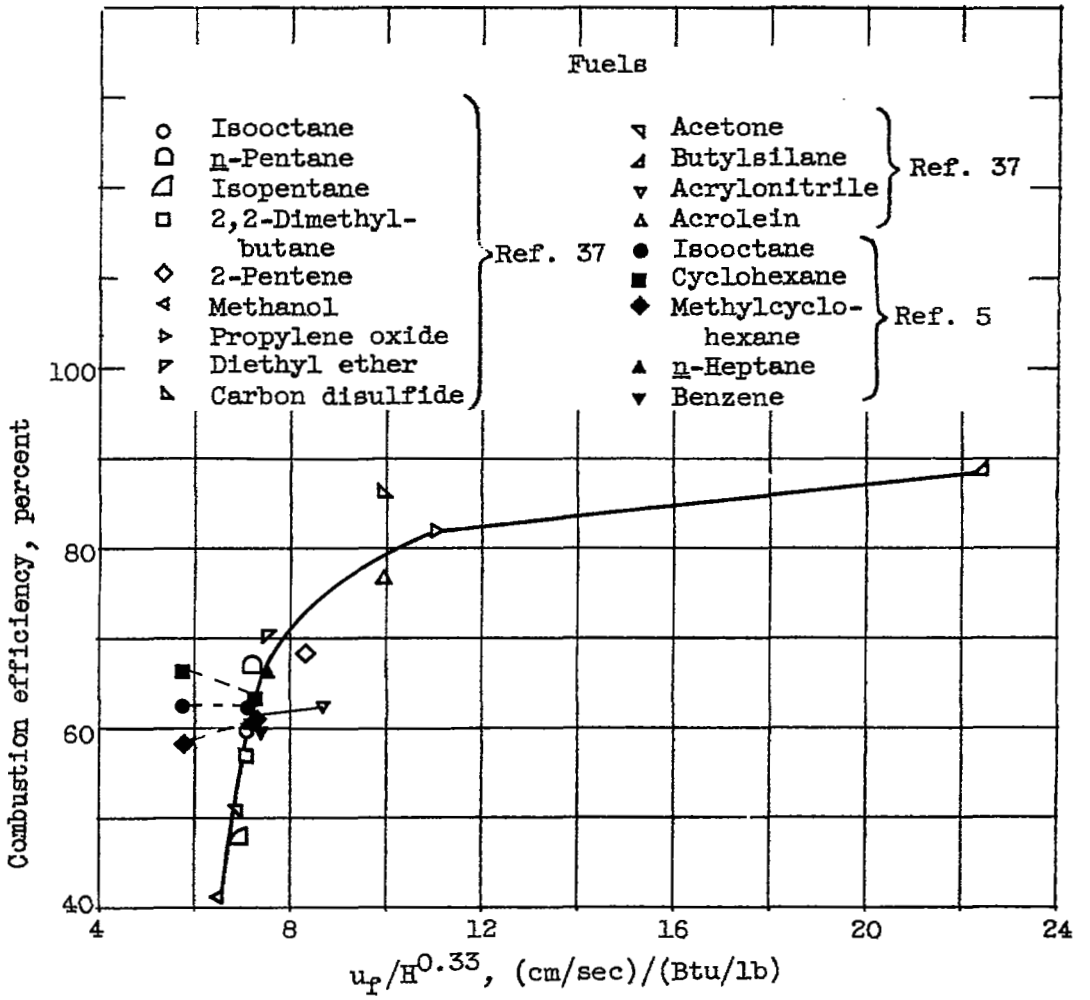

Figure 100. - Correlation of combustion efficiency with parameter $u_f/H^{0.33}$. Single tubular combustor; inlet-air pressure, 7 pounds per square inch absolute; inlet-air temperature, 500° R; heat input, 250 Btu per pound of air; air-flow rate, 1.0 pound per second.

[redacted]

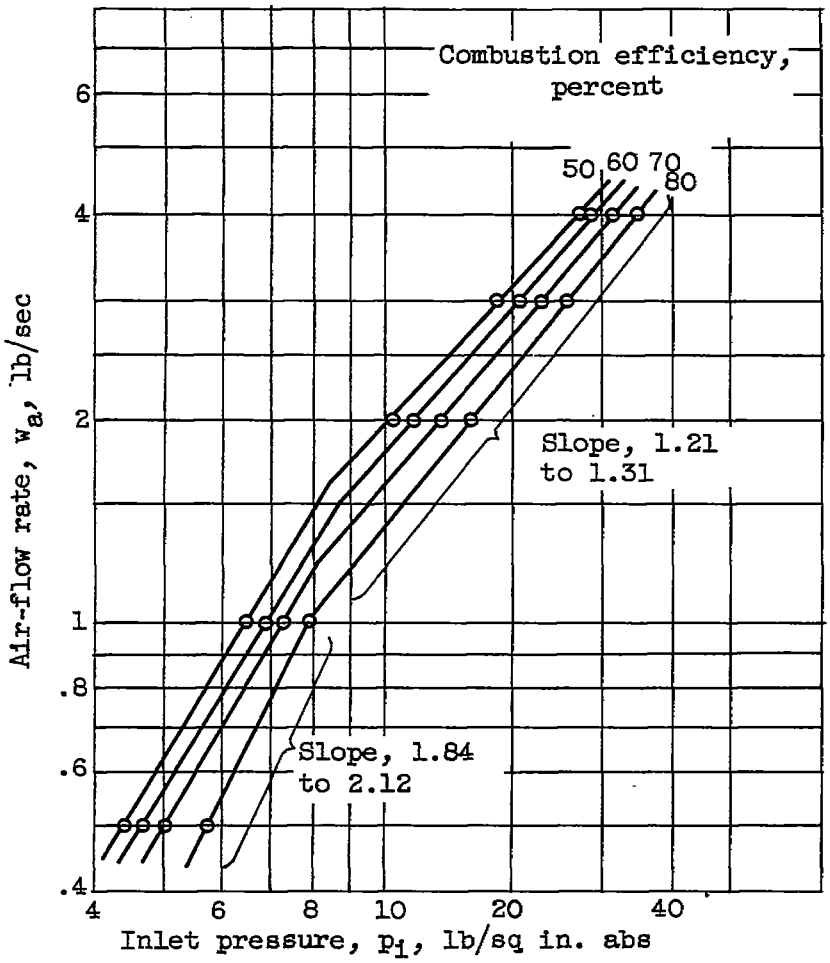

Figure 101. - Relative effects of inlet pressure and air-flow rate on combustion efficiency. Fuel-air ratio, 0.012 (ref. 40).

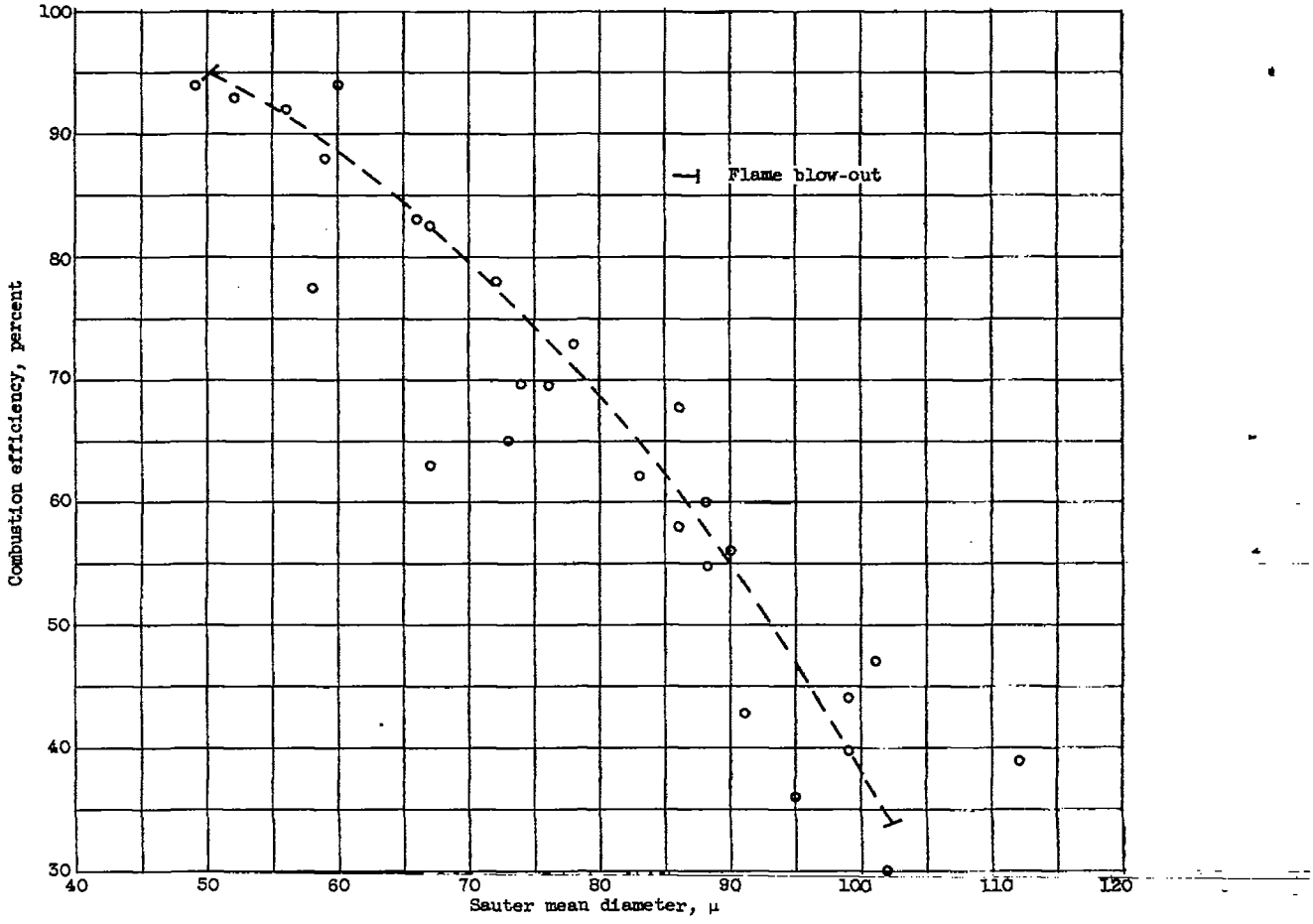

Figure 102. - Relation between combustion efficiency and Sauter mean diameter of fuel spray. Single combustor operating at simulated altitudes from 30,000 to 55,000 feet (ref. 42).

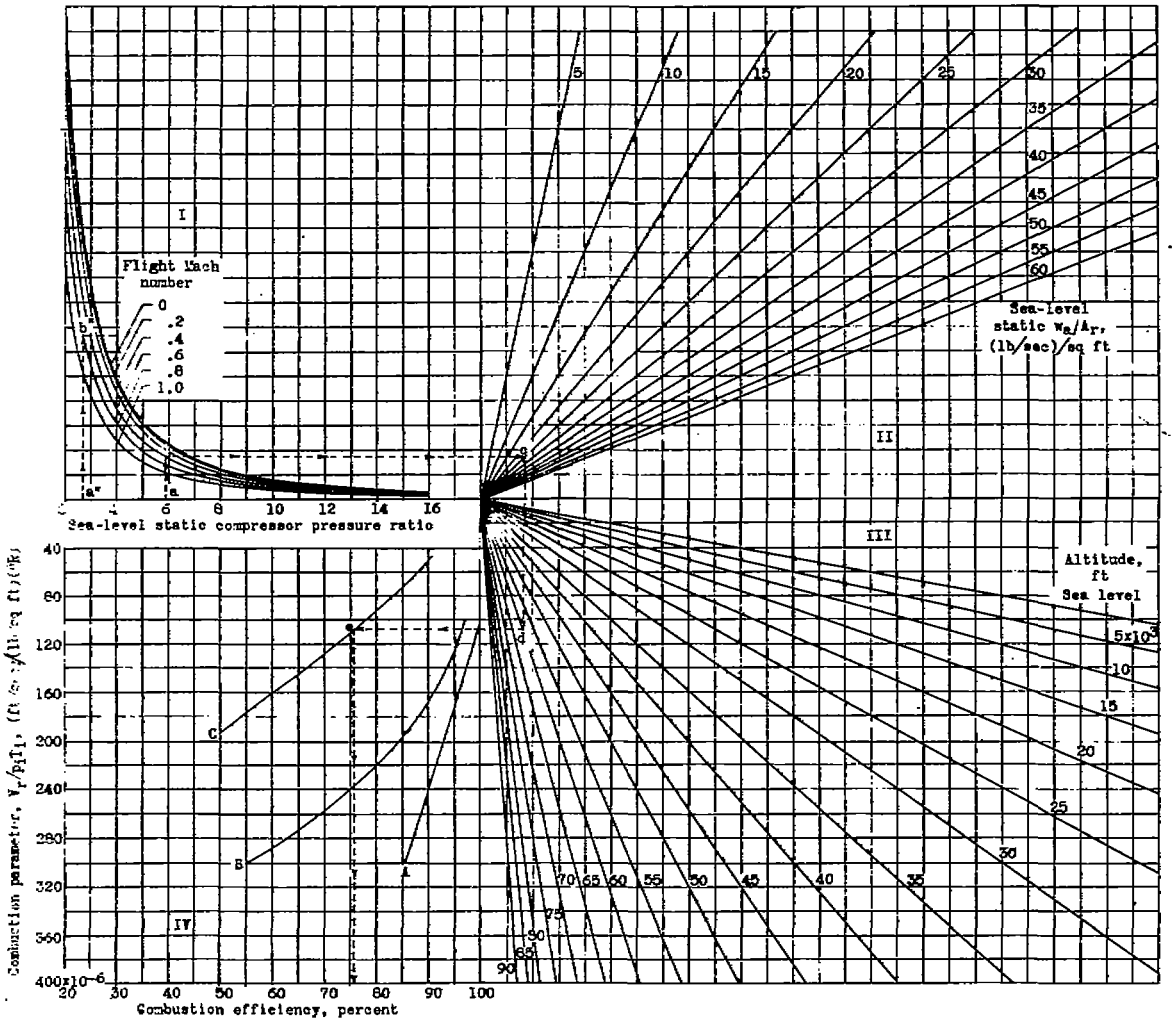

Figure 103. - Chart for estimating combustion efficiency of turbojet combustors at altitude flight conditions. Corrected engine speed, constant; diffuser total-pressure recovery factor, 0.95 (ref. 43).

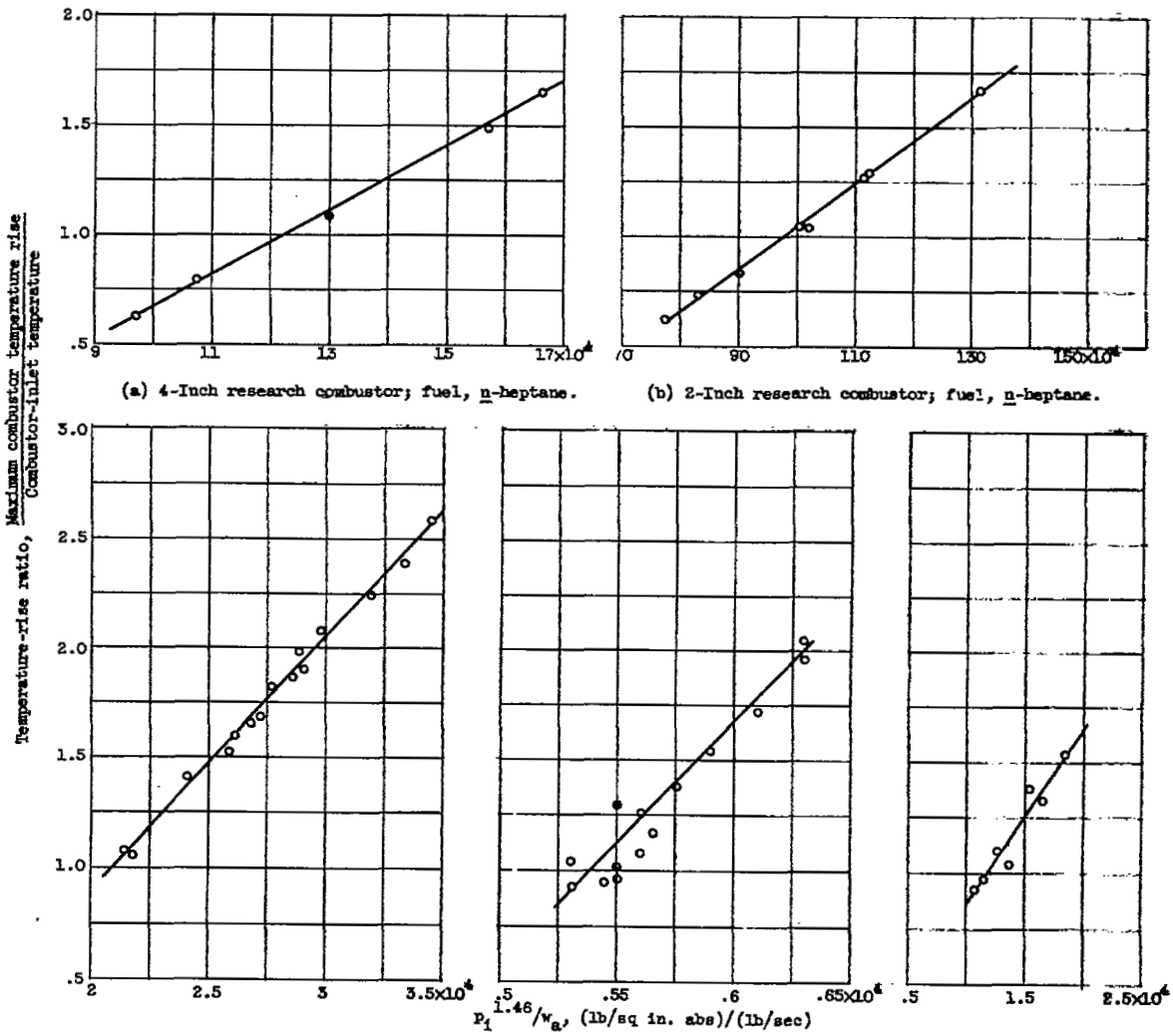

(a) 4-Inch research combustor; fuel, n-heptane.

(b) 2-Inch research combustor; fuel, n-heptane.

(c) 9.5-Inch annular combustor; fuel, n-heptane.

(d) 19-Inch annular combustor; fuel, AN-F-28.

(e) Tubular combustor; fuel, AN-F-28.

Figure 104. - Correlation of temperature-rise ratio with severity parameter $P_i^{1.46}/w_a$ for several combustors (ref. 44).

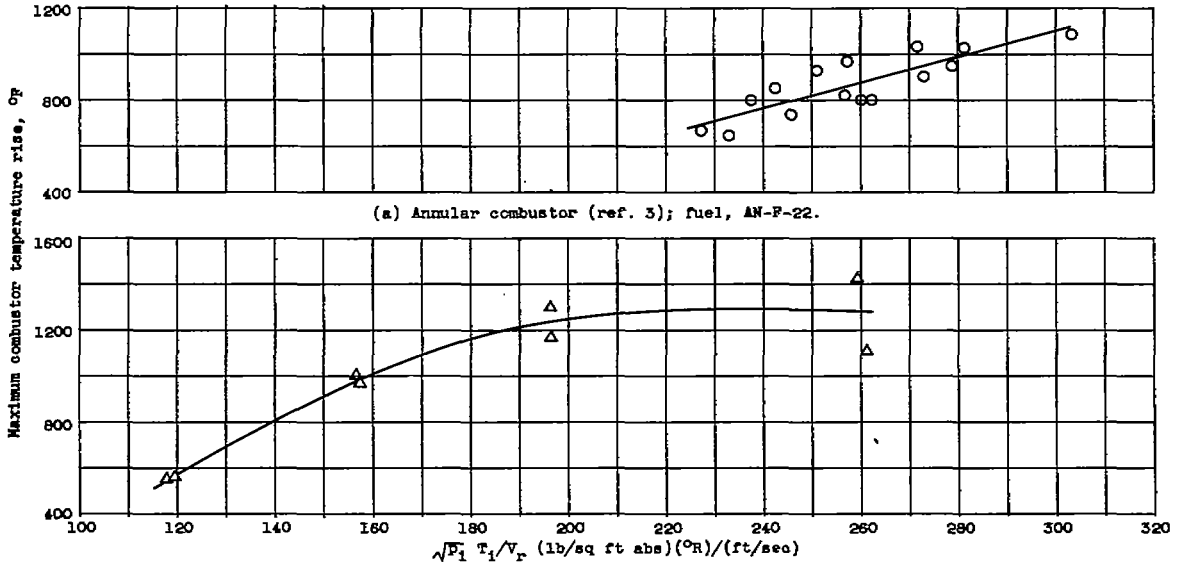

(a) Annular combustor (ref. 3); fuel, AN-F-22.

(b) Tubular combustor (ref. 5); fuel, isooctane.

Figure 105. - Correlation of maximum temperature rise with parameter $\sqrt{p_i}\ T_i/V_r$ for two full-scale combustors.

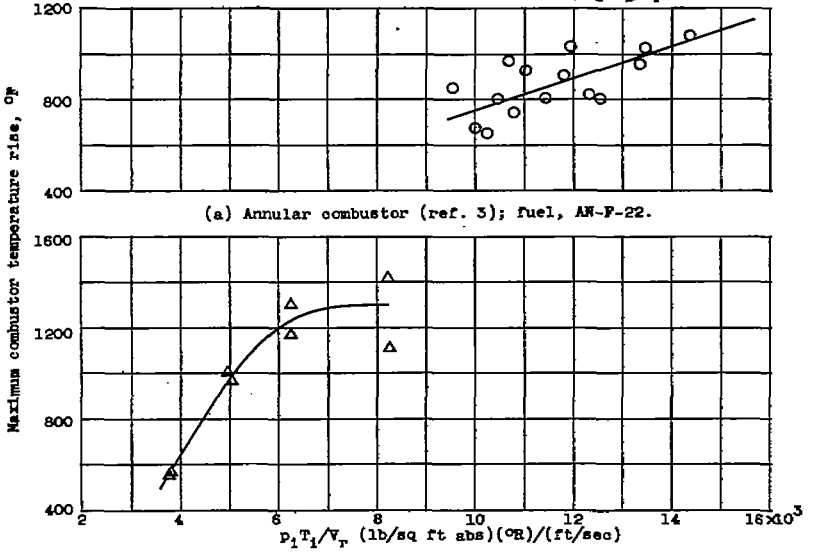

(a) Annular combustor (ref. 3); fuel, AN-F-22.

(b) Tubular combustor (ref. 5); fuel, isooctane.

Figure 106. - Correlation of combustor maximum temperature rise with parameter $p_i T_i/V_r$ for two full-scale combustors.

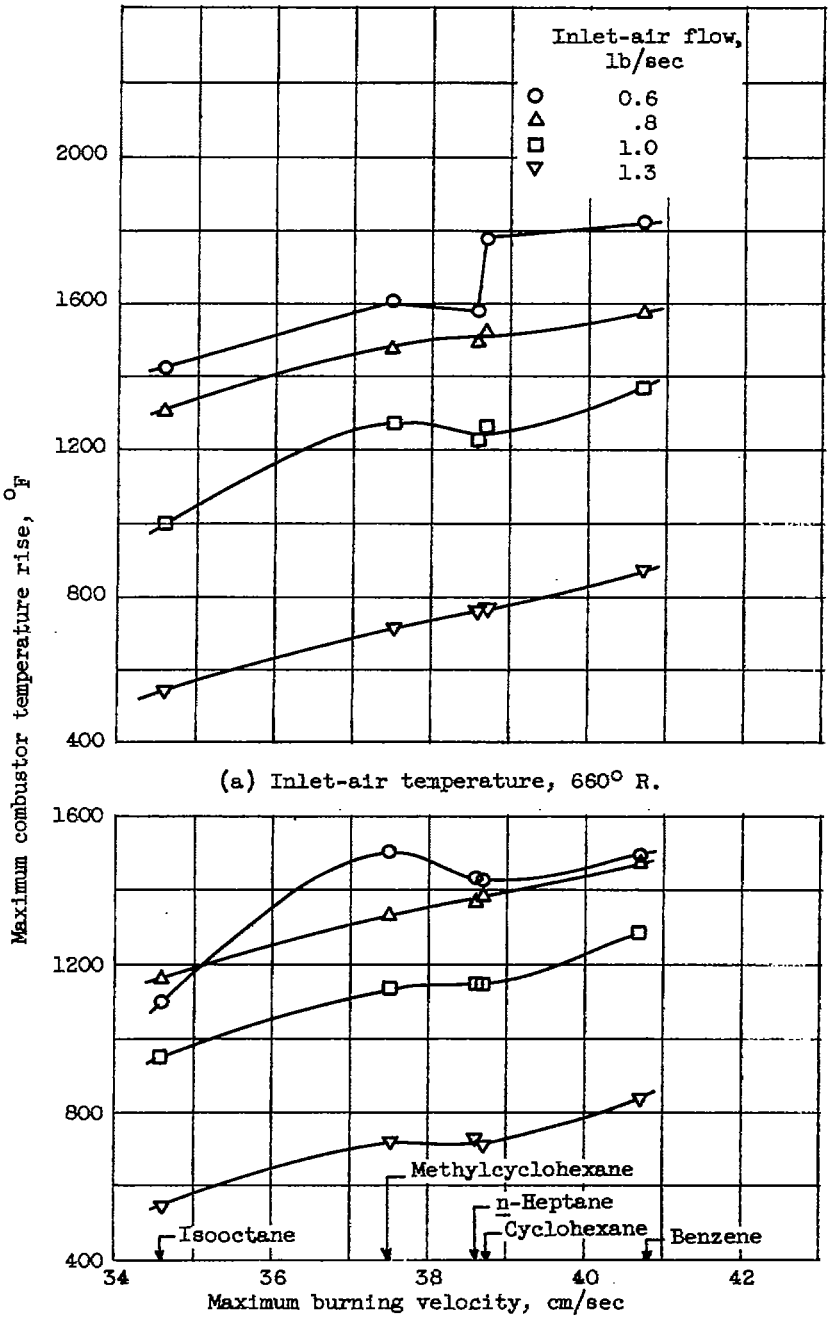

Figure 107. - Variation of maximum combustor temperature rise obtained with pure hydrocarbon fuels with maximum burning velocity in tubular combustor. Combustor inlet-air pressure, 7 pounds per square inch absolute (ref. 5).

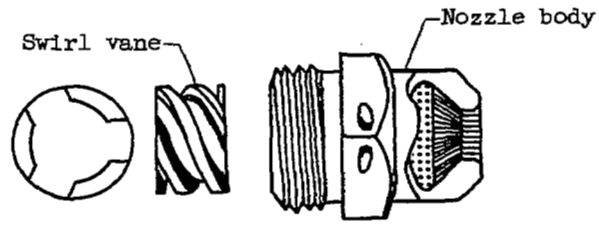

(a) Water-alcohol injection nozzle.

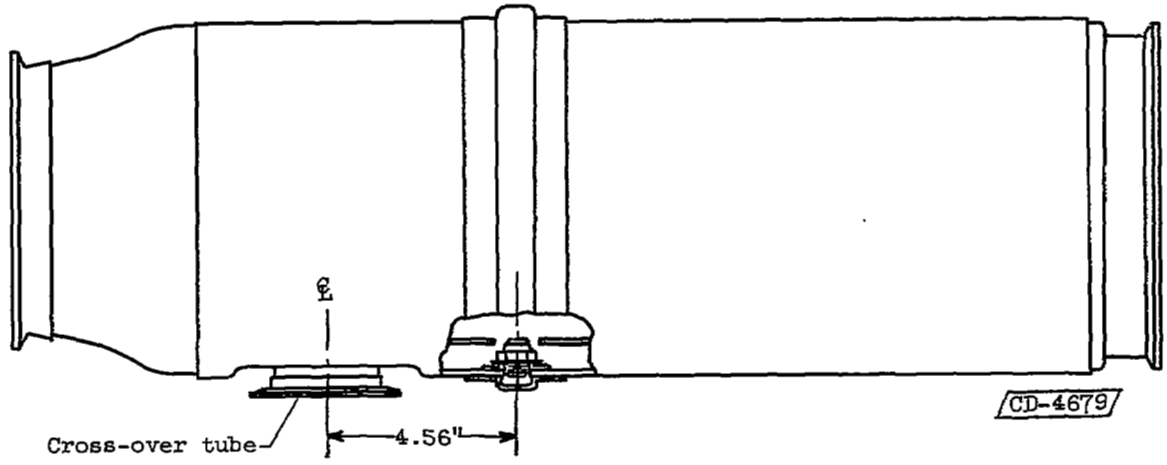

(b) Location of nozzle in combustion chamber (four nozzles per combustion chamber equally spaced around periphery).

Figure 108. - Water-alcohol injection nozzle and its location in tubular combustion chamber (ref. 47).

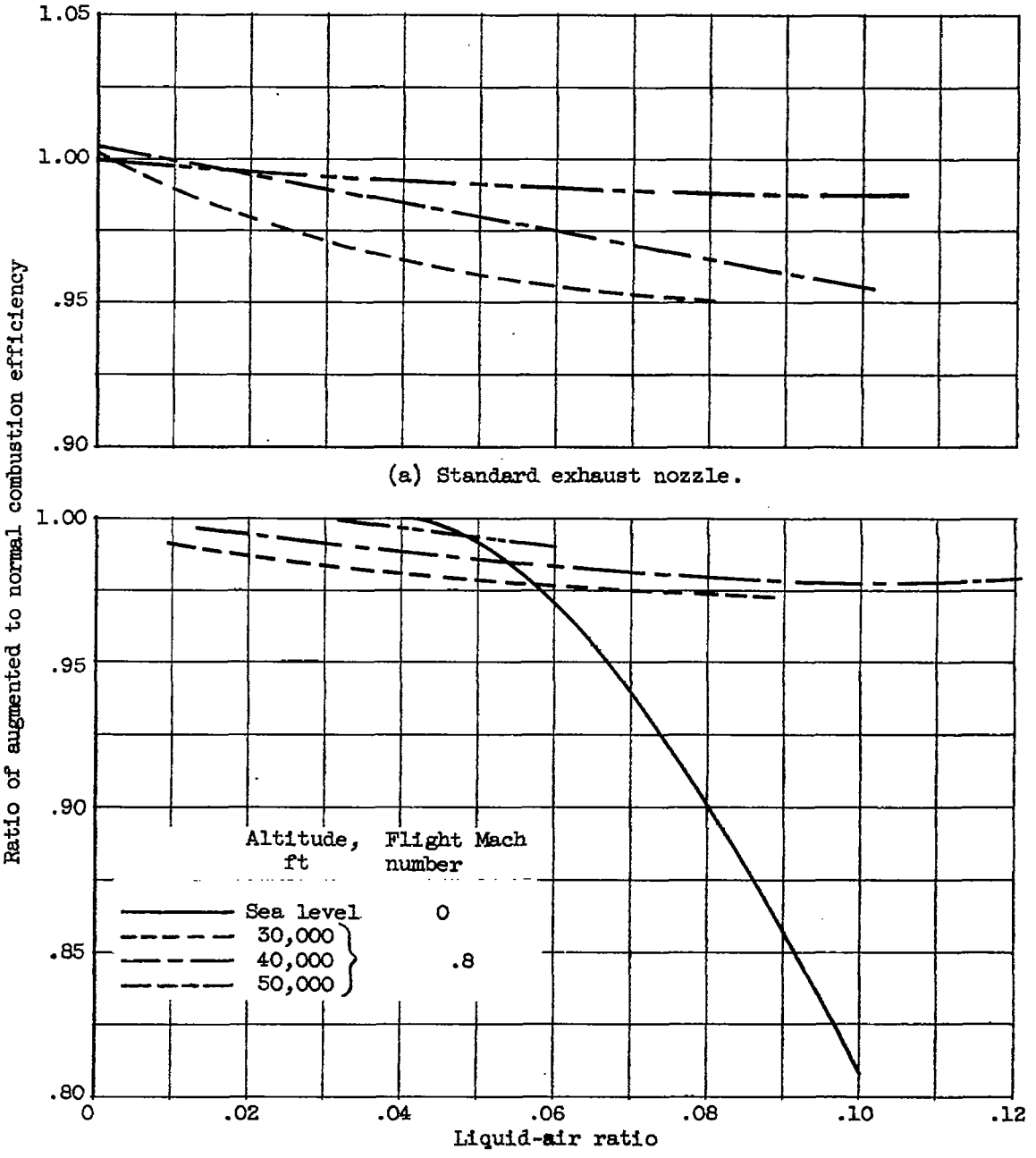

(a) Standard exhaust nozzle.

(b) Variable-area exhaust nozzle.

Figure 109. - Effect of liquid-air ratio on combustion efficiency of turbojet engine equipped with combustion-chamber water-alcohol injection and standard or variable-area exhaust nozzle. Engine speed for augmented operation, 7950 rpm; engine speed for normal operation determined by rated turbine-outlet temperature (ref. 47).

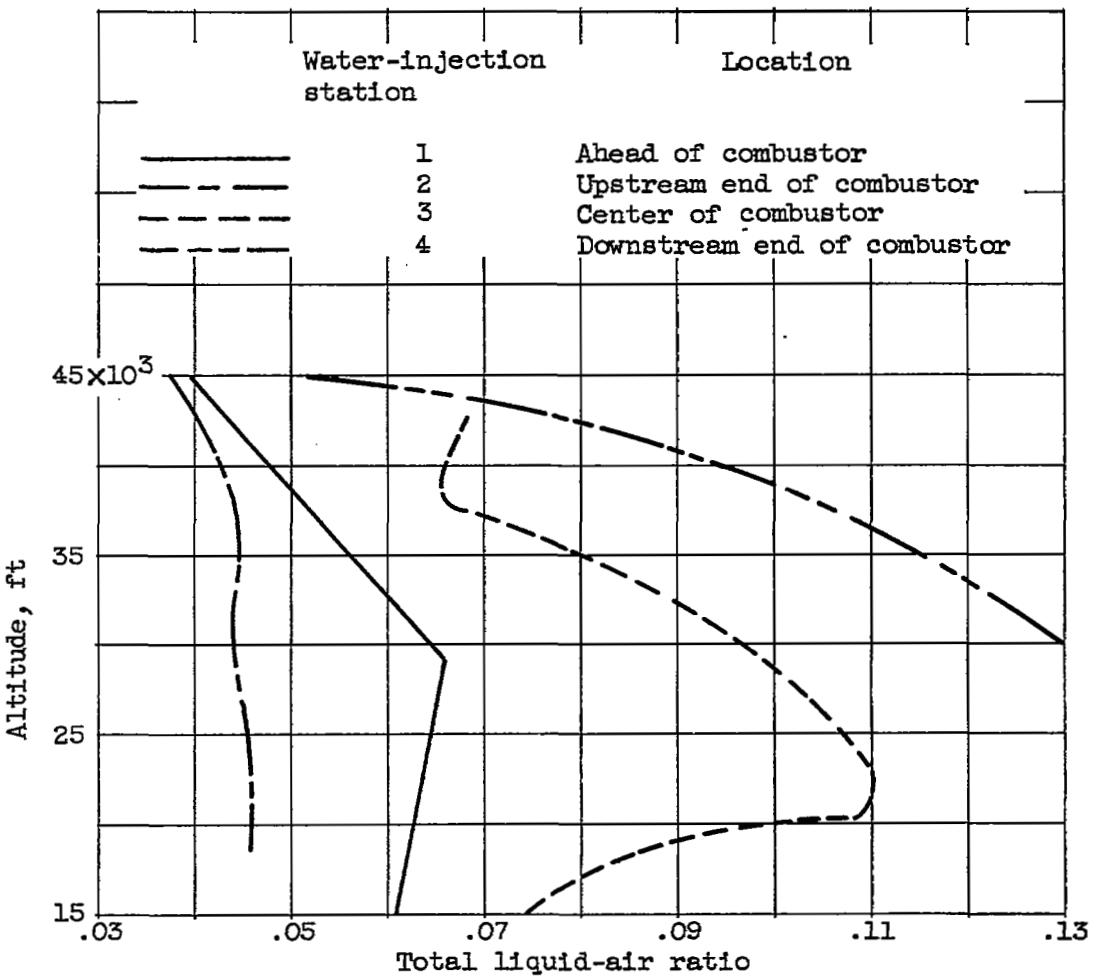

Figure 110. - Effect of altitude on maximum total liquid-air ratio with water injection at various stations in tubular combustor. Simulated operating conditions, zero ram pressure and rated engine speed (ref. 51).

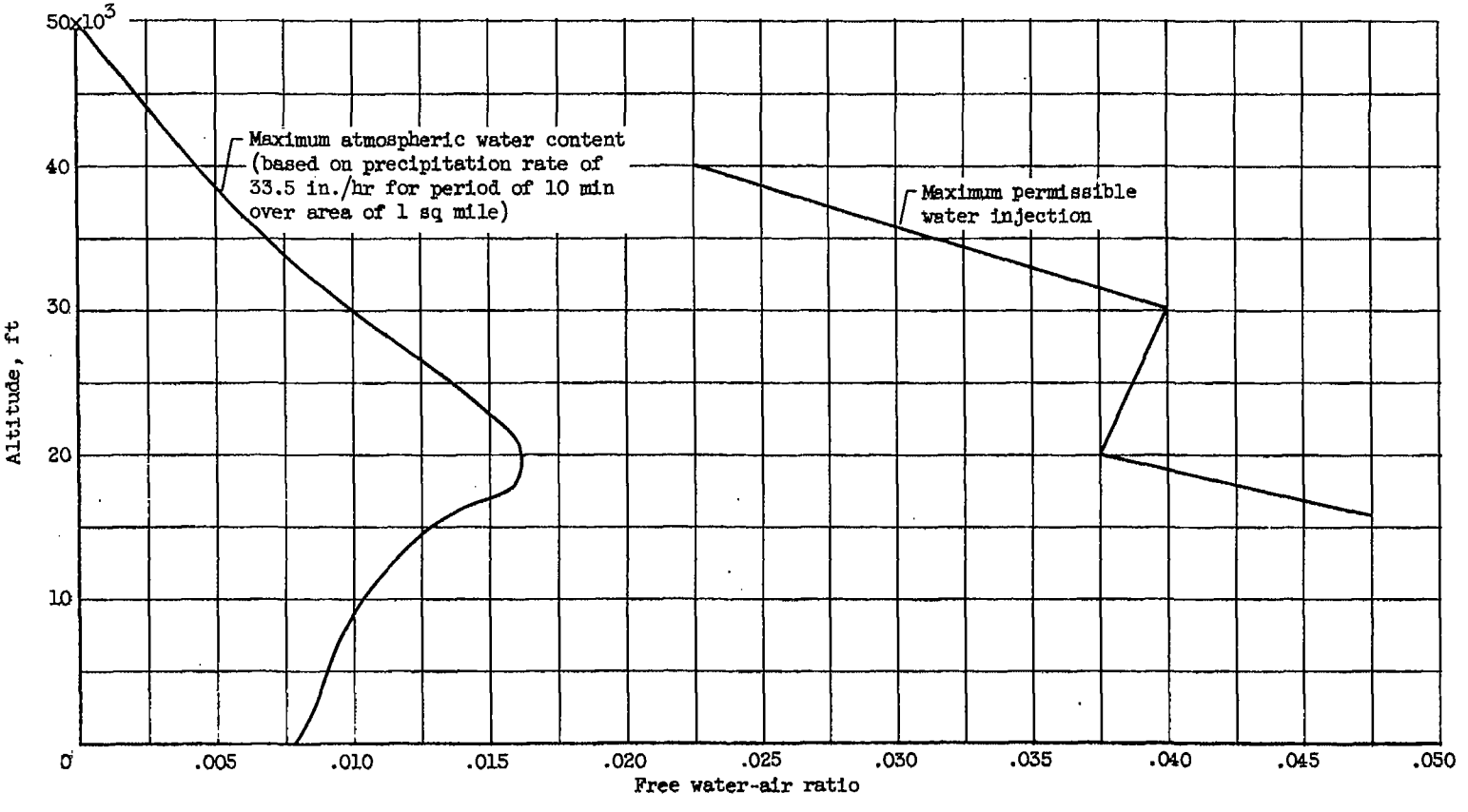

Figure 111. - Comparison of maximum water-air ratios that have been encountered in the atmosphere with those that can be tolerated in single tubular combustor operating at zero-ram and rated-engine-speed conditions (ref. 52).

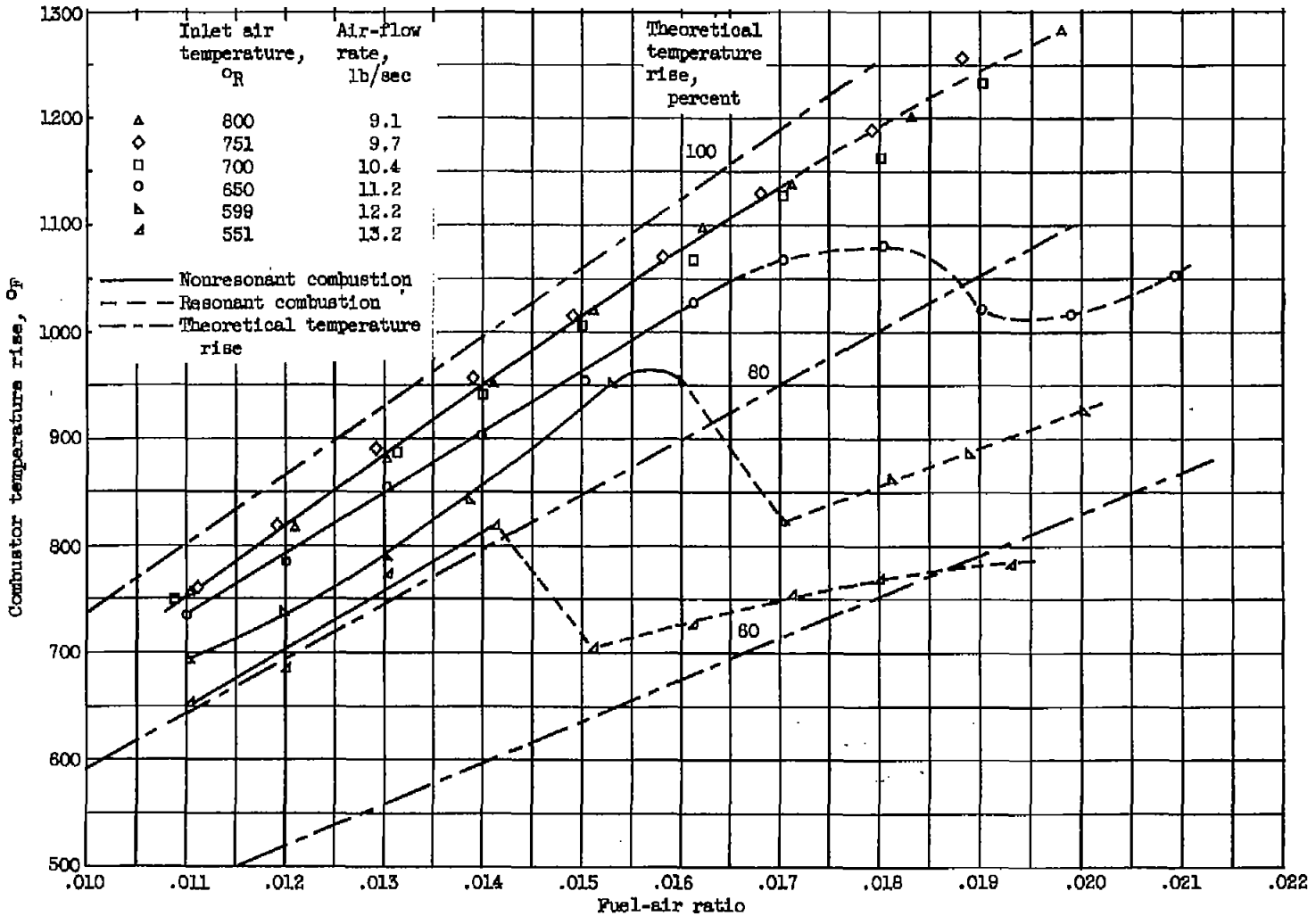

(a) Annular turbojet combustor. Inlet-air pressure, 16 pounds per square inch absolute; reference velocity, 103 feet per second; fuel, AN-F-22 (ref. 3).

Figure 112. - Combustor performance obtained during resonant and nonresonant combustion.

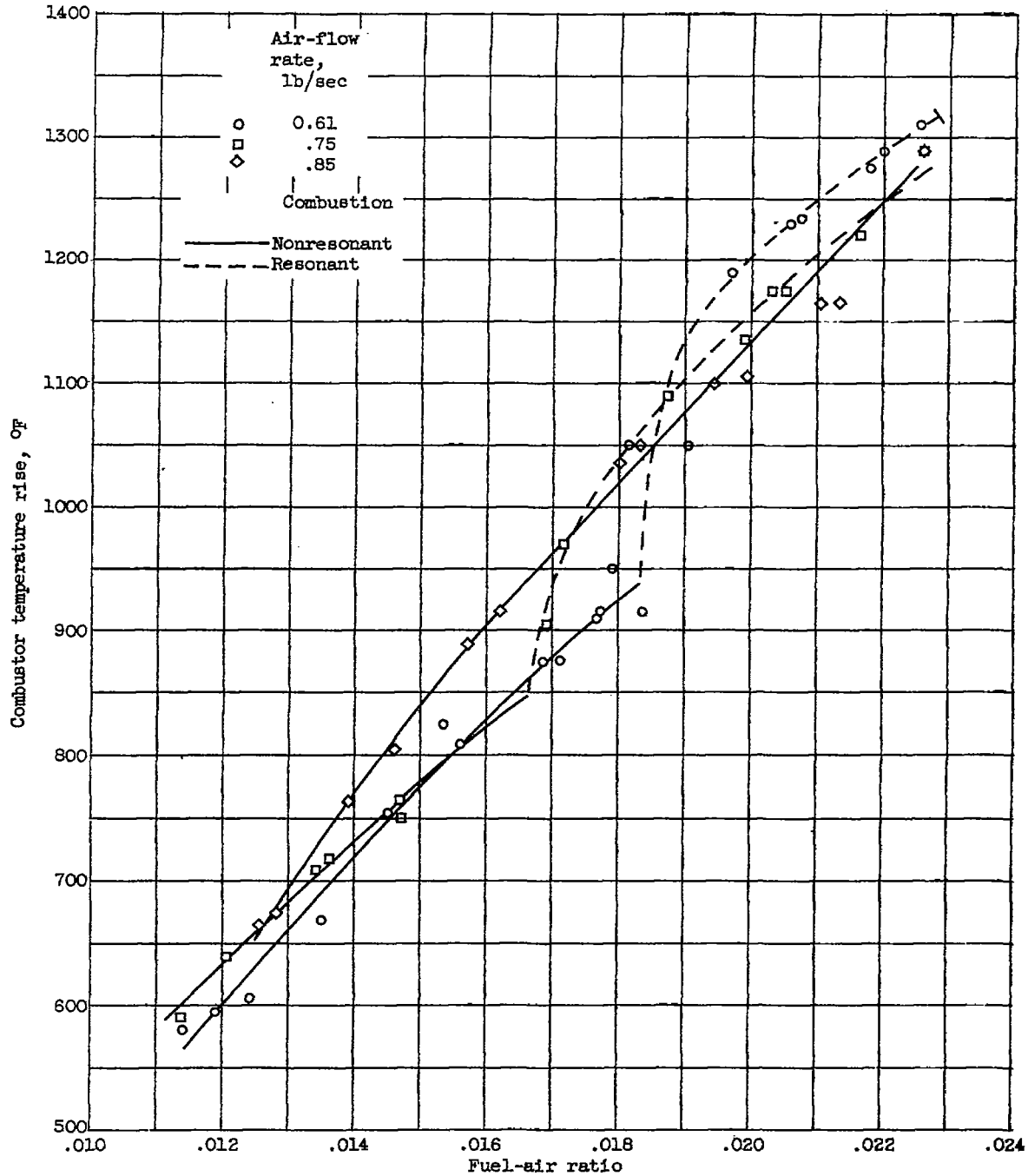

(b) Single tubular combustor. Inlet-air pressure, 7 pounds per square inch absolute; inlet-air temperature, 500° R; fuel, high-boiling paraffin.

Figure 112. - Concluded. Combustor performance obtained during resonant and nonresonant combustion.

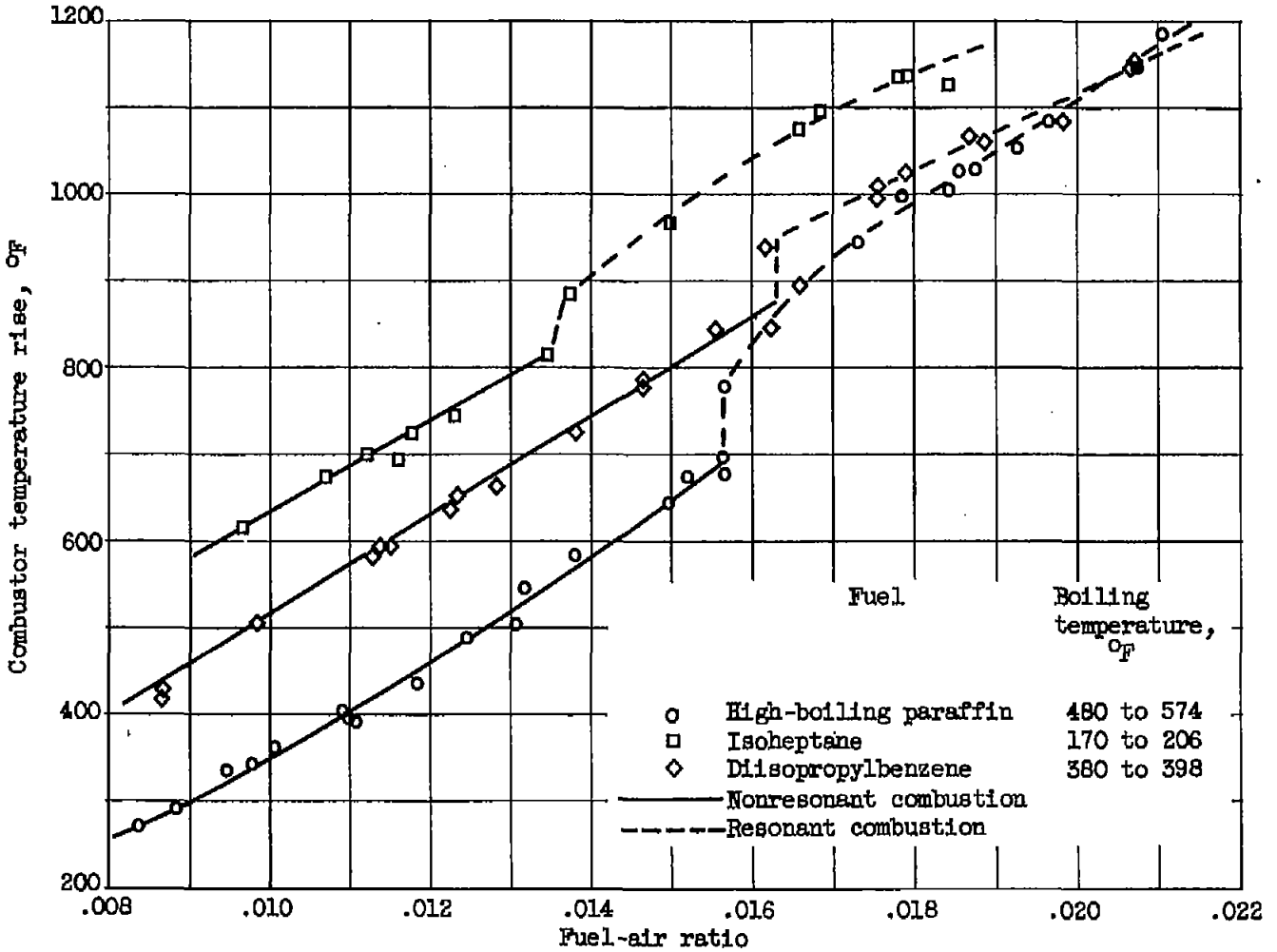

Figure 113. - Effect of fuel characteristics on combustion resonance in single tubular combustor. Inlet-air pressure, 7 pounds per square inch absolute; inlet-air temperature, 500° R; air-flow rate, 0.61 pound per second; variable-area fuel nozzle.

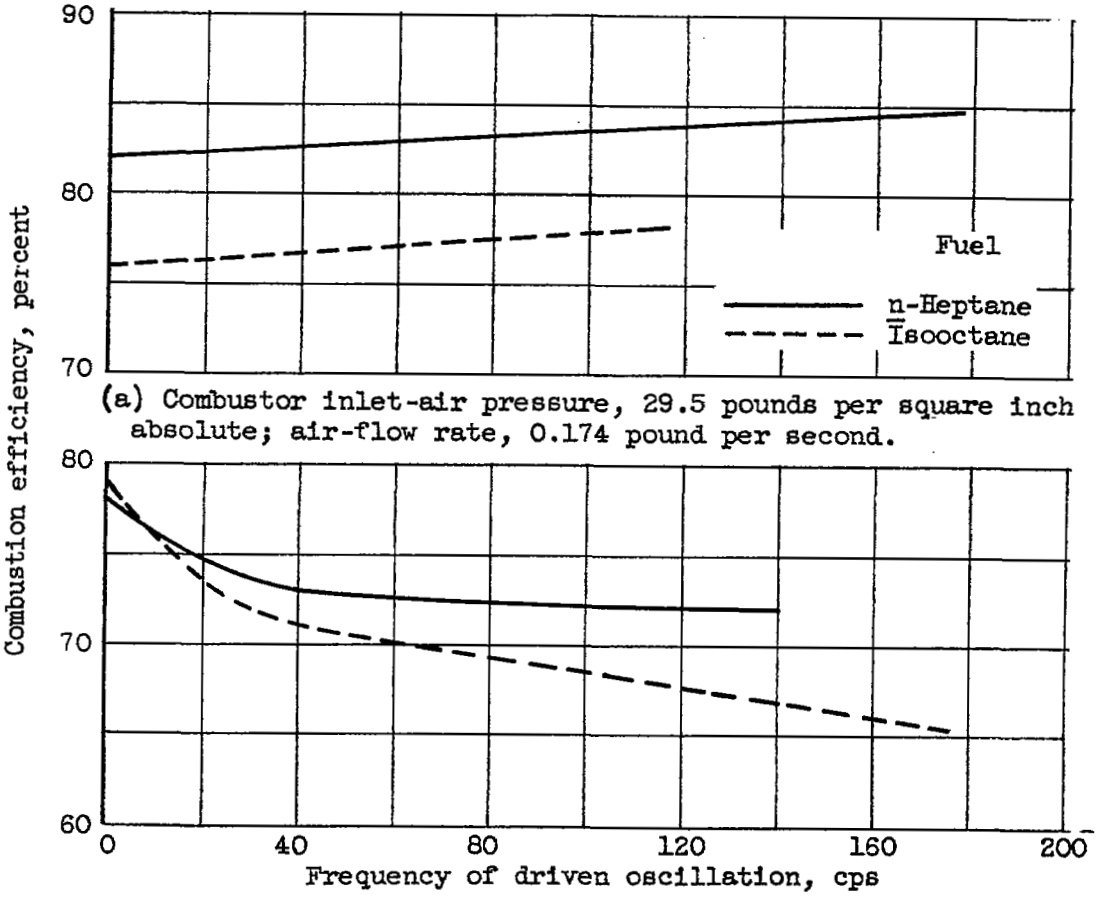

(a) Combustor inlet-air pressure, 29.5 pounds per square inch absolute; air-flow rate, 0.174 pound per second.

(b) Combustor inlet-air pressure, 18.7 pounds per square inch absolute; air-flow rate, 0.093 pound per second.

Figure 114. - Effect of oscillating combustor air supply on combustion efficiency of 2-inch-diameter combustor. Fuel-air ratio, 0.005 to 0.015 (ref. 53).

CC-26 back

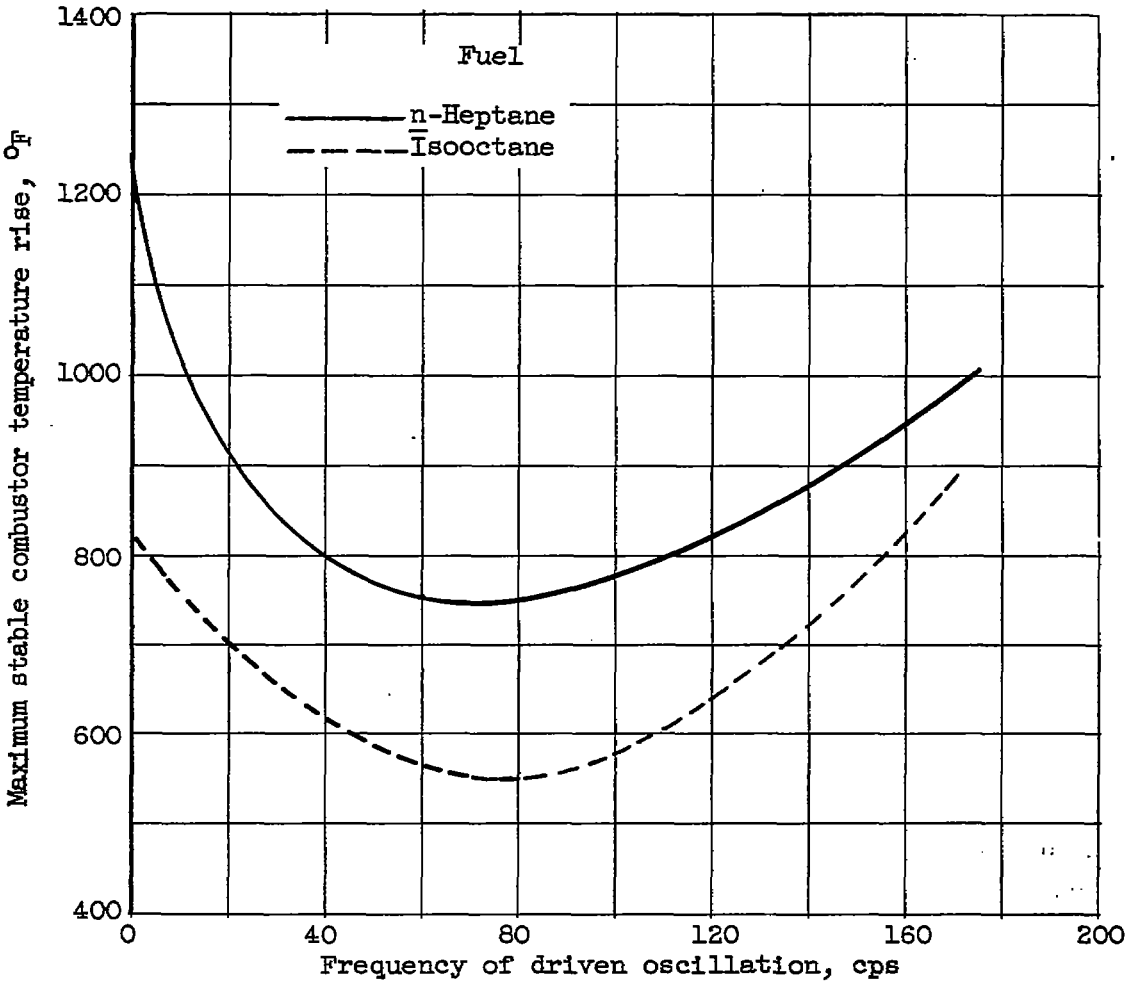

Figure 115. - Effect of oscillating combustor air supply on maximum stable temperature rise of 2-inch-diameter combustor. Inlet-air pressure, 29.5 pounds per square inch absolute; inlet-air temperature, 660° R; air-flow rate, 0.174 pound per second (ref. 53).

[redacted]

CHAPTER XIII

COKE DEPOSITION AND SMOKE FORMATION IN TURBOJET ENGINES

By Jerrold D. Wear and Robert R. Hibbard

INTRODUCTION

In the early development of jet engines, it was occasionally found that excessive amounts of coke or other carbonaceous deposits were formed in the combustion chamber. Sometimes a considerable amount of smoke was noted in the exhaust gases. Excessive coke deposits may adversely affect jet-engine performance in several ways. The formation of excessive amounts of coke on or just downstream of a fuel nozzle (figs. 116(a) and (b)) changes the fuel-spray pattern and possibly affects combustor life and performance. Similar effects on performance can result from the deposition of coke on primary-air entry ports (fig. 116(c)). Sea-level or altitude starting may be impaired by the deposition of coke on spark-plug electrodes (fig. 116(b)), deposits either grounding the electrodes completely or causing the spark to occur at positions other than the intended gap. For some time it was thought that large deposits of coke in turbojet combustion chambers (fig. 116(a)) might break away and damage turbine blades; however, experience has indicated that for metal blades this problem is insignificant. (Cermet turbine blades may be damaged by loose coke deposits.) Finally, the deposition of coke may cause high-temperature areas, which promote liner warping and cracking (fig. 116(d)) from excessive temperature gradients and variations in thermal-expansion rates. Smoke in the exhaust gases does not generally impair engine performance but may be undesirable from a tactical or a nuisance standpoint. Appendix B of reference 1 and references 2 to 4 present data obtained from full-scale engines operated on test stands and from flight tests that indicate some effects on performance caused by coke deposits and smoke.

Some information about the mechanism of coke formation is given in reference 5 and chapter IX. The data indicate that (1) high-boiling fuel residuals and partly polymerized products may be mixed with a large amount of smoke formed in the gas phase to account for the consistency, structure, and chemical composition of the soft coke in the dome and (2) the hard deposits on the liner are similar to petroleum coke and may result from the liquid-phase thermal cracking of the fuel.

During the early development period of jet engines, it was noted that the excessive coke deposits and exhaust smoke were generally obtained when fuel-oil-type fuels were used. Engines using gasoline-type fuels were relatively free from the deposits and smoke. These results indicated that some type of quality control would be needed in fuel specifications. Also noted was the effect of engine operating conditions on coke deposition. It is possible that, even with a clean-burning fuel, an excessive amount of coke could be formed at some operating conditions. In this case, combustor redesign could possibly reduce the coke to a tolerable level. This chapter is a summary of the various coke-deposition and exhaust-smoke problems connected with the turbojet combustor. Included are (1) the effect of coke deposition on combustor life or durability and performance; (2) the effect of combustor design, operating conditions, inlet variables, and fuel characteristics on coke deposition; (3) elimination of coke deposits; (4) the effect of operating conditions and fuel characteristics on formation of exhaust smoke; and (5) various bench test methods proposed for determining and controlling fuel quality.

COKE DEPOSITION IN TURBOJET ENGINES

The coke deposits in a turbojet-engine combustor are formed on the liner walls from 2 to 6 inches downstream of the dome, in the dome, on the fuel

nozzle, and on the spark plug (fig. 116(e)). The deposits on the liner are generally hard and of a medium gray color, show erosion marks or streaks caused by the hot gases, and adhere strongly to the liner walls. The dome and nozzle deposits are sometimes softer than liner deposits and generally darker in color. These deposits are probably not heated to as high temperatures as are the liner deposits. The amount of coke deposit obtained in one tubular combustor of a full-scale engine has been as much as 170 grams (fig. 116(a)); 250 grams has been obtained from full-scale annular combustors. Although most investigators consider deposit weight as a measure of the amount of coke, it is possible that volume instead of weight should be considered.

Effect of Coke on Combustor Life and Performance

As stated previously, large deposits on liner walls can cause severe temperature gradients that may result in warping and cracking of the liner. Coke deposits on or just downstream of the fuel nozzle may cause alterations in the fuel-spray patterns with possible effects on performance.

Life or durability. - Severe liner warping that occurred just downstream of a large coke formation is shown in figure 116(d). Figure 1 of reference 6 also indicates quite clearly the effect of coke formations on liner warping. Information presented in reference 6, which was obtained from military flight bases and overhaul stations, indicates that severe coke deposition can cause liner failure in as little time as 30 hours. In some engines, five out of eight liners had failed at the 30-hour check time. Generally, flight stations that reported heavy coking in their engines had much higher rates of liner replacement than did stations that reported only small amounts of coke build-up. In some cases where the coke deposition was generally quite low, liner life was as long as 200 hours. Liner life can also be shortened because of a distortion or deflection of the fuel spray by coke formations that causes actual burning of part of the liner. This type of failure is also reported in reference 6.

Combustion efficiency and stability. - Loss in fuel heating value due to coke formation in the combustion chamber is unimportant even under the worst conditions. As explained in chapter IX, for such conditions, the loss due to coke deposition is only of the order of 0.004 percent. However, coke formation can affect efficiency by other means. For example, an increase in efficiency at low fuel-air ratios accompanied the formation of coke on fuel nozzles in an early type tubular combustor (fig. 117). The periods of operation shown in this figure were conducted under various test conditions. This unexpected increase in efficiency was attributed to a change in the fuel-spray characteristics. Photographs of the fuel sprays in still air, obtained before and after the coke had been deposited, indicated that the deposits caused a large increase in fuel-spray angle and provided improved fuel drop distribution at low fuel-flow rates. It is noted that cleaning the fuel nozzle after $6\frac{1}{2}$ hours of operation reduced combustion efficiency to the original values. The insertion of a nozzle shield that prevented the formation of coke on the nozzle tip resulted in constant combustion efficiency with run time. An opposite effect of coke deposits on full-scale-engine performance is reported in reference 6. It was reported from one flight station that if the domes and liners were not cleaned, a significant loss in engine power and efficiency (increased tail-pipe temperature for a given engine speed) was observed within 60 hours.

Results of an investigation reported in reference 7 show the effect of coke deposits on altitude limits of a single tubular combustor. The altitude limits were

determined before and after an 80-hour test run, during which the coke deposit pictured in figure 118 was accumulated. The operational limits were reduced somewhat as a result of the coke deposits, as shown in figure 119. In general, there seems to be no reason to expect coke deposits to improve either the efficiency or the altitude limits of well-designed combustors. Decreases in efficiency and altitude limits would appear more likely, although adequate substantiating data are not available.

Effect of Combustor Design and Operating Conditions on Coke Deposition

The coke deposits in a combustor are affected by combustor design and operating conditions or inlet variables. The amount of the coke deposit is determined by the operating time and by the rates of formation, burning, and erosion. These rates are in turn affected to different degrees by design and by inlet variables. As previously mentioned, coke deposits may result from liquid-phase thermal cracking of the fuel on the liner walls. The softer coke found in the dome is probably high-boiling fuel residuals mixed with a larger amount of smoke that was formed in the gas phase. Therefore, a combustor design that permits a large amount of liquid fuel to impinge on the hot liner walls should accumulate more coke, provided that the temperature of the liner walls is proper for thermal cracking of the liquid. Preventing the liquid fuel from getting to the liner walls or using vapor-fuel injection should decrease the coke deposits.

The direct effects of engine operating conditions or combustor-inlet variables on combustor deposits are somewhat obscured by the interdependence of these variables, which include inlet-air pressure, temperature, velocity, and fuel-air ratios. Investigators employing small-scale or full-scale single tubular combustors have tried to determine the singular effect of pressure, for example, by holding mass air flow, temperature, and fuel-air ratio constant. In this case, the inlet-air velocity varies with pressure. Then to determine whether the pressure or velocity is affecting the quantity of deposits, tests must be made with constant pressure, temperature, and fuel-air ratio and varying velocity. The change in mass air flow, to vary velocity, requires a change in fuel flow to maintain constant fuel-air ratio which in turn requires tests to determine the effect of total fuel flow on deposition. Because of the large number of tests required, most investigators have not determined the singular effects of all the combustor-inlet variables. From the available data, however, some indications can be obtained as to whether or not the effect of the inlet variables on combustor deposits is in agreement with the deposit formation mechanisms previously postulated.

Combustor design. - Several investigators have determined the effect of change in "air wash" along the liner walls on coke deposition. Data of reference 8 show a 58- to 77-percent reduction in weight of coke deposits in a small-scale combustor when the gaps in the liner-wall louvers were increased from 0.030 to 0.050 inch. Information presented in reference 9 (full-scale tubular combustor) indicated an appreciable increase in coke deposition when one-third of the liner louvers were closed. Unpublished NACA data (full-scale single combustor) show a reduction in coke deposits from about 30 grams to 1 gram when the combustor was modified so that an annulus of air was directed downstream surrounding the fuel spray. This annulus of air was obtained by modifying the upstream end of the combustor dome as follows: A 3-inch-diameter hole was cut in the end of the dome, and a flat plate $2\frac{1}{2}$ inches in diameter was installed at the back of the fuel nozzle so that the plate was centered in the 3-inch opening. The primary air entering the $\frac{1}{4}$-inch annulus ($1\frac{1}{4}$ in. from the fuel

nozzle) prevented most of the liquid fuel from impinging on the liner walls. This method also decreased the amount of liquid fuel recirculating into the dome; smoke formed in the gas phase could not adhere as readily to the dome surface.

Injection of vaporized fuel (considered as part of combustor design) has an effect on coke deposits, as shown by data presented in reference 10. Less liner deposit was obtained in a small-scale tubular fuel-vaporizing combustor than in a similar design of a fuel-atomizing combustor operated at comparable conditions. However, if the fuel is not completely vaporized, the liner deposit may be increased over the values obtained with the atomizing combustor. Also, deposits may form in the vaporizing tubes and cause a decrease in fuel flow that will probably result in tube failure.

Inlet-air pressure. - Increasing the pressure increases the smoke-forming tendency of hydrocarbon flames (ref. 11); thus, combustor deposits should increase with increase in inlet pressure. This is generally substantiated by information presented in references 12 and 13 (small-scale tubular combustors; fuel-atomizing and -prevaporizing, respectively) and reference 14 (full-scale single tubular combustor). For example, data in figure 120 show a continued increase in total deposit weight with increase in pressure. In this case, velocity, temperature, and fuel-air ratio were relatively constant while fuel flow varied. Deposit weight per unit of fuel, which tends to minimize the variable-fuel-flow effect, also increased with pressure, but at a decreasing rate. This leveling off of combustor deposits at higher pressures is similar to the pressure effect on the rate of smoke formation shown in reference 11. This may be caused, in part, by an increased rate of erosion with increase in air density.

Inlet-air temperature. - An increase in the combustor inlet-air temperature should decrease combustor deposits because of the increased evaporation rate of the liquid fuel from the liner walls and the resultant decrease in fuel residence time. Investigations reported in references 13 and 15 (small-scale tubular combustors; fuel-vaporizing and -atomizing, respectively) and reference 16 (full-scale single tubular combustor) were conducted to determine the effect of inlet-air temperature on coke deposition. Results of these investigations are somewhat conflicting regarding the temperature effect on combustor deposits. For example, data taken at a constant air velocity (ref. 13) show that the flame-tube deposit of a high-deposit fuel increased with increase in air temperature up to 250° F, then decreased as temperature was further increased up to 400° F. Similar data (ref. 15) are shown in figure 121(a). The data were obtained in a small-scale tubular fuel-atomizing combustor at constant mass air flow. Increase in the air temperature from 100° to 250° F increased the amount of deposits; however, further increase in temperature to 325° F caused a decrease in deposits. Data for a full-scale single tubular combustor (ref. 16) for both constant mass air flow and constant inlet-air velocity indicate a decrease in deposits as inlet-air temperature was increased from 100° to 300° F. As the air temperature was increased from 300° to 500° F, the deposit quantity increased. Data obtained in a small-scale tubular fuel-atomizing combustor (ref. 17) at constant reference air velocity show an increase in deposits as air temperature was increased from 100° to 350° F. The inlet-air pressure was varied from 20 to 50 pounds per square inch absolute. Varying inlet-air temperature from 200° to 860° F (ref. 18) caused a decrease in deposits at inlet pressures from 60 to 173 pounds per square inch absolute, as shown in figure 121(b). The data were obtained at constant reference air velocity and fuel-air ratio.

It is apparent that the processes that cause combustor deposits are affected to different degrees by change in inlet-air temperature. With some particular inlet-air temperature, combustor geometry, and fuel, one process may predominate;

with other combinations another process may predominate. In some cases the increase in temperature will increase the vaporization rate of the fuel, thereby decreasing the fuel residence time on the walls; in other cases the thermal-cracking rate (with increase in inlet-air temperature) may become greater, relative to the vaporization rate, and therefore deposits will increase. Of course, if the inlet-air temperature is high enough, the liner temperature will be above the minimum temperature at which coke will burn, and, therefore, combustor deposits will not build up on the liner (fig. 121(b)).

Inlet-air velocity. - An increase in the inlet-air velocity would be expected to decrease combustor deposits because (1) the increased scrubbing action of the air on the liquid fuel decreases fuel residence time on the walls, (2) less fuel impinges on the liner walls, and (3) the erosion of deposits is greater. Conversely, the fuel recirculation increases with increase in air velocity, and the greater amount of liquid fuel in the dome may increase deposits. The relative importance of these different processes is not known. Data of references 14 and 19 (full-scale single tubular atomizing combustors) show an increase in deposits as the velocity was increased. Information presented in reference 17 for a small-scale tubular atomizing combustor indicates a decrease in deposits as velocity was increased. Data shown in figure 122 indicate that, depending on the fuel-air ratio, there will be either an increase, no change, or a decrease in combustor deposits with increasing inlet velocity, which is proportional to mass air flow. It is apparent that the effect of inlet velocity on combustor deposits is similar to the inlet-air-temperature effect. Depending on the operating conditions and combustor geometry, combustor deposits may increase or decrease with increase in velocity.

Fuel-air ratio. - Increase in fuel-air ratio of fuel flow should increase combustor deposits because of higher local fuel-air ratios and the increased amount of residual wall fuel. The increased primary-zone temperature resulting from the increased fuel-air ratio should cause either an increase in deposits through increased thermal cracking or a decrease in deposits because of increased burning and erosion of the deposits. Investigations reported in reference 13 (small-scale fuel-vaporizing tubular combustor) and references 14 and 19 (full-scale single tubular combustors) indicate a general increase in combustor deposits with increase in fuel-air ratio. Data presented in figure 123 show an increase in total combustor deposits with increase in fuel-air ratio, with all other variables constant except, of course, exhaust-gas temperature. However, deposit weight per unit of fuel is constant with increase in fuel-air ratio. Data shown in figure 122 also indicate an increase in combustor deposits with increase in fuel-air ratio.

Run time. - The amount of deposit in a combustor depends on the length of the run time. However, because of increased burning and erosion of deposits as the deposit quantity increases, deposition rate remaining constant, the rate of deposit build-up decreases, and finally at some value of run time a maximum quantity of deposits is obtained. This tendency is shown in figure 124.

Summary of effects of combustor design and operating variables. - In summary, it is noted that certain changes in combustor design and inlet variables affect combustor deposits in the way expected. For example, increased "air wash" along the liner walls or injection of vaporized fuel caused a decrease in amount of deposits. Increases in inlet-air pressure and fuel-air ratio both generally caused increases in coke deposits. Deposit weight increased with run time until an equilibrium level was reached; the rate of erosion and burning becomes approximately equal to the deposition rate. Increases in inlet-air temperature or velocity, or both, were expected to decrease deposits. However, results were conflicting; in some cases deposits increased and in others decreased as air temperature was increased. If the air temperature was high enough (>850° F), little deposit was formed. The inlet-air-velocity

[redacted]

effect on deposits was similar to the temperature effect; depending on the operating conditions and combustor design, the deposits either increased or decreased with increase in velocity.

Effect of Fuel Characteristics on Coke Deposition

A substantial quantity of data has been obtained by numerous investigators describing the effects of various fuel properties on combustor deposits. Since all inlet variables or operating conditions can be maintained relatively constant, the direct effect of fuel type on combustor deposits can be determined.

Volatility. - It is indicated earlier in this chapter that combustor deposits are smaller with gasoline-type fuels than with higher-boiling fuels. This result is in agreement with the supposition that more easily vaporized fuels should produce less combustor deposits because of the decrease in fuel residence time. Other data that substantiate this theory are given in references 9 and 19 (full-scale single tubular combustors), reference 20 (small-scale tubular combustor), and reference 21 (full-scale annular combustor, $10\frac{3}{8}$-in. diam.). For example, information presented in figure 125(a) shows a considerable increase in combustor deposit with increase in the volumetric average boiling temperature (decrease in volatility) at constant hydrogen-carbon weight ratio. This result suggests that decreasing the liquid-fuel residence time on the liner walls results in decreased combustor deposits. Hence, it would seem that the use of vapor fuel would eliminate deposits. However, as indicated in reference 22, some deposits were obtained on the vapor-fuel nozzle and in the combustor dome when a vapor fuel (propane) was used. These deposits were formed during incomplete combustion of the fuel in the complete absence of a liquid phase.

Fuel composition. - The effect of hydrocarbon type or composition on the tendency of diffusion flames to produce smoke is presented in chapter IX. The fuel types in order of decreasing tendency to smoke are naphthalene and substituted naphthalene compounds, aromatics, alkynes, olefins, and normal paraffins. The aromatics are about 12 times as smoky as the olefins and about 24 times as smoky as the normal paraffins. Naphthalene, with its high smoking tendency would be expected to cause large amounts of combustor deposit. Data of reference 21 (full-scale annular combustor, $10\frac{3}{8}$-in. diam.) show that 139 grams of coke was obtained with a mixture of α- and β-monomethylnaphthalene, 88 grams with triisopropylbenzene, 34 grams with benzene, and 2 grams with a normal paraffin fuel. Other investigators have shown that aromatic-type fuels generally cause a large amount of coke deposit. Some of this data is reported in references 9, 23, and 24 (full-scale single tubular combustors) and references 12, 20, and 25 (small-scale tubular combustors). An example of these data is shown in figure 125(b), where the combustor deposits increase with increase in aromatic content for constant values of volumetric average evaporated temperature. Some investigators have surmised that the highest-boiling fraction of the aromatic portion may be causing much of the combustor deposits. Information presented in reference 12 (small-scale tubular combustor) shows that combustor deposits increase as the percentage of aromatics boiling above 420° F increases. However, the quantity of coke deposits was not necessarily the same for different types of fuels that had the same percentage of aromatics boiling above 420° F.

Information concerning the effects of normal paraffins, isoparaffins, and cycloparaffins on combustor deposits indicates that these different fuel types have about the same coke-forming tendencies and that the amount deposited is appreciably less

than that obtained from aromatic-type fuels. As shown in chapter IX, except for the normal paraffins, olefinic-type hydrocarbons have the lowest values of smoking tendency. In spite of these low values, larger deposits could possibly form because of the polymerizing characteristics of olefins. However, data from investigations reported in references 9, 23, and 26 (full-scale single tubular combustors) and reference 18 (full-scale annular combustor, $10\frac{3}{8}$-in. diam.) show that the quantity of deposits obtained with olefinic fuels is similar to that obtained from paraffin fuels of the same boiling range. One investigator (ref. 27) reported heavy deposits in a full-scale single tubular combustor from a fuel containing a considerable amount of diolefins. Unreported investigations conducted in a full-scale single tubular combustor with a fuel blend consisting of 50 percent JP-3 fuel and 50 percent dipentene showed an increase of about 25 percent in combustor deposits over those obtained with JP-3 fuel alone. For the same operating conditions, an aromatic fuel blend with an average boiling point of about 380° F caused an increase in deposits of about 230 percent over those for JP-3 fuel.

SL79

CC-27 back

Nonhydrocarbon fuel components. - Sulfur compounds and gum are minor nonhydrocarbon components present in petroleum-derived aviation fuels that can have an effect on combustor deposits. Investigations conducted to determine the effects of sulfur on combustor deposits indicate that the quantity of sulfur in the fuel can be increased a considerable amount above the present specification MIL-F-5624C maximum of 0.4 percent before an appreciable increase in deposits is obtained. Results of some of these (full-scale single tubular combustor) investigations are shown in the following table:

Fuel	Additive for increasing sulfur content	Sulfur in fuel, percent by weight	Weight of deposit, g	Reference
Straight-run kerosene	None	0.05	4.1	9
	↓	.5	3.1	↓
		1.0	5.0	
		3.0	7.2	
AN-F-58	None	0.034	3.1	28
	Thiophene	.39	2.3	↓
	Thiophene	.91	1.2	
	Disulfide oil	1.00	3.6	
MIL-F-5624A, grade JP-3	None	0.04	7.0	26
	Disulfide oil	.55	8.8	↓
	Disulfide oil	1.03	8.4	
	None	.04	5.6	
	Mixed butyl mercaptans	1.05	6.5	

It is noted that the sulfur content of a fuel can be increased to 1 percent or more before a significant increase in combustor deposits is obtained. Thiophene added to a fuel in amounts of 1 and 3 percent (0.39 and 0.91 percent sulfur) actually caused a decrease in deposits.

The majority of investigations that have been conducted to determine the effect of gum, either existent or potential, on combustor deposits show, in general, that the specification MIL-F-5624C maximum limits of 7 and 14 milligrams per 100 milliliters of fuel may be increased several times before an appreciable effect on combustor deposits is obtained. The following data were obtained from some of these investigations:

Fuel	Combustor	Gum, mg/100 ml		Weight of deposit, g	Reference
		Existent	Potential		
MIL-F-5624A, grade JP-3	Full-scale single tubular	7 77 165	12 445 560	12.6 14.7 15.4	26
MIL-F-5624A, grade JP-3	Full-scale single tubular fuel-vaporizing	9 95	12 103	2.1 2.6	26
AN-F-58	Full-scale single tubular	6.5 4.3 21.1 34.1	3.5 4.2 25.3 55.8	4.3 3.3 4.1 4.8	28

The existent and potential gum contents were determined by the A.S.T.M. Standards D381-46 and D525-46, respectively. It can be seen that a large increase in gum content is possible before any significant increase in combustor deposits is obtained. In the data from reference 26, the gum content of the fuels was increased without any appreciable change in other fuel characteristics. Information obtained from reference 29 showing the effect of existent gum content of fuels on deposits in small-scale tubular combustors (fuel-atomizing and fuel-vaporizing) is presented in the following table:

Fuel	Existent gum, mg/100 ml	Deposit weight, mg/hr			
		Atomizing-combustor flame tube or liner	Vaporizing combustor		
			Flame tube or liner	Outside vaporizer tube	Inside vaporizer tube
A174 (base) A76	6.1 58.5	260 ---	9.0 81.2	1.5 7.5	16.2 377.5
A84 (base) A98	5.2 59.2	216 185	16.6 49.0	7.0 16.5	13.5 425.0

The data indicate that an existent gum content of about 8 or 9 times the maximum specification limit may cause large increases in the deposits in the vaporizing-combustor flame tube or liner and inside the vaporizer tube. Information presented in reference 30 shows that the vaporizing tubes plugged after about $1\frac{1}{2}$ hours of operation with a low-aromatic fuel with a gum content of 100 milligrams per 100 milliliters of fuel. This plugging caused rough burning and unsatisfactory operation of the combustor. Continued combustion with a plugged vaporizer tube would probably result in a complete tube failure.

[redacted]

Elimination of Coke Deposits

The effects on combustor deposits of changes in combustor design and fuel injection, variation in combustor inlet-air variables, and changes in fuel quality can be qualitatively estimated from deposit formation mechanisms previously presented. From these considerations, methods for decreasing or eliminating combustor deposits can be proposed.

Combustor design. - Any design changes in the combustor that decrease or prevent liquid-fuel impingement on the liner walls decrease combustor deposits. Among the design changes by which deposit reduction may be effected are provisions for (1) fuel prevaporization, (2) increased "air wash" to the liner walls, (3) change of fuel-spray angle, and (4) liner temperatures either low enough to prevent thermal decomposition of the fuel or high enough to burn off the deposits. With fuel prevaporization, additional problems are encountered, such as plugging of vaporizing tubes, and these problems may overshadow the advantages of decreased combustor deposits. Increased "air wash" and changed fuel-spray angle may have adverse effects on combustion efficiency, stability, or altitude blow-out. It may be impracticable to keep liner temperatures below the fuel-decomposition temperature, and very high liner temperatures shorten liner life (ref. 18). It is apparent that the final combustor design must be a compromise involving several factors, and combustor coke deposition is only one of these factors.

Fuel-quality control. - Combustor deposits can be greatly affected by choice of fuel. As previously shown, deposits generally increase as the state of the fuel is varied from vapor to liquid and as the type of the fuel is varied from high to low volatility or from paraffin to aromatic. From the standpoint of reducing combustor deposits, the vapor fuel would be best. As previously mentioned, the special equipment needed to obtain vaporized fuel may be sensitive to coke deposits. However, continued research may overcome this problem. High-volatility fuels cannot be used in aircraft because tank losses due to fuel boiling and slugging become excessive (ref. 31). For liquid-fuel-atomizing combustors, the paraffin-type fuels cause less deposits than aromatic fuels. However, the availability of paraffin or nonaromatic fuels is limited. It can be seen that the final fuel will be a compromise depending on the amount of importance that is assigned to the various considerations.

Fuel additives. - Another means of reducing combustor deposits is by use of fuel additives. Additives effective in reducing or eliminating coke from commercial furnaces and Diesel engines may also be effective in turbojet combustors. Data of reference 32 (full-scale single tubular combustor) show a decrease in deposits when small amounts of tetraethyl lead were added to the fuel. Deposits decreased about 45 percent with a lead concentration of about 0.002 percent. Further increases in lead concentration eventually cause an increase in deposits because of increased amounts of lead oxides. With the need of JP fuels and military aviation gasoline in a national emergency estimated as about 1,000,000 and 300,000 barrels per day, respectively, the metallic lead needed per day for JP fuels (0.002 percent by weight) would be about $2\frac{3}{4}$ tons and lead required for aviation gasoline (4.6 ml TEL/gal) would be 55 tons per day. Other additives that reduced deposits were lead naphthenate, secondary amylnitrate, and commercial fuel-oil additives (refs. 16, 32, and 33; full-scale single tubular combustors). In small-scale combustors (refs. 34 to 36), the decreases in deposits were negligible with additives such as lead naphthenate, U.O.P. Inhibiter No. 5, amylnitrates, ditertiary butyl peroxide, and a commercial additive. Aviation tetraethyl lead in a concentration of 4 cubic centimeters per gallon (0.12 percent lead by weight) caused a considerable increase in deposits because of the lead deposits added to the coke. Reference 37 presents data for a large number of

additives tested in small-scale atomizing and vaporizing combustors. The additives consisted of halogen compounds, antioxidants, organometallics, silicates, carbonyls, high-molecular-weight organics, and water. Tetraethyl lead (0.01 percent by volume) and iron pentacarbonyl (0.1 percent by volume) were the only additives that caused any appreciable decrease in combustor liner deposits, and water was the only additive that caused a decrease of fuel-vaporizer-tube internal deposits.

The results of various investigations to decrease combustor deposits by special fuel additives are not conclusive enough at the present time to determine whether the advantages are sufficient to offset such problems as storage stability, deleterious effects on engine fuel systems and hot engine parts, and perhaps availability. The over-all benefits must be determined by further research.

3176

SMOKE FORMATION IN TURBOJET ENGINES

As previously indicated, smoke formation in turbojet combustion is less important than is coke deposition. There is no measurable loss in performance due to smoke, and, in fact, operating conditions conducive to smoke formation are the same conditions that yield generally high combustion efficiencies. For this reason, less work has been done in the field of smoke research in full-scale engines and in single combustors than has been done in the study of coking. The reverse has been true in bench-scale experimentation (ch. IX).

Bench-scale studies reported in chapter IX have shown that smoke can be formed only in a fuel-rich environment. The primary zone in turbojet combustors certainly contains local areas that are fuel-rich under most operating conditions, and it is likely that smoke is often generated in considerable quantities. The fact that smoke is not found in much higher concentrations in the turbojet exhaust indicates that much of this material is consumed in passing through the burner. This theory is confirmed by electron microscopy studies of turbojet smoke (ch. IX).

Smoke formation has been determined qualitatively in full-scale engines and single combustors by visual observation. Smoke has been determined quantitatively by either filtration and optical measurements or by collection and weighing. In the filtration method, the exhaust is passed through a filter at a given rate for a given time, and the darkening of the filter is then determined by either visual rating or by optical methods. This method was used in references 13, 14, 20, and 38. In references 27, 39, and 40, the smoke was trapped by bubbling the exhaust gases through water, and the smoke was weighed after filtration and drying. There has been no attempt to report absolute smoke values by either method; the data only indicate the effect obtained when a small and unreported fraction of the exhaust gas is sampled. Comparison between laboratories on an absolute basis is obviously impossible, and the results reported herein are given only as trends.

Effect of Operating Variables on Smoke Formation

A systematic study of the effect of inlet variables on smoke production was made in a full-scale tubular combustor using the filter-darkening technique (ref. 38). With a typical JP-3 fuel, the exhaust smoke increased from two- to tenfold as the inlet pressure increased from 35 to 65 inches of mercury absolute. The controlled variables were fuel type, inlet temperature, fuel-air ratio and inlet-air velocity. This effect of a marked increase in smoke with increasing pressure is also reported in reference 14 for pressures up to 350 inches of mercury absolute and in reference 13 for pressures up to 150 inches of mercury absolute. This effect of pressure is also fully confirmed in the bench-scale work reported in reference 11 and by the fact that, in flight, turbojet-powered aircraft leave the heaviest smoke trails at low altitudes.

With the other variables constant, it was also shown in the work of reference 38 that smoke production increased from two- to four fold as the fuel-air ratio increased from 0.008 to 0.016. Above a fuel-air ratio of 0.016, there was a slight decrease in smoke up to a fuel-air ratio of 0.022. In the tests of reference 13, fuel-air ratios were varied up to 0.015 and in the tests of reference 20 up to 0.020. In both cases, the smoke production increased with increasing fuel-air ratio up to the highest ratios tested. These values are over-all fuel-air ratios, and the smoke was obviously formed in much richer mixtures. Bench-scale data plotted in figure IX-4 show that smoke continually increases with increasing fuel-air ratio. In general, there is agreement that smoke increases with increasing fuel-air ratio. The slight decrease at higher ratios reported in reference 38 is accounted for by the probability that increasing flame length at high fuel-air ratios consumed a large fraction of the smoke that was initially formed.

3179

Both references 13 and 38 show that smoke formation is substantially independent of inlet-air temperature over the range between 100° and 400° F. This result is in full agreement with the bench-scale work reported in reference 41.

It is difficult to fully isolate the effect of inlet-air velocity as a variable in reference 38 since other air parameters vary simultaneously. However, it appears that smoke increases slightly with increasing velocity at low fuel-air ratios and decreases slightly with increasing velocity at high fuel-air ratios. Reference 13 shows a considerable decrease in smoke with increasing velocity at low fuel-air ratios, but the data are few and scattered. The effect of inlet-air velocity on smoke would be expected to be a function of combustor geometry, but little agreement is likely between investigators regarding this relation.

Smoke tests have been made on a full-scale engine running at near-sea-level conditions with a JP-3 fuel (ref. 38). Engine speed and exhaust-nozzle area were the controlled variables and fuel-air ratio and inlet-air pressure, temperature, and velocity were the dependent variables. Because the various inlet parameters cannot be independently varied in full-scale-engine testing, the independent effect of the parameters on smoke cannot be determined. In the tests of reference 38, smoke increased 3 to 4 times as engine speed increased from 5300 to 8000 rpm. Smoke increased to a lesser extent as nozzle area was decreased by 33 percent. The changes in engine operating conditions that increased smoke also increased fuel-air ratio, pressure, and temperature. It seems probable that increases in fuel-air ratio and pressure were the main factors contributing to increased smoke, a theory confirmed by the observations from both bench-scale and single-combustor studies.

Effect of Fuel Quality on Smoke Formation

A small amount of work has been done in several laboratories relating smoke formation to fuel quality. Four fuels of low aromatic content but of varying volatility were tested in a full-scale single combustor (ref. 38). As fuel volatility increased, the maximum values of smoke density did not change appreciably, but the fuel-air ratio at which maximum smoke was produced shifted to lower ratios. Data presented in references 19 and 20 and chapter IX indicate that smoke formation is less dependent on fuel volatility than on other fuel factors. Chapter IX shows that smoking tendency does not vary greatly with molecular weight in the range of molecular weights covered by the usual petroleum-derived fuels. However, the effect of hydrocarbon type on smoke production is quite pronounced, the aromatic fuels yielding considerably more smoke than the nonaromatic ones. References 19, 20, and 40 show this effect in combustor studies, and chapter IX shows it for bench-scale flames.

Liner coke is quite dependent on both the hydrocarbon type and the volatility characteristics of fuels, the latter presumably being important since it relates to the residence time of liquid fuels on combustor walls. Smoke, on the other hand, is largely dependent on hydrocarbon type but is little affected by fuel volatility. Therefore, a poor correlation might be expected between the coking and smoking tendencies of fuels, and this poor correlation is, in fact, noted in references 20, 27, and 40.

EVALUATION OF FUEL DEPOSIT-FORMING CHARACTERISTICS

Since the influence of fuel quality on coke deposition is a matter of considerable importance affecting the performance and reliability of turbojet engines, it would be desirable to have laboratory tests that could be used to evaluate and control the quality of such fuels. In general, the most accurate deposit-forming evaluation of fuels is made by operating complete engines under service conditions. This approach is prohibitively expensive, and easier methods have been sought.

A fairly close approach to the prototype testing of turbojet fuels has been made by taking single combustors from full-scale engines and using these in connected-duct facilities. A considerable amount of deposit-formation work has been done in such test units. In order to determine whether results of tests with single full-scale combustors can be related to full-scale-engine coke deposition, several full-scale-engine tests were conducted. The full-scale engines were operated on test stands (refs. 2 and 4). Results of some flight test data are also available and can be used for comparison (appendix B of ref. 1 and refs. 3 and 6). The results show, in general, a good relation between deposits in full-scale single combustors and full-scale engines. However, even full-scale single-combustor testing is too costly in terms of facilities, power, fuels, and time to permit its use for the control of fuel quality by manufacturers.

Therefore, considerable effort has gone into the development of either a simple bench-scale test which will correlate with the performance of fuels in engines or the correlation of other easily determinable fuel properties with full-scale-engine performance. Since little quantitative full-scale engine data are available on the coke-forming tendencies of turbojet fuels, much of this effort has been toward correlating bench-scale results with the results from single-combustor testing. There has been no complete agreement concerning the best correlating test. The following discussion describes the progress that has been made to date.

Correlation of Fuel Properties With Coke Deposit Formation

Certain fuel characteristics and related properties are considered to affect coke deposits. These include hydrogen-carbon ratio, aromatic content, A.S.T.M. distillation temperatures, gravity, and aniline point. These properties have been used singly and in combinations to help indicate the coke-forming tendency of a fuel. One drawback to the use of fuel properties to relate combustor deposits to the fuel is that these properties do not give any indication of the effect of special fuel additives on deposits.

Hydrogen-carbon ratio and volatility. - Early investigators attempted to relate the carbon and hydrogen contents of a fuel and some measure of its volatility to combustor deposits. Deposits from several fuels obtained in a small-scale combustor (ref. 20) were empirically related to the fuel as follows:

$$\text{Weight of deposits} = \frac{\log (n_C/n_H + C_1)}{C_2} + \frac{T}{C_3} + C_4 \qquad (1)$$

where

$C_1 \ldots C_4$ constants

n_C/n_H ratio of carbon atoms to hydrogen atoms

T A.S.T.M. 10-percent distillation temperature, °F

The fuels varied from low-boiling or high-volatility cycloparaffins to low-volatility aromatics, and also included high- and low-volatility fuel blends. In general, the combustor deposits increased with an increase in the value of equation (1), although a considerable scatter was obtained.

The logarithm of the combustor-deposit values obtained from 19 fuels (ref. 21; full-scale annular combustor, $10\frac{3}{8}$-in. diam.) were empirically related to the fuels by a factor designated as the NACA K factor and shown as

$$\text{Log of combustor deposits} = a + b\,K \qquad (2)$$

$$K = (t + 600)(0.7)\,\frac{H/C - 0.207}{H/C - 0.259} \qquad (3)$$

where

a,b constants

t fuel volumetric average evaporated temperature, °F

H/C hydrogen-carbon weight ratio

The fuels consisted of high- and low-volatility paraffins, olefins, aromatics, and fuel blends. Examples of the relation of the NACA K factor to deposits of various fuels obtained in a small-scale tubular combustor, a full-scale single tubular combustor, and a full-scale tubular combustor engine are shown in figure 126. The deposits from most of the fuels can be estimated by this relation, although some fuel deposits show wide variations.

Aromatic content and volatility. - Both the total aromatic content of a fuel and the aromatics boiling above 400° or 420° F have been used in attempts to relate combustor deposits to fuel properties. Some of this type of data is presented in references 12 (small-scale combustor) and 23 (full-scale single combustor). The full-scale-combustor data show a regular increase in deposits with increase in total aromatic content. Although the small-scale-combustor data indicate an increase in deposits with aromatics and aromatics boiling above 420° F, the increase does not show any regular trend, and different fuels with the same aromatic content gave different deposit values.

Other investigators have used aromatic content of a fuel and some measure of volatility as a means of relating combustor deposits to the fuels. For example, as shown in reference 23 (full-scale single tubular combustor), the logarithms of the

combustor-deposit values of several fuels are plotted against the percentage of aromatics by weight plus one-tenth of either the 80- or 90-percent A.S.T.M. distillation temperature. The combustor deposits of some fuels can be estimated with reasonable accuracy by this relation; however, wide variations are obtained with other fuels.

Volatility, density, and aniline-gravity constant. - Fuel properties such as specific gravity or density, volatility, and aniline point are easily determined and therefore are desirable for use in a bench or control test to determine the combustor deposit-forming tendency of fuels. Data of reference 19 (full-scale single tubular combustor) show how combustor deposits of several fuels vary with molal average boiling point of the fuel and Universal Oil Products (U.O.P.) characterization factor.

$$\text{U.O.P. factor} = \frac{(T_b)^{1/3}}{\text{Sp.gr. } 60^\circ/60^\circ \text{ F}} \tag{4}$$

where

T_b mean average boiling point, $^\circ$R

There is a general trend of increased combustor deposits with decrease in U.O.P. factor, although some fuels vary from this trend. Information presented in reference 40 for a full-scale single tubular combustor also shows a similar relation of combustor deposits to the U.O.P. characterization factor.

The U.O.P. characterization factor, the hydrogen-carbon ratio, and, to some extent, gravity are all related to the aromaticity of a fuel. Therefore, different combinations of these various fuel properties should give about the same trend of deposits with fuel.

The aniline-gravity constant (product of the aniline point in $^\circ$F and the A.P.I. gravity) is another fuel property that has been used to rate fuels for their coke-forming tendencies (ref. 1, full-scale single tubular combustors). With this fuel property there was wide variation in the data.

The A.P.I. gravity has been used to estimate the coking tendency of fuels. Data presented in reference 1 (full-scale single tubular combustors) show examples of a general decrease in deposits with increase in A.P.I. gravity (decrease in sp. gr.) and other examples where this trend is not so evident. Data of reference 42 show a regular decrease in deposits with increase in A.P.I. gravity.

Laboratory Measurement of Fuel Coke-Forming Characteristics

There does not appear to be a chemical or physical or combination chemical-physical property of a fuel that will consistently give an accurate estimation of the coke-forming tendency of a fuel. Therefore, investigations were conducted to determine whether some type of laboratory combustion test would give a satisfactory coke-forming rating among fuels.

The investigations included smoke-lamp, flame-plate, and small-pot-burner methods. Although small-scale combustors could be classed as laboratory equipment, for the data presented herein, they are discussed along with the full-scale combustors.

Smoke-lamp method. - One simple bench test that has been used by several investigators is the fuel smoke-point determination by some type of smoke lamp. A simple wick lamp is used to determine the maximum height of a smoke-free flame of a particular fuel. The different types of lamp and test procedure are described in chapter IX. The smoke point is defined as the maximum height of a smoke-free flame in millimeters h; smoking tendency of a fuel is defined as $\frac{320}{h}$. Information presented in references 1 (full-scale single tubular combustors) and 12 (small-scale tubular combustor) shows a trend of increasing deposits with decrease in the smoke point; however, there is considerable variation in the data. The average deviation of some of the deposit data of reference 1 from a curve faired through the data is about 16 percent. The data from reference 12 indicate an average deviation of about 60 percent. An example of some of these data is given in figure 127, which is a plot of smoking tendency (320/h) and combustor deposits of 16 fuels tested in a full-scale single tubular combustor. This figure indicates some relation between smoke point and combustor deposits, although some of the data show wide variations. The smoke-point test is not affected by small amounts of special fuel additives (ch. IX), but combustor deposits may be decreased by addition of small amounts of these same additives.

In an attempt to eliminate variations in the data, investigators have included the boiling point of a certain fraction of the fuel or a certain function of the boiling point. Data in reference 43 show the relation of combustor deposits obtained with 16 fuels in a full-scale annular combustor ($10\frac{3}{8}$-in. diam.) to a function of boiling temperature and smoke point. A somewhat different relation is presented in reference 44 (small-scale tubular combustor) relating combustor deposits to a function of smoke point and boiling point. Coke deposits are related to

$$0.1\,(\text{90-Percent distillation temperature, }^{\circ}\text{F}) + \frac{100\,(\text{Volume percent boiling above }400^{\circ}\text{ F})}{\text{Smoke point of fuel boiling above }400^{\circ}\text{ F, mm}} - \text{smoke point, mm} \qquad (5)$$

The average deviation of data from a faired curve was about 21 percent for the annular combustor (ref. 43) and about 14 percent for the small-scale combustor (ref. 44).

The following relation for Smoke Volatility Index (SVI) (ref. 15) has been used with some success to determine which fuels will produce above average amounts of combustor deposits in full-scale engines:

$$\text{SVI} = \text{smoke point} + \frac{\text{volume percent of fuel boiling under }400^{\circ}\text{ F}}{\frac{\text{A.S.T.M. distillation temperature}}{2.4}} \qquad (6)$$

This relation is used in current military procurement fuel specification MIL-F-5624C, grades JP-3 and JP-4, to limit the carbon-forming tendency of these fuels. The specification requires that fuels have SVI values greater than 54. Figure 3(a) of reference 46 shows the SVI values of 21 fuels plotted against deposits obtained in a full-scale single combustor. The average deviation from a faired curve is about 27 percent. Data showing the relation of the SVI and liner deposits obtained in a full-scale single fuel-vaporizing combustor are given in reference 30. These data indicate a much larger average deviation.

Flame-plate method. - Another bench test that has been used to determine the coke-forming tendency of a fuel is known as the flame-plate test. Fuel is delivered

dropwise to the surface of a tared stainless steel plate maintained at a constant elevated temperature. The vaporized fuel is ignited by a bunsen burner pilot, and, after a specified amount of fuel is burned, the plate is reweighed to determine the amount of deposits. The apparatus and procedure are more fully described in references 12, 47, and 48. Results presented in reference 48 show good agreement between the deposits obtained from the flame-plate test and deposits obtained from the same fuels tested in a full-scale single tubular combustor. The effect of such fuel properties as gravity, percent aromatics, and percent aromatics boiling above 420° F on flame-plate-deposit quantity is shown in reference 12. In reference 35, information is presented showing the effect of special fuel additives on flame-plate deposits. Use of tetraethyl lead, U.O.P. Inhibitor No. 5, and amylnitrate resulted in decreased flame-plate deposits of 50 to 90 percent. Small amounts of tetraethyl lead and secondary amylnitrate also reduced deposits in full-scale single combustors. However, the effect of amylnitrate and U.O.P. Inhibitor No. 5 on deposits in a small-scale combustor appeared negligible. One drawback to this bench test is the considerable amount of time required to complete the test ($6\frac{1}{2}$ hr).

Pot-burner method. - Another bench test apparatus that has been used to a limited extent is the "pot burner" (ref. 49). Fuel is fed to a small combustion chamber at a known rate and burns as it enters the chamber. The weight of deposit is determined by weighing the residue scraped from the combustion chamber after a predetermined run time.

Summary of laboratory tests. - In summary, several laboratory and bench tests have been used for determining the deposit-forming tendency of fuels. The tests included methods using the smoke point, the smoke point in combination with a particular boiling point, a flame plate, and a "pot burner." None of the methods listed consistently predicts the combustor-deposit-forming characteristics of various fuels. However, a method that can be used as a first approximation is the smoke-point method with some function of the distillation temperature. This type of test also has the advantage of requiring simple apparatus and only a little time for the determination. The Smoke Volatility Index defined by equation (6) appears to give as consistent results as do any of the methods.

SIGNIFICANCE OF COKE DEPOSITION AND SMOKE-FORMING RESEARCH IN APPLICATION TO JET-ENGINE FUEL SPECIFICATION AND COMBUSTOR DESIGN

The information presented in chapters IX and XIII indicates that coke in a jet-engine combustor liner may be formed from liquid-fuel cracking on the hot liner walls. The softer coke in the dome appears to be a combination of high-boiling fuel fractions and partly polymerized products mixed with a large amount of smoke.

A high-volatility paraffin-type fuel will cause the least deposits. Decrease in fuel volatility causes an increase in combustor deposits but has no significant effect on exhaust smoke. Increase in aromatic content of a fuel causes large increases in combustor deposits and also exhaust smoke. Minor fuel components, such as sulfur and gum, have no effect on combustor deposits until their concentrations are considerably above the maximum permitted by present fuel specifications.

Combustion-chamber inlet-air variables of pressure and fuel-air ratio cause increases in combustor deposits and exhaust smoke; however, the effects of combustor inlet-air temperature and velocity on deposits are not conclusive. Future turbojet engines will have higher inlet-air pressures and mass air flows; these are both conducive to combustor-deposit formations. The higher mass air flows which require

more fuel cause an increase in combustor deposits. Because of these considerations, it may be more practical to use special fuel additives to hold the deposits down to a tolerable level. In some investigations very small amounts of tetraethyl lead and lead naphthanate (0.002 percent lead) caused a significant decrease in combustor deposits.

Any combustion-chamber and fuel-injector design that prevents liquid fuel from impinging on the combustor walls or decreases the residence time of liquid fuel on the hot combustor liner walls will decrease combustor deposits. For example, increasing "air wash" to liner walls should decrease fuel residence time, and, therefore, combustor deposits. Combustion with a properly designed vapor-fuel-injection system should be relatively free of liner deposits.

As previously indicated, a high-volatility paraffin-type fuel will give the least combustor deposits. However, considerations of availability require the final fuel to be a blend of the various types. In an attempt to determine whether the deposit-forming tendency of various fuel blends can be related to fuel properties, investigations were made of properties such as aromatic content, aromatics and volatility, hydrogen-carbon ratio and volatility, density, and aniline-gravity constant. Of these properties, a function of hydrogen-carbon ratio and the 50-percent-evaporated temperature seemed to give the best relation of fuel properties to combustor deposits.

Laboratory and bench test methods for determining the coke-forming characteristics of fuels include the smoke-point method with some measure of volatility, the flame-plate method, and the "pot-burner" method. The Smoke Volatility Index $\left(\text{smoke point} + \frac{\text{volume percent boiling under } 400^\circ \text{ F A.S.T.M. distillation temperature}}{2.4}\right)$ seemed to be the best method because of the accuracy of the results, the simple equipment needed, and the short time required for the determination.

Lewis Flight Propulsion Laboratory
National Advisory Committee for Aeronautics
Cleveland, Ohio, December 7, 1955

REFERENCES

1. Jonash, Edmund R., Wear, Jerrold D., and Hibbard, Robert R.: Relations Between Fuel Properties and Combustion Carbon Deposition. NACA RM E52B14, 1952.

2. Wear, Jerrold D.: Combustor Deposits Obtained with MIL-F-5624A Fuels in a Full-Scale Single Combustor and in Three Full-Scale Engines. NACA RM E54D16, 1954.

3. Anon.: Survey of Service Performance of JP-4 Fuel. Bur. Aero., Dept. Navy.

4. Wear, Jerrold D., and Useller, James W.: Carbon Deposition of Several Special Turbojet-Engine Fuels. NACA RM E51C02, 1951.

5. Clark, Thomas P.: Examination of Smoke and Carbon from Turbojet-Engine Combustors. NACA RM E52I26, 1952.

6. Anon.: Second BuAer Survey on Service Experience with Jet Fuels. Res. and Dev. Dept., Phillips Petroleum Co., Oct. 1, 1953. (Contract NOas 52-132-c.)

7. Wear, Jerrold D., and Douglass, Howard W.: Carbon Deposition from AN-F-58 Fuels in a J33 Single Combustor. NACA RM E9D06, 1949.

8. Rogers, J. D.: Combustion Characteristics of Gas Turbine Fuels. Prog. Rep. No. 34, Calif. Res. Corp., Mar. 1951. (Air Force Contract W-33-038ac-9083, AMC Proj. MX-587.)

9. Horstman, W. W.: Gas Turbine Fuels. Summary Rep. No. 1345, Wood River. Res. Lab., Shell Oil Co., June 15, 1950. (Air Force Contract W-33-038-ac-9813 (14169).)

10. Schirmer, R. M., Fromm, E. H., and Kittredge, G. D.: Evaluation of Fuel Characteristics in Thermojet Engine Combustion Processes. Prog. Rep. No. 3, Rep. 403-14-52R, Res. Div., Phillips Petroleum Co., Apr. 15, 1952. (Navy Contract NOas 52-132-C.)

11. Schalla, Rose L., Clark, Thomas P., and McDonald, Glen E.: Formation and Combustion of Smoke in Laminar Flames. NACA Rep. 1186, 1954. (Supersedes NACA RM's E51E15, E52G24, E52I22, E52I26, E53E05, E53J12, and E54E03.)

12. McLean, C. D.: Combustion Characteristics of Gas Turbine Fuels. Summary Rep., Calif. Res. Corp., Dec. 1952. (Air Force Contract AF 18(600)-152.)

13. Fromm, E. H.: Evaluation of Fuel Characteristics in Thermojet Engine Combustion Processes. Prog. Rep. No. 2, Rep. 403-22-53R, Res. Div., Phillips Petroleum Co., May 28, 1952. (Navy Contract NOas 52-132-c, Amendment I.)

14. Wear, Jerrold D., and Butze, Helmut F.: Preliminary Investigation of the Performance of a Single Tubular Combustor at Pressures up to 12 Atmospheres. NACA RM E53K09, 1954.

15. Marshall, E. F.: Progress Report, Jan. 1-Feb. 28, 1951. Prog. Rep. No. 35, Automotive Lab., Sun Oil Co., Feb. 19, 1951. (Contract No. W-33-038-ac-9086.)

16. Moore, R. A., and Donnelly, J. J.: Summary Rep. No. 2, Rep. No. 48-1-DX, Res. and Dev. Div., Socony-Vacuum Labs., Jan. 9, 1948. (U.S. Gov't. Contract W-33-038-ac-8527, AMC Proj. MX-587.)

17. McLean, C. D.: Combustion Characteristics of Gas Turbine Fuels. Summary Rep., Calif. Res. Corp., Jan. 15, 1954. (Air Force Contract AF 18(600)-152.)

18. Butze, Helmut F., and Wear, Jerrold D.: Performance of a Tubular Turbojet Combustor at High Pressures and Temperatures. NACA RM E55A24, 1955.

19. Moore, R. A., and Giaccone, F. W.: Summary Rep. No. 46.23-DX, Res. and Dev. Div., Socony-Vacuum Labs., Nov. 8, 1946. (U.S. Gov't. Contract W-33-038-ac-8527, AMC Proj. MX-587.)

20. Starkman, E. S., and Cattaneo, A. G.: The Influences of Fuel Characteristics on Performance in a Reduced Scale Gas Turbine Combustion Chamber. Rep. No. S-9861, Shell Dev. Co., Nov. 7, 1945.

21. Wear, Jerrold D., and Jonash, Edmund R.: Carbon Deposition of 19 Fuels in an Annular Turbojet Combustor. NACA RM E8K22, 1949.

22. McCafferty, Richard J.: Vapor-Fuel-Distribution Effects on Combustion Performance of a Single Tubular Combustor. NACA RM E50J03, 1950.

[redacted]

23. Marshall, E. F.: Progress Report No. 19, May 1, 1947-June 30, 1948. Dev. Div., Sun Oil Co., July 22, 1948. (Contract No. W-33-038-ac-9086 (13420).)

24. Jonash, Edmund R., Wear, Jerrold D., and Cook, William P.: Carbon-Deposition Characteristics of MIL-F-5624A Fuels Containing High-Boiling Aromatic Hydrocarbons. NACA RM E52G11, 1952.

25. Marshall, E. F.: Progress Report, May 1-June 30, 1952. Prog. Rep. No. 43, Automotive Lab., Sun Oil Co., Aug. 1, 1952. (Contract No. W-33-038-ac-9086.)

26. Wear, Jerrold D., and Cook, William P.: Effect of Fuel Properties on Carbon Deposition in Atomizing and Prevaporizing Turbojet Combustors. NACA RM E52C24, 1952.

27. Rogers, J. D.: J-33 Jet Propulsion Burner Tests on Carbon Deposition and Effects of Wide-Cut Fuel Properties. Summary Rep. for period July 1, 1948 to June 30, 1949, Calif. Res. Corp., Aug. 29, 1949. (Army Contract W-33-038-ac-9083, AMC Proj. MX-587.)

28. Moore, R. A.: Summary Report No. 4, Rep. No. 49.17-DX, Res. and Dev. Div., Socony-Vacuum Labs., June 26, 1950. (U.S. Gov't. Contract W-33-038-ac-8527, AMC Proj. MX-587.)

29. Fromm, E. H.: Evaluation of Fuel Characteristics in Thermojet Engine Combustion Processes. Prog. Rep. No. 5, Rep. 403-16-52R, Res. Div., Phillips Petroleum Co., Aug. 13, 1952. (Navy Contract NOas 52-132-c.)

30. Horstman, W. W., and Jackson, J. L.: Fuel Requirements of Pre-Vaporizing Type Gas Turbine Combustors - Materials Section. Rep. No. 1451, Final Rep. Mar. 17, 1952-June 17, 1954, Wood River Res. Lab., Shell Oil Co., July 30, 1954. (USAF Contract No. AF 33(616)-76.)

31. Barnett, Henry C., and Hibbard, R. R.: Fuel Characteristics Pertinent to the Design of Aircraft Fuel Systems. NACA RM E53A21, 1953.

32. Jonash, Edmund R., Wear, Jerrold D., and Cook, William P.: Effect of Fuel Additives on Carbon Deposition in a J33 Single Combustor. I - Three Metallic-Organic Additives. NACA RM E52H21, 1952.

33. Hlavin, Vincent F., and Cook, William P.: Effect of Fuel Additives on Carbon Deposition in a J33 Single Combustor. II - Seven Commercial Organo-Metallic Additives. NACA RM E54H23, 1954.

34. Marshall, E. F.: Progress Report, Jan. 1-Feb. 28, 1953. Prog. Rep. No. 47, Automotive Lab., Sun Oil Co., Mar. 11, 1953. (Contract No. W-33-038-ac-9086.)

35. Bert, J. A.: Combustion Characteristics of Gas Turbine Fuels. Prog. Rep. No. 35, Calif. Res. Corp., May 1951. (AF Contract W-33-038-ac-9083, AMC Proj. MX-587.)

36. Marshall, E. F.: Progress Report, Sept. 1-Oct. 31, 1952. Prog. Rep. No. 45, Automotive Lab., Sun Oil Co., Dec. 31, 1952. (Contract No. W-33-038-ac-9086.)

37. Kittredge, G. D., and Fromm, E. H.: Evaluation of Fuel Characteristics in Thermojet Engine Combustion Processes. Prog. Rep. No. 6, Rep. No. 403-17-52R, Res. Div., Phillips Petroleum Co., 1952. (Navy Contract NOas 52-132-C.)

38. Butze, Helmut F.: Effect of Inlet-Air and Fuel Parameters on Smoking Characteristics of a Single Tubular Turbojet-Engine Combustor. NACA RM E52A18, 1952.

39. Bert, J. A.: G.E. I-16 Jet Propulsion Burner Tests. Prog. Rep. No. 12, Calif. Res. Corp., Apr. 19, 1947. (Army Contract W-33-038-ac-3083, AMC Proj. MX-587.)

40. Rogers, J. D.: G.E. J-33 Jet Propulsion Burner Tests. Prog. Rep. No. 23, Calif. Res. Corp., Apr. 30, 1949. (Air Force Contract No. W-33-038ac-9083, AMC Proj. MX-587.)

41. Clark, T. P.: Influence of External Variables on Smoking of Benzene Flames. NACA RM E52G24, 1952.

42. Sharp, J. G.: Fuels for Gas-Turbine Aero-Engines. Aircraft Eng., vol. XXIII, no. 263, Jan. 1951, pp. 2-8.

43. Busch, Arthur M.: Correlation of Laboratory Smoke Test with Carbon Deposition in Turbojet Combustors. NACA RM E9K04, 1950.

44. Marshall, E. F.: Progress Report Nov. 1-Dec. 31, 1952. Prog. Rep. No. 46, Automotive Lab., Sun Oil Co., Feb. 4, 1953. (Contract No. W-33-038-ac-9086.)

45. Eaffy, Allan: Method of Predicting the Carbon Forming Tendencies of Jet Fuels. Tech. Note WCLP 53-204, Power Plant Lab., Wright Air Dev. Center, Wright-Patterson Air Force Base, July 9, 1953. (E.O. No. R-531-357A.)

46. Jonash, Edmund R., Butze, Helmut F., and Cook, William P.: Correlation of Turbojet Combustor Carbon Formation with Smoke-Volatility Index, Smoke Point, and NACA K Factor. NACA RM E55D28, 1955.

47. Rogers, J. D., and Jones, D. R.: Combustion Characteristics of Gas Turbine Fuels. Prog. Rep. No. 27, Calif. Res. Corp., Dec. 31, 1949. (Air Force Contract W-33-038ac-9083, AMC Proj. MX-587.)

48. Rogers, J. D., and Jones D. R.: Combustion Characteristics of Gas Turbine Fuels. Prog. Rep. No. 28, Calif. Res. Corp., Feb. 28, 1950. (Air Force Contract W-33-038ac-9083, AMC Proj. MX 587.)

49. Anon.: Deposit Forming Tendencies of Several AN-F-58 Jet Engine Fuels Observed in Bench Tests and in Full Scale Combustor Tests. Refining Dept., Tech. and Res. Div., Beacon Labs., The Texas Co., July 6, 1950.

50. Jonash, Edmund R., Barnett, Henry C., and Stricker, Edward G.: Investigation of Carbon Deposition in an I-16 Jet-Propulsion Engine at Static Sea-Level Conditions. NACA RM E6K01, 1947.

51. Wear, Jerrold D., and Locke, Theodore E.: Effect of Retractable Ignition Plug on Plug Fouling by Carbon Deposits. NACA RM E50F14, 1950.

52. Dittrich, Ralph T.: Effects of Fuel-Nozzle Carbon Deposition on Combustion Efficiency of Single Tubular-Type, Reverse-Flow, Turbojet Combustor at Simulated Altitude Conditions. NACA TN 1618, 1948.

(a) On liner after 2-hour run with Diesel fuel oil (ref. 50).

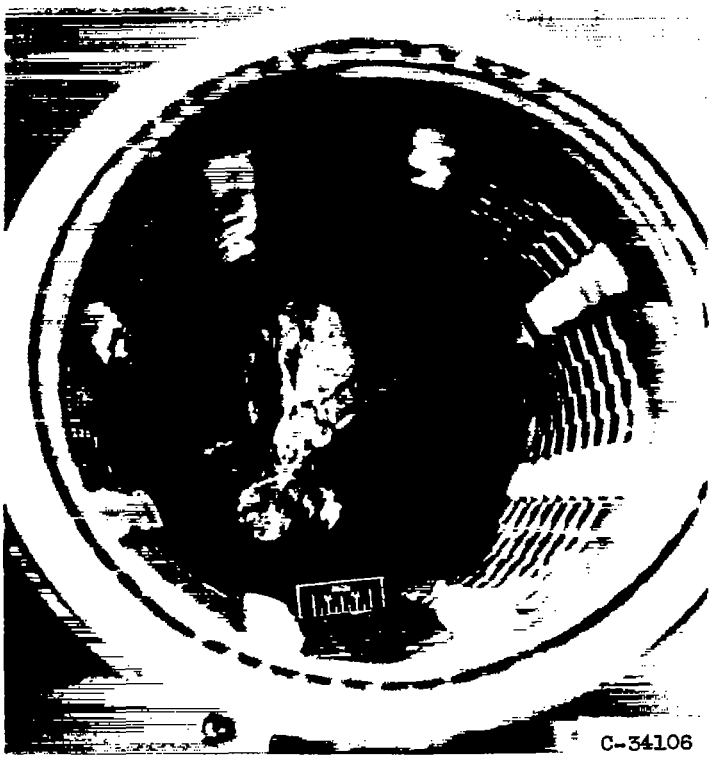

(b) On liner after 25-hour run with JP-4 fuel.

Figure 116. - Coke deposits in full-scale-engine combustors.

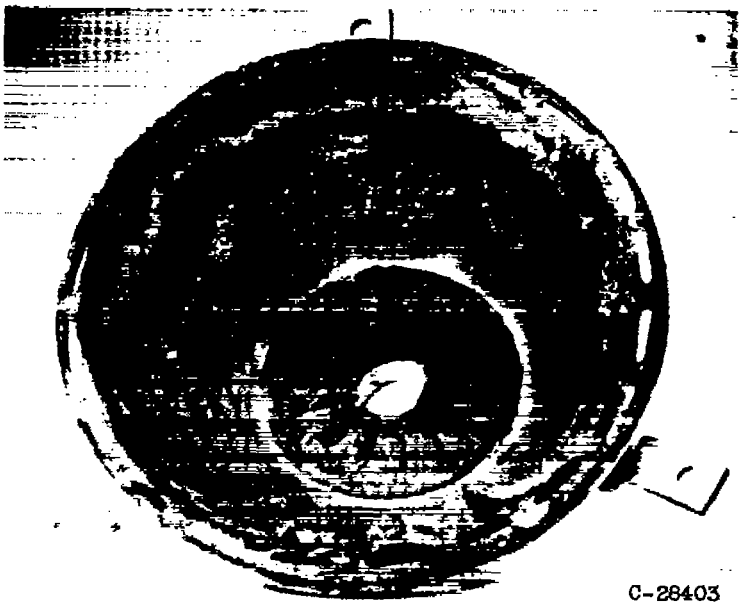

(c) On dome and primary-air entry ports after 30-hour run with JP-3 fuel.

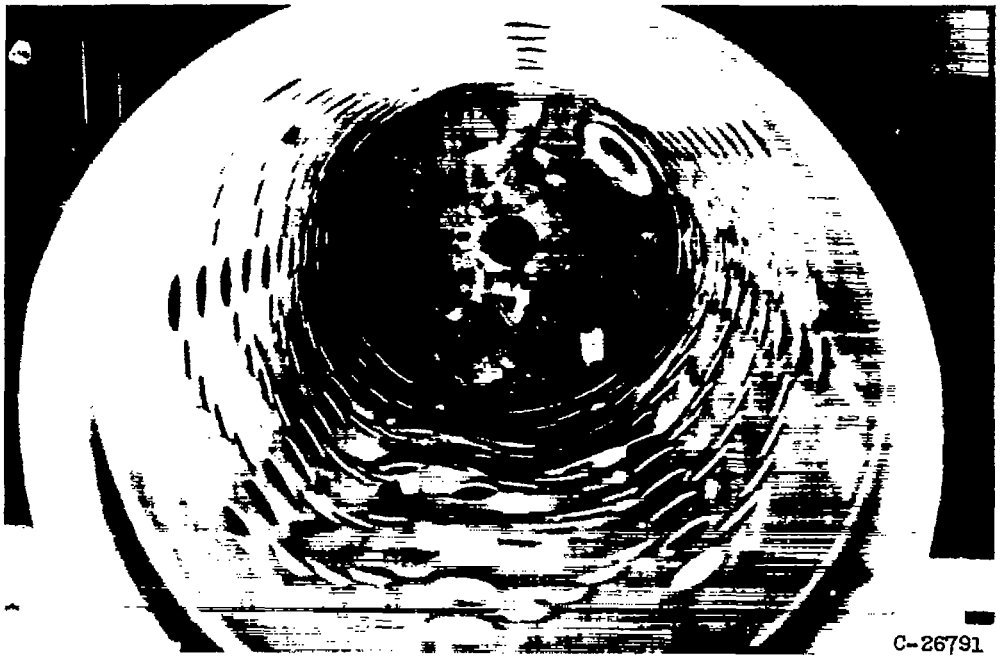

(d) On liner near warped and cracked area after 25-hour run with JP-3 fuel (ref. 4).

Figure 116. - Continued. Coke deposits in full-scale-engine combustors.

CC-29 back 3179

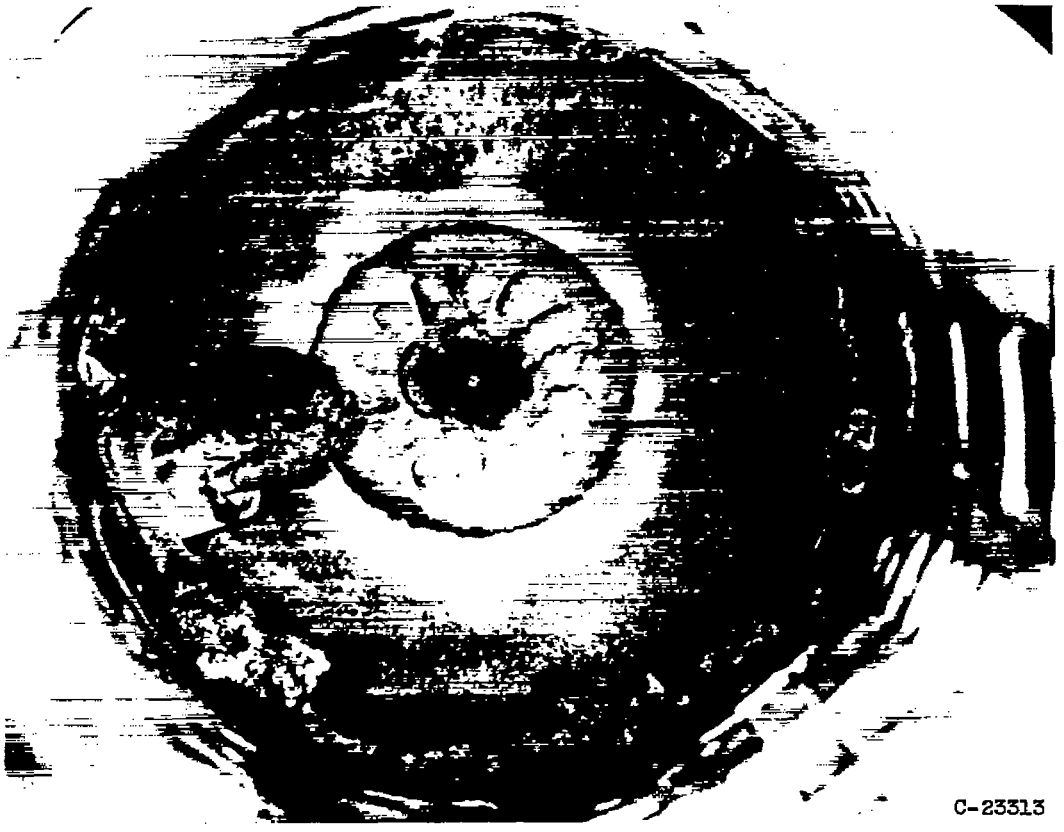

(e) On liner, fuel nozzle, primary-air entry ports, and spark plug after 12-hour run with aromatic fuel (ref. 51).

Figure 116. - Concluded. Coke deposits in full-scale-engine combustors.

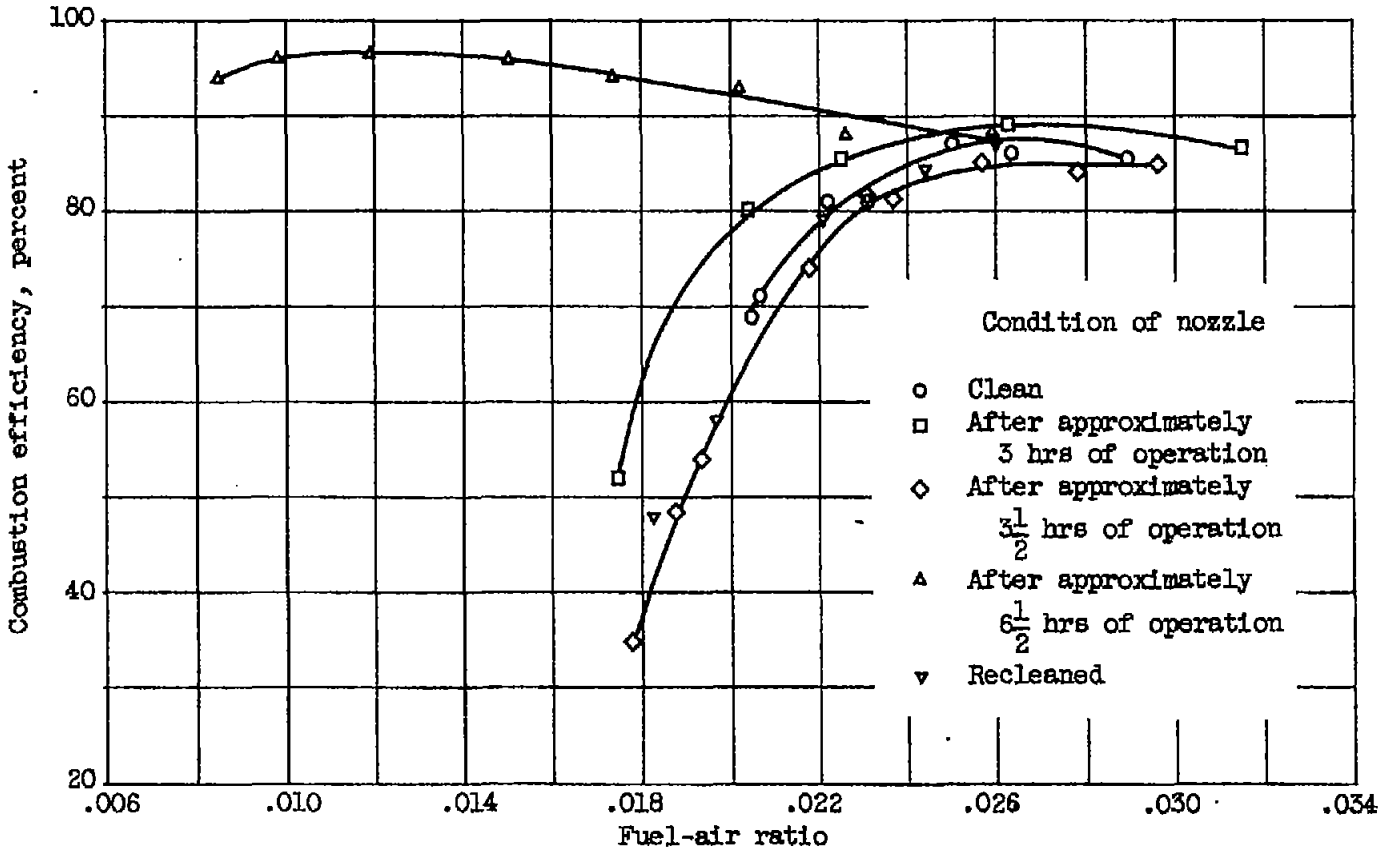

Figure 117. - Variation of combustion efficiency with fuel-air ratio as affected by coke formation on fuel nozzle of single tubular turbojet combustor. Inlet-air pressure, 6.1 pounds per square inch absolute; inlet-air temperature, 550° R; air-flow rate, 0.457 pound per second (ref. 52).

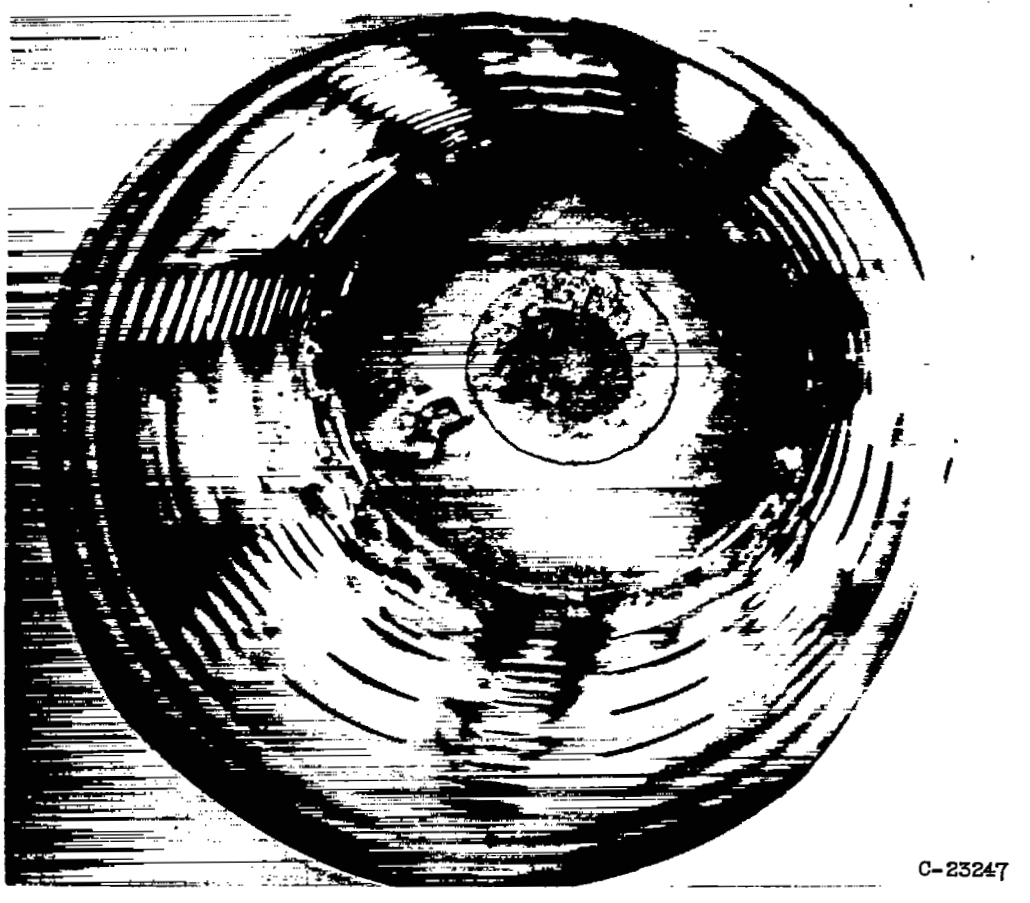

Figure 118. - Coke deposits obtained in single tubular combustor during 80-hour test run. Fuel, high-aromatic MIL-F-5624A, grade JP-3; engine conditions: altitude, 20,000 feet; 90-percent normal rated engine speed; flight Mach number, zero (ref. 7).

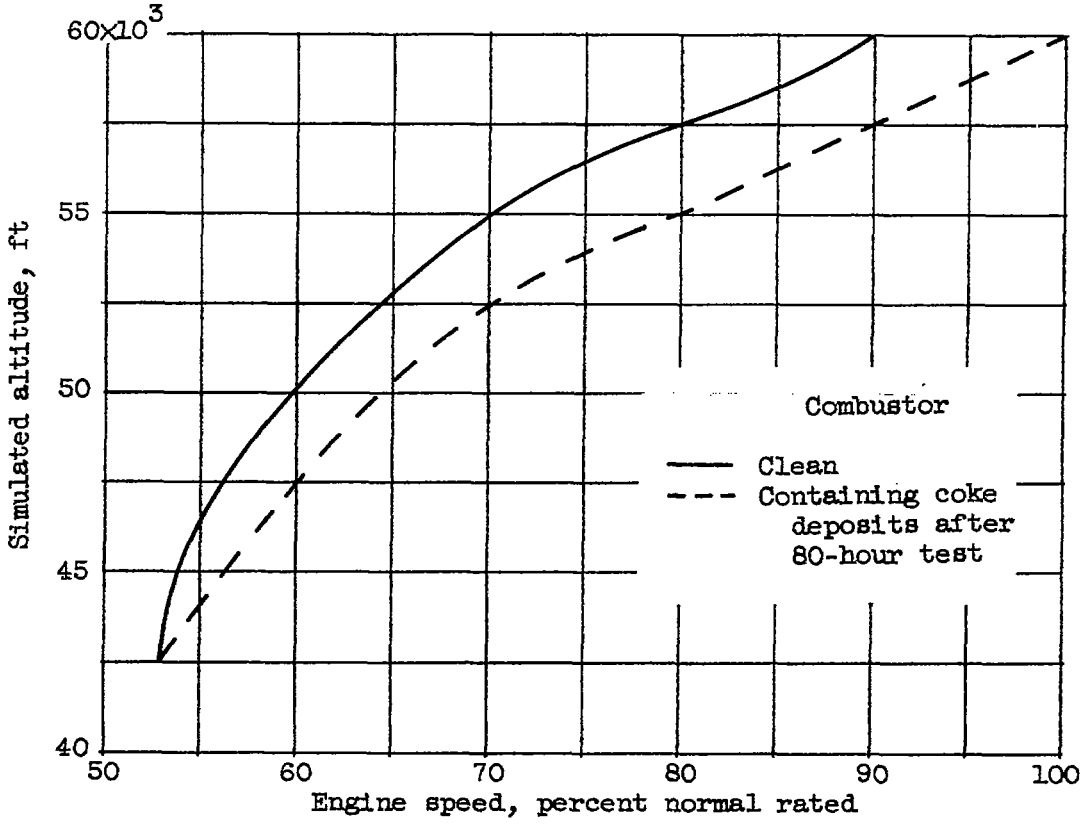

Figure 119. - Altitude operational limits obtained in clean single tubular combustor and in combustor containing coke deposited during 80-hour test. Fuel, minimum-quality MIL-F-5624A, grade JP-3 (ref. 7).

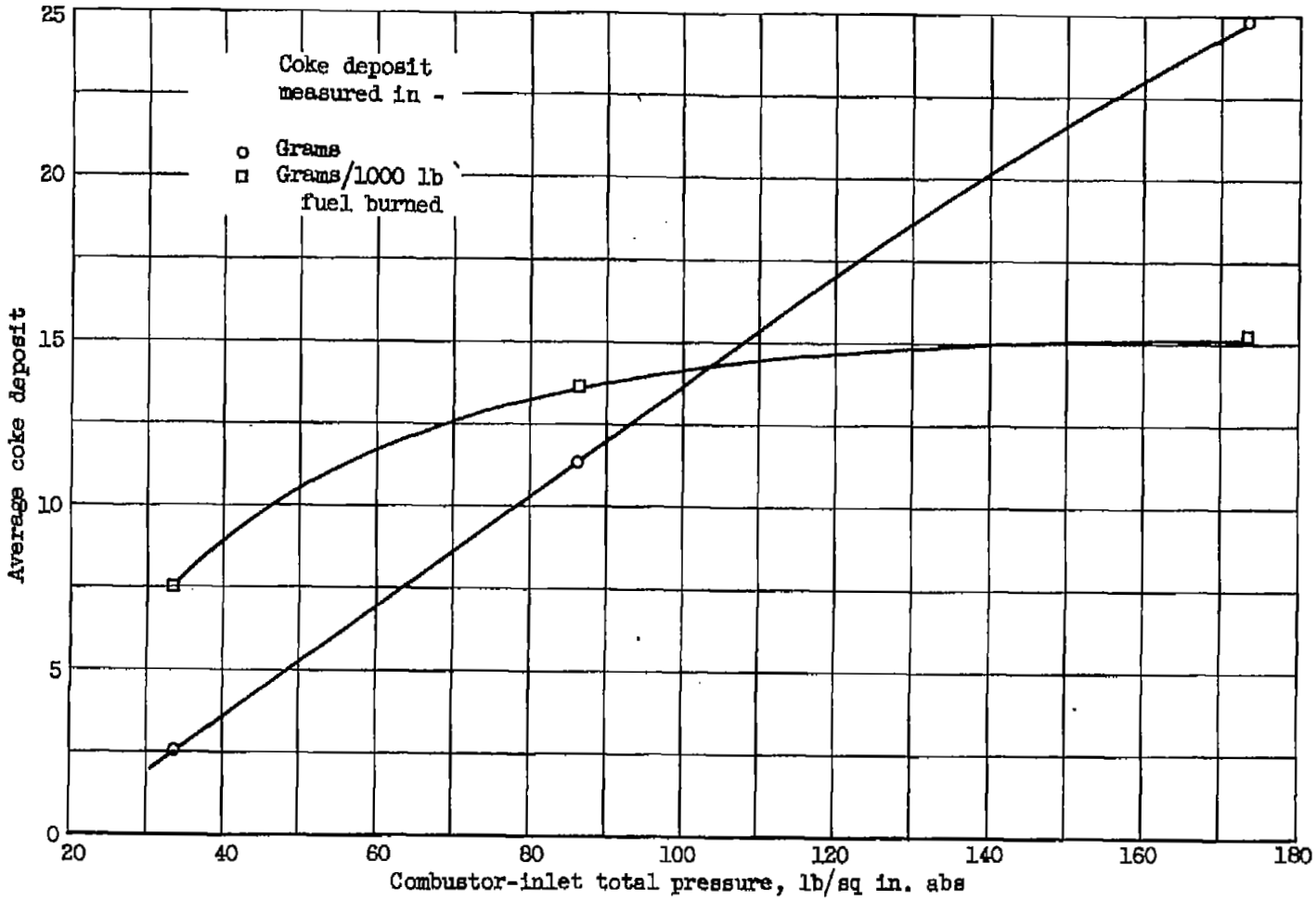

Figure 120. - Effect of combustor-inlet total pressure on coke deposition in full-scale single tubular combustor. Combustor reference velocity, 78 feet per second; inlet-air temperature range, 218° to 253° F; fuel-air-ratio range, 0.0166 to 0.0174; JP-4 fuel; run time, 2 hours (ref. 14).

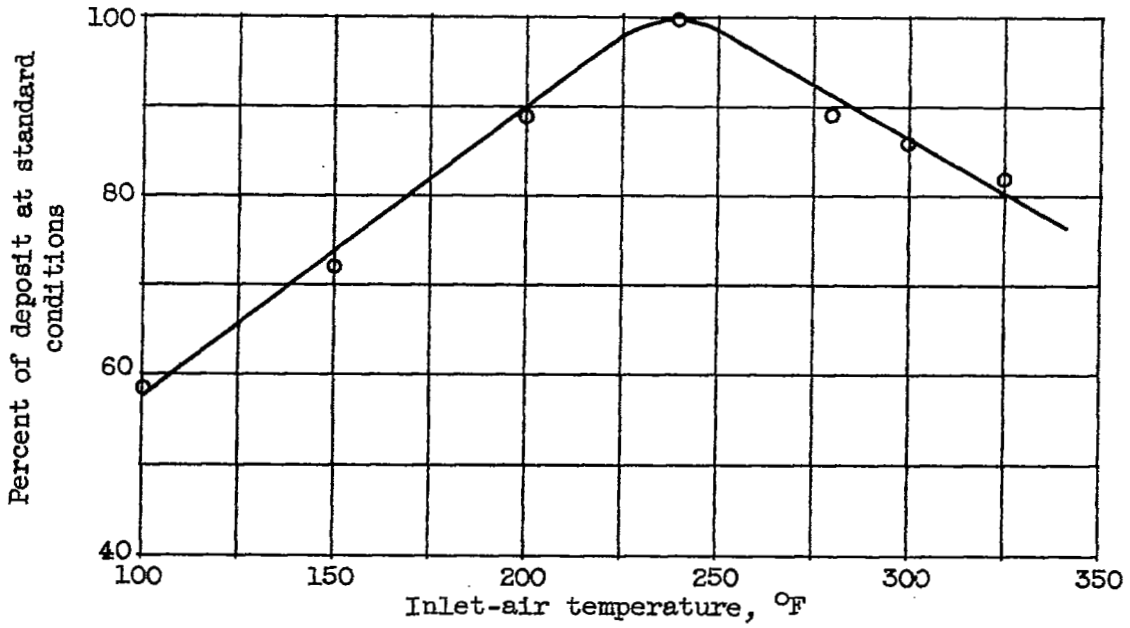

(a) Small-scale combustor. Inlet pressure, 48 inches of mercury absolute; total mass air flow, 435 pounds per hour; fuel-air ratio, 0.0133; JP-1 fuel; run time, 2 hours (ref. 15).

Figure 121. - Effect of inlet-air temperature on coke deposition in tubular combustors.

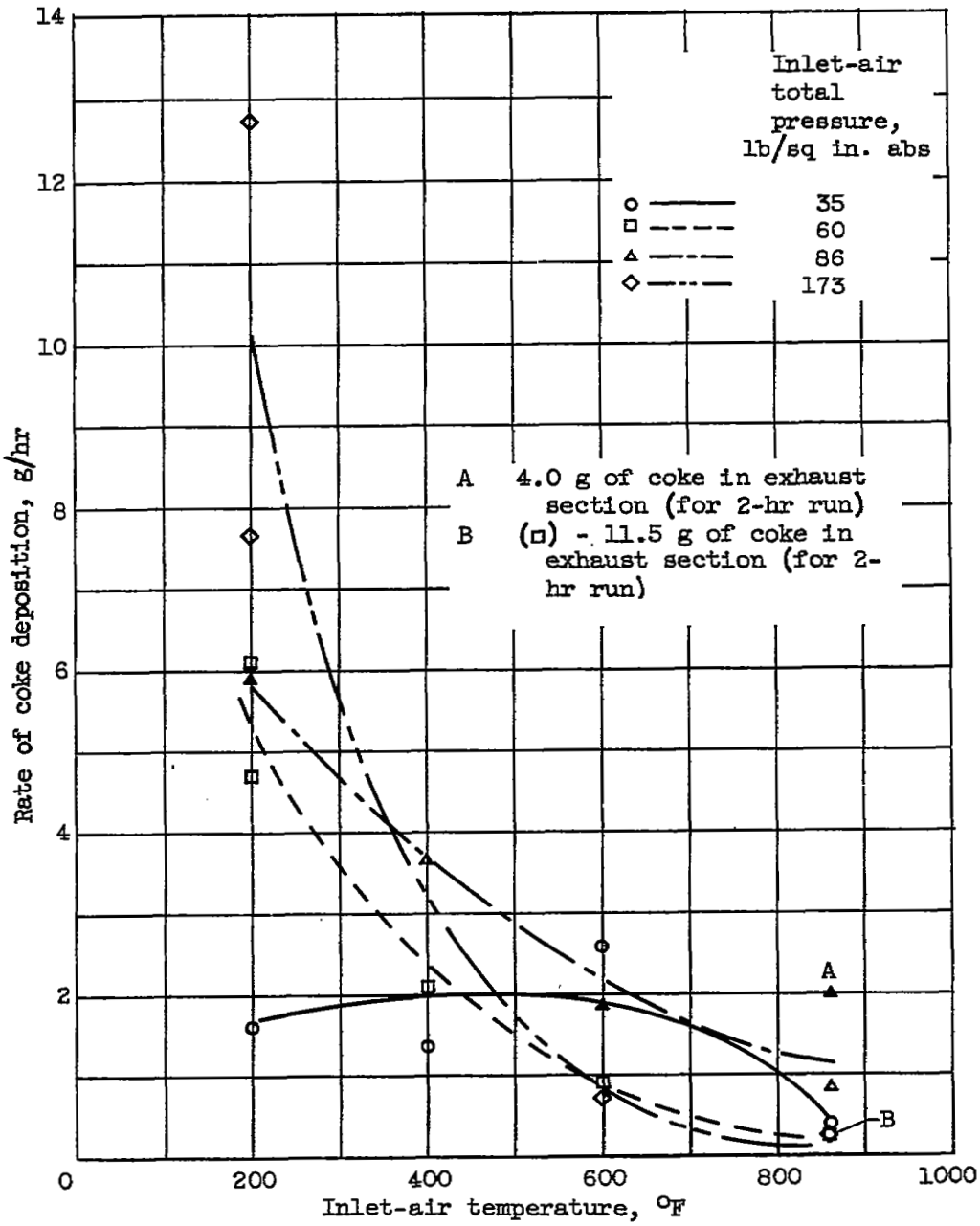

(b) Full-scale single combustor. Inlet reference velocity, 78 feet per second; combustor temperature rise, 1165° F (ref. 18).

Figure 121. - Concluded. Effect of inlet-air temperature on coke deposition in tubular combustors.

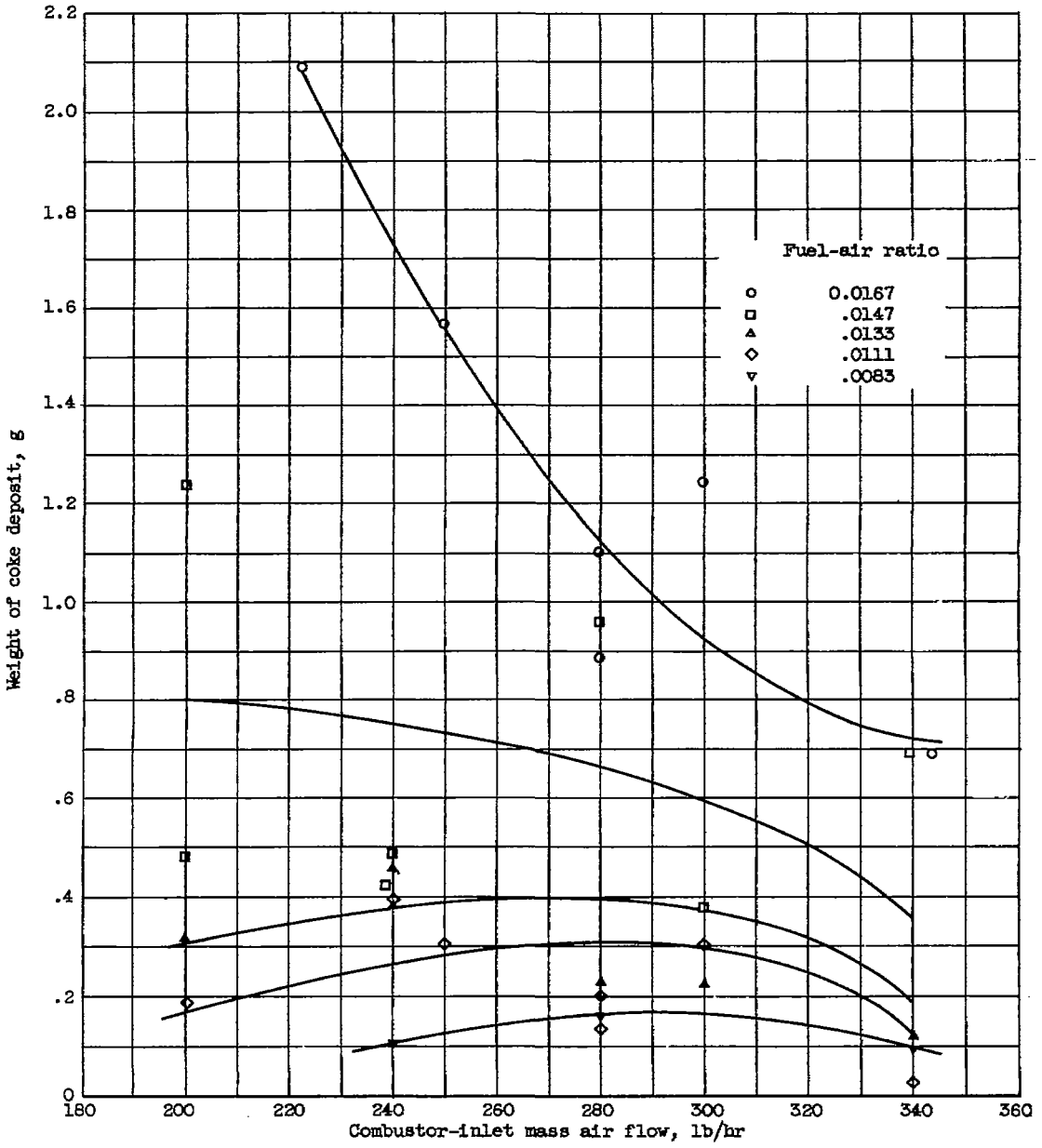

Figure 122. - Effect of combustor-inlet mass air flow and fuel-air ratio on coke deposition in small-scale tubular combustor. Combustor-inlet pressure, 20 pounds per square inch; JP-1 fuel; run time, 15 minutes (ref. 20).

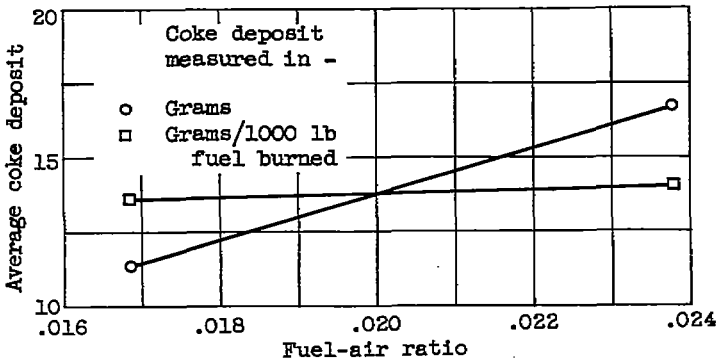

Figure 123. - Effect of fuel-air ratio on carbon deposition in full-scale single tubular combustor. Inlet-air total pressure, 86.2 pounds per square inch absolute; combustor reference velocity, 78 feet per second; inlet-air temperature range, 239° to 246° F; JP-4 fuel; run time, 2 hours (ref. 14).

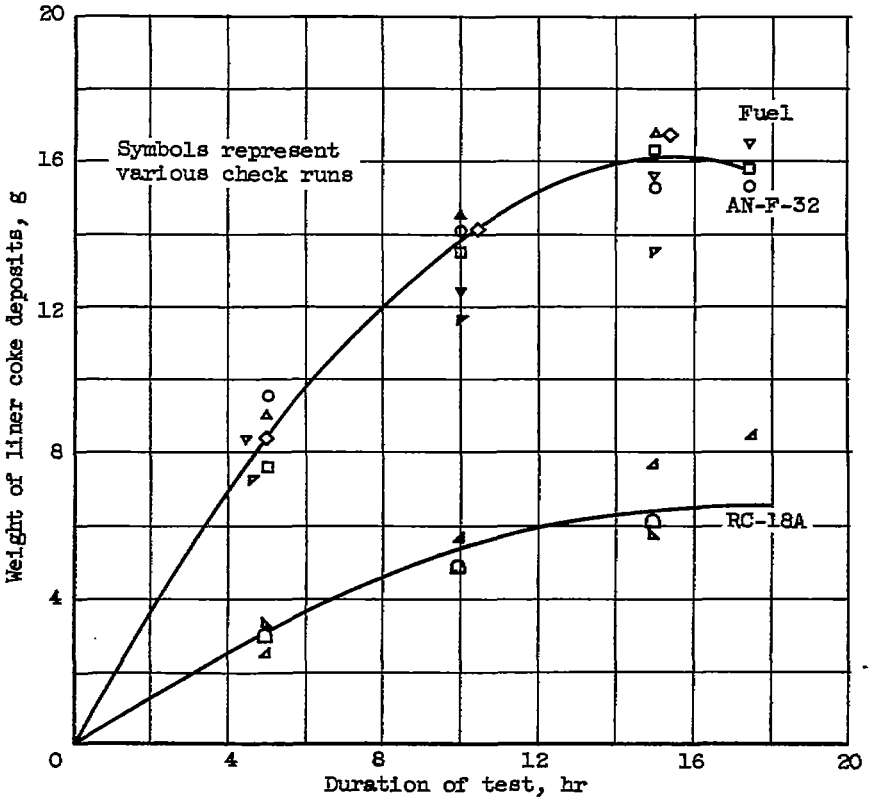

Figure 124. - Effect of run time and fuel type on coke deposition in full-scale single combustor. Combustor operated at cyclic conditions (ref. 28).

[redacted]

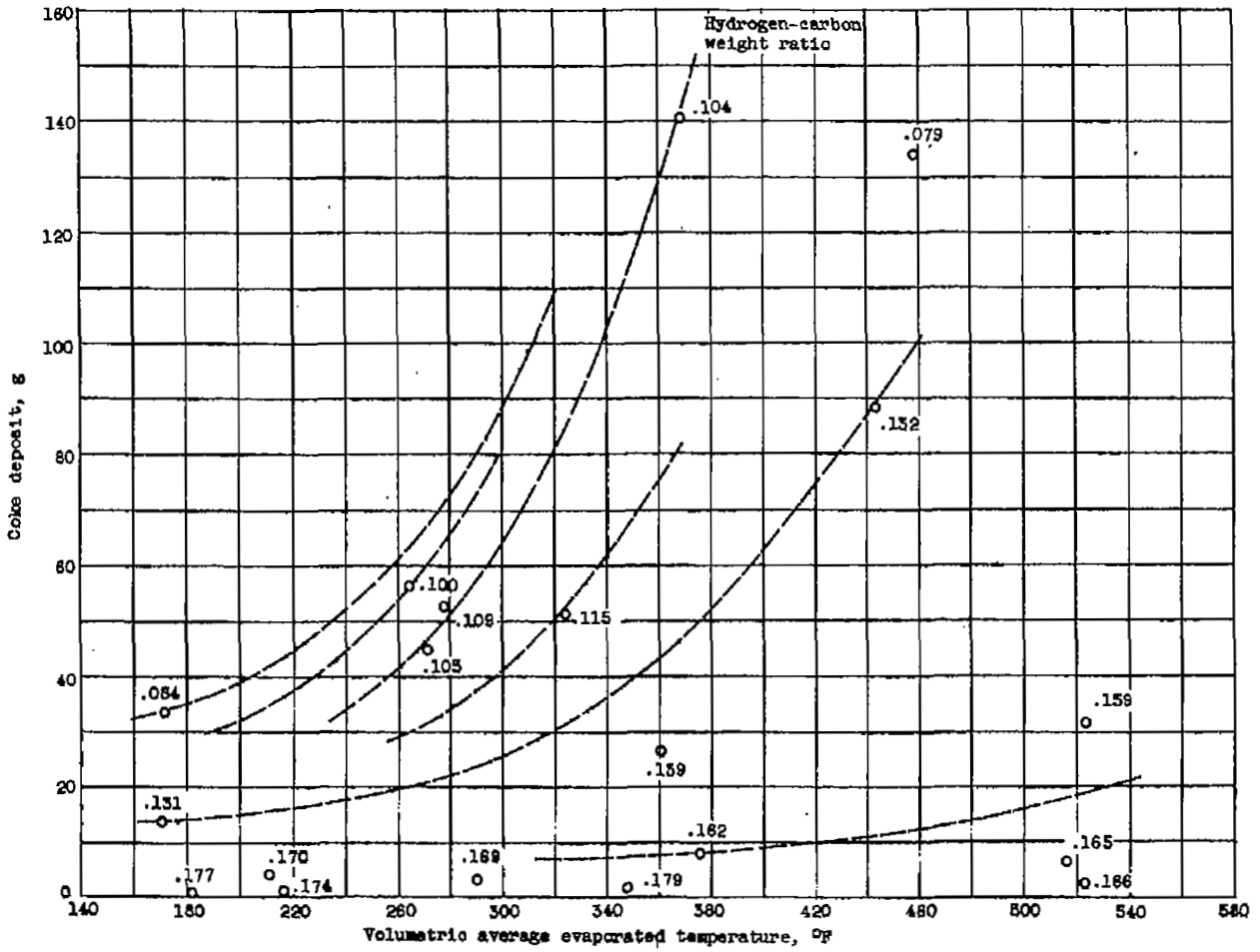

(a) As function of hydrogen-carbon weight ratio.

Figure 125. - Coke deposition of 19 fuels as determined by volumetric average evaporated temperature. Annular-combustor diameter, $10\frac{3}{8}$ inches; inlet-air total pressure, 40 inches mercury absolute; inlet-air total temperature, 100° F; fuel flow, 157.5 pounds per hour; fuel-air ratio, 0.0175; run time, 2 hours (ref. 21).

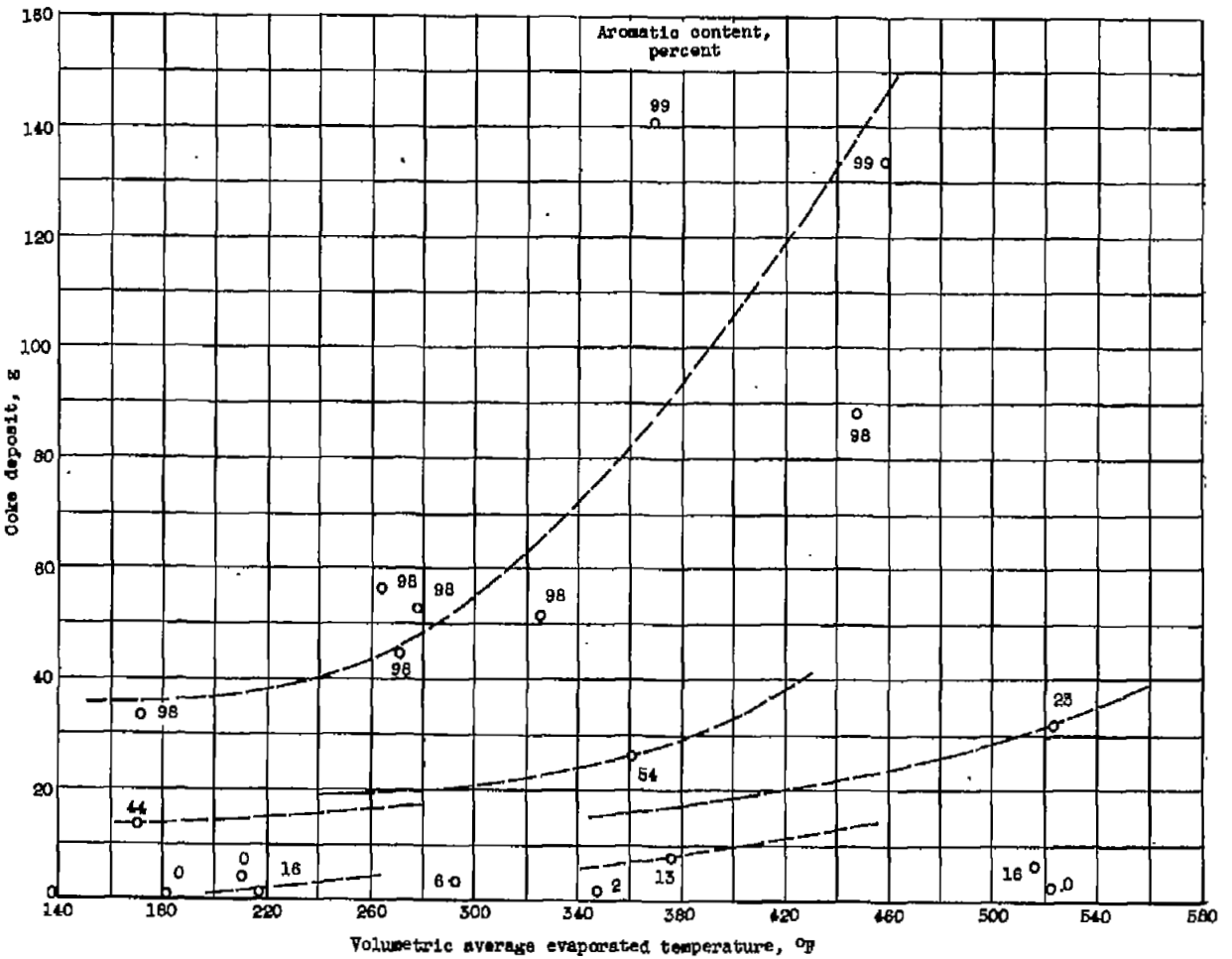

(b) As function of aromatic content.

Figure 125. - Concluded. Coke deposition of 19 fuels as determined by volumetric average evaporated temperature. Annular-combustor diameter, $10\frac{3}{8}$ inches; inlet-air total pressure, 40 inches mercury absolute; inlet-air total temperature, 100° F; fuel flow, 157.5 pounds per hour; fuel-air ratio, 0.0175; run time, 2 hours (ref. 21).

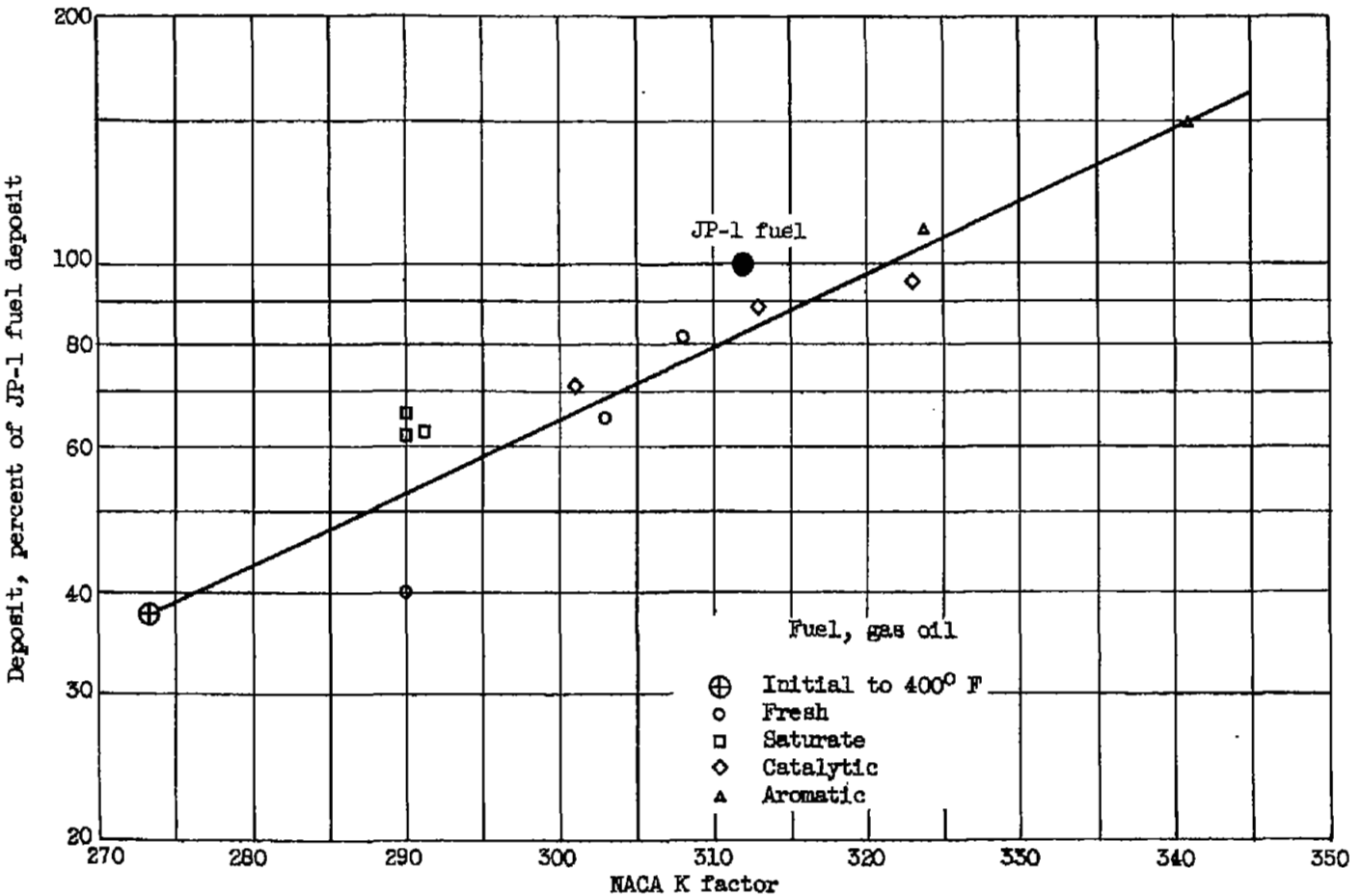

(a) In small-scale tubular combustor. Combustor-inlet air pressure, 48 inches of mercury absolute; inlet-air temperature, 240° F; total mass air flow, 435 pounds per hour; fuel-air ratio, 0.0133; run time, 2 hours (ref. 44).

Figure 128. - Effect of NACA K factor on coke deposition of several fuels.

3179

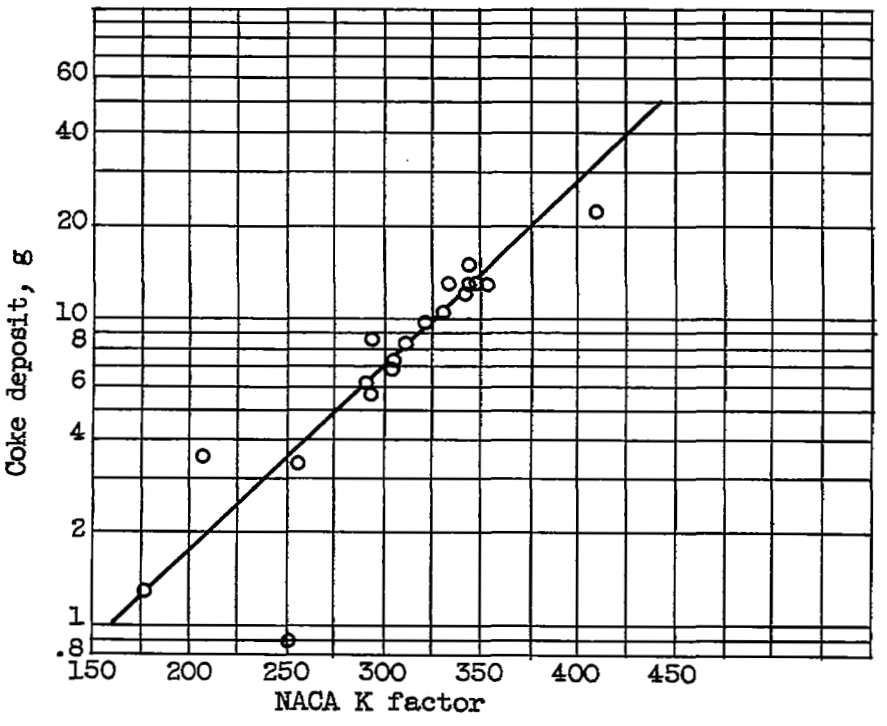

(b) In full-scale single tubular combustor. Combustor-inlet air total pressure, 53.9 inches of mercury absolute; inlet-air temperature, 271° F; fuel flow, 127.0 pounds per hour; fuel-air ratio, 0.0123; run time, 4 hours (ref. 1).

Figure 126. - Continued. Effect of NACA K factor on coke deposition of several fuels.

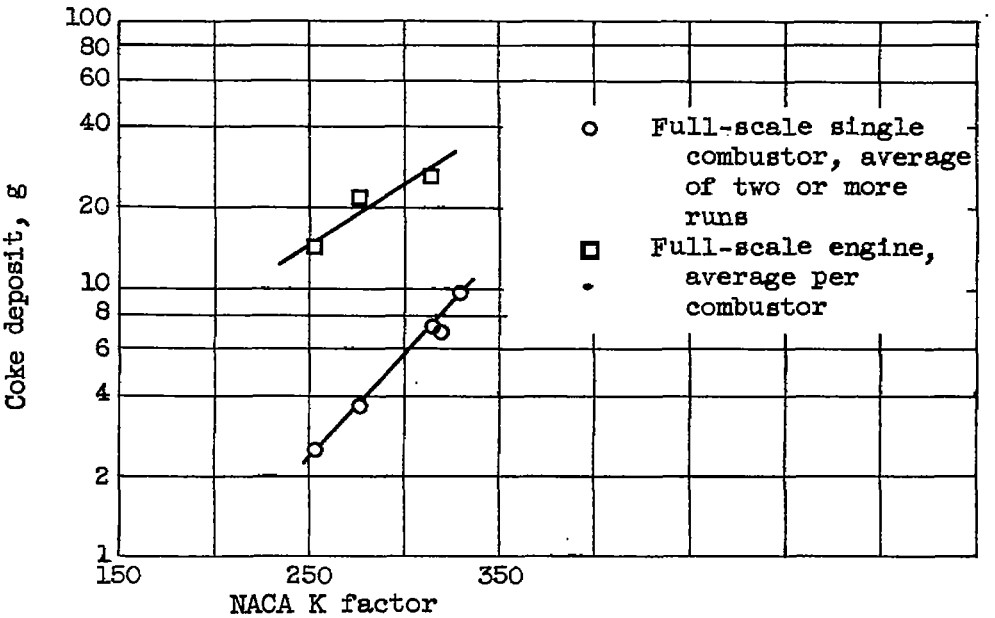

(c) In full-scale single combustor and in full-scale engine. Single combustor-inlet total pressure, 53.9 inches of mercury absolute; inlet-air temperature, 271° F; fuel flow, 127.0 pounds per hour; fuel-air ratio, 0.0123. Full-scale engine cyclic running schedule, 15 minutes at take-off speed and 5 minutes at idle speed; total run time, about 50 hours (ref. 2).

Figure 126. - Concluded. Effect of NACA K factor on coke deposition of several fuels.

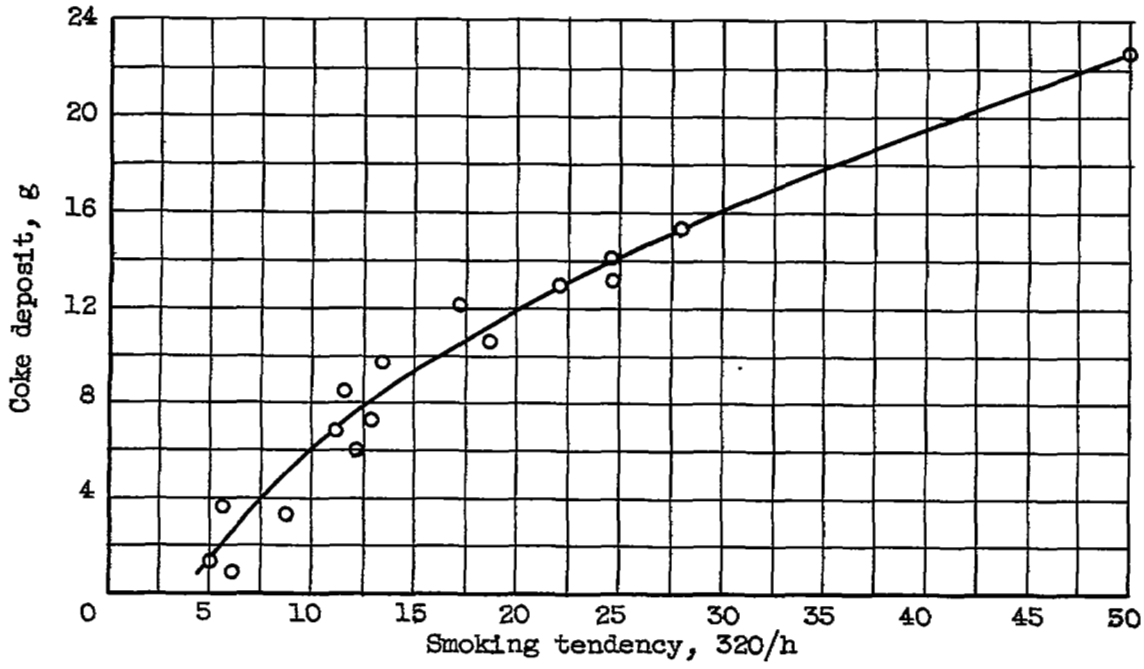

Figure 127. - Effect of smoking tendency on coke deposition of several fuels in full-scale single tubular combustor. Combustor-inlet total pressure, 53.9 inches mercury absolute; inlet-air temperature, 271° F; fuel flow, 127.0 pounds per hour; fuel-air ratio, 0.0123; run time, 4 hours (ref. 1).

CHAPTER XIV

RAM-JET PERFORMANCE

By A. J. Cervenka and R. Friedman

INTRODUCTION

The ram jet is basically one of the most simple types of aircraft engine. It consists only of an inlet diffuser, a combustion system, and an exit nozzle. A typical ram-jet configuration is shown in figure 128. The engine operates on the Brayton cycle, and ideal cycle efficiency depends only on the ratio of engine to ambient pressure. The increased engine pressures are obtained by ram action alone, and for this reason the ram jet has zero thrust at zero speed. Therefore, ram-jet-powered aircraft must be boosted to flight speeds close to a Mach number of 1.0 before appreciable thrust is generated by the engine.

Since pressure increases are obtained by ram action alone, combustor-inlet pressures and temperatures are controlled by the flight speed, the ambient atmospheric condition, and by the efficiency of the inlet diffuser. These pressures and temperatures, as functions of flight speed and altitude, are shown in figure 129 for the NACA standard atmosphere and for practical values of diffuser efficiency. It can be seen that very wide ranges of combustor-inlet temperatures and pressures may be encountered over the ranges of flight velocity and altitude at which ram jets may be operated. Combustor-inlet temperatures from 500° to 1500° R and inlet pressures from 5 to 100 pounds per square inch absolute represent the approximate ranges of interest in current combustor development work.

Since the ram jet has no moving parts in the combustor outlet, higher exhaust-gas temperatures than those used in current turbojets are permissible. Therefore, fuel-air ratios equivalent to maximum rates of air specific impulse or heat release can be used, and, for hydrocarbon fuels, this weight ratio is about 0.070. Lower fuel-air ratios down to about 0.015 may also be required to permit efficient cruise operation. This fuel-air-ratio range of 0.015 to 0.070 used in ram jets can be compared with the fuel-air ratios up to 0.025 encountered in current turbojets.

Ram-jet combustor-inlet velocities range from 150 to 400 feet per second. These high linear velocities combined with the relatively low pressure ratios obtainable in ram jets require that the pressure drop through the combustor be kept low to avoid excessive losses in cycle efficiency. It has been estimated that, for a long-range ram-jet engine, an increase in pressure loss of one dynamic head would require a compensating 1-percent increase in combustion efficiency. Therefore, combustor pressure-loss coefficients (pressure drop/impact pressure) of the order of 1 to 4 are found in most current engines.

The operating conditions described impose major problems in the design of stable and efficient ram-jet combustion systems. This chapter presents a survey of ram-jet combustor research and, where possible, points out criteria that may be useful in the design of ram-jet combustion systems.

EXPERIMENTAL METHODS

Data Sources

Ram-jet combustor performance data have been obtained in connected-pipe, free-jet, tunnel, and flight tests. A connected-pipe facility (e.g., ref. 1) consists of

a subsonic diffuser, a combustion chamber, and an exhaust nozzle connected by suitable ducting to air supply and exhaust pumps. A free-jet test installation (e.g., ref. 2) consists of a ram-jet engine complete with supersonic diffuser installed downstream of a supersonic nozzle. In subsonic or supersonic tunnel tests (e.g., ref. 3), the ram-jet engine has been installed either directly in the main air stream or downstream of a connecting air supply duct. Ram-jet-combustor data have also been obtained with engines attached to subsonic aircraft (ref. 4), with free-falling engines dropped from high-flying aircraft (ref. 5), and with engines launched by rocket power (ref. 6).

Data Reduction Methods

Combustion efficiency, one of the most important performance parameters for evaluating ram-jet combustors, is defined as the ratio of the actual enthalpy rise across the combustor to the theoretical heating value of the fuel. Combustion-efficiency data for a ram-jet engine are difficult to obtain directly from inlet and exhaust-gas temperature measurements because of the high exhaust-gas temperatures. For this reason, indirect methods have been evolved whereby combustion-chamber pressures, engine thrust, or heat-balance measurements are reduced to give combustion efficiency. For applications where thrust measurements are obtained, ram-jet performance is usually expressed in terms of impulse efficiency, which is defined as the ratio of actual to theoretical specific impulse.

Pressure method. - In the pressure method, the increase in momentum of the gases flowing through the combustion chamber is determined by means of total- and static-pressure measurements. These pressures can be related to the temperature rise across the combustor by the following compressible-flow equation (ref. 7):

$$T_4 = \frac{p_5^2 A_5^2 g}{(w_a + w_f)^2} \frac{\gamma_{st,5}(\gamma_{av} + 1)}{2R} \qquad (1)$$

where

A area

g acceleration due to gravity

p static pressure

R gas constant

T total temperature

w weight flow

γ specific-heat ratio

γ_{av} average specific-heat ratio between static and total temperature at exhaust-nozzle throat

Subscripts:

a air

f fuel

[redacted]

st static ;

4 combustor outlet

5 exhaust-nozzle throat

Equation (1) is based on a choked exhaust nozzle where the Mach number M_5 is 1 and the temperatures at the combustor outlet and at the exhaust-nozzle throat are assumed to be equal. This equation is rendered more exact if the nozzle throat area is corrected by a discharge coefficient.

Exhaust total-pressure measurements are also used to determine combustion efficiency directly without calculation of exhaust temperatures by defining combustion efficiency by the relation (ref. 8)

$$\eta_b = \frac{(f/a)'}{f/a} \tag{2}$$

where

f/a fuel-air ratio

(f/a)' ideal fuel-air ratio that would produce same burner total pressure as actual fuel-air ratio

η_b combustion efficiency

The calculation of (f/a)' is based on the fact that air flows for burning and nonburning conditions are the same for an engine with a diffuser operating supercritically. Thus, total pressure at the nozzle throat for a choked exhaust nozzle is calculated by compressible-flow equations similar to equation (1). By assuming no change in total pressure and temperature between the combustor outlet and the nozzle throat, the ratio of total pressures for burning and nonburning conditions is obtained (refs. 8 and 9):

$$\frac{P_{4,b}}{P_{4,nb}} = \sqrt{\frac{T_{4,b}}{T_0}}\left(1 + \frac{w_f}{w_a}\right)\sqrt{\frac{\left[\left(\frac{\gamma+1}{2}\right)^{\frac{\gamma+1}{\gamma-1}}\left(\frac{R}{\gamma}\right)\right]_b}{\left[\left(\frac{\gamma+1}{2}\right)^{\frac{\gamma+1}{\gamma-1}}\left(\frac{R}{\gamma}\right)\right]_{nb}}} \tag{3}$$

where

P total pressure

Subscripts:

b burning

nb nonburning

0 free stream

From measured values of $P_{4,b}/P_{4,nb}$, $T_{4,b}$ is calculated; (f/a)' is computed from tables of ideal combustion temperature as a function of fuel-air ratio. Efficiencies are then calculated by means of equation (2).

Thrust-measurements method. - Combustor exhaust total temperatures are also calculated from jet-thrust measurements in wind-tunnel installations where engines are mounted on thrust balances. The exhaust-nozzle total temperature, essentially equal to combustor-exhaust total temperature, is computed by the following energy equation derived in early NACA work:

$$T_4 = T_5 = \frac{p_5 A_5 F}{gR(w_a + w_f)^2} - \frac{p_5 A_5^2 (p_5 - p_0)}{gR(w_a + w_f)^2} + \frac{F - A_5(p_5 - p_0)^2}{2gJ(c_p)_5(w_a + w_f)^2} \tag{4}$$

where

$(c_p)_5$ constant-pressure specific heat at exhaust-nozzle throat

F jet thrust

J mechanical equivalent of heat

Combustor efficiency is then calculated from the exhaust-gas temperature in the same way as described for the pressure method.

Heat-balance method. - Combustion efficiencies obtained by the pressure and thrust-measurement methods are only close approximations to true chemical combustion efficiencies if these efficiencies are defined as ratios of actual to ideal temperature rise or as ratios of fuel-air ratio (eq. (2), e.g.). An exact combustion efficiency is defined as a ratio of actual to ideal enthalpy rise. A method of obtaining this true combustion efficiency involves the use of a water quench spray at the nozzle exit. The temperature of the resulting steam-exhaust-gas mixture is measured at a station sufficiently past the spray to allow complete evaporation of the water. From enthalpy values corresponding to this measured temperature, combustion efficiency is determined by the following heat-balance equation (ref. 10):

$$\eta_b = \frac{(\Delta H_w + \Delta H_e + \Delta H_j)}{h(f/a)} \tag{5}$$

where

h lower heating value of fuel

ΔH enthalpy rise

Subscripts:

e exhaust gases

j cooling-jacket water

w quench water for exhaust gases

Equation (5) is used for fuel-air mixtures leaner than stoichiometric. For mixtures richer than stoichiometric, the enthalpy rise of exhaust gases ΔH_e is determined from

$$\Delta H_e = \Delta H_s + \left[(f/a)_{ac} - (f/a)_s\right]\left[(L_v)T_i + (c_p)_m(T_e - T_i)\right] \tag{6}$$

where

$(c_p)_m$ mean constant-pressure heat capacity of fuel

L_v latent heat of vaporization of fuel

Subscripts:

ac actual

i inlet mixture

s stoichiometric

FLAMEHOLDER AND COMBUSTION-CHAMBER GEOMETRY

General Considerations

The problem encountered in ram-jet combustors is that of initiating a stable flame in a fuel-air mixture traveling at velocities as high as 800 feet per second. This stabilization can be accomplished by placing a bluff body such as a rod or disk in the gas stream. A flame initiated in the fuel-air mixture attaches itself to the eddy region behind the bluff body, and this stabilized flame serves to ignite the oncoming fuel-air mixtures. The subject of flame stabilization by bodies within the gas stream is covered in chapters IV to VI, and this chapter is concerned only with the direct ram-jet-combustor applications of flame stabilization.

The simplest type of flameholder is a baffle placed at a single plane normal to the gas flow. Baffles may take the form of rods, disks, cones, or combinations of these. More advanced baffle designs consist of U- or V-shaped gutters with the open end facing downstream, arranged singly or in annular, radial, or grid-like planar combinations (fig. 130(a)).

Ram-jet flameholders are also designed in three-dimensional forms in which the axial dimension of the flameholder is appreciable. A gutter-type flameholder may be constructed with axial sloping gutters to form a three-dimensional flameholder (fig. 130(b)). A refined type of three-dimensional flameholder of wide use is the conical can where the flameholder consists of a conical surface perforated to allow the desired open flow area (fig. 130(c)).

Integral piloting systems are often used to assist flameholders in maintaining combustion under adverse conditions. The pilot creates the low-velocity region for stable combustion by channeling a small portion of the combustible mixture into a relatively large flow passage. Pilots are frequently combined with simple-baffle flameholders or with three-dimensional flameholders.

A number of other flameholder designs have also been investigated in ram-jet combustors. Immersed-surface types in which plates or blades have been placed downstream of a gutter flameholder directly in the flame zone have been employed successfully. Some work has been done with types that have the fuel-injection and flameholding systems combined in one unit.

The following section does not aim to select one of those general types of flameholder as being superior to the others. In general, flameholder research has aimed at perfecting each of the various types of flameholder for its own specified purposes rather than in competing one type against another.

Simple-Baffle Types

Stability limits. - Some information concerning flame stability of simple baffles is treated in chapters III and VI. In addition, recent reviews of the subject have been published (refs. 11 and 12). A theoretical analysis of the effect of flameholder dimensions and inlet-gas variables upon stability has been developed by considering the fact that blow-out occurs when the heat supply rate from the eddy region behind the flameholder is infinitesimally less than the heat required to ignite the approaching fresh gases.

If viscosity is regarded as a function of the 0.7 power of temperature, then the following equation for fuel-air-ratio stability limits may be derived (ref. 13):

$$\frac{f}{a} = \Phi\left(\frac{V_{bl}}{p_i^{0.95} D^{0.856} T_i^{1.70}}\right) \tag{7}$$

where

D diameter of disk-type flameholder normal to flow

V velocity

Φ functional notation

Subscript:

bl blow-out

In additional studies of stability limits reported in references 14 to 21, the effects of such variables as fuel type, mixture temperature, stabilizer size and type, temperature, pressure, and turbulence were investigated experimentally.

In actual engines, the most common simple-baffle flameholder system consists of gutters arranged in grids or annular-radial combinations. Some work has been done on a flameholder system as simple as a sudden expansion in cross section from diffuser to combustor (ref. 22).

The blow-out limits obtained in free-flight investigations of ram-jet engines with V-gutter grid flameholders are described in references 4 and 23. Reference 23 reports that increasing the blocked area of the flameholder by increasing the number of gutters in the grid tended to widen the stability limits. The gutters were all 3/4 inch wide; the effect of gutter width was not determined. A comparison of U- and V-gutter grids of approximately the same blocked area in another investigation (ref. 24) showed no difference in stability limits between these types of gutters.

Results of a series of investigations with V-gutters arranged in annular-radial combinations are reported in references 7, 25, and 26. The flameholders consisted of several rings of annular V-gutters of varying widths, staggered longitudinally, and interconnected by radial V-gutters or flat-plate struts similar to the configuration shown in figure 130(a). Changes in blocked area had little effect on stability limits, but the increased gutter widths improved these limits. A correlation representing a simplification of equation (7) applies to the data of these investigations (ref. 25) in the form

$$\left(\frac{f}{a}\right)_{bl} = \Phi\left(\frac{M_3}{n^{0.45}}\right) \tag{8}$$

where

$(f/a)_{bl}$ fuel-air ratio at either lean or rich blow-out

M_3 combustor-inlet Mach number based on entire cross section

n nominal gutter width

The correlation is shown in figure 131, where the velocity - gutter-width parameter is plotted against blow-out fuel-air ratio. A similar plot (ref. 17) shown in figure 132 correlates fuel-air-ratio limits with a parameter r/V_3, where r is a nominal circular-baffle flameholder radius and V_3 the combustor inlet velocity. In this case, an exponent of unity for the flameholder dimension correlates stability limits as well as the exponent of 0.45 in equation (8).

Some work has also been reported on the use of ceramic or ceramic-filled baffles rather than steel or nickel alloy types. A comparison between a steel flameholder consisting of four radial V-gutters and a similar flameholder of alundum and silicon carbide shows a much wider range of stability limits for the ceramic baffle, especially at the rich limits (refs. 27 and 28). The wider stability range with ceramic flameholders is probably due to the reduction of heat losses by conduction from the flame zone. This is in conformity with the analysis previously presented which shows that blow-out occurs when heat losses exceed the heat supply rate to the flame zone.

Combustion efficiency. - An analysis of the combustion processes must necessarily consider fuel-air preparation and inlet parameters as well as flame stabilization and oxidation. Thus in order to compare flameholders, it is essential to control the fuel-air preparation and inlet variables. The role of the flameholder is discussed in this section, with particular reference to the simple-baffle type.

Preliminary combustion-efficiency investigations were performed on a variety of flameholder configurations (e.g., ref. 29). In early NACA work, screens, solid and perforated strips, flat plates, disks, cones, and V-gutters were used as flameholders in a 20-inch-diameter ram jet. Another investigation (ref. 30) showed that V-gutters in series were very successful for high combustion efficiency. In general, the most widely used simple-baffle type of flameholder is formed of V-gutters, although ramjet engines have been designed with perforated-gutter flameholders (ref. 31), corrugated gutters (refs. 32 and 33), and the simple sudden-expansion type of flameholder (ref. 22) often with vortex blades at the entrance to the combustor (ref. 34).

The principles underlying the operation of efficient simple-baffle flameholders can be stated briefly. The stagnation region downstream of the baffle is a stable, high-temperature zone which acts as a torch for the adjacent high-velocity mixture. For stability, a wide baffle is desired, but this in turn increases the velocity of the unburned mixture past the flameholder; therefore, a compromise between efficiency and stability must be made (ref. 12). A second principle observed is that a continuous flame path connecting all of the flameholder baffles is desired. Thus, reignition can proceed if flame is locally snuffed out.

These principles are illustrated in the investigation reported in reference 35. The four gutter-grid flameholders used, shown in figure 133, are typical of he simple-baffle type. Their combustion efficiencies were about the same, with a slight advantage for the standard-gutter flameholder. In general, the configurations that gave the highest peak efficiencies had the narrowest fuel-air-ratio range of operation. This compromise of efficiency with stability limits has been noted repeatedly in combustor investigations. As noted previously, this is the case

primarily because large-width baffles for wide stability limits increase the velocity of the unburned gases and reduce efficiency. A further explanation may lie in the fact that low-pressure-drop flameholders operated at high temperature ratios favorable for high efficiency tend to amplify pressure disturbances introduced in the diffuser (ref. 36). The intensified pressure fluctuations no doubt decrease stability. Also reported in reference 35 is an investigation of an adjustable gutter-grid flameholder having a gutter angle that could be varied from 0° to 53° during operation to give a variation in the blocked frontal area from 14.2 to 59.5 percent of the combustion-chamber area. The combustion efficiency of the adjustable-gutter flameholder as a function of gutter angle is shown in figure 134, where the data show that variations in gutter angle from 25° to 50° had little effect on combustion efficiency. However, other results of the investigation showed that the stable limits of operation were improved slightly with increased gutter angle.

Gutter-grid flameholders were also used in the free-flight tests reported in reference 23. Three grids of 49, 55, and 60 percent blocked area were constructed of 3/4-inch V-gutters. The maximum combustion efficiencies obtained with the two grids of smaller blocked area were greater than those obtained with the third flameholder of 60 percent blocked area. Perhaps flame blow-out at some portions of the grid for the holder with 60 percent blocked area was responsible for these results.

The staggered annular-radial V-gutter combinations previously cited in the discussion of stability limits (refs. 7, 25, and 26) were also employed in a combustion-efficiency test program to determine the effect of flameholder geometry on performance. Figure 135 (ref. 26) indicates the effects of flameholder blocked area and gutter width upon combustion efficiency. Unlike stability, combustion efficiency is not greatly influenced by gutter width, and the gains afforded by increased area blockage are very slight.

Piloting Systems

A pilot is a portion of the combustor in which a reduced air velocity is maintained by expanding part of the air stream. This low-velocity region provides a stable burning zone from which flame may be propagated to the rest of the combustor. Theories of flame propagation from a low-velocity region to a high-velocity region are discussed in chapters III, IV, and V. A typical pilot configuration is shown in figure 136. Since the pilot contains a low-velocity region, the design principles are different from those used for the main combustor. In the pilot a large pressure-loss coefficient may be tolerated and heat release per unit volume is small. Fuel-air ratios can be maintained at fixed optimum values and special fuels may be used.

Pilot heat release. - A program was conducted (ref. 37) to determine whether the heat release of a pilot or the production of active particles controls flame propagation from the pilot. Experiments were performed in a 2-inch-diameter burner with a pilot zone supplied with hydrogen and oxygen. The burner itself was run under fixed conditions of pentane flow, air velocity, temperature, and pressure. Specific impulse increased almost linearly as the heat release from the pilot was raised by increasing the flow of stoichiometric hydrogen-oxygen mixture. When more hydrogen was added, with the same oxygen flow, the heat release was kept constant while the production of hydrogen atoms dropped more than a hundredfold; nevertheless, the specific impulse remained nearly constant. Reference 37 takes this to be a negative type of evidence in favor of the importance of pilot heat release, as opposed to the production of actual particles in the pilot flame. However, it is by no means conclusive evidence, because the effects of the temperature of the pilot exhaust gas were not considered.

Design and use of pilots. - The physical size of a piloting zone is an important factor in the design of combustors. It has been found experimentally that a circular pilot cross section is better than a rectangular one (ref. 38), and that a length equal to a diameter is adequate before pilot recirculation air is admitted (ref. 39). Reference 40 states that the sum of the diameters of the first row of recirculation air holes should equal 40 percent of the pilot circumference.

A one-dimensional aerodynamic analysis of the required size of a pilot combustor is shown for one set of initial conditions in reference 41. A more extensive treatment of optimum pilot size is given in reference 42. In this report, an ideal piloting system is considered in which all the combustion takes place in a low-velocity stoichiometric pilot zone. Secondary air is mixed with the exhaust products downstream of the pilot combustor to give the desired over-all fuel-air ratio. The study shows that it is possible to maintain a large pilot area for efficient low-velocity combustion without incurring excessive total-pressure losses.

Percent pilot is defined as the percent of total fuel sent to the pilot zone. This percentage may vary from 0 to 100, the latter value corresponding to the idealized pilot of reference 42. An example of an experimental investigation of a ram-jet combustor operated at varying percent pilot is found in reference 43, where percent pilot ranged from 12 to 100 percent. In some cases, where low-drag flameholders are employed (refs. 9 and 44), piloting of 1 percent or less is sufficient for large gains in stability limits. Figure 137 illustrates the increase in efficiency with small percent pilot for a single V-gutter flameholder described in reference 45.

Pilot operation is not required where inlet conditions are very favorable for combustion and over-all fuel-air ratios near stoichiometric are employed. In the investigation of reference 26, for lean over-all fuel-air ratios, where the fuel was concentrated locally, pilot operation was beneficial, but at rich fuel-air ratios where uniform fuel distribution was required, pilot operation was of little help.

Piloted flameholders. - Integral piloting systems have been combined with such well-known simple-baffle systems as V-gutter grids (ref. 46), radial gutters (ref. 47), annular-radial gutter combinations (ref. 48), and staggered annular-radial gutter combinations (refs. 8, 26, and 49). In general, the effects of flameholder geometry on combustion performance of the piloted flameholders were not different from those of nonpiloted flameholders. Reference 47, for example, reports no appreciable effect of varied area blockage on combustion efficiency. Comparisons between otherwise similar piloted and nonpiloted configurations are given in references 26, 44, and 49. The piloted designs offered no improvement in peak combustion efficiency, but they did tend to widen the fuel-air-ratio range of operation. A comparison is made in reference 50 of three types of piloted configurations intended for use in a ram-jet combustor at low pressures and rich fuel-air ratios. The configurations consisted of a can that acted as a 100-percent pilot and two gutter combinations, one with five can-type pilots (fig. 138) and the other with a sloping-gutter pilot. The third type was the most satisfactory design. This configuration (also described in ref. 51) consisted of a perforated conical flow divider enclosing a sloping V-gutter basket (fig. 139). The sloping V-gutter and flow divider served first to confine the mainstream fuel to a portion of the air and then to promote good mixing of the pilot combustion products with the mainstream combustibles. Another example of this type of design is given in reference 52.

Three-Dimensional Flameholders

Three-dimensional baffle. - In contrast to the planar, simple-baffle flameholder, the three-dimensional baffle has appreciable axial depth. The advantage of

this design is that the volume of the primary zone can be large, and a means for controlling the introduction of dilution air is provided. The pilot configurations of references 50 and 51 (fig. 139) are an approach to the three-dimensional type.

Flameholder designs have been evolved (refs. 43 and 53) in which the radial gutters slope at a comparatively small angle to the combustor axis and provide a conical flame-holding surface. The sloping-baffle configuration investigated in a 16-inch connected-pipe facility described in reference 53 consisted of two sets of U-shaped baffles separated by a conical section (fig. 130(b)). The 6 baffles in the primary zone and the 12 baffles in the secondary zone were inclined at 30° angles to the combustor axis. The fuel-mixing control sleeve, which extended from the fuel injectors to the flameholder, intercepted approximately 20 percent of the total engine air mass flow and ducted this air into the primary combustion zone. Combustion originated in the wake of the upstream set of baffles and was substantially complete in the sheltered region downstream of these baffles. The use of a sloping baffle and conical shielded zone provided an expanding volume for the combustion region, thereby maintaining a low flow velocity which permitted combustion to be completed in a relatively short length. 3105

The combustion performance of this configuration as a function of fuel-air ratio is compared in figure 140 with that of a baffle-pilot configuration investigated in the same facility and at the same test conditions. The advantage of providing fuel-air mixing control downstream of the point of initiation of combustion is an increase in combustion efficiency at low fuel-air ratios.

Another type of three-dimensional flameholder is the rake type, which consists of a pilot body with petal-like fins extending downstream and radially from the pilot (fig. 141). Usually several of these flameholder combinations are positioned at an axial station in the combustor. Multiple-rake flameholders were used in free-flight investigations reported in references 5 and 54 to 57, where these configurations were found to be superior to piloted gutter flameholders in stability limits and efficiency. Another comparison of a rake-type flameholder with a piloted serrated baffle flameholder also showed improved results with the former type (ref. 58). Further gains would have been possible with improved fuel injection systems. An investigation of more complex rake designs (ref. 59) showed that best performance was obtained with a rake-type flameholder which had alternate rakes connected to the pilot burner outlet by V-gutters. The three rakes that were connected in this manner appeared to be more effective as flameholders than the other three rakes because of the continuous flame path from pilot to baffle.

Can flameholder. - The principle of an expanding combustion zone is inherent in the design of a conical can-type flameholder. Can combustors fall into two general types of designs: simple cans and annular cans. A typical simple can is shown in figure 142(a). The flameholder consists of a continuous or segmented conical surface, expanding in a downstream direction with a pilot assembly usually situated at the upstream end of the cone. An annular can (ref. 60), shown in figure 142(b), consists of two conical cans, the vertex of inner can facing downstream, and the vertex of the outer can facing upstream. Can flameholders may differ in cone angle, distribution of holes and hole sizes, arrangement of holes, and shape of holes. Cans are usually specified in terms of open area and pitch alinement. Open area is the ratio of the area of the perforations to the cross-sectional area of the combustion chamber; the pitch alinement is the number of rows of perforations that spiral around the conical surface counted along the intersection of an axial plane on the surface.

The effect of cone angle on combustion performance has not been systematically investigated in the literature, the standard half angles being from 5° to 15°. However, the effect of pitch alinement on combustion efficiency and stability limits

has been investigated (ref. 61). A slight improvement in efficiency was found through the use of a two-pitch-alinement can rather than a zero-pitch-alinement can, but stability limits were unaffected by the alinement.

In an investigation of can combustors intended mainly for piloting applications (ref. 38), stability limits were unaffected by hole size, total open area, or pitch alinement. Reference 41, on the other hand, reports that for a single-rowed can flameholder, increasing hole size increases the rich limits but does not affect the lean limits.

3105

The effect of open area and hole type on combustor performance is described in reference 62 for a 10-inch-diameter quarter-segment combustor in a free-jet installation. Figure 143 compares the combustion efficiency of four can configurations, three having open areas of 100, 145, and 177 percent with round holes the same size in each case, and one having an open area of 100 percent with transverse rectangular slotted holes. The flameholder with 100 percent open area yielded a maximum efficiency of 94 percent, a value slightly higher than the maximum combustion efficiency obtained with the cans of greater open area. The transverse-slotted can exhibited a maximum efficiency close to that of the corresponding round-hole can, but efficiencies at low fuel-air ratios were much less for the slotted can, probably because the increased frontal area of the slots admitted too much air to the primary portion of the can.

Immersed-Surface Flameholders

The use of surfaces in the flame zone of a combustor stems from the observed catalytic effects of certain materials in the ignition of quiescent combustibles. The employment of similar materials in a high-velocity combustor was a logical extension of this principle. In addition to the thermal effect, a beneficial increase in mixing rate was envisioned. Some of the effects of immersed surfaces on combustion efficiency and stability are described in the following paragraphs.

A systematic program of investigations of immersed surface combustors was conducted and is reported in references 10, 44, 63, and 64. In reference 63, the flameholder employed was a wedge-shaped block of graphite that had been spray-coated with aluminum. Two such wedges placed parallel across the cross section of the combustor represented a conventional type flameholder. Additional rows of similar wedges were introduced downstream of the original row to evaluate the effect of surfaces immersed in the flame zone. The flameholder configurations used in this program are shown schematically in figure 144. The effect of the immersed surfaces on pressure loss and combustion efficiency was slight, but the additional surfaces did widen the combustion stability limits.

In reference 64, Inconel surfaces were employed because carbon blocks have inadequate shock resistance. The results indicated that, within the requirements of providing a low-velocity path for flame propagation, the number of surfaces and their geometry were unimportant. A conventional V-gutter configuration is compared in reference 10 with another in which 12 Inconel blades were positioned in the flame zone. Variation of the immersed-surface temperatures confirmed that the performance gains were due to aerodynamic rather than thermal influences. Both stability limits and combustion efficiency were improved by the immersed surfaces. The combustion-efficiency effect is illustrated in figure 145, where efficiency is plotted against equivalence ratio. The difference between efficiency of cooled and uncooled blades is small in comparison with the difference between efficiencies of the configurations with and without immersed surfaces.

A systematic investigation of simplified immersed-surface configurations in reference 44 concluded that the greatest gains in combustion efficiency could be effected by the use of a single blade in the flame zone close to the flameholder. Optimum efficiency results were obtained with a blade across the combustor perpendicular to and 4 inches downstream of the single V-gutter flameholder (figs. 146 and 147). Apparently the flame-immersed blade is best positioned close to the flameholder, but not close enough to disturb the normal wake region behind the flameholder (less than 4 in. in this case). At a slight compromise in efficiency and pressure drop, a considerable improvement in stability limits was obtained by combining this single perpendicular blade with three parallel blades farther downstream. A further widening of stability limits was possible by removal of all of the flame-immersed surfaces.

In studies described in reference 65, the effect on combustion of a grill of heated, coated molybdenum strips submerged in the combustion zone of a 6-inch-diameter combustor was determined. The anticipated acceleration of combustion was not realized because the strips did not act as surface combustion aids, but instead conducted heat from the flame zone to the combustor walls.

The advisability of employing immersed surfaces in the combustion zone appears controversial, even though the aerodynamic influence of these surfaces was shown to be important (ref. 10). Mixing can possibly be controlled in a simpler manner, for example, by proper spacing and sizing of holes in a can-type flameholder. However, these tests very dramatically emphasized the fact that the rate of mixing of unburned and burned gases can be the controlling step in the combustion process.

IGNITION

The basic principles of ignition discussed in chapter III apply to ram-jet combustors. The techniques generally used in starting ram-jet combustors incorporate either pyrotechnic flares or spark plugs located within the pilot zone. The spark system is more desirable for ground tests since repeated starts can be obtained. However, under certain operating conditions, chronic failures of the spark system have been experienced, and ignition with a hypergolic fuel such as aluminum borohydride is advantageous. Flight-test data reported in reference 4 show that up to pressure altitudes of 14,000 feet spark systems are satisfactory, but above that altitude flare systems are necessary. However, in recent tests with a 48-inch ram jet (ref. 66), reliable spark ignition was obtained at 1/8 atmospheric pressure. A further aid to spark ignition at low pressure is the addition of small amounts of hydrogen in the region of the spark (ref. 12). A magnesium-flare ignition system that has proved to be very satisfactory is described in reference 6. Additional ease in starting flight models is afforded by the use of magnesium flares in conjunction with rake-type flameholders (refs. 6 and 67).

FUELS AND FUEL SYSTEMS

Combustion proceeds most favorably in a near stoichiometric fuel-air mixture, where flame speed and temperature are at a maximum. Thus, the principles underlying the design of a fuel system are the achievement of a near stoichiometric mixture and complete vaporization of fuel in the precombustion zone.

Fuel Injection

Fuel-injection types. - In ram-jet combustors, the energy of the high-velocity air stream is used to atomize the fuel, thus allowing simple fuel-injector designs

and low fuel pressures to be used. Air-blast atomization is discussed in chapter I, where it is shown that drop size can be predicted from certain fuel properties and the relative air and fuel velocities and volumes by the following equation:

$$d_{32} = \frac{585\sqrt{\sigma_f}}{U_r\sqrt{\rho_f}} + 597\left(\frac{\mu_f}{\sqrt{\sigma_f\rho_f}}\right)^{0.45}\left(1000\,\frac{Q_f}{Q_a}\right)^{1.5} \qquad (9)$$

where

d_{32} Sauter mean diameter, microns

Q_f/Q_a fuel-air volume ratio

U_r relative air-fuel velocity, meters/sec

μ viscosity, poises

σ surface tension, dynes/cm

ρ density

Subscripts:

a air

f fuel

For a typical ram-jet combustor-inlet velocity of 300 feet per second and with JP-4 fuel, the drop-size calculation can be approximated by $d_{32} = \frac{585\sqrt{\sigma_f}}{U_r\sqrt{\rho_f}}$, since Q_f/Q_a is small. The value of d_{32} at this condition is about 35 microns. This drop-size diameter is roughly one-third that predicted for a 17.5-gallon-per-hour Monarch spray nozzle in still air by the following equation from chapter I:

$$d_{32} = 251\Delta P^{-0.17} \text{ microns} \qquad (10)$$

where

ΔP pressure drop across nozzle

For a pressure differential of 100 pounds per square inch, d_{32} is 115 microns.

These drop-size estimates show that the air flow past the fuel injector provides remarkably good atomization and that further mechanical improvements are unnecessary. Thus it is not surprising that injector types of a wide variety have proved satisfactory. At low fuel-air ratios it is reported (ref. 41) that simple fixed-orifice nozzles give the highest efficiencies because less dilution of the fuel-air mixture occurs. However, fewer injection points are required with the Monarch nozzle because the radial component of the fuel-droplet velocity distributes the fuel over a greater area than the simple-orifice type. At higher fuel-air ratios, air-atomizing types of nozzles provide a more homogeneous mixture and are more satisfactory. Variable-area spring-loaded nozzles appear promising for ram-jet applications, but difficulty has been encountered in providing equal flow through each nozzle in multinozzle installations.

A program was conducted (ref. 68) to determine the effect of nozzle size in a configuration of six fixed-area nozzles evenly spaced at an axial station. The results showed that there is an optimum size of nozzle for maximum efficiency. With overly large nozzles, distribution is poor; similarly, with undersized nozzles, fuel pressure is so high that fuel particles strike and flow along the chamber wall and do not mix with air properly, decreasing efficiency.

Other methods of fuel injection include impinging jets and spray bars. Excellent efficiencies are reported (refs. 69 and 70) for fuel-injection systems consisting of multiple impinging jets of compressed air and fuel. Spray bars, usually perforated tubes, are also widely used since they have the advantage of low area blockage.

3105

Location and direction of fuel sprays. - The location and direction of fuel sprays are determined by the combustor-inlet conditions and the type of fuel injector. Since it is desired that a vaporized, locally stoichiometric mixture be produced at the flameholder, the direction of fuel spray is of some importance, particularly for fuel injectors just upstream of the flameholder. Injection of fuel in a contrastream direction allows a greater path of travel of the fuel droplets and produces a more homogeneous mixture than injection in the costream direction. Thus reference 51 reports excellent combustion efficiencies at rich fuel-air ratios by contrastream injection, but recommends costream or cross-stream injection, which produce a more concentrated fuel mixture, at lean fuel-air ratios.

The significance of fuel-injector location is best illustrated by some examples from reference 71. Combinations of upstream fuel injection, flameholder injection, and split injection between the two positions were employed, as shown in figure 148. The combustion efficiencies of the four injector configurations are shown in figure 149 as a function of fuel-air ratio. The broadest range of operation was obtained with flameholder injection, where operation was possible from fuel-air ratios of 0.012 to 0.047. The upstream-injection case gave only a narrow range of operation near stoichiometric fuel-air ratio and peak efficiencies of less than 80 percent. This range was broadened by the use of split injection, and the peak efficiency increased slightly by the use of flameholder split injection. Thus the results indicate that upstream or split injection, which gives a nearly homogeneous mixture, produces the best performance at rich fuel-air ratios, and localized flameholder injection produces the best performance at lean fuel-air ratios.

These findings have been widely confirmed. Results from reference 72 plotted in figure 150(a) show that for a can-type combustor peak efficiencies at low fuel-air ratios are obtained with internal (flameholder) injection; peak efficiencies at high fuel-air ratios are obtained with upstream injection. For operation over a wide range of fuel-air ratios, a combination of internal and upstream operation was most satisfactory.

The principle of fuel-mixture stratification to obtain efficient combustion at lean fuel-air ratios also applies to the radial positioning of the fuel injector. Figure 150(b) (ref. 72) shows that for upstream fuel injection, efficiency is better at low fuel-air ratios for injector positions near the centerbody but the reverse is true at high fuel-air ratios. Figure 151(a) shows the effect of injector-ring diameter on combustion efficiency (ref. 73). The fuel-air ratio for peak efficiency increases with increasing fuel-ring diameter as seen in the cross plot (fig. 151(b)). The solid line in figure 151(a) illustrates the fact that injector rings of two different diameters may be combined to broaden the range of operation.

Staged fuel injection. - For operation over a wide range of fuel-air ratio, the principle of fuel-injection staging is used. A set of injectors, denoted as primary fuel injectors, supply fuel for low-fuel-air-ratio operation. For operation at richer fuel-air ratios, additional fuel is injected through secondary sets of injectors, which are positioned for the most efficient combustion.

The performance of a combustor operated with careful proportioning of primary and secondary fuel flows is shown in figure 152 (ref. 72). High efficiencies were achieved by operating with primary fuel up to fuel-air ratios of 0.034 and then by maintaining the primary fuel-air ratio constant at 0.014 and increasing the secondary fuel flow. A mixture control sleeve of the type described in the following section separated the primary and secondary fuel-air mixtures.

Such combinations of primary and secondary fuel injection are very common in all types of ram-jet combustors. A three-stage fuel-injection system for a can flameholder is described in reference 62, one stage located at the can entrance and the other two downstream of the first stage. Best results were obtained when the first stage was used for very lean fuel-air ratios, the first and second stages for ratios up to 0.045, and all three stages for ratios above 0.045. It is important to reduce the primary fuel flow to a low value at rich fuel-air ratios, as is illustrated in figure 152 and further shown in a plot from reference 73 (fig. 153), where the rich limits of combustion narrow as primary fuel flow is increased from 18 to 34 percent of the total fuel flow.

Mixture control sleeves. - Good combustion efficiency at lean fuel-air ratios can be obtained with upstream injection as well as with flameholder injection if excessive mixture dilution upstream of the flameholder is prevented by a control sleeve. The combustor configurations shown in figures 130(b) and (c) and 152 illustrate the placement of such a control sleeve. Although primary and secondary fuel injection are from the same axial station upstream of the flameholder, the primary fuel-air mixture within the control sleeve is channeled directly to the upstream portion of flameholder where it maintains a rich concentration. The control sleeve produces the same effect as does the near-stoichiometric pilot zone of reference 42, described in the section on piloting.

An early type of mixture control sleeve is described in reference 74, but the device had not been fully exploited until recently (refs. 1, 9, 34, 43, 53, 75, and 76). An increase in combustion efficiency from 30 to 75 percent at a fuel-air ratio of 0.025 with no increase in combustor pressure loss is reported in reference 75. The advantages of a sleeve system are reviewed in reference 34. Besides the improvement of combustion efficiency at low fuel-air ratios provided by rich local mixtures, the control sleeve produces more consistent fuel distribution and sharp-edged fuel-air profiles and allows the use of simple fuel orifices rather than atomizing nozzles.

Effect of Fuel Variables

Fuel type. - The effect of fuel type on combustion performance in a ram jet would depend on the controlling step in the combustion process. The combustion process may be considered as successive steps of fuel vaporization, mixing, and chemical oxidation. If the vaporization step were controlling, then the physical properties of the fuel would be of great importance; if oxidation were controlling, the chemical properties would determine the performance of the fuel. Small-scale tests of efficiencies of several fuels bear out these hypotheses. (Fundamental combustion properties are discussed in chapters I to VI.) Investigations of gaseous fuel-air mixtures (ref. 45) where fuel volatility is eliminated as a factor show that fuels of low ignition energy, or short ignition lags, such as hydrogen, acetylene, carbon disulfide, or propylene oxide, produce the best efficiencies.

Although large-scale engine tests cannot be as easily analyzed, the same conclusion may be reached regarding the effect of fuel properties. In reference 77, the use of gasoline rather than JP-3 fuels increased combustion efficiency 10 percent at an inlet-air temperature of 920° R. These results indicate that a 53-inch length for a 20-inch-diameter combustor was insufficient for complete vaporization of the less-volatile fuels. Similarly, in other investigations where low inlet temperatures and short combustor lengths caused the vaporization of liquid fuels to govern the over-all combustion efficiency, gasoline was superior to the less-volatile kerosene (refs. 32 and 45). Other studies have found n-heptane to be superior to the less-volatile Diesel oil (refs. 26 and 78) and propylene oxide superior to kerosene (refs. 3, 32, 58, 59, 79, and 80), but this effect with the latter pair of fuels may be attributed to flame speed as well as to increased volatility.

Where nearly complete vaporization is ensured, fuels that differ from one another mainly in volatility give nearly the same performance in ram-jet combustors. Reference 81 reports little difference in combustion efficiencies between 80-octane gasoline, JP-3 fuel, and special low-vapor-pressure fuels. Similarly, almost identical results with gasoline and JP-4 fuel were found in the work of reference 82, and samples taken in this investigation at an inlet-air temperature of 1060° R confirmed that vaporization was substantially complete in 17 inches of mixing length.

In ram-jet combustors where vaporization does not control the over-all efficiency, appreciable gains in efficiency result from the use of high-flame-speed fuels. For premixed and prevaporized fuel mixtures, reference 83 states that combustion efficiency increases with the 1.1 power of flame speed.

Octane rating of gasoline-type fuels is of little consequence in ram-jet combustors. Reference 84 shows that 62-octane gasoline performed as well as 100-octane gasoline.

Fuel preheating. - For combustor operating conditions where fuel vaporization is an important factor, increased preheating of fuel aids combustion efficiency. Reference 85 reports a 10-percent increase in combustion efficiency with preheating of 62-octane gasoline from 40° to 200° F. In combustors where vaporization of the fuel is complete for cold injection, such as the combustor discussed in reference 82, preheating the fuel is of no consequence.

OPERATING VARIABLES

Pressure

Effect on combustion efficiency. - Because pressure affects all of the fundamental processes in the combustor, finding occasional contradictory results from pressure investigations is not too surprising. Evaporation of liquid fuels is retarded by increased combustor pressures (ch. I), whereas this pressure increase aids the oxidation reaction (ch. III). Thus, in general, at low and moderate pressures where fuel vaporization is rapid, efficiency increases with pressure. Conversely, where vaporization is the controlling step, as at high pressures or with low-volatility fuels, efficiency may remain independent of pressure or even decrease slightly with pressure.

Results for a 2-inch-diameter gaseous-propane - air burner (fig. 154) show a continuous increase in combustion efficiency with pressure increases from 5 to 85 inches of mercury absolute (ref. 45). Similar plots of combustion efficiency as a function of inlet pressure have been established from larger-scale tests of combustors with simple-baffle flameholders (ref. 86), rake-type flameholders (ref. 55)

and can flameholders (ref. 87) over pressure ranges as great as from 8 to 85 inches of mercury absolute. The more usual findings, however, are that efficiency increases with pressure up to a certain value and then remains independent of pressure. Figure 155 illustrates this trend from results given in reference 77, where at a fuel-air ratio of 0.06, combustion efficiency increases with pressures from 7 to 55 inches of mercury absolute and remains constant at higher pressures.

In combustors where fuel vaporization is more critical, the pressure effects shown in figures 154 and 155 may not apply. In reference 60, for example, data are presented for can combustors where efficiency increases with pressure only up to a pressure of 20 inches of mercury absolute, above which efficiency decreases slightly. References 3 and 71 state that efficiency was virtually independent of pressure at pressures as low as 17 to 28 inches of mercury absolute. That these results are due to an increased importance of fuel vaporization is confirmed by the work of reference 88, where over a pressure range of 30 to 65 inches of mercury absolute, combustion efficiency decreased with pressure when radial simple-orifice fuel injectors were used and increased with pressure when hollow-cone spray nozzles were used. The spray nozzles had better vaporization characteristics than the fixed-orifice injectors.

Effect on stability limits. - Increased inlet pressure usually tends to widen both the lean and rich limits of combustion, especially at very low pressures (refs. 55, 56, 73, 77, and 86). As in the case of combustion efficiency, where fuel vaporization is a critical factor, pressure may have an adverse effect upon limits. In figure 156, the effect of pressure on stability limits is shown for three inlet temperatures (ref. 73). At the two higher temperatures, the expected widening of the limits with increased pressures is seen; but at 810° R, where vaporization may control, the limits are independent of pressure above 18 inches of mercury absolute. A fundamental treatment of the effect of pressure on flame stabilization is given in chapter VI.

Temperature

Effect on combustion efficiency. - The two important combustion steps of vaporization and oxidation are both accelerated by increased temperatures (chs. I and III); hence, combustion efficiency would be improved appreciably by increased inlet temperatures. This effect of temperature has been confirmed by many combustion studies, although the results of some of these reports are of doubtful significance because of lack of control of other variables, principally pressure. Investigations where inlet temperature was the only variable have shown that combustion efficiency increases almost linearly with increasing inlet temperature (e.g., refs. 34, 59, 62, 77, 78, and 88). Since the temperature contribution to combustion efficiency is not the result of two competing effects, efficiencies increase asymptotically with temperature to limiting values of 100 percent. Studies of ram-jet combustors are presented in which increased inlet temperature improved combustion efficiency greatly under conditions of low inlet pressure (ref. 60) and off-stoichiometric fuel-air ratios (ref. 76). However, at atmospheric pressure and near-stoichiometric fuel-air ratios, where efficiencies were normally near 100 percent, increasing inlet temperatures could not improve combustion efficiency.

Effect on stability limits. - The stability curves for three inlet temperatures shown in figure 156 indicate that increased inlet temperatures widen stability limits, especially the rich limits. These findings of the effect of temperature on stability limits are in agreement with those of other investigations (refs. 27, 78, 81, 89, and 90). A discussion of the effect of temperature on stability is also given in chapter VI.

Velocity

Effect on combustion efficiency. - Increased inlet velocity improves fuel atomization (ch. I); but, for a given chamber length, increased velocities allow shorter reaction times for the evaporation and oxidation steps in the combustor. Thus, as with inlet pressure, competing contributions to combustion efficiency are influenced by inlet velocity. Experimental information has been presented wherein combustion efficiencies may increase up to maximum and then decrease with increasing velocity (ref. 61), decrease with increasing velocity (refs. 78 and 88), or be unaffected by velocity changes (ref. 3). These contradictory findings are apparently due to different relative importances of the atomization, vaporization, and oxidation steps in the combustor. This has been borne out by the work of reference 71, where combustion efficiency reached a maximum with velocity for upstream or split fuel injection runs and decreased with increasing velocity for flameholder fuel injection. The most usual findings, however, are that combustion efficiency decreases with increasing air velocity.

Effect on stability limits. - Increased velocity has been found to both widen (ref. 74) and narrow (refs. 4 and 78) lean limits. With a homogeneous fuel-air mixture, increased velocity would normally result in poorer lean limits of combustion. However, under certain conditions of stratified fuel-air-mixture distribution, the increased mixing rates associated with increased velocity would tend to improve the local combustible concentration. The only available literature on rich limits (ref. 73) shows that the limits are decreased by increased inlet velocities.

Angle of Attack

Angle-of-attack operation distorts the velocity profile at the combustor, and therefore would be expected to be detrimental to combustion efficiency. Investigations of 16-inch can-type combustors at several angles of attack (refs. 91 and 92) showed that efficiency decreased about 10 percent with an increase in angle of attack from 0° to 10°, but stability limits were unaffected.

Correlations of Operating Variables

It is obvious from the experimental literature that the same change in an inlet variable may affect combustor performance in opposite directions, depending on which step in the over-all process predominates. Semitheoretical correlations must of necessity assume a controlling step in the combustor. Most combustor investigations are conducted under conditions to which an oxidation-controlled mechanism would be most closely analogous. For this particular case, the usual correlation of combustion efficiency takes the form

$$\eta_b = \Phi\left(\frac{pTl\,\frac{f}{a}}{V}\right) \tag{11}$$

where

l combustion length

as proposed in reference 14. A function of this type was successful (ref. 93) in correlating the performance of turbojet combustors under conditions of constant combustor length and limited fuel-air-ratio ranges. With these limitations, the simplified parameter pT/V will suffice for correlation.

[redacted]

A correlation similar to the preceding was derived for application to ram-jet combustors (ref. 94). The theoretical basis for the correlation was the assumption that the mixing of burned and unburned gases and their movement through the flame front controlled the over-all combustion rate. Thus, combustion efficiency was defined as the ratio of the mass flow of gases through the flame front to the over-all mass flow of unburned gases through the combustor

$$\eta_b = \frac{\rho_u A_{ff} u}{\rho_u A_c V} \tag{12}$$

where

u fundamental flame speed

Subscripts:

c combustor cross section

ff flame front

u unburned gases

Flame-front area and flame speed were evaluated in terms of inlet variables to give a function of inlet pressure, temperature, and velocity. Empirical data from runs with a 5-inch ram-jet combustor with V-gutter flameholders could be correlated by the expression

$$\eta_b = \Phi\left(\frac{p^{0.3}\,T}{V^{0.8}}\right) \tag{13}$$

This expression could be applied to data of many different fuels by multiplying the correlation parameter by the term $(u_f/u_{ref})^{1.1}$, where u_f is the flame speed of the fuel employed and u_{ref} is the flame speed of a reference fuel (ref. 83). The reference fuel used in references 83 and 94 was gasoline with a flame speed of 1.4 feet per second. The correlation is shown in figure 157, where combustion efficiency is plotted against the correlating parameter. Reasonable agreement between the results with different fuels is shown with the exception of carbon disulfide, a compound with a very low ignition energy. A linear relation between combustion efficiency and the correlation parameter is exhibited up to efficiencies of 80 percent, above which the effect of the parameter on efficiency is slight. At high values of the inlet variable parameter, therefore, combustion efficiency would be high and would be unaffected by moderate changes in inlet variables. This conclusion has also been shown in tests in a 16-inch combustor reported in reference 76.

SUMMARY OF RAM-JET COMBUSTION PRINCIPLES

Ram-jet combustion work has been conducted mainly along experimental lines. Because the field is comparatively new, considerable effort was expended in exploratory programs, and only a few of the many variables affecting ram-jet combustor performance have been investigated systematically. Some of the ram-jet design principles which have been evolved are briefly reviewed in the following discussion.

Flameholder Geometry

The single-plane, simple-baffle flameholder can be applied satisfactorily at favorable inlet-air conditions and at rich fuel-air ratios. Its simplicity, low weight and drag, and structural reliability are very desirable. However, at less-favorable inlet conditions (particularly at inlet pressures below one-half atmosphere and at lean fuel-air ratios), the three-dimensional flameholder, as exemplified by the can type, has more desirable performance characteristics. The most satisfactory simple-baffle shape was a V-gutter arranged to form an annular-, radial-, or grid-type flameholder. Combustion performance is insensitive, within certain limits, to variations in baffle width, spacing, angle, and area blockage. Baffle widths of 1 to 2 inches and angles from 30° to 60° have been most generally used.

The three-dimensional flameholder type most widely investigated is the conical can. It is believed that the superior performance of this type at lean fuel-air ratios and at low pressures is due to fuel-air mixing control downstream of the point of initiation of combustion, which is absent in the simple-baffle flameholder. Within the range investigated for the can flameholder, geometric variables of hole number, size, shape, pitch, and open area do not influence combustion efficiency appreciably, and most of the geometric investigations were directed toward reduction of flameholder pressure loss. The flameholders investigated had open areas ranging from 75 to 175 percent.

The sloping-baffle flameholder, a combination of the simple-baffle and the can-type flameholders, appears to have the desirable performance characteristics of the can type. However, the many variables involved in this design have not as yet been investigated.

In reference 95 a comparison is made of five configurations tested in the same 20-inch ram-jet engine. From these tests of can, sloping-baffle, annular-piloted, and piloted V-gutter flameholder designs, it was found that all types gave combustion efficiencies of 80 to 90 percent. A comparison on the basis of specific impulse, where the effect of friction loss is included, showed the same high level of performance for all designs.

Piloting

The use of a large-size pilot in conjunction with either the simple-baffle or the can flameholder is a desirable design principle for improved combustion performance, particularly at lean-fuel-air-ratio conditions. It has been shown analytically and experimentally that a shielded, low-velocity pilot zone can occupy a relatively large percentage of the combustor area without causing or producing excessive pressure losses (ref. 42).

Both high combustion efficiency and wide stability limits are desired in pilots; but it has been found experimentally that a pilot which has wide stability limits usually has poor combustion efficiency. The importance of pilot burning efficiency on over-all combustion performance has not been definitely established, except to the extent that, where the pilot heat release represents a large portion of the total heat release, the pilot combustion efficiency should be high. A circular pilot cross section gave better efficiency than a rectangular cross section, and a pilot length equal to its diameter was adequate. Pilot performance was insensitive to hole size, number, and spacing within the limits investigated. For large-size combustors, an annular-shaped pilot is believed to have an advantage over the centerbody pilot, since for a given pilot cross-sectional area, the radial distance from pilot to outer wall can be reduced.

Fuel Injection

Location of injectors. - The location of the fuel injector with respect to the flameholder is one of the most significant variables influencing ram-jet combustor performance. In general, for efficient combustion at lean fuel-air ratios it is desirable to stratify the fuel-air mixture, thereby producing a locally stoichiometric region. For near-stoichiometric operation, a homogeneous mixture gives best results. Information on mixture distribution downstream of fuel injectors is given in chapter I. A stratified mixture can be obtained with some degree of effectiveness by radial and axial location of the fuel injector so that the fuel mixes with only a portion of the combustion air. A more effective technique for obtaining stratification is mechanical control of fuel-air mixing by means of a mixing control sleeve (refs. 1 and 75).

5105

For efficient combustion at lean as well as rich operation, the use of dual fuel-injection systems is necessary. For best combustion efficiency, the primary injector supplies the fuel at lean fuel-air ratios, and both primary and secondary injectors are used for rich mixtures. At increasingly rich operation, a smaller fraction of the fuel is supplied by the primary and the remainder by the secondary injector.

Locating the fuel injector upstream of the flameholder is a generally accepted practice. However, care must be exercised to prevent flame from seating upstream of the flameholder, especially with the can-type flameholder. It is possible to inject the fuel within the flameholder, and combustion efficiency, though not impaired at lean fuel-air ratios by this method of injection, is poor at rich conditions.

Types of injectors. - Simple-orifice, solid, and hollow-cone sprays have been used with equal success. The spray bar with multiple orifices provides a large number of injection points with little area blockage; this is desirable for rich operation. However, spray nozzles do not plug as easily, and changes in nozzle tip size can be readily made. Variable-area fuel nozzles also seem suited for ram-jet application.

Fuel Type

The majority of the investigators have concluded that for inlet-air temperatures corresponding to flight Mach numbers of 2.0 or greater, combustion is satisfactory with either gasoline or JP fuels. High-volatility and high-flame-speed fuels such as propylene oxide show some gains at severe operating conditions such as at low inlet-air temperatures or with short combustor lengths.

Inlet-Air Conditions

The combustion efficiency of ram-jet combustors follows well known trends with inlet-air conditions. Efficiency under usual conditions increases with pressure and temperature and decreases with velocity. These effects have been correlated for an idealized combustor in which the vaporization and mixing steps have been eliminated as possible rate-controlling mechanisms (ref. 94). For these reasons, and because the effects of other variables such as combustor length and operating fuel-air ratio have not been definitely established, these correlations can be applied specifically only in certain cases.

[redacted]

REFERENCES

1. Cervenka, A. J., and Dangle, E. E.: Effect of Fuel-Air Distribution on Performand of a 16-Inch Ram-Jet Engine. NACA RM E52D08, 1952.

2. Wentworth, Carl B., Hurrell, Herbert G., and Nakanishi, Shigeo: Evaluation of Operating Characteristics of a Supersonic Free-Jet Facility for Full-Scale Ram-Jet Investigations. NACA RM E52I08, 1952.

3. Sterbentz, W. H., and Nussdorfer, T. J.: Investigation of Performance of Bumblebee 18-Inch Ram Jet with a Can-Type Flame Holder. NACA RM E8E21, 1948.

4. Disher, John H.: Flight Investigation of a 20-Inch-Diameter Steady-Flow Ram Jet. NACA RM E7I05a, 1948.

5. Carlton, William W., and Messing, Wesley E.: Free-Flight Performance of 16-Inch-Diameter Supersonic Ram-Jet Units. I - Four Units Designed for Combustion-Chamber-Inlet Mach Number of 0.12 at Free-Stream Mach Number of 1.6 (Units A-2, A-3, A-4, and A-5). NACA RM E9F22, 1949.

6. Disher, John H., Kohl, Robert C., and Jones, Merle L.: Free-Flight Performance of a Rocket-Boosted, Air-Launched 16-Inch-Diameter Ram-Jet Engine at Mach Numbers up to 2.20. NACA RM E52L02, 1953.

7. Jones, W. L., Shillito, T. B., and Henzel, J. G., Jr.: Altitude-Test-Chamber Investigation of Performance of a 28-Inch Ram-Jet Engine. I - Combustion and Operational Performance of Four Combustion-Chamber Configurations. NACA RM E50F16, 1950.

8. Smolak, George R., and Wentworth, Carl B.: Altitude Performance of a 20-Inch-Diameter Ram-Jet Engine Investigated in a Free-Jet Facility at Mach Number 3.0. NACA RM E52K24, 1953.

9. Smolak, George R., and Wentworth, Carl B.: Altitude Investigation of Can-Type Flame Holder in 20-Inch-Diameter Ram-Jet Combustor. NACA RM E54D08, 1954.

10. Male, Donald W.: Use of Flame-Immersed Blades to Improve Combustion Limits and Efficiency of a 5-Inch Diameter Connected-Pipe, Ram-Jet Combustor. NACA RM E53B16, 1953.

11. Longwell, J. P.: Flame Stabilization by Bluff Bodies and Turbulent Flames in Ducts. Fourth Symposium (International) on Combustion, The Williams & Wilkins Co. (Baltimore), 1953, pp. 90-97.

12. Longwell, J. P., and Petrein, R. J.: Ramjet Technology. Ch. 10 - Design of Baffle-Type Combustors. APL/JHU TG 154-10, Esso Labs., Standard Oil Dev. Co. (Publ. by The Johns Hopkins Univ.)

13. DeZubay, E. A.: Characteristics of Disk-Controlled Flame. Aero. Digest, vol. 61, no. 1, July 1950, pp. 54-56; 102-104.

14. Friedman, J., Bennet, W. J., and Zwick, E. B.: The Engineering Application of Combustion Research to Ram-Jet Engines. Fourth Symposium (International) on Combustion, The Williams & Wilkins Co. (Baltimore), 1953, pp. 756-764.

15. Williams, G. C.: Basic Studies on Flame Stabilization. Jour. Aero. Sci., vol. 16, no. 12, Dec. 1949, pp. 714-722.

16. Williams, G. C., Hottel, H. C., and Scurlock, A. C.: Flame Stabilization and Propagation in High Velocity Gas Streams. Third Symposium on Combustion and Flame and Explosion Phenomena, The Williams & Wilkins Co. (Baltimore), 1949, pp. 21-40.

17. Longwell, J. P., Chenevey, J. E., Clark, W. W., and Frost, E. E.: Flame Stabilization by Baffles in a High Velocity Gas Stream. Third Symposium on Combustion and Flame Explosion Phenomena, The Williams & Wilkins Co. (Baltimore), 1949, pp. 40-44.

18. Caldwell, Frank R., Ruegg, Fillmer W., Olsen, Lief O., and Broida, Herbert P.: Sixty-fifth Report on Progress of the Combustion Chamber Research Program Jan.-Mar. 1950. U.S. Dept. Commerce, Nat. Bur. Standards, Apr. 15, 1950.

19. Caldwell, Frank R., Ruegg, Fillmer W., Olsen, Lief O., and Broida, Herbert P.: Sixty-sixth Report on Progress of the Combustion Chamber Research Program Apr.-June 1950. U.S. Dept. Commerce, Nat. Bur. Standards, July 15, 1950.

20. Caldwell, Frank R., Ruegg, Fillmer W., Olsen, Lief O., and Broida, Herbert P.: Sixty-seventh Report on Progress of the Combustion Chamber Research Program July-Sept. 1950. U.S. Dept. Commerce, Nat. Bur. Standards, Oct. 15, 1950.

21. Williams, Glenn C., and Shipman, C. W.: Some Properties of Rod-Stabilized Flames of Homogeneous Gas Mixtures. Fourth Symposium (International) on Combustion, The Williams & Wilkins Co. (Baltimore), 1953, pp. 733-742.

22. Annunziata, F. J., and Edwards, A. E.: Low Altitude Performance of the UAC 5-Inch Diameter Ramjet Engine at JHU/APL-Jan. 1949. Meteor Rep. UAC-40, Res. Dept., United Aircraft Corp., Sept. 1949. (U.S. Navy, Bur. Ord. Contract NOrd 9845 with M.I.T.)

23. Black, Dugald O., and Messing, Wesley E.: Effect of Three Flame-Holder Configurations on Subsonic Flight Performance of a Rectangular Ram Jet over Range of Altitudes. NACA RM E8I01, 1948.

24. Douglass, Wm. M.: Tests of a Direct Connect Segment of a Rectangular Wing Ramjet. USCAL Rep. 3-5, Aero. Lab., Univ. Southern Calif., Dec. 1, 1947. (Navy Contract NOa(s) 8164.)

25. Shillito, T. B., Jones, W. L., and Kahn, R. W.: Altitude-Test-Chamber Investigation of Performance of a 28-Inch Ram-Jet Engine. II - Effects of Gutter Width and Blocked Area on Operating Range and Combustion Efficiency. NACA RM E50H21, 1950.

26. Shillito, T. B., and Nakanishi, Shigeo: Effect of Design Changes and Operating Conditions on Combustion and Operational Performance of a 28-Inch Diameter Ram-Jet Engine. NACA RM E51J24, 1952.

27. Anon.: Survey of Bumblebee Activities. Rep. No. 54, Appl. Phys. Lab., The Johns Hopkins Univ., Feb. 1947. (Contract NOrd 7386 with Bur. Ord., U.S. Navy.)

28. Anon.: Survey of Bumblebee Activities. Rep. No. 64, Appl. Phys. Lab., The Johns Hopkins Univ., July 1947. (Contract NOrd 7386 with Bur. Ord., U.S. Navy.)

[redacted]

29. Weedman, J. A.: An Initial Digest of the Literature on Combustion in a Ram Jet. CAE Rep. No. 324, Continental Aviation and Eng. Corp., Detroit (Mich.), Feb. 3, 1947.

30. Longwell, J. P., Eames, J. P., Yahnke, R. L., and Newhall, R. M.: Study of Combustors for Supersonic Ram-Jet for period Feb. 1-Mar. 31, 1946. Rep. PDN-4174, Esso Labs., Process Div., Standard Oil Dev. Co., Apr. 30, 1946. (Contract NOrd-9233.)

31. Lustenader, E.: Hermes B-1 Ramjet Combustion Tests in a Twelve-Inch Duct. Rep. No. R50A0524, Apparatus Dept., General Electric Co., Dec. 1950. (Proj. Hermes (TU1-2000 A).)

32. Nussdorfer, T. J., Sederstrom, D. C., and Perchonok, E.: Investigation of Combustion in 16-Inch Ram Jet under Simulated Conditions of High Altitude and High Mach Number. NACA RM E50D24, 1951.

33. Perchonok, Eugene, and Farley, John M.: Internal Flow and Burning Characteristics of 16-Inch Ram Jet Operating in a Free Jet at Mach Numbers of 1.35 and 1.73. NACA RM E51C16, 1951.

34. Chamberlain, John: Development of an 11-Inch Unit for a 30-Inch Diameter Multi-Unit Ramjet. Rep. R-50484-33, Res. Dept., United Aircraft Corp., Sept. 1952. (Contract NOa(s) 9661, U.S. Navy, Bur. Aero.)

35. Wilcox, Fred A., Perchonok, Eugene, and Wishnek, George: Some Effects of Gutter Flame-Holder Dimensions on Combustion-Chamber Performance of 20-Inch Ram Jet. NACA RM E8C22, 1948.

36. Dangle, E. E., Cervenka, A. J., and Perchonok, Eugene: Effect of Mechanically Induced Sinusoidal Air-Flow Oscillations on Operation of a Ram-Jet Engine. NACA RM E54D01, 1954.

37. Garmon, R. C., Moomaw, C. E., and Fenn, J. B.: Pilot Heat and Altitude Burner Performance. TM-150, Experiment, Inc., July 26, 1949.

38. Frost, E. E., Morris, K. G., Petrein, R. J., and Weiss, M. A.: Quarterly Progress Report on Study of Combustors for Supersonic Ram-Jet for period Jan. 1-Mar. 31, 1951. Rep. No. PDN 5621, Esso Labs., Standard Oil Dev. Co., June 15, 1951. (Contract NOrd-9233.)

39. Frost, E. E., Morris, K. G., Petrein, R. J., and Weiss, M. A.: Quarterly Progress Report on Study of Combustors for Supersonic Ram-Jet for period Oct. 1-Dec. 31, 1950. Rep. No. PDN 5591, Esso Labs., Standard Oil Dev. Co., Feb. 5, 1951. (Contract NOrd-9233.)

40. Longwell, J. P., Weiss, M. A., and Van Swerigen, R. A., Jr.: Report on Design Variables in Small-Scale Ram-Jet Altitude Pilots. Rep. No. PDN 5582, Esso Labs., Process Div., Standard Oil Dev. Co., Jan. 9, 1951. (Contract NOrd-9233, SOD/CM 656.)

41. Farley, John M., Smith, Robert E., and Povolny, John H.: Preliminary Experiments with Pilot Burners for Ram-Jet Combustors. NACA RM E52J23, 1953.

42. Dangle, E. E., Friedman, Robert, and Cervenka, A. J.: Analytical and Experimental Studies of a Divided-Flow Ram-Jet Combustor. NACA RM E53K04, 1954.

43. Henzel, James G., Jr., and Wentworth, Carl B.: Free-Jet Investigation of 20-Inch Ram-Jet Combustor Utilizing High-Heat-Release Pilot Burner. NACA RM E53H14, 1953.

44. Reynolds, Thaine W., and Male, Donald W.: Effect of Immersed Surfaces in Combustion Zone on Efficiency and Stability of 5-Inch-Diameter Ram-Jet Combustor. NACA RM E54C25, 1954.

45. Mullen, James W., II, and Fenn, John B.: Burners for Supersonic Ram Jets. Some Factors Influencing Performance at High Altitudes - A Resumé. Tech. Memo. No. TM-188, Experiment, Inc., Richmond (Va.), Jan. 11, 1950.

46. De Vault, R. T.: Summary of Subsonic Ramjet Development. USCAL Rep. 2-11, Aero. Lab., Univ. Southern Calif., Apr. 15, 1947. (Contract NOa(s) 7598, Navy Res. Proj.)

47. Beckelman, B. F.: Ram-Jet Burner Development. Doc. No. D-9487, Boeing Jet Lab., Boeing Airplane Co., Seattle (Wash.), Dec. 21, 1948. (Contract W-33-038 ac-13875.)

48. Justice, D. A.: Progress Report for November and December, 1952 - Development of XRJ-30-MA-8 Subsonic Ram Jet Model MA19G and Model FM8 Fuel Control. Reps. PR-36-20 and PR-36-21, Marquardt Aircraft Co., Dec. 31, 1952. (Contract NOa(s) 51-762-c.)

49. Shillito, Thomas B., Younger, George G., and Henzel, James G., Jr.: Altitude-Test-Chamber Investigation of Performance of 28-Inch Ram-Jet Engine. III - Combustion and Operational Performance of Three Flame Holders with a Center Pilot Burner. NACA RM E50J20, 1951.

50. Meyer, Carl L., and Welna, Henry J.: Investigation of Three Low-Temperature-Ratio Combustion Configurations in a 48-Inch-Diameter Ram-Jet Engine. NACA RM E53K20, 1954.

51. Rayle, Warren D., and Koch, Richard G.: Design of Combustor for Long-Range Ram-Jet Engine and Performance of Rectangular Analog. NACA RM E53K13, 1954.

52. Henzel, James G., Jr., and Trout, Arthur M.: Altitude Investigation of 20-Inch-Diameter Ram-Jet Engine with Annular-Piloted Combustor. NACA RM E54G12, 1954.

53. Cervenka, A. J., Bahr, D. W., and Dangle, E. E.: Effect of Fuel Air Ratio Concentration in Combustion Zone on Combustion Performance of a 16-Inch Ram-Jet Engine. NACA RM E53B19, 1953.

54. Messing, Wesley E., and Simpkinson, Scott H.: Free-Flight Performance of 16-Inch-Diameter Supersonic Ram-Jet Units. II - Five Units Designed for Combustion-Chamber-Inlet Mach Number of 0.16 at Free-Stream Mach Number of 1.60 (Units B-1, B-2, B-3, B-4, and B-5). NACA RM E50B14, 1950.

55. Disher, John H., and Rabinowitz, Leonard: Free-Flight Performance of 16-Inch-Diameter Supersonic Ram-Jet Units. III - Four Units Designed for Combustion-Chamber-Inlet Mach Number of 0.245 at Free-Stream Mach Number of 1.8 (Units D-1, D-2, D-3, and D-4). NACA RM E50D07, 1950.

56. Rabb, Leonard, and North, Warren J.: Free-Flight Performance of 16-Inch-Diameter Supersonic Ram-Jet Units. IV - Performance of Ram-Jet Units Designed for Combustion-Chamber-Inlet Mach Number of 0.21 at Free-Stream Mach Number of 1.6 over a Range of Flight Conditions. NACA RM E50L18, 1951.

[redacted]

57. North, Warren J.: Summary of Free-Flight Performance of a Series of Ram-Jet Engines at Mach Numbers from 0.80 to 2.20. NACA RM E53K17, 1954.

58. Wilcox, Fred, Baker, Sol, and Perchonok, Eugene: Free-Jet Investigation of a 16-Inch Ram Jet at Mach Numbers of 1.35, 1.50, and 1.73. NACA RM E50G19, 1950.

59. Howard, Ephraim M., Wilcox, Fred A., and Dupree, David T.: Combustion-Chamber Performance with Four Fuels in Bumblebee 18-Inch Ram Jet Incorporating Various Rake- or Gutter-Type Flame Holders. NACA RM E8I01a, 1948.

60. Anon.: Bumblebee Semi-Annual Survey. Convair Rep. 5001-9, July-Dec. 1950, Consolidated Vultee Aircraft Corp. (Contract NOrd 9028.)

61. Dupree, D. T., Nussdorfer, T. J., and Sterbentz, W. H.: Altitude-Wind-Tunnel Investigation of Various Can-Type Burners in Bumblebee 18-Inch Ram Jet. NACA RM E8L20, 1949.

62. McFarland, H. W.: Development of Supersonic Ramjet Burners. USCAL Rep. 8-2, Aero. Lab., Univ. Southern Calif., Feb. 19, 1951. (U.S. Navy Bur. Aero. Contract NOa(s) 9961, Item 2.)

63. Breitwieser, Roland: Performance of a Ram-Jet-Type Combustor with Flame Holders Immersed in the Combustion Zone. NACA RM E8F21, 1948.

64. Male, Donald W., and Cervenka, Adolph J.: Design Factors for 4- by 8-Inch Ram-Jet Combustor. NACA RM E9F09, 1949.

65. Cunningham, W., ed.: Summary Report on Jet Engine Development. Continental Aviation and Eng. Corp., Detroit (Mich.), Aug. 1, 1949. (Air Forces Contract W-33-038-ac-13371.)

66. Rayle, Warren D., Smith, Ivan D., and Wentworth, Carl B.: Preliminary Results from Free-Jet Tests of a 48-Inch-Diameter Ram-Jet Combustor with an Annular-Piloted Baffle-Type Flameholder. NACA RM E54K15, 1955.

67. Anon.: Survey of Bumblebee Activities. Rep. No. 82, Appl. Phys. Lab., The Johns Hopkins Univ., June 1948. (Contract NOrd 7386 with Bur. Ord., U.S. Navy.)

68. Messing, Wesley E., and Black, Dugald O.: Effect of Variation in Fuel Pressure on Combustion Performance of Rectangular Ram Jet. NACA RM E8I28, 1948.

69. Reid, J.: Development of Six Inch Diameter Ramjet Combustion Chamber. Rep. No. AERO 2282, British R.A.E., Sept. 1948.

70. Reid, J.: The Further Development of a Six Inch Diameter Ramjet Combustion Chamber. Rep. No. G.W. 12, British R.A.E., Mar. 1952.

71. Sterbentz, W. H., Perchonok, E., and Wilcox, F. A.: Investigation of Effects of Several Fuel-Injection Locations on Operational Performance of a 20-Inch Ram Jet. NACA RM E7L02, 1948.

72. Cervenka, A. J., Perchonok, Eugene, and Dangle, E. E.: Effect of Fuel Injector Location and Mixture Control on Performance of a 16-Inch Ram-Jet Combustor. NACA RM E53F15, 1953.

73. Bennet, W. J., and Maloney, J.: Altitude Tests of the Convair 20 Inch Diameter Can Type Combustor. Rep. No. ZM-9136-010, Consolidated Vultee Aircraft Corp., San Diego (Calif.), May 10, 1950.

74. Huber, Paul W.: Preliminary Tests of a Burner for Ram-Jet Applications. NACA RM L6K08b, 1947.

75. Trout, Arthur M., and Wentworth, Carl B.: Free-Jet Altitude Investigation of a 20-Inch Ram-Jet Combustor with a Rich Inner Zone of Combustion for Improved Low-Temperature-Ratio Operation. NACA RM E52L26, 1953.

76. Cervenka, A. J., Dangle, E. E., and Friedman, Robert: Effect of Inlet-Air Temperature on Performance of a 16-Inch Ram-Jet Combustor. NACA RM E53I03, 1953.

77. Beam, Thomas T.: Results of Direct-Connected Altitude Proof Tests of the XRJ-43-MA-1 Model C20-2.5A6 Test Ramjet at the W-P AFB May 12-June 22, 1950. Memo. Rep. No. M-1207, Ramjet Design Section, Marquardt Aircraft Co., Dec. 5, 1950.

78. Kahn, Robert W., Nahanishi, Shigeo, and Harp, James L., Jr.: Altitude-Test-Chamber Investigation of Performance of 28-Inch Ram-Jet Engine. IV - Effect of Inlet-Air Temperature, Combustion-Chamber-Inlet Mach Number, and Fuel Volatility on Combustion Performance. NACA RM E51D11, 1951.

79. Wilcox, Fred A.: Free-Jet Performance of 16-Inch Ram-Jet Engine with Several Fuels. NACA RM E50I06, 1950.

80. Wilcox, Fred A., and Howard, Ephraim M.: Comparison of Two Fuels in Bumblebee 18-Inch Ram Jet Incorporating Rake-Type Flame Holder. NACA RM E8F11, 1948.

81. Lundquist, W. G.: Third Quarterly Progress Report on Ram Jet Development. W.A.C. Ser. Rep. No. 1485, Wright Aero. Corp. (N.J.), Oct. 16, 1950. (Contract AF 33(038)-9000.)

82. Dangle, E. E., Cervenka, A. J., and Bahr, D. W.: Effects of Fuel Temperature and Fuel Distribution on the Combustion Efficiency of a 16-Inch Ram-Jet Engine at a Simulated Flight Mach Number of 2.9. NACA RM E52J14, 1953.

83. Reynolds, Thaine W.: Effect of Fuels on Combustion Efficiency of a 5-Inch Ram-Jet-Type Combustor. NACA RM E53C20, 1953.

84. Perchonok, Eugene, Sterbentz, William H., and Wilcox, Fred A.: Performance of a 20-Inch Steady-Flow Ram Jet at High Altitudes and Ram-Pressure Ratios. NACA RM E6L06, 1947.

85. Perchonok, Eugene, Wilcox, Fred A., and Sterbentz, William H.: Invetigation of the Performance of a 20-Inch Ram Jet Using Preheated Fuel. NACA RM E6I23, 1946.

86. Curry, Richard: Development of a Four-Inch Ramjet Burner Unit for Multi-Unit Test Burner Application. Rep. R-50133-17, Res. Dept., United Aircraft Corp., June 1950. (U.S. Navy, Bur. Aero. Contract NOa(s) 9661, Lot II.)

87. Dailey, C. L., and McFarland, H. W.: Development of Ramjet Components. UECAL Rep. 13-5, Prog. Rep. June through Sept. 1951, Aero. Lab., Univ. Southern Calif., Oct. 8, 1951. (U.S. Navy, Bur. Aero. Contract NOas 51-116-c.)

88. Cervenka, A. J., and Miller, R. C.: Effect of Inlet-Air Parameters on Combustion Limit and Flame Length in 8-Inch-Diameter Ram-Jet Combustion Chamber. NACA RM E8C09, 1948.

89. Anon.: Survey of Bumblebee Activities. Rep. No. 46, Appl. Phys. Lab., The Johns Hopkins Univ., Nov. 1946. (Contract NOrd 7386 with Bur. Ord., U.S. Navy.)

[redacted]

3105

90. Anon.: Survey of Bumblebee Activities. Rep. No. 49, Appl. Phys. Lab., The Johns Hopkins Univ., Dec. 1946. (Contract NOrd 7386 with Bur. Ord., U.S. Navy.)

91. Perchonok, Eugene, Wilcox, Fred, and Pennington, Donald: Effect of Angle of Attack and Exit Nozzle Design on the Performance of a 16-Inch Ram Jet at Mach Numbers from 1.5 to 2.0. NACA RM E51G26, 1951.

92. Hearth, Donald P., and Perchonok, Eugene: Performance of a 16-Inch Ram-Jet Engine with a Can-Type Combustor at Mach Numbers of 1.50 to 2.16. NACA RM E54G13, 1954.

93. Childs, J. Howard: Preliminary Correlation of Efficiency of Aircraft Gas-Turbine Combustors for Different Operating Conditions. NACA RM E50F15, 1950.

94. Reynolds, Thaine W., and Ingebo, Robert D.: Combustion Efficiency of Homogeneous Fuel-Air Mixtures in a 5-Inch Ram-Jet Combustor. NACA RM E52I23, 1952.

95. Wentworth, Carl B.: Performance of Five Low-Temperature-Ratio Ram-Jet Combustors over Range of Simulated Altitudes. NACA RM E54H13, 1954.

[redacted]

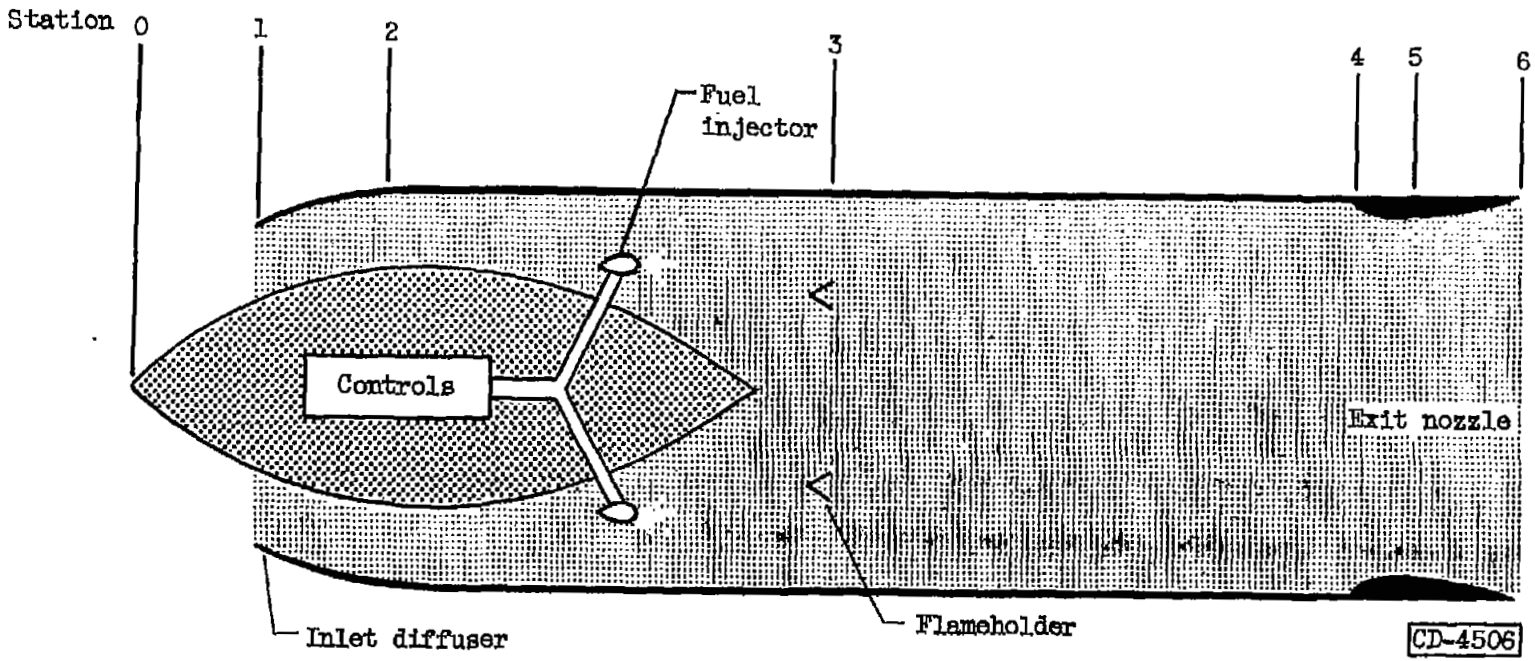

Figure 128. - Typical ram-jet configuration.

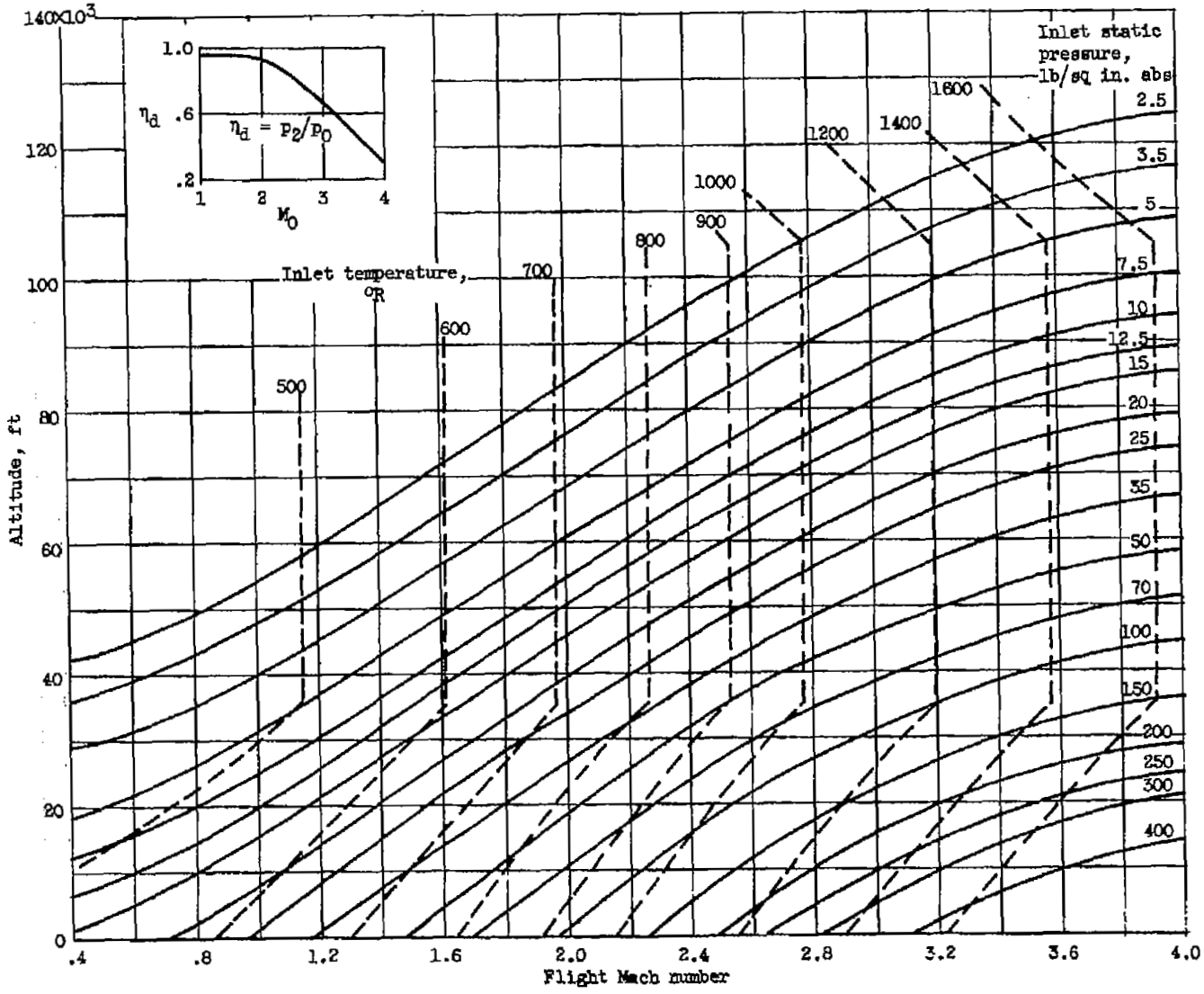

Figure 129. - Ram-jet inlet conditions for various flight speeds and altitudes. Inlet-air velocity, 200 feet per second; assumed diffuser recovery η_d ranges from 0.95 at Mach 1 to 0.30 at Mach 4.

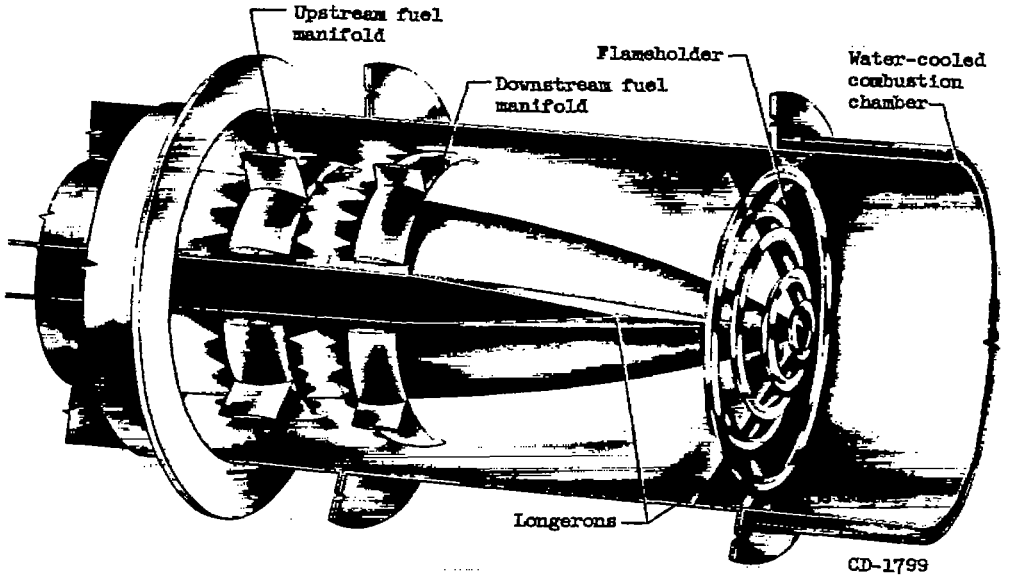

(a) V-gutter flameholder.

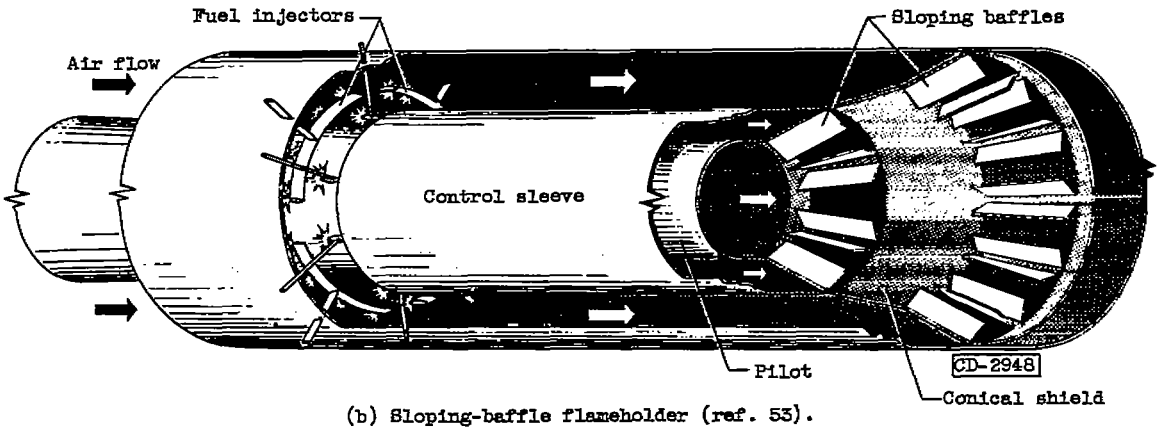

(b) Sloping-baffle flameholder (ref. 53).

Figure 130. - Typical ram-jet flameholder configurations.

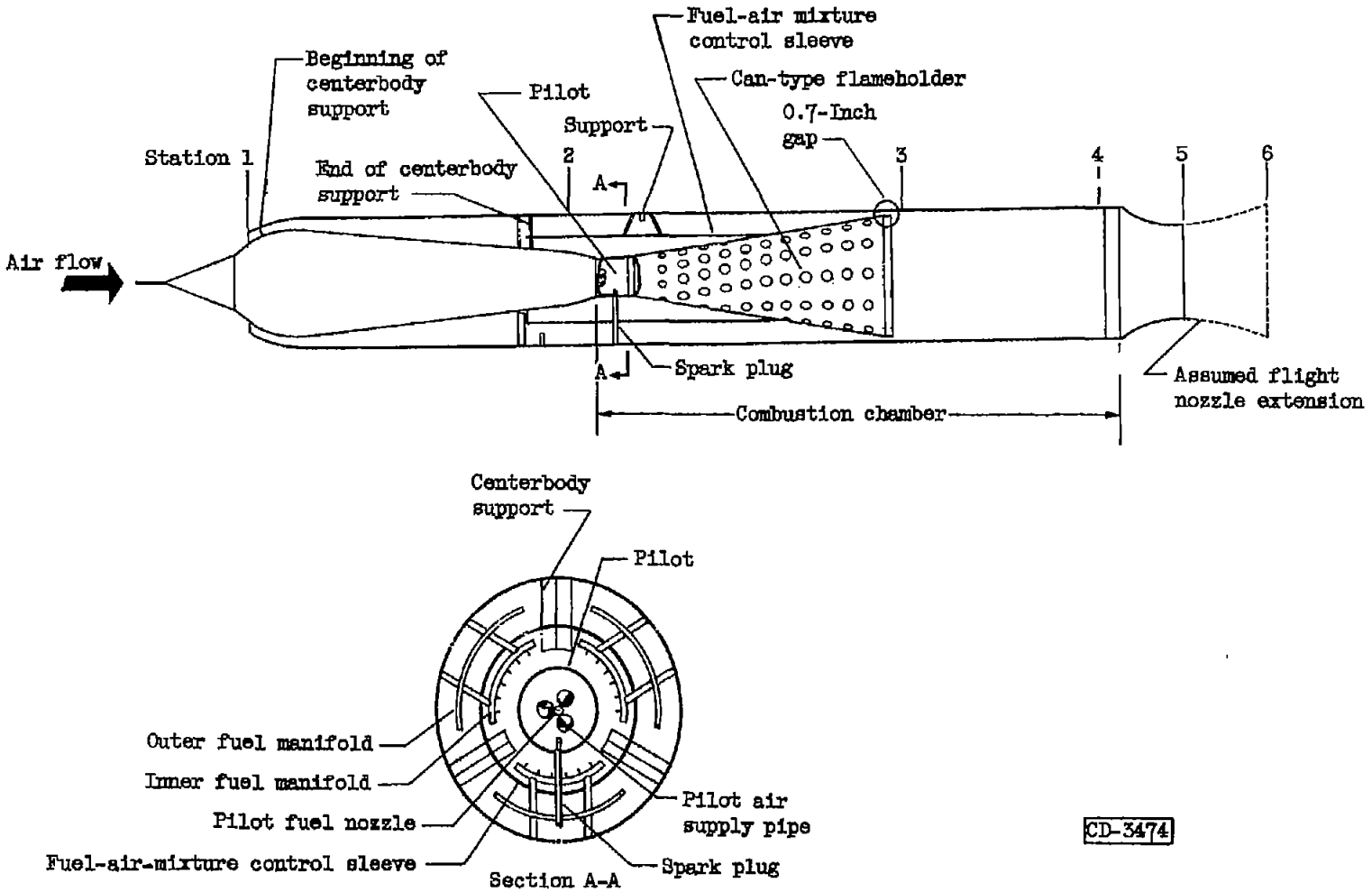

(c) Can-type flameholder.

Figure 130. - Concluded. Typical ram-jet flameholder configurations.

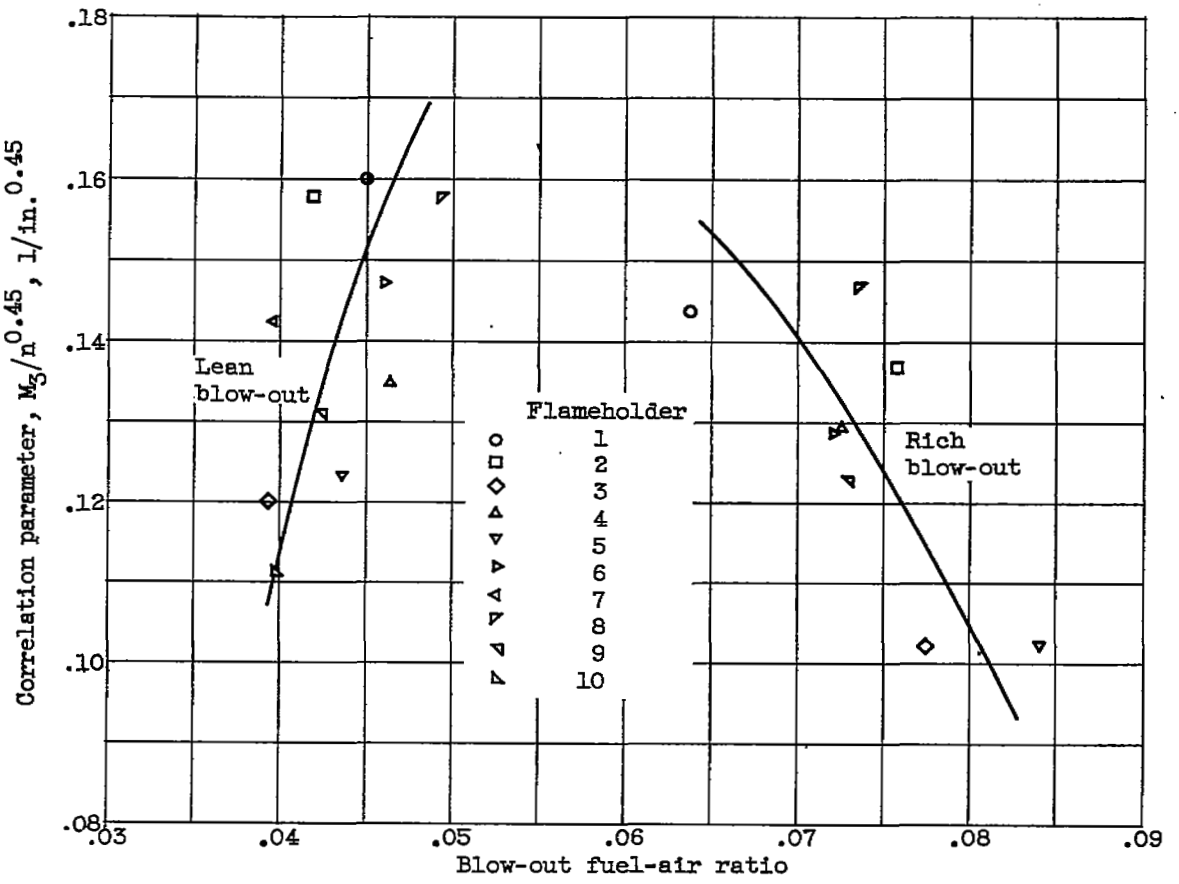

Figure 131. - Correlation of blow-out data with gutter size. Combustion-chamber-outlet total pressure, 2000 pounds per square foot absolute.

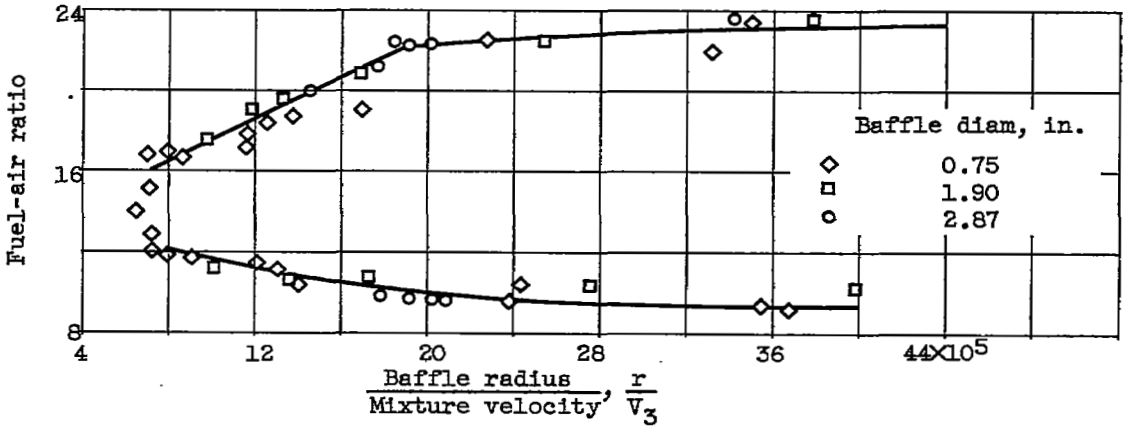

Figure 132. - Effect of mixture velocity and baffle size on stability range. Pressure, 1 atmosphere; temperature, 300° F (ref. 17).

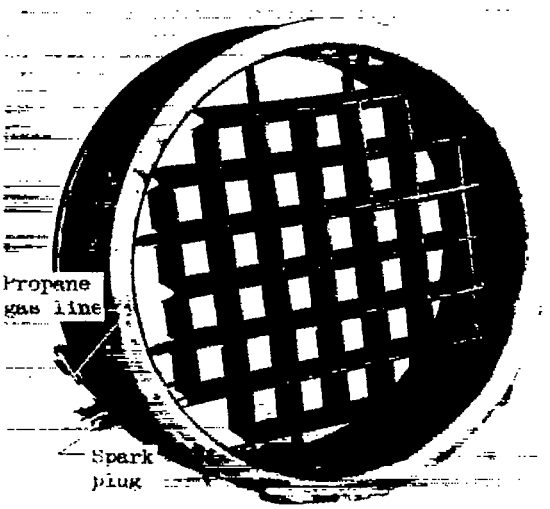

(a) Standard flameholder mounted in flameholder section.

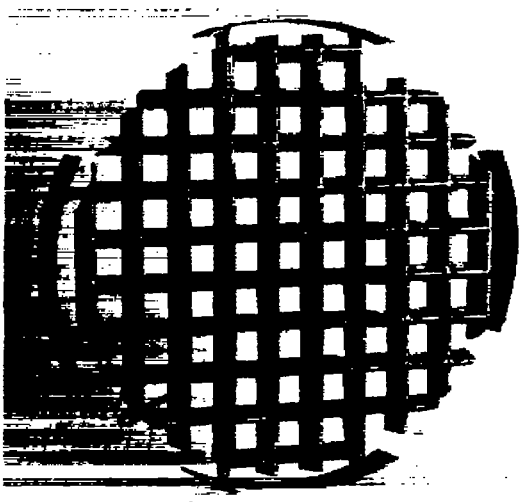

(b) Three-quarter-scale flameholder.

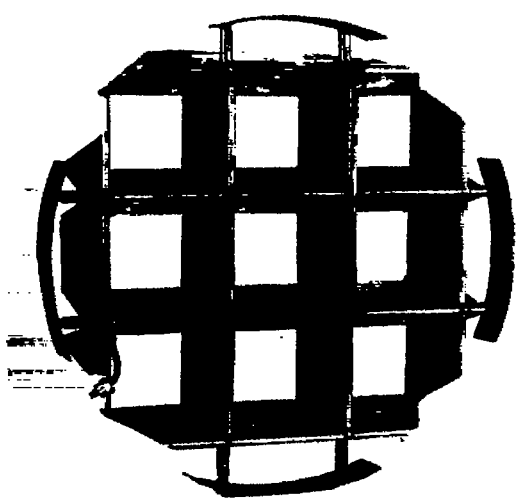

(c) Double-scale flameholder.

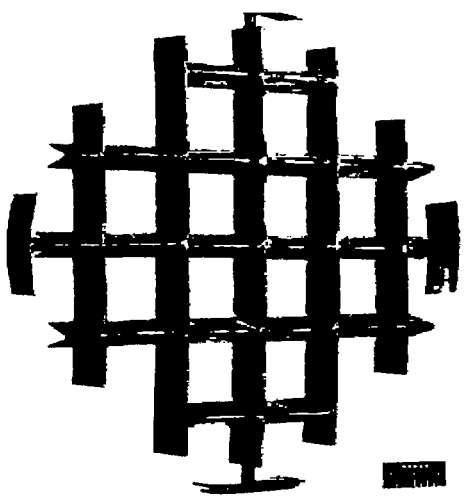

(d) 1.4 Spaced flameholder.

Figure 133. - Gutter-grid flameholders used in 20-inch ram jet (ref. 35).

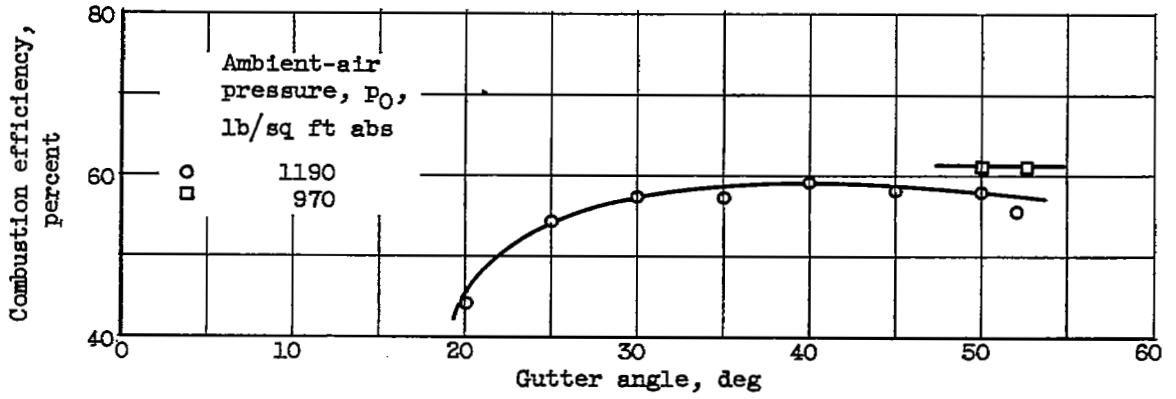

Figure 134. - Effect on combustion efficiency of gutter angle of adjustable three-gutter flameholder. 20-Inch ram jet with 5-foot combustion chamber; fuel-air ratio, 0.072 to 0.078; combustion-chamber-inlet static pressure, 1500 pounds per square foot absolute (ref. 35).

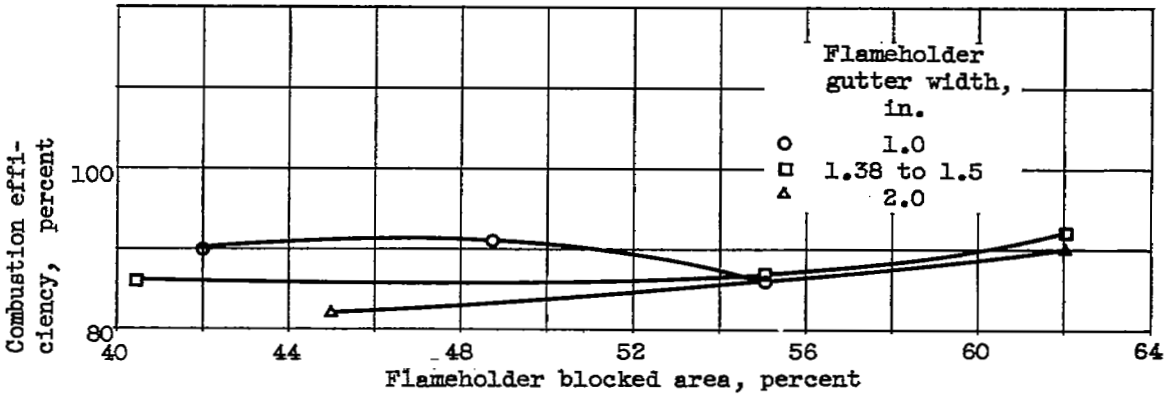

Figure 135. - Effect of flameholder blocked area on combustion efficiency. Fuel-air ratio, 0.050; combustion-chamber-exit pressure, 1800 pounds per square foot absolute (ref. 26).

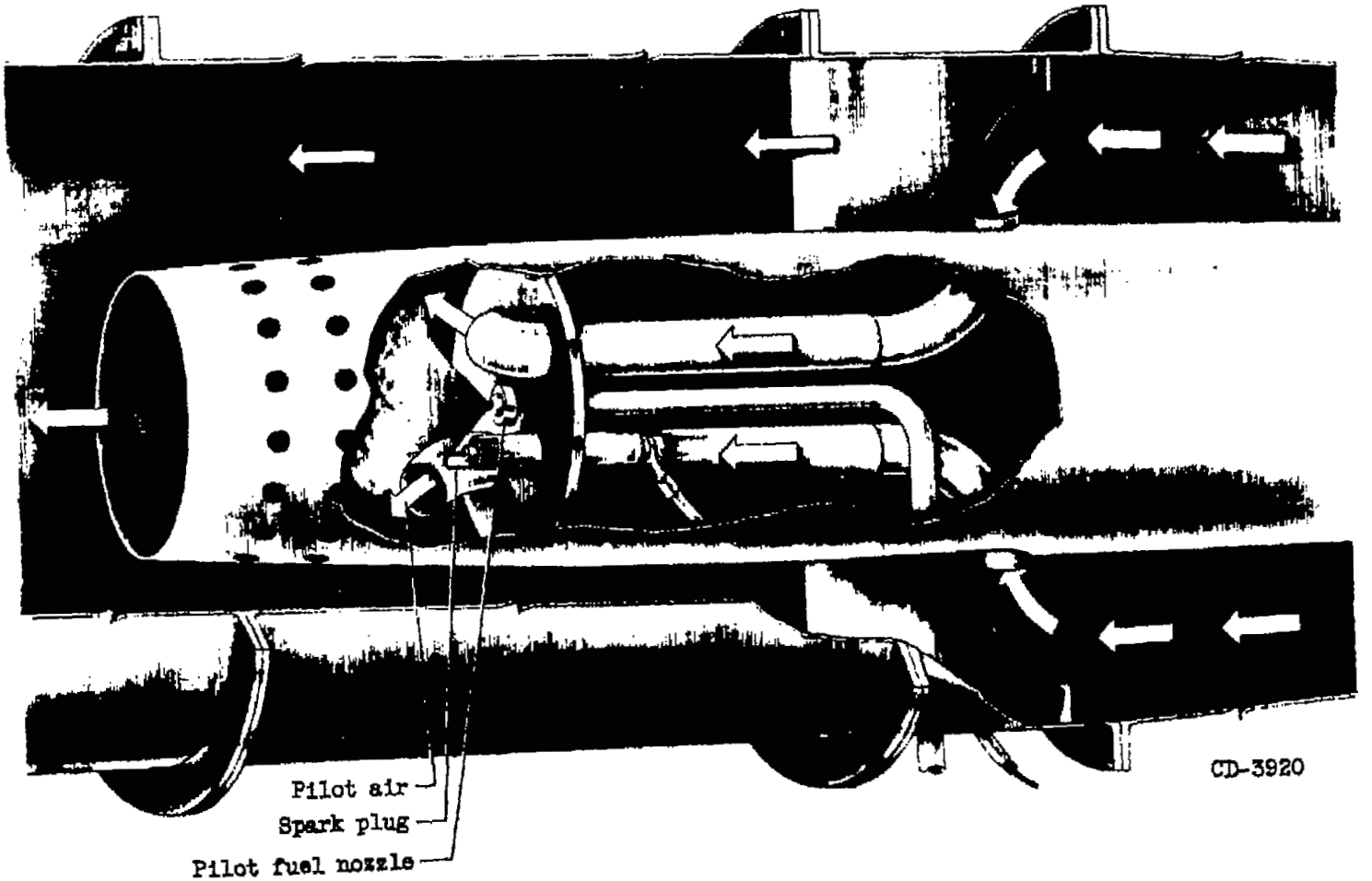

Figure 136. - Typical pilot configuration.

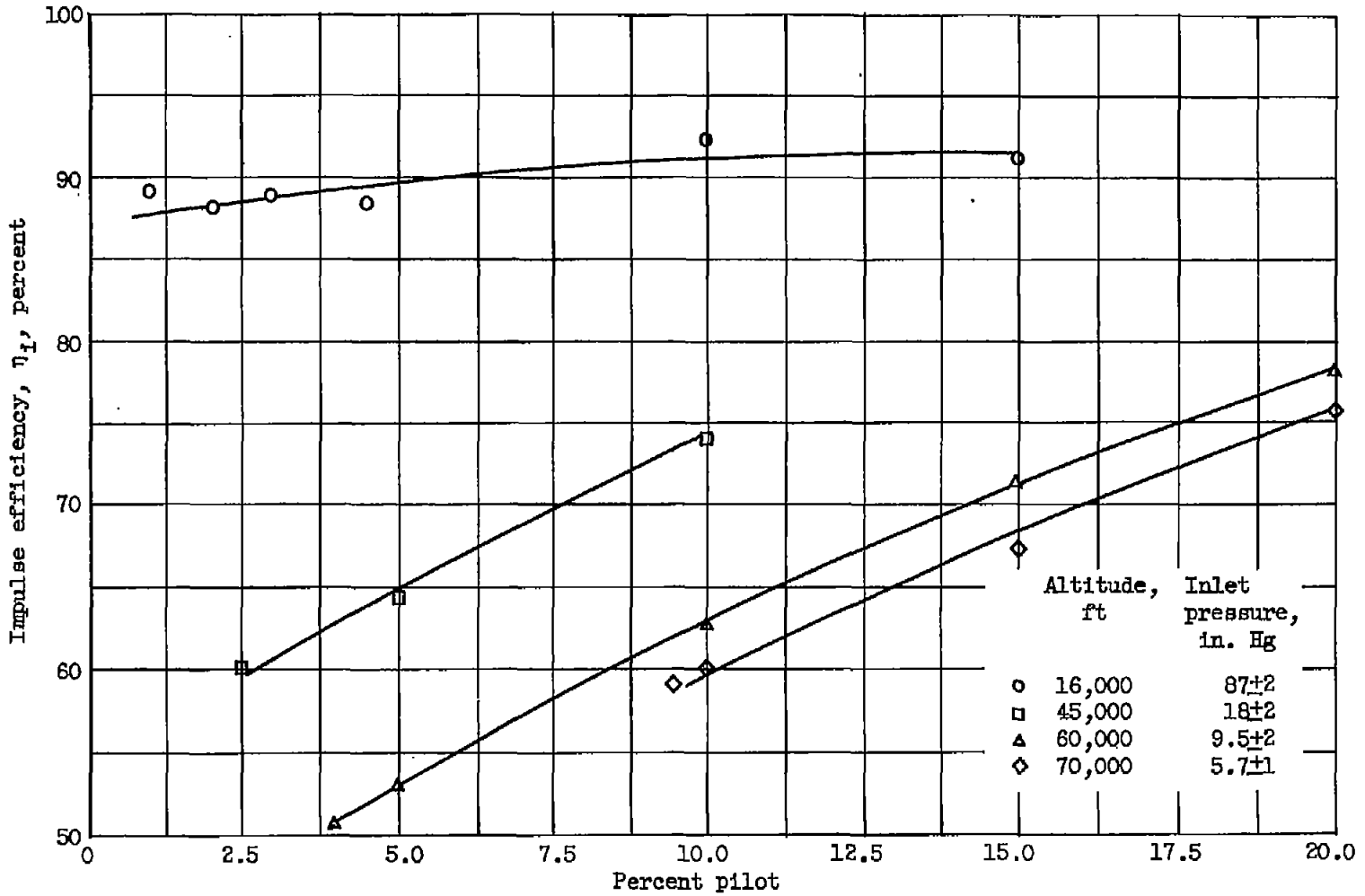

Figure 137. - Effect of pilot heat on burner efficiency. Burner length, 14 inches; fuel, pentane; stoichiometric conditions (ref. 45).

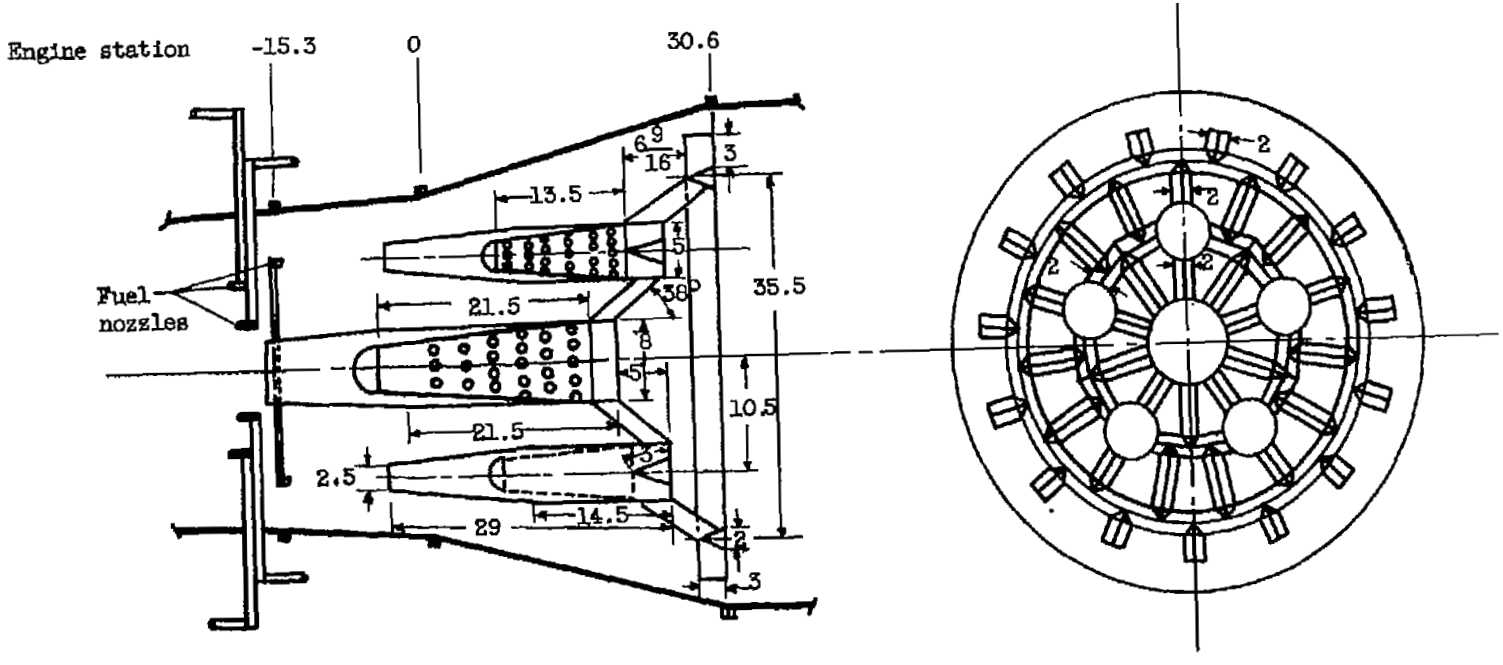

Figure 138. - Flameholder configuration employing five pilot zones (ref. 50). (Dimensions in inches.)

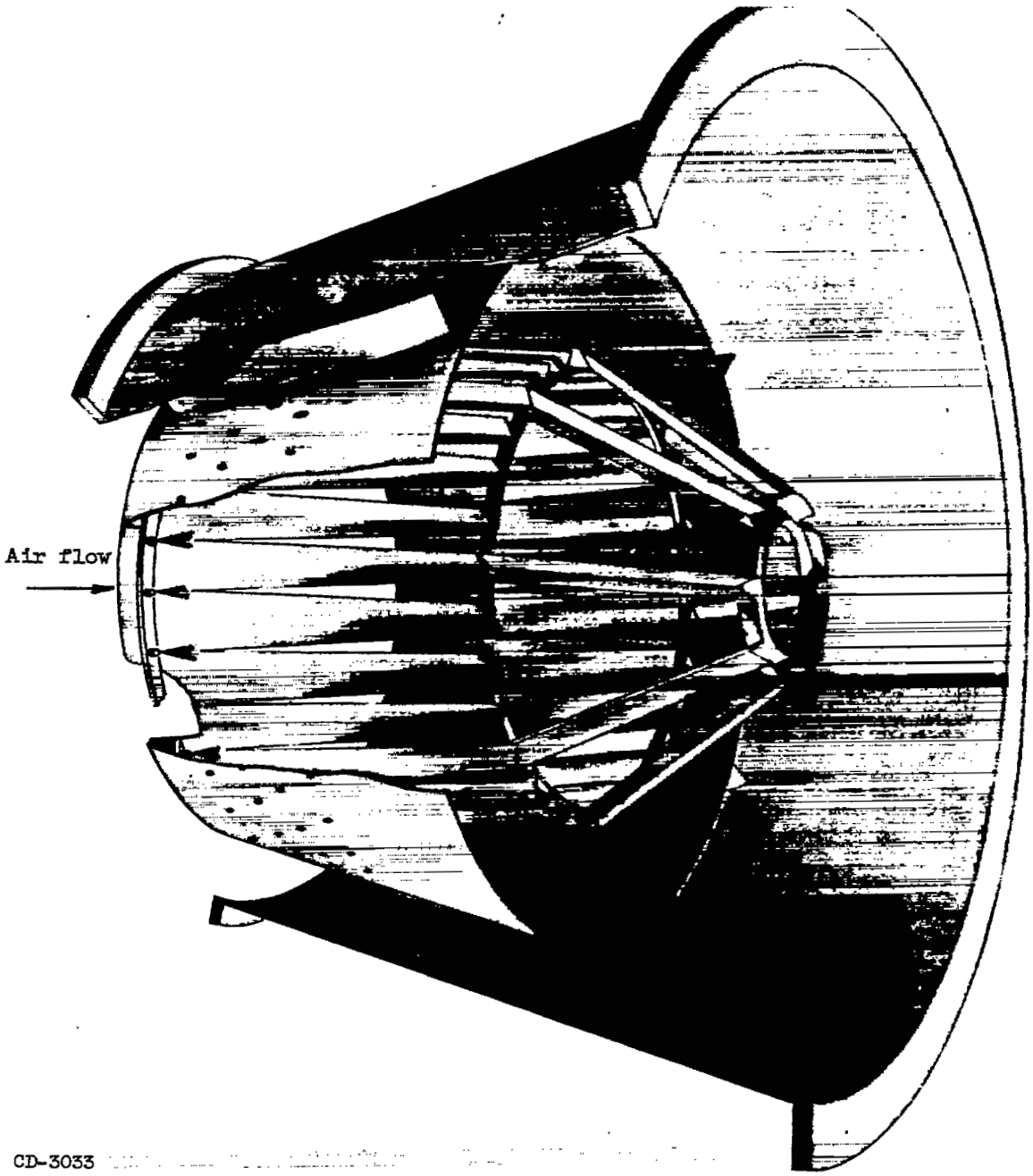

Figure 139. - Annular-piloted combustor configuration (refs. 50 and 51).

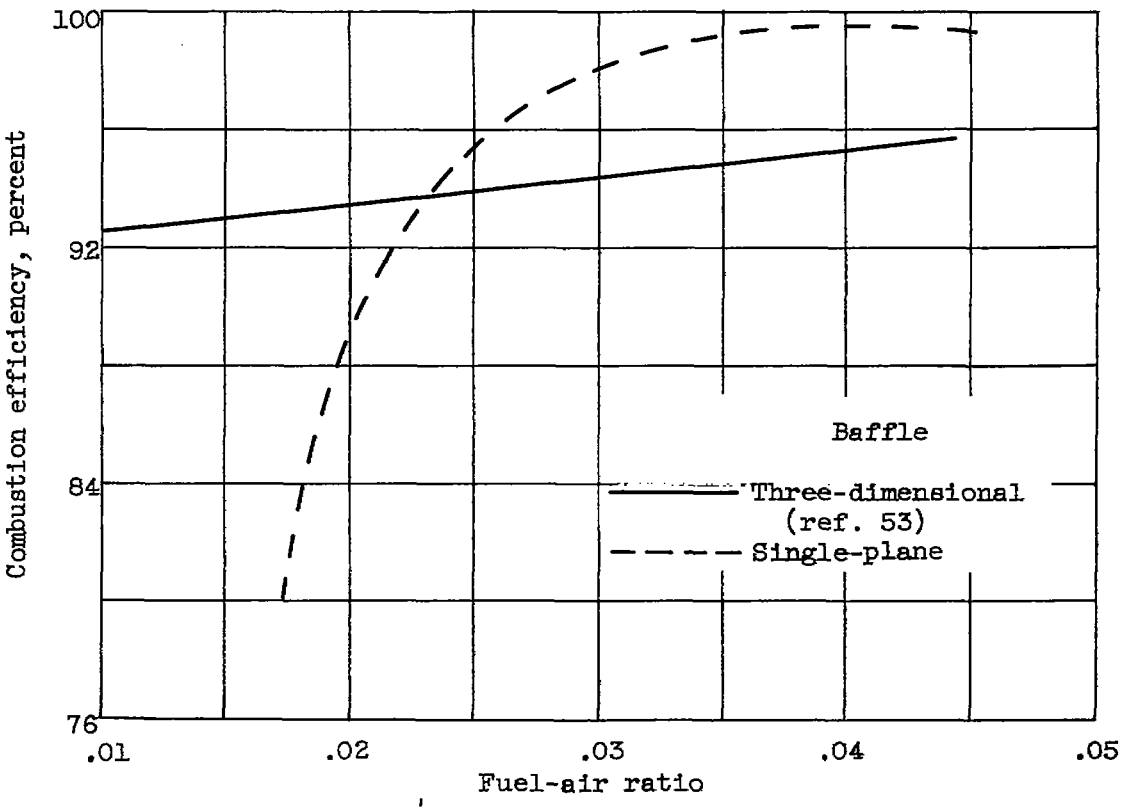

Figure 140. - Comparison of combustion performance of planar and three-dimensional flameholders. Inlet-air temperature, 600° F; velocity, 230 to 260 feet per second; pressure, 31 to 35 inches of mercury absolute.

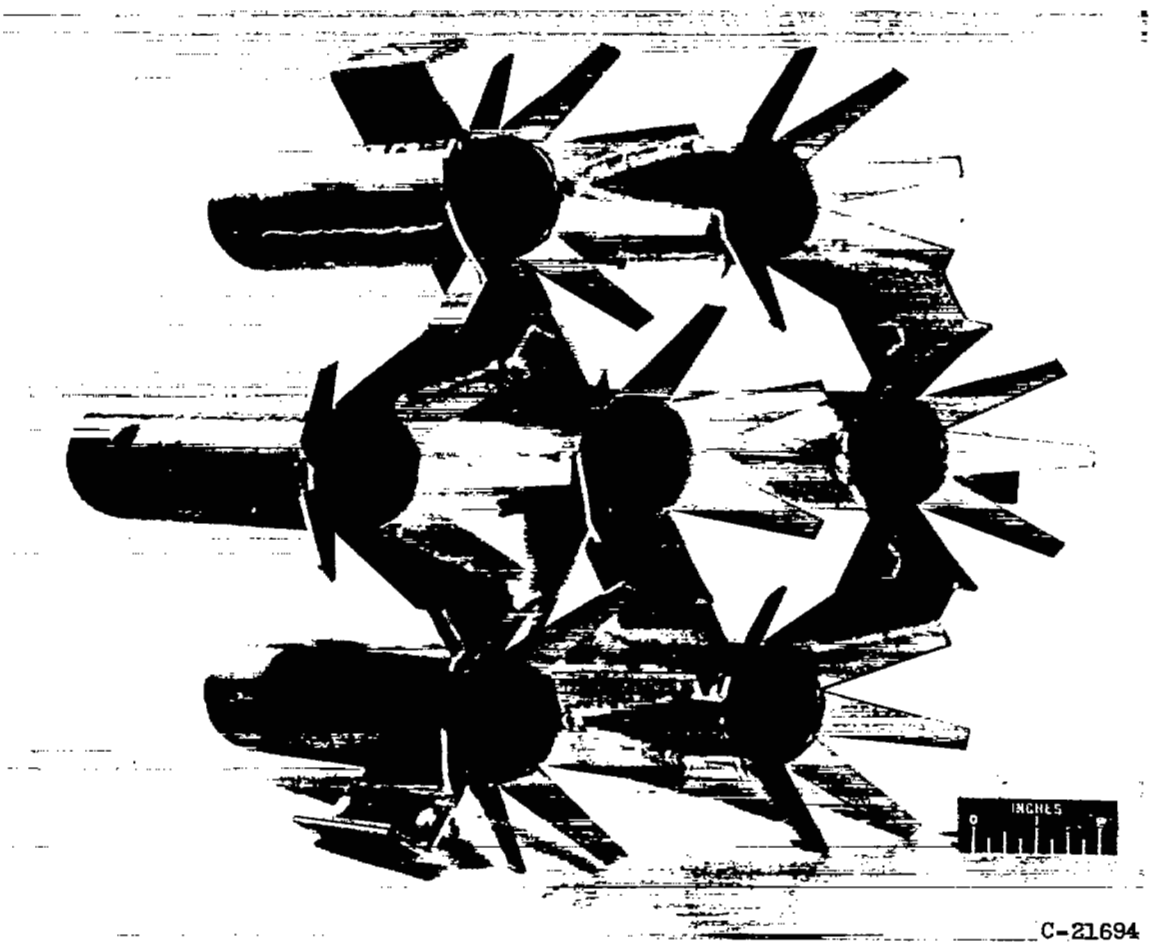

Figure 141. - Rake-type flameholder with flare pilots.

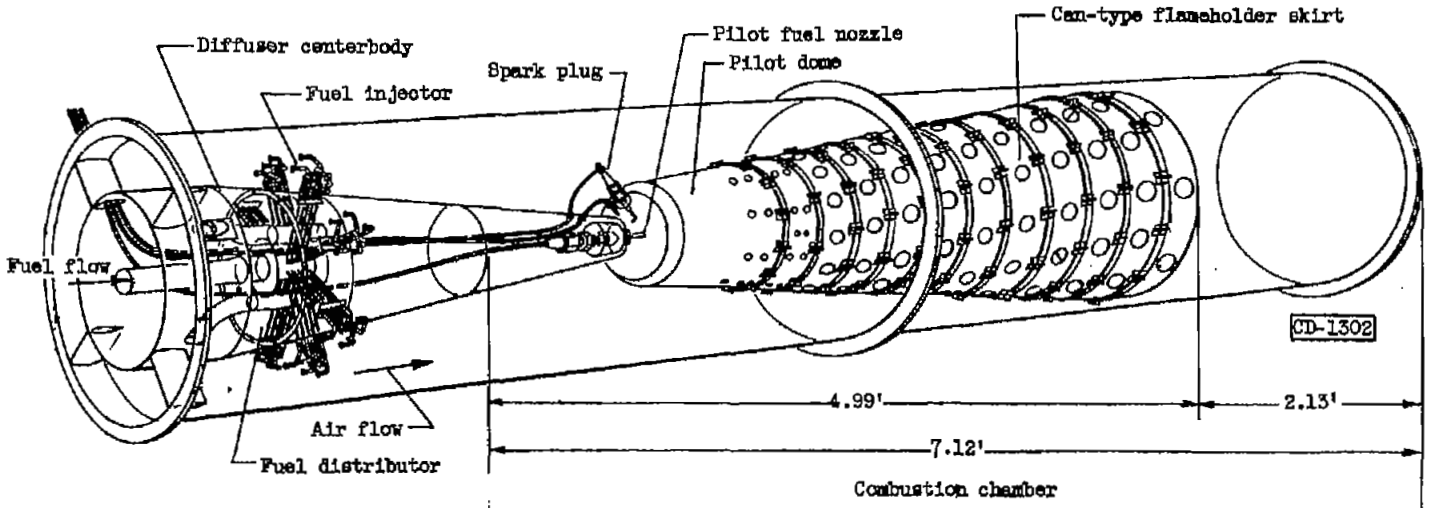

(a) Simple can flameholder installed in ram-jet engine.

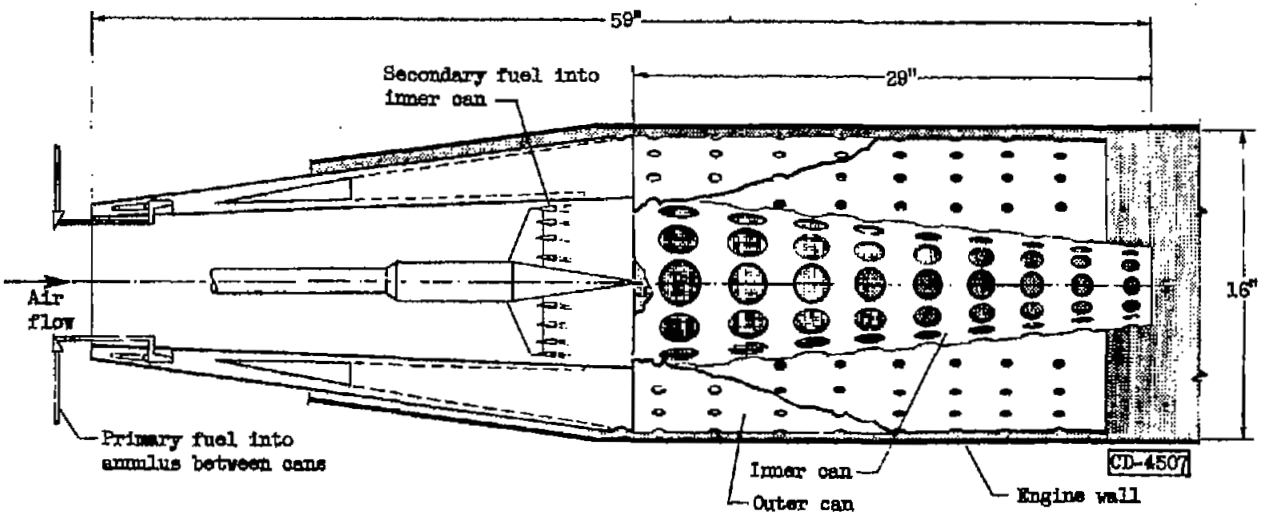

(b) Annular can flameholder (ref. 60).

Figure 142. - Typical can flameholder.

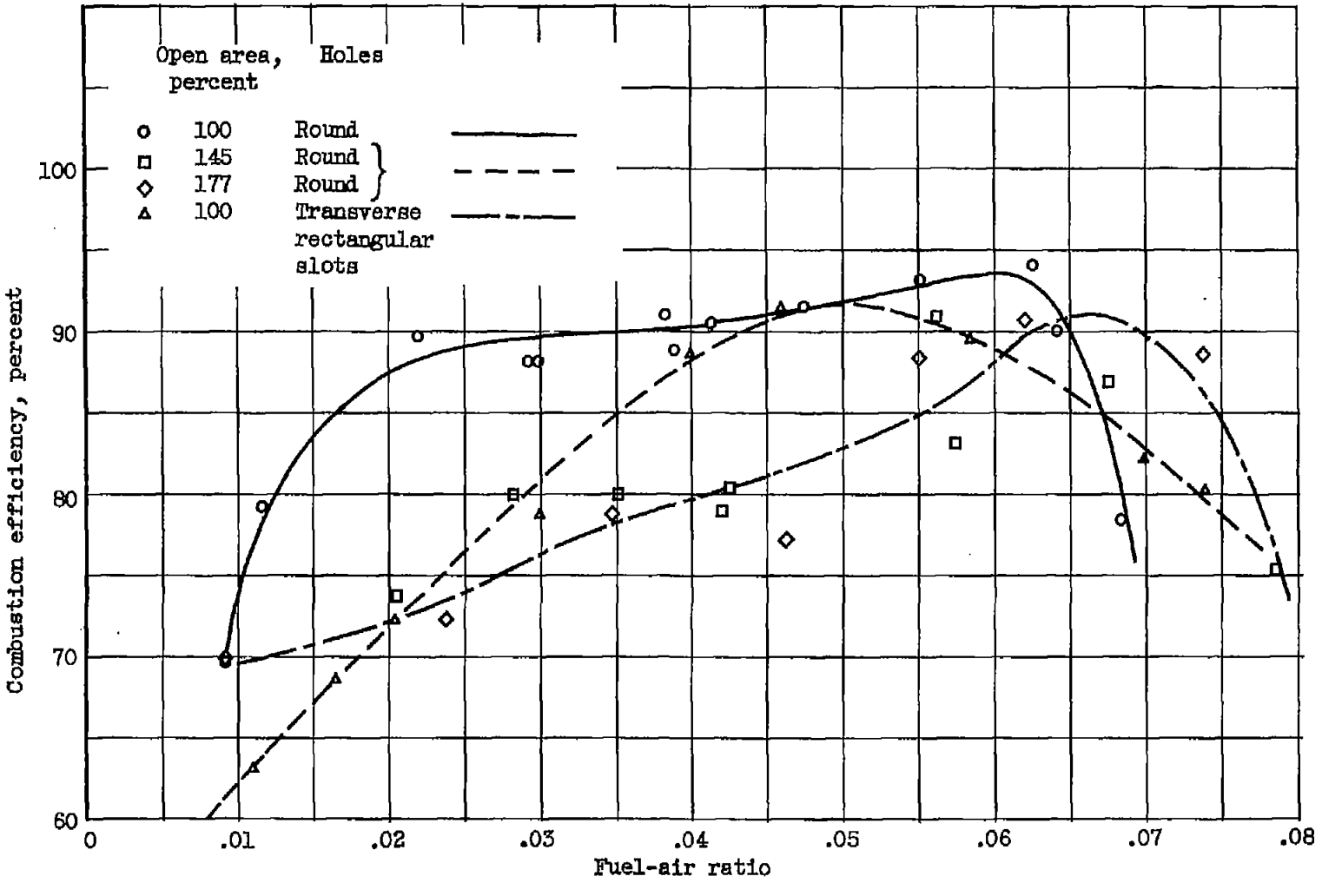

Figure 143. - Effect of can open area upon combustion efficiency of 10-inch-diameter, quarter-segment combustor during free-jet tests. Inlet-air temperature, 180°±10° F; atmospheric exhaust (ref. 62).

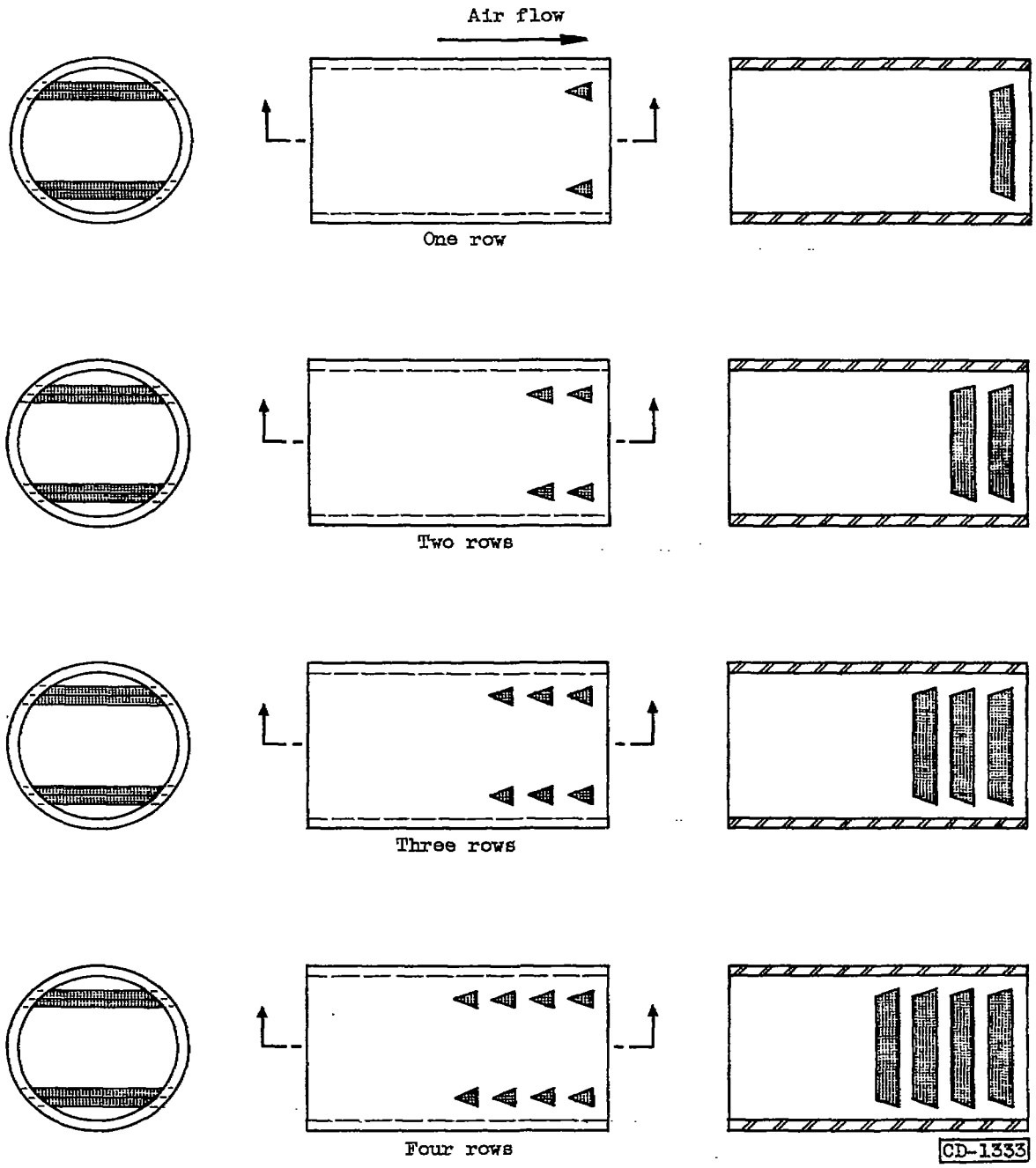

Figure 144. - Flameholder configuration employing immersed surfaces (ref. 63).

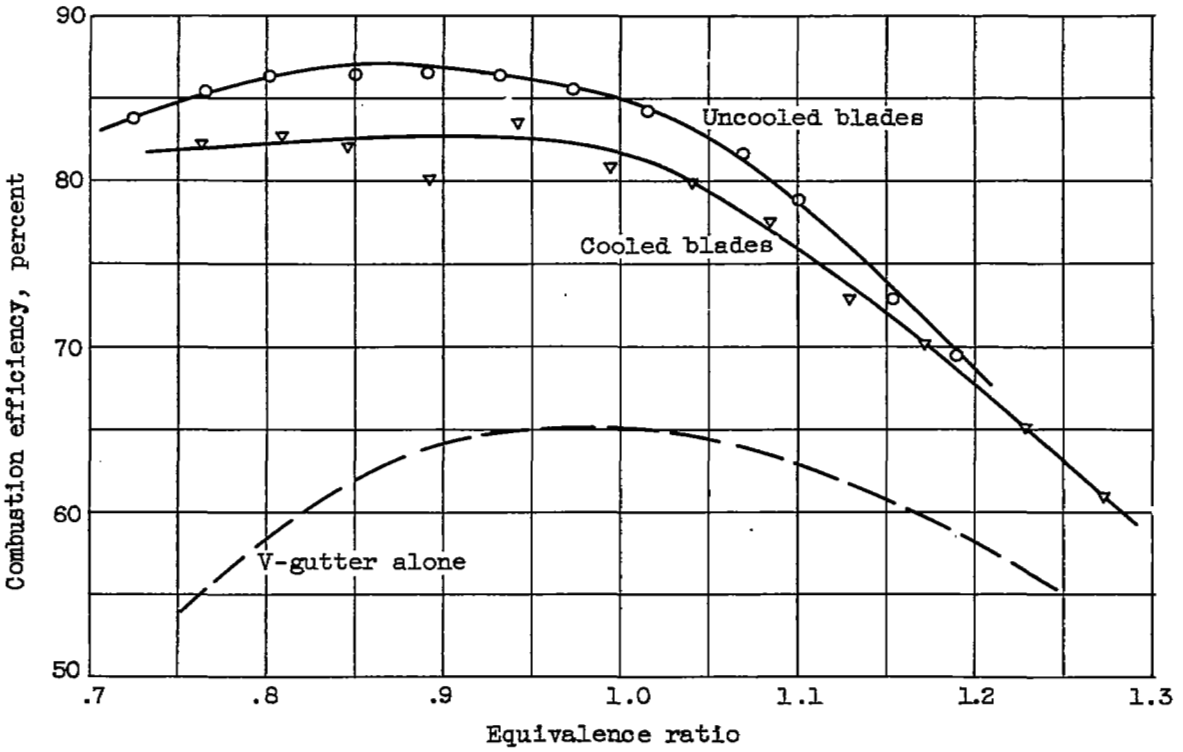

Figure 145. - Combustion efficiencies of immersed-surface configurations with both cooled and uncooled blades. Inlet-air pressure, 1 atmosphere; inlet-air temperature, 660° R; velocity, 200 feet per second; fuel, gasoline with high-pressure injection.

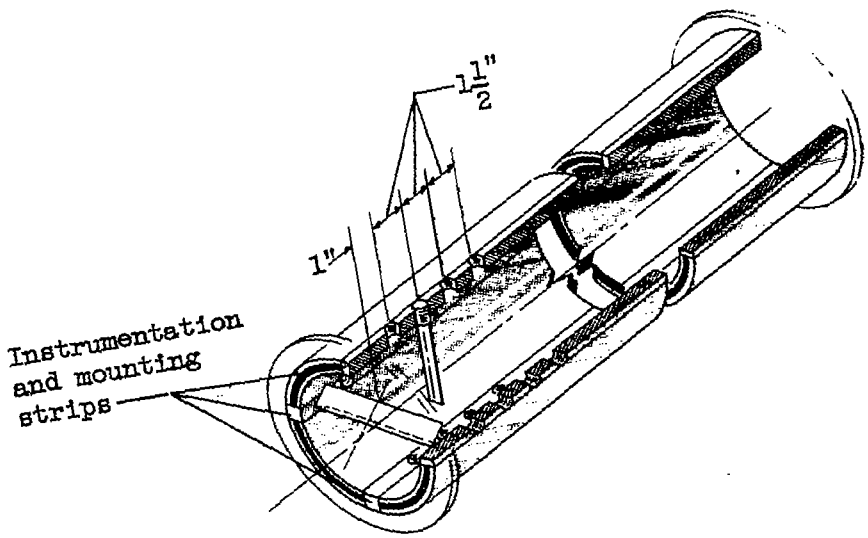

(a) Single-perpendicular-blade configuration.

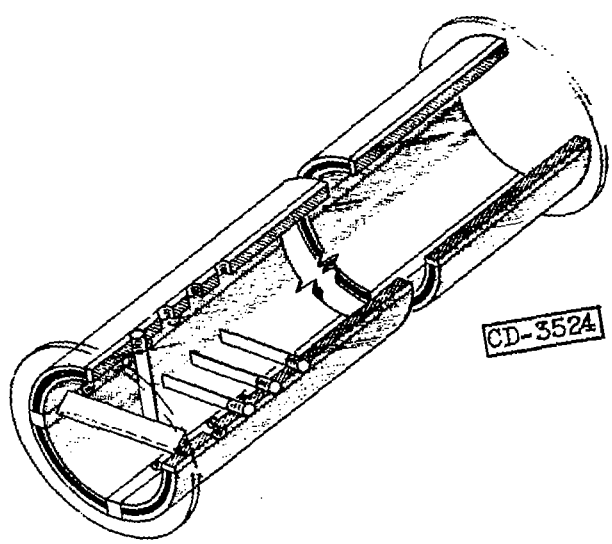

(b) Four-blade configuration.

Figure 146. - Typical arrangements of blades (immersed surfaces).

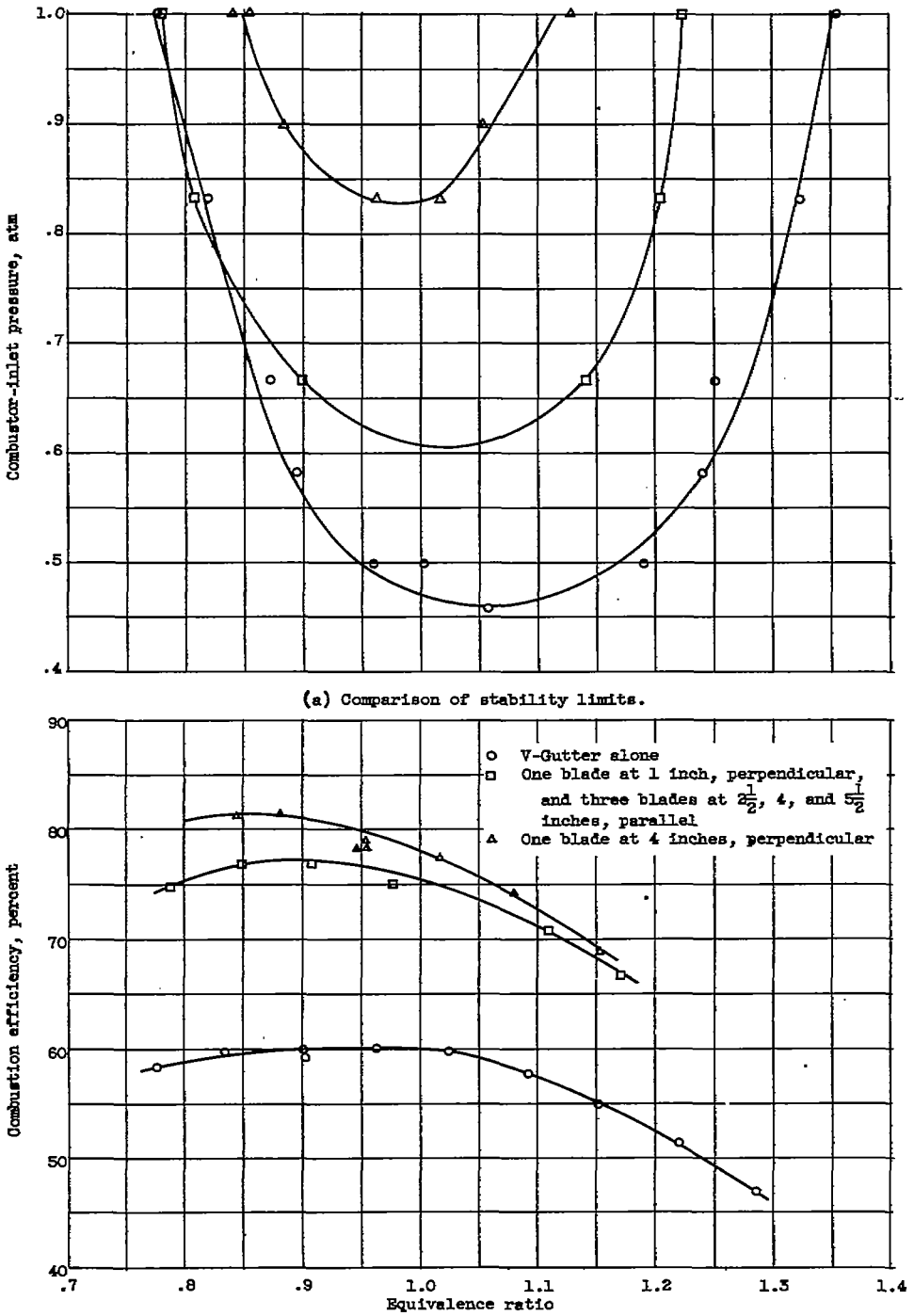

(a) Comparison of stability limits.

(b) Comparison of combustion efficiency.

Figure 147. - Effect of location of immersed surfaces on combustion efficiency and stability limits of 5-inch-diameter combustor. Inlet-air temperature, 660° R; inlet-air velocity, 220 feet per second.

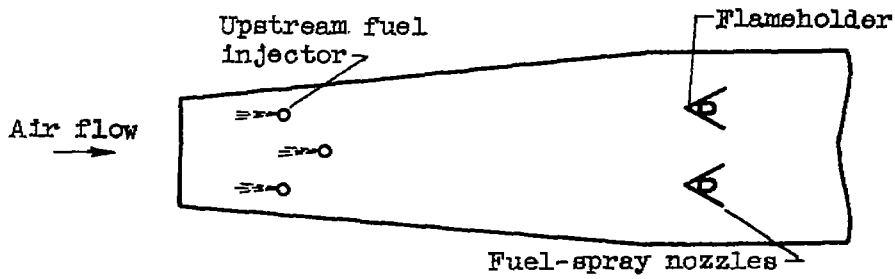

(a) Upstream-injection burner.

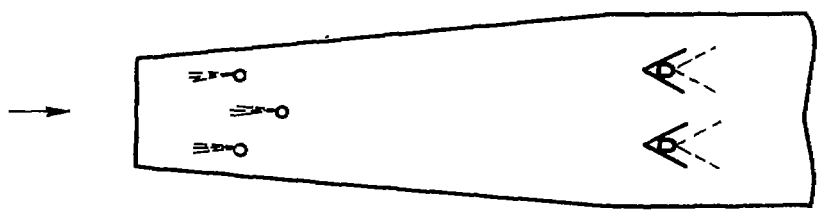

(b) Split-injection burner.

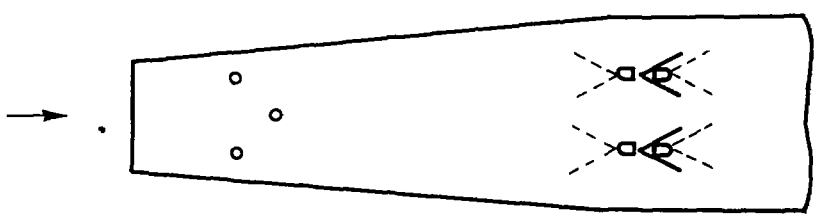

(c) Flameholder split-injection burner.

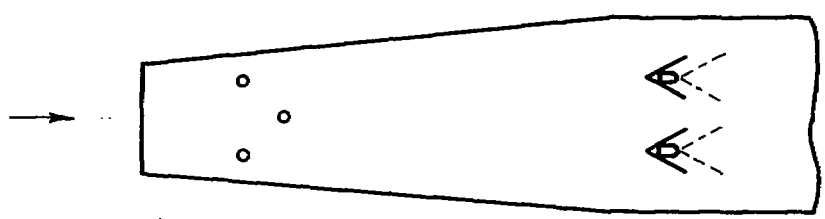

(d) Flameholder injection burner.

Figure 148. - Fuel-injection arrangements used in operational performance investigation of 20-inch ram jet (ref. 71).

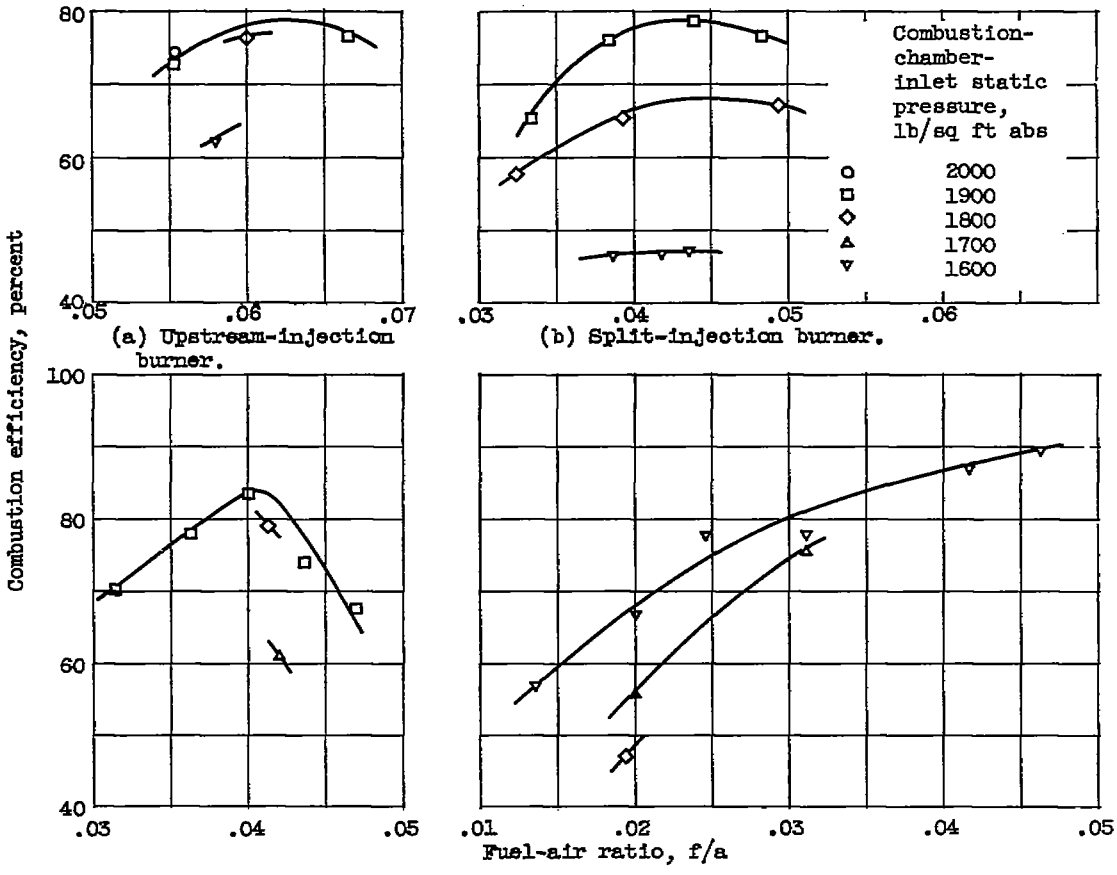

Figure 149. - Effect of fuel-injector location on combustion efficiency at various conditions of combustion-chamber-inlet static pressure. 20-Inch ram jet with 8-foot combustion chamber and 17-inch-diameter exhaust nozzle; ambient-air pressure, 20 inches of mercury absolute; equivalent pressure altitude, 10,100 feet (ref. 71).

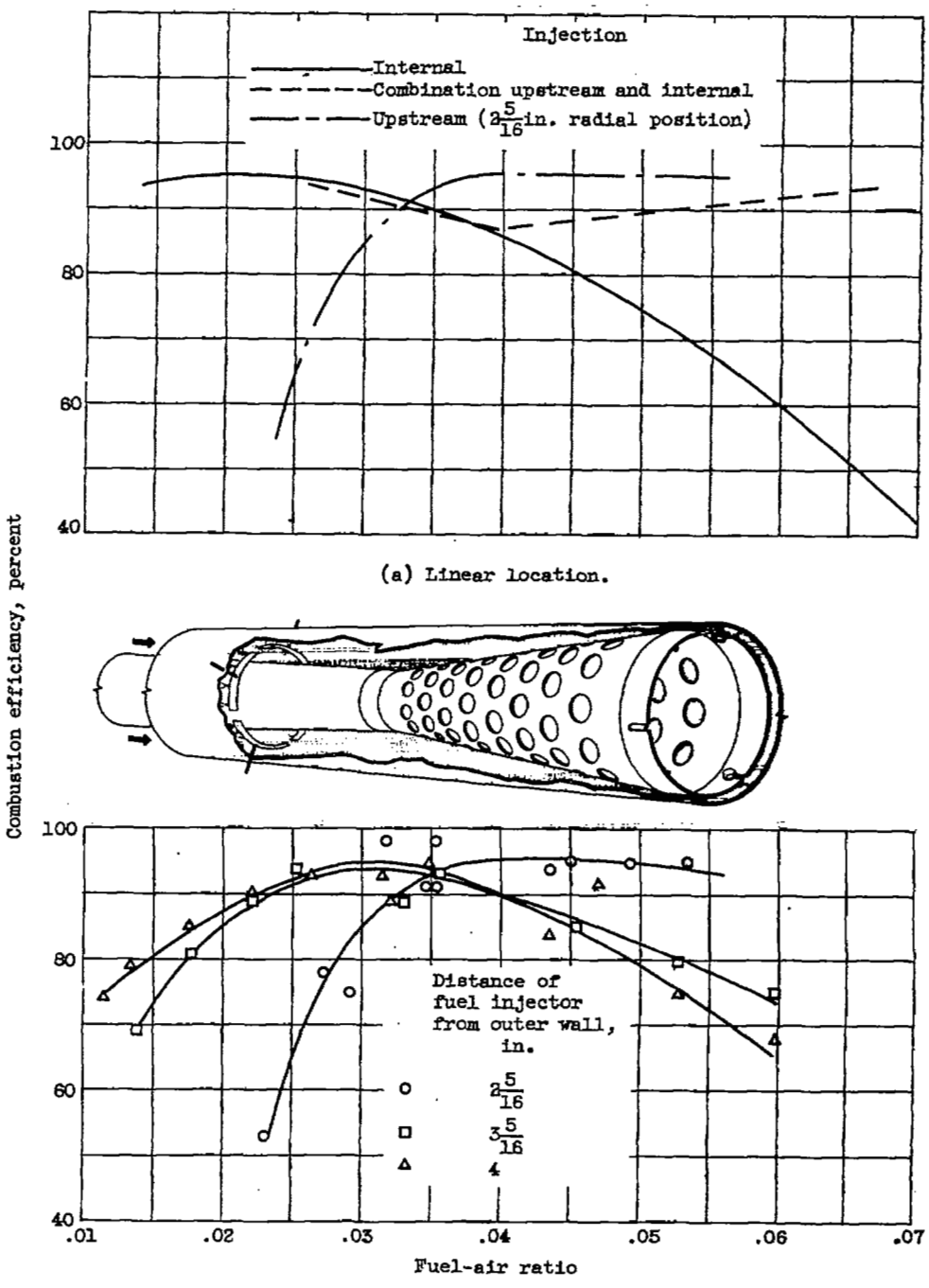

(a) Linear location.

(b) Radial location.

Figure 150. - Effect of fuel-injector location on performance of can-type combustor. Inlet-air pressure, 32 to 36 inches of mercury absolute; inlet-air temperature, 1050° to 1070° R; velocity, 230 to 260 feet per second; fuel, MIL-F-5624A grade JP-4 (ref. 72).

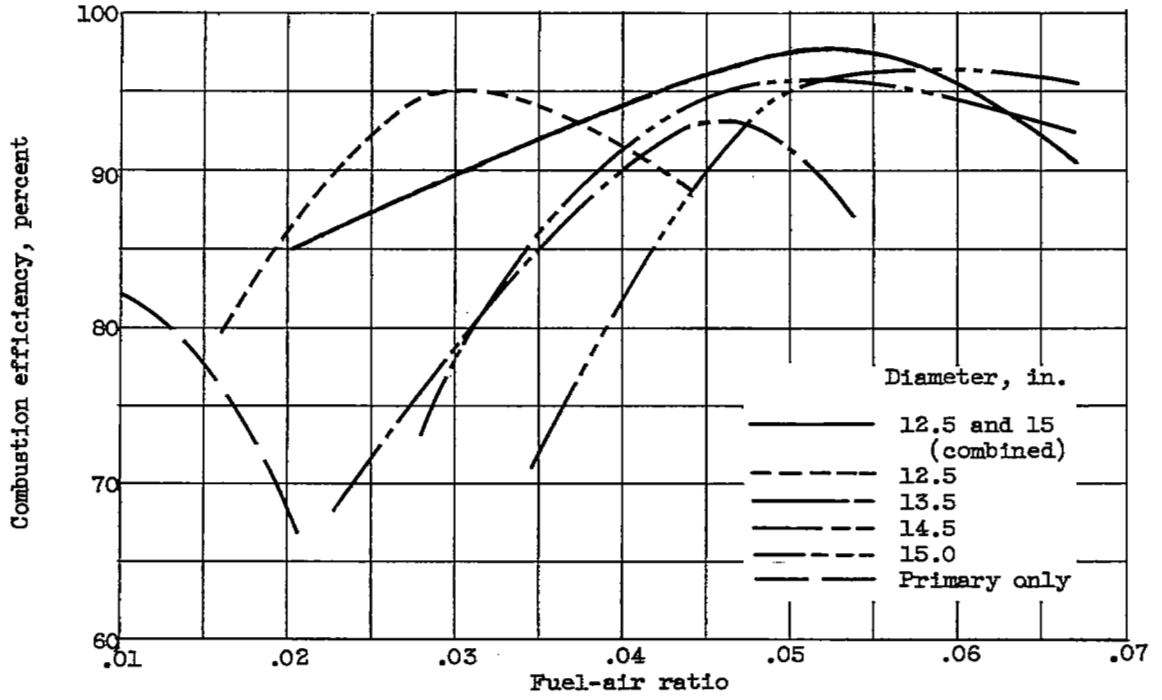

(a) Combustion efficiencies.

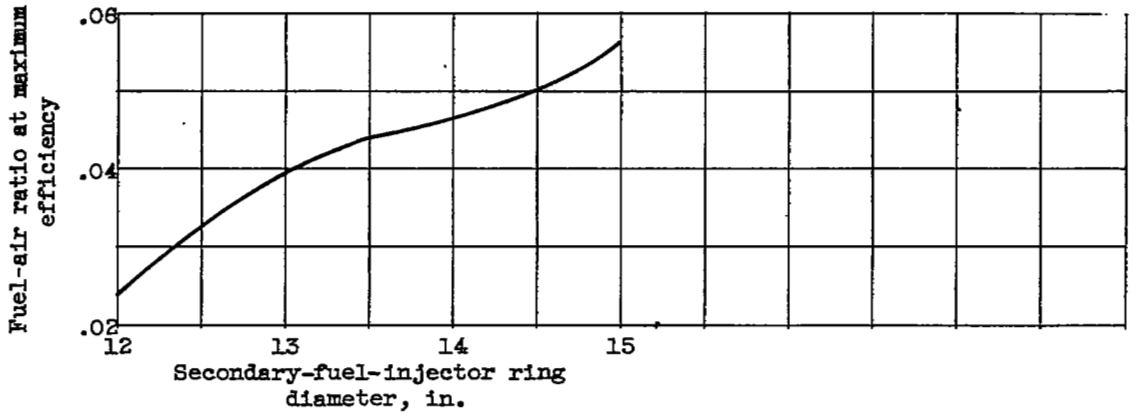

(b) Fuel-air ratio at maximum efficiency.

Figure 151. - Effect of secondary-fuel-injector ring diameter on combustion. Inlet-air pressure, 15 inches of mercury absolute; inlet-air temperature, 580° R; fuel, ANF-48; 20-inch-diameter combustor; 20-percent primary flow (ref. 73).

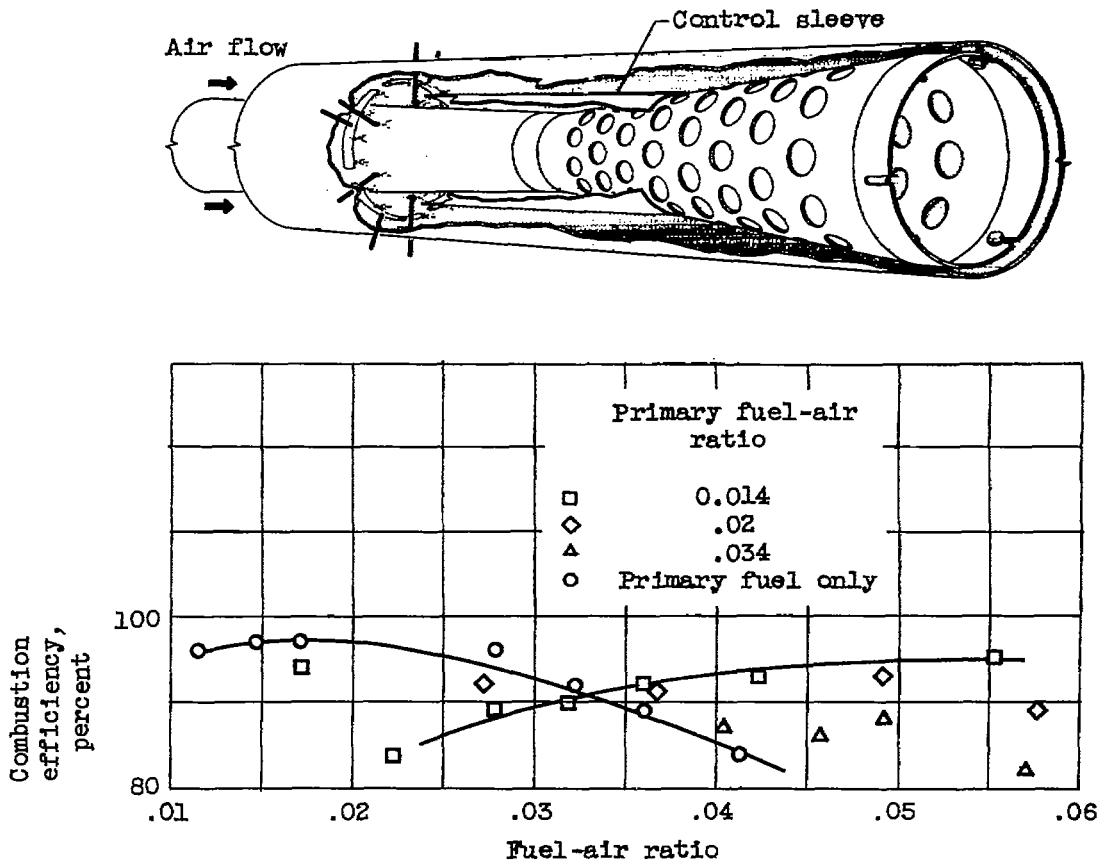

Figure 152. - Effect of fuel staging on combustor performance. Inlet-air pressure, 32 to 36 inches of mercury absolute; inlet-air temperature, 1050° to 1070° R; velocity, 230 to 260 feet per second; fuel, MIL-F-5624A (ref. 72).

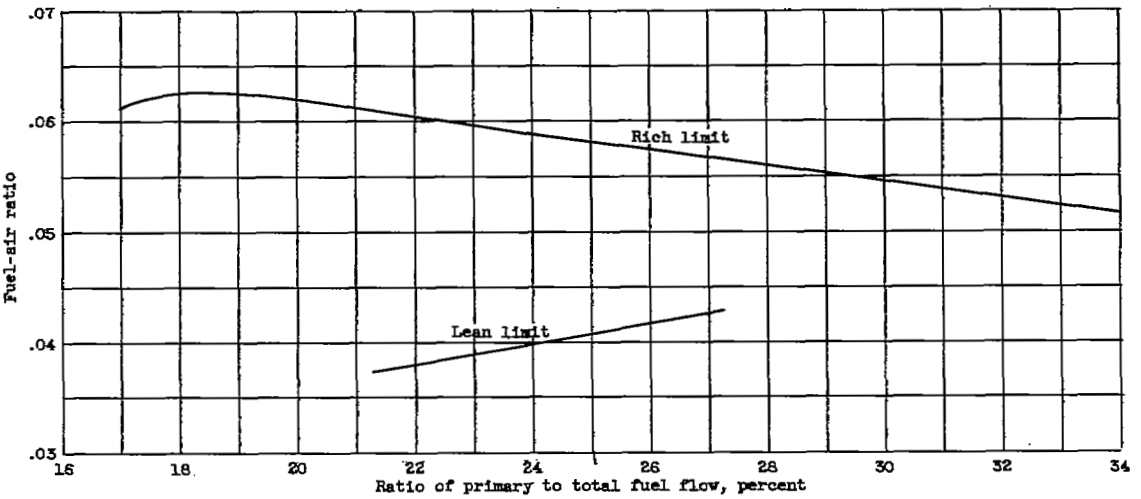

Figure 153. - Effect of primary fuel flow on combustor operating limits of 20-inch-diameter can combustor. Inlet-air pressure, 15 inches of mercury absolute; temperature, 910° R; velocity, 280±40 feet per second; fuel, ANF-48 (ref. 73).

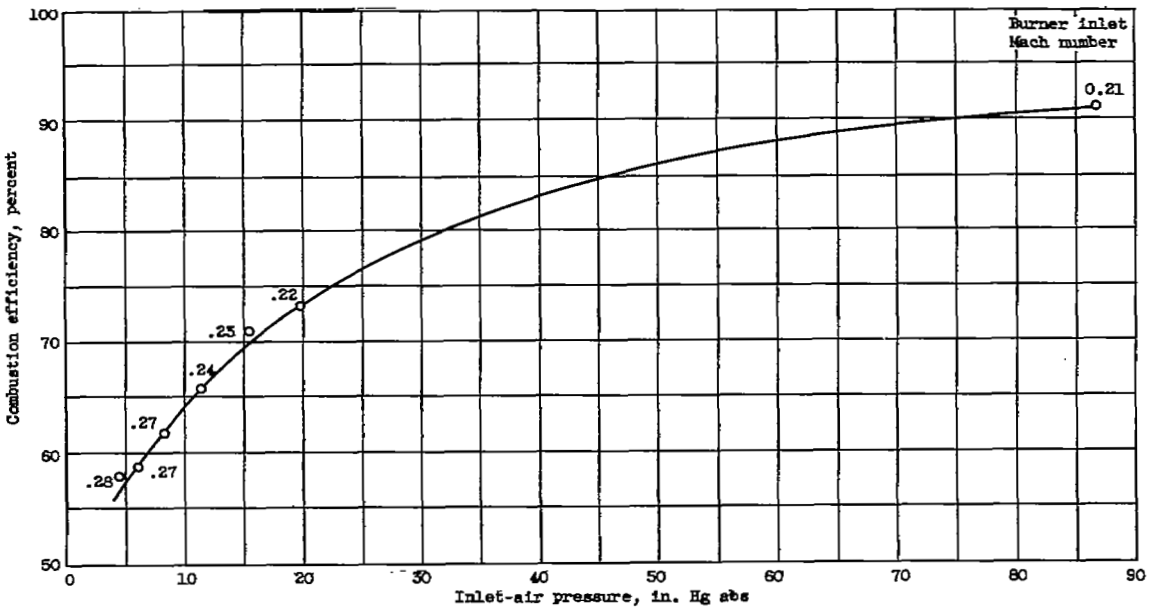

Figure 154. - Effect of inlet-air pressure on burner efficiency. Burner length, 14 inches; fuel, pentane; stoichiometric conditions; pilot heat, 10 percent (ref. 45).

[redacted]

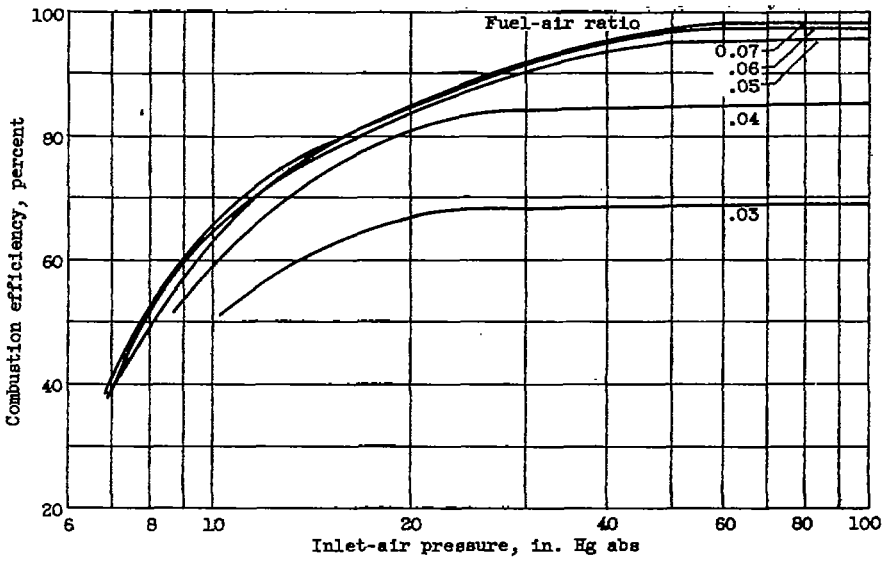

Figure 155. - Combustion efficiency of 20-inch-diameter ram-jet combustor as function of fuel-air ratio and burner inlet pressure. Inlet-air temperature, 920° R; fuel, ANF-58; exit nozzle, 55 percent (ref. 77).

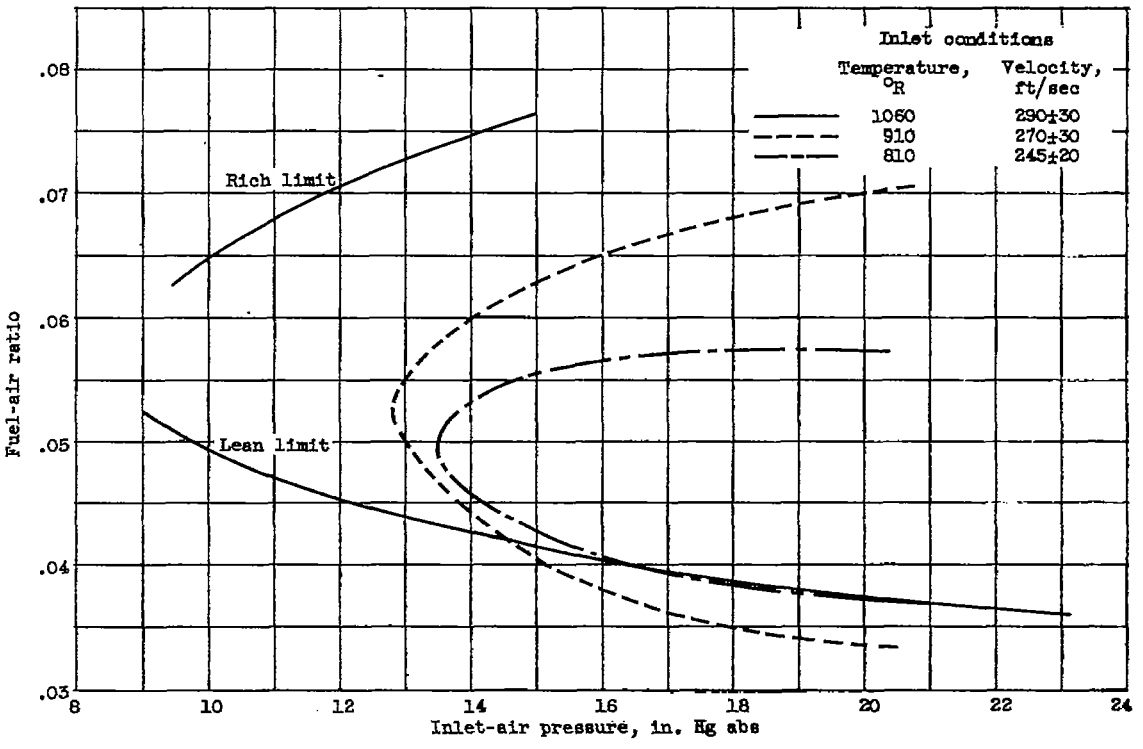

Figure 156. - Effect of inlet-air pressure on combustion limits for three inlet temperatures in 20-inch-diameter ram jet with can-type flameholder. Fuel, ANF-48 (ref. 73).

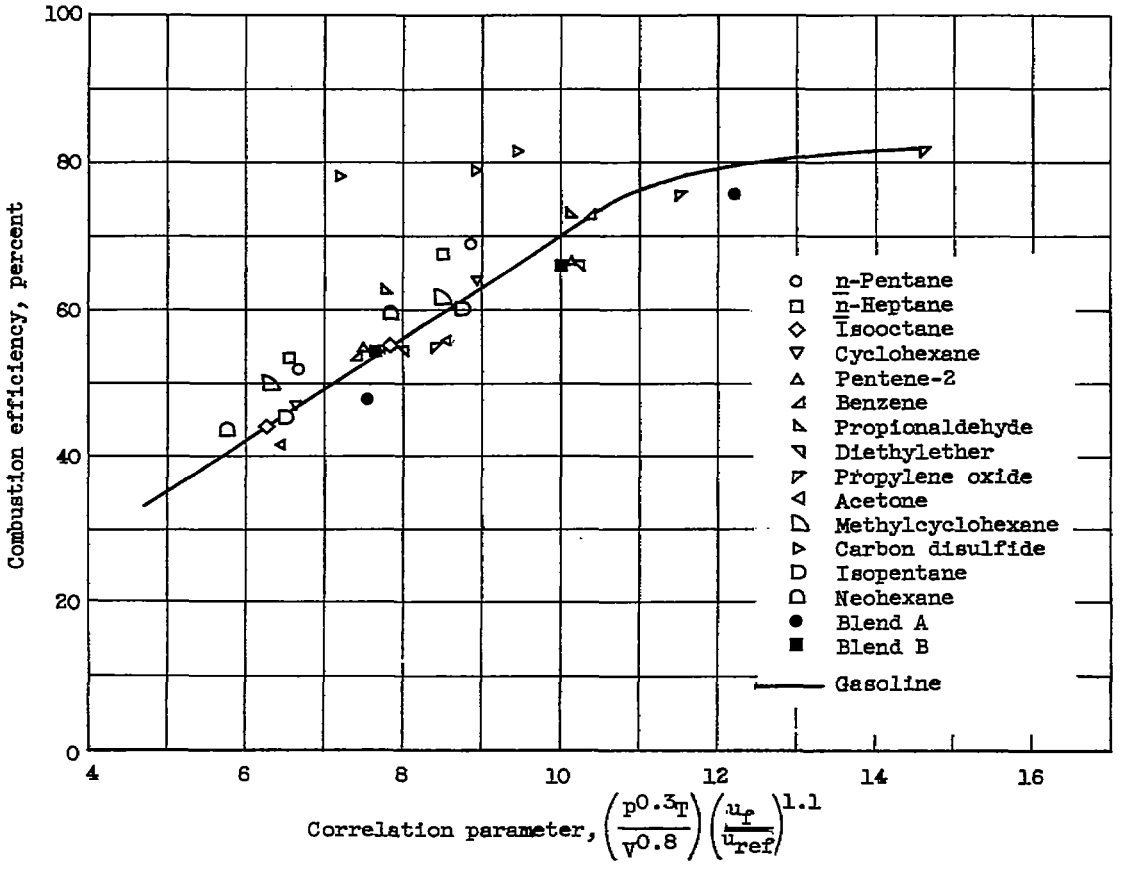

Figure 157. - Correlation of combustion efficiency for V-gutter flameholder in 5-inch ram-jet combustor for 14 pure fuels, a gasoline, and 2 fuel blends. (Blend A contains 2/3 propylene oxide plus 1/3 isopentane by weight; blend B, 1/3 propylene oxide plus 2/3 isopentane by weight.)

CHAPTER XV

EFFECT OF OPERATING CONDITIONS AND DESIGN ON AFTERBURNER PERFORMANCE

By Bruce T. Lundin, David S. Gabriel, and William A. Fleming

INTRODUCTION

Afterburners for turbojet engines have, within the past decade, found increasing application in service aircraft. Practically all engines manufactured today are equipped with some form of afterburner, and its use has increased from what was originally a short-period thrust-augmentation application to an essential feature of the turbojet propulsion system for flight at supersonic speeds.

The design of these afterburners has been based on extensive research and development effort in expanded laboratory facilities by both the NACA and the American engine industry. Most of the work of the engine industry, however, has either not been published or is not generally available owing to its proprietary nature. Consequently, the main bulk of research information available for summary and discussion is of NACA origin. However, because industrial afterburner development has closely followed NACA research, the omission is more one of technical detail than method or concept.

One principal difficulty encountered in summarizing the work in this field is that sufficient knowledge does not yet exist to rationally or directly integrate the available background of basic combustion principles into combustor design. A further difficulty is that most of the experimental investigations that have been conducted were directed chiefly toward the development of specific afterburners for various engines rather than to the accumulation of systematic data. This work has, nonetheless, provided not only substantial improvements in the performance of afterburners but also a large fund of experimental data and an extensive background of experience in the field. Consequently, it is the purpose of the present chapter to summarize the many, and frequently unrelated, experimental investigations that have been conducted rather than to formulate a set of design rules. In the treatment of this material an effort has been made, however, to convey to the reader the "know-how" acquired by research engineers in the course of afterburner studies.

The material presented is divided into the following topics:

(1) Experimental procedures

(2) Burner-inlet diffusers

(3) Ignition, starting, and transient performance

(4) Fuel-injection systems

(5) Flameholder design

(6) Combustion space

(7) Effect of operating variables on performance

(8) Combustion instability (screech)

(9) Effects of diluents on performance

Each topic is treated somewhat independently, although interacting considerations are discussed where known or important. Numerous references are listed for the convenience of those who may desire more detailed treatment than is possible herein.

No attempt is made to describe the details of the apparatus and test procedures used, although they are available in many of the references. The general range of afterburner operating conditions discussed comprise burner-inlet velocities from 400 to 600 feet per second, burner-inlet pressures from 500 to 3500 pounds per square foot absolute, inlet temperatures of approximately 1700° R, and afterburner fuel-air ratios from about 0.03 to about 0.08. Most of the data were obtained with afterburners operating on full-scale engines in either an altitude test chamber or an altitude wind tunnel. Some data were also obtained from static-test-stand engine setups and from full-scale afterburners connected to a preheater and an air-supply duct.

EXPERIMENTAL PROCEDURES

The blower-rig setup was provided with a preheater and an annular burner-inlet diffuser to simulate turbine-outlet conditions and was connected to central laboratory combustion-air and exhaust equipment. A choked, fixed-area exhaust nozzle that discharged into an exhaust plenum chamber was provided at the afterburner outlet. The full-scale turbojet engines used for most of the investigations were installed either in an altitude wind tunnel or in an altitude test chamber; some data were also obtained from static sea-level test stands. All engines were installed on thrust-measuring platforms.

In the engine installations, the principal independent operating variables were afterburner fuel-air ratio and inlet pressure. Variations in fuel-air ratio required simultaneous variation in exhaust-nozzle area by use of either a variable-geometry nozzle or a series of fixed nozzles in order to maintain constant turbine-inlet temperature; control of afterburner-inlet pressure was obtained by varying the simulated altitude of engine operation. Variations in afterburner-inlet velocity could be made independently of other operating variables only by changes in afterburner diameter. Afterburner-inlet temperature was established by engine operating requirements, and was not an independent variable of operation. Because the blower-rig setup was divorced from engine operating requirements, changes in inlet velocity could be made at constant values of inlet pressure and of fuel-air ratio by variations of the exhaust-nozzle area.

The type of fuel used in the various investigations was determined primarily by availability or, in the case of specific engine development programs, by military requirements. Most of the early experiments were therefore conducted with gasoline or kerosene, and later experiments with JP-3 or JP-4 fuel. Only a few experiments have been conducted in which a given afterburner was operated on more than one type of fuel. Specific data on the effect of fuel type are therefore not available. Except for differences in spontaneous ignition characteristics, as discussed later, however, no large effect of fuel type within the range used has become apparent in the general course of the work.

When the afterburner on the engine setups was equipped with a fixed-area exhaust nozzle, the afterburner-outlet temperature was determined by two methods. One is based on flow continuity through the nozzle throat and the other on momentum, or jet thrust, considerations. With the flow-continuity method, the actual measurements required to compute exhaust temperature are nozzle-outlet total pressure, effective nozzle flow area, and total gas flow; with the momentum method they are

nozzle-outlet total pressure, jet thrust, and total-gas flow. With proper instrumentation and by use of appropriate gas properties and nozzle coefficients, satisfactory agreement between the two methods is usually obtained. When the afterburner was equipped with a variable-area exhaust nozzle, the outlet temperature was usually computed only by the momentum method because of the uncertainty of the effective nozzle flow area under all conditions of operation. In the blower-rig setup, the burner thrust was not measured, and outlet temperature was therefore computed only by the flow-continuity method.

The combustion efficiency of an afterburner has been computed on at least four different bases in the various references cited. These four definitions of combustion efficiency are: (1) ratio of actual enthalpy rise to heat input in the fuel, (2) ratio of the ideal fuel flow for the actual temperature rise to the actual fuel flow, (3) ratio of the actual temperature rise to the ideal temperature rise for the fuel flow, and (4) ratio of actual enthalpy rise to ideal enthalpy rise based on the corresponding temperature rises. At fuel-air ratios above stoichiometric, methods (3) and (4) give values of efficiency appreciably greater than those computed by methods (1) and (2); at lower fuel-air ratios, all four methods substantially agree. The data presented herein from different sources are, however, either for fuel-air ratios at which the differences in efficiency are only 3 or 4 percent or the results from any one investigation, or within any one figure, are consistent within themselves. It was therefore considered unnecessary, for the purpose of this summary report, to reduce all efficiency data to a common basis. Because of the differences in efficiency calculations, however, and because different types of afterburners in various states of development were used, the results presented herein should not be compared from one unrelated figure to another.

For all calculations, the fuel-flow to the afterburner was taken to be the sum of the fuel directly injected into the afterburner and the unburned fuel entering the afterburner because of incomplete combustion in the primary engine combustor. The afterburner is thus made liable for unburned primary-combustor fuel. The afterburner fuel-air ratio is defined as the ratio of this weight of fuel to the weight of unburned air from the primary engine combustor (or preheater).

AFTERBURNER-INLET DIFFUSERS

The aerodynamic characteristics of the diffuser between the turbine exhaust and the afterburner inlet have an important influence on the performance of the afterburner. These characteristics, in conjunction with those of the turbine, determine both the velocity distribution and the mass-flow distribution entering the afterburner. The effectiveness of the diffuser in reducing gas velocity below the turbine-discharge value is important, because high burner-inlet velocities have a detrimental effect on afterburner performance. The mass-flow distribution determines the required fuel-flow distribution and, hence, the design of the fuel-injection system. In addition, diffuser pressure losses have a first-order effect on thrust.

Turbine-exhaust gases are discharged from the turbine into the annular inlet of the afterburner diffuser at average axial Mach numbers from 0.4 to 0.8, and at flow directions that may be axial or as much as 40° from the axial, depending on the turbine design. To provide satisfactory velocities at the afterburner inlet, the diffuser is usually required to have an area ratio between 1.5 and 2.0. Space and weight considerations usually dictate maximum diffuser length less than twice the afterburner diameter.

These are extreme diffuser requirements and in most cases they lie outside the realm of known diffuser-design techniques. It is not surprising that large pressure and velocity gradients usually exist at the outlet of afterburner diffusers, or that an appreciable loss in total pressure occurs in the diffuser.

Effect of Diffuser-Outlet Velocity on Afterburner Performance

No precise criteria are known that relate the performance of an afterburner to the magnitude of the velocity gradient at the burner inlet. Experience has shown, however, that afterburner performance is sensitive to magnitude of the velocity of the gases flowing around the flameholders, deteriorating as the gas velocity near the flameholders increases. A typical example from reference 1 of the effect of velocity on the performance of a highly developed afterburner is shown in figure 158. The afterburner was about $4\frac{1}{2}$ feet long and had a conventional V-gutter flameholder and conventional fuel-system components. As shown in figure 158(a), the inlet velocity at the center of the burner was low (typical of most afterburner diffusers) compared with the velocity in the region of the flameholders. When the average velocity through the afterburner was about 380 feet per second, the velocity near the flameholders was approximately 440 feet per second. As the average velocity increased, the velocity in the center of the burner remained about the same but the velocity near the flameholders increased. At an average velocity of 675 feet per second, the velocity near the flameholders was as high as 800 feet per second.

The combustion efficiency, as shown in figure 158(b), decreased considerably as the average inlet velocity increased. At a burner-inlet pressure of 570 pounds per square foot the efficiency decreased from about 0.88 at an average inlet velocity of 380 feet per second to about 0.60 at an average inlet velocity of 680 feet per second. It is apparent that, in this burner, the velocity in the region of the flameholders may not exceed 450 to 500 feet per second if combustion efficiencies of 0.85 or higher are to be maintained at low burner-inlet pressures; to maintain efficiencies of 0.8, local velocities should not exceed about 600 feet per second. At high afterburner-inlet pressures, the performance is considerably less sensitive to velocity. As shown in the figure, at a burner-inlet pressure of about 1100 pounds per square foot, combustion efficiencies above 0.80 may be obtained with local velocities of about 750 feet per second, corresponding in this case to an average velocity of about 675 feet per second.

Similar trends have been found in other investigations. For example, in one afterburner development (ref. 2) in which the velocity in the region of the flameholder was about 700 feet per second, combustion efficiencies above 0.72 could not be obtained at low burner-inlet pressures, even though a relatively long burner length was used and extensive development effort was expended on the flameholder and fuel system.

A qualitative measure of the merit of an afterburner-inlet diffuser is, therefore, the magnitude of the gas velocities it provides in the region of the flameholder. For an afterburner about $4\frac{1}{2}$ feet long that is to operate at low inlet pressures, the diffuser should provide velocities in the region of the flameholder that do not exceed 500 to 600 feet per second. For high inlet pressures, local velocities as high as 750 feet may be acceptable.

In the absence of a rigorous method of diffuser design, two general types of diffuser have been developed. One is a long diffuser having a gradually increasing

flow area, and the other is a short diffuser in which the inner body ends abruptly at some convenient length. With the short diffuser, the blunt end of the inner body can serve as part of the flameholding surface. With long diffusers, the average velocity of the gases entering the burner is low, but some combustion length is sacrificed (for a given over-all afterburner length); with short diffusers, combustion length is greater but gas velocities are higher. It is evident that one of the parameters of primary importance in determining the effect of diffuser performance on afterburner performance is the diffuser length. Other design features of interest are the shape of the diffuser inner body and the type of control devices, such as vortex generators, or vanes, that may be added to improve performance.

Effect of Diffuser Length

The effects of diffuser length on diffuser-outlet velocity profiles and pressure losses are reported in reference 3, which presents the performance of the series of four diffusers represented in figure 159. Diffuser length varied from less than 0.1 diameter to 1.05 diameter; all had an outlet-inlet area ratio of 1.92. Accompanying the variation in length was a variation in the shape of the inner body that, as will be discussed in a subsequent paragraph, probably had little effect on performance. The diffusers were tested in a duct that imposed a diffuser-inlet velocity distribution approximating fully developed pipe flow. This velocity distribution is an approximate simulation of the diffuser-inlet velocity conditions in some engines.

Velocity profile at the diffuser outlet and the pressure loss for the four diffusers are shown in figure 160. As discussed in reference 3, because of the errors inherent in measuring total pressures in highly turbulent streams, the values of pressure drop presented should be considered qualitative and indicative of relative losses only. Pressure loss data for diffuser 4 have no intrinsic significance, inasmuch as the diffuser consists simply of a sudden expansion. As diffuser length was increased the loss in total pressure increased but the velocity profile improved.

With diffuser 3 (fig. 160(b)), the velocity in the region in which flameholders would be located was above 0.8 of the diffuser-inlet velocity. If diffuser 3 were to be used with an afterburner, the average burner-inlet velocity could not exceed approximately 400 feet per second (corresponding to a diffuser-inlet velocity of about 700 ft/sec), if velocities in the flameholder region are to be maintained below the 500 to 600 feet per second required for good high-altitude performance. Increasing the length-diameter ratio from 0.51 (diffuser 3) to 1.05 (diffuser 1) would permit an increase in average burner-inlet velocity to approximately 470 feet per second without exceeding velocities of 500 to 600 feet per second in the flameholder region. The average burner-inlet velocity requirement for most modern engines is generally between 450 and 550 feet per second. It is apparent that although the increase in length from 0.51 to 1.05 diameters considerably improves the performance of this series, a length-diameter ratio of 1.0 (at an area ratio of 1.92) is not great enough to assure efficient burner operation at high altitudes for all modern engines.

Data are not available to show directly the effect on velocity profile of increasing the length of the 1.92-area-ratio diffusers beyond the 1.05 length-diameter ratio. In figure 161 the performance of the three diffusers shown in figure 160 is plotted as the ratio of the average burner-inlet velocity to the approximate velocity of the gases flowing through the portion of the burner inlet in which flameholders would be located, against the length-diameter ratio. The improvement in this velocity ratio as diffuser length increases is evident. Extrapolation of these data indicates that a diffuser length-diameter ratio of about 1.5 would permit the

[redacted]

use of average burner inlet velocities of about 500 feet per second. Figure 161 also presents data for two diffusers having greater values of length-diameter ratio. One, with an area ratio of 1.5, has a length-diameter ratio of 2.35; the other, with an area ratio of 1.3, has a length-diameter ratio of 1.85. An improvement in velocity ratio is evident for the longer, lower area-ratio diffusers as compared with the 1.92-area-ratio diffusers. Although a direct quantitative comparison of the data for the five diffusers can not be made because of differences in diffuser-inlet conditions, the improvement undoubtedly is the combined results from both the increase in length and the decrease in area ratio. Sufficient data are not available to separate the two effects. It appears, however, that with reasonably uniform diffuser-inlet conditions, maldistribution of velocity at the burner inlet will limit the average velocity that may be tolerated without large performance losses only for installations in which the length-diameter ratio is less than about 2, and the area ratio is greater than $1\frac{1}{2}$.

Diffusers with Truncated Inner Bodies

In many diffusers, the flow separates from the inner body several inches upstream of the diffuser outlet. Such flow separation occurred, for example, in diffusers 2 and 3 (fig. 159). In such cases, the presence of an inner body downstream of the separation point probably has no effect on diffuser performance. The diffuser inner body could therefore have been cut off at the separation point, thus providing a reduction in over-all length without altering the performance. If, however, the inner body is cut off appreciably upstream of the separation point, an effect of length on performance would be expected. Performance of some diffusers altered in this manner is presented in reference 4; the data are summarized in figure 162. This figure presents the pressure losses and the diffuser-outlet velocity profile for truncated diffusers of two lengths and of two inner-body angles (or diffuser area ratio) for a given length.

Increasing the length-diameter ratio from 0.35 to 0.5 resulted in a significant improvement in velocity profile and a reduction in total-pressure losses of over 50 percent. Performance of the two diffusers having a length-diameter ratio of 0.5 was not affected by the small difference in outlet-to-inlet area ratio.

As previously discussed, cutting off the diffuser before the separation point results in an increase in velocity at the diffuser outlet compared with a diffuser that extends to the separation point. The ratio of average burner-inlet velocity to local velocity in the flameholder region for the two longest cut-off diffusers of figure 162 is approximately 0.7. Such diffusers could therefore be used in afterburners with average inlet velocities of about 390 feet per second without sacrifice in altitude performance or increase in burner length. Although the velocity ratio of 0.7 is about the same as that presented in figure 161 for a 1.92-area-ratio diffuser with a length-diameter ratio of 0.51, no generality is implied by the results because of differences in area ratio and diffuser-inlet conditions.

Effect of Inner-Body Shape

As discussed previously, it was assumed in the investigation of diffuser length that the shape of the inner body has a negligible effect on diffuser performance. The validity of this assumption is supported by the results of previously unpublished NACA tests, shown in figures 163 and 164. Figure 163 shows the configurations and axial area variation of two diffusers with different inner bodies that were tested in an afterburning engine. The rate of change of flow area with length was

greatly different for the two inner bodies up to a length of about 34 inches. The velocity distribution was measured at the 34-inch station. As shown in figure 164, the velocity profiles were very nearly the same with the two inner bodies. These results indicate that inner-body shape (for a constant diffuser length) has only a minor effect on diffuser-outlet velocity profile. The data also showed pressure losses for the two diffusers were very nearly the same.

Flow-Control Devices

Of the numerous flow-control devices that have been used in flow passages, only vortex generators have been comprehensively investigated in diffusers suitable for afterburner inlets. Brief investigations have, however, also been made of annular vanes and annular shrouds or splitter ducts.

Vortex generators. - References 3, 5, 6, and 7, discuss tests in which vortex generators were used to energize the boundary layer along the inner cone (and in some cases along the outer shell as well). Their action is to delay flow separation, and thereby permit the use of slightly shorter diffusers without loss in performance or slightly improve performance for the same diffuser length. It has been found that differences in diffuser-inlet velocity profile, diffuser length, inlet whirl, and diffuser shape all influence the optimum vortex generator configuration. In general, it has been found that effective vortex generators must be placed several chord lengths upstream of the diffuser separation point and must be long enough radially to extend through the boundary layer into the free stream. For diffusers 2 or 3 feet in diameter, from 20 to 40 equally spaced vortex generators are required. Chord length was between 1 and 3 inches and angle of attack was between 13° and 15° in most tests. Within this range, the effectiveness of the vortex generators was not sensitive to chord length or angle of attack. The optimum values of axial location and vortex generator span must be determined experimentally for each configuration.

Typical effects of vortex generators on diffuser performance are shown in figure 165. Outlet-velocity distributions are given for diffusers 1 and 3 of figures 159 and 160. The vortex generator configurations used in these tests were considered to be approximately optimum on the basis of preceding investigations. Twenty-four vortex generators were installed 1 inch upstream of the confluence of the cylindrical section of the diffuser inlet section and the curved portion of the inner body. Each was an NACA 0012 untwisted airfoil of 3-inch chord and 1/2-inch span with the chord skewed 15° to the axis of the diffuser. Alternate vortex generators were skewed to the left, and the intermediate ones skewed to the right. With both long and short diffusers, the vortex generators improve the velocity profile only slightly. The effect of vortex generators on pressure drop has also been found to be very small.

Annular vanes. - Cascades of annular vanes are suggested in reference 8 as a device to improve velocity distribution in diffusers. A brief investigation of annular vanes for afterburner diffusers is reported in reference 6. Three configurations investigated and their outlet-velocity distributions are shown in figure 166. In configuration A, a cascade of five annular vanes was installed, with a blunt inner cone. The vanes were simple, slightly cambered, sheet metal hoops with rounded leading edges. Successive vanes had slightly different angles of attack as suggested in reference 8. As shown in figure 166, the outlet-velocity profile with this configuration was fairly uniform, neglecting small gradients caused by wakes off the vanes. The pressure loss of configuration A was very high, however, (7 percent of diffuser-inlet total pressure). Configuration B had a longer inner cone, with vortex generators attached and no annular vanes. Although the pressure

loss was only about two-thirds that of diffuser A, the velocity profile was poor with a large separated region in the center of the burner. The vortex generators were removed from configuration B, and the two upstream vanes of diffuser A were installed to form configuration C. Both pressure loss and velocity profile were about the same for configuration C as for configuration B.

On the basis of these preliminary tests, annular cascades are effective in preventing large gradients in burner-inlet velocity, but only at the expense of large pressure losses. Additional development may produce a more favorable combination of inner body and vanes.

Splitter shrouds. - The use of splitter shrouds to divide the diffuser into two concentric annular passages was briefly investigated in reference 9. The short diffuser represented in figure 167 was tested with and without a splitter shroud surrounding the inner body. The splitter produced a lower velocity in the outer 4 inches of the diffuser outlet, but velocity in the center of the annulus was increased to an undesirably high value. With the splitter, diffuser pressure loss was slightly higher.

These results have been generally confirmed by tests in other types of diffusers. The use of the splitter reduces the velocity in one passage, but the reduction is usually accompanied by an increase in velocity in the other passage to undesirably high values. Although the data available are by no means conclusive, splitter shrouds seem to be of doubtful advantage.

Effects of Whirl on Diffuser and Afterburner Performance

Depending on engine design and to some extent on engine operating conditions, the direction of flow at the turbine outlet (diffuser inlet) may be as much as 20° to 30° from axial. Typically, as the flow progresses through the diffuser the angle of whirl increases, with the greatest increase occurring near the center body. As a result, a diffuser-inlet whirl angle of about 20° may result in an average diffuser-outlet (afterburner-inlet) whirl angle as high as 40° or 50° with local whirl angles near the center body as high as 70° or 80° (ref. 3). The effects of this whirl on afterburner and diffuser performance have been investigated in reference 10, and some typical results are reviewed in the subsequent paragraphs.

Effects of whirl on afterburner performance. - In figure 168, the effects of whirling flow on the combustion efficiency of the typical afterburner of reference 10 are shown. The whirl angles at the diffuser outlet (without straightening vanes) were greater than 30° (fig. 168(a)) over most of the flow passage. Performance of the afterburner with this large whirl and with most of the whirl eliminated by straightening vanes is compared in figure 168(b). It is evident that whirl has no significant effect on afterburner combustion efficiency. Similar results were obtained over a range of altitudes between 30,000 and 50,000 feet. Because changes in whirl angle result in changes in velocity and mass flow distribution at the afterburner inlet, it was necessary to revise the fuel distribution to obtain an optimum distribution when the whirl angle was changed. The afterburner was otherwise unchanged for the comparative tests.

Although whirl angle has little effect on combustion efficiency, large whirl angles can lead to operational problems. In burners with a large amount of whirl and with fuel injection ahead of inner-body support struts, flame may seat in the wakes from these struts and cause warping and buckling of the diffuser parts. To avoid these operational difficulties, it seems advisable to reduce whirl at the burner inlet. Experience indicates that whirl angles at the burner inlet up to approximately 20° may be tolerated without operational difficulty.

Flow-straightening vanes. - Airfoil-shaped flow-straightening vanes have been installed at the turbine discharge in several investigations to reduce whirl. Some of the vanes were fabricated from sheet metal and some were cast. Typical effects of straightening vanes on the diffuser-inlet whirl angle are shown in figure 169. Without straightening vanes whirl angle in excess of 20° (corresponding to diffuser-outlet whirl angles of approximately 40°) occurred over most of the passage. With straightening vanes, the whirl angle was 10° or less. Similar results have been obtained in other investigations (see fig. 168(a)).

The shape of the straightening vanes used is illustrated in figure 170. The vanes, designed to produce axial discharge, have the leading edge skewed to the diffuser axis at the approximate whirl angle. This inlet angle varies radially to match the local whirl angle, and chord length is greatest in the region of greatest whirl. Maximum effectiveness is obtained with vanes spanning the full passage. A ratio of vane spacing to vane chord of about 3/4 has provided satisfactory performance in several designs.

The presence of vanes in the high-velocity gas stream at the turbine discharge has been found to approximately double the pressure loss in the diffuser-vane combination. However, the reduction in whirl caused by the vanes reduces the resultant velocity over the flameholder (by reduction of the tangential component) and thereby reduces the flameholder pressure loss. As a consequence, it has been found that in most installations the over-all afterburner pressure losses are approximately the same with and without straightening vanes.

Summary

Typical afterburner-inlet diffusers produce varying degrees of nonuniformity in the velocity profile at the burner inlet, with high velocities near the outer wall in the region of the flameholder and lower velocities in the center of the burner. Because the gas velocity at the flameholder is usually limited by combustion considerations, the allowable average burner-inlet velocity, and hence the burner diameter, is largely a function of the uniformity of this velocity profile. One of the most significant design variables affecting the outlet-velocity distribution is diffuser length. Although data are not available to provide detailed design rules, several investigations have demonstrated that increasing diffuser length results in a more uniform velocity profile although with some increase in pressure loss. The shape of the diffuser inner body has no appreciable effect on its performance. Vortex generators provide small improvements in diffuser velocity profile, but other flow-control devices such as annular vanes and splitter ducts have not been successfully applied. Afterburner-inlet whirl has a negligible effect on combustion efficiency but may lead to burning in the wakes of support struts and attendant overheating and warping of adjacent parts of the diffuser. Turbine-outlet whirl may be reduced to acceptable values by relatively simple straightening vanes.

IGNITION, STARTING, AND TRANSIENT PERFORMANCE

The afterburner starting cycle includes three steps: (1) introduction of the fuel, (2) ignition of the fuel, and (3) control of exhaust-nozzle area to obtain steady-state afterburner operation. The ignition phase of afterburner starting has been investigated in somewhat greater detail than the other two phases because of the need for repeated starts during afterburner investigations in altitude facilities.

Introduction of Fuel

A significant portion of the time required to start an afterburner after the control lever is advanced to the afterburning position is consumed in accelerating the fuel pump and filling the afterburner fuel lines and manifold. The time required to fill the fuel piping and manifolds is obviously directly proportional to the volume of the piping that must be filled at each start and inversely proportional to the fuel-flow rate set by the starting control. The time required to accelerate the conventional turbine-driven fuel pump usually does not exceed 1 second at any flight condition. Likewise, the time required to fill the afterburner fuel piping at low altitudes where the fuel-flow rates are high is also very short. At high-altitude conditions, however, the time required to fill a given volume of fuel piping becomes quite significant because of the reduced fuel-flow rate.

The effect of this set, or starting, fuel-flow rate on the time required to reach operating manifold pressure is shown in figure 171. Data are presented for a 6000-pound sea-level-thrust engine (ref. 11) and for a 10,000-pound-thrust engine. The afterburner fuel systems of the two engines were similar and utilized air-turbine-driven fuel pumps, with the turbine driven by compressor bleed air. The volume of piping that had to be filled prior to each start (neglecting any residual fuel downstream of the fuel shut-off valve) was approximately 135 cubic inches for the 6000-pound-thrust engine and 200 cubic inches for the 10,000-pound-thrust engine.

In figure 171, the time required to reach the operating manifold pressure is plotted against the ratio of the fuel-system volume to the starting fuel-flow rate. Data are presented for several flight conditions, which define a single curve. The time required to fill the fuel systems varied from 2 to 9 seconds, with the longer times occurring at the higher altitude conditions, where the flow rates were lowest. Agreement of the two sets of data indicates that the time required to accelerate the fuel pump to delivery speed was about the same for both systems. Measurements on the 10,000-pound-thrust engine showed that about 1 second of the total time was required to accelerate the pump from rest. These data thus indicate that to avoid delays in filling the fuel system before the afterburner can be ignited, it is important to keep to a minimum the volume of fuel piping that must be filled prior to each afterburner start.

Ignition

Three general methods of igniting afterburner fuel have been used: (1) spark ignition, (2) spontaneous ignition, and (3) hot-streak ignition. Some of the early research on these methods of ignition is summarized in reference 12. The spark ignition method utilizes a spark plug to ignite a combustible mixture provided within a sheltered region of the burner. Spontaneous ignition is obtained in an afterburner when the pressure, temperature, velocity, and fuel-air ratio conditions within the burner are such that the fuel-air mixture ignites without addition of energy from an outside agency. In the hot-streak method, afterburner ignition is obtained by momentarily increasing the fuel-air ratio in one of the primary engine combustors to about twice the normal operating value. This momentary excess of fuel produces a streak of flame that extends through the turbine and into the afterburner and thus provides the ignition source for the afterburner fuel.

Spark ignition. - Most of the early afterburners utilized a spark-ignition system (ref. 13 and an unavailable NACA publication). The spark plug was generally installed in a sheltered region at the downstream end of the afterburner diffuser inner body, as illustrated in figure 172. Experience with this type of system

indicated that ignition could seldom be initiated at altitudes above about 30,000 feet, and the systems were not particularly reliable at lower altitudes.

Three factors contribute to the poor reliability of the spark ignition method. One factor is breakdown of the electrical insulation in the region of high gas temperature, which causes a short circuit in the ignition lead. A second factor is melting or burning of the electrodes during afterburner operation, which prevents reignition of the burner. A third factor often preventing ignition is that the spark is either improperly located or releases too little energy to initiate ignition. The ignition systems used provided a spark energy of only about 0.02 joule per spark at a repetition rate of several hundred sparks per second. Although higher spark energies, such as those provided by the capacitor-type systems discussed in chapter III of reference 14, would be expected to improve the ability of the spark to effect ignition, no good solution to the problems of electrode insulation breakdown or electrode burning has been obtained. Because other methods of afterburner ignition held promise of being more reliable, further development of a spark system for afterburner ignition was discontinued.

3925

Spontaneous ignition. - Methods of spontaneously igniting the afterburner fuel have also been investigated to determine the applicability and degree of effectiveness of this method. Although this method of ignition was seldom employed in gasoline-fueled afterburners without an explosive light-off, the conversion to kerosene and later to JP-3 and JP-4 fuels sufficiently lowered the spontaneous-ignition temperature of the fuel to provide satisfactory spontaneous-ignition characteristics in some afterburners. The spontaneous-ignition temperature of several fuels is indicated by the following values from chapter III of reference 14.

Fuel	Spontaneous-ignition temperature, °F
Grade 100/130 aviation gasoline	844
Kerosene	480
JP-3 fuel	484
JP-4 fuel	484

These temperatures were measured in a static system and are much lower than the temperatures required for ignition in afterburners. Nevertheless they should indicate the relative ease with which different types of fuels can be spontaneously ignited under afterburner conditions. Although the above fuels ignited spontaneously in some afterburners, in other afterburner configurations spontaneous ignition could not be obtained at turbine-outlet temperatures up to current maximum values of 1700° to 1750° R.

There are no consistent results available to indicate the specific differences in afterburner design that result in some burners' being readily ignitable spontaneously while others are not. It is, in fact, concluded in chapter III of reference 14 that the effects of various design or operating variables on spontaneous ignition (designated therein as ignition by hot gases) are incompletely understood. However, it has been observed in various afterburner experiments that relatively minor alterations in radial fuel distribution may have marked effects on the spontaneous-ignition characteristics. In general, it is believed that the two afterburner design factors having a major influence on the ability to obtain

[redacted]

ignition in this manner are the fuel-air-ratio distribution and the velocity profile within the burner. Fuel-air ratios that are somewhat richer than stoichiometric in a sheltered zone, with low velocities in and near such a zone, are believed to promote spontaneous ignition.

Spontaneous ignition has been obtained at burner-inlet pressures as low as about 500 pounds per square foot absolute; both burner-inlet pressure and burner-inlet temperature have been found to exert a pronounced effect on ignition limits (ref. 15). The effects of inlet pressure and temperature on the limits of spontaneous ignition with JP-3 in one afterburner configuration are shown in figure 173. Each data point on this figure represents a single afterburner start; the fuel-air-ratio value is that at which ignition occurred as the afterburner fuel flow was gradually raised. Each curve thus represents a boundary between the ignition and no-ignition regions at a given pressure. The region to the left of each curve represents the fuel-air ratios at which spontaneous ignition could not be obtained. At a burner-inlet pressure of about 1500 pounds per square foot absolute, the inlet temperature had no effect on the fuel-air ratio required for successful ignition, but at lower pressures, large increases in fuel-air ratio were required to obtain spontaneous ignition as the burner-inlet temperature was reduced. Similarly, these data show that for a given fuel-air ratio a reduction in burner-inlet pressure required a large increase in burner-inlet temperature for spontaneous ignition to occur. Spontaneous ignition of this afterburner was unobtainable at a burner-inlet pressure of 500 pounds per square foot.

The effect of burner-inlet pressure on the fuel-air ratio required to obtain spontaneous ignition for several other afterburner configurations is illustrated in figure 174. As in the previous figure, each data point represents a single afterburner start as afterburner fuel flow was being increased. These data also indicate that higher fuel-air ratios are required to obtain spontaneous ignition as the burner-inlet pressure is reduced. It should also be noted that there are appreciable differences in the required fuel-air ratio among the several configurations. The poor reproducibility of spontaneous-ignition limits is indicated by the wide band of fuel-air ratio over which ignition occurred in the several configurations.

The effect of altitude on the time required for spontaneous ignition to occur after the preset fuel manifold pressure is reached differs greatly among various afterburners. In one installation, the time required for spontaneous ignition increased from about 4 seconds at an altitude of 15,000 feet to 40 seconds at an altitude of 45,000 feet (unpublished NACA data). In contrast to this result, another quite similar afterburner (ref. 11) exhibited little effect of altitude on spontaneous ignition time, with the time for ignition varying between 4 and 8 seconds at altitudes between 30,000 and 50,000 feet.

These data, as well as related experience on other afterburners, indicate that the ability of an afterburner to ignite spontaneously cannot be predicted, nor can any practical modifications necessary to provide reliable spontaneous ignition in any given afterburner be specified. Therefore, spontaneous ignition, although it may be fortuitously obtained in some afterburners, is not a method that can be generally relied upon.

Hot-streak ignition. - Because of its high degree of reliability and simplicity, the hot-streak ignition method has received widespread application in research afterburners. The earliest hot-streak ignition systems provided supplemental fuel through one of the main engine fuel nozzles. The system was operated manually to supply the excess flow at the discretion of the operator for a period of about 1 second. This method of injection was subsequently modified to isolate the hot-streak fuel from the engine fuel manifold and thereby simplify the installation.

This later system utilized a fuel-injection orifice located about one-half of the distance down the combustor from the main fuel nozzle, as shown in figure 175. Details of a typical hot-streak injector installation are shown in figure 176(a). For can-type combustors, the injector is designed to approximately double the fuel-air ratio of the combustor in which it is located. In annular-type combustors, the injector is designed to provide a similar increase in local fuel-air ratio and thus handles a flow of 10 to 15 percent of the main engine fuel flow. A large number of afterburners utilizing this type of system have been consistently ignited at altitudes up to 50,000 or 55,000 feet, which correspond to burner-inlet pressures down to about 500 pounds per square foot absolute (refs. 11 and 12). The system has been used with equal success on engines having one-, two-, or three-stage turbines. In each case it has been found that once the fuel-air ratio in the afterburner has reached a combustible level, the hot-streak fuel need be injected for only 1/2 to 1 second to ignite the afterburner.

3925

To explore the effect of the hot-streak-injector location on the ignition limits, the effectiveness of several hot-streak injectors located immediately upstream of the turbine nozzle was investigated and compared with that of the more conventional upstream location. Details of the turbine-inlet injector installation are shown in figure 176(b). This injector was also designed to double the fuel-air ratio in one combustor can. The time required before a burst from the hot-streak system would ignite the afterburner using both types of hot-streak injectors is compared in figure 177 for altitudes of 30,000 to 50,000 feet. Also included for comparison is the time required to ignite this afterburner spontaneously. The time required for ignition is defined as the period between the time at which full afterburner fuel manifold pressure was obtained after a throttle burst and (1) the time at which the burner ignited spontaneously, or (2) the time at which a 1/2 to 1 second burst of hot-streak fuel flow would provide ignition. Minimum ignition times for several preset fuel-air ratios are plotted in the figure. Minimum time for the hot-streak systems was determined by progressively reducing the time between the throttle burst and actuation of the hot-streak ignitor until ignition could no longer be obtained from the burst of hot-streak fuel flow.

In general, the data of figure 177 indicate a relatively minor effect of either afterburner fuel-air ratio or altitude on the time for hot-streak ignition, with about 1 or 2 seconds being required in most cases. At the lower altitudes, ignition occurred slightly sooner with the turbine-inlet fuel injector than with the upstream injector, but at an altitude of 50,000 feet the turbine-inlet injector failed to provide ignition because of the absence of flame through the turbine. Increasing the injector flow two- to threefold did not improve the ignition characteristics of the turbine-inlet injector. Furthermore, when the turbine-inlet injector flow was reduced by one-half or more, afterburner ingition was unobtainable at any altitude investigated.

Failure of the turbine-inlet injector to provide flame through the turbine at high altitude was attributed to insufficient time for the fuel to ignite before entering the turbine. This premise was borne out by the fact that moving the turbine-inlet injector 3 inches farther upstream resulted in ignition characteristics comparable to those observed with the upstream injector.

Although the improvements in ignition that have been described and which result from proper installation of the ignition system are considered to apply to most afterburners, the ignition times shown in figure 177 do not apply to all afterburner designs. In some afterburners subjected to extensive ignition tests, hot-streak ignition has occurred during the process of filling the fuel manifolds so that the ignition time, as defined herein, was essentially zero.

[redacted]

Because the time required to fill the fuel piping and obtain a combustible mixture in the afterburner following a throttle burst varies with altitude and varies from engine to engine, a single burst of hot-streak fuel for a period of 1/2 to 1 second would have to be very accurately scheduled to provide reliable ignition at all flight conditions. However, continuous injection of hot-streak fuel for periods much longer than 1/2 to 1 second would, in all probability, overheat the turbine stator. Therefore, to provide reliable afterburner ignition without endangering turbine life, the hot-streak ignition system should be designed to provide intermittent bursts of fuel for periods of 1/2 to 1 second from the time the throttle burst occurs until the control senses that the afterburner has ignited. Of course, it is important that the control system be designed so that in the event of failure the hot-streak fuel cannot be continuously injected into the engine.

Hundreds of afterburner starts with the hot-streak ignition system injecting fuel into an engine combustor for periods up to 1 second have resulted in no apparent effect on the turbine rotor blades or on the stator blades located in the path of the hot-streak flame. The absence of any rotor or stator blade deterioration attributable to the hot streak indicates that although the gas temperature may suddenly rise as much as 1000° R, the increase in metal temperature is much less because of the thermal capacity of the turbine blades. To support and explain these practical observations, transient metal temperatures were measured at the stator-blade leading edge in a single-stage turbine assembly as large step increases were made in engine fuel flow. The actual response in stator-blade metal temperature to the sudden changes in gas temperature can be characterized by a time constant. Typical values of this time constant, defined as the time to reach 63 percent of the final value in response to a step input, are shown in figure 178; the data cover a range of turbine-inlet pressures from 3000 to 12,500 pounds per square foot absolute. These pressures correspond to an altitude variation from 7000 to 45,000 feet at a Mach number of 0.8 for the engine used.

The significance of these time constants is illustrated by the computed values of stator-blade temperature rise shown in figure 179. These values were computed using the time constants of figure 178, with the assumption that the engine was operating at an average turbine-inlet temperature of 2000° R and that the temperature in the path of the hot-streak flame increased in a stepwise fashion to 3000° R for periods of 1/2 to 1 second. The values of blade-temperature rise thus calculated are seen to be considerably less than the sudden rise in gas temperature in the path of the hot streak.

The turbine rotor-blade temperatures are, of course, affected to a much lesser extent by the hot-streak flame than are the stator blades. This insensitivity of the rotor blades to the hot streak is due to the speed with which the rapidly rotating blades pass through the local hot region.

The foregoing discussion of the hot-streak ignition system indicates that, with proper installation, the system is a simple and reliable method of initiating afterburner ignition.

Turbine-outlet hot-streak ignition. - In view of the requirement that the preturbine hot-streak fuel be injected for only short intervals to avoid overheating the turbine, and in view of the possibility that accidental prolongation of the injection period would cause turbine-stator failure, the feasibility of obtaining dependable ignition with a hot-streak ignitor located immediately downstream of the turbine was investigated on one engine. Three hot-streak fuel-injector configurations were investigated. Details of these injectors are shown in figure 180. The principal difference among the fuel injectors was the size, location, and number of fuel orifices. One injector consisted of a straight tube with seven orifices

directed toward the turbine, another injector consisted of a bent tube pointed toward the turbine with four orifices in the end of the tube, and the third injector was a similar tube with the end left open to the full inner diameter of the tube. The afterburner on which these injectors were evaluated was of conventional design with a double V-gutter flameholder, having relatively uniform values of fuel-air-ratio distribution and velocity profile upstream of the flameholder.

Afterburner ignition limits of the three turbine-outlet hot-streak fuel injectors are compared in figure 181, which also indicates ignition limits with the conventional preturbine hot streak. Each data point represents an attempt to ignite the afterburner. All starting attempts were made at a turbine-outlet temperature of 1710° R. Although the ignitor fuel-air ratio does not represent the fuel-air ratio in the region of the fuel injector, it serves to generalize the ignitor fuel flows for all altitudes as a fraction of the engine air flow.

The three turbine-outlet hot-streak injectors were equally effective, although they were inferior to the preturbine hot-streak system. With the turbine-outlet injector, the maximum altitude for dependable ignition was between 50,000 and 55,000 feet. In comparison, the preturbine hot-streak system ignited this afterburner at altitudes up to 60,000 feet, which was the operating limit of the afterburner.

Stabilization of Operation

The greater part of the time consumed in the afterburner starting sequence occurs while the control is stabilizing engine conditions immediately following ignition. This fact is illustrated by the investigation of reference 11 (and unpublished NACA data), in which a production-type electronic control and a continuously variable exhaust nozzle were used on an engine. An example of how the control and engine variables are affected by the starting cycle is illustrated by a typical oscillograph trace in figure 182. There is a 6- or 7-second interval between advance of the throttle and ignition, followed by 7 or 8 seconds of oscillatory operation of the engine afterburner before steady-state conditions are reached. The oscillations are caused by an interaction of the various loops of the control, in conjunction with the dynamic behavior of the engine. In this particular control system, engine speed is controlled by primary engine fuel flow, and turbine-outlet temperature is controlled by exhaust-nozzle area.

The following sequence of events occurs in the engine afterburner and the control during ignition and stabilization of operation: the fuel-air mixture in the afterburner ignites while the exhaust nozzle is in a closed or nonafterburning position, because the exhaust nozzle restricts flow, the pressure in the afterburner increases, raising the pressure level throughout the engine and tending to decrease the engine speed; to maintain engine speed constant, the speed control increases the primary engine fuel flow; this increase in engine fuel flow, along with the increase in pressure level at the turbine outlet, tends to drive the turbine-outlet temperature over the limiting value; this over-temperature condition then causes the exhaust-nozzle control to open the exhaust nozzle; because the temperature-error signal is usually large, the nozzle starts to open very rapidly, which decreases the pressure level in the afterburner; this decrease in afterburner pressure tends to make the engine overspeed, which causes the control to reduce the engine fuel flow, both the increase in nozzle area and the decrease in engine fuel flow cause the turbine-outlet temperature to decrease rapidly and thus reduce the temperature-error signal to the control. The signal reduction causes the control to stop the nozzle opening and, in some cases, actually to start closing the nozzle before the required area is obtained; the turbine-outlet temperature is driven over the limit and the cycle is again repeated but with diminishing magnitude. The cycling is

continued until the proper nozzle area is reached. Amplitude of the oscillations may be reduced by changing the constants of the control system, but such a modification would make the control action slower.

The period of oscillation depends on the time constant of the engine and on the control-system constants. Because the engine time constant (rotor inertia divided by change in torque for a given change in engine speed) increases with altitude, the period of each oscillation and thus the time to reach equilibrium is greater at altitude. This increase in duration of the oscillations with altitude is shown in figure 183, for both hot-streak and spontaneous ignition. With hot-streak ignition, the duration of the oscillations increased from about 7 to 17 seconds, as the altitude was increased from 30,000 to 50,000 feet. The duration of the unsteady operation was about 2 seconds longer with spontaneous ignition than with hot-streak ignition at altitudes of 30,000 to 40,000 feet and was as much as 30 seconds longer at an altitude of 50,000 feet. The greater length of time required for the control to stabilize engine operation following spontaneous ignition is due to the more violent manner in which the fuel is ignited. The high fuel-air ratios required to obtain spontaneous ignition, particularly at high altitude, are probably the main contributors to the violent ignition of the fuel.

3925

Complete Starting Sequence

The time required for each phase of the starting sequence and the total time consumed from throttle burst to stabilized afterburner operation at three altitudes and for both spontaneous and hot-streak ignition are summarized in figure 184. The time required for the complete starting sequence with hot-streak ignition increased from $11\frac{1}{2}$ to 27 seconds as the altitude increased from 30,000 to 50,000 feet. The same altitude variation increased the total starting time with spontaneous ignition from $16\frac{1}{2}$ to 60 seconds.

Of the total time for starting, the time required to obtain preset fuel manifold pressure amounted to only about 2 seconds at an altitude of 30,000 feet, although as long as 8 seconds were required at an altitude of 50,000 feet. After the manifold pressure reached the preset value, only 1 to 2 seconds were required to obtain ignition with the hot-streak system, as compared to 4 to 6 seconds for spontaneous ignition. Although ignition times significantly shorter than that provided by the hot-streak system cannot be expected, reductions in the time required to obtain a preset fuel manifold pressure would be obtainable by reducing the volume of the fuel lines that must be filled prior to each afterburner start.

As mentioned previously, the greatest portion of the starting time at each altitude is consumed in reaching equilibrium following ignition. Although the length of this stabilizing period is significant, it should be noted that the afterburner provides a substantial thrust increase shortly after ignition occurs. During the time that afterburner operation is becoming stabilized, the thrust will be oscillatory and may periodically equal or even exceed the final stabilized value. Because the hot-streak system provided smoother ignition than did spontaneous ignition, particularly at high altitudes, the oscillation was less severe with the hot-streak system; consequently the time required to stabilize operation was appreciably shorter at all altitudes.

Summary

The complete starting cycle of an afterburner consists of filling the fuel pipes and manifolds with fuel, igniting the fuel, and establishing equilibrium engine-afterburner operation. Ignition of the fuel by means of a spark plug has proven to be unreliable; and spontaneous ignition, while successful and consistent in some afterburners, cannot be considered a generally reliable method. Hot-streak ignition, which produces a torch of flame into the afterburner by momentarily augmenting the fuel flow to a primary combustor, has been very successful in many types of afterburners. The time required to obtain ignition by this method varies from 1 to 3 seconds. The greatest length of time in the complete starting cycle is involved in establishing equilibrium operation of the engine-afterburner combination following ignition of the fuel. With a representative current control system, the time required for the exhaust-nozzle area, the primary engine fuel flow, and other engine variables to complete their oscillatory behavior and reach their final steady-state values increased from 11 to 27 seconds as the altitude was increased from 30,000 to 50,000 feet.

FUEL-INJECTION SYSTEMS

The primary function of the fuel-injection systems of an afterburner is to provide the proper distribution of fuel and air within the burner and adequate preparation of this fuel-air mixture for combustion. Proper distribution requires that the fuel be introduced into the gas stream at the correct locations, dependent upon the mass distribution of the turbine-discharge gases and the flameholder-area distribution. Adequate fuel preparation comprises thorough mixing of the fuel with the turbine-discharge gases, and vaporization of the mixture before it reaches the flameholder location, where combustion occurs. The basic processes involved in this union of fuel and air have been discussed in chapter I and II of reference 14.

Fuel-Spray Bars and Their Installation

The type of fuel-injection systems used almost exclusively at the Lewis laboratory and that has received widespread industrial acceptance is that of radial spray bars. These bars are located some distance upstream of the flameholder, usually within the turbine-discharge diffuser. The use of a relatively large number of spray bars, each with several fuel-injection orifices, provides the multiplicity of fuel-injection locations that is necessary for good dispersion of fuel across the gas stream. A distinct research advantage of spray-bar systems is that they can be easily removed for inspection and readily altered in both orifice number and orifice location.

A photograph of a typical fuel-spray bar is presented in figure 185. These spray bars are fabricated from commercial stainless-steel tubing; they are closed at the end and equipped with some means of attachment to the shell of the burner or burner-inlet diffuser. The inside diameter of the spray bar is usually between 1/8 and 1/4 inch; the bars are frequently left round, although in many installations they have been flattened somewhat, as shown in the photograph, to form a more streamlined cross section. The fuel orifices are simply holes drilled through the wall of the tubing at appropriate locations.

As illustrated in figure 186, the spray bars are evenly spaced circumferentially in a single plane across the burner or diffuser. They are usually cantilevered from their point of attachment on the inner or the outer shell; additional structural support is seldom necessary. For simplicity, all the spray bars are usually connected to a single manifold.

In the following presentation, the distribution of fuel-air ratio upstream of the flameholder under burner conditions is discussed for various afterburners. This discussion presents (1) the types of radial and circumferential fuel-air-ratio distribution afforded by various injection systems, and (2) the effects of fuel-air-ratio distribution on the over-all performance of the afterburner. Attention is also given to the degree to which the actual fuel-air-ratio distribution may be predicted from consideration of the injection-system design and the mass-flow profile of turbine exhaust gases. The accuracy of such predictions is not only pertinent to design, but the predictions are useful in evaluating the effects of fuel-air distribution on performance when actual measurements are not available. The effects of fuel mixing length, orifice size, injection pressure, and direction of fuel injection on afterburner performance are also summarized.

Radial Fuel-Air-Ratio Distribution in Afterburner

Measurements of the fuel-air ratio across the gas stream immediately upstream of the flameholder under burning conditions have been of considerable aid to afterburner research and development. These measurements have been obtained with the NACA mixture analyzer described in detail in reference 16.

Effect of spray-bar design on distribution. - A typical effect of a change in location of the fuel-injection orifices in a matched set of spray bars on the radial fuel-air distribution is shown in figure 187. These data, obtained from a full-scale afterburner installed on a blower rig (ref. 17), represent the fuel-air distributions measured 22.5 inches downstream of the fuel-spray bars. The fuel was injected in a transverse direction from 24 spray bars; this number, as will be illustrated subsequently, provides about the same distribution at all circumferential locations. Sketches of the spray bars, approximately to scale, are included in the figure to show the locations of the fuel-injection orifices.

With the six-orifice spray bar, the fuel-air ratio varied from approximately 0.070 near the center of the burner to less than half this value near the outer shell of the burner. By addition of two orifices near the outer shell of the burner to form the eight-orifice bar, the fuel-air ratio was made nearly the same all the way across the burner. The addition of a pair of orifices to the spray bar thus altered the fuel-air-ratio distribution from a 2 to 1 variation across the burner to an essentially uniform distribution.

Similar data on the effect of orifice location on fuel distribution are shown in figure 188 for a full-scale afterburner operating on a turbojet engine. A 16-orifice spray bar, with orifices spaced as shown in the sketch, provided the somewhat uneven fuel-air-ratio distribution shown by the solid curve. To increase the fuel-air ratio near the outer shell of the burner, a second set of spray bars was used that incorporated a closer spacing of fuel orifices near the outer shell. This spray bar, shown in the left portion of the figure, produced the fuel-air-ratio distribution indicated by the dashed curve. Although the fuel-air-ratio distribution obtained with this spray bar was slightly low in the mid-radial location, the fuel-air ratio near the outer shell was substantially increased.

Comparison of measured and calculated distribution. - The data of figures 187 and 188 show that changes in the location of the fuel-injection orifices produce, in at least a qualitative manner, the expected changes in actual fuel-air-ratio distribution. To determine the accuracy with which such changes may be quantitatively predicted, calculations of radial fuel-air-ratio distribution were made that were based on the radial location of the fuel orifices and the measured mass-flow profile of the turbine exhaust gases at the spray-bar location. These calculations were

thus based on a simple radial proportionment of fuel and air, neglecting such effects as inertial separation of the fuel and the air and diffusion of fuel vapor beyond the stream tube of air passing each orifice.

In figure 189, the results of such a calculation for the two fuel systems represented in figure 187 are compared with the measured fuel-air-ratio distribution. Although the minor variations of fuel-air-ratio distribution across the radius for each separate fuel system are not closely predicted, the general trends and the differences between the two fuel systems are predicted with fair accuracy. For both the uniform distribution of the eight-orifice bar and the decidedly nonuniform distribution produced by the six-orifice bar, the calculated fuel-air ratio is within 0.013 of the measured distribution.

3925

Further evidence that these simple calculations of fuel-air-ratio distribution will predict general trends but not minor, or detailed, variations is presented in figure 190. The measured distributions of this figure are those previously presented in figure 188. Again, the calculated distributions agree with the measured distributions with regard to both general trend and level; the quantitative agreement is within about 0.018. Further inspection of these data, as well as other data not presented herein, shows that the measured fuel-air ratio is generally greater than the calculated values in the outer one-third of the burner. This rather general characteristic is attributed to a centrifugal separation of the fuel and air in passing through the annular diffuser, with the fuel tending to follow the initial axial direction of gas flow and the gases following more closely the curved walls of the diffuser inner cone.

From the foregoing, it may be concluded that the gross or principal effects of changes in spray-bar design on the resulting radial fuel-air-ratio distribution under burning conditions may be predicted with satisfactory accuracy from very simple considerations of the radial proportionment of the fuel and air. More detailed considerations of fuel vaporization and turbulent diffusion such as discussed in reference 18 therefore do not appear necessary for general afterburner development. In practice, a fuel-injection system for an afterburner is usually developed in two successive steps. First, the spray bar is designed to give the desired distribution on the basis of simple calculation of radial fuel and gas distribution, utilizing for this calculation the actual, and usually nonuniform, mass-flow profile at the spray-bar location. Detailed alterations to the spray bar are then made on the basis of measurements of the actual fuel-air-ratio distribution. The radial fuel distribution delivered by a spray bar may, of course, be altered by changing the location of the fuel orifices, the relative size of the orifices, or by a combination of both. As discussed in reference 17, it has been found that changing the radial location of the fuel orifices produces somewhat more predictable results than does changing the orifice size.

Effect of Radial Fuel-Air-Ratio Distribution on Performance

The effect of distribution of fuel-air ratio on the combustion performance of afterburners has been noted by many investigators over the past 4 or 5 years. This research was, until recently, conducted without the aid of actual measurements of the fuel-air-ratio distribution existing within the burner. It was generally observed, however, that fuel systems which would be expected on the basis of their design to provide most uniform distribution provided the highest combustion efficiency at high over-all fuel-air ratios, and hence provided highest maximum exhaust-gas temperatures. Some early work reported in both reference 19 and in the summary report of reference 12 indicated that progressive alterations to the fuel injectors made to obtain a more homogeneous mixture of fuel and air raised the peak combustion

efficiency and shifted the region of peak efficiency to higher over-all fuel-air ratios. Reference 12 also observed that the attainment of such "homogeneous" mixtures requires that the radial fuel distribution be tailored for each engine because of variations in turbine-outlet mass-flow profiles from one engine to another.

Spray-bar fuel-injection system. - Data that show the effect of a change in the radial distribution of fuel-air ratio on combustion efficiency and exhaust-gas temperature are presented in figures 191 and 192, respectively. A sketch illustrating the radial distribution of fuel-air ratio for one point of operation of each fuel system is included in the figures. The over-all fuel-air ratio at which each of these radial distributions was measured is indicated by the leader from the sketch. From considerations of the spray-bar design (as discussed later) and the constancy of the mass-flow profile of the gases as discussed in reference 17, it is believed that the radial distribution for each system stays about the same throughout the fuel-air-ratio range presented. The two fuel systems used for the data of these figures are those previously illustrated in figures 187 and 189, herein; they are described in greater detail as fuel-system configurations 1 and 3 in reference 17.

3925

For fuel-air ratios higher than about 0.035, the uniform fuel-air-ratio distribution produced higher values of combustion efficiency and exhaust-gas temperature; for lower fuel-air ratios, the nonuniform fuel-air-ratio distribution gave slightly higher values. The nonuniform distribution also resulted in a slightly lower lean blow-out limit, as indicated by the small cross-hatched regions in the figure. This somewhat better combustor performance at low fuel-air ratios with the nonuniform distribution is due to the existence of localized regions within the burner in which the fuel-air ratio is high enough for good combustion, even at the low over-all values of fuel-air ratio. These locally rich regions are also the cause of the reduction in combustion efficiency at higher fuel-air ratios, because the local fuel-air mixture becomes greater than stoichiometric and thus too rich to burn completely. It is evident from these data, as well as from many other similar observations, that a uniform fuel-air-ratio distribution is desirable except for an afterburner intended primarily for very low temperature-rise operation.

Concentric manifold fuel system. - Data from another series of tests with a full-scale engine in which the radial distribution of fuel injection was varied is presented in figure 193. In this afterburner, fuel was injected from three concentric manifolds, each incorporating a large number of simple fuel orifices. The three manifolds were so connected to separate fuel throttles that the radial distribution of fuel could be varied during operation. A more complete description of this fuel system as well as the complete afterburner may be found in reference 6. Although the fuel-air-ratio distribution was not measured during the tests, the distribution provided by one method of operation relative to another was computed on the basis of the number and the location of fuel-injection orifices in operation, the distribution are illustrated by the sketches in the upper part of the figure. While no claims can be made for quantitative accuracy of fuel-air-ratio distribution, it is apparent that systems A, B, and C provided progressively more uniform radial distributions of fuel.

The combustion efficiencies concomitant with the three different fuel systems are shown in the lower part of the figure. Although the peak efficiency has the same value for all three systems, the fuel-air ratio at which peak efficiency occurred shifted to progressively higher values of over-all fuel-air ratio as the fuel distribution became more uniform. These data illustrate the desirability of a multiple, or at least, a dual orifice system if efficient operation is required over a wide range of fuel-air ratios. Such a dual orifice system, which could provide a nonuniform (locally rich) fuel distribution for low-temperature operation and a uniform mixture for high temperature, is mentioned in reference 12 also. Dual

systems have not been put into actual use in full-scale afterburners because their primary requirement is usually that of high thrust output; they have, however, found effective application to ram-jet combustors where efficient operation over a wide range of conditions is required (refs. 20 to 22).

Locally rich fuel injection. - A particularly striking, though extreme, example of the good combustion performance that may be obtained at low values of fuel-air ratio with a nonuniform fuel-air-ratio distribution is shown in figure 194. The fuel-injection system used in this afterburner consisted of 12 radial spray bars, each having four fuel orifices. At an over-all fuel-air ratio of 0.055, the local fuel-air ratio (fig. 194(a)) varied from about 0.02 to 0.11 across the radius of the burner, with the rich region located near the position of the single-ring flameholder. The combustion efficiency of this burner is shown in figure 194(b); the performance of the burner with the uniform distribution of figure 191 is included for comparison. As previously noted, operation with the uniform fuel distribution produced a peak efficiency at a fuel-air ratio of about 0.05 and a lean blow-out limit of about 0.03. With the very nonuniform fuel-air-ratio distribution, on the other hand, lean blow-out did not occur until an over-all fuel-air ratio of 0.004 was reached. Although the combustion efficiency decreased rapidly as the fuel-air ratio was increased, efficiencies approaching 100 percent were measured at the lowest fuel-air ratios.

Summary. - A summary of the manner in which afterburner fuel-air ratio for peak combustion efficiency varies with the degree of uniformity of radial fuel-air-ratio distribution is presented in figure 195. The abscissa of this figure is the integral across the burner of the absolute value of the difference between the local and the average fuel-air ratio, divided by the average fuel-air ratio. A value of zero thus indicates perfect uniformity of fuel-air-ratio distribution, and a value of 0.5, for example, means that the mean deviation of local fuel-air ratios from the average value is 50 percent of the average.

Included in figure 195 are all available data from tests in which the fuel-air-ratio distribution was systematically varied and the fuel-air ratio for peak combustion efficiency was observed. Data from references 17 and 23 are based on actual measurements of fuel-air-ratio distribution within the burner, while that from references 6 and 19 are, in the absence of actual measurements, based upon the arrangement of fuel-injection orifices across the burner flow passage. The greater degree of nonuniformity of distribution indicated by the fuel-injector design compared to the actual measurements is a result of the spreading and softening of the distribution between the point of fuel injection and the flameholder.

For both types of data, a rapid decrease in the fuel-air ratio at which peak efficiency occurs is apparent as the fuel-air-ratio distribution becomes less uniform. In order to have a peak combustion efficiency at a fuel-air ratio between 0.055 and 0.06, or to provide maximum temperature rise and thrust augmentation, the mean deviation in local fuel-air ratio should be no greater than 10 percent of the average value.

Circumferential Distribution of Fuel-Air Ratio in Burner

Just as the radial fuel-air-ratio distribution in an afterburner is determined by the number and location of the fuel orifices in each radial spray bar (if such a fuel system is used), so will the circumferential distribution be affected by the spacing between the spray bars and the amount of crossflow penetration of the fuel jet into the gas stream. The spacing between spray bars is, of course, determined directly by the number of bars used and the burner diameter, while the jet penetration is a function of orifice size, gas velocity, fuel-jet velocity, and other

properties affecting the vaporization rate of the fuel. These various factors are not independent but are, instead, closely interrelated. In the following discussion, the effect of the number of spray bars on both the circumferential fuel-air-ratio distribution and the burner performance is first examined at various gas velocities for a given orifice size. The effects of changing the orifice diameter are then presented for two gas velocities and different numbers of bars. Although data covering complete ranges of all the pertinent variables are not available, a review of the available data permits certain general conclusions to be drawn.

Although radial nonuniformity in distribution of fuel-air ratio may be desirable in those applications where efficient operation at low temperature rise is desired, it is logical to assume that the circumferential distribution should always be fairly uniform because of the circumferential symmetry of the flameholders in general use. It remains, therefore, to determine the type of fuel system required to give a sufficiently uniform circumferential distribution of fuel-air ratio at various gas velocities.

Effect of number of spray bars on fuel-air-ratio distribution. - The circumferential distributions of fuel-air ratio provided by 12 and by 24 radial spray bars are compared in figure 196. All spray bars were the same, with eight fuel orifices of 0.030-inch diameter in each. The gas velocity for these tests was between 500 and 600 feet per second; fuel was injected in a radial plane. The burner diameter was approximately 26 inches. A measure of the circumferential distribution of fuel-air ratio is provided in this figure by comparing the fuel-air ratios along two radii some 15 inches downstream from the spray bars; one radius was directly aft of a spray bar, and the other in a plane midway between adjacent spray bars. As indicated in the upper part of the figure, the radial fuel-air-ratio distribution is about the same for both radii when 24 spray bars were used, this result indicating a circumferentially uniform distribution. When 12 spray bars were used, however, the fuel-air ratio along the two radii differed by more than 2 to 1 over most of the area of the burner. As would be expected, the difference was greatest near the outer shell of the burner, where the spray bars were farther apart, and almost disappeared at the center of the burner. Thus, with 12 spray bars in this afterburner, there existed a combined radial and circumferential distortion in fuel-air-ratio distribution.

It should be noted that the poorer circumferential distribution of fuel with the 12 spray bars existed in spite of the higher fuel-injection pressures associated with the smaller number of fuel orifices. This result is contrary to what would be expected for nonvaporizing liquid jets, inasmuch as the correlation of reference 24 for liquid jets indicates that the higher injection pressures should have essentially offset the greater spacing between the bars for the conditions of this test; therefore, vaporization of the fuel had a significant influence on the circumferential fuel distribution. As might be expected, however, the jet penetrations generally indicated by the data of figure 196 are somewhat greater than would have been predicted from the data of reference 25 for air jets. Although more exact quantitative comparisons are not possible, it is apparent that the penetration characteristics of fuel jets in afterburners are between those of liquid jets and air jets, with the specific characteristics depending on the various factors that influence the vaporization rate of the fuel.

Effect of number of spray bars on performance. - The effects of the nonuniform circumferential fuel-air-ratio distribution illustrated in figure 196 on the combustion efficiency of the afterburner are presented in figure 197. Although the effects of this nonuniformity do not appear to be as large as those resulting from a radial nonuniformity, the combustion efficiency is 7 or 8 percentage points higher with the 24-spray-bar fuel system than with the 12-spray-bar system over most of the range of fuel-air ratio.

[redacted]

The data of figure 197 were obtained at a burner-inlet velocity of 500 to 600 feet per second; they indicate that, for these conditions, the higher fuel-injection pressures associated with the smaller number of spray bars did not provide sufficient penetration to give a uniform fuel distribution. It might be expected, however, that the fuel penetration across the gas stream would be greater at a lower gas velocity and the effect of the number of fuel-spray bars on the performance of the afterburner would be less. That this is actually the case is illustrated in figure 198, where the combustion efficiency at a burner-inlet velocity of 380 to 480 feet per second is shown to be the same for both 12 and 24 spray bars. For comparison, the combustion efficiency obtained at these lower gas velocities with the fuel-air-ratio distribution nonuniform in a radial direction, as obtained for the six-orifice spray bars of figure 187, is included as the dashed curve. In this case, the combustion efficiency decreased very rapidly with increasing fuel-air ratio, as previously discussed. Therefore, while low gas velocities permit the number of spray bars used to be reduced because of greater fuel penetration across the gas stream, the fuel orifices must be located radially to give good coverage across the burner if good performance is desired at high over-all fuel-air ratios.

Effect of orifice size on performance. - The results presented in the preceding section are for an orifice diameter of 0.030 inch. As was mentioned, a reduction in orifice diameter may increase the rate of fuel vaporization sufficiently to decrease the jet penetration and thereby have an adverse affect on burner performance. This effect would be reduced, of course, if a large number of spray bars were used. Data from reference 17 comparing the combustion efficiency with 0.030- and 0.020-inch-diameter fuel orifices are presented in figure 199; 24 spray bars were used in a 26-inch-diameter afterburner. It is apparent that in this case the jet penetration was not reduced enough by the reduction in fuel-orifice size to affect the performance appreciably. This result was, furthermore, obtained at the relatively high gas velocity of 500 to 600 feet per second.

If the spacing between spray bars is similar to that provided by 24 bars in a 26-inch-diameter burner, orifice diameters as small as 0.020 inch may, therefore, be used even at high gas velocities. If, on the other hand, only 12 spray bars are used, an orifice diameter of 0.020 inch does not appear to be large enough to provide good fuel distribution, even at gas velocities no higher than 400 feet per second. This conclusion is based on a comparison of figure 198 with 200, which is replotted from the data of reference 25. As indicated in figure 200, the spray-bar system for these data comprised 12 long spray bars, each having 8 orifices, and 12 shorter spray bars with 6 orifices per bar. The performance obtained when all 24 spray bars were used is compared with that obtained when only the 12 long spray bars were used. Although an exact comparison between the data of figures 198 and 200 is not possible because different afterburners were used, values of gas velocity, burner-inlet pressure, and burner diameter were about the same. The principal difference is that 0.020-inch orifices were used for the data of figure 200 as compared to the 0.030-inch orifices for the data of figure 198.

Contrary to the satisfactory performance indicated in figure 198 for the 12 spray bars having 0.030-inch orifices, the performance shown in figure 200 for 0.020-inch orifices was appreciably reduced when the number of spray bars was decreased from 24 to 12. Not only was the maximum gas temperature reduced from 3400° to 3000° R, but the combustion efficiency at the condition of maximum temperature was also about 20 percentage points lower. Although the fuel-injection pressure at stoichiometric fuel-air ratio was increased from 25 to 75 pounds per square inch for the smaller number of spray bars, the fuel penetration with the small orifices was obviously inadequate to overcome the wider spacing between the bars.

[redacted]

To recapitulate, the use of as few as 12 spray bars in a 26-inch-diameter afterburner provided good performance only when the gas velocity was relatively low (380 to 480 ft/sec) and the fuel orifices were as much as 0.030 inch in diameter. The performance of the 12-bar system was inferior to that of the 24-bar system at high gas velocities with 0.030-inch orifices, and at low gas velocities with 0.020-inch orifices. A spray-bar spacing corresponding to 24 spray bars in a 26-inch-diameter burner provided good performance at high gas velocities (500 to 600 ft/sec) with either 0.020- or 0.030-inch diameter orifices. Other combinations of orifice diameter and number of spray bars within these limits should, of course, be possible.

Effect of ratio of orifice size to spray-bar diameter. - The foregoing discussion indicates the possibility of reducing the number of spray bars somewhat if the jet penetration is increased by increasing the orifice diameter. Early fuel vaporization is apparently less with the larger orifices, and the penetration characteristics approach those of a purely liquid jet. (As discussed later, large axial mixing distances permit adequate fuel preparation for combustion.) If the fuel orifice becomes too large relative to the internal diameter of the spray bar, however, the static pressure within the bar and the effective flow area of the several orifices will vary. The effect of this ratio of orifice area to spray-bar area on the proportion of fuel delivered by each orifice is reproduced from the data of reference 17 in figure 201. Plotted against the ratio of total fuel-orifice area to spray-bar flow area is the ratio of fuel-flow through each orifice relative to that through the number 1 orifice (at the shank of the spray bar). For each value of total orifice area, all orifices were the same size. As this ratio of total orifice area to spray-bar area increases, the fuel orifices located toward the tip of the spray bar deliver proportionally greater amounts of the total fuel-flow. This variation in fuel delivery is a result of the higher static pressure within the bar at the tip and the higher relative flow coefficient of the tip orifices. Although the effects of these variations are probably negligible for area ratios of less than 0.5, the tip orifices deliver as much as 50 percent more fuel than the shank orifices for an area ratio of 1.0.

As discussed in reference 17, other factors affecting the amount of fuel delivered by each orifice are the length-diameter ratio of the orifice and the method of drilling the hole. Orifices having small length-diameter ratios, with the hole drilled undersize and reamed to final size, produced the greatest uniformity of flow from one orifice to another. Orifices produced in this manner have flow coefficients in the range of 0.5 to 0.6, based on the fuel pressure in the spray bar.

Effect of direction of fuel injection. - The data presented so far on fuel-injection systems were obtained with the fuel injected in a transverse direction, that is, across the gas stream. It might be expected that this direction of injection would be somewhat better than an upstream or downstream direction, simply because it would provide a better fuel coverage of the gas stream. This premise is substantiated in figure 202(a), which compares the combustion efficiencies obtained when fuel was injected alternatively in a transverse, upstream, or downstream direction from an otherwise identical system. Although the effect of the direction of fuel injection is not large at low fuel-air ratios, the combustion efficiency at the higher fuel-air ratios is considerably higher when fuel is injected in a transverse direction than when injected either upstream or downstream. It should be noted that this rather significant effect of the direction of fuel injection was obtained with a fuel-mixing distance of 29.5 inches; if a shorter fuel-mixing distance had been used, the effects might have been even greater.

A further comparison of the combustion efficiency of an afterburner with upstream and with downstream injection is presented in figure 202(b). In this burner, three concentric fuel manifolds were used; in one case fuel was injected in a downstream direction from all three manifolds, and in the other case the direction of injection of two of the manifolds was reversed. At the higher burner-inlet pressure, the effect of this change in direction of fuel injection was not large, but performance at the pressure of 620 pounds per square foot absolute was considerably better with upstream injection, particularly at the high fuel-air ratios. The very small fuel-mixing distance used in this afterburner (1.5 inches) probably accounts for this rather large effect of changing from a downstream to an upstream direction in this case.

Effect of fuel-mixing distance on performance. - There are few data indicating the isolated effect of change in the fuel-mixing distance (the distance between the fuel injector and the flameholder). Theoretical analyses of the evaporation of fuel sprays summarized in chapter I of reference 14 are not applicable, and experimental results are quite meager. Also, little work has been done on the subject of the mixing of fuel sprays with air (chapter II of ref. 14). It has been a matter of almost universal experience in full-scale afterburner research, however, that relatively large mixing distances (approaching 2 ft) are required for satisfactory performance, particularly at low burner-inlet pressures. The summary report of reference 12, for example, indicates an appreciable improvement in high-altitude performance of an afterburner when the fuel-mixing length was increased from $17\frac{1}{2}$ to $25\frac{1}{2}$ inches. The improvement in performance of one series of afterburners relative to that of another series described in reference 26 is also largely attributed to an increase in fuel-mixing distance. Although there is probably some basis for the viewpoint that large mixing distances tend to aggravate the problem of combustion instability, all available experience with afterburners of many types indicates that the combustion performance at high altitude will not be satisfactory with mixing distances of only a few inches. The fuel-mixing distances of all known afterburners that have what might be considered satisfactory high-altitude performance have been of the order of 20 inches or more.

Summary

The distribution of fuel-air ratio across the burner in both a radial and a circumferential direction has an important influence on both the combustion efficiency and on the fuel-air ratio at which maximum efficiency occurs. In general, uniform mixtures are required for high efficiencies at high fuel-air ratios, and nonuniform, or locally rich regions, are necessary for good efficiency at low fuel-air ratios. The required orientation of a nonuniform fuel-air-ratio distribution is related to the arrangement or type of flameholder. The radial fuel-air-ratio distribution provided by a fuel-injection system can be predicted with satisfactory accuracy by simple considerations of the radial proportionment of the injected fuel and gas flow. The uniformity of the circumferential pattern of fuel-air ratio will depend on both the spacing of the radial fuel-spray bars and the penetration characteristics of the fuel jet across the gas stream. The penetration characteristics of fuel jets in afterburners appear to be between those of pure liquid jets and air jets, with the relative position depending on the various factors that influence the rate of fuel vaporization. Highest combustion efficiency at high fuel-air ratios is obtained with fuel injection in a transverse direction to the gas stream and with mixing distances of at least 12 to 15 inches between the point of injection and the flameholder.

[redacted]

FLAMEHOLDER DESIGN

As in most of the various aspects of combustor design, knowledge of flameholder design principles has been accumulated empirically. The first experiments with afterburners showed that various bluff bodies in the air stream successfully anchored flame and provided a source for further propagation of combustion throughout the burner. Following these early results, numerous experiments have been performed to explore the size, shape, and arrangement of bluff-body flameholders with the objective of obtaining high combustion efficiency, high altitude limits, and low pressure drop. Because these experiments were necessarily carried out simultaneously with experiments to improve the design of other parts of afterburners, such as fuel-injection systems and inlet diffusers, the relations among the results of tests on different afterburners are obscure in many cases. Wherever possible, however, the results presented herein are selected from experiments that covered a range of pertinent burner designs. In this manner, the degree of generality of the results is revealed. Although types of flameholders other than bluff bodies (such as pilots and cans) may have considerable merit, the absence of information about them makes it necessary to limit the present discussion to bluff-body flameholders. Basic aspects of flow and combustion around flameholders may be found in chapters II and III of reference 14.

The flameholders that will be discussed are all formed of annular rings, or gutters, constructed in a manner similar to that shown in figure 203. The flameholders are usually attached to the wall of the burner with several streamlined struts. Although several methods of fabrication have been employed, the most satisfactory method from the standpoint of durability and ease of manufacture has usually been to weld sheets of Inconel about 1/8 of an inch thick into the shape required (in this case a V) and smooth off the weld on the external surfaces by grinding. Radial interconnecting gutters are similarly formed and attached by welding.

Effects of Cross-Sectional Shape

In references 27 and 28, a theory is advanced to explain the nature of stabilization of flames on gutters. According to the theory, hot gases from the burning boundaries of the fuel-air mixture surrounding the wake from a bluff body are recirculated upstream and enter the relatively cool boundary near the body. These hot gases increase the temperature of the mixture and carry ignition sources into the mixture. By this process, ignition of fresh mixture is initiated, and a continuous process of ignition is maintained.

Isothermal wake flow. - An experimental evaluation of the effect of cross-sectional shape on the recirculation characteristics of bluff bodies in isothermal flow is given in reference 29. "Bluffness" of a body is considered to be qualitatively proportional to the sum of the angles between the body's trailing edges and its axis of symmetry. It was reasoned that the recirculation characteristics of a bluff body were directly related to vortex strength (ratio of tangential velocity to vortex radius) and to shedding frequency of the vortices formed in the wake. Bluff bodies of twelve shapes were investigated; with the aid of hot-wire and flow-visualization techniques, the strength and shedding frequency of the vortices were determined. Some of the principal results are shown in figure 204.

In figure 204, the ratio of vortex strength to approaching gas velocity is plotted against the ratio of shedding frequency to gas velocity for five representative shapes. The various shapes investigated are shown in the sketches in the symbol key. The flameholders were circumferentially symmetrical except for the V-gutter flameholder with the vortex generators installed on the upstream splitter plate. The vortex generators of this flameholder were essentially small vanes

installed on both the inner and outer surfaces of the splitter vane or projecting cylinder. The vanes were inclined at an angle of about 16° to the axis of the burner and were about 3/4 inch high and 1.2 inches in chord. The gutter width of each flameholder at the open end was 3/4 inch. In figure 204, the general trend of increasing strength and decreasing frequency with increased bluffness of the flameholder is apparent. The changes in vortex strength and frequency are large.

Combustion efficiency. - To determine the possible relation of these isothermal-wake characteristics to combustion performance, tests were made in a simulated afterburner facility to evaluate combustion efficiency, stability limits, and pressure-loss characteristics of flameholders with cross-sectional shapes similar to those tested in cold flow. The results of this investigation are reported in reference 1 and additional tests of two shapes are reported in reference 30. Typical results are shown in figure 205, where combustion efficiency is plotted against afterburner-inlet pressure. The two upper curves represent typical data selected from reference 1 and the two lower curves are from the afterburner study of reference 30. Although the efficiency levels of the two afterburners differed by about 25 percent (because of differences in flameholder size, fuel distribution, burner length, and burner-inlet velocity), the changes in efficiency with change in flameholder cross-sectional shape are about the same for both. In both afterburners, combustion efficiency was 2 to 20 percentage points lower with the U-shape gutter than with the V-shape gutter. For both burners, the difference in efficiency was greater at the lower inlet pressures.

In figure 206, the afterburner combustion efficiency is plotted as a function of afterburner-inlet velocity and pressure for various shapes of flameholder gutters. Parts (a) to (c) of this figure are for a fuel-air ratio of 0.047, and parts (d) to (f) for a fuel-air ratio of 0.067. Data are shown for ten flameholder cross-sectional shapes. The general trend of decreasing combustion efficiency with increasing afterburner velocity or decreasing inlet pressure is consistent for all shapes investigated, but scatter of the data obscures any general effect of shape on performance.

To aid in comparing the efficiencies of the various flameholders, the arithmetical average difference between the efficiency observed with the V-shape flameholder and with each of the other shapes was calculated; these differences in efficiency are plotted in the bar graphs of figure 207. Included in the calculations are a large number of data points that cover values of fuel-air ratio between 0.02 and 0.08, burner-inlet velocity between 400 and 700 feet per second, and burner-inlet pressure between 500 and 1200 pounds per square foot. Because insufficient data are available to isolate the effects of these variables, the observed values of efficiency at all operating conditions for a given flameholder were averaged together. In view of the trend of decreasing efficiency difference with increasing pressure shown in figure 205, the over-all average differences shown in figure 207 are probably conservative for low pressures and extreme for high pressures.

The results of figure 207 show that the U-shape flameholder is inferior to the flameholders of other shapes by amounts varying from 4 to 10 percent. Among the several shapes with highest efficiency, differences of only 2 or 3 percent were obtained. Below the bar for each flameholder shape is given the corresponding value of cold-flow vortex strength from reference 29. There is no apparent correlation between combustion efficiency and cold-flow vortex strength. It is evident from these results that although the U-shape gutter is inferior to gutters of most other shapes (particularly at low pressures), only small differences in combustion efficiency are obtained by using flameholders with cross-sectional shapes other than the V-shape.

[redacted]

Blow-out limits. - The effect of cross-sectional shape on operable fuel-air-ratio range is shown for several typical shapes in figure 208. Data from references 1 and 30 are included. The effect of gutter shape on the lean and the rich fuel-air-ratio limits is small (0.005 to 0.01). The principal effect of shape appears to be that the minimum pressure for stable combustion is from 50 to 200 pounds per square foot higher for the U-shape flameholder than for the other shapes investigated.

Pressure loss. - The effect of flameholder shape on total-pressure loss between burner inlet and outlet (excluding pressure losses in the diffuser) is shown in figure 209. Without burning (temperature ratio of 1.0), the pressure loss is from 1 to 2 percent of the burner-inlet pressure. With the exception of the flameholder with knife edges mounted on the sides of the gutter (square symbols), the pressure losses are the same with the various flameholders within ±1 percent over the range of burner-temperature ratio investigated. Data for pressure drop with the U-shape gutter are available from reference 1 only for the nonburning condition, and are shown for the temperature ratio of 1.0 in figure 209. During cold flow, the pressure drop for the U-shape gutter is approximately the same as for the V-gutter. Data from reference 30 indicate, however, that during burning the pressure-loss ratio is 0.01 to 0.02 less with the U-shape flameholder than with a V-gutter flameholder of the same size ($22\frac{1}{2}$-percent blockage).

3925

In summary, the experimental investigations have shown that afterburner combustion efficiency may vary as much as 10 percent with flameholder cross-sectional shape. Of the various shapes investigated, the U-shape flameholder was inferior in both stability limit and combustion efficiency to all others. Combustion efficiency and stability limits of several shapes were comparable to the V-shape flameholder. Pressure losses for most of the shapes were approximately the same.

Effects of Gutter Width, Number of Gutters, and Blockage on Combustion Performance

The size and arrangement of flameholders is one of the dominant factors affecting afterburner performance. The best arrangement of flameholders is a function of the factors of environment in which the flameholder must operate such as velocity and fuel-air-ratio distribution at the flameholder and type of wall-cooling system used. It is evident, therefore, that a single optimum location (axial and radial spacing) of flameholders does not exist for all possible environmental conditions. Some general trends and qualitative indications of best location are, however, discussed in a subsequent section. In this section the effects of gutter width, number of gutters, and blockage will be shown for a wide range of environmental conditions; general trends that are to a large degree independent of environment are discussed. All the results are for unstaggered flameholders.

Gutter width. - Some effects of gutter width are illustrated in figure 210. It is, of course, impossible in any experiment to isolate the individual effects of gutter width, gutter diameter, number of gutters, and percent blockage. The effects shown in figure 210 may, therfore, be influenced to some degree by variables other than gutter width and number of gutters. An attempt was made in each test to minimize the extraneous effects. In most cases, the flameholders were located in regions of nearly uniform afterburner-inlet velocity to avoid large effects of small changes in gutter diameter. Particular emphasis was placed on providing a uniform fuel-air-ratio distribution at the flameholder location.

In figure 210(a), some results from reference 20 are shown. Combustion efficiency at a fuel-air ratio of 0.04 is plotted against burner-inlet pressure for two flameholders, each having two rings and the same blockage but with gutter widths of 2 and 1.6 inches. The 2-inch-wide gutter produced a combustion efficiency two to five points lower than the 1.6-inch gutter. Tests in the same afterburner showed that with 1/2-inch-wide gutters combustion could not be maintained at all pressure levels below approximately 1000 pounds per square foot absolute. The data shown in figure 210(b), taken from unpublished NACA tests, are contrary to the width trend indicated in figure 210(a). For this afterburner, a flameholder with a 2-inch-wide gutter had a combustion efficiency 2 to 6 percentage points higher than a flameholder with a $1\frac{5}{8}$-inch-wide gutter. In figure 210(c), the results from reference 31 are shown for two flameholders each having three V-gutter rings. The $1\frac{1}{2}$-inch-wide gutter had 48-percent blockage, and the 3/4-inch-wide gutter had 29-percent blockage. At inlet pressures near 1000 pounds per square foot absolute, the differences in gutter width and blockage had no appreciable effect on combustion efficiency. At lower pressures, the flameholder with narrower gutters and less blocked area produced a combustion efficiency as much as 5 percentage points less than the wide flameholder. Observation of the flame during the tests showed that at pressures less than 800 pounds per square foot absolute the flame was partially blown out with the 3/4-inch gutter, whereas the flame with the $1\frac{1}{2}$-inch gutter was steady and complete. It is thus indicated that the reduction in efficiency at low pressures was due to the narrow gutters rather than the smaller blocked area.

Although there are inconsistencies in the data, it appears that increases in gutter width above $1\frac{1}{2}$ inches have no large effect on combustion efficiency. Reduction in gutter width from $1\frac{1}{2}$ inches to 3/4 inch has no large effect on combustion efficiency, but may cause instability of the flame at low pressures. Gutter widths of 1/2 inch did not support combustion at inlet pressures less than 1000 pounds per square foot absolute. These results were obtained with several afterburners and are apparently independent of burner-inlet velocity over the range between 450 and 620 feet per second. Because all of the burners investigated were 4 feet or more in length, the applicability of the results to shorter afterburners is not known.

Blow-out limits for flameholders having different gutter widths (same afterburners that provided data of figures 210(a) and (c) are shown in figure 211. Although the minimum pressure limits are not clearly defined, it is evident from the consistent trends of lean and rich blow-out limits that the minimum pressure for combustion is higher for the narrower gutters. The magnitude of the increase in minimum pressure limit as gutter width decreases from 2 inches to 3/4 inch is probably of the order of 100 pounds per square foot. Effects of number of gutters on blow-out limits for the afterburners investigated in references 30 and 31 were negligible.

Number of gutters. - Some data showing the effects of the number of flameholder gutters or rings on combustion efficiency are presented in figure 212. In this figure, a $1\frac{1}{2}$-inch-wide, three-ring flameholder is compared with a 3/4-inch-wide, three-ring flameholder and a $1\frac{1}{2}$-inch-wide, two-ring flameholder. As discussed previously in connection with the effects of gutter width, the lower efficiency of the 3/4-inch-wide, three-ring flameholder at low pressures relative to the $1\frac{1}{2}$-inch-wide, three-ring flameholder is attributed to partial blow-out (a gutter-width effect) of the narrower gutters. The three-ring, 3/4-inch-wide flameholder and the two-ring, $1\frac{1}{2}$-inch-wide flameholder both had a blockage of 29 percent. The three-ring,

$1\frac{1}{2}$-inch-wide flameholder had a blockage of 48 percent. Comparison of these three flameholders shows that except in the region of partial blow-out for the 3/4-inch gutters, there is an improvement of about 5 percentage points in combustion efficiency, if three rather than two flameholder rings are used. It is, of course, not possible to separate completely the effects of blockage from the effects of number of rings. Comparison of the three curves at an inlet pressure of 1000 pounds per square foot (above the region of partial blow-out for the 3/4-inch gutters) indicates that blockage in the range from 29 to 48 percent has no separate effect on combustion efficiency. At lower pressures, the effects of number of gutters and blockage on combustion efficiency are not separable, but as is shown subsequently, it is probable that blockage effects are small.

The observed effects of number of gutters, as pointed out in reference 31, are probably due to the increased average burning time obtained by using three rings (six flame fronts or $1\frac{1}{2}$- or 2-inch spacing between gutters), rather than two rings (four flame fronts or about 3-inch spacing between gutters). If the flame front always extends downstream from the gutter edges at approximately the same angle, it is obvious that the fuel particles will, on the average, encounter a flame front farther upstream in the case of the three-ring flameholder than in the case of the two-ring flameholder. Hence, the average burning time is greater for the larger number of flame fronts.

Although the available data are meager, it appears that, if the gutters are wide enough (approximately $1\frac{1}{2}$ in.) to prevent partial blow-out at low pressures, gains in efficiency of 5 to 7 percent are possible at burner-inlet pressures between 500 and 1000 pounds per square foot, by using three rather than two flameholder rings. Data are not available to determine the magnitude of the effects at higher pressures. In view of the apparent insensitivity of combustion efficiency to flameholder design at high afterburner-inlet pressures, it is probable that an afterburner sufficiently long to operate efficiently at low inlet pressure would not be appreciably improved in performance at high pressure by using three flameholder rings instead of two.

Blockage. - Effects of blockage on afterburner combustion efficiency are shown in figure 213 for several afterburners at a high and a low pressure level. Data for this figure were obtained with six afterburners, of which three were fitted with different flameholders to vary the blockage. The number of flameholder gutters used is indicated by the symbols. Included among the tests are a wide variety of fuel-air-ratio and velocity distributions at the burner inlet, average velocity level at the burner inlet, number of flameholder rings, and gutter widths. All the afterburners are similar, however, in that fuel was injected sufficiently far upstream to ensure adequate mixing and vaporization time and burner length was great enough to provide adequate burning time. Although the data at high pressures are few and no one afterburner was investigated over a range of blockages at this high pressure, it is evident that blockage effects at pressure levels near 3000 pounds per square foot are very small. These effects are confirmed by many results, such as those discussed in reference 32, which reports afterburners that operated with high efficiency at burner-inlet pressures of the order of 3000 pounds per square foot with blockages as low as 15 to 20 percent.

At lower pressures (fig. 213(b)), gains in efficiency by increasing blockage beyond 30 percent appear to be negligible. The data for the upper curve of figure 213(b) are representative of three of the best current afterburner designs (afterburners of refs. 6, 31, and 33) in approximately the same state of development.

[redacted]

The small effect of flameholder blockage on combustion efficiency for blockages greater than 30 percent is particularly apparent in these data.

For blockages less than 30 percent, the combustion efficiency decreases as blockage decreases. As indicated in the figure, however, the decrease in efficiency with blockage is greater when blockage is reduced by decreasing the number of flameholder gutters than when blockage is reduced by decreasing the width of the gutters and retaining the same number of gutters. The reduction in efficiency at the lowest blockage may, therefore, be due at least in part to the use of single-gutter flameholders. The lower curve of figure 213(b)(ref. 30), is for flameholders having two gutters, and it is evident that in this case the decrease in efficiency as blockage decreases below 30 percent is much less than for the other two curves. These results are further confirmation of the effects of number of flameholder gutters discussed previously in connection with figure 212.

Although the effects of blockage on operable fuel-air-ratio range and minimum pressure for stable combustion have not been well documented, isolated observations do not indicate any large or consistent trend with blockage.

All the results presented in figure 213 are for flameholders with four to six radial gutters interconnecting the annular gutters. Several experiments have shown that these interconnecting gutters have little effect on combustion efficiency, except at conditions near the minimum pressure limit. It has been shown that in some cases use of interconnecting gutters improves combustion efficiency and operating range of fuel-air ratio at very low inlet pressures without any appreciable penalty in flameholder pressure loss.

Summary. - The number, arrangement, and size of flameholders (of the V-gutter type) are important design considerations. For stable and efficient combustion at afterburner-inlet pressures down to 600 pounds per square foot, minimum gutter width appears to be about $1\frac{1}{2}$ inches. At very high burner-inlet pressures, both two- and three-ring flameholders have about the same combustion efficiency; at intermediate and low pressures, three-ring flameholders are superior. At burner-inlet pressures around 3000 pounds per square foot, change in flameholder blockage over the range from approximately 25 to 40 percent has negligible effect on combustion efficiency. At low pressures (800 lb/sq ft or less), in order to provide a sufficient number of flameholder rings of adequate width, blockages of 30 percent or more must be used for maximum combustion efficiency. Gutter width has a first-order effect on minimum pressure for stable combustion and on fuel-air-ratio range of afterburners; radial gutters interconnecting the annular flameholder rings have a favorable effect on low-pressure limits.

Effect of Flameholder Blockage on Pressure Drop

The pressure drop in the afterburner is due to losses in the diffuser or cooling liners, to the aerodynamic drag of the flameholders, and to the momentum changes associated with combustion of fuel. Numerous approximate methods of calculation of these pressure drops have been published (e.g., refs. 34, 35, and chapter II ref. 14). Some measurements of pressure loss in an afterburner (ref. 31) without burning are shown in figures 214 and 215. The flameholders used were simple nonstaggered V-gutters; the various blockages and sizes are indicated in the keys at the top of the figures. A comparison (fig. 214) of the pressure drops observed with flameholders of the same blockage (29 percent), but having different numbers and sizes of gutters, indicates that number and size have no separate effects on the cold-burner pressure losses. It is evident that velocity has a very large effect on pressure loss and

that, in general, there is a value of velocity at which the rate of change of pressure loss with velocity increases very rapidly.

A cross plot of the data of figure 214 is given in figure 215. At each inlet Mach number, pressure losses increase appreciably only after blocked area is increased above about 30 percent. For a blocked area of 35 percent, the pressure loss increases from about 0.007 to 0.024 of the inlet total pressure as burner-inlet Mach number increases from 0.2 (400 ft/sec) to 0.3 (600 ft/sec). It appears that blockages as high as 30 percent may be used at an inlet Mach number of 0.3, or as high as 37 percent at an inlet Mach number of 0.2, with a cold pressure loss of only 1 percent. Pressure losses at a burner-inlet Mach number of 0.306 computed by a method similar to that of reference 35 are shown by the dashed line. The method used in reference 35 employs an analytic solution for the flow conditions at the downstream, or exit, plane of the flameholder and application of empirically determined coefficients to compute the pressure drop. The agreement between the calculations and the experimental data is good for pressure losses of 0.04 or less. It has been previously shown that blockages of 35 percent are adequate for good performance at high altitudes; it is thus apparent that the "cold-pressure" losses introduced by such a flameholder in an afterburner amount to only 1 or 2 percent.

In figure 216(a), the combined pressure losses due to drag of the flameholder and cooling liner and to combustion of fuel are shown. The pressure loss is shown as a function of temperature ratio across the burner for several flameholder blockages. It is apparent that a change in blockage over the range between 22 and 31 percent has little effect on pressure losses during burning. Although the absolute values of the pressure loss shown in figure 216(a) are high because of an unusual cooling liner that was used, the relative effects of flameholder blockage are valid.

In figure 216(b), a comparison is made between the measured pressure loss and the pressure loss computed by the method of reference 34. Good agreement between the measured and calculated values indicates that, in the absence of cooling liners or other extraneous devices, the method of reference 34 is adequate for the prediction of internal afterburner pressure losses during burning.

COMBUSTION SPACE

The combustion efficiency and maximum obtainable temperature rise in an afterburner are, of course, functions of the space available for combustion. As length is reduced, the time available for the completion of combustion (residence time) is reduced and, in addition, the distance available for the spread of flame across the burner from the flameholders is decreased. Inasmuch as burner-inlet conditions influence these combustion processes, it would be expected that the effects of the combustion space on performance would be different for different pressure, temperature, and velocity levels. The arrangement of the flameholders across the burner cross-section and the amount of wall taper would also be expected to influence the combustion space requirements. Some of these effects for two different classes of afterburners are discussed in the following paragraphs.

Effects of Afterburner Length

Take-off afterburner. - In some afterburner installations, such as in subsonic bombers, it may be desirable to obtain a moderate amount of thrust augmentation at take-off and to carry the afterburner inoperative at altitude conditions. In these applications, minimum afterburner size is required in order to reduce weight and drag penalties to a minimum; internal pressure losses, with their attendant penalties on engine fuel consumption, are also of greater relative importance than the combustion efficiency.

An afterburner designed for take-off application is shown in figure 217. The diffuser, flameholder, fuel system, and perforated liner were designed for minimum pressure loss, as discussed in reference 4, and in part, elsewhere herein. Flameholder blockage amounted to about 14 percent of the burner cross-sectional area. The length of the burner from the flameholder to the exhaust-nozzle outlet was varied from 20 to 62 inches by adding or removing spool sections in the 31-inch-diameter section of the burner. The burner-inlet pressure for the tests was 3800 pounds per square foot absolute, and the burner-inlet velocity (at the flameholder location) was 350 feet per second.

The effect of the afterburner length on the combustion efficiency is shown in figure 218(a). As the length was reduced from 62 to 20 inches, the combustion efficiency decreased from over 90 percent to less than 60 percent. Although the efficiency decreased rather rapidly as the length was reduced below 3 feet, such a change may not be important for a take-off application because the afterburner operates for only a short time. Of greater importance is the thrust augmentation obtainable with different burner lengths shown in figure 218(b). For the reduction in length from 62 to 20 inches, the thrust augmentation ratio (ratio of augmented thrust to normal thrust with the standard tail pipe) decreased from about 1.50 to 1.36. It is evident, therefore, that for an afterburner designed for take-off use only, where the burner-inlet pressures are relatively high and combustor efficiency is not of primary importance, a length of 20 to 30 inches may be adequate.

The total-pressure losses across this afterburner were relatively low. For nonafterburning operation, the loss in total pressure from turbine outlet to exhaust-nozzle outlet was about 5 percent for the burner lengths investigated. This loss is slightly less than the total-pressure loss that usually occurs in a standard, nonafterburning tail pipe.

Altitude afterburner. - Some effects of afterburner length on performance for a limited range of conditions are reported in reference 36; more recent and previously unpublished data over a wide range of conditions and with an afterburner designed to have good performance at high-altitude conditions are discussed herein. A sketch of the afterburner used is shown in figure 219. A two-ring V-gutter flameholder of 29.5-percent blockage was installed. Fuel was injected from 24 fuel-spray bars located 32 inches upstream of the flameholder. The afterburner was cylindrical and its length was varied in four equal steps from 30 to 66 inches. With each burner length investigated, burner-inlet total pressure, total temperature, and velocity were varied over a wide range.

The variation of combustion efficiency with burner length is summarized in figure 220 for the range of burner-inlet conditions investigated. Although reducing inlet pressure and temperature, or raising inlet velocity lowered the general level of combustion efficiency, all the data showed the same general trend of increased combustion efficiency with burner length. Increasing burner length from 30 to 66 inches raised the combustion efficiency by 25 to 35 percentage points over the range of conditions investigated. The major portion of this efficiency variation occurred between burner lengths of 30 and 42 inches.

As a result of the sizeable drop in combustion efficiency at reduced burner-inlet pressures, it follows that a substantial increase in burner length is required to obtain a given efficiency as burner-inlet pressure is lowered. For example, maximum combustion efficiency at a burner-inlet pressure of 750 pounds per square foot was obtained with a burner length of about 66 inches. However, the same efficiency required a burner length of only about 42 inches at a burner-inlet pressure of 1800 pounds per square foot. In addition, the data of figure 218 indicate the same efficiency was attainable with a burner length of only about 32 inches at a burner-inlet pressure of 3800 pounds per square foot.

The data of figures 220(c) and (d) also illustrate the possible trades between burner length and burner-inlet velocity or temperature for operation at constant combustion efficiency. With relatively short burners, an increase in length of only a few inches is required to offset the efficiency reduction accompanying a 200° F drop in inlet temperature or a 100-foot-per-second increase in inlet velocity. However, for burners longer than about 42 inches the added length required to offset efficiency losses resulting from such changes in inlet conditions becomes very large. In fact, if the burner is already relatively long, further additions in length will fail to restore efficiency losses resulting from increased velocity or reduced temperature.

The pressure loss across this afterburner increased with inlet velocity in the manner indicated in figure 214. As might be expected, there was a negligible effect of burner length on pressure loss. For a burner temperature ratio of 2.0 and a burner-inlet temperature of 1200° F, the pressure loss increased from 0.04 to 0.11 of the burner-inlet total pressure as inlet velocity was increased from 400 to 600 feet per second.

3935

Effect of Flameholder Gutter Diameter

Variations in flameholder gutter diameter have been observed to significantly influence the combustion efficiency of an afterburner operating at high altitudes. To demonstrate these effects, a brief investigation was conducted using the afterburner of figure 219 as the reference configuration. Data indicating the effect of flameholder gutter diameter were obtained by using a flameholder with gutter diameters slightly smaller than the one used in the reference configuration. A comparison of these two flameholders is shown in figure 221. The advantage of moving the gutters farther away from the burner wall is that it eases the problem of shell cooling, as is discussed in a later section.

The combustion efficiency obtained with the modified flameholder and that for the reference configuration (fig. 220) are compared in figure 222. The modified flameholder was tested with burner lengths of 42 and 66 inches, and the data for these configurations are shown by the solid symbols. Comparison is made with the performance of the reference flameholder over a range of lengths previously presented in figure 220. Moving the outer gutter away from the burner wall requires added length for the flame front to reach the wall, and thus, as shown here, lowers the combustion efficiency by 5 to 10 percent with a 66-inch burner length and as much as about 30 percent with the 42-inch burner length. This means that moving the flameholder gutters inward to ease shell cooling is equivalent to reducing afterburner length. For the cases investigated, the net effect of the flameholder modification was to reduce the combustion efficiency by about the same amount as would a 15- to 20-inch reduction in length of the reference configuration.

Effect of Afterburner-Shell Taper

To demonstrate the effect of burner-shell taper on performance, the afterburner described in figure 219 was operated with a tapered burner section having a length of 42 inches. A sketch of this configuration is shown in figure 223.

The combustion efficiencies obtained with the 42-inch-large tapered afterburner are compared with those for the cylindrical reference afterburner in figure 224. The data of figure 224(a) indicate that a drop in combustion efficiency of 13 to 18

percent resulted from tapering the burner. The primary reason for this drop in combustion efficiency is reduced residence time, inasmuch as the volume of the tapered burner was only 78 percent of that for the cylindrical burner of equal length. To illustrate this point, the combustion efficiencies of the two afterburners are compared in figure 224(b) on the basis of afterburner volume instead of length. For the single point of comparison (and for two pressure levels), the efficiency is the same for a given afterburner volume, independent of the taper of the outer shell. Such agreement indicates that the secondary factors associated with tapering the burner are relatively unimportant.

Because combustion efficiency is relatively insensitive to length variations for burners about 60 inches long, it might be expected that tapering burners of this length would result in a smaller efficiency reduction than was observed with the 42-inch burner. Unfortunately, data for longer afterburners of sufficiently similar design and operating conditions for inclusion on figure 224 are not available. However, some slightly tapered afterburners about 60 inches in length have been found to operate with combustion efficiencies of about 90 percent at burner-inlet total pressures down to about 1000 pounds per square foot. These observations, therefore, offer some substantiation to the premise that tapering of afterburners having a length greater than about 60 inches will have a relatively minor effect on combustion efficiency.

EFFECTS OF OPERATING VARIABLES ON PERFORMANCE OF A TYPICAL AFTERBURNER

Performance of an afterburner of fixed design is affected by inlet values of velocity, pressure, temperature, and by fuel-air ratio. The effects of inlet conditions on afterburner performance are illustrated to some degree in numerous reports. Reference 2, for example, discusses effects of inlet pressure and velocity in detail. Because most turbojet engines operate at about the same turbine-outlet (afterburner-inlet) temperature, data have not been obtained to show the effect of afterburner-inlet temperature on afterburner performance. Although the quantitative effect of these inlet variables on combustion efficiency differs with afterburner design, as is illustrated elsewhere in this report, the general trends of efficiency with changes in inlet conditions are similar for all burners. With this generality in mind, only a brief summary of the principal trends is given here.

The afterburner selected for the discussion is illustrated in figure 225. The burner is 53 inches long and $25\frac{3}{4}$ inches in diameter. A two-ring V-gutter with a gutter width of $1\frac{1}{2}$ inches and a blocked area of 29 percent was used. Fuel was injected through radial spray bars located approximately 30 inches upstream of the flameholder. Particular attention was given in the design to achieving reasonably uniform fuel-air-ratio distribution at the afterburner inlet. The afterburner had an inlet-velocity distribution (fig. 226) typical of current afterburners.

In figure 227, the effects of inlet velocity and inlet pressure on the combustion efficiency of the burner are illustrated. As shown in figure 227(a), combustion efficiency decreases as burner-inlet pressure decreases. At an inlet velocity of 450 feet per second, the efficiency decreases about 5 percentage points as pressure decreases from 1000 to 570 pounds per square foot. At higher velocities, however, the effects of pressure are greater; at an inlet velocity of 600 feet per second, the efficiency falls off about 13 percentage points for this decrease in pressure. As shown in figure 227(b), this divergence continues for velocities up to 700 feet per second. A loss in efficiency of about 18 percentage points results from decreasing pressure from 1060 to 566 pounds per square foot at an inlet velocity of 650 feet per second.

[redacted]

Although these results are for a fuel-air ratio of 0.047, similar trends are obtained at other fuel-air ratios. Because of the manner in which the particular burner under consideration was operated, individual effects of fuel-air ratio at constant values of pressure and velocity were not obtained. Fuel-air-ratio effects are illustrated, however, for several burners in the section on fuel-injection systems.

The effect of inlet velocity on the blow-out limits is illustrated in figure 228. The minimum pressure for stable combustion at a given fuel-air ratio increases slightly as burner-inlet velocity increases. The minimum pressure at any fuel-air ratio, which occurs at a fuel-air ratio of about 0.060, increases from about 350 pounds per square foot at an inlet velocity of 500 feet per second to 400 pounds per square foot at a velocity of 600 feet per second.

It may be concluded that the effects of inlet velocity on blow-out limits are small but that the inlet velocity and pressure greatly affect the combustion efficiency, even in an afterburner of good design. Although changes in inlet velocity and inlet pressure affect the performance of various burners to different degrees, the trends shown by these data are general and are probably representative of many current afterburner designs.

COMBUSTION INSTABILITY (SCREECH)

The phenomenon commonly known as "screech" in afterburners is a combustion instability characterized by high-frequency, high-amplitude pressure oscillations. Combustion-chamber pressure has been observed to oscillate in various afterburners at frequencies between 800 and 4000 cycles per second and with amplitudes between one-third and one-half the burner-inlet pressure. The oscillations are usually accompanied by increased burner-shell temperature and improved combustion efficiency. The combination of high burner-shell temperature and high-frequency pressure variations frequently leads to structural failure. Numerous failures have been encountered in the afterburner shells, flameholders, and fuel-system components after only a few minutes of operation with screeching combustion. A photograph of a typical failure due to screeching combustion is shown in figure 229. Other oscillations of lower frequency, often referred to as buzz or rumble, sometimes occur in afterburners, but screech is the only type of instability that has become a severe operational problem. Some fundamental considerations of various types of combustion instability, including screech, are discussed in chapter VIII of reference 14.

The afterburner-inlet conditions at which screech occurs differ widely for various afterburner designs. The occurrence of screech has been shown, however, to be consistently related to fuel-air ratio and afterburner-inlet pressure. In general, screeching combustion is observed to occur over a wider range of fuel-air ratios as inlet pressure is increased in the range between 500 and 4000 pounds per square foot. Recent unpublished data indicate that at pressures above 4000 pounds per square foot the range of fuel-air ratio for screech may be reduced. The effects of afterburner-inlet velocity on screech have not been defined completely.

Because of the destructive nature of screeching combustion, considerable effort has been expended in attempts to find methods of suppressing or preventing the occurrence of screech. The principal results of these investigations are summarized in references 37 and 38; they are repeated, in part, in the following discussion. Early experiments, conducted before special transient pressure and flame-front detection instrumentation was available, consisted of determining the effects on screech limits (screech limits are defined as the fuel-air ratio and pressure conditions at which screech starts or stops) of various systematic changes in the de-

sign features of afterburners. Later experiments with both small-scale burners and full-scale afterburners, utilizing special transient instrumentation, were made to identify the mode of oscillation and to develop special devices for preventing screech.

Effect of Afterburner Design on Screech Limits

In the early experiments on effects of afterburner design on screech limits, variations in nearly all afterburner components were investigated. Included in these tests were variations in radial distribution of fuel-air ratio, in distance between fuel injectors and flameholder, in shape of the inlet-diffuser centerbody, in radial velocity distribution at the flameholder, in radial location of the gutters, in flameholder cross-sectional shape, and in gutter width. Results of these tests showed that the centerbody shape, the distance between flameholders, and the distance between the flameholder and the outer wall had no consistent effect on screech limits.

In contrast to these results, the velocity distribution at the flameholder influenced the screech limits to a considerable degree in one afterburner. A high degree of whirl originally existed at the turbine outlet in the particular afterburner investigated. This large whirl resulted in the velocity distribution at the burner inlet (diffuser outlet) shown by the circled points in figure 230. With this velocity distribution, screech was encountered over a fairly wide range of fuel-air ratio, as shown in figure 230(b). The addition of antiwhirl vanes (diamond symbols) eliminated the whirl and also eliminated the low-velocity region at the inner diffuser wall. With the improved velocity profile, screech was not encountered. To determine whether removal of the whirl or of the low-velocity region had eliminated screech, the flow was tripped off the diffuser inner cone by an obstruction. The resultant velocity profile at the burner inlet was very close to the original profile, but no whirl was present. With this configuration, screech again occurred at approximately the same conditions as with the original configuration. It was concluded that the change in velocity profile rather than the change in whirl was responsible for the improved screech limits. It is evident, therefore, that at least in this case the occurrence of screech was dependent upon the velocity profile at the flameholder.

An effect of the radial distribution of fuel-air ratio on screech limits has been observed in several experiments. The results have, however, been erratic and inconclusive. In some cases, a change of as little as 1/8 inch in the immersion of fuel-spray bars eliminated screech at a particular operating condition. In other cases, larger variations in radial fuel distribution have been ineffective in altering the screech limits. Reducing the mixing distance between the fuel injectors and the flameholder has also successfully eliminated screech, but the required reduction in mixing distance has always been so great that altitude performance was sacrificed. Although further research into these effects may reveal some useful design criteria for avoiding screech, it seems unlikely at the present time that alteration in fuel distribution will yield significant benefits in screech suppression without some performance sacrifice.

As illustrated in figure 231, the flameholder gutter width may influence the screech limits. In this figure, the number of times various flameholders of different gutter widths were tested in a particular afterburner is shown; the solid bars represent configurations that screeched, and the open bars those that did not screech. It is then apparent that the wider the gutter, the greater the probability that screech will occur. No screech was encountered in the particular afterburner

investigated if gutters of $1\frac{1}{2}$ inches or less in width were used. This result is not general; other burners using gutters as narrow as 1/2 inch have produced screech, although of lower severity. The general trend of lower screech tendency with narrower gutters has, however, been confirmed in several other investigations. The blockage areas of the flameholders used in these tests were substantially the same. Separate blocked-area effects have not been determined.

A few experiments conducted with various radial locations of the flameholder revealed no effects on screech limits. Similarly, effects of changing the cross-sectional shape from a "V" to a "U" were negligible. However, the addition of an aft splitter plate (such as those shown schematically in fig. 232) to annular V-gutters had appreciable effect on screech limits. As shown in figure 232, a 9-inch splitter was effective in eliminating screech at some conditions. Other experiments have shown that longer splitter plates are even more effective in preventing screech. Although the 9-inch splitter plate was not adversely affected by the surrounding hot gases, the necessity for cooling longer splitters may make them impractical. The effects of splitter plates on combustion efficiency are not known.

These experiments show that the conditions under which an afterburner will screech may be controlled at least partially by proper design of the diffuser, the fuel system, and the flameholder. Proper selection of these components may enable many afterburners to operate over the required range of inlet conditions without encountering screech. In addition, it appears from the large effects of flameholder design and velocity distribution on screech limits that the origin or mechanism of sustenance of screech is associated with the aerodynamics of the flow upstream of the combustion region as well as with the combustion process itself. This relation of the aerodynamic and combustion processes in screech has been appreciated by many investigators, although several different theories to explain the nature of the driving force or "feedback" mechanism have been advanced. It is suggested in reference 39, for example, that vortex shedding from the flameholders may account for the relation between screeching combustion and aerodynamic phenomena. Reference 40 goes farther by stating that the screech oscillations are driven by vortex-induced variations in the flame area with time. Satisfactory verification of either of these hypotheses has not been obtained, however.

Identification of Mode of Oscillation

The tests to determine the effect of burner configuration on screech limits were ineffective in revealing the origin or nature of the pressure oscillations encountered during screech. To identify the mode of oscillation, additional tests were conducted on two afterburners in which transient pressure instrumentation was used to measure temperal variations in pressure and to determine the phase relation between components of the pressure oscillations at various stations around the burner circumference and along the burner length.

A typical oscilloscope record from one of these tests is shown in figure 233. A cross-sectional sketch of the burner used showing the relative positions of the pressure pickups around the circumference and the flameholder location is shown at the bottom of the figure. The oscilloscope record shows that the variation of pressure with time is small at stations 1 and 3 and large at stations 2 and 4. It is evident that the pressure pulses at stations 2 and 4 are 180° out of phase. Similar phase relations were measured for other types of flameholders and for burners of different size. Analysis of the possible modes of oscillation (refs. 14 or 38) shows that the indicated phase relation can occur only in the mode of pressure oscillation called the first transverse mode.

A diagram schematically illustrating the first transverse mode (fig. 234) indicates that the particle paths are curved transverse lines. For the first transverse mode, two nodes exist; for higher-order transverse modes, additional nodes exist, with appropriate increases in frequency. Phase and frequency measurements indicate, as shown in figure 235, that for small afterburners (about 6 in. in diam.) without inlet-diffuser centerbodies, the first mode most frequently exists. Modes up to the fourth apparently occur in larger afterburners (up to 36 in. in diam.) with diffuser centerbodies. The shaded areas of figure 235 indicate the ranges of frequencies that are encompassed by the first and fourth modes of oscillation over the range of gas temperature (speed of sound) in the burner. Similar areas, which would lie between the two shown, can be computed for the second and the third modes; they are omitted in figure 235 for clarity.

Oscillation Damping by Perforated Walls

After it was established that screeching combustion is associated with a transverse oscillation, attempts were made to prevent or suppress screech by dampening the oscillation with various devices arranged inside the burner shell. Experiments were made with an afterburner having fins attached to the wall of the burner that extended the entire length of the combustion chamber. The fins were radial and had various heights and circumferential spacings. The fins altered the screech limits and the oscillation frequency, but did not eliminate screech at all operating conditions. Other investigations of the use of fins are reported in reference 41. The results were generally similar to the NACA experience, in that the fins prevented screech in some, but not all, of the configurations investigated. The use of burner-shell taper is also reported in reference 41 to have successfully prevented screech. This result is, however, not supported by similar NACA tests, in which it was found that shell taper of reasonable amounts would not prevent screech. The difference between the results of reference 41 and of the NACA investigation is probably due to differences in flameholder design, fuel-injection systems, and burner-inlet conditions. It may be concluded that the use of fins or shell taper, while beneficial in some cases, will not prevent screech in all burners or under all conditions of operation.

In another attempt to dampen the pressure oscillations, a perforated liner was installed in an afterburner, as shown in figure 236. The liner, spaced concentrically 3/4 inch from the burner wall, had 3/16-inch-diameter holes throughout, spaced on 1/2-inch centers. The liner extended from a few inches upstream of the flameholder to the end of the 24-inch-long combustion chamber. The use of this liner completely prevented screech with several flameholders at burner-inlet pressures up to approximately 3000 pounds per square foot, which was the maximum pressure investigated.

Many additional tests with similar perforated liners in other afterburners have demonstrated that these liners are effective in eliminating screech over the full operable range of fuel-air ratio and for burner-inlet pressures up to 6500 pounds per square foot absolute. The combustion-chamber length of these afterburners was about 5 feet; liner lengths of 3 feet were sufficient to eliminate screech at all conditions investigated. Corrugated, louvered liners have appeared to be more effective than plain cylindrical, perforated liners.

Summary

It is evident that the design of the flameholder, the fuel system, and the inlet diffuser have an appreciable influence on the screech limits (conditions of inlet pressure and fuel-air ratio) of afterburners. These facts indicate that the

aerodynamics of the flow approaching the burner are linked with the screech mechanism. By proper selection of flameholder, fuel system, and diffuser, many burners may be designed to be screech-free over their required range of operation. Phase and frequency measurements of pressure oscillations in several afterburners have led to identification of the modes of oscillation. The oscillations are transverse and occur in the first to fourth mode in most afterburners investigated. Perforated combustion-chamber liners have prevented screeching combustion in every afterburner investigated over a wide range of fuel-air ratio and pressure conditions.

EFFECT OF DILUENTS ON PERFORMANCE

The combination injection of refrigerants into the compressor or combustion chamber of a turbojet engine with afterburning may, as discussed in reference 42, result in higher thrust augmentation than can be achieved by either injection or afterburning alone. The jet-thrust ratio ideally obtainable with the combined systems is, in fact, approximately the product of the thrust ratios obtainable from the individual systems. Experimental investigation of combined refrigerant injection and afterburning are reported in references 43 and 44. In these experiments, afterburning was combined with injection of ammonia or a water-alcohol mixture. Alcohol is normally added to the water because it depresses the freezing point of the mixture and because it serves as a convenient source of the additional heat needed to vaporize the water. Because a water-alcohol mixture provides appreciable gains in thrust only at moderately high inlet-air temperatures, tests with these fluids were confined to sea-level, zero-ram conditions. Ammonia injection, on the other hand, provides useful thrust gains at low ambient temperatures and, consequently, tests with ammonia injection were conducted at conditions simulating flight above the tropopause at a Mach number of approximately 1.0.

In reference 43, augmentation ratios as high as 1.7 were obtained by combined water-alcohol injection and afterburning as compared to about 1.5 for afterburning alone and 1.22 for injection alone. In reference 44, appreciable thrust increases with combined ammonia injection and afterburning over that obtainable with either system alone were demonstrated. The thrust increases obtainable by the combined augmentation systems depend, however, upon the coolant used, the characteristics of the engine, and the gas-temperature limitations in the afterburner. Because of this dependence of thrust output on factors other than afterburner performance, the effect of the presence of the injected coolants (diluents) on the performance of the afterburner is discussed in this section with regard to operating limits and combustion efficiency of the afterburner rather than with regard to thrust augmentation obtainable.

The afterburners used in the experiments (figs. 237 and 238) were representative of the best current design practices as discussed in other sections of this report. The afterburners were over 5 feet long and had two- or three-ring V-gutter flameholders with blockages of about 35 percent. The fuel-injection systems were located to provide adequate mixing length.

Effect of Water-Alcohol Injection

In figure 239 are shown the effects of the presence of water and alcohol on the combustion efficiency and outlet-gas temperature of the afterburner. The mixture used was 30 percent alcohol and 70 percent water by volume; the alcohol was a blend of 50 percent ethyl and 50 percent methyl alcohol. The value of fuel-air ratio presented in the figure is the weight ratio of fuel flowing to the afterburner (including alcohol not consumed in the engine combustors) to unburned air flowing

to the afterburner. Values of equivalence ratio presented are based on total flow of all fuels (engine fuel, afterburner fuel, and alcohol) and total air flow. At each fuel-air ratio, or equivalence ratio, increasing the flow of coolant decreases the combustion efficiency. These effects are particularly pronounced at the higher equivalence ratios. With an equivalence ratio of 0.93, the efficiency decreases more than 35 percent as the coolant-to-air ratio increases from zero to 0.072. The effects of water-alcohol injection on gas temperature are shown in figure 239(b). Outlet temperature decreases 17 percent over the same range of coolant-to-air ratios. The temperature could not be increased by raising the equivalence ratio beyond the value of 0.93 because the decrease in combustion efficiency offset the increase in fuel flow. The large reduction in combustion efficiency as water-alcohol flow is increased is probably due to a reduction in reaction rate, as discussed in reference 45.

The maximum equivalence ratios that could be used in the engine were limited by afterburner screech. The limits of stable combustion are shown in figure 240. The afterburner fuel-air ratio at which screech occurred was approximately constant over most of the coolant flow range and occurred at a value greater than the fuel-air ratio for maximum temperature. The over-all equivalence ratio was also nearly constant over the range of injected flows.

Although afterburner blow-out was not encountered in the full-scale work of reference 43, some small-scale combustor work reported in reference 46 indicates that for some burner designs, blow-out limits may be affected by water injection. Results of blow-out tests on a 6-inch-diameter V-gutter-type combustor (ref. 48) are shown in figure 241. Afterburner equivalence ratio is plotted against the injected water-air ratio. With the burner operating with JP-3 fuel, the possible range of operation decreases as water-air ratio increases, and operation was not possible at water-air ratios above 0.07.

Also shown in figure 241 are operating points for a slurry fuel of 60 percent magnesium (approximately 3-micron particle size) and 40 percent JP-3 fuel. As indicated by the stable operation obtained at equivalence ratios over 1.0 at water-air ratios as high as 0.15 (limited only by water-pumping capacity), the effect of water injection on blow-out limits is eliminated in the practical range of water injection rates by the use of the slurry fuel.

The small-scale burner results with the slurry fuel have been partially confirmed in a full-scale afterburner. Unpublished full-scale afterburner tests with a slurry of 50 percent magnesium and JP-4 fuel have shown that stable screech-free operation is possible with a water-air ratio of about 0.10 at stoichiometric fuel-air ratio in the afterburner.

Effect of Ammonia Injection

The effect on combustion efficiency and outlet-gas temperature of ammonia injection in the afterburner of figure 238 is shown in figure 242. In this afterburner, maximum combustion efficiency and highest gas temperature over the range of equivalence ratios covered occurred at an over-all equivalence ratio of 1.0 for all ammonia flows. Increasing the ammonia-air ratio decreased both the combustion efficiency and the maximum gas temperature. This effect, while quite small at an equivalence ratio of 1.0, became much greater as the equivalence ratio was decreased.

Although screech was not encountered during these tests, the effect of ammonia injection on blow-out limits shown in figure 243 was observed. At the higher ammonia-injection rates, the afterburner was operable over only a very narrow range

of equivalence ratios. At ammonia-air ratios above 0.05, afterburner operation was not possible at any equivalence ratio at these inlet conditions. A similar, though less pronounced, trend of decreasing limits of flame propagation with increases in ammonia-air ratio above 0.02 is noted in reference 47.

The relative effects of water and ammonia on afterburner combustion efficiency cannot be determined by direct comparison of the results because the tests were run on different afterburners with somewhat different inlet conditions. It is probable that the superior performance of the afterburner of figure 238 with ammonia injection as compared to the afterburner in figure 237 with water injection is due, at least in part, to its greater length.

3925

REFERENCES

1. Nakanishi, S., Velie, W. W., and Bryant, L.: An Investigation of Effects of Flame-Holder Gutter Shape on Afterburner Performance. NACA RM E53J14, 1954.

2. Schulze, F. W., Bloomer, H. E., and Miller, R. R.: Altitude-Wind-Tunnel Investigation of Several Afterburner Configurations Having Moderately High Burner-Inlet Velocities. NACA RM E54G22, 1954.

3. Wood, Charles C., and Higgenbotham, James T.: Effects of Diffuser and Center-Body Length on Performance of Annular Diffusers with Constant-Diameter Outer Walls and with Vortex-Generator Flow Controls. NACA RM L54G21, 1954.

4. Ciepluch, Carl C., Velie, Wallace W., and Burley, Richard R.: A Low-Pressure-Loss Short Afterburner for Sea-Level Thrust Augmentation. NACA RM E55D26, 1955.

5. Wood, Charles C.: Preliminary Investigation of the Effects of Rectangular Vortex Generators on the Performance of a Short 1.9:1 Straight-Wall Annular Diffuser. NACA RM L51G09, 1951.

6. Conrad, E. William, Schulze, Frederick W., and Usow, Karl H.: Effect of Diffuser Design, Diffuser-Exit Velocity Profile, and Fuel Distribution on Altitude Performance of Several Afterburner Configurations. NACA RM E53A30, 1953.

7. Conrad, E. William, and Campbell, Carl E.: Altitude Wind Tunnel Investigation of High-Temperature Afterburners. NACA RM E51L07, 1952.

8. Patterson, G. N.: Modern Diffuser Design. Aircraft Eng., vol. X, no. 115, Sept. 1938, pp. 267-673.

9. Mallett, William E., and Harp, James L., Jr.: Performance Characteristics of Several Short Annular Diffusers for Turbojet Engine Afterburners. NACA RM E54B09, 1954.

10. Braithwaite, Willis M., Walker, Curtis L., and Sivo, Joseph N.: Altitude Evaluation of Several Afterburner Design Variables on a J47-GE-17 Turbojet Engine. NACA RM E53F10, 1953.

11. Renas, P. E., Harvey, R. W., Sr., and Jansen, E. T.: Altitude Starting Characteristics of an Afterburner with Autoignition and Hot-Streak Ignition. NACA RM E53B02, 1953.

[redacted]

11. Renas, P. E., Harvey, R. W., Sr., and Jansen, E. T.: Altitude Starting Characteristics of an Afterburner with Autoignition and Hot-Streak Ignition. NACA RM E53B02, 1953.

12. Fleming, W. A., Conrad, E. William, and Young, A. W.: Experimental Investigation of Tail-Pipe-Burner Design Variables. NACA RM E50K22, 1951.

13. Thorman, H. Carl, and Campbell, Carl E.: Altitude-Wind-Tunnel Investigation of Tail-Pipe Burner with Converging Conical Burner Section on J35-A-5 Turbojet Engine. NACA RM E9I16, 1950.

14. Fuels and Combustion Research Division: Adaptation of Combustion Principles to Aircraft Propulsion. Vol. I - Basic Considerations in the Combustion of Hydrocarbon Fuels with Air. NACA RM E54I07, 1955.

15. Conrad, E. William, Bloomer, Harry E., and Sobolewski, Adam E.: Altitude Operational Characteristics of a Prototype Model of the J47D (RX1-1 and RX1-3) Turbojet Engines with Integrated Electronic Control. NACA RM E51E08, 1952.

16. Gerrish, Harold C., Meem, J. Lawrence, Jr., Scadron, Marvin D., and Colnar, Anthony: The NACA Mixture Analyzer and Its Application to Mixture-Distribution Measurement in Flight. NACA TN 1238, 1947.

17. Jansen, Emmert T., Velie, Wallace W., and Wilsted, H. Dean: Experimental Investigation of the Effect of Fuel-Injection-System Design Variables on Afterburner Performance. NACA RM E53K16, 1954.

18. Longwell, John P., and Weiss, Malcolm A.: Mixing and Distribution of Liquids in High-Velocity Air Streams. Ind. and Eng. Chem., vol. 45, no. 3, Mar. 1953, pp. 667-677.

19. Johnson, LaVern A., and Meyer, Carl L.: Altitude Performance Characteristics of Turbojet-Engine Tail-Pipe Burner with Variable-Area Exhaust Nozzle Using Several Fuel Systems and Flame Holders. NACA RM E50F28, 1950.

20. Trout, Arthur M., and Wentworth, Carl B.: Altitude Investigation of a 20-Inch Ram-Jet Combustor with a Rich Inner Zone of Combustion for Improved Low-Temperature-Ratio Operation. NACA RM E52L26, 1953.

21. Henzel, James G., Jr., and Wentworth, Carl B.: Free-Jet Investigation of 20-Inch Ram-Jet Combustor Utilizing High-Heat-Release Pilot Burner. NACA RM E53H14, 1953.

22. Dangle, E. E., Friedman, Robert, and Cervenka, A. J.: Analytical and Experimental Studies of a Divided-Flow Ram-Jet Combustor. NACA RM E53K04, 1954.

23. Huntley, S. C., Auble, Carmon M., and Useller, James W.: Altitude Performance Investigation of a High-Temperature Afterburner. NACA RM E53D22, 1953.

24. Chelko, Louis J.: Penetration of Liquid Jets into a High-Velocity Air Stream. NACA RM E50F21, 1950.

25. Callaghan, Edmund E., and Ruggeri, Robert S.: Investigation of the Penetration of an Air Jet Directed Perpendicularly to an Air Stream. NACA TN 1615, 1948.

[redacted]

26. Huntley, S. C., and Wilsted, H. D.: Altitude Performance Investigation of Two Flame-Holder and Fuel-System Configurations in Short Afterburner. NACA RM E52B25, 1952.

27. Nickolson, H. M., and Field, J. P.: Some Experimental Techniques for the Investigation of the Mechanism of Flame Stabilization in the Wakes of Bluff Bodies. Third Symposium on Combustion and Flame and Explosion Phenomena, The Williams & Wilkins Co. (Baltimore), 1949, pp. 44-68.

28. Williams, Glenn C.: Basic Studies on Flame Stabilization. Jour. Aero. Sci., vol. 16, no. 12, Dec. 1949, pp. 714-722.

29. Younger, George G., Gabriel, David S., and Mickelsen, William R.: Experimental Study of Isothermal Wake-Flow Characteristics of Various Flame-Holder Shapes. NACA RM E51K07, 1952.

30. Renas, Paul E., and Jansen, Emmert T.: Effect of Flame-Holder Design on Altitude Performance of Louvered-Liner Afterburner. NACA RM E53H15, 1953.

31. Henzel, James G., Jr., and Bryant, Lively: Investigation of Effect of Number and Width of Annular Flame-Holder Gutters on Afterburner Performance. NACA RM E54C30, 1954.

32. Lundin, Bruce T., Dowman, Harry W., and Gabriel, David S.: Experimental Investigation of Thrust Augmentation of a Turbojet Engine at Zero Ram by Means of Tail-Pipe Burning. NACA RM E6J21, 1947.

33. Braithwaite, Willis M., Renas, Paul E., and Jansen, Emmert T.: Altitude Investigation of Three Flame-Holder and Fuel-Systems Configurations in a Short Converging Afterburner on a Turbojet Engine. NACA RM E52G29, 1952.

34. Hawthorne, W. R., and Cohen, H.: Pressure Losses and Velocity Changes Due to Heat Release and Mixing in Frictionless, Compressible Flow. Rep. No. E.3997, British R.A.E., Jan. 1944.

35. Sterbentz, William H.: Analysis and Experimental Observation of Pressure Losses in Ram-Jet Combustion Chambers. NACA RM E9H19, 1949.

36. Useller, James W., Braithwaite, Willis M., and Rudey, Carl J.: Influence of Combustion-Chamber Length on Afterburner Performance. NACA RM E54E06, 1954.

37. Harp, James L., Jr., Velie, Wallace W., and Bryant, Lively: Investigation of Combustion Screech and a Method of Its Control. NACA RM E53L24b, 1954.

38. Lewis Laboratory Staff: A Summary of Preliminary Investigations into the Characteristics of Combustion Screech in Ducted Burners. NACA RM E54B02, 1954.

39. Bragdon, Thomas A., Lewis, George D., and King, Charles H.: Interim Report on Experimental Investigation of High Frequency Oscillations in Ramjet Combustion Chambers. M.I.T. Meteor Rep. UAC-53, Res. Dept., United Aircraft Corp., Oct. 1951. (BuOrd Contract NOrd 9845.)

40. Kaskan, W. E., and Noreen, A. E.: High-Frequency Oscillations of a Flame Held by a Bluff Body. A.S.M.E. Trans., vol. 77, no. 6, Aug. 1955, pp. 855-891; discussion, pp. 891-895.

41. Newton, R. T., and Truman, J. C.: An Approach to the Problem of Screech in Ducted Burners. General Eng. Lab., General Electric Co., Schenectady (N.Y.), Mar. 12, 1954.

42. Hall, Eldon W., and Wilcox, E. Clinton: Theoretical Comparison of Several Methods of Thrust Augmentation for Turbojet Engines. NACA Rep. 992, 1950. (Supersedes NACA RM E8H11.)

43. Useller, James W., and Povolny, John H.: Experimental Investigation of Turbojet-Engine Thrust Augmentation by Combined Compressor Coolant Injection and Tail-Pipe Burning. NACA RM E51H16, 1951.

44. Useller, James W., Harp, James L., Jr., and Fenn, David B.: Turbojet-Engine Thrust Augmentation at Altitudes by Combined Ammonia Injection into the Compressor Inlet and Afterburning. NACA RM E52L19, 1953.

45. Kapp, N. M., Snow, B., and Wohl, K.: The Effect of Water Vapor on the Normal Burning Velocity and on the Stability of Butane-Air Flames Burning above Tubes in Free Air. Meteor Rep. UAC-30, United Aircraft Corp., Nov. 1948. (U. S. Navy, BuOrd Contract NOrd-9845 with M.I.T.)

46. Tower, Leonard K.: Effect of Water Vapor on Combustion of Magnesium-Hydrocarbon Slurry Fuels in Small-Scale Afterburner. NACA RM E52H25, 1952.

47. O'Neal, Cleveland, Jr.: Effect of Ammonia Addition on Limits of Flame Propagation for Isooctane-Air Mixtures at Reduced Pressures and Elevated Temperatures. NACA TN 3446, 1955.

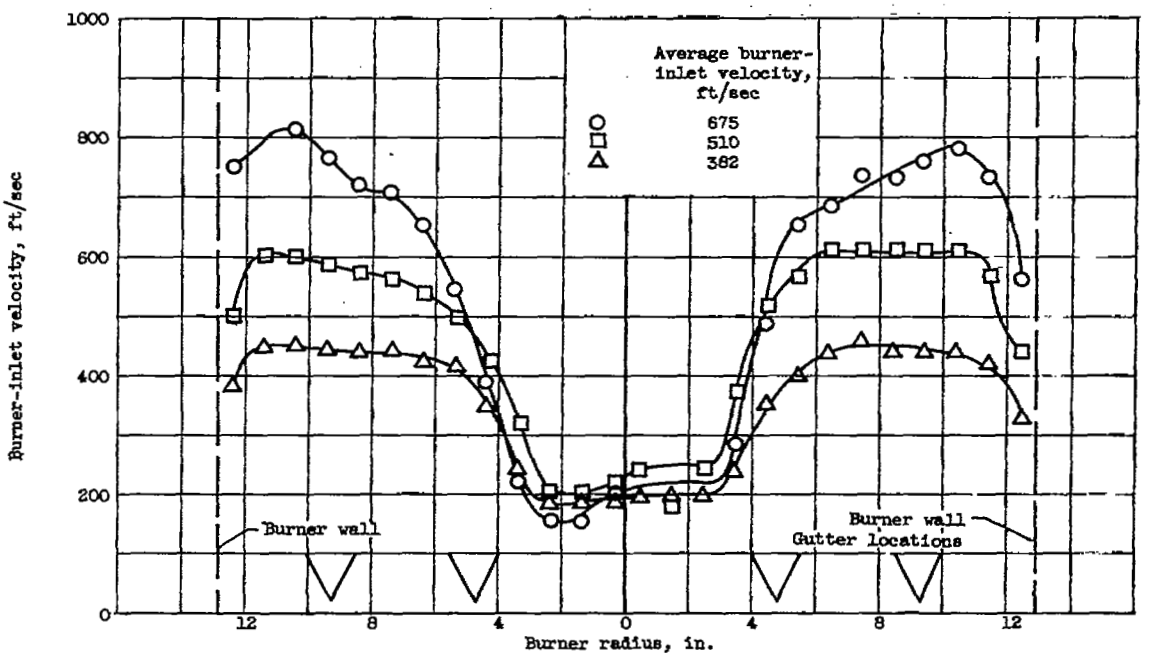

(a) Velocity profiles.

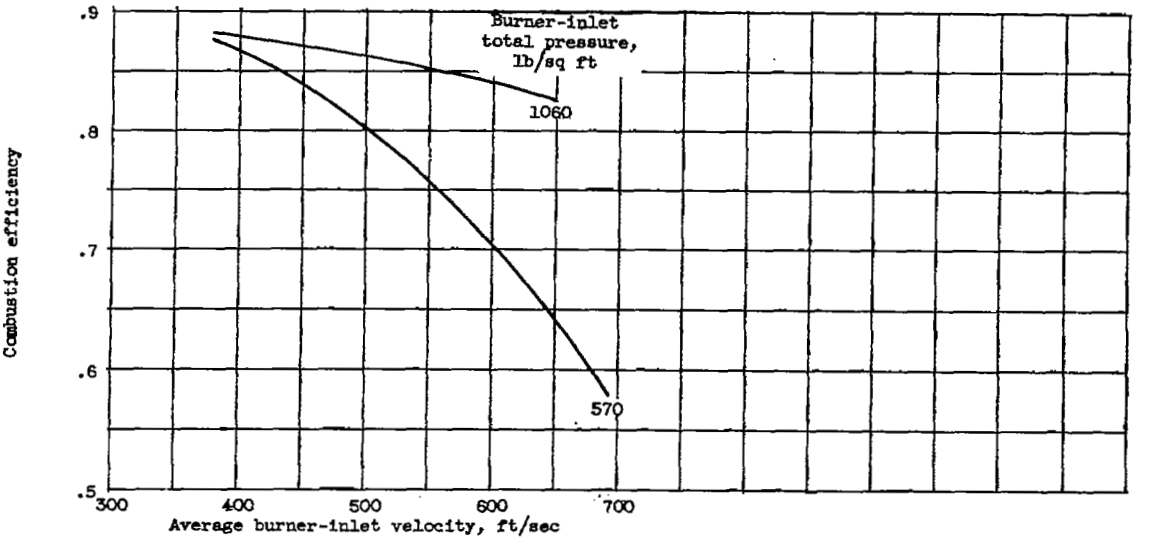

(b) Combustion efficiency at fuel-air ratio of 0.047.

Figure 158. - Effect of velocity in region of flameholders on afterburner performance.

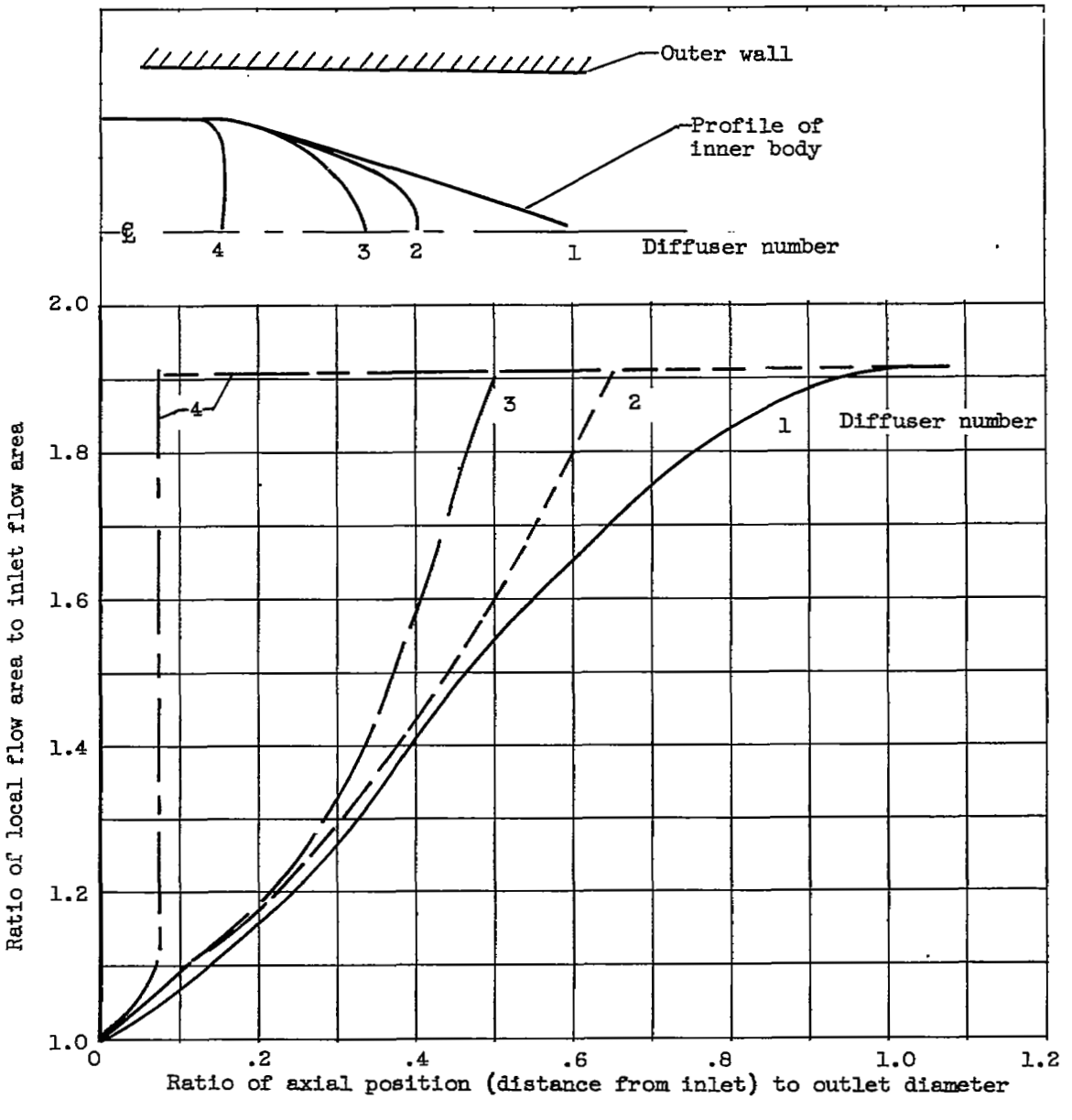

Figure 159. - Geometric relations of diffusers investigated to determine length effects.

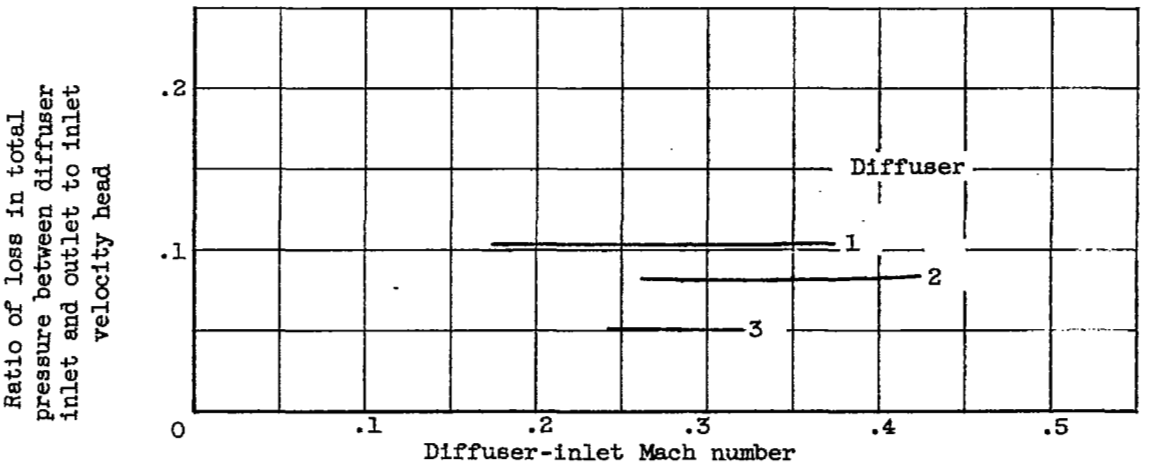

(a) Pressure loss.

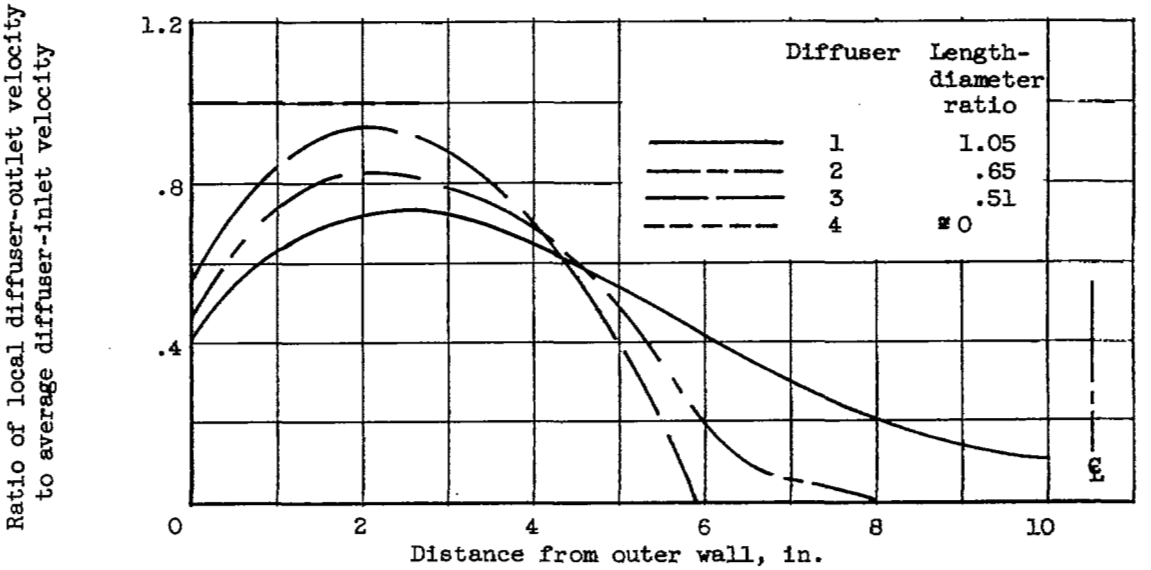

(b) Velocity profile.

Figure 160. - Performance of four diffusers of different length.

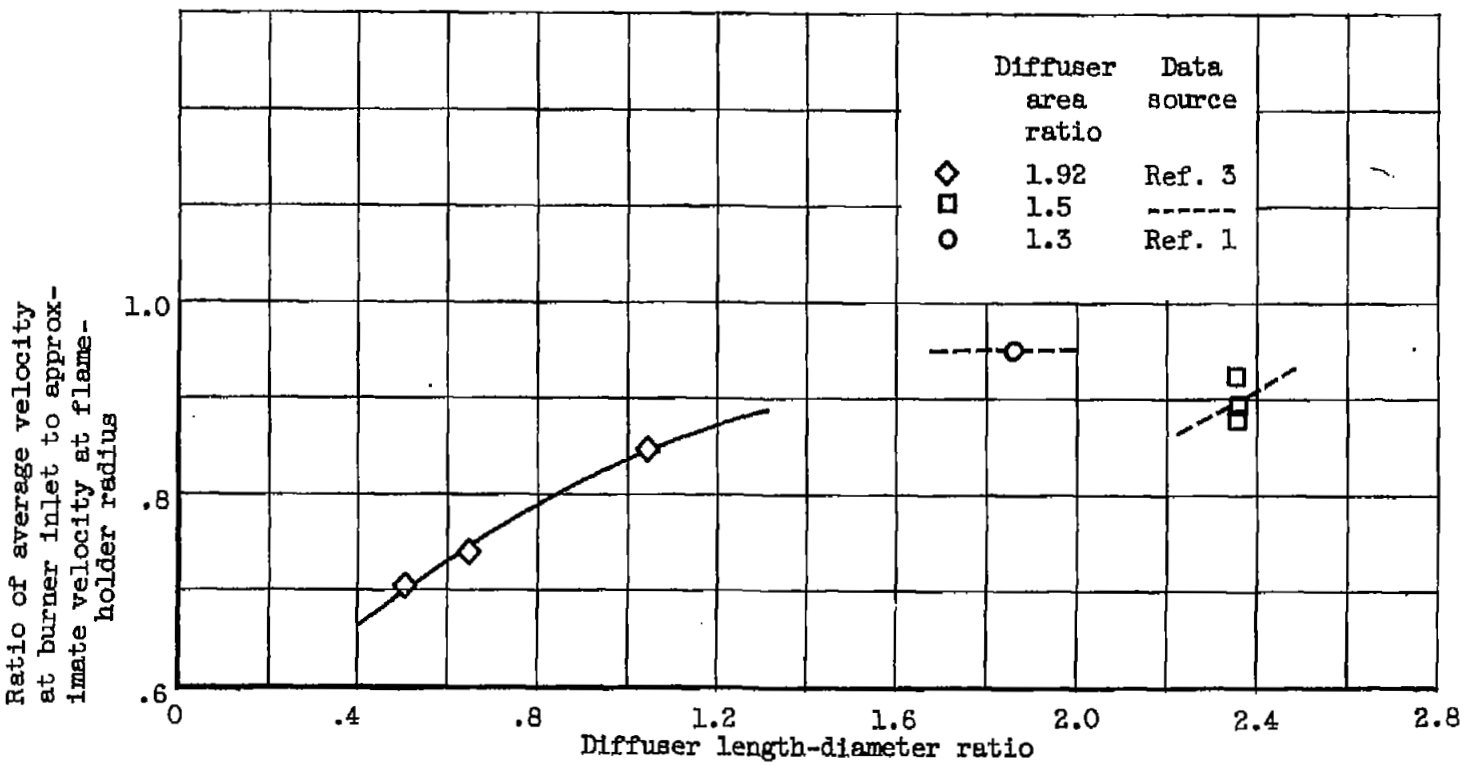

Figure 161. - Effect of diffuser length-diameter ratio on velocity near flameholder.

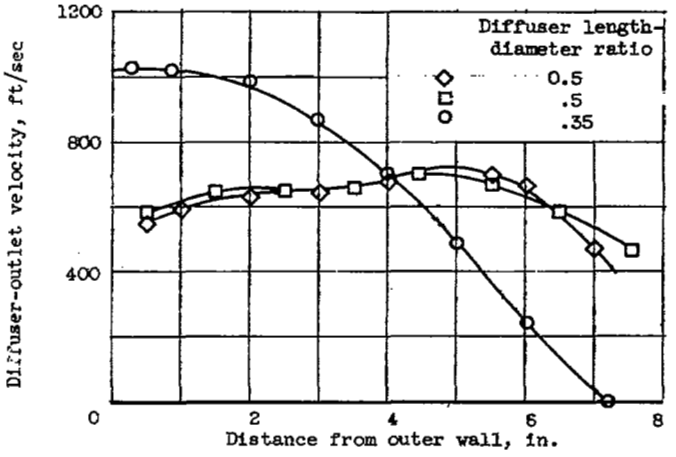

(a) Velocity profiles.

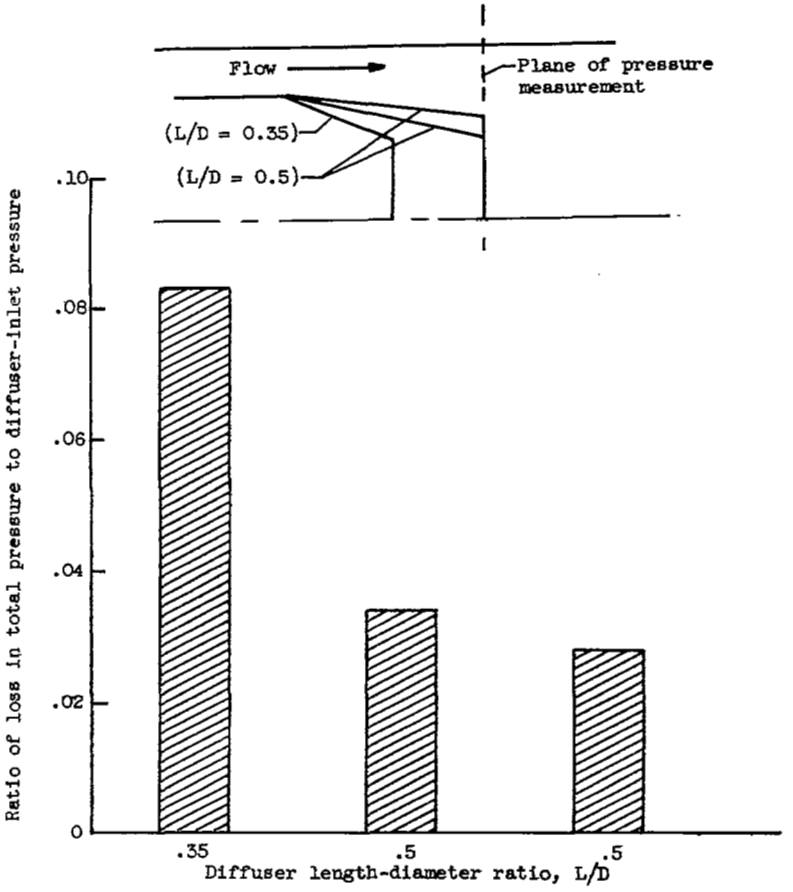

(b) Pressure loss.

Figure 162. - Effect of length on diffuser performance.

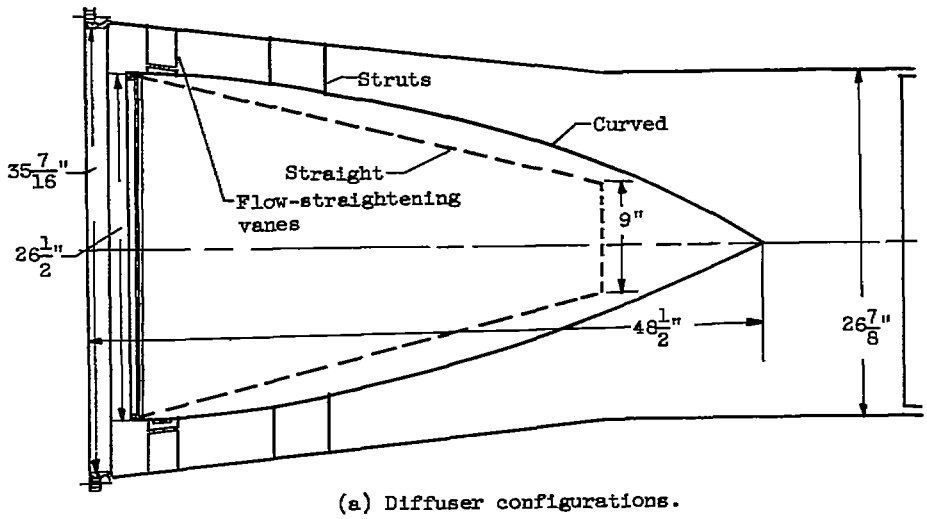

(a) Diffuser configurations.

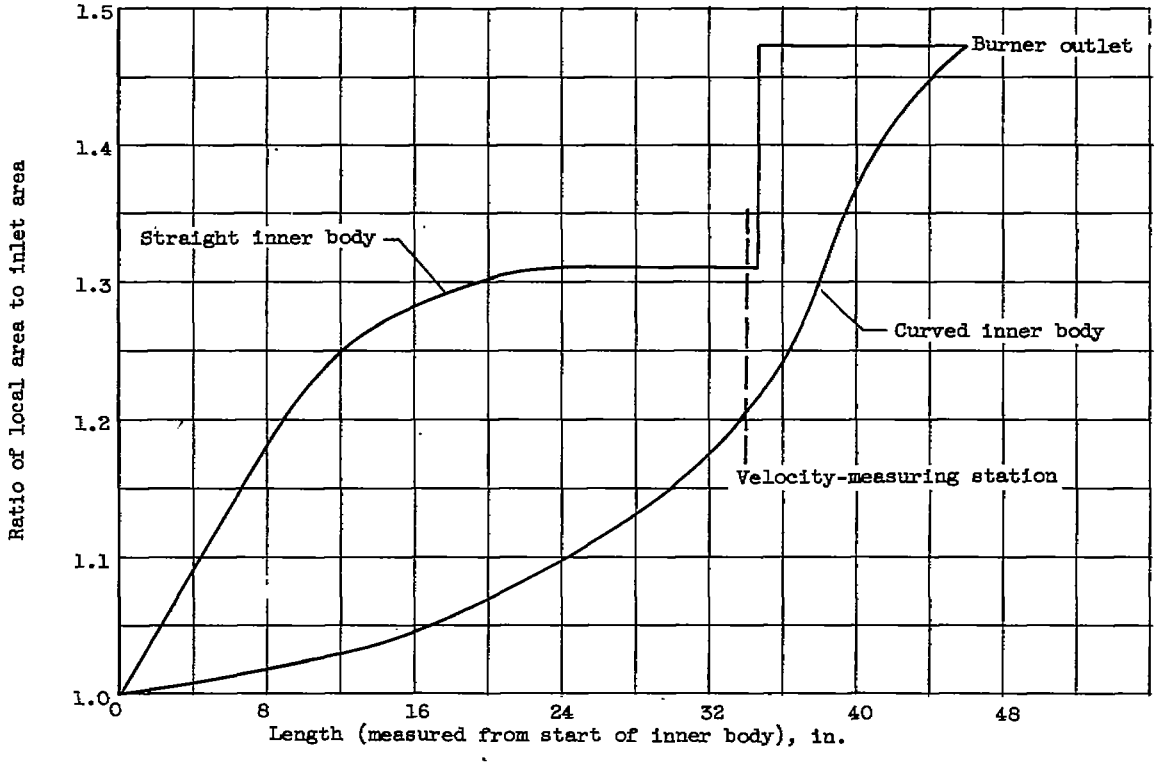

(b) Diffuser area variation.

Figure 163. - Diffusers used in investigation of inner-body shape.

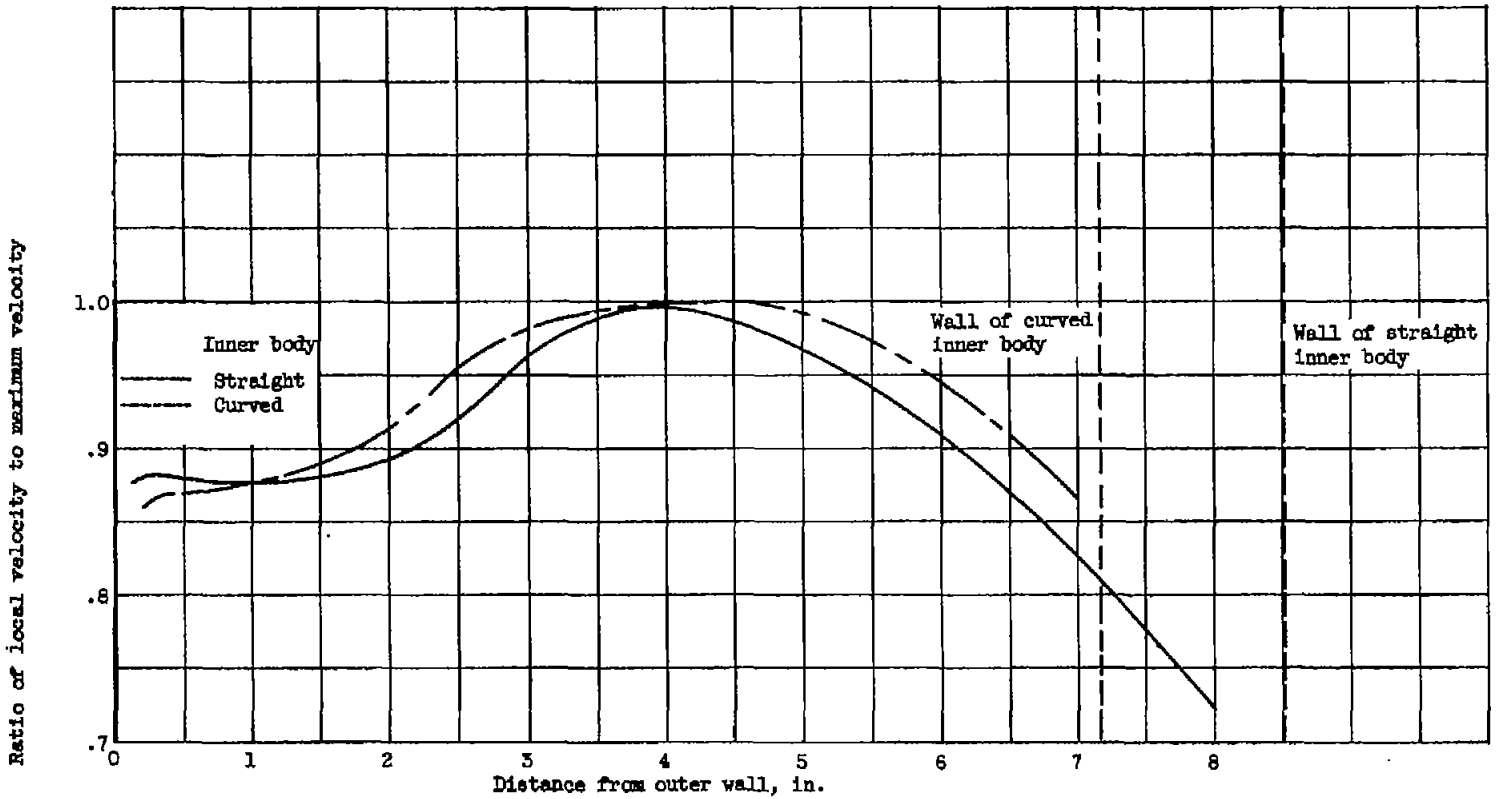

Figure 164. - Radial velocity profiles 34 inches from diffuser inlet with two inner-body shapes.

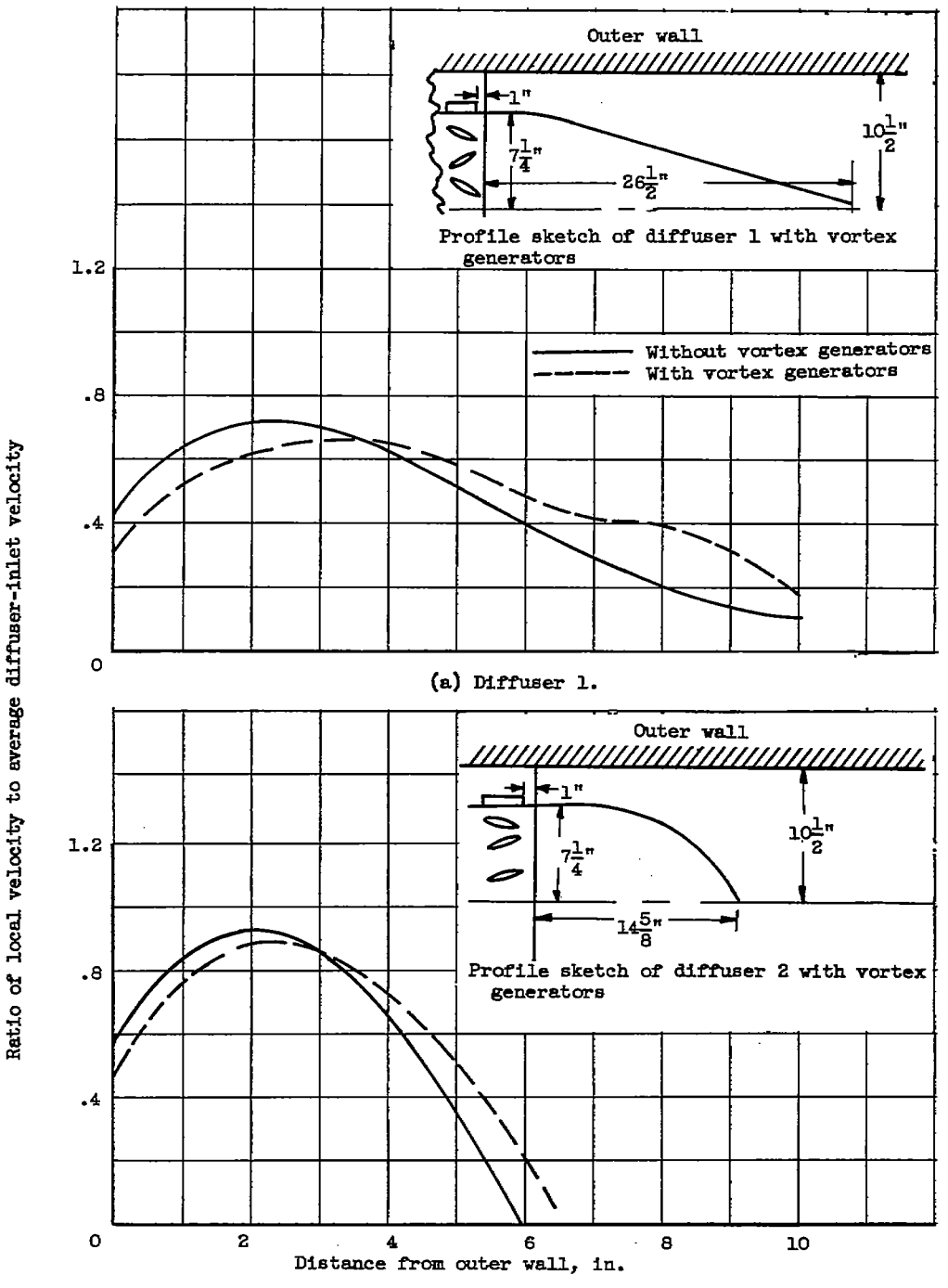

(a) Diffuser 1.

(b) Diffuser 2.

Figure 165. - Effect of vortex generators on diffuser-outlet velocity profiles.

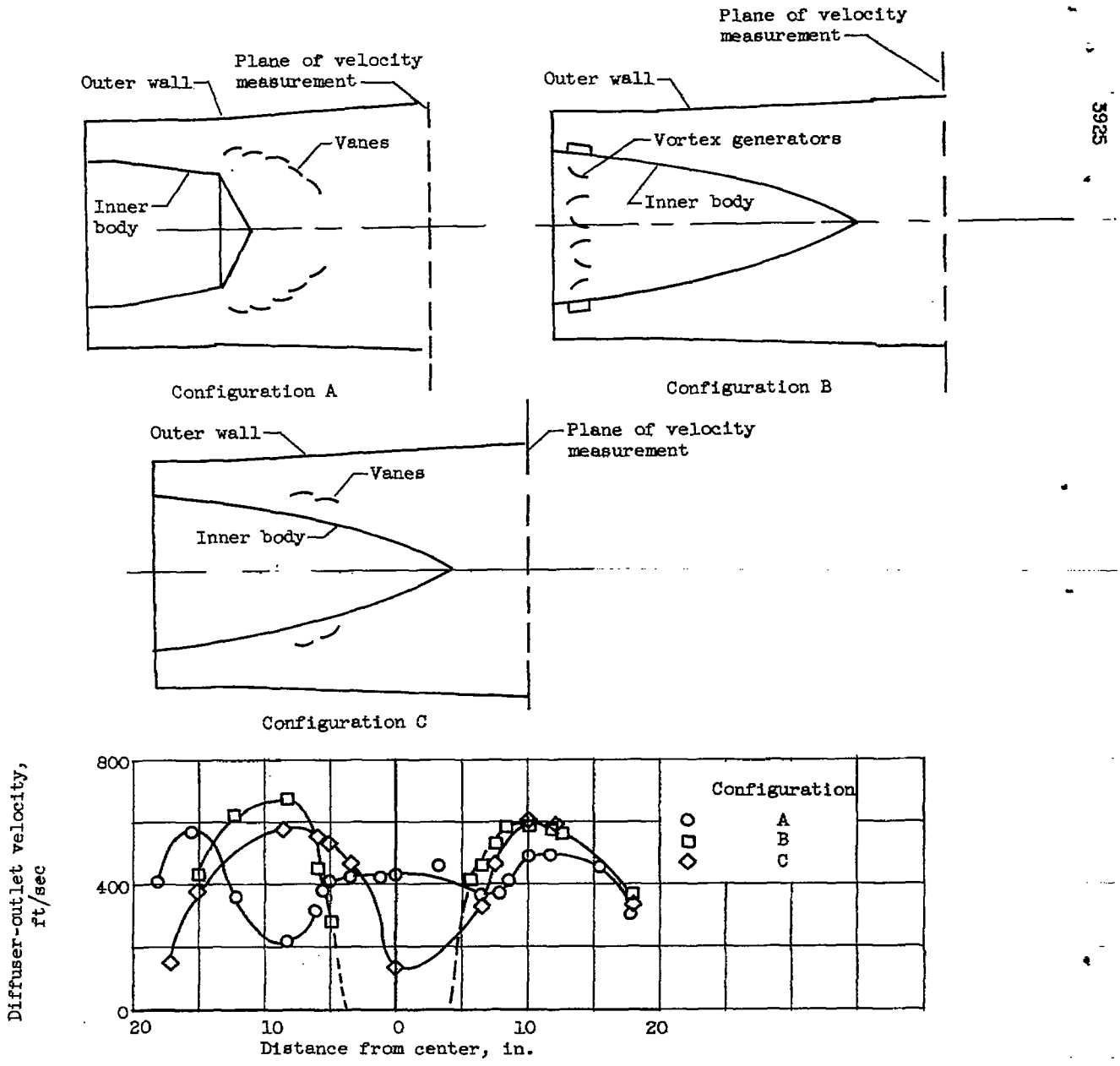

Figure 166. - Effect of annular vanes on diffuser-outlet velocity profiles.

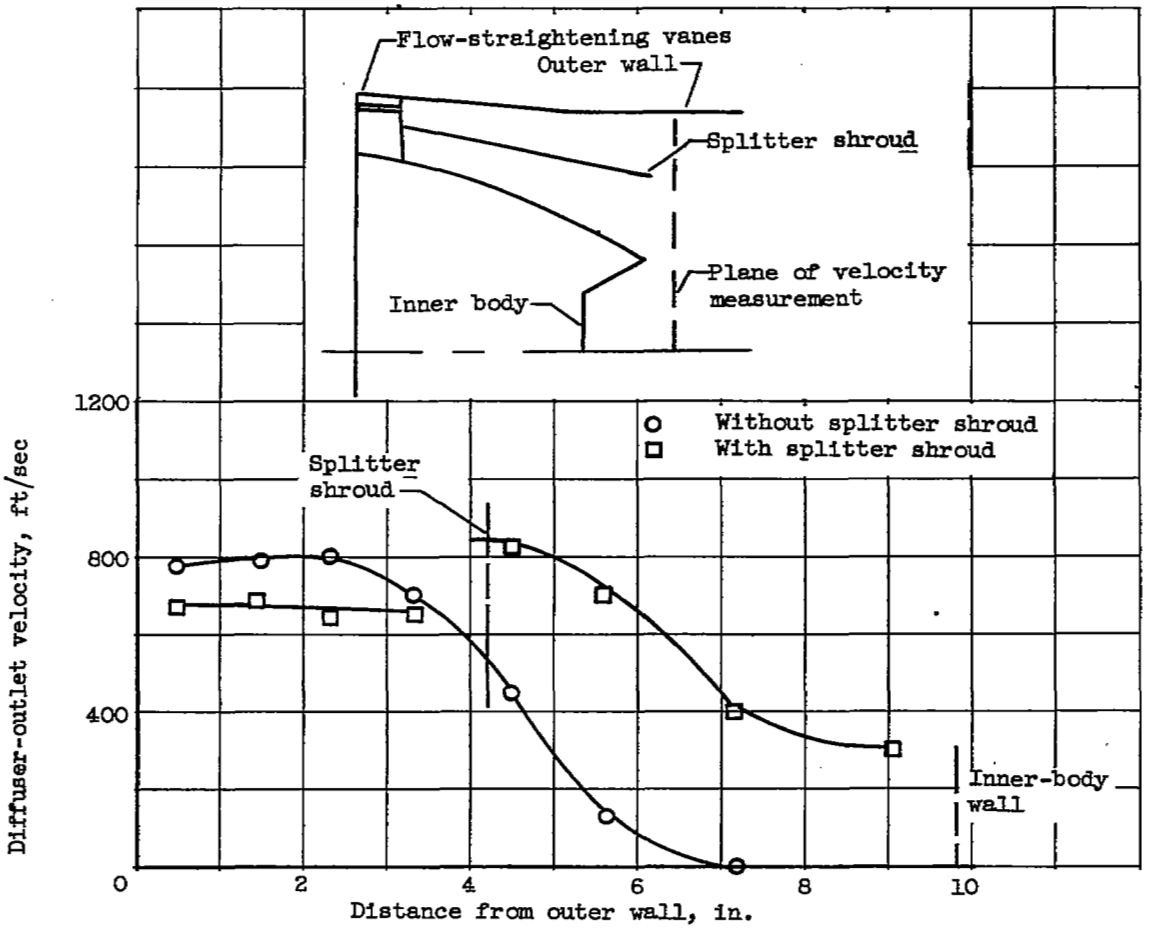

Figure 167. - Effect of splitter shroud on diffuser-outlet velocity profile.

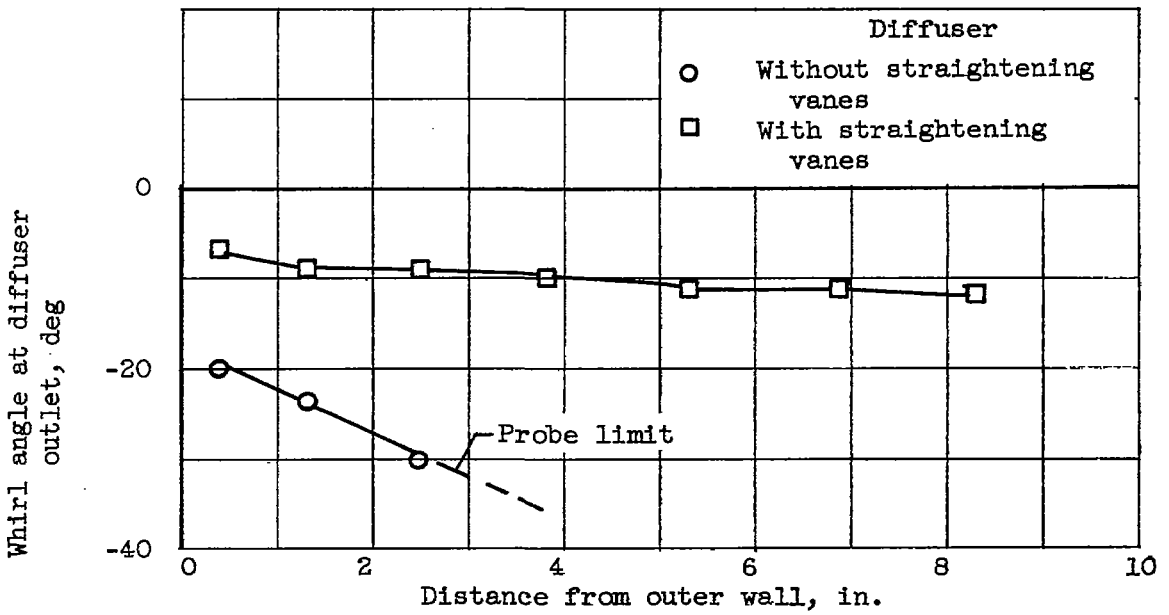

(a) Representative diffuser-outlet whirl angles.

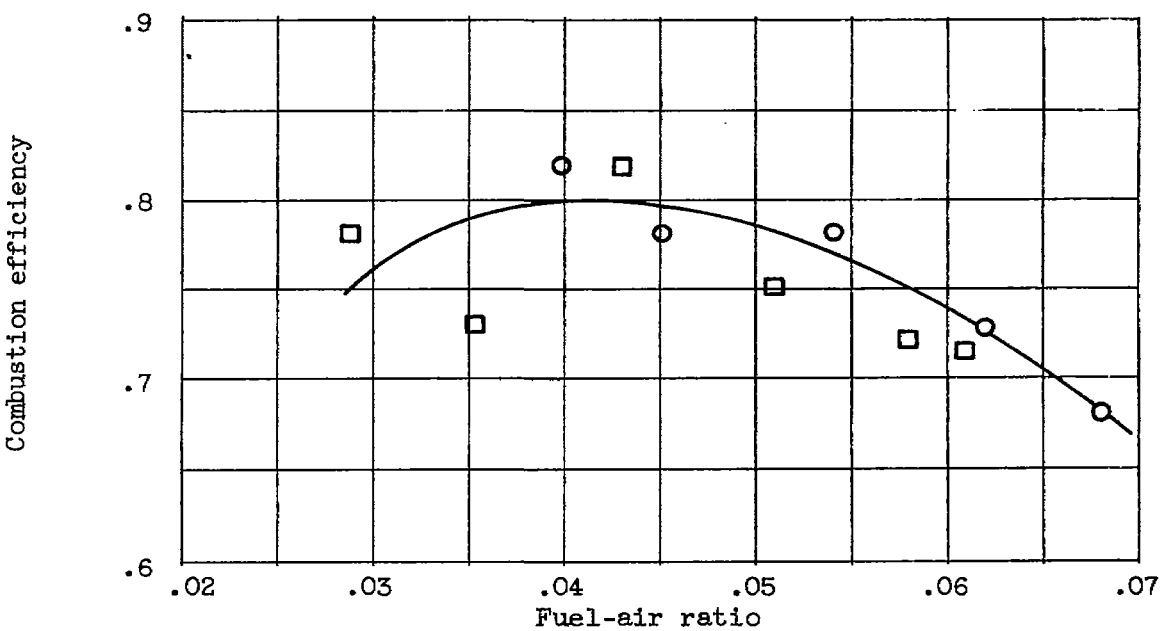

(b) Effect of diffuser-outlet whirl on combustion efficiency at altitude.

Figure 168. - Effect of diffuser-outlet whirl on afterburner performance.

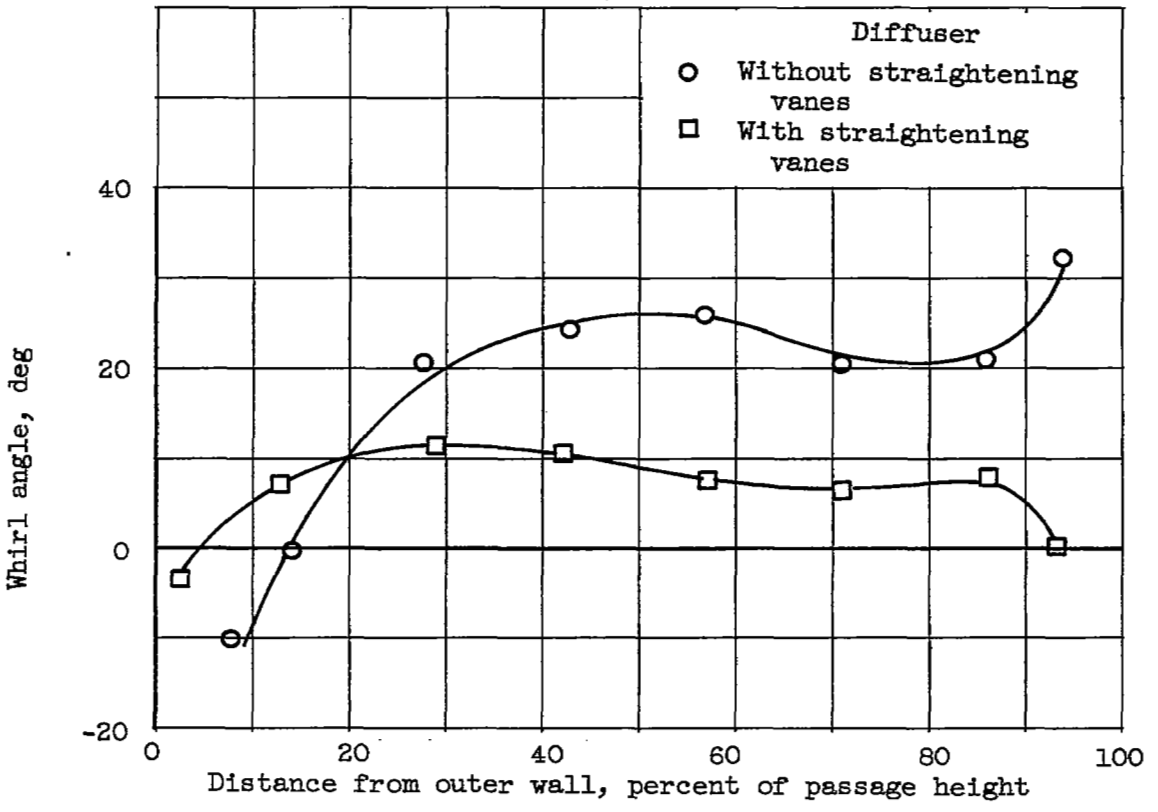

Figure 169. - Effect of straightening vanes on whirl angles near diffuser inlet.

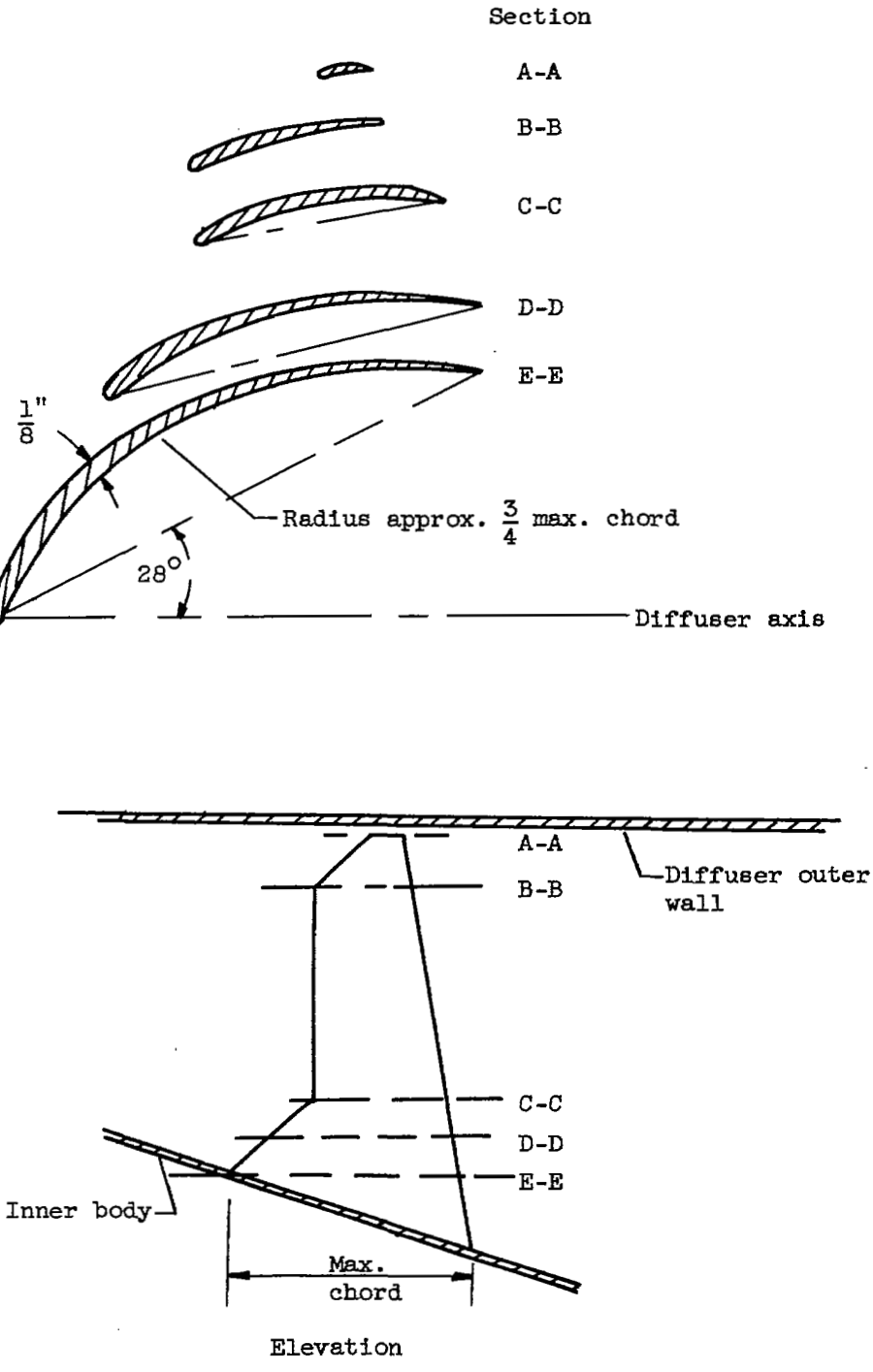

Figure 170. - Typical flow-straightening vane at turbine outlet.

3925

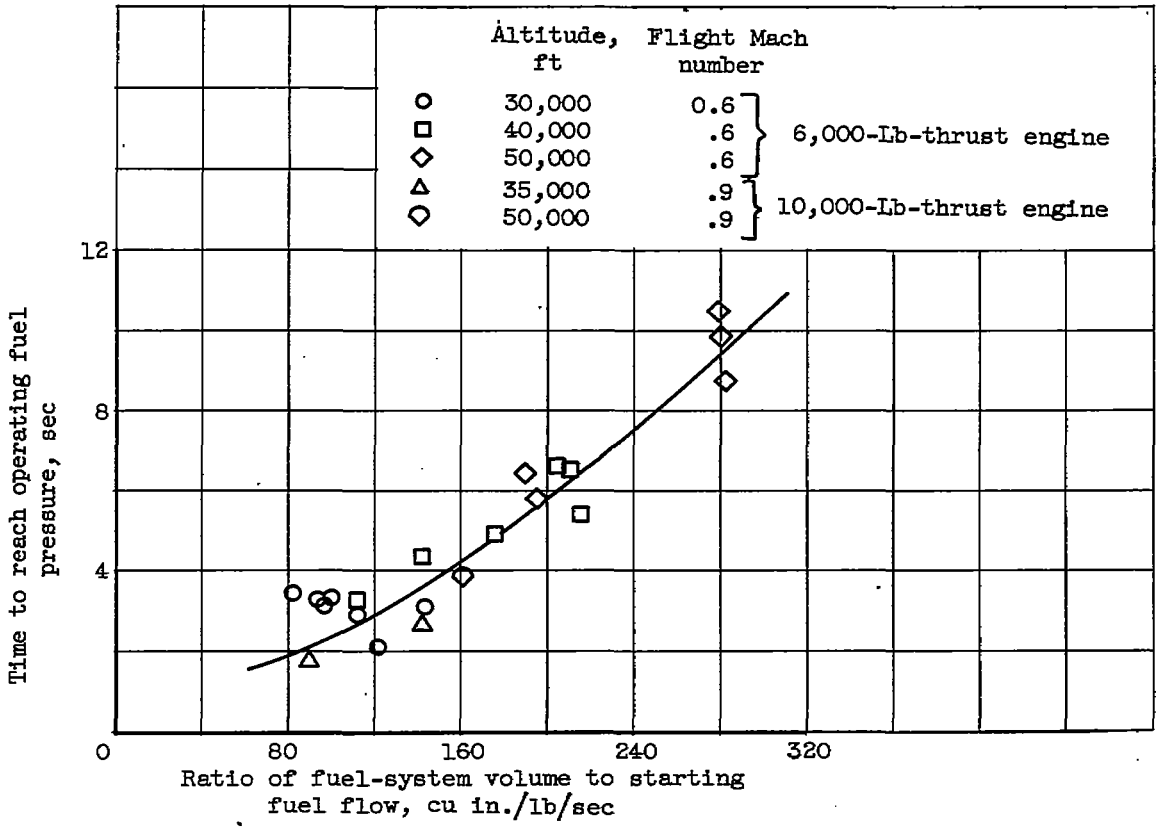

Figure 171. - Time required to reach operating fuel-manifold pressure for an afterburner start.

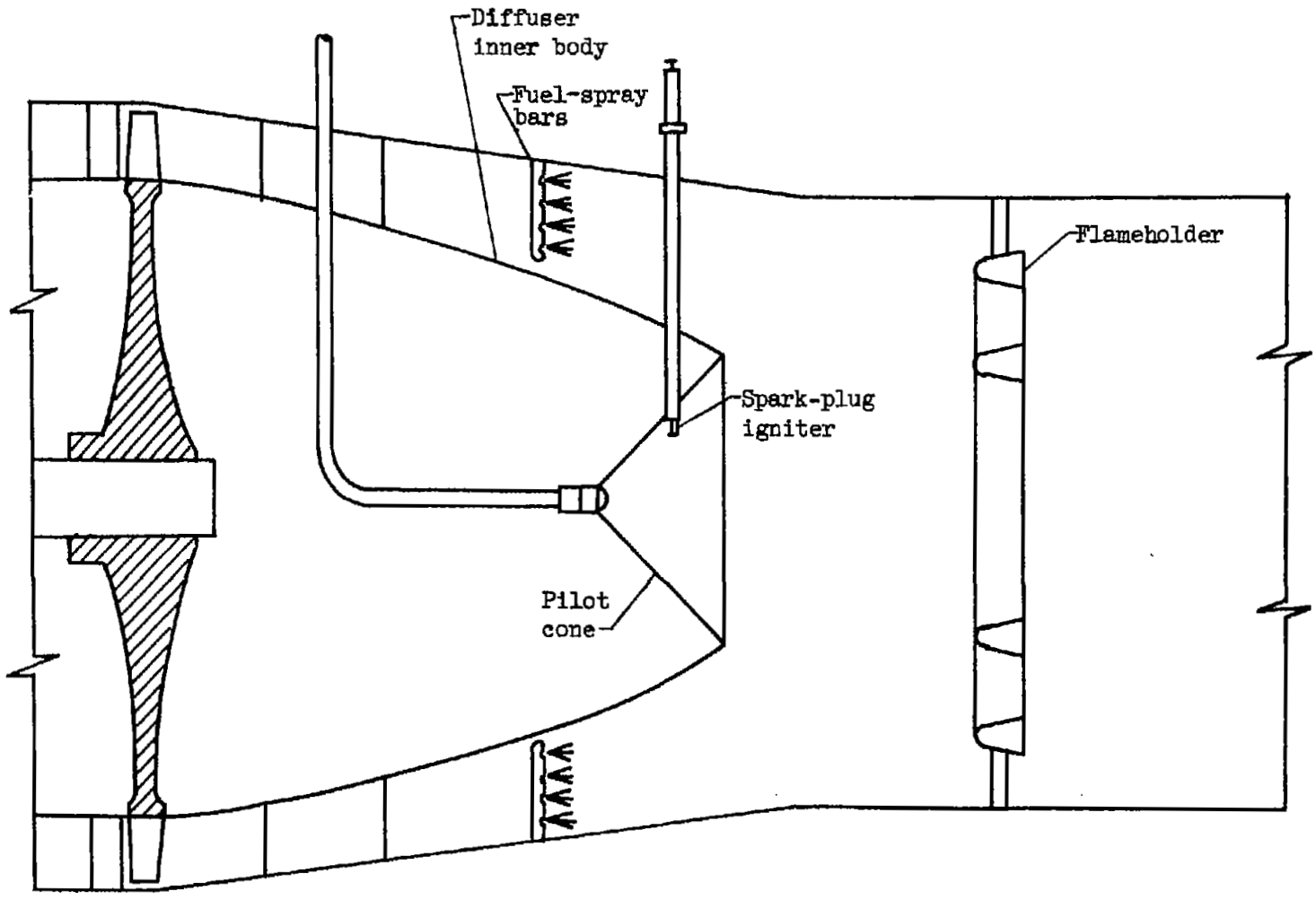

Figure 172. - Typical spark-plug igniter installation in afterburner.

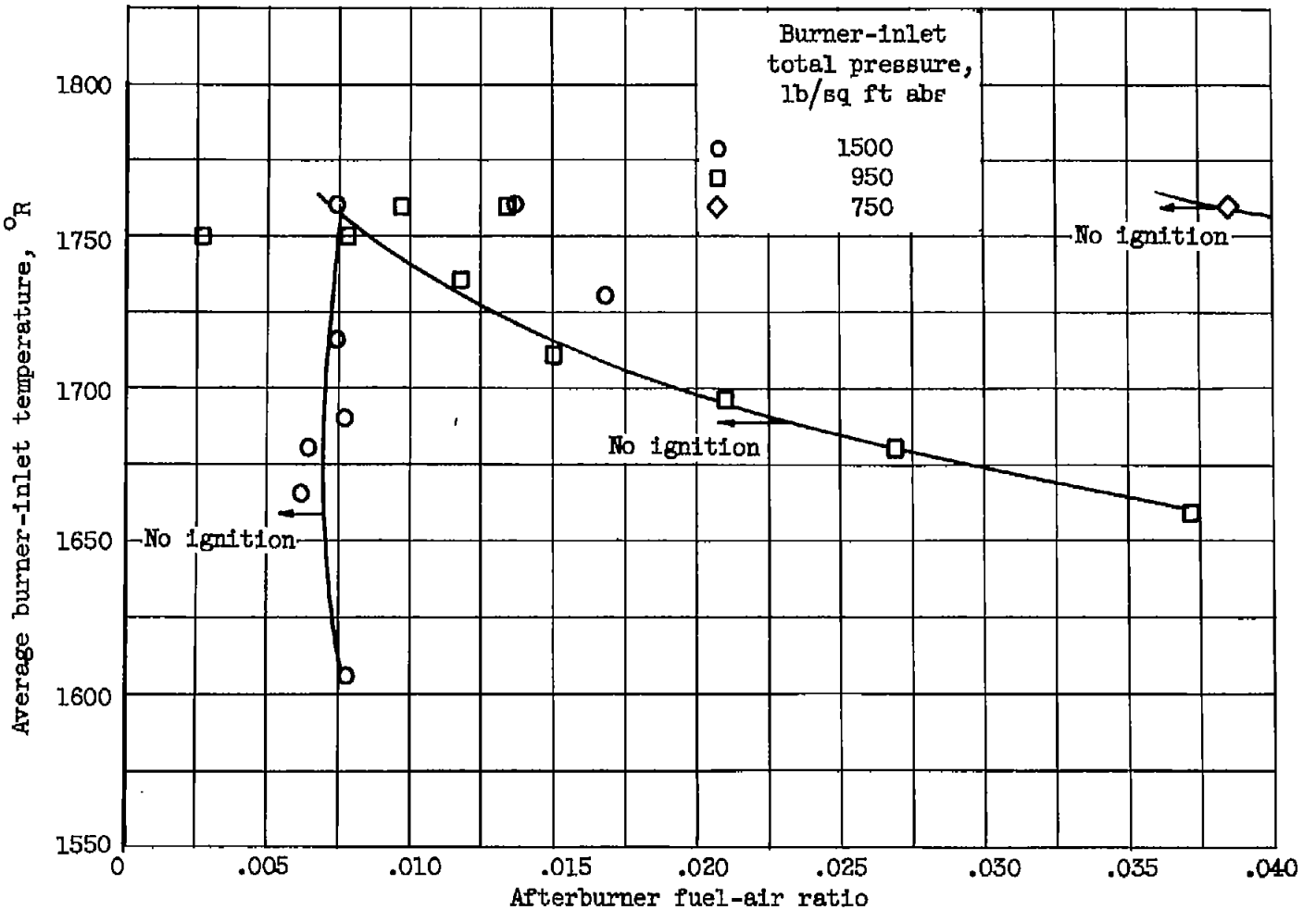

Figure 173. - Effect of afterburner-inlet pressure and temperature on limits of spontaneous ignition. Fuel, MIL-F-5624, grade JP-3, with Reid vapor pressure of 7 pounds per square inch.

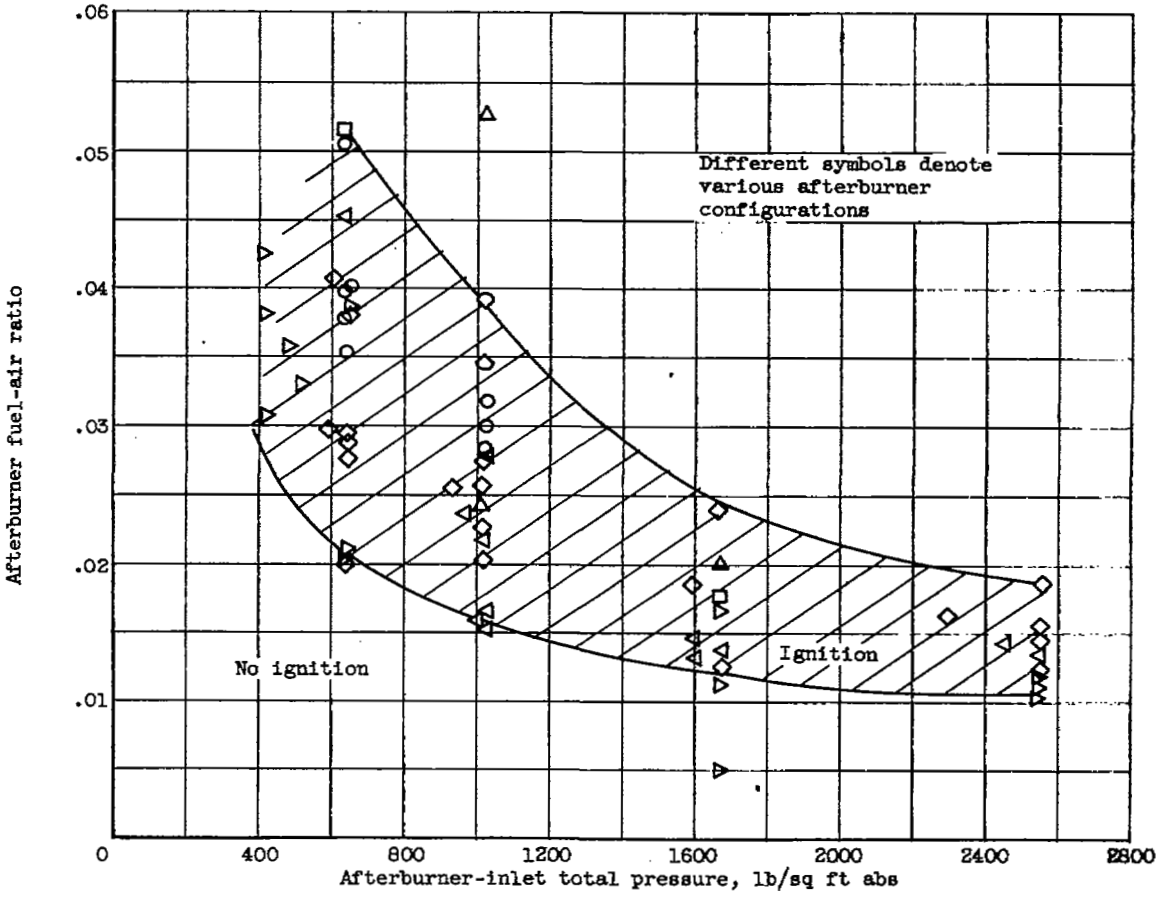

Figure 174. - Minimum afterburner fuel-air ratios at which autoignition occurred with several afterburner configurations. Fuel, MIL-F-5624, grade JP-3; burner-inlet temperature, 1710° to 1760° R.

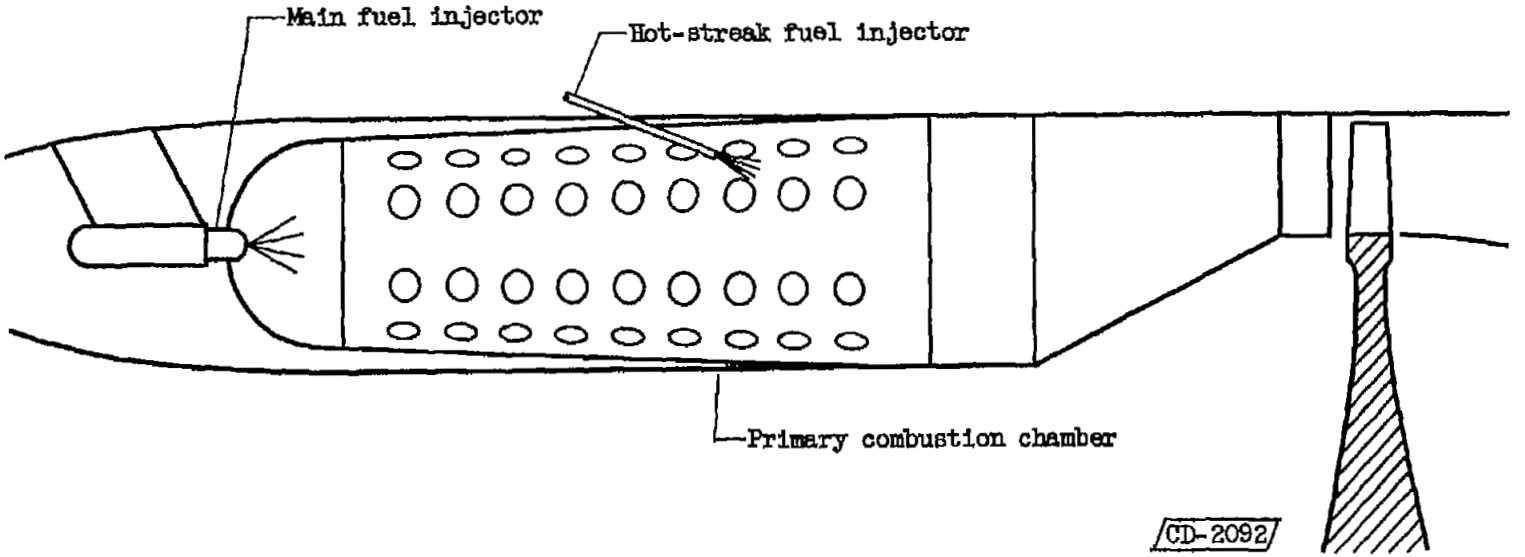

Figure 175. - Schematic diagram of hot-streak ignition system.

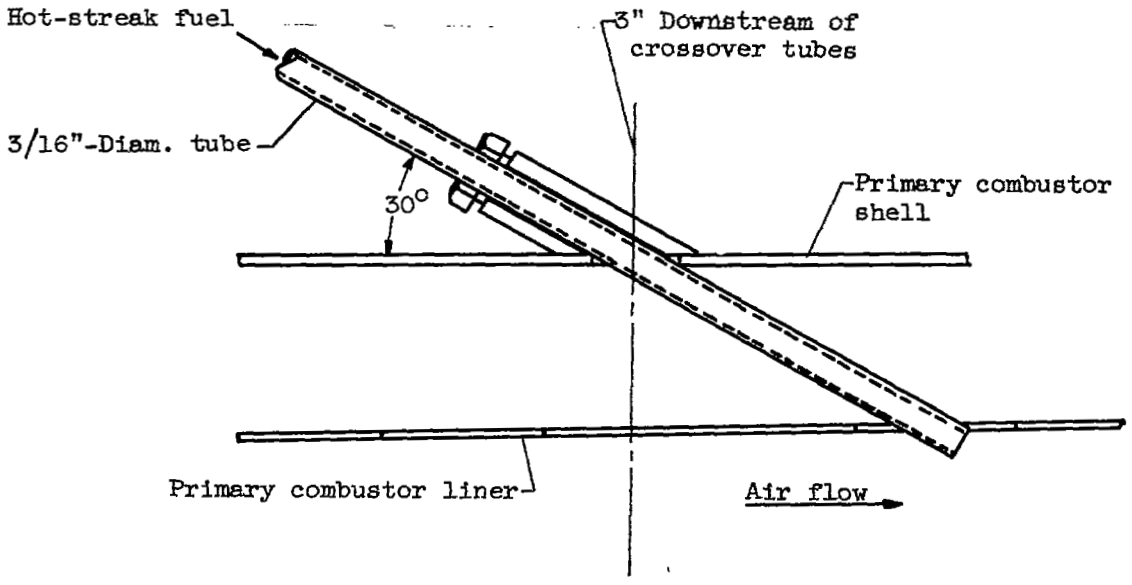

(a) Igniter A.

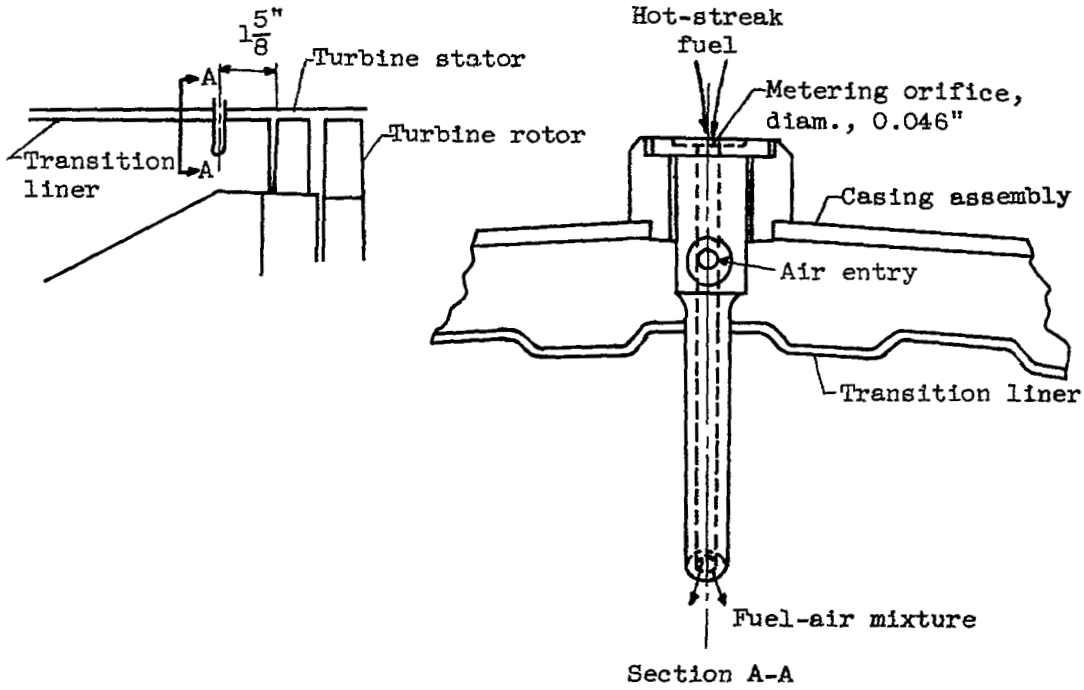

(b) Igniter B.

Figure 176. - Details of two hot-streak igniters.

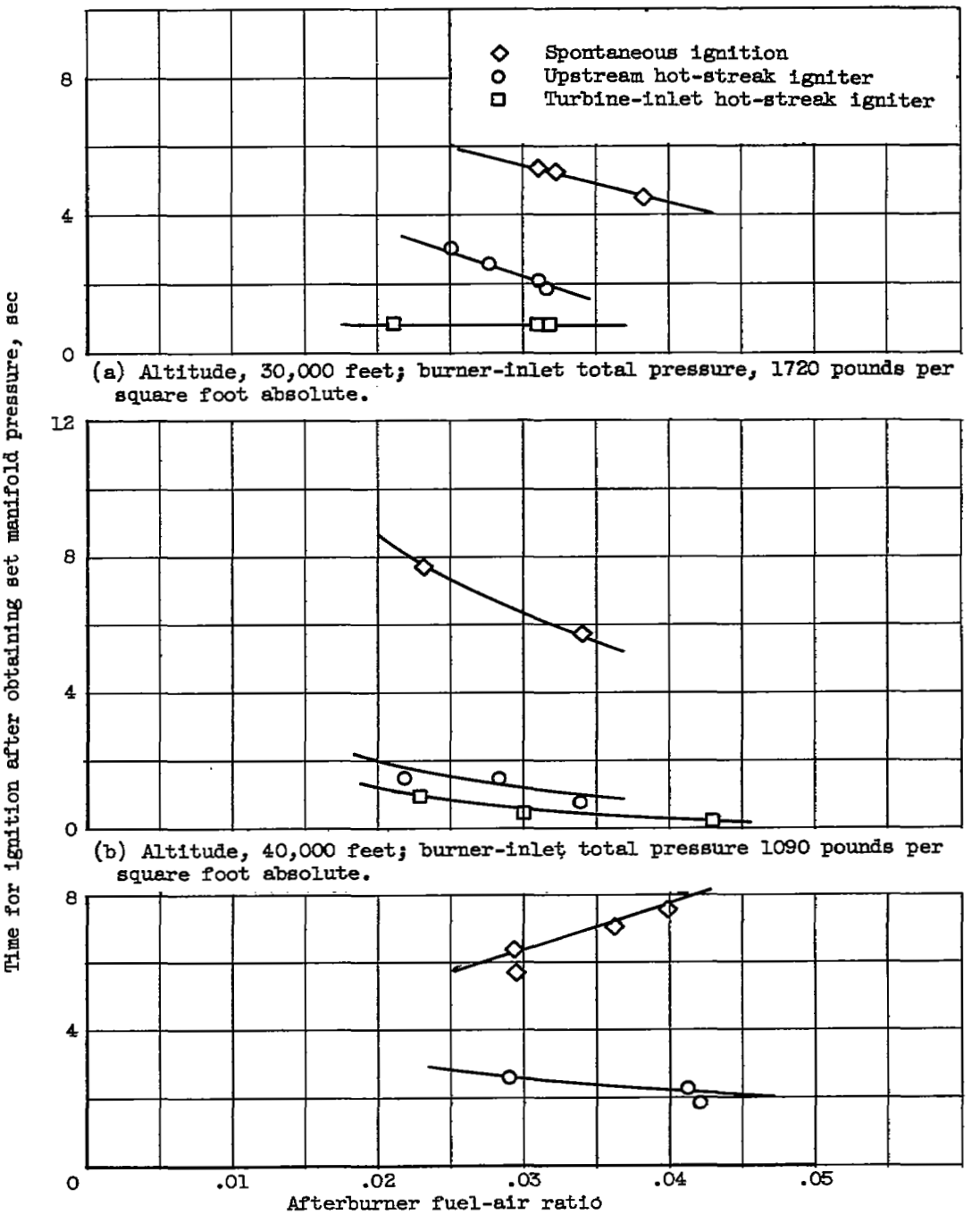

(a) Altitude, 30,000 feet; burner-inlet total pressure, 1720 pounds per square foot absolute.

(b) Altitude, 40,000 feet; burner-inlet total pressure 1090 pounds per square foot absolute.

(c) Altitude, 50,000 feet; burner-inlet total pressure, 660 pounds per square foot absolute.

Figure 177. - Effect of altitude on time for afterburner ignition. Flight Mach number, 0.6.

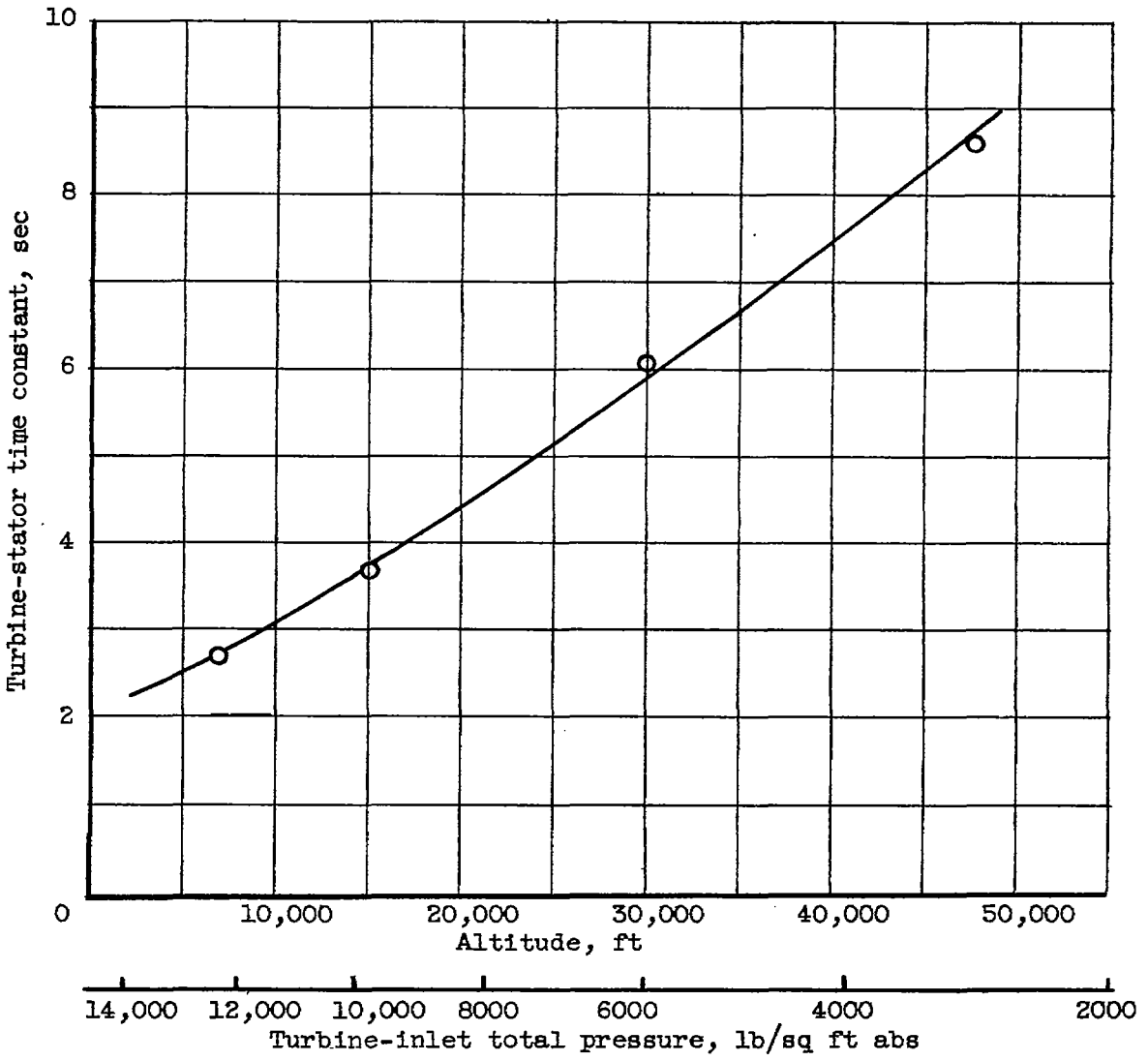

Figure 178. - Variation of turbine-stator time constant with altitude. Flight Mach number, 0.8.

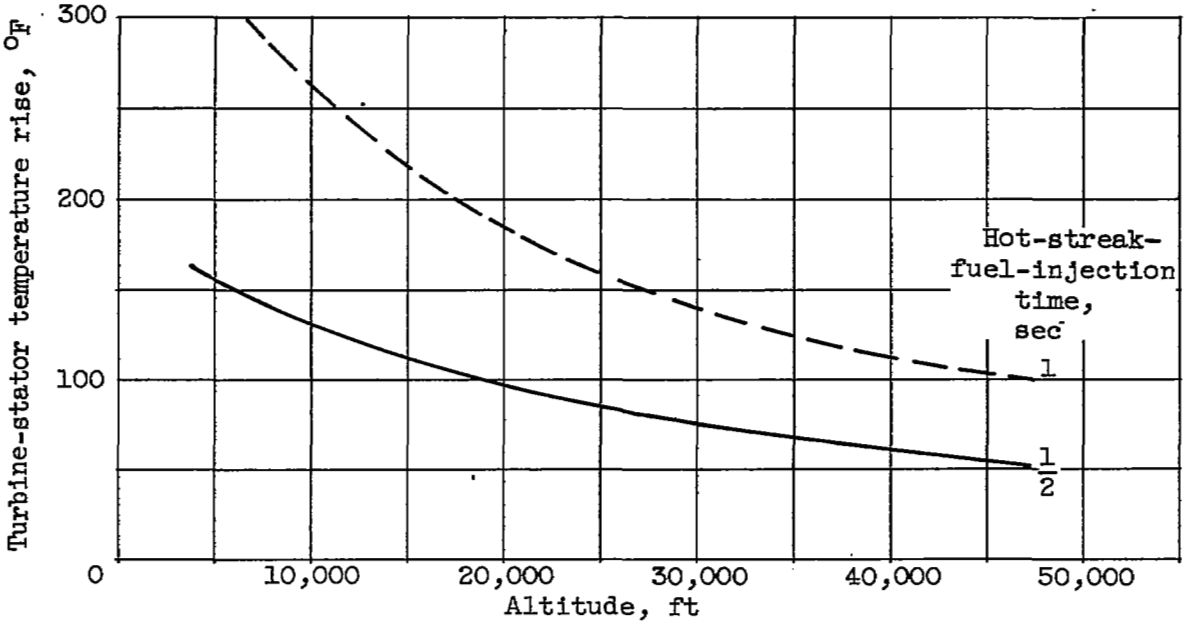

Figure 179. - Effect of hot-streak-fuel-injection time on variation of turbine-stator-blade temperature rise with altitude. Initial gas temperature, 2000° R; local gas temperature, 3000° R; equilibrium blade temperature equal to 0.93 gas temperature; flight Mach number, 0.8.

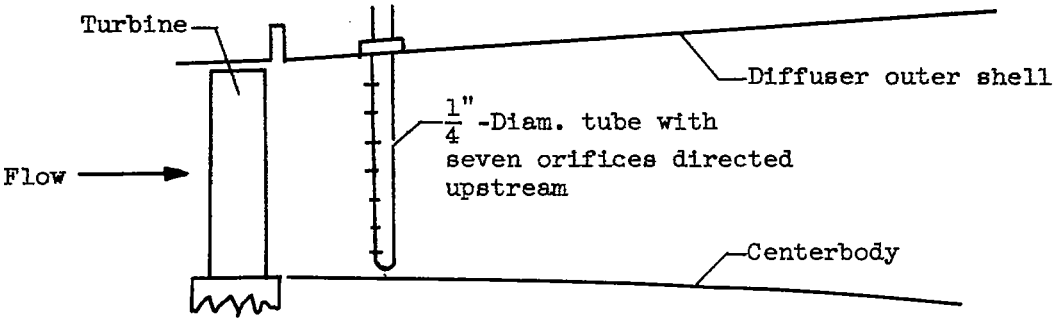

(a) Configuration A, multiorifice bar.

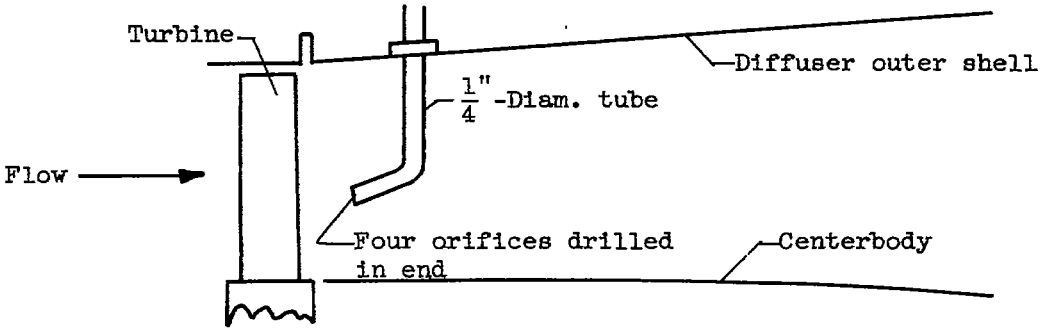

(b) Configuration B, four-orifice bar.

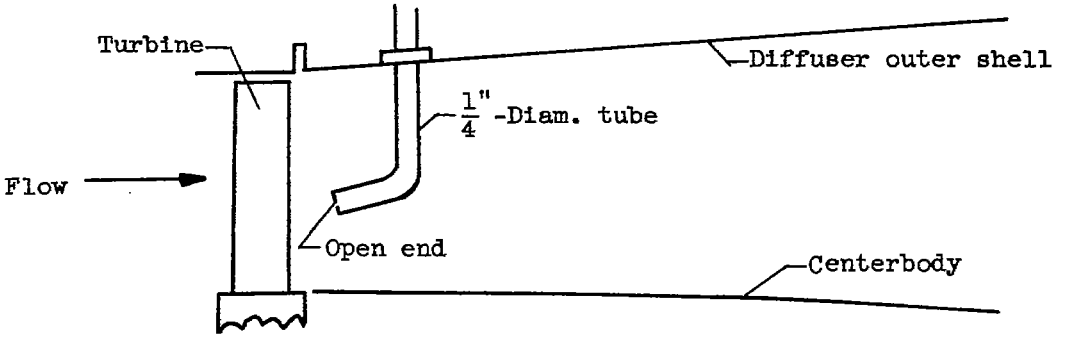

(c) Configuration C, open-end tube.

Figure 180. - Turbine-outlet hot-streak systems evaluated.

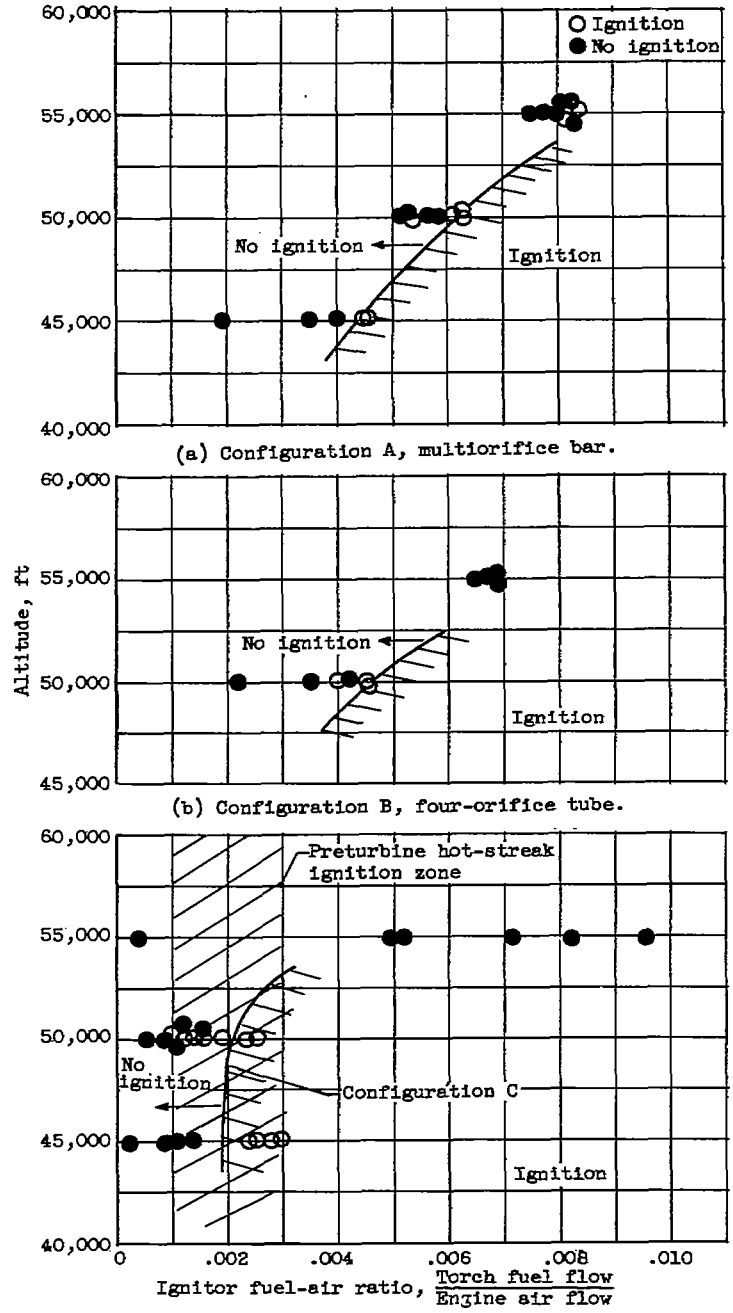

(a) Configuration A, multiorifice bar.

(b) Configuration B, four-orifice tube.

(c) Configuration C, open-end tube, compared with typical preturbine hot-streak configuration.

Figure 181. - Ignition limits of turbine-outlet hot-streak systems in comparison with typical preturbine hot streak. Turbine-outlet temperature, 1710° R.

[redacted]

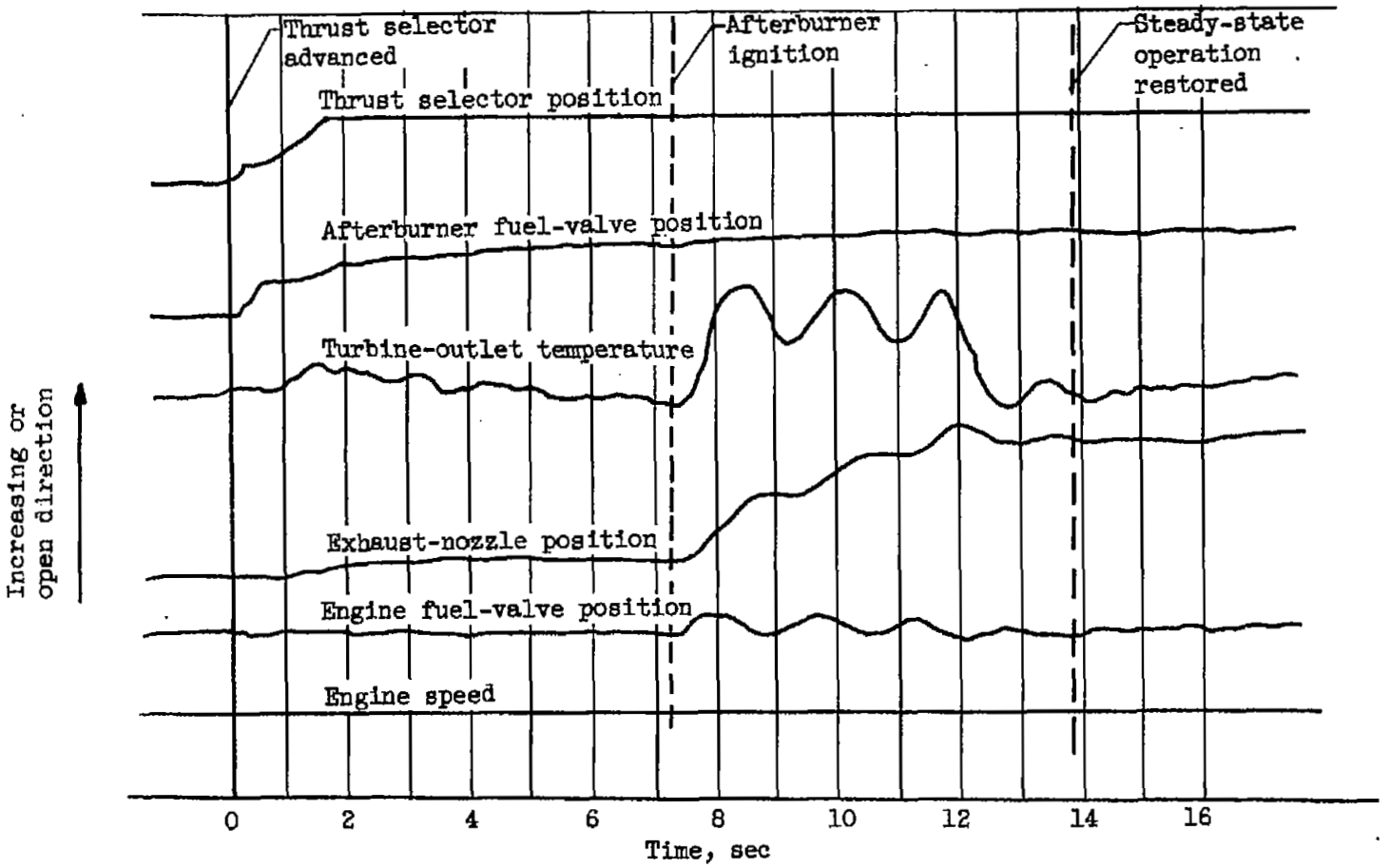

Figure 182. - Oscillograph indications of control-parameter variations during afterburner ignition and transient to steady-state operation. Altitude 30,000 feet; flight Mach number, 0.6.

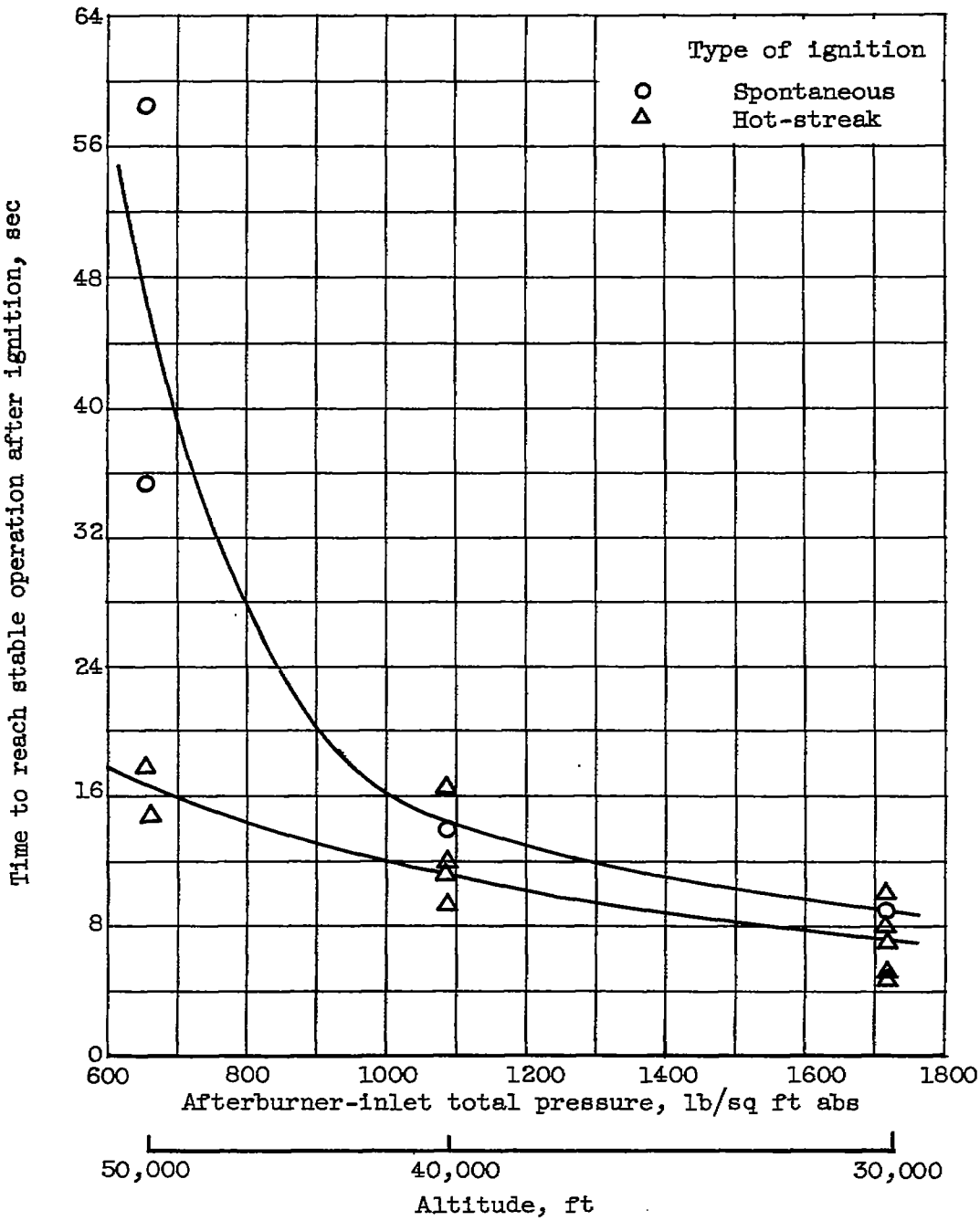

Figure 183. - Effect of afterburner-inlet total pressure on time to reach stable operation after ignition. Flight Mach number, 0.60.

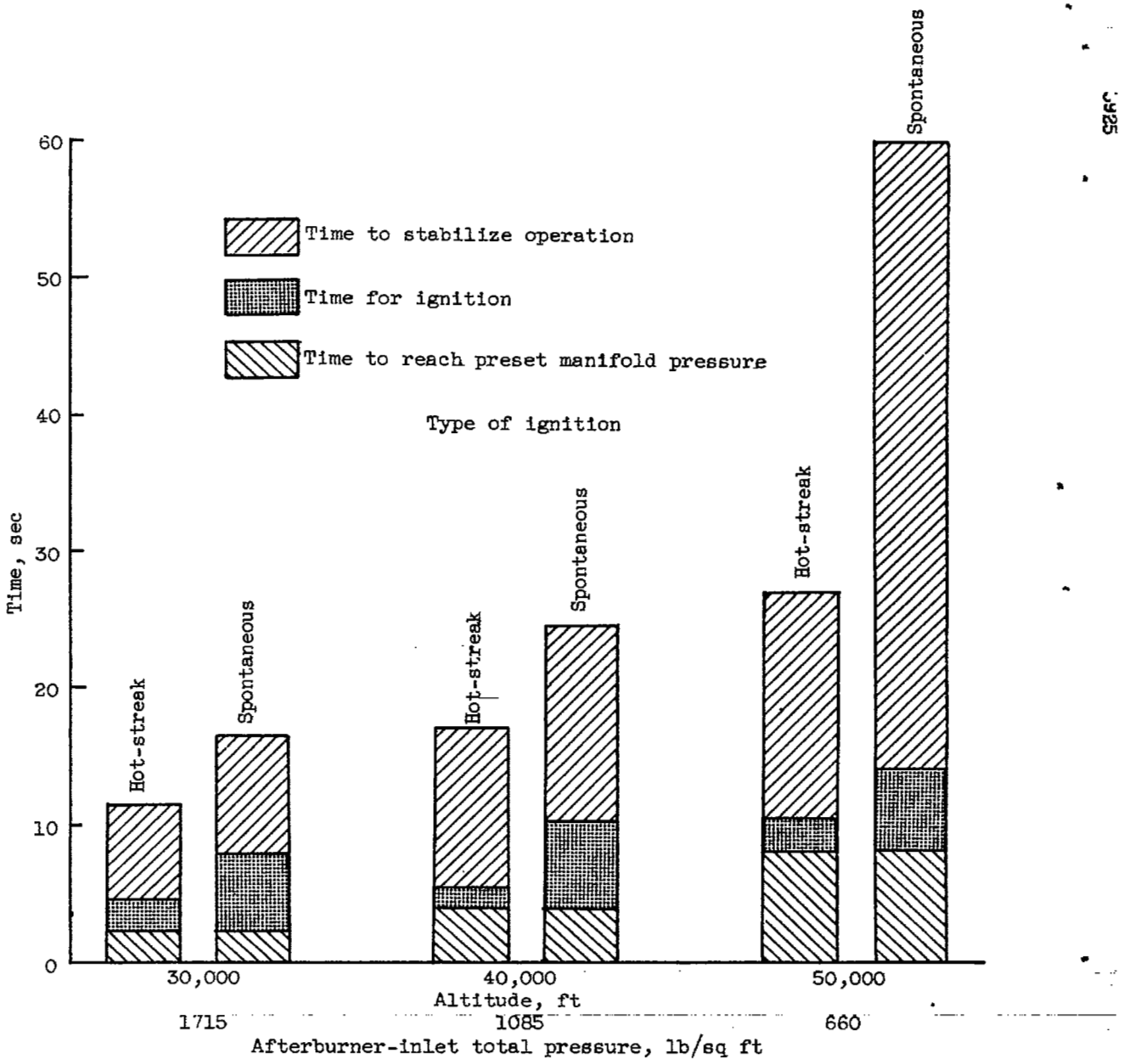

Figure 184. - Effect of altitude on over-all time required for afterburner starting. Preset fuel-air ratio, 0.03; flight Mach number, 0.6.

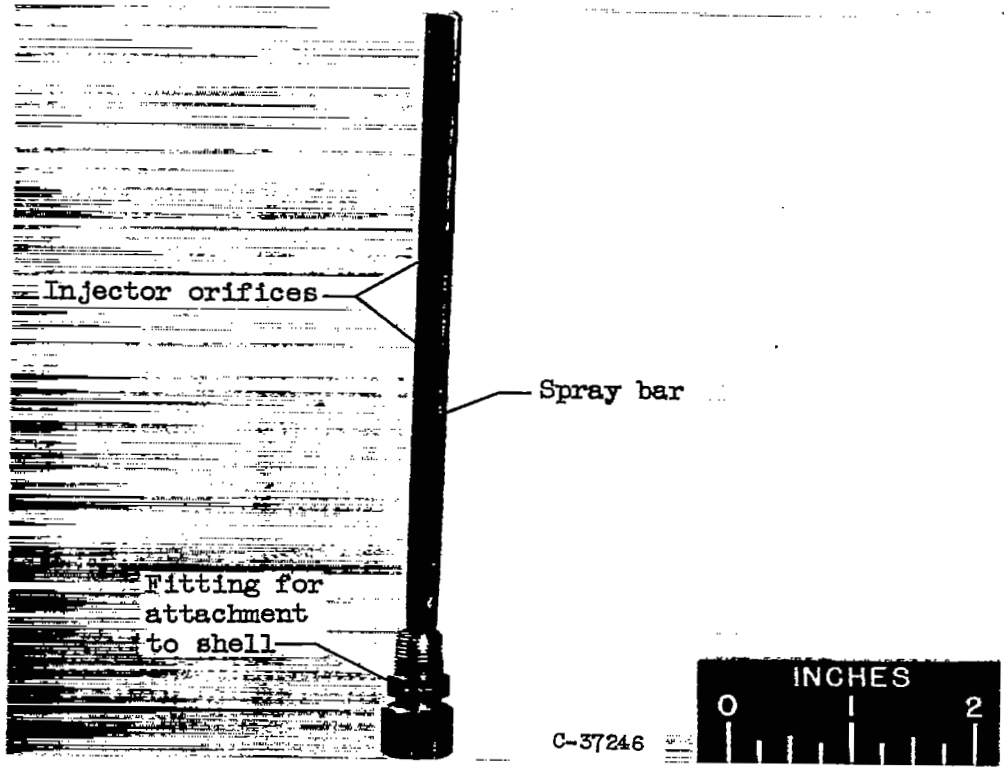

Figure 185. - Typical fuel-spray bar for full-scale afterburner.

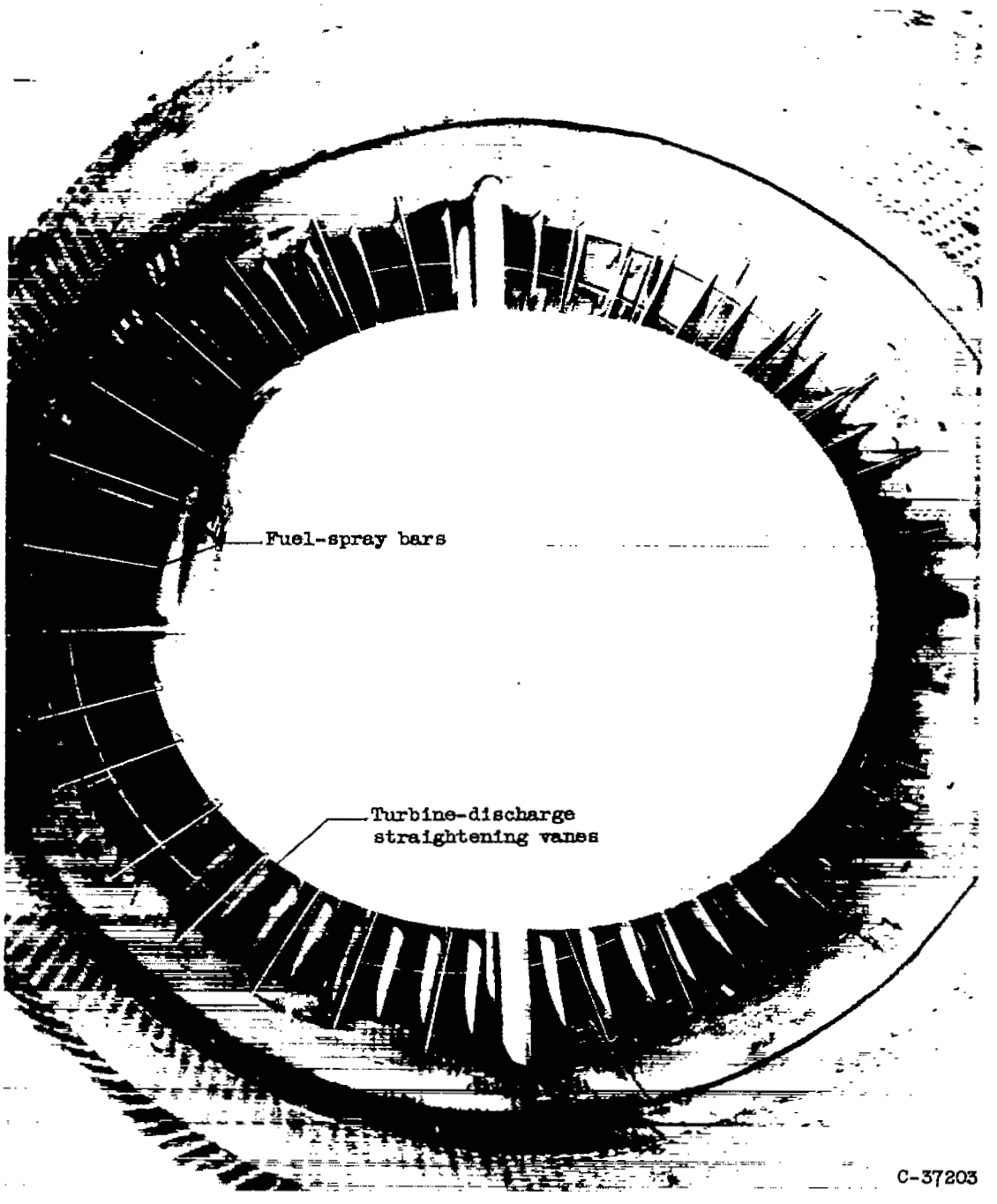

Figure 186. - View looking upstream into full-scale afterburner diffuser showing typical installation of fuel-spray bars at turbine discharge.

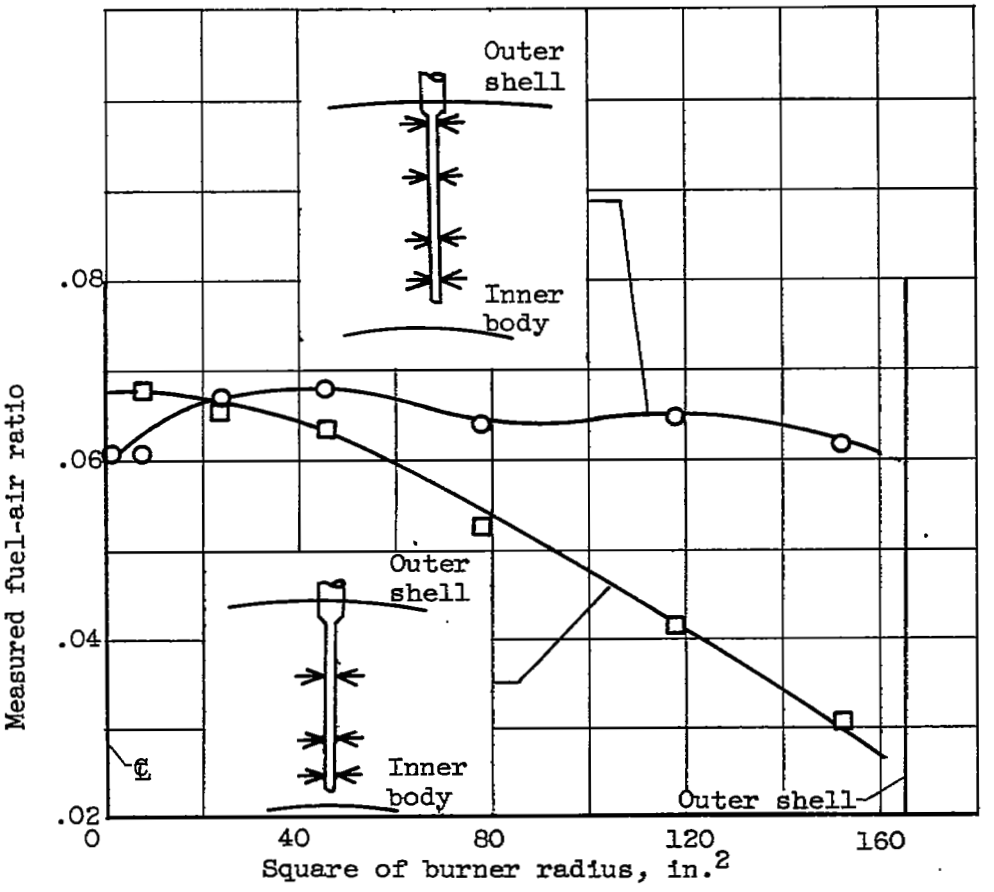

Figure 187. - Effect of spray-bay design on fuel-air-ratio distribution 22.5 inches downstream of spray bars. Transverse injection from 24 spray bars having 0.030-inch-diameter orifices.

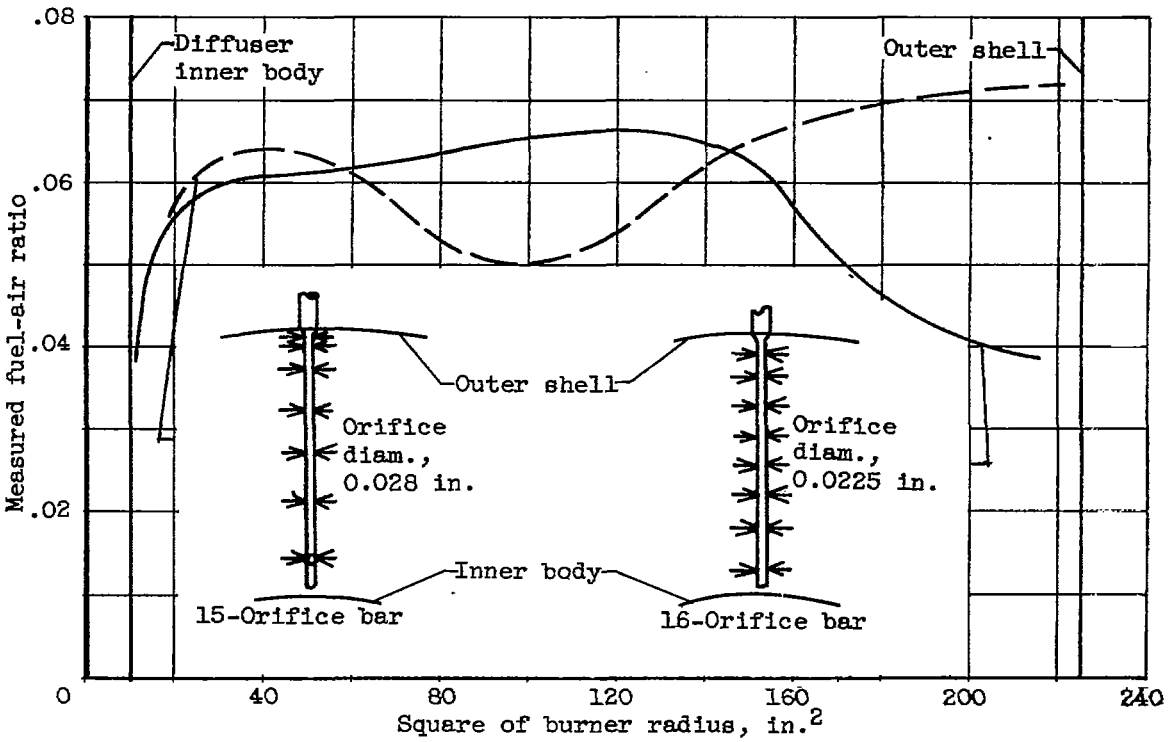

Figure 188. - Effect of radial location of fuel orifices on fuel-air-ratio distribution 15 inches downstream of spray bars. Transverse injection from 20 spray bars.

3925

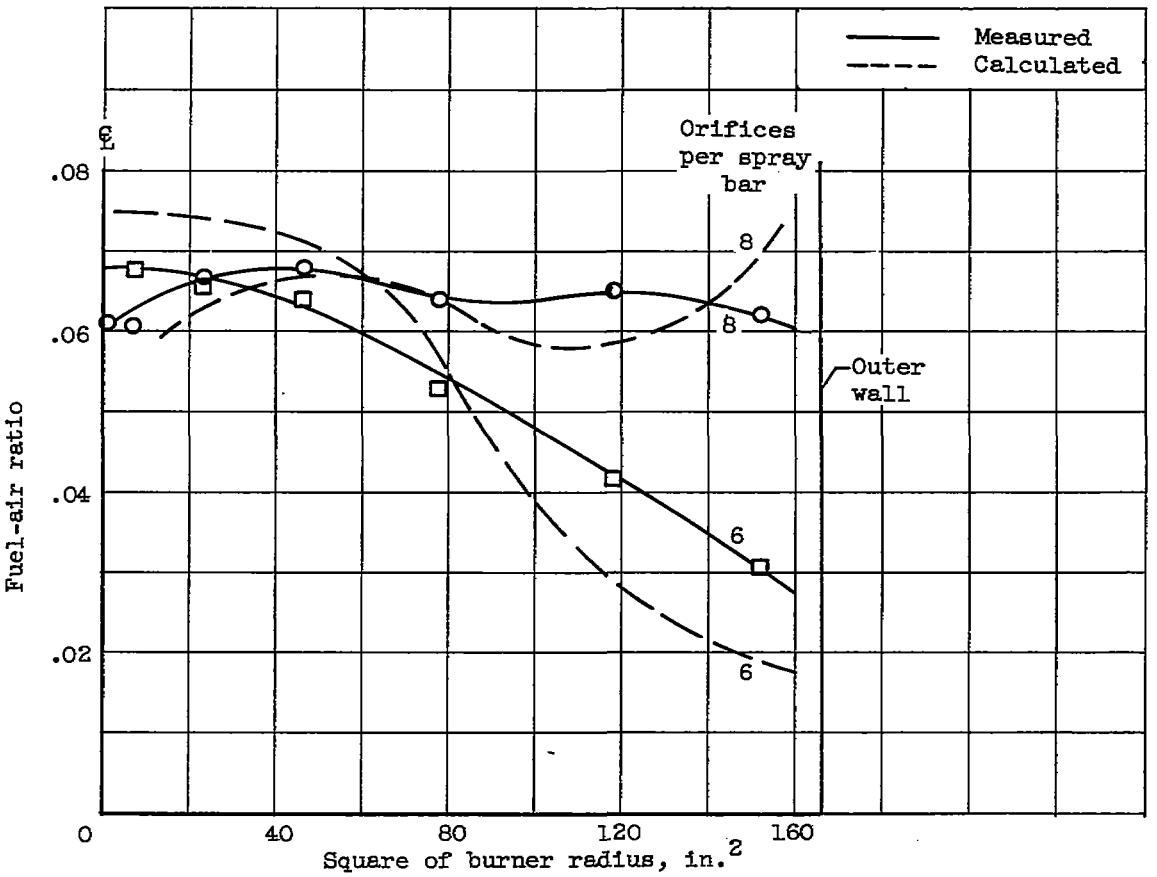

Figure 189. - Comparison of calculated fuel-air-ratio distribution with measured values from figure 187. Fuel mixing distance, 22.5 inches.

[redacted]

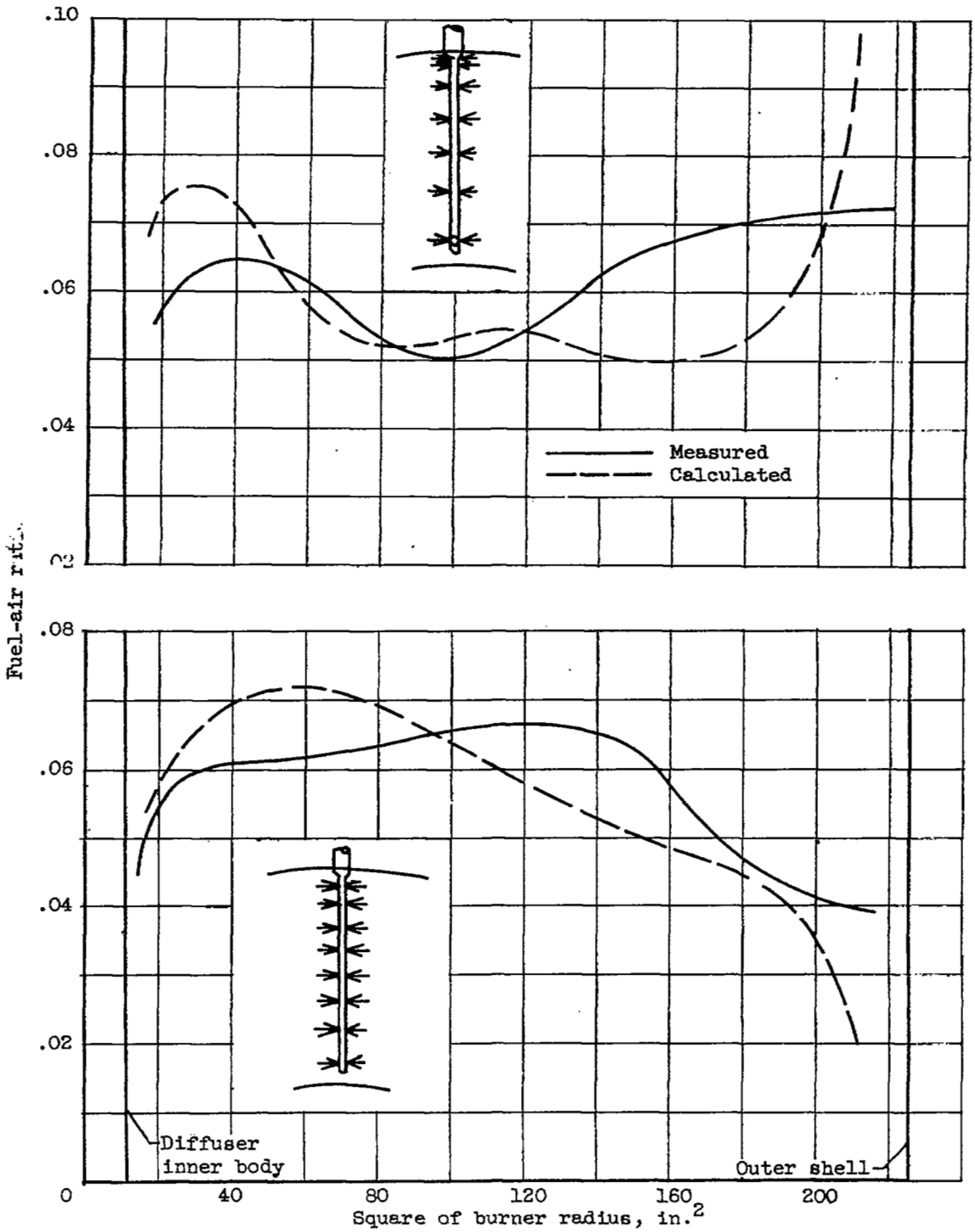

Figure 190. - Comparison of calculated fuel-air-ratio distribution with measured values of figure 188. Fuel mixing distance, 15 inches.

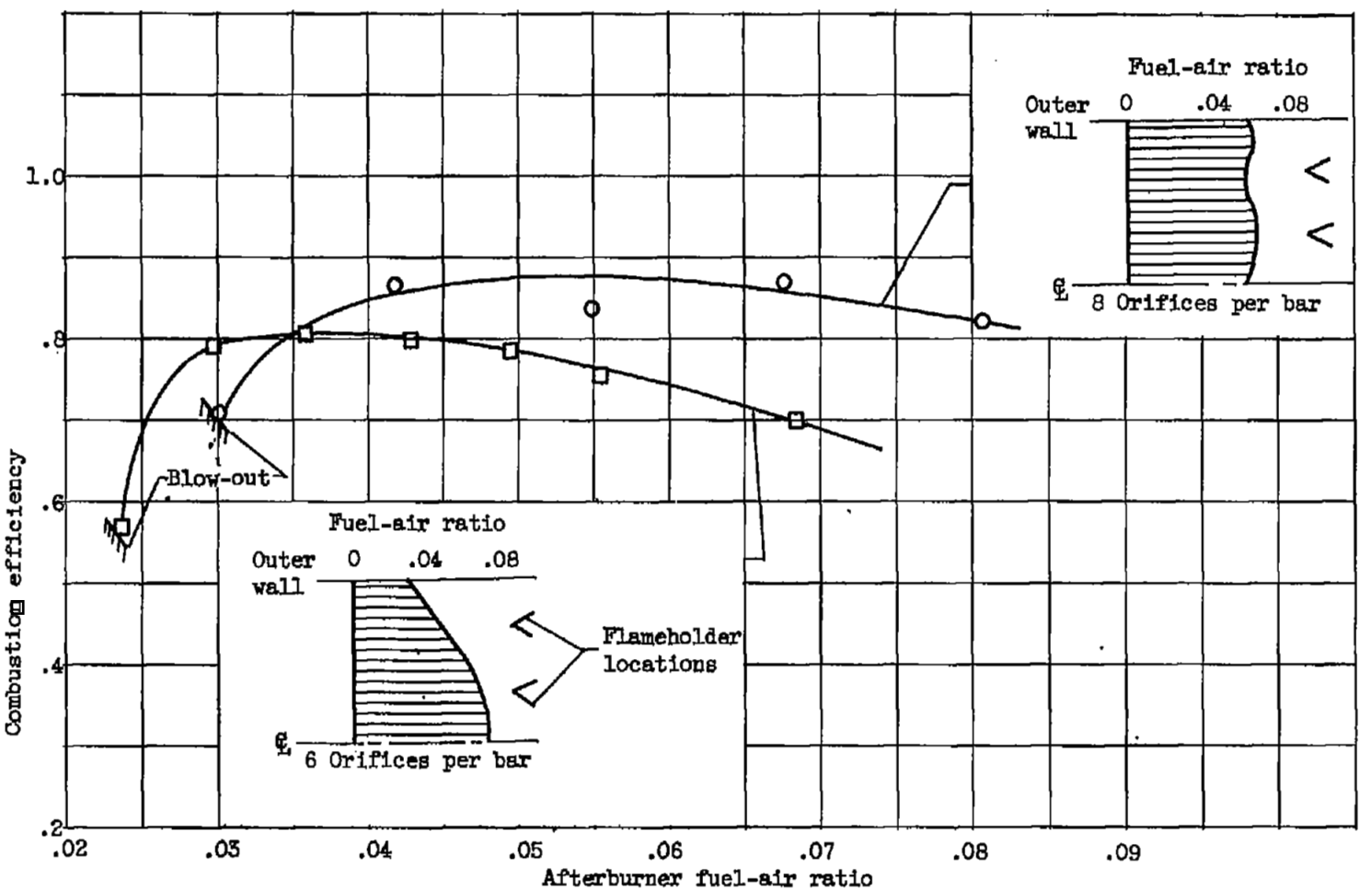

Figure 191. - Effect of radial fuel-air-ratio distribution on combustion efficiency.

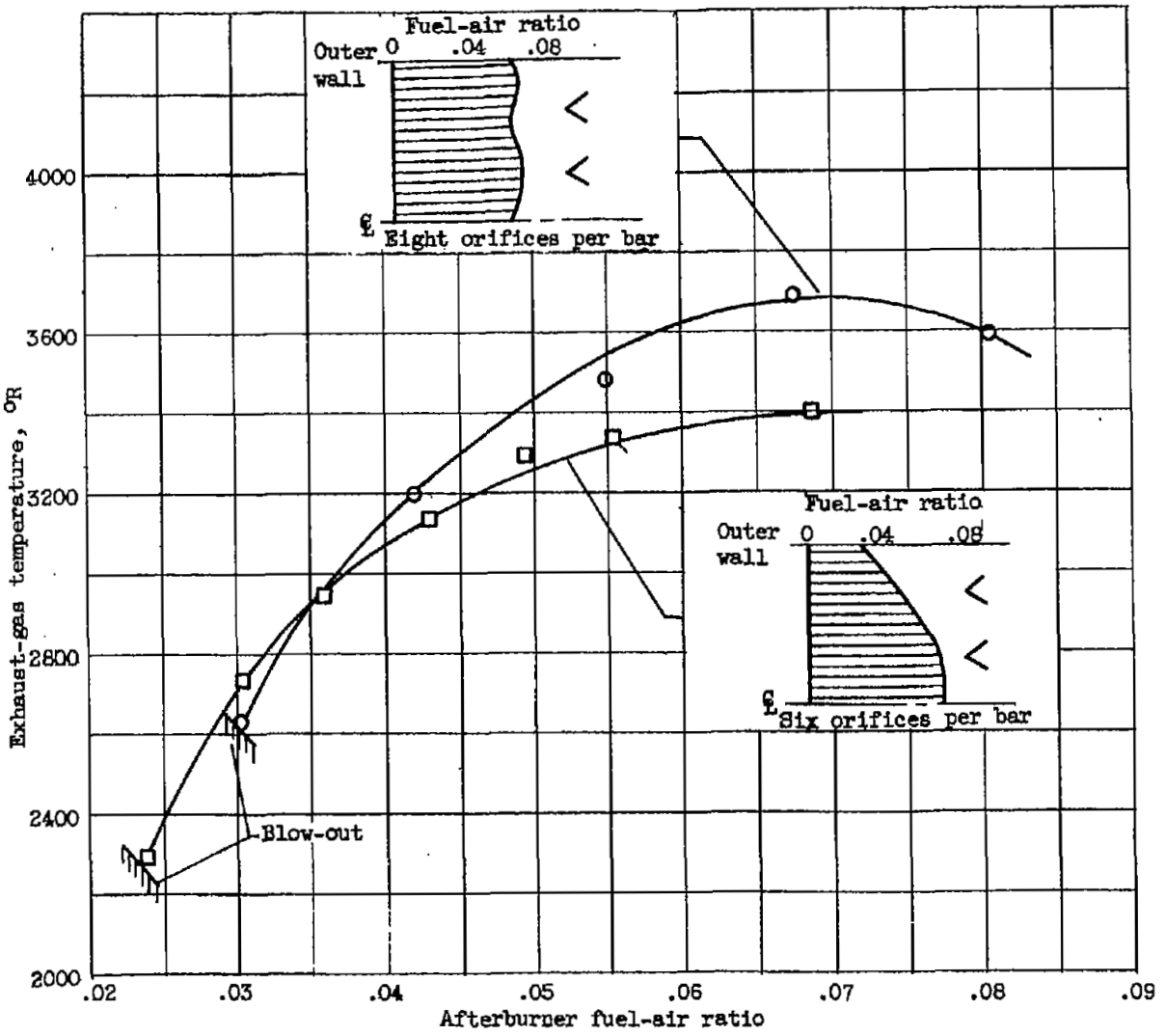

Figure 192. - Effect of radial fuel-air-ratio distribution on exhaust-gas temperature.

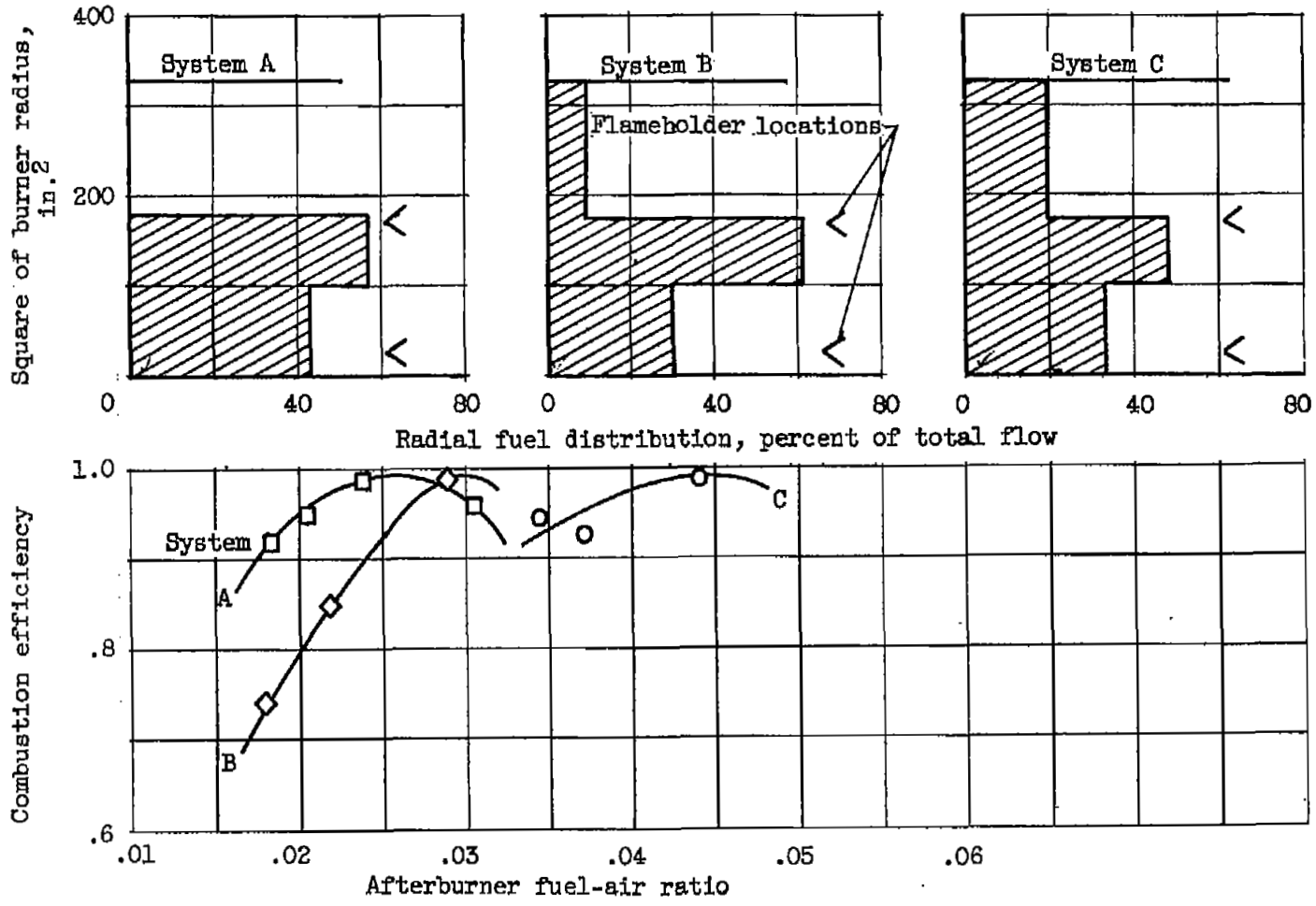

Figure 193. - Effect on combustion efficiency of varying radial distribution of fuel.

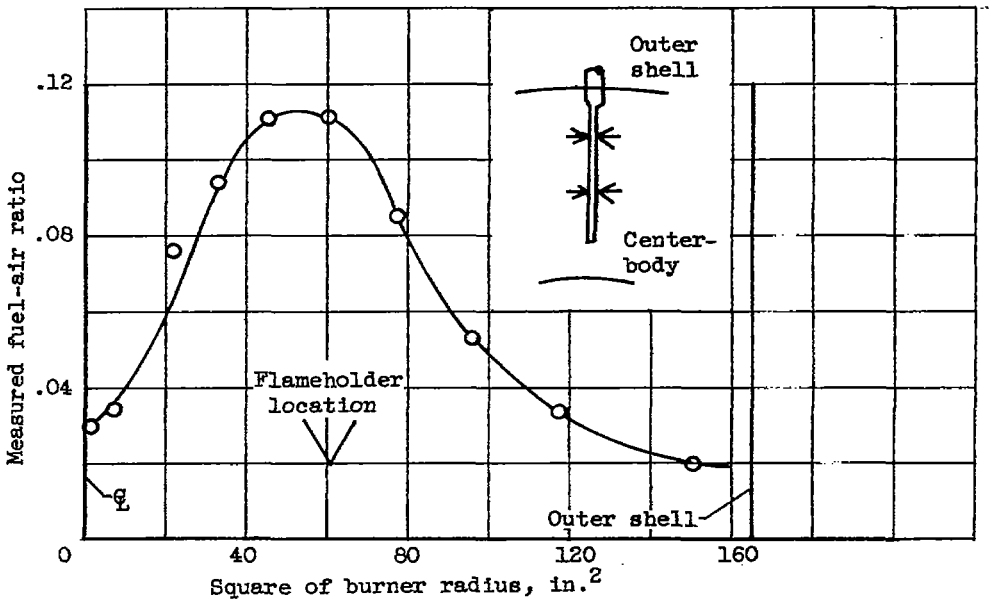

(a) Fuel-air-ratio distribution. Average fuel-air ratio, 0.055.

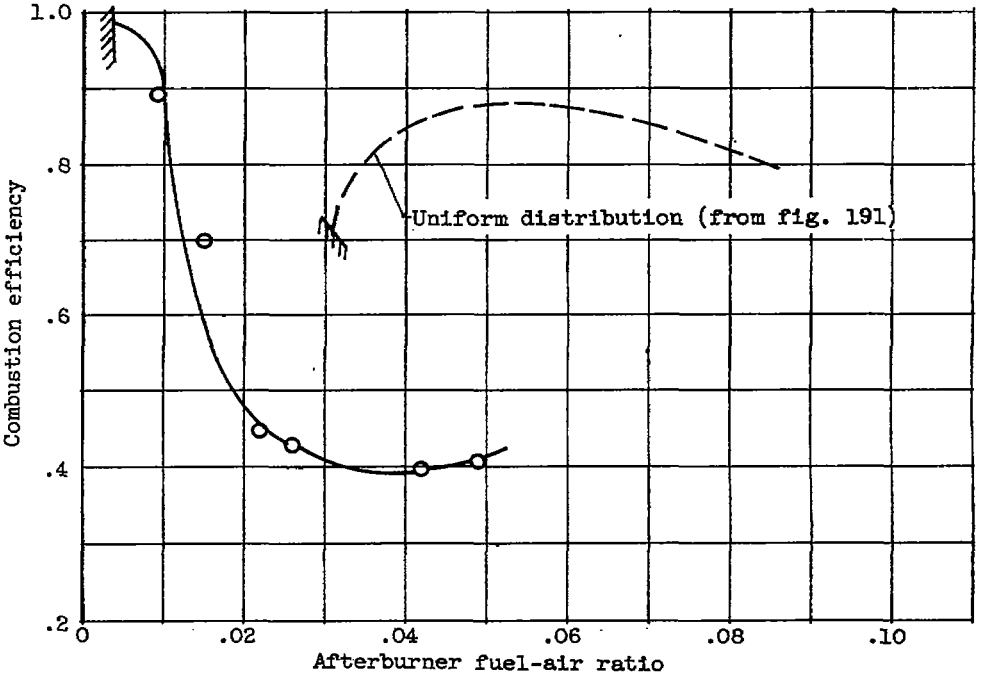

(b) Combustion efficiency.

Figure 194. - Combustion performance of afterburner with locally rich fuel injection. Transverse fuel injection from 12 bars having four 0.030-inch-diameter orifices.

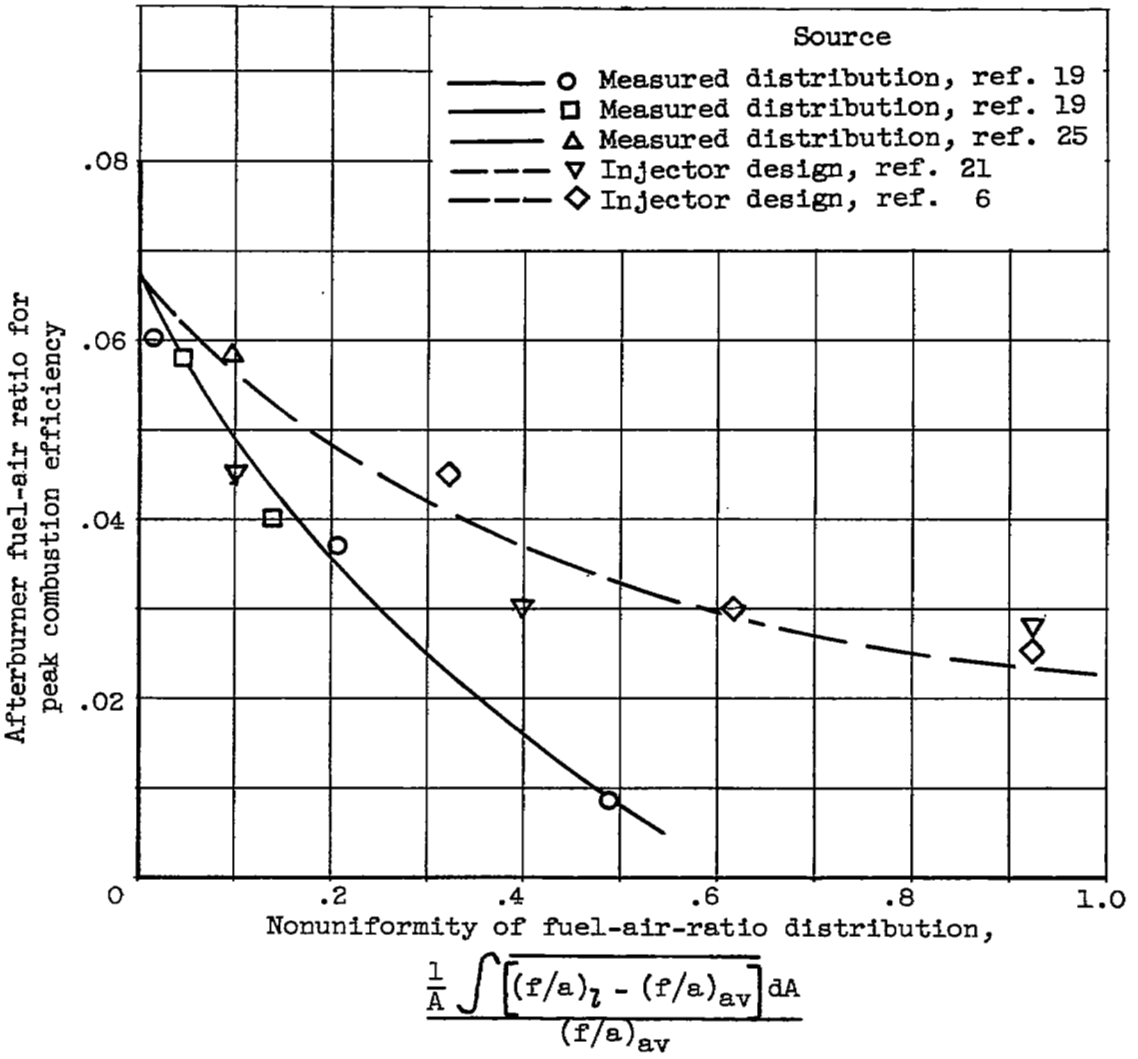

Figure 195. - Variation of fuel-air ratio at which peak combustion efficiency occurs with uniformity of fuel-air ratio distribution.

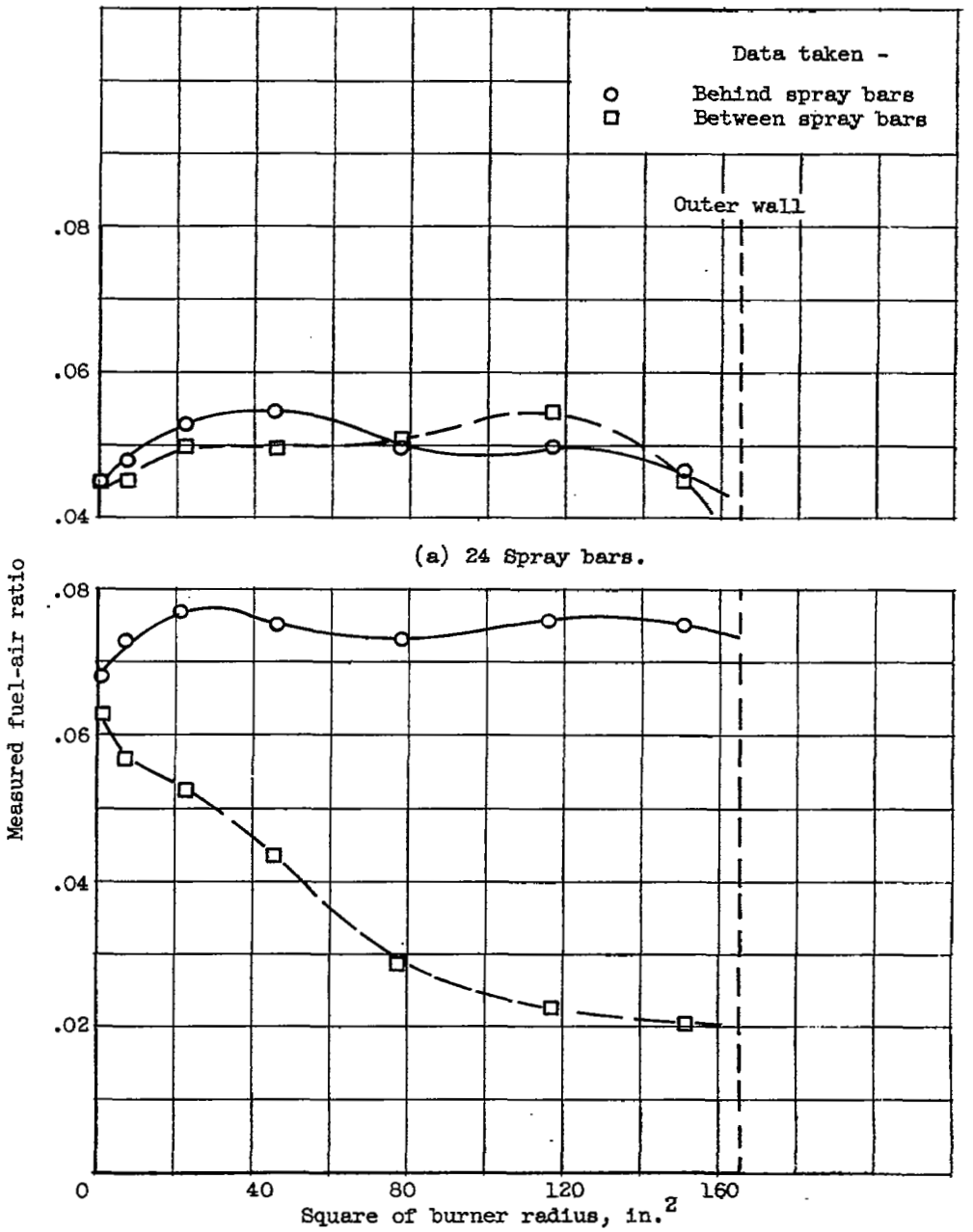

Figure 196. - Effect of number of spray bars on circumferential fuel-air-ratio distribution. Transverse injection from eight 0.030-inch-diameter orifices in each bar. Gas velocity, 500 to 600 feet per second; burner diameter, 26 inches.

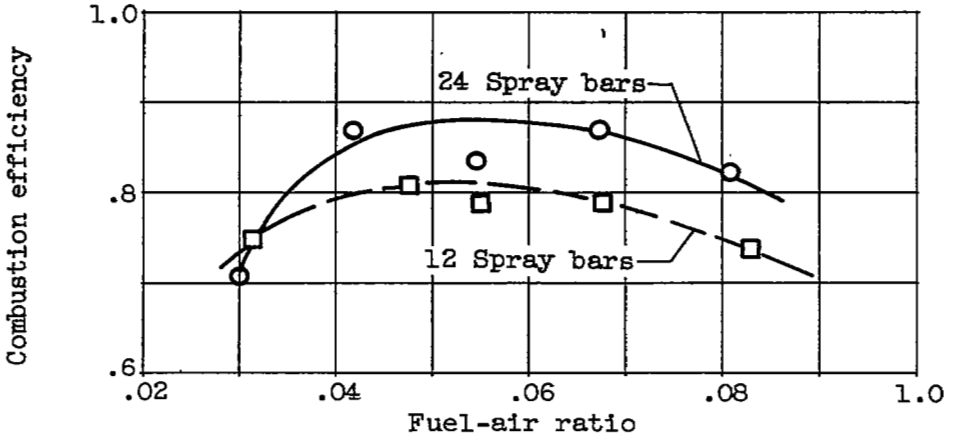

Figure 197. - Effect of number of spray bars on combustion efficiency. Transverse injection. Eight 0.030-inch-diameter orifices per spray bar; gas velocity, 500 to 600 feet per second.

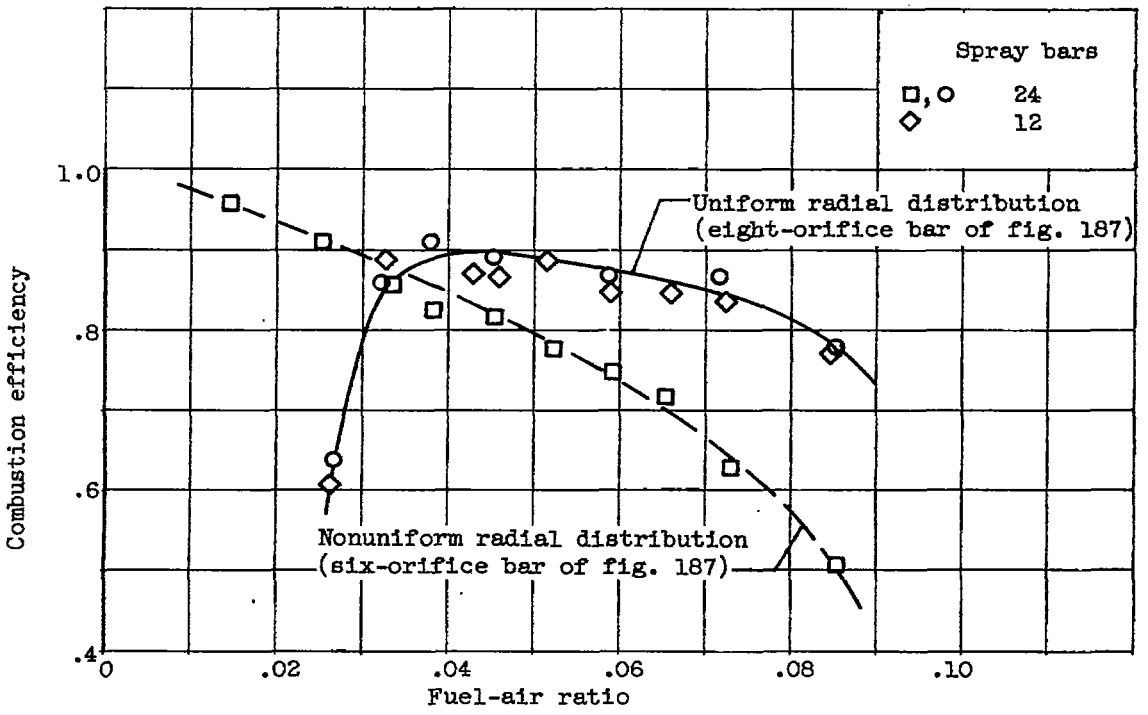

Figure 198. - Effect of radial and circumferential fuel-air-ratio distribution on combustion efficiency. Orifice diameter, 0.030 inch; burner-inlet velocity, 380 to 480 feet per second.

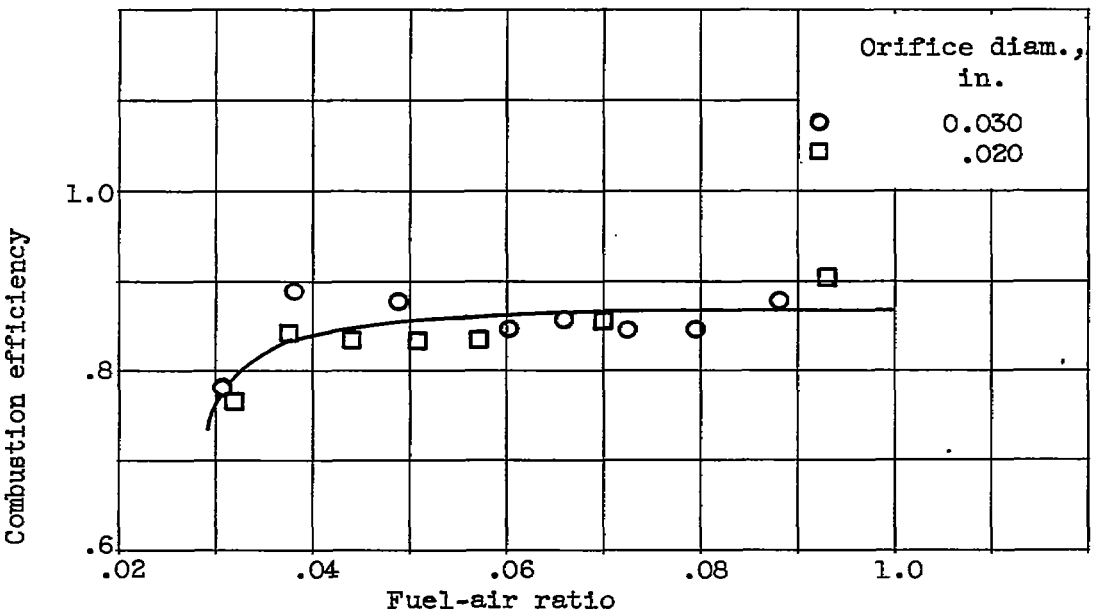

Figure 199. - Effect of spray-bar-orifice size on combustion efficiency. Transverse injection from 24 spray bars, each having eight orifices. Gas velocity, 500 to 600 feet per second; burner diameter, 26 inches.

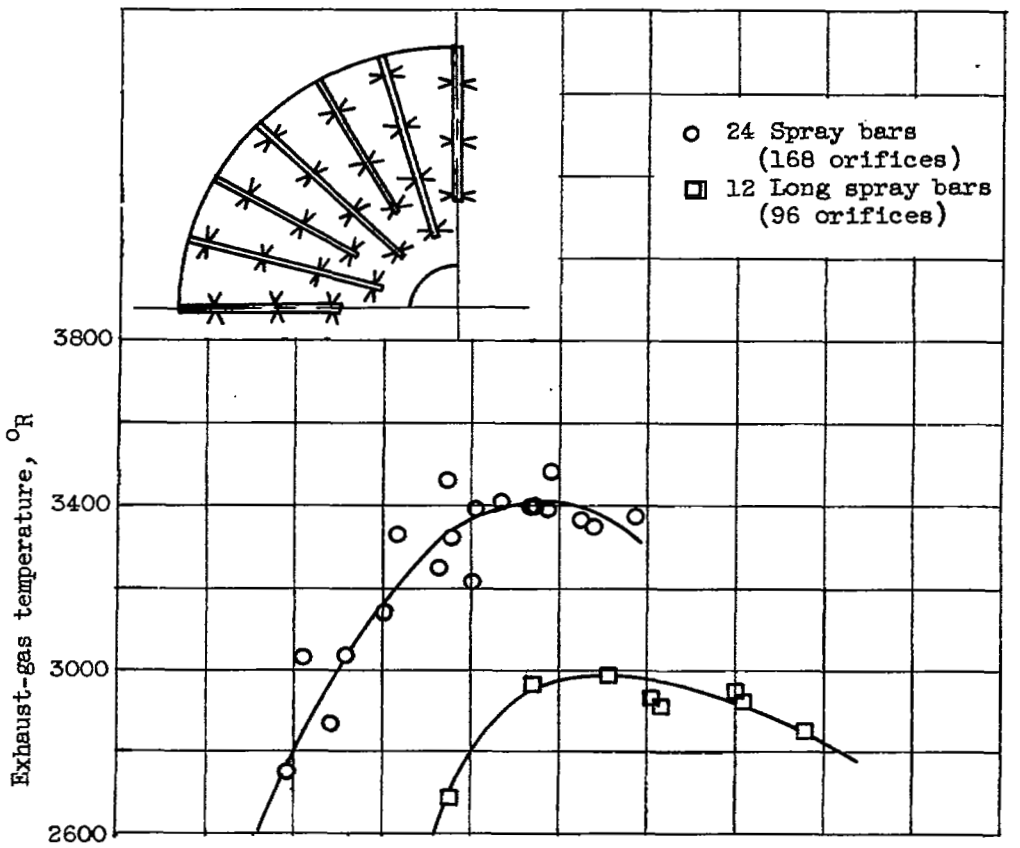

(a) Exhaust-gas temperature.

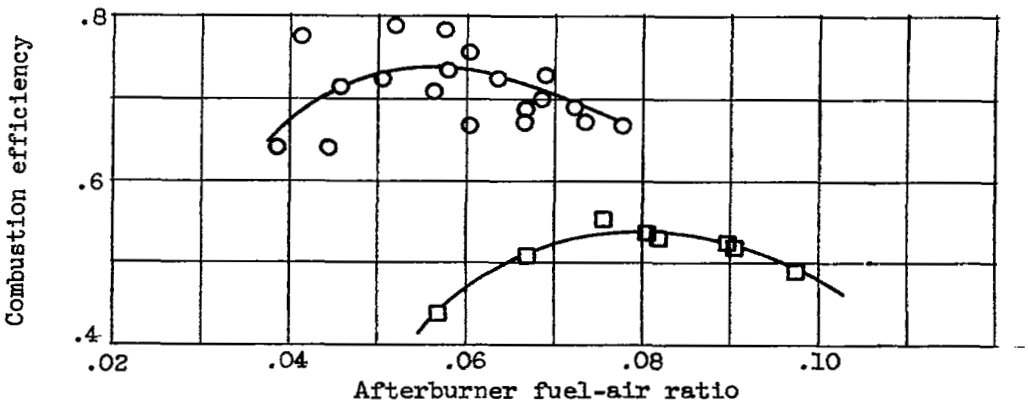

(b) Combustion efficiency.

Figure 200. - Effect of number of fuel-spray bars on combustion efficiency and exhaust-gas temperature. Burner-inlet velocity, approximately 400 feet per second; diameter of transverse injection orifice, 0.020 inch.

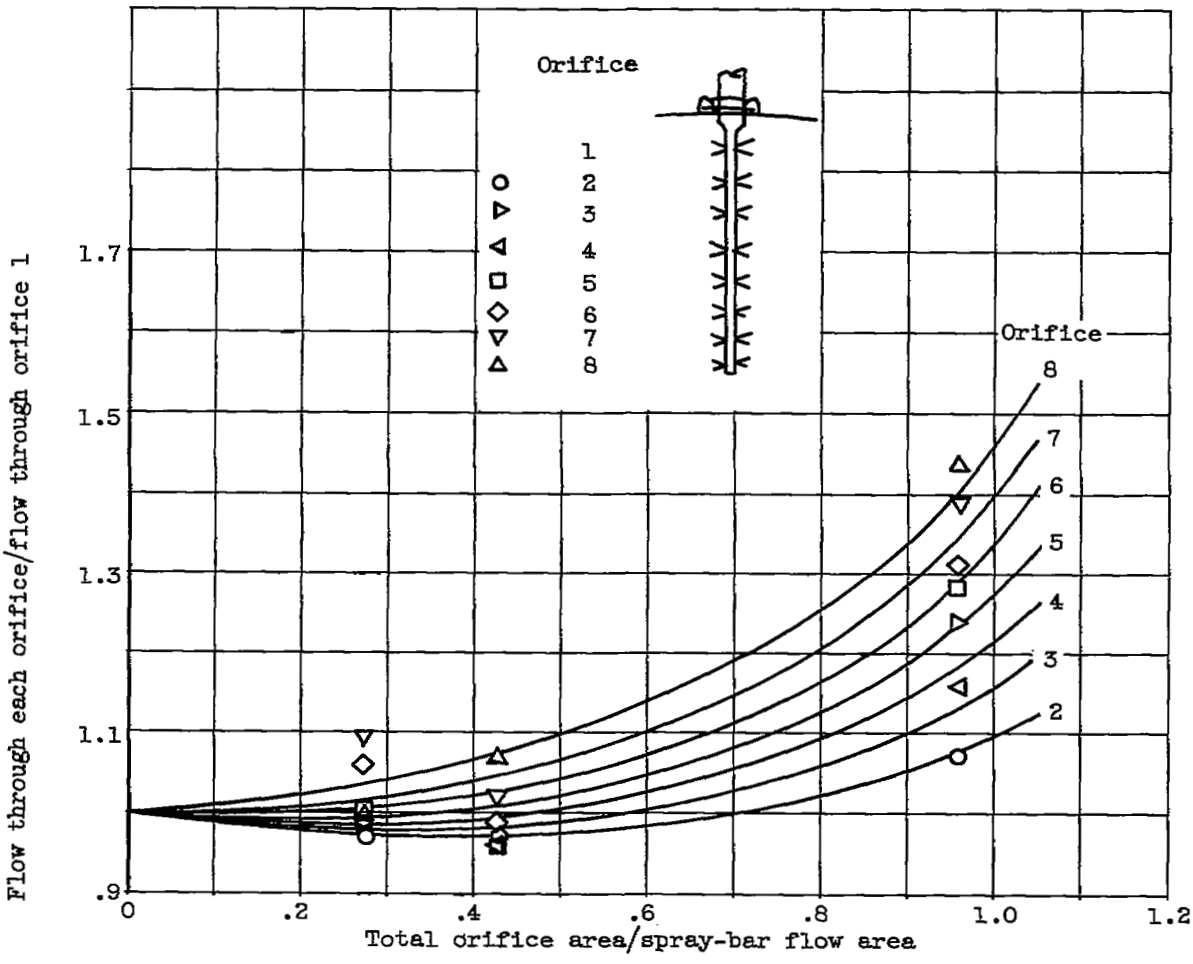

Figure 201. - Flow distribution among orifices of spray bars having various ratios of total orifice area to spray-bar flow area.

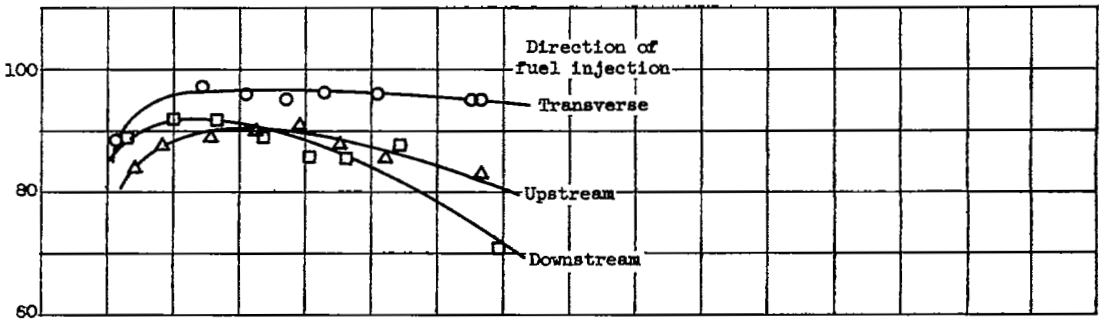

(a) Twenty-four eight-orifice spray bars. Gas velocity, 460 to 540 feet per second; burner-inlet pressure, 1060 to 1350 pounds per square foot absolute.

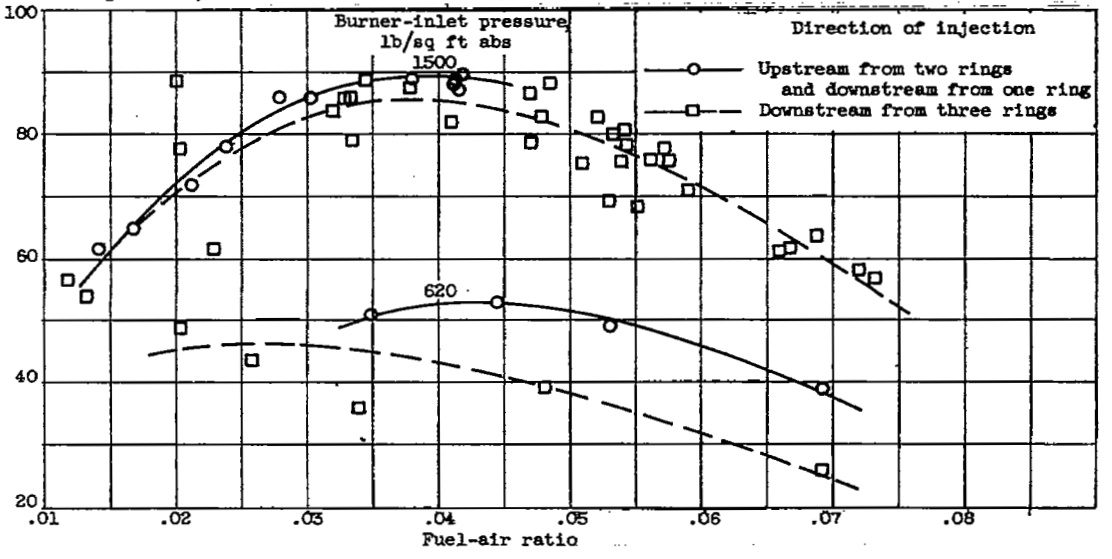

(b) Three concentric manifold rings having total of 144 orifices. Orifice diameter, 0.041 inch.

Figure 202. - Effect of direction of fuel injection on combustion efficiency.

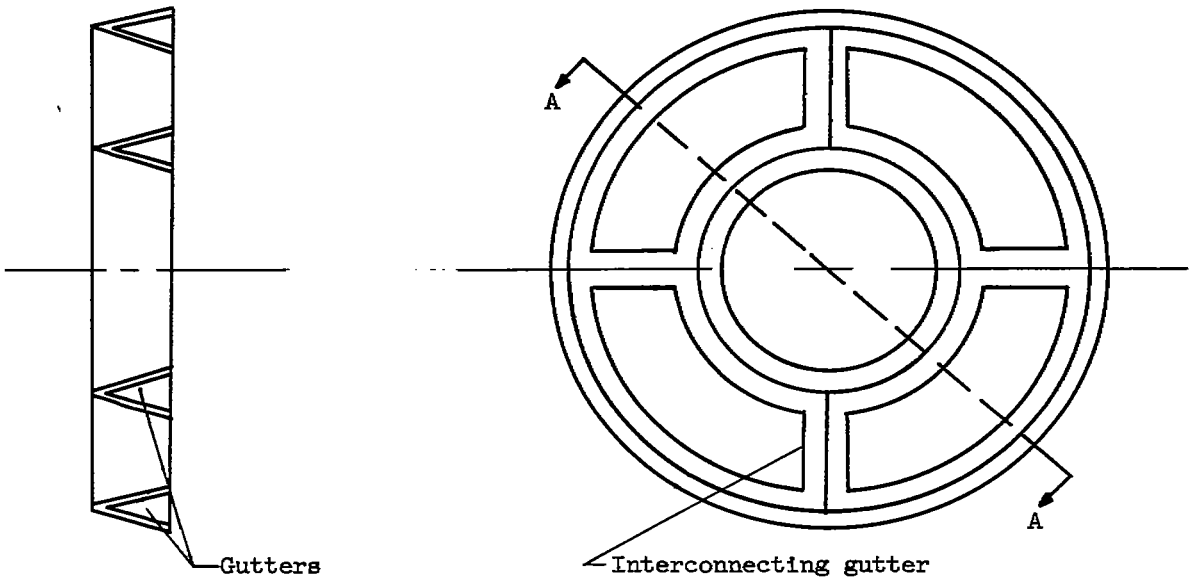

Section A-A Downstream view

Figure 203. - Typical two-ring V-gutter flameholder.

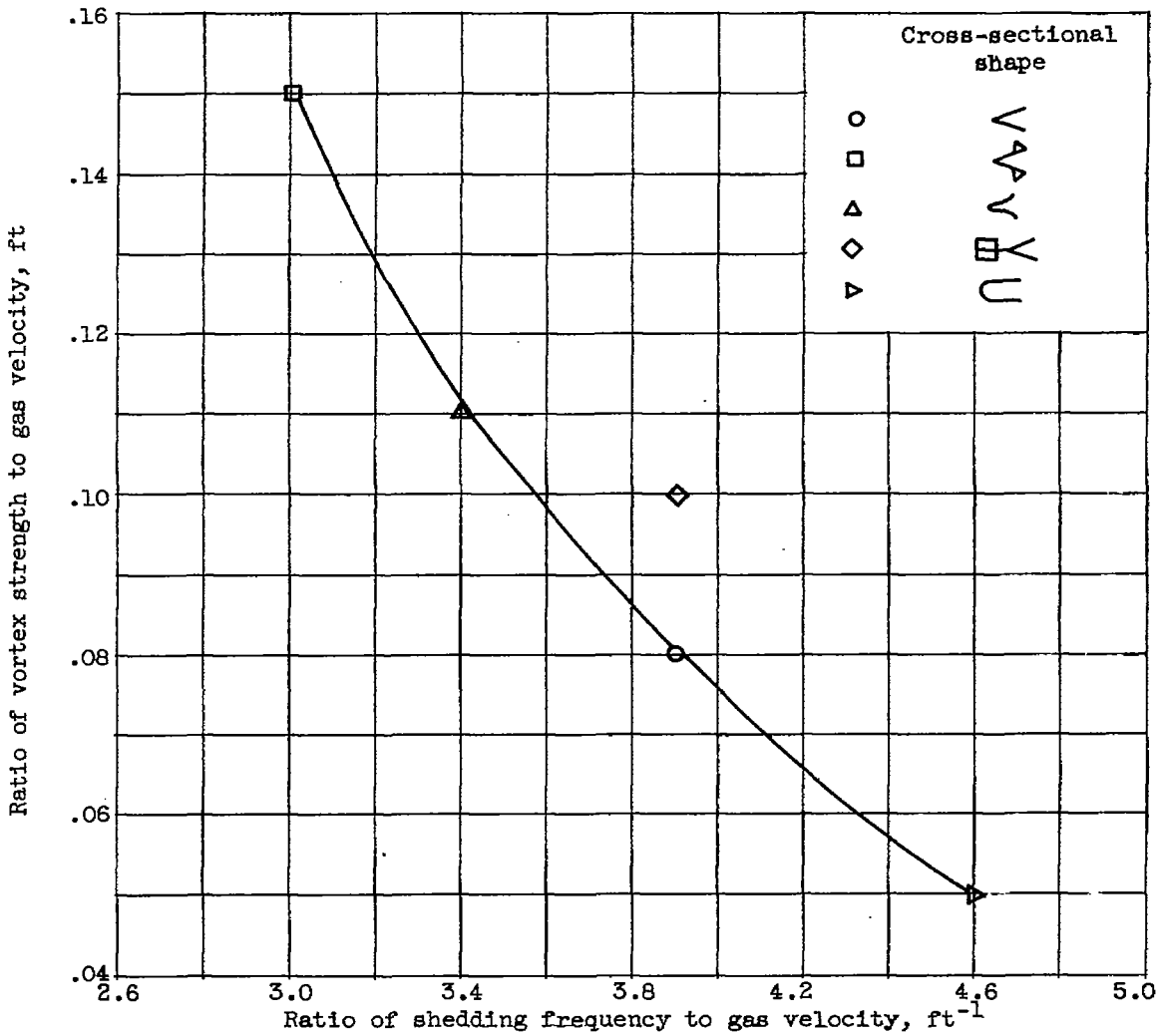

Figure 204. - Effect of cross-sectional shape on isothermal wake characteristics. Gutter width, 3/4 inch.

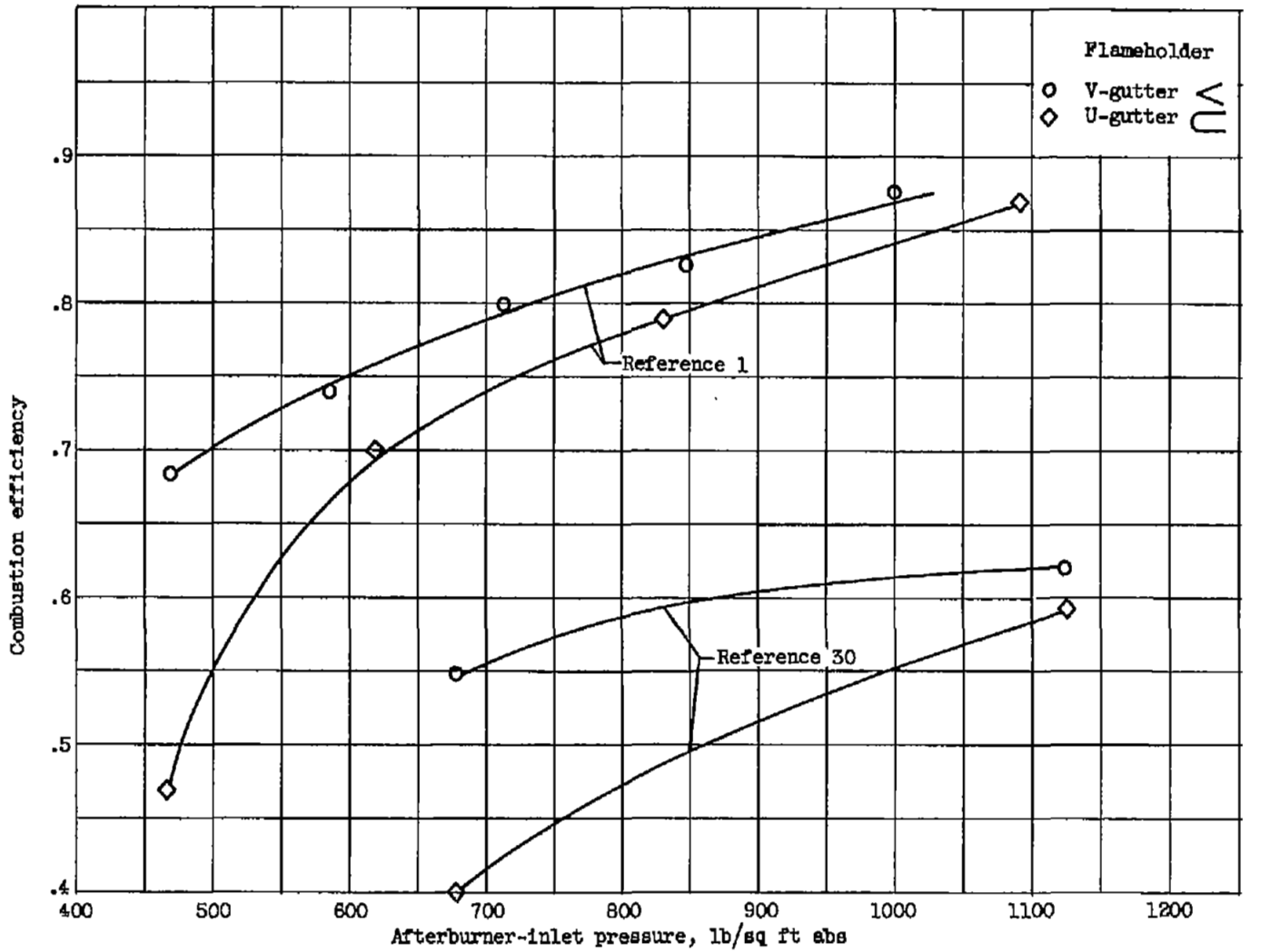

Figure 205. - Effect of flameholder cross-sectional shape on afterburner combustion efficiency as function of afterburner-inlet pressure. Afterburner fuel-air ratio, approximately 0.045.

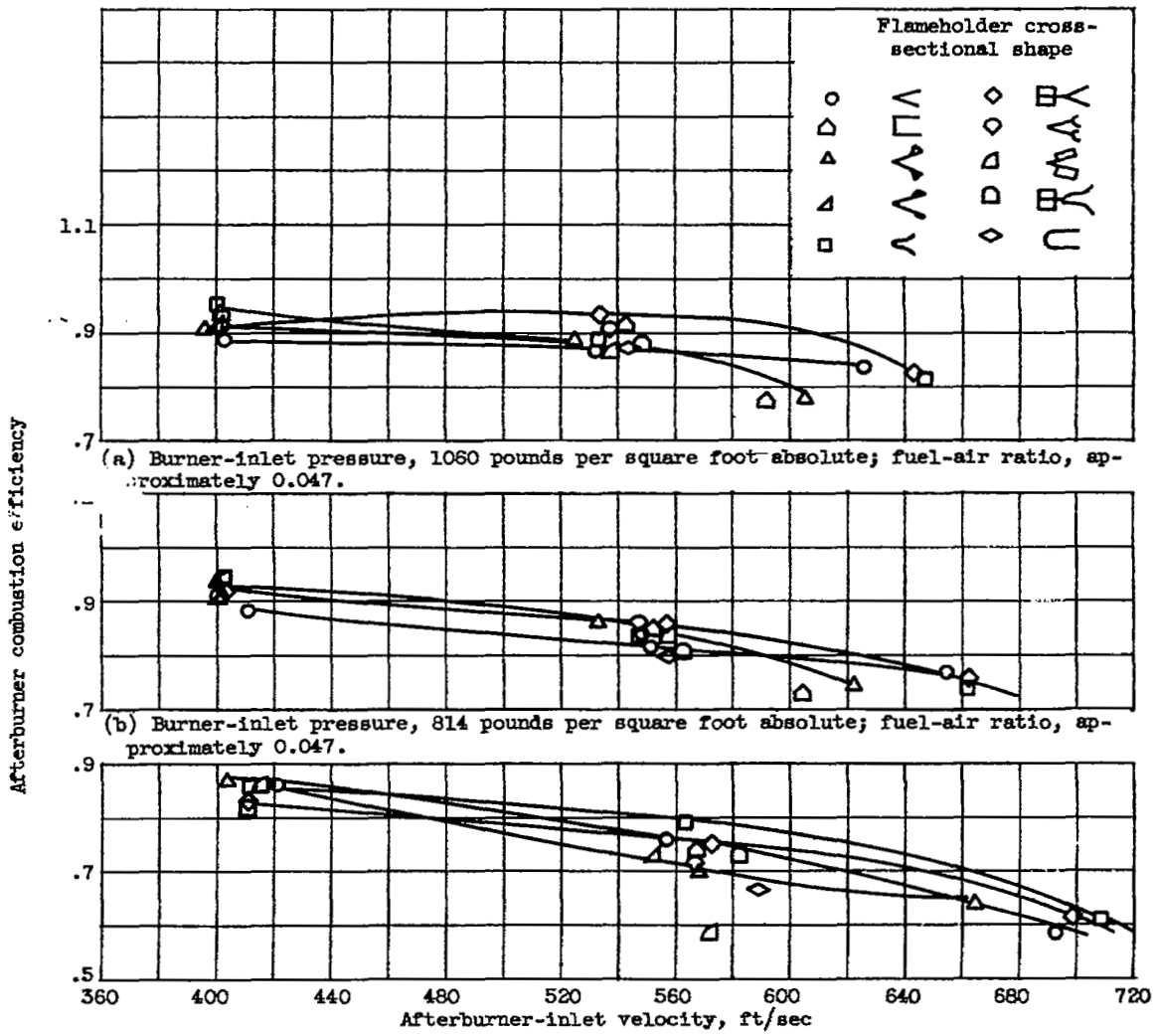

(a) Burner-inlet pressure, 1060 pounds per square foot absolute; fuel-air ratio, approximately 0.047.

(b) Burner-inlet pressure, 814 pounds per square foot absolute; fuel-air ratio, approximately 0.047.

(c) Burner-inlet pressure, 566 pounds per square foot absolute; fuel-air ratio, approximately, 0.047.

Figure 206. - Effect of flameholder cross-sectional shape on afterburner as function of afterburner-inlet velocity.

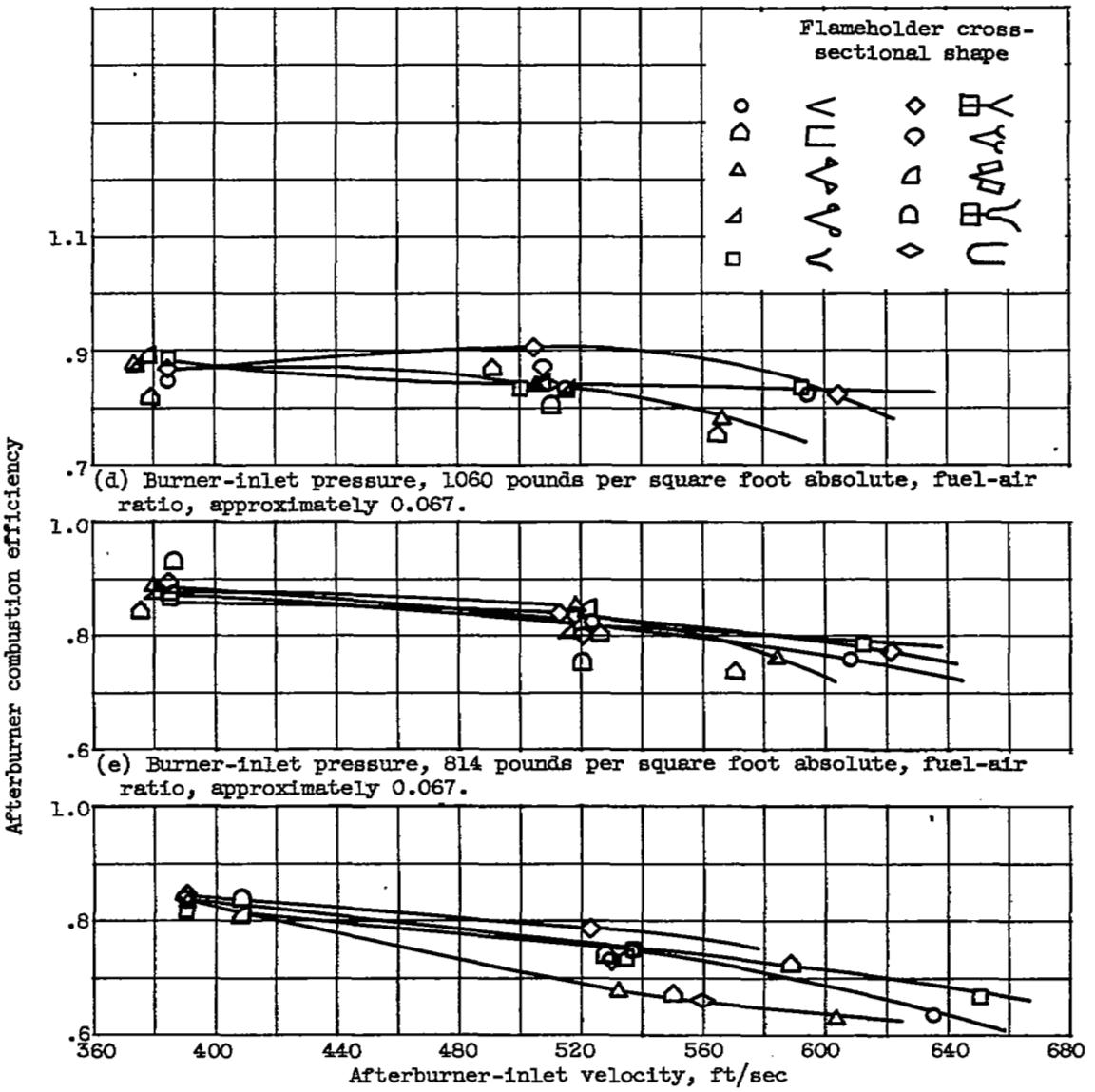

(d) Burner-inlet pressure, 1060 pounds per square foot absolute, fuel-air ratio, approximately 0.067.

(e) Burner-inlet pressure, 814 pounds per square foot absolute, fuel-air ratio, approximately 0.067.

(f) Burner-inlet pressure, 566 pounds per square foot absolute; fuel-air ratio, approximately 0.067.

Figure 206. - Concluded. Effect of flameholder cross-sectional shape on afterburner as function of afterburner-inlet velocity.

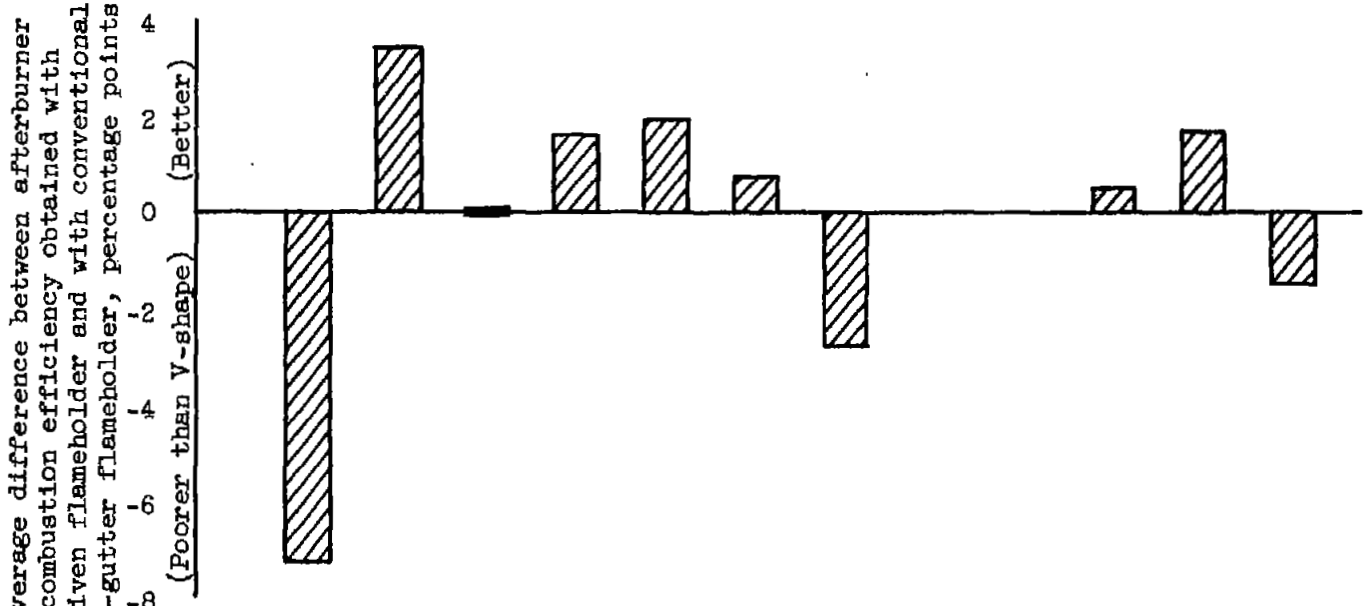

Cross-sectional shape	⊂	⌇	<	∝	≺	≷	⌇	∝	⋖	⊏
Ratio of vortex strength to shedding frequency, K/N	.086	.156	.156	.208	.226	.300	.310	---	--	---
Number of experimental runs	48	29	259	49	212	139	132	105	38	119

Figure 207. - Average difference in afterburner combustion efficiency obtained with various flameholder shapes.

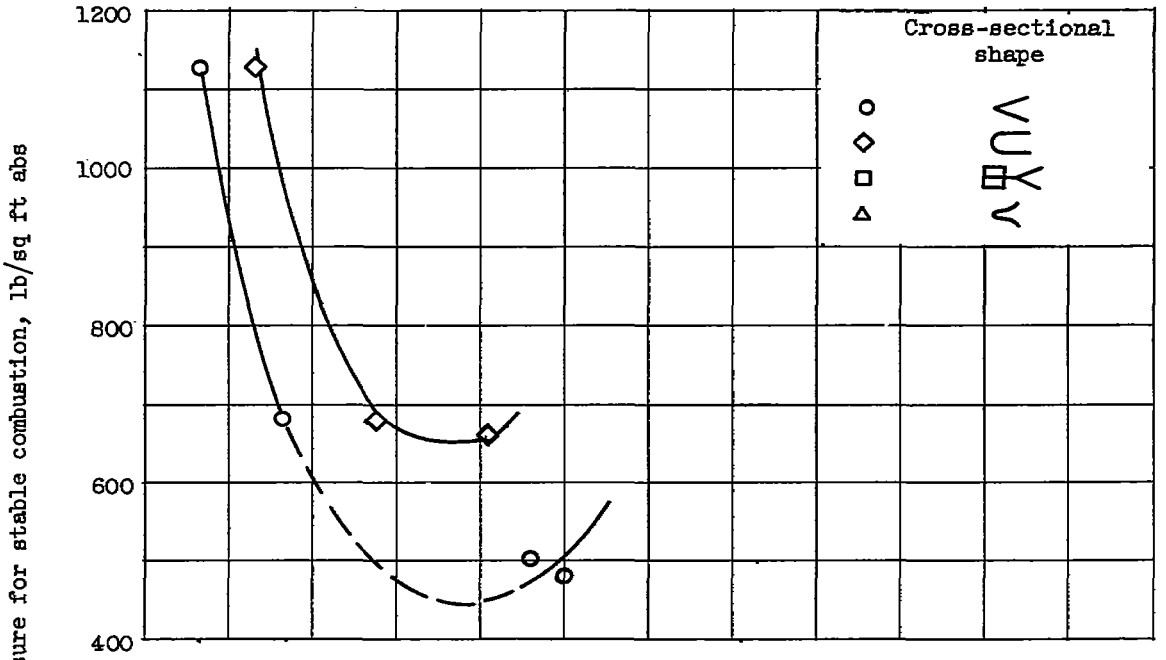

(a) Engine afterburner tests (ref. 32).

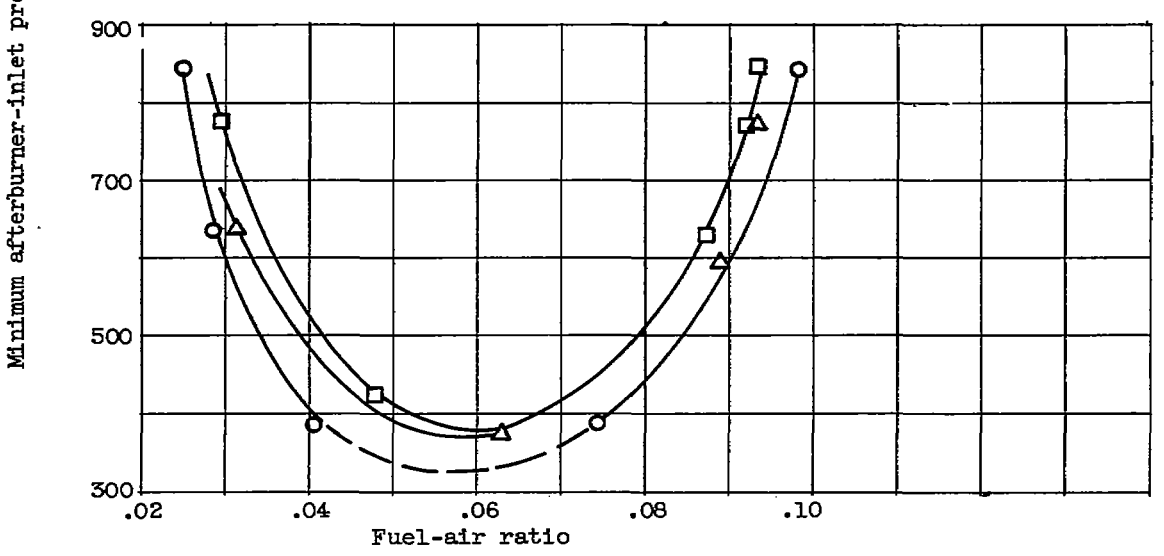

(b) Simulated afterburner facility (ref. 1).

Figure 208. - Effect of flameholder cross-sectional shape on blow-out limits.

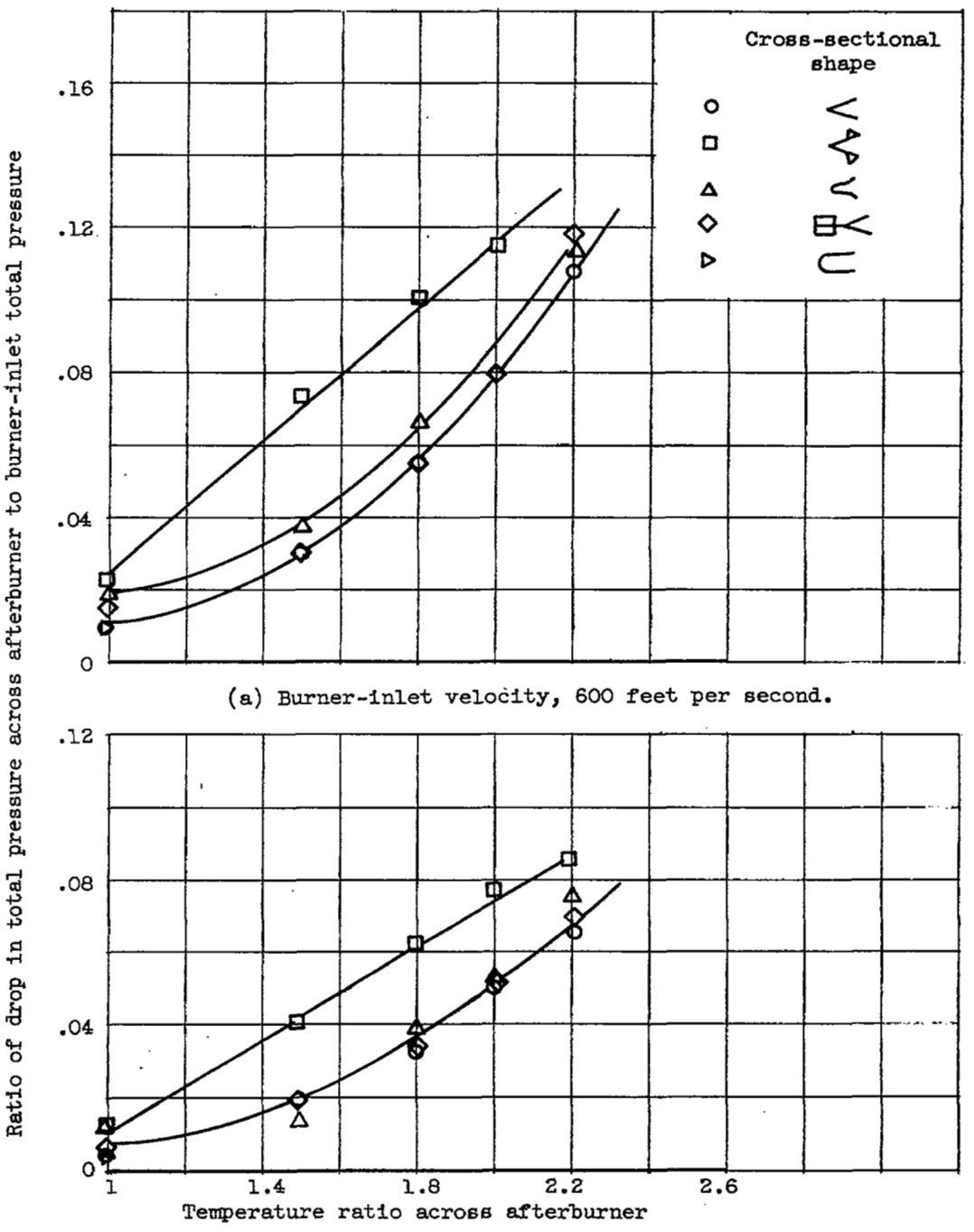

(a) Burner-inlet velocity, 600 feet per second.

(b) Burner-inlet velocity, 500 feet per second.

Figure 209. - Effect of flameholder cross-sectional shape on afterburner pressure loss. Blockage, 29 percent.

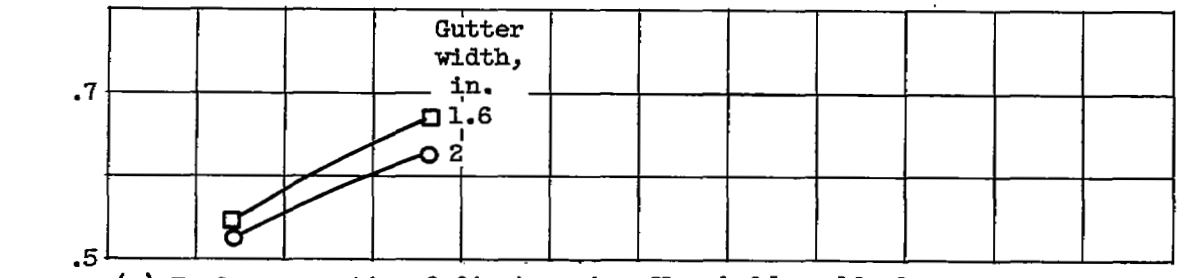

(a) Fuel-area ratio, 0.04; two-ring flameholder; blockage, 27 percent; burner-inlet velocity, 450 feet per second.

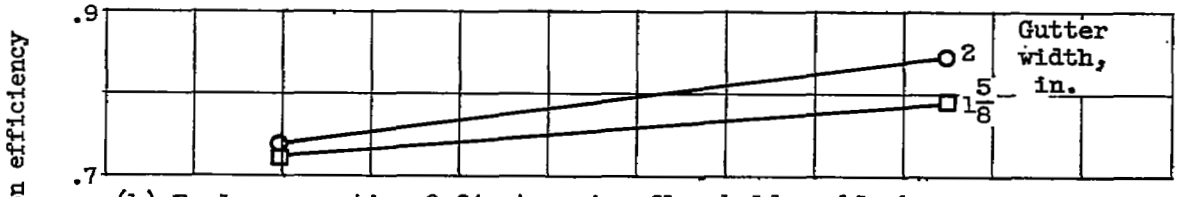

(b) Fuel-area ratio, 0.04; two-ring flameholder; blockage, 35 percent; burner-inlet velocity, 620 feet per second.

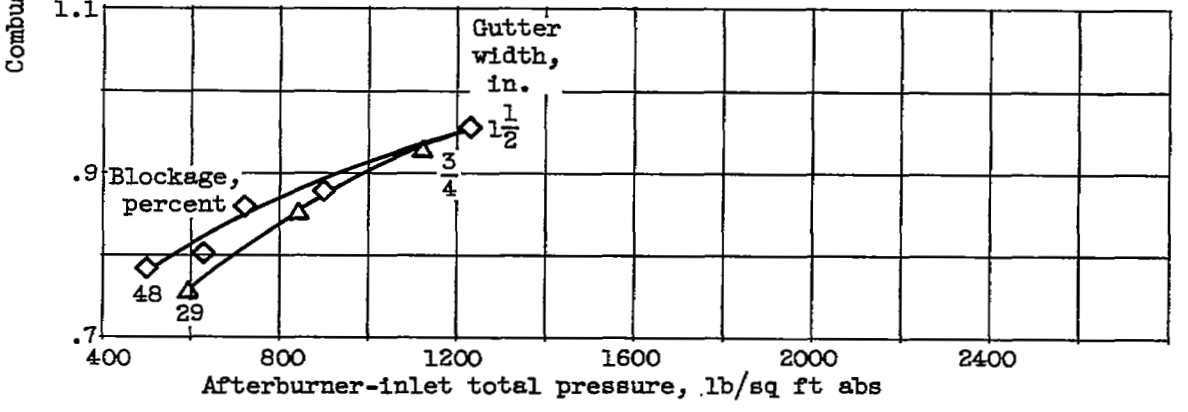

(c) Fuel-air ratio, 0.05; three-ring flameholder; burner-inlet, velocity, 520 feet per second.

Figure 210. - Effect of flameholder V-gutter width on afterburner combustion efficiency.

[redacted]

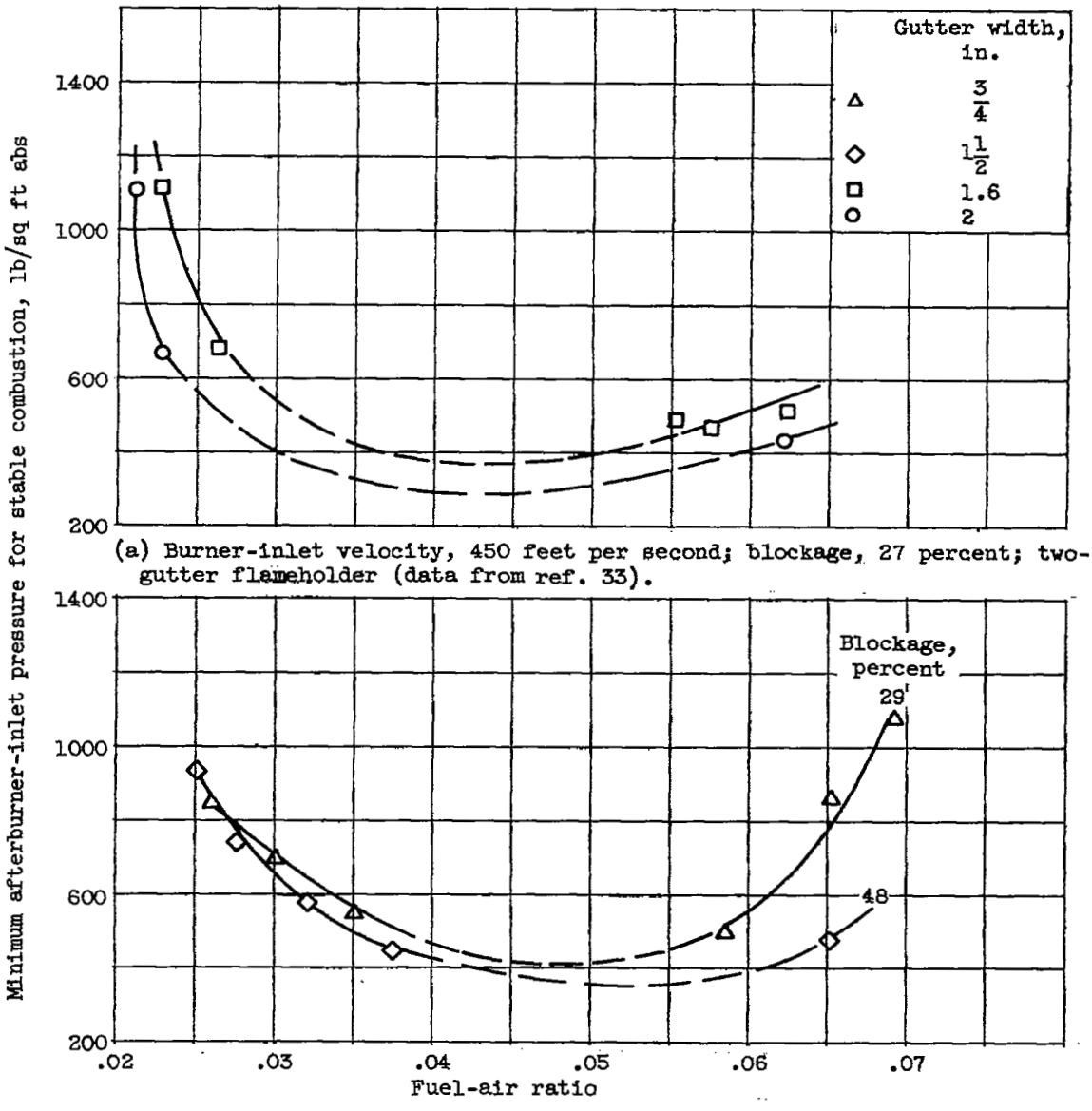

(a) Burner-inlet velocity, 450 feet per second; blockage, 27 percent; two-gutter flameholder (data from ref. 33).

(b) Burner-inlet velocity, 520 feet per second; three-gutter flameholder (data from ref. 32).

Figure 211. - Effects of flameholder gutter width on afterburner blow-out limits.

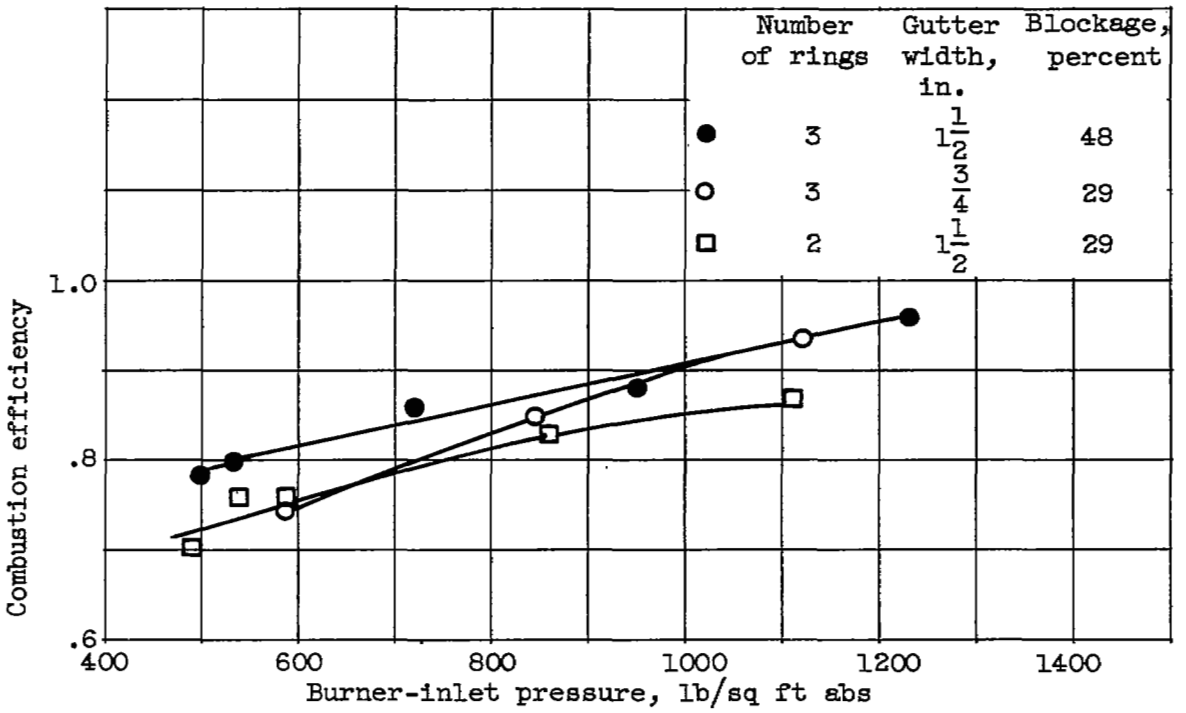

Figure 212. - Effect of number of gutters on afterburner combustion efficiency. Afterburner-inlet velocity, 520 feet per second; fuel-air ratio, 0.05.

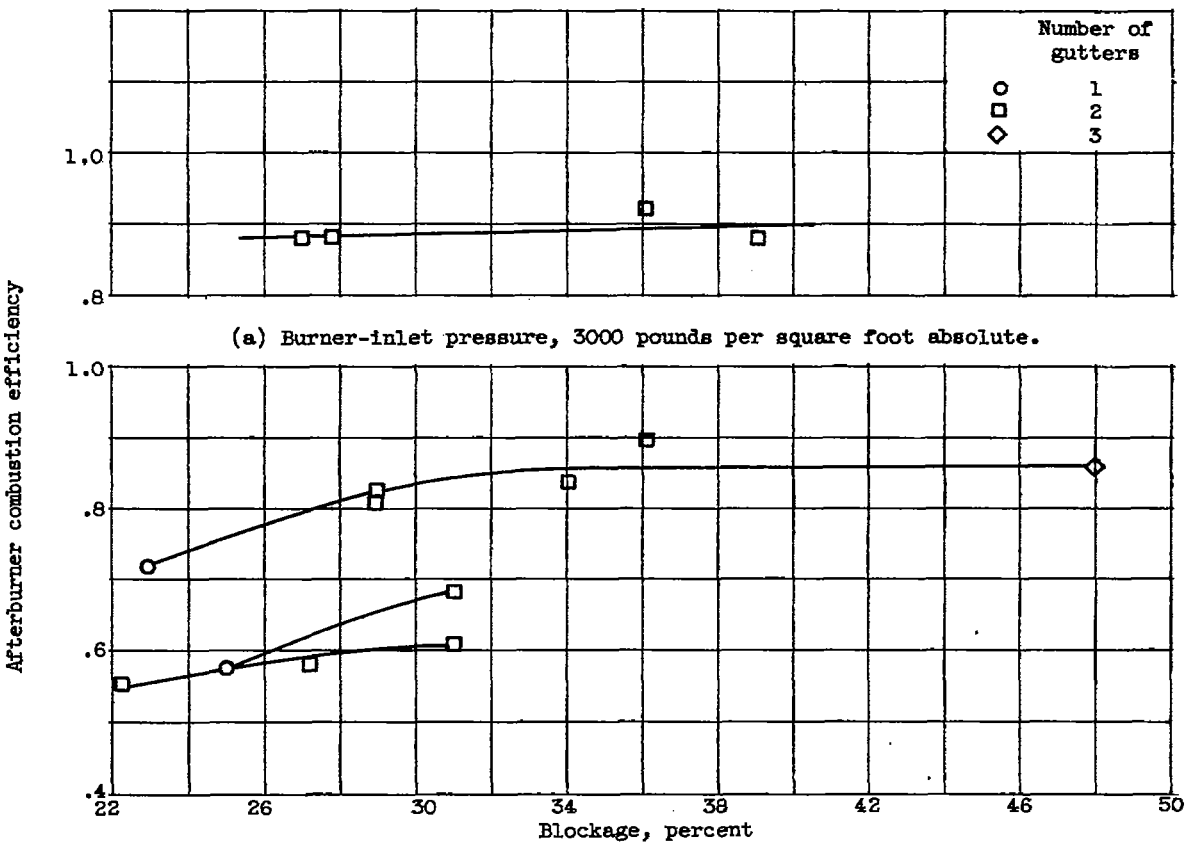

(a) Burner-inlet pressure, 3000 pounds per square foot absolute.

(b) Burner-inlet pressure, 800 pounds per square foot absolute.

Figure 213. - Effect of blockage on afterburner combustion efficiency. Fuel-air ratio, between 0.04 and 0.05.

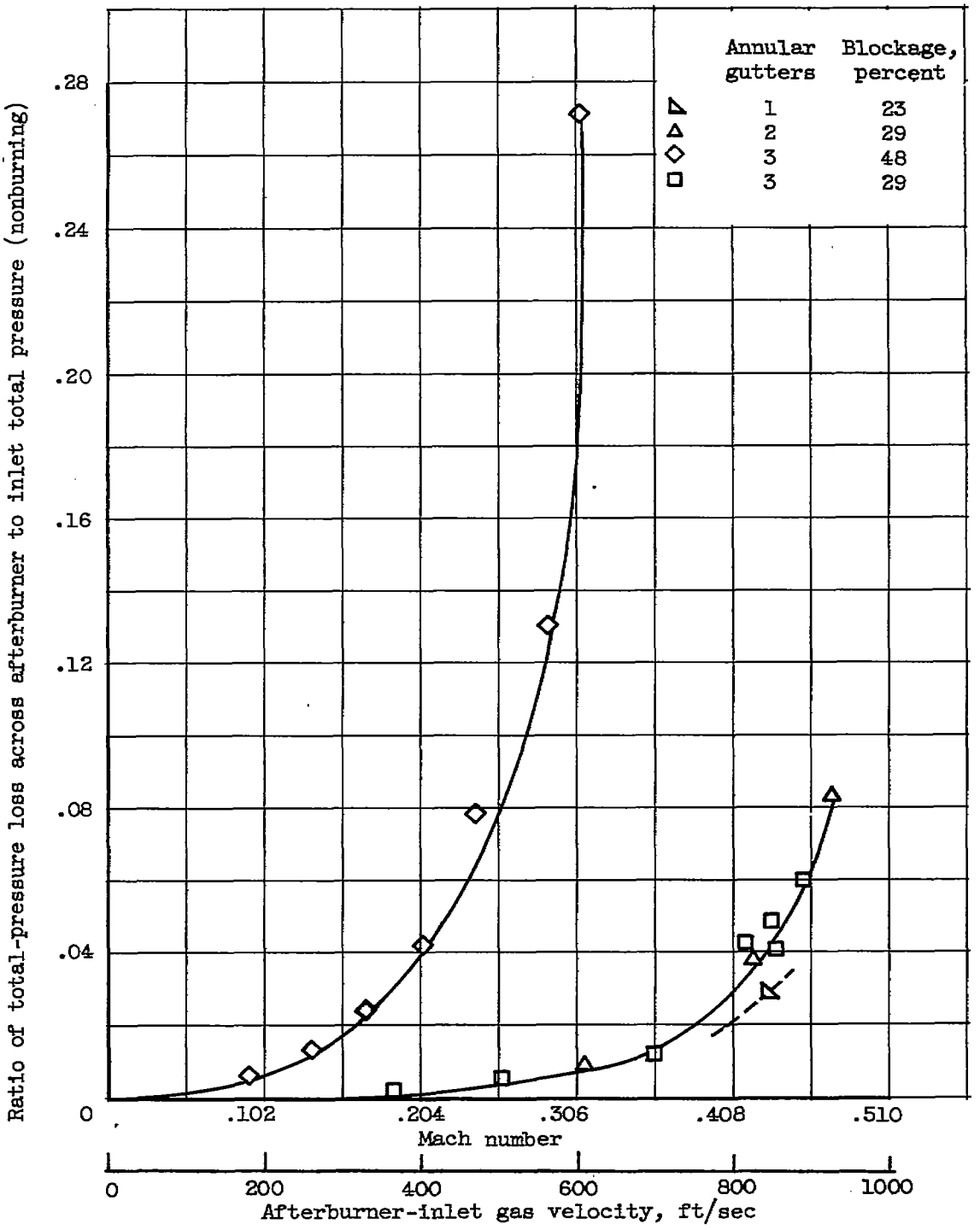

Figure 214. - Effect of afterburner-inlet gas velocity on nonburning total-pressure loss.

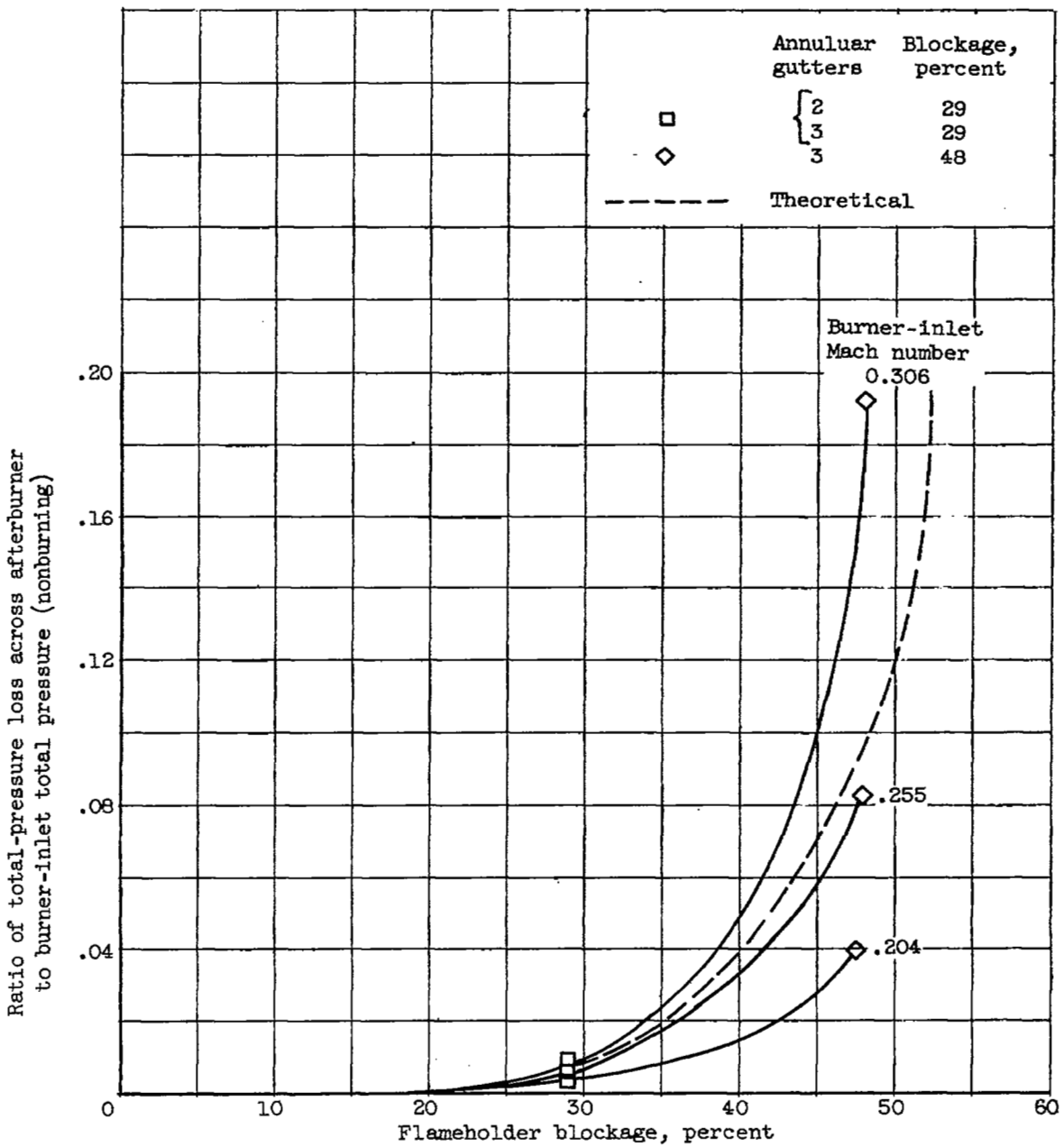

Figure 215. - Effect of flameholder blockage on nonburning total-pressure loss.

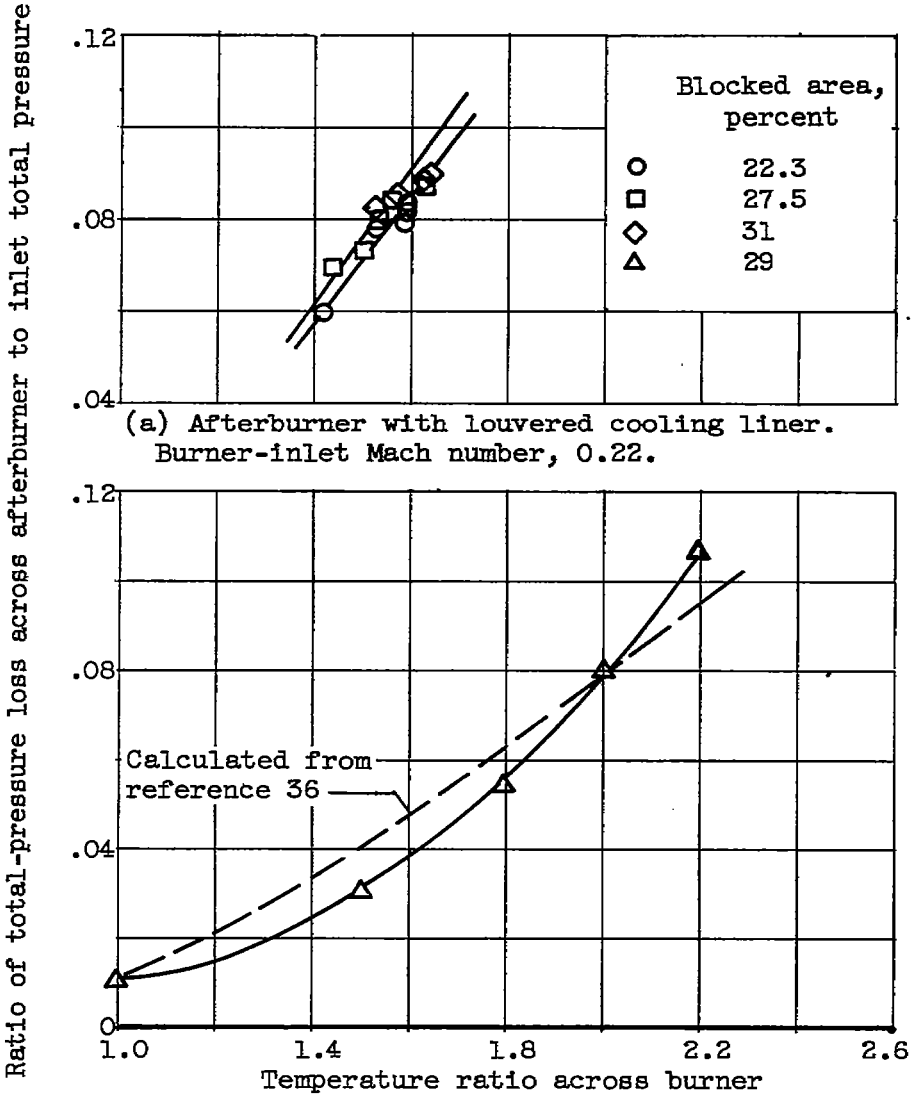

(b) Afterburner without cooling liner. Burner-inlet Mach number, approximately 0.30.

Figure 216. - Effect of temperature ratio and blocked area on pressure losses, with burning.

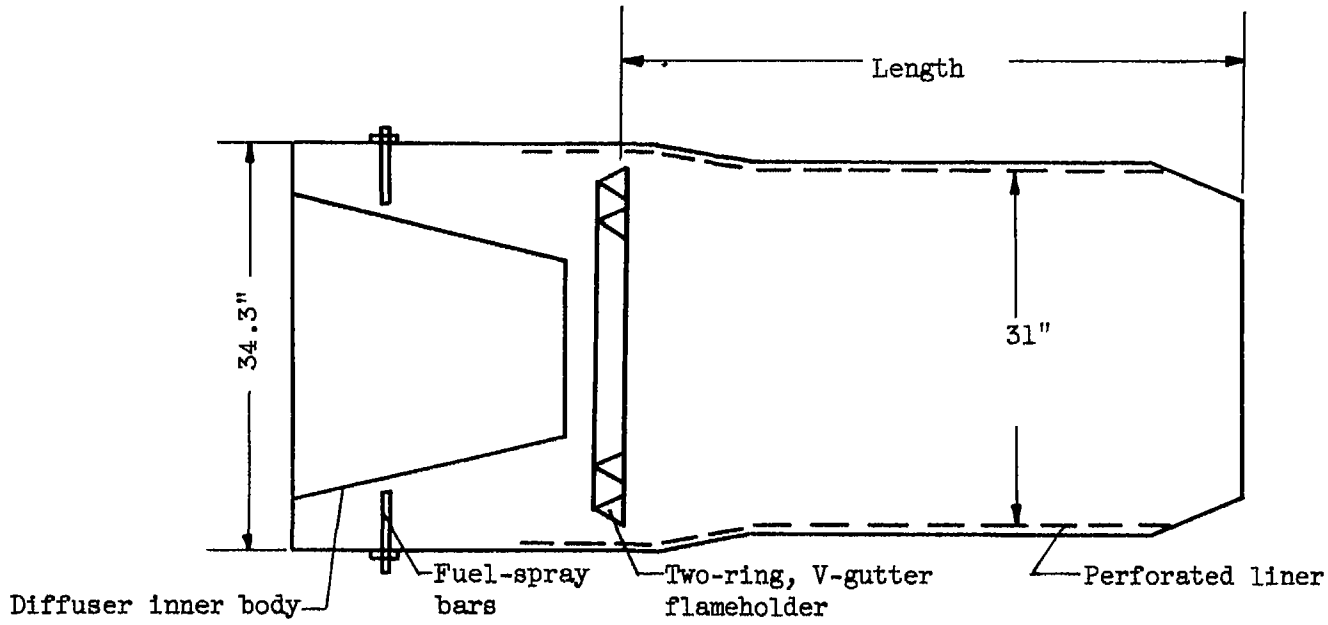

Figure 217. - Afterburner designed for take-off application.

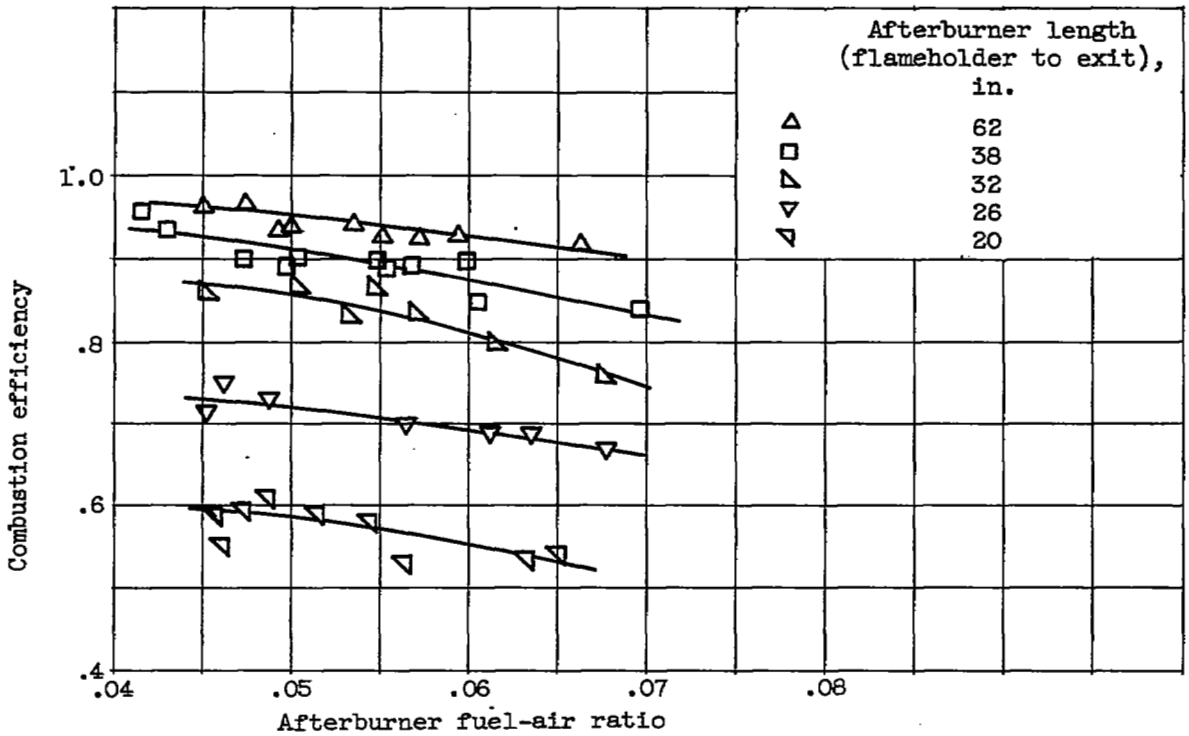

(a) Combustion efficiency.

Figure 218. - Effect of afterburner length on performance of take-off afterburner. Burner-inlet pressure, 3800 pounds per square foot absolute.

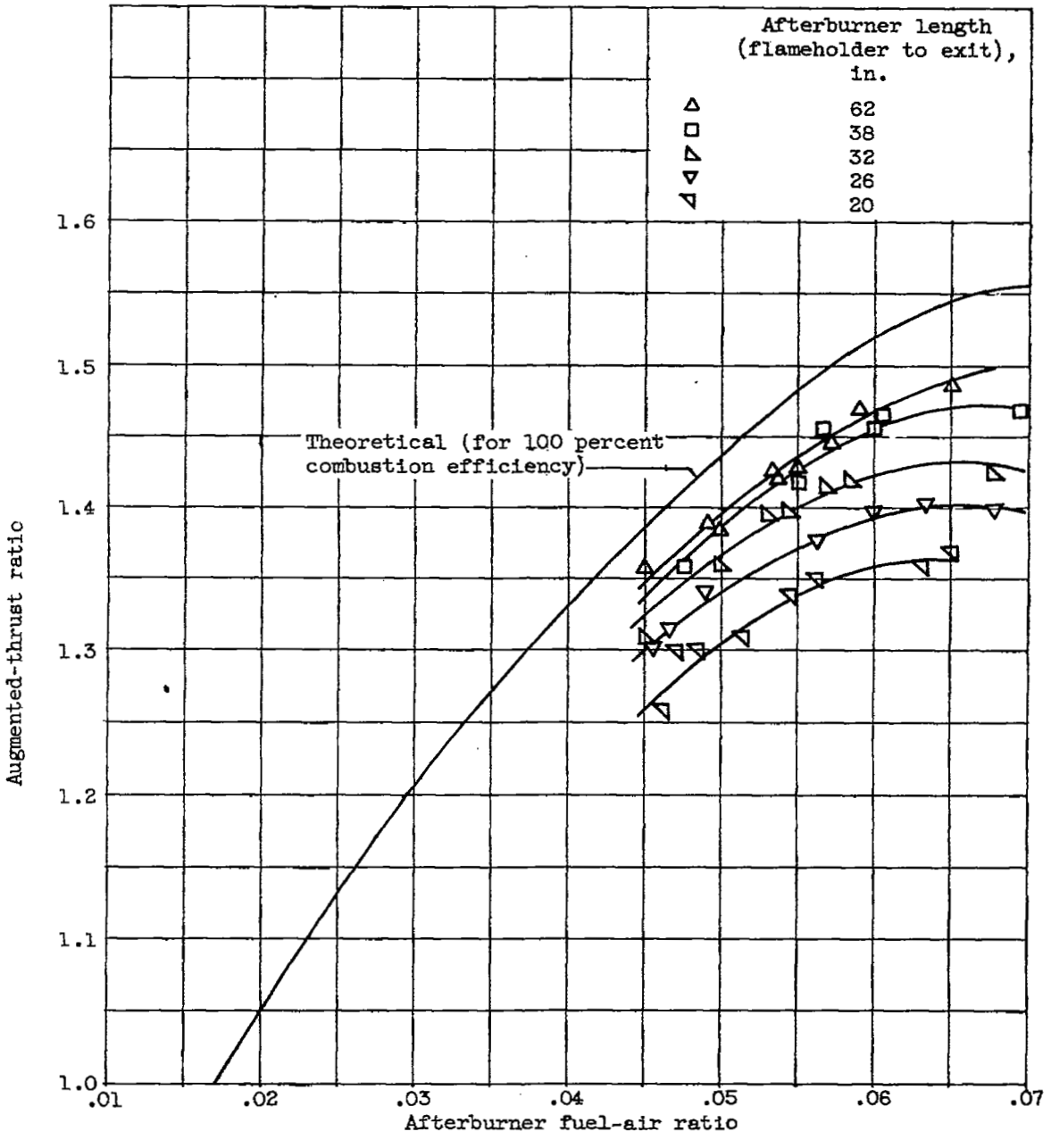

(b) Augmented-thrust ratio.

Figure 218. - Concluded. Effect of afterburner length on performance of take-off afterburner. Burner-inlet pressure, 3800 pounds per square foot absolute.

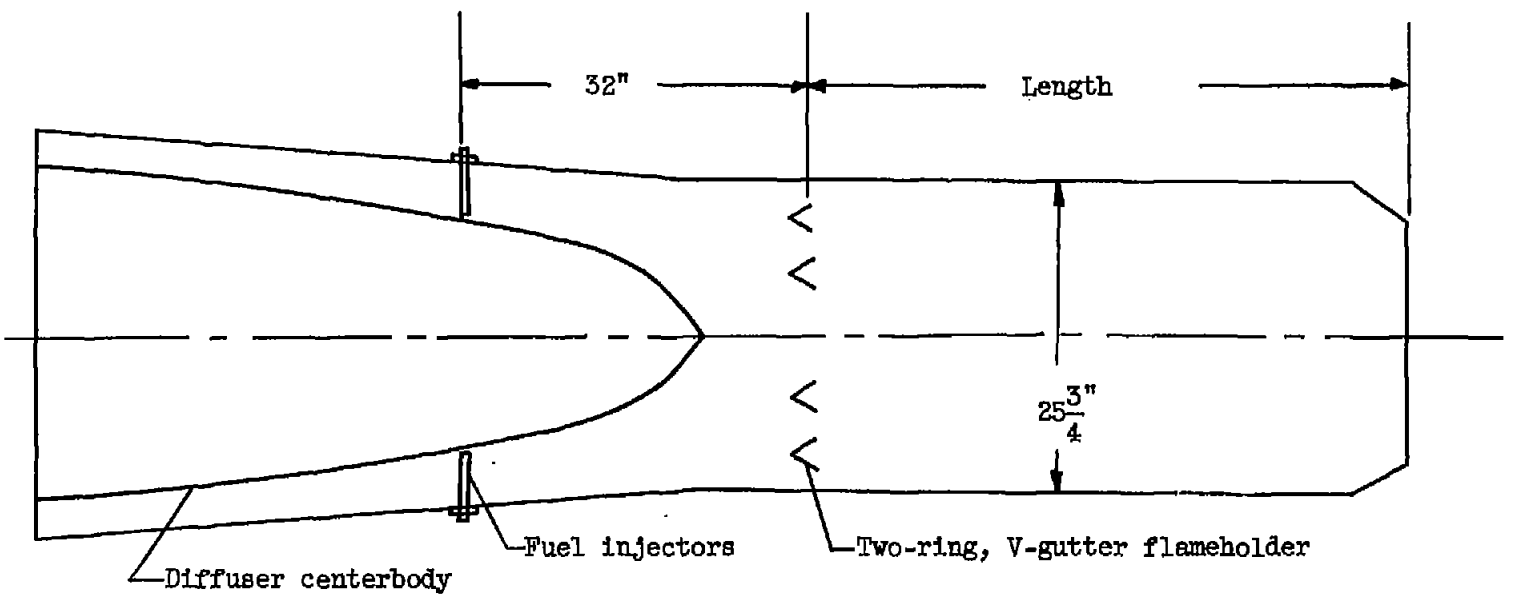

Figure 219. - Afterburner designed for high-altitude conditions.

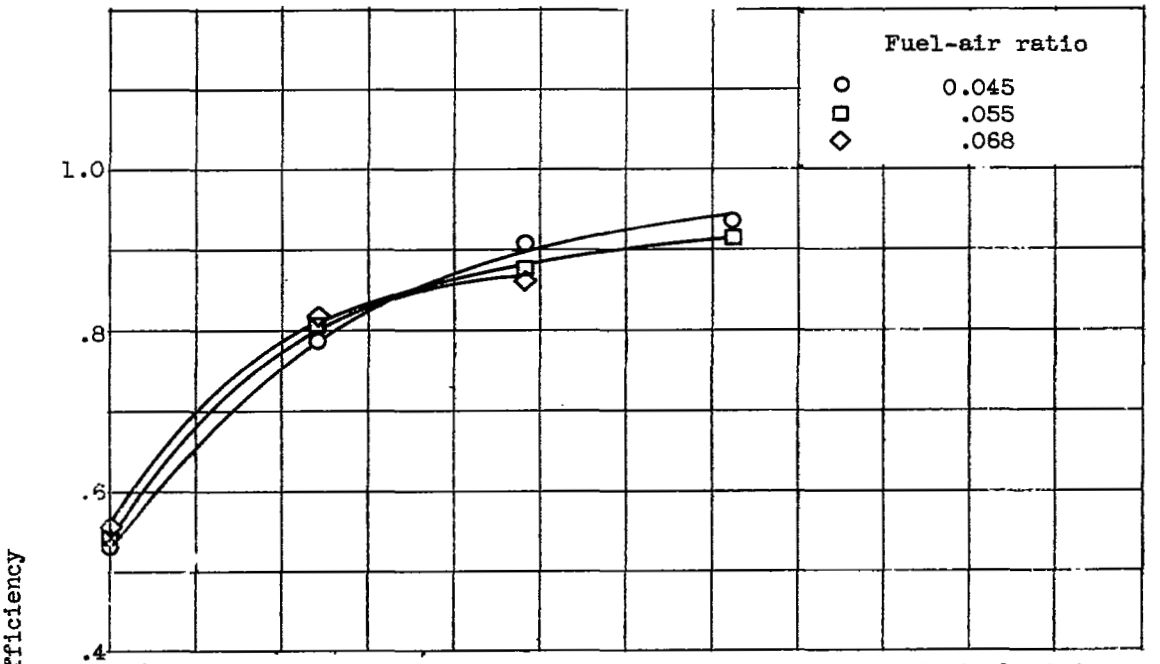

(a) Burner-inlet total pressure, 1275 pounds per square foot absolute; inlet velocity, 500 feet per second; inlet total temperature, 1200° F.

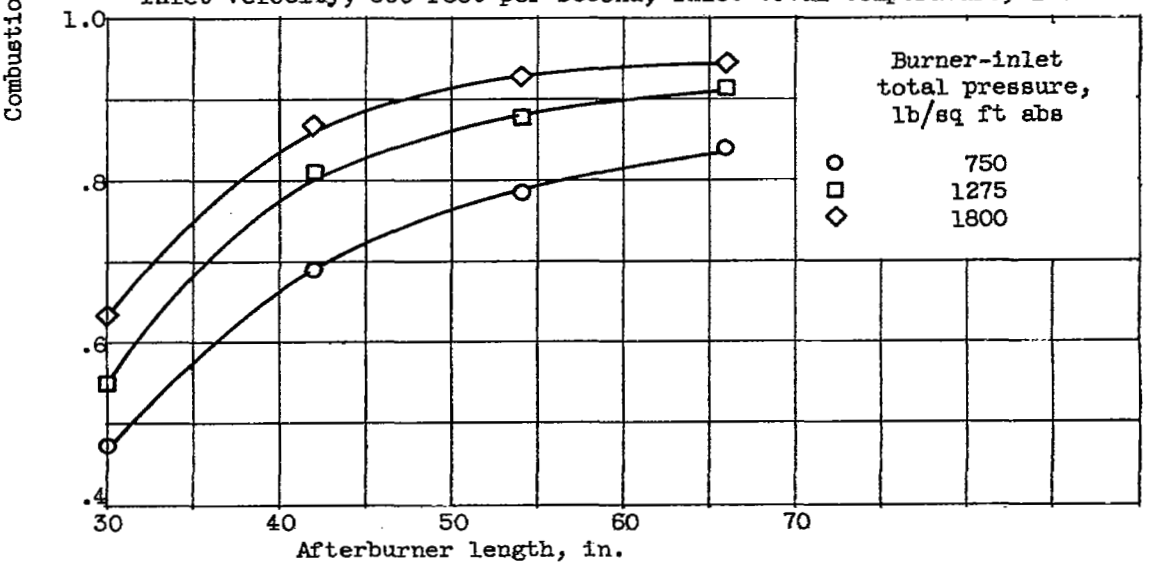

(b) Burner-inlet velocity, 500 feet per second; inlet temperature, 1200° F; fuel-air ratio, 0.055.

Figure 220. - Effect of afterburner length on performance of high-altitude afterburner.

[redacted]

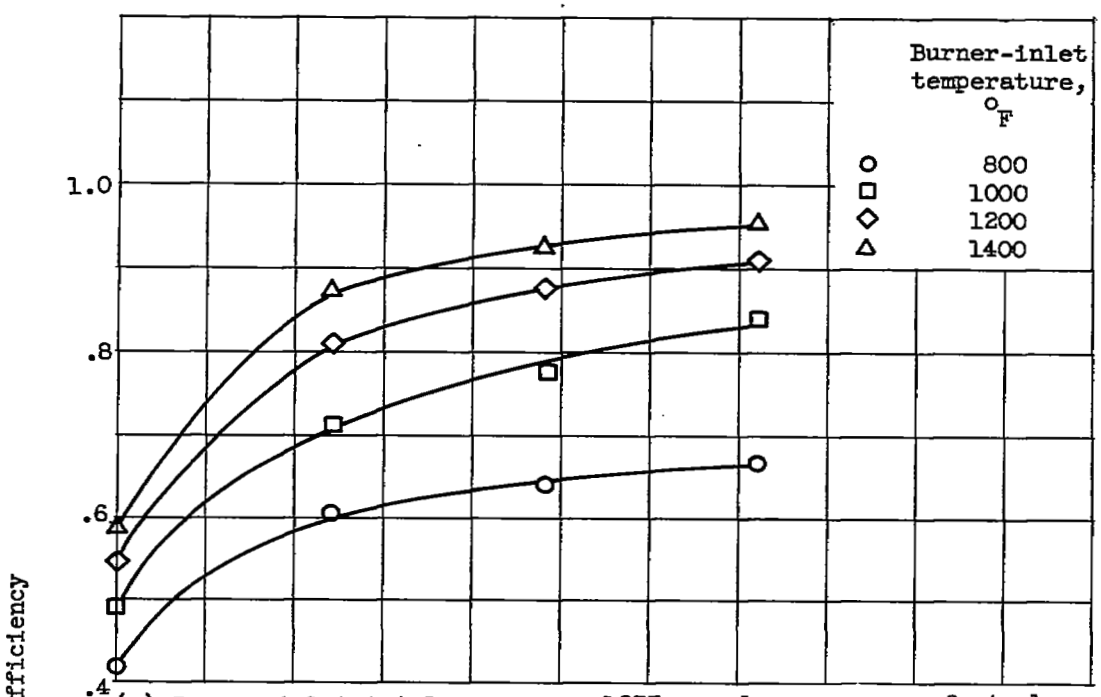

(c) Burner-inlet total pressure, 1275 pounds per square foot absolute; inlet velocity, 500 feet per second; fuel-air ratio, 0.055.

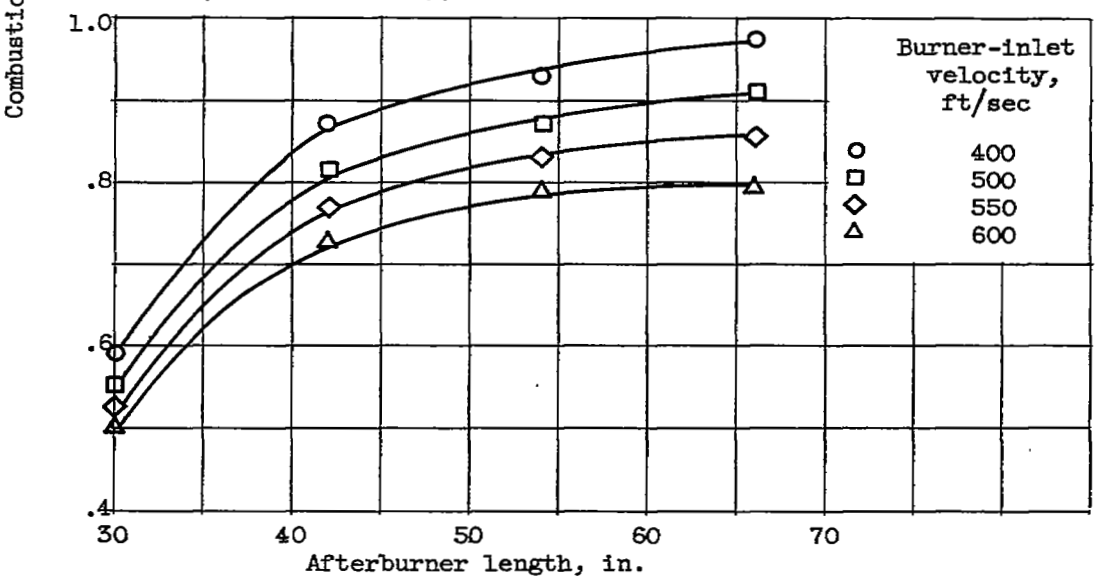

(d) Burner-inlet total pressure, 1275 pounds per square foot absolute; inlet temperature, 1200° F; fuel-air ratio, 0.055.

Figure 220. - Concluded. Effect of afterburner length on performance of high-altitude afterburner.

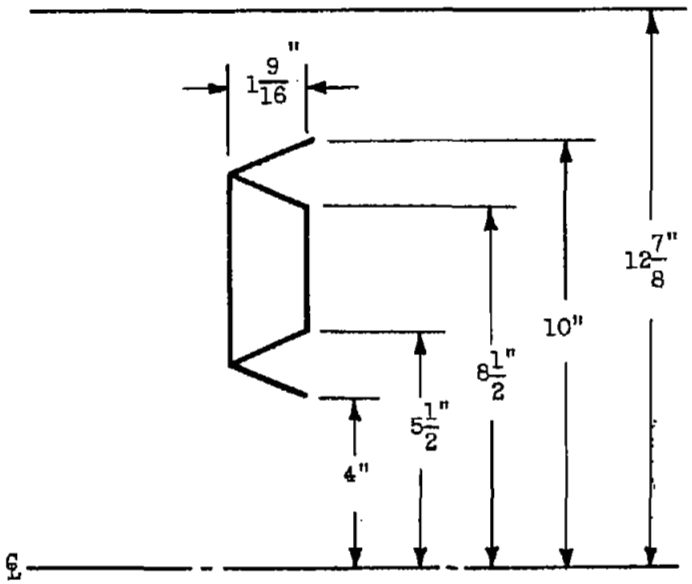

(a) Original flameholder with optimum gutter diameters.

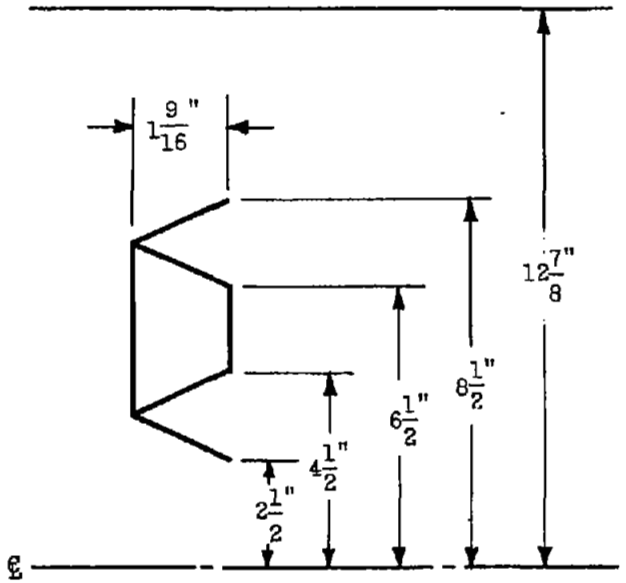

(b) Modified flameholder with reduced gutter diameters.

Figure 221. - Comparison of flameholders with optimum and reduced gutter diameters.

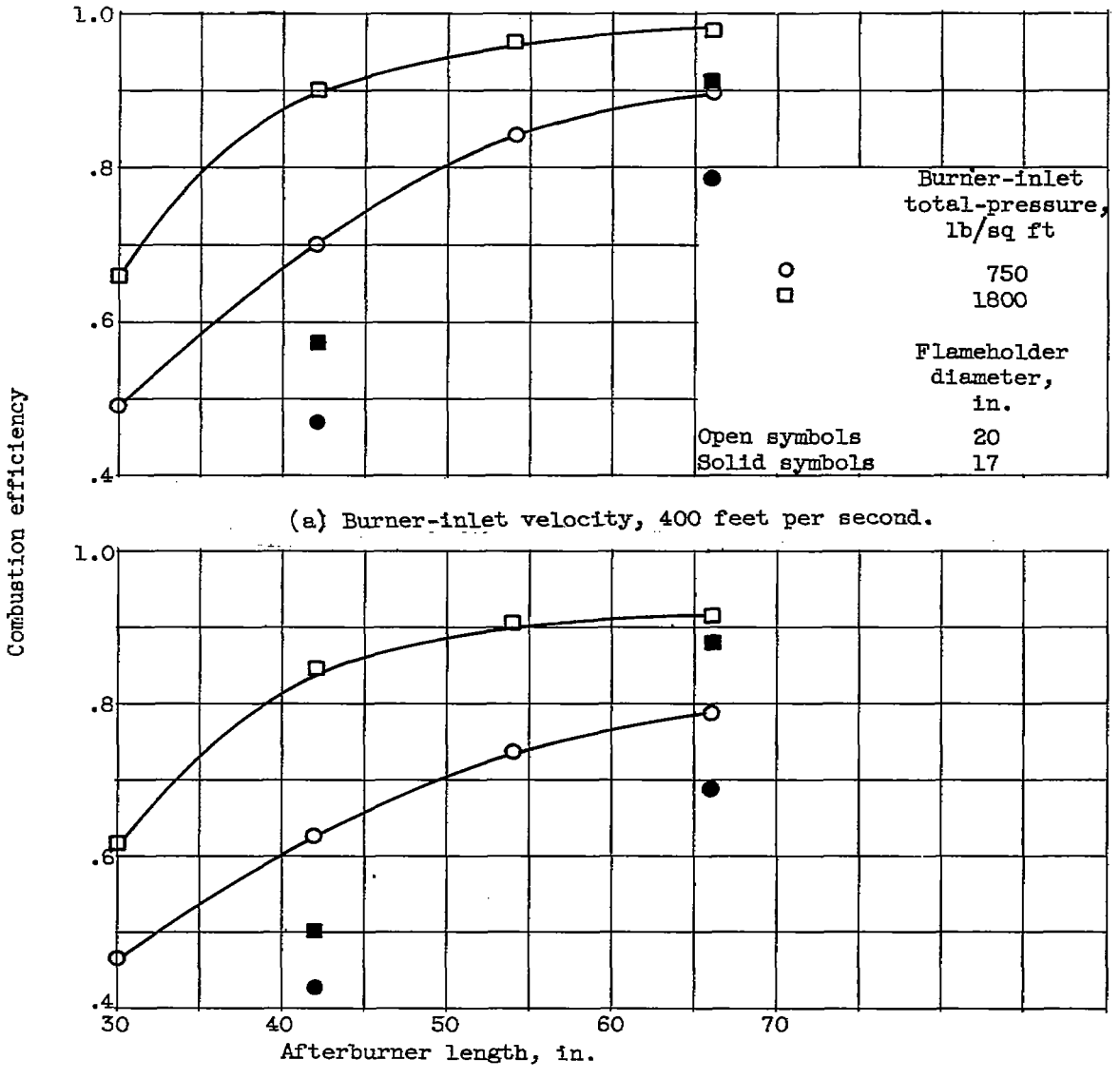

(a) Burner-inlet velocity, 400 feet per second.

(b) Burner-inlet velocity, 550 feet per second.

Figure 222. - Effect of reduced flameholder-gutter diameter on combustion efficiency. Burner-inlet total temperature, 1200° F; fuel-air ratio, 0.055.

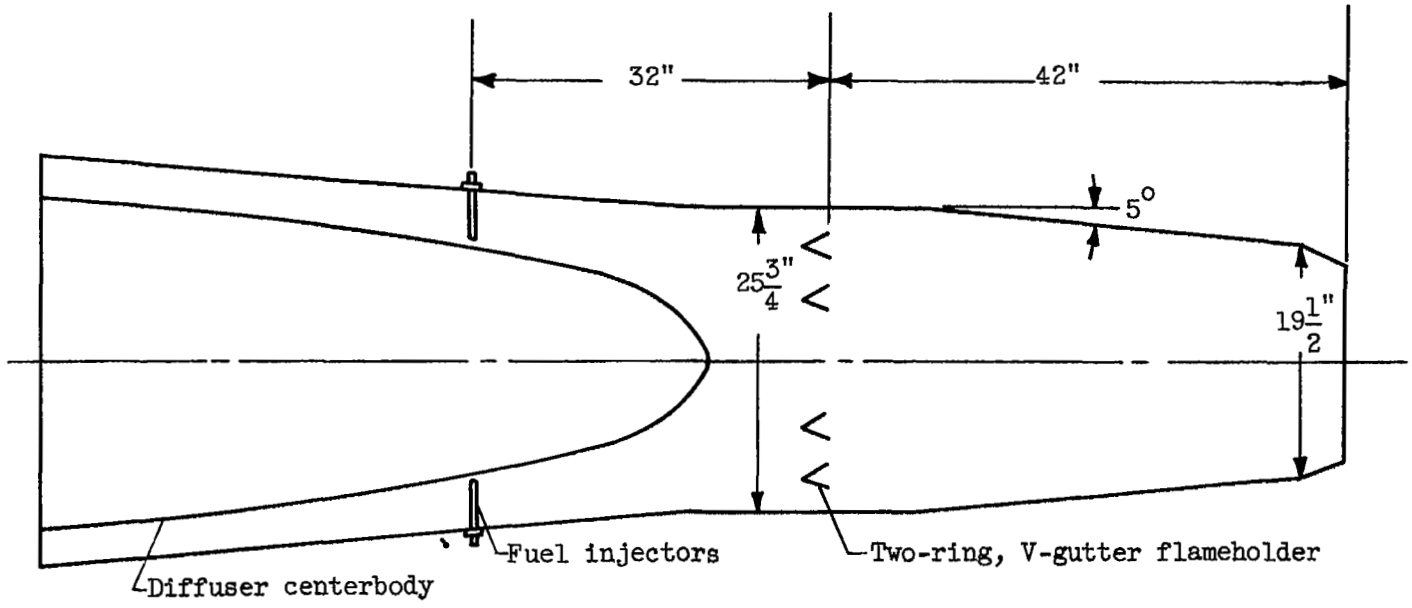

Figure 223. - Tapered afterburner designed for high-altitude operation.

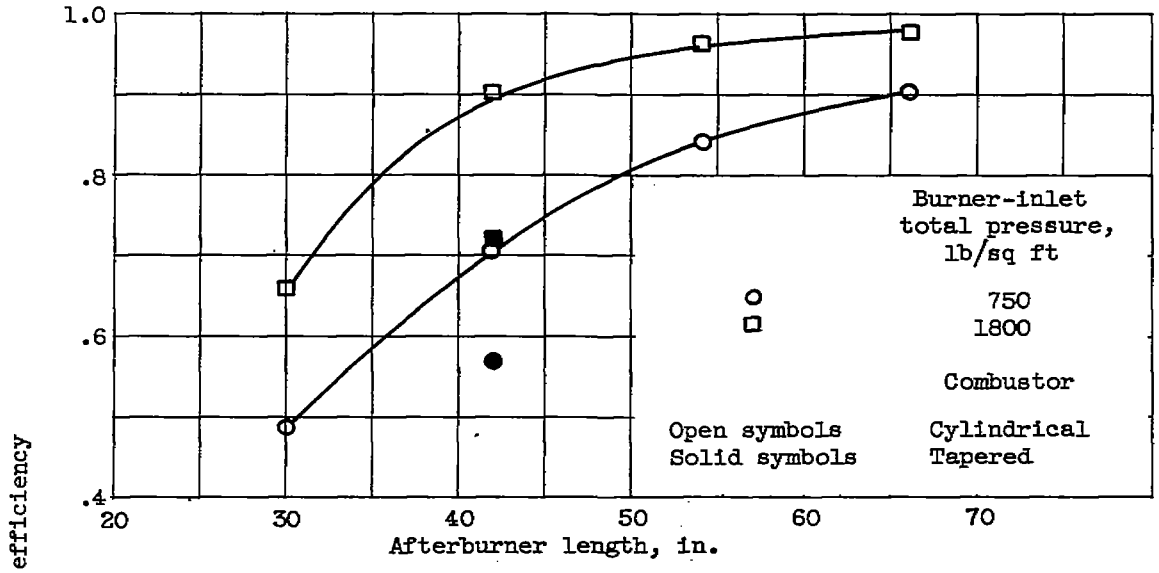

(a) Variation of efficiency with afterburner length.

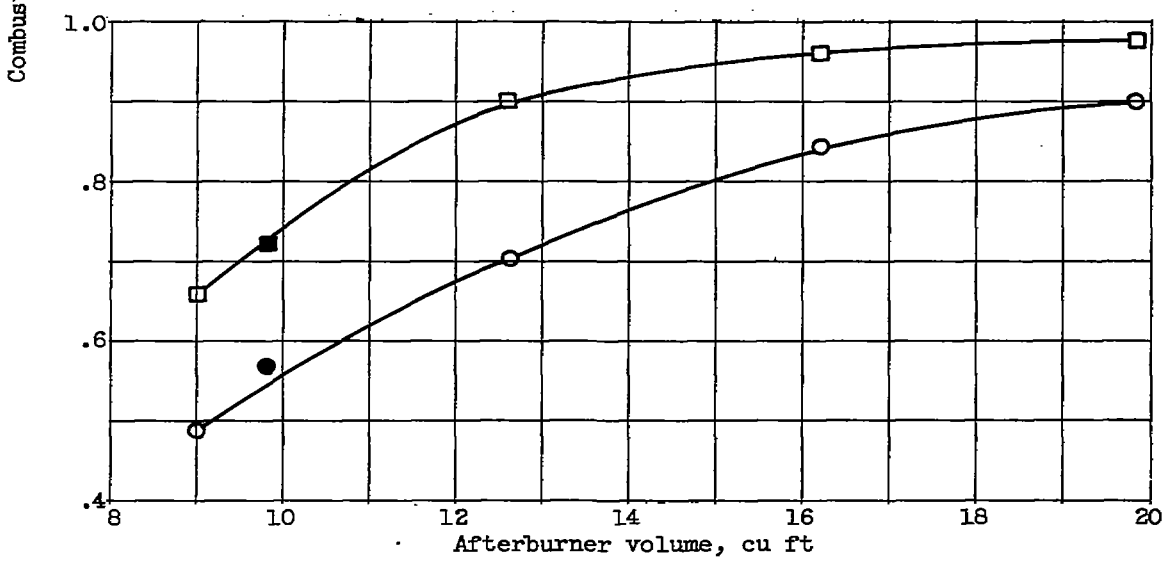

(b) Variation of efficiency with afterburner volume.

Figure 224. - Effect of afterburner-shell taper on combustion efficiency. Burner-inlet velocity, 400 feet per second; inlet total temperature, 1200° F; fuel-air ratio, 0.055.

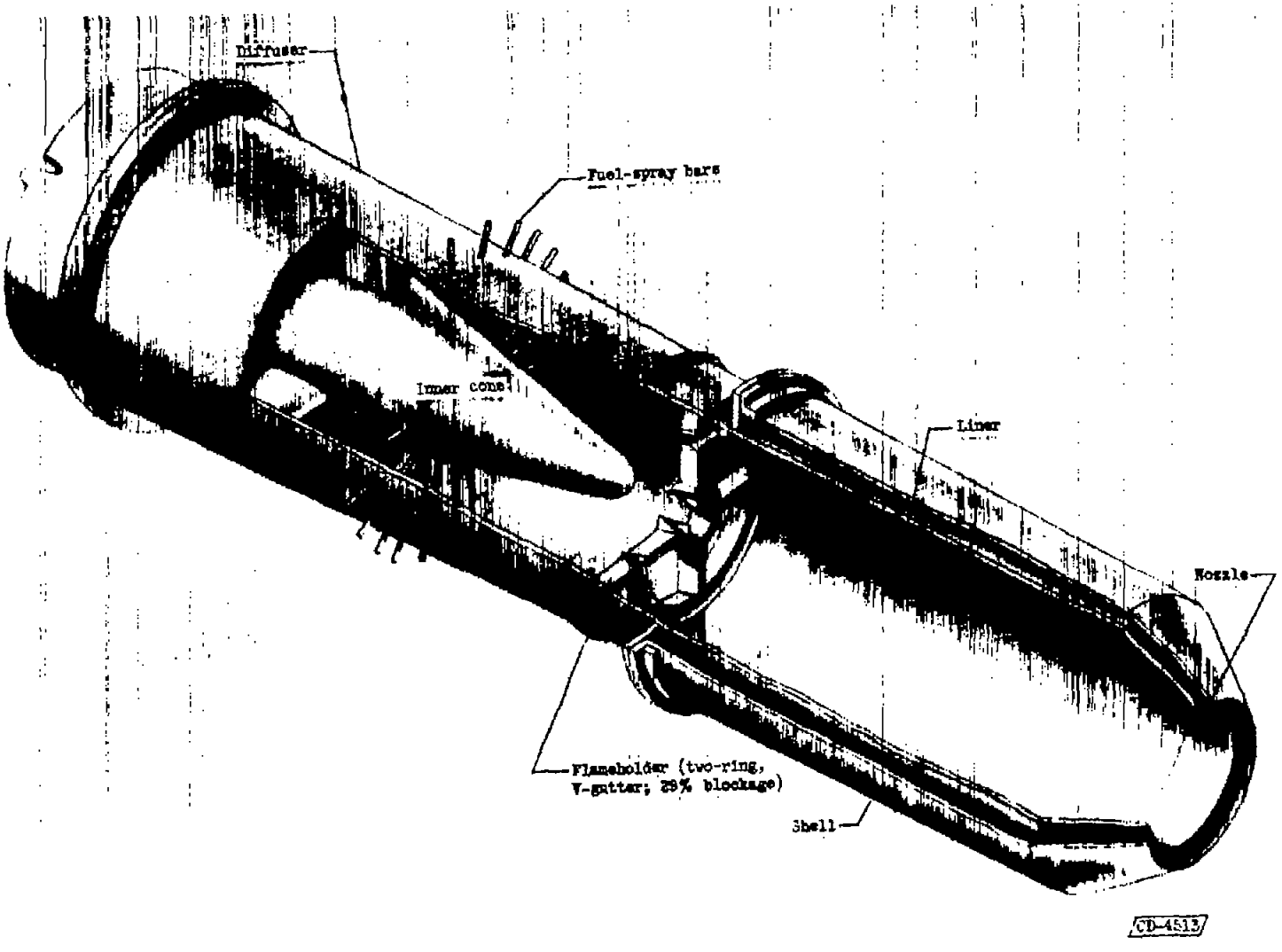

Figure 225. - Cutaway view of afterburner.

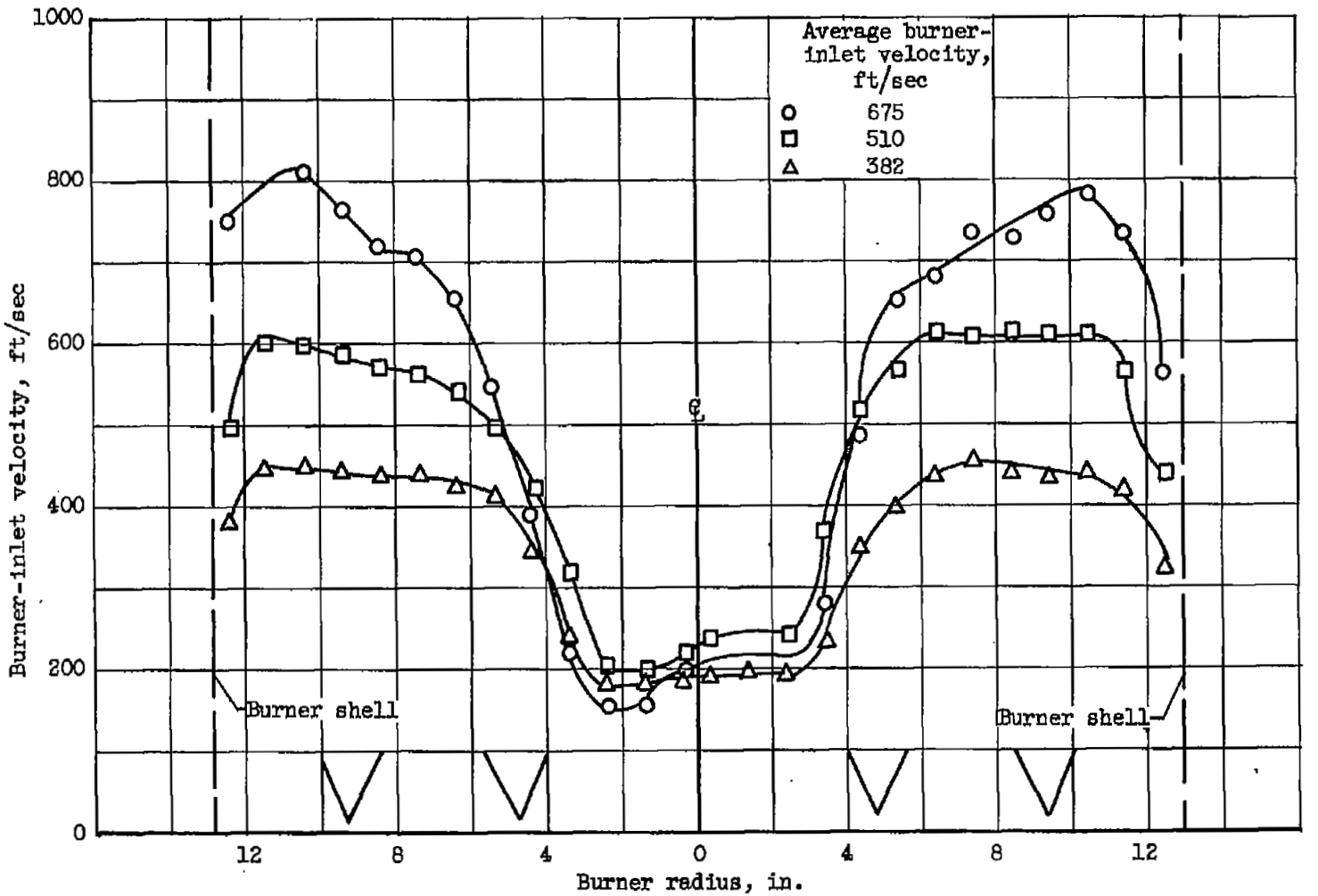

Figure 226. - Velocity profile at burner inlet showing relative location of flameholder gutters.

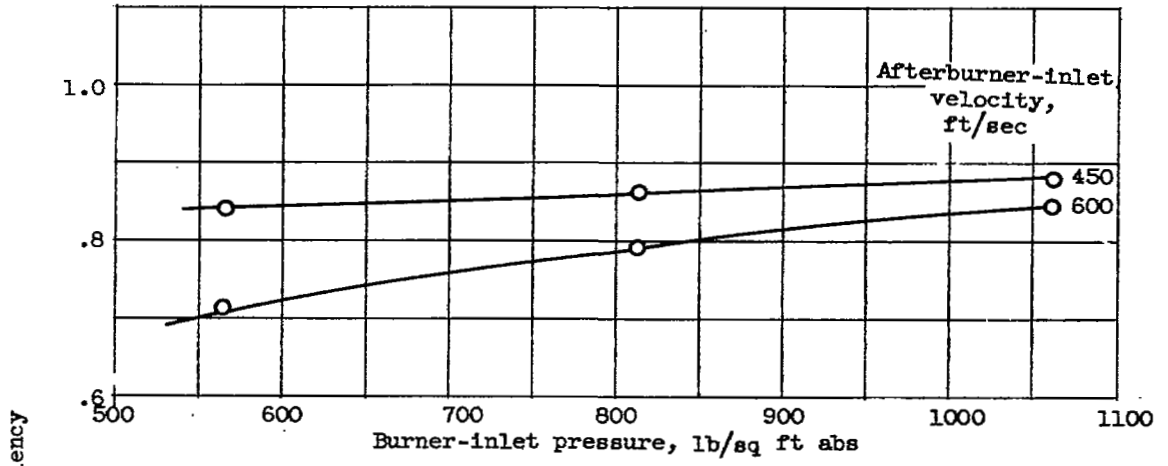

(a) Effect of burner-inlet pressure.

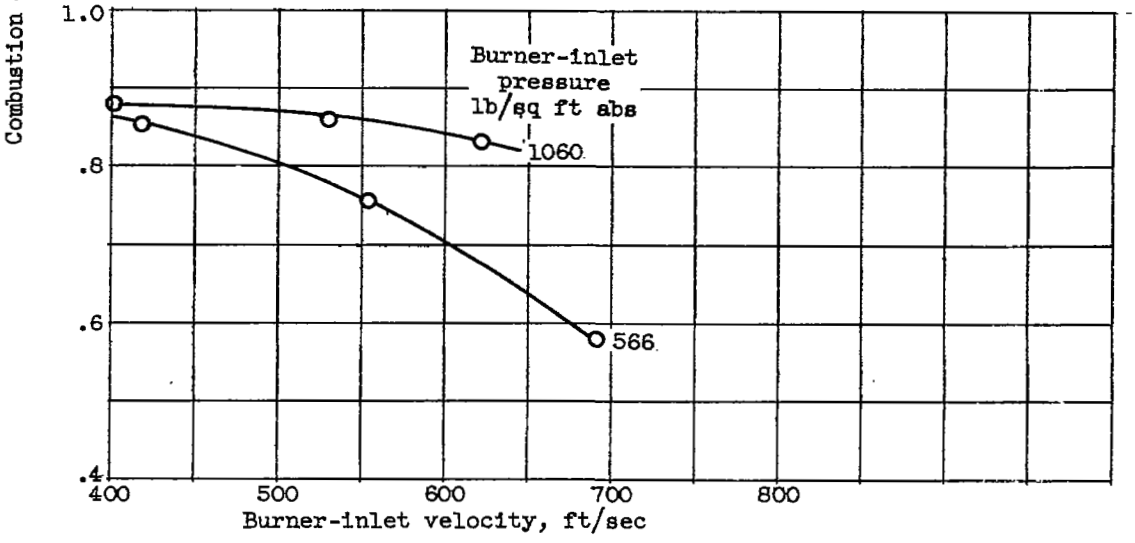

(b) Effect of burner-inlet velocity.

Figure 227. - Effect of inlet pressure and inlet velocity on combustion efficiency of afterburner. Blockage, 30 percent; V-gutter flameholder; fuel-air ratio, 0.047.

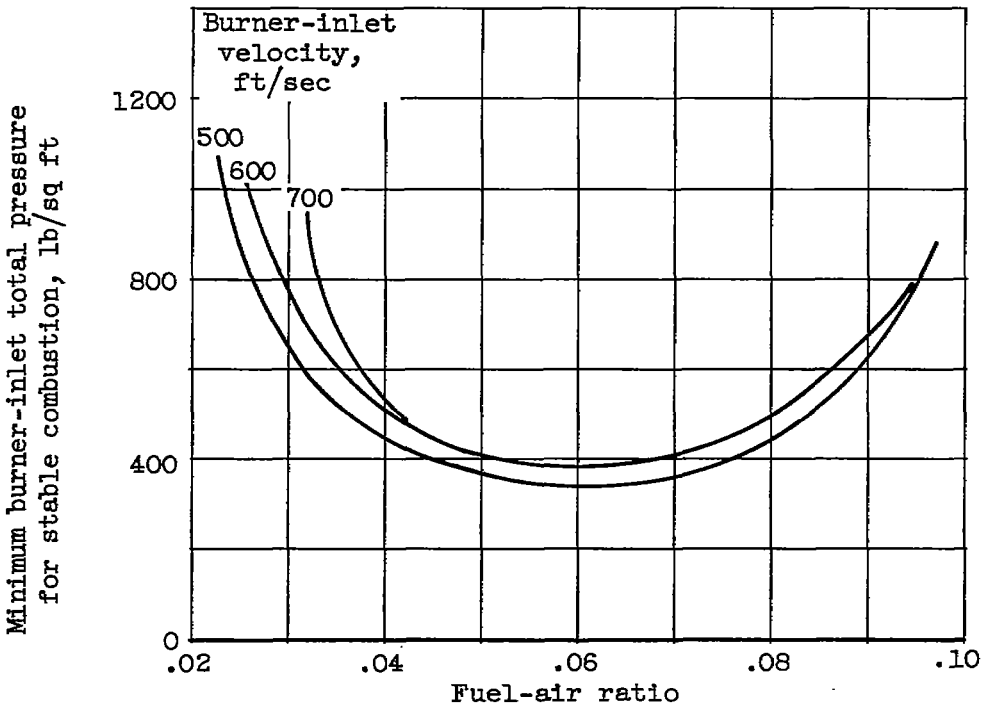

Figure 228. - Effect of velocity on stable operating range of afterburner with 30-percent-blocked-area V-gutter flameholder.

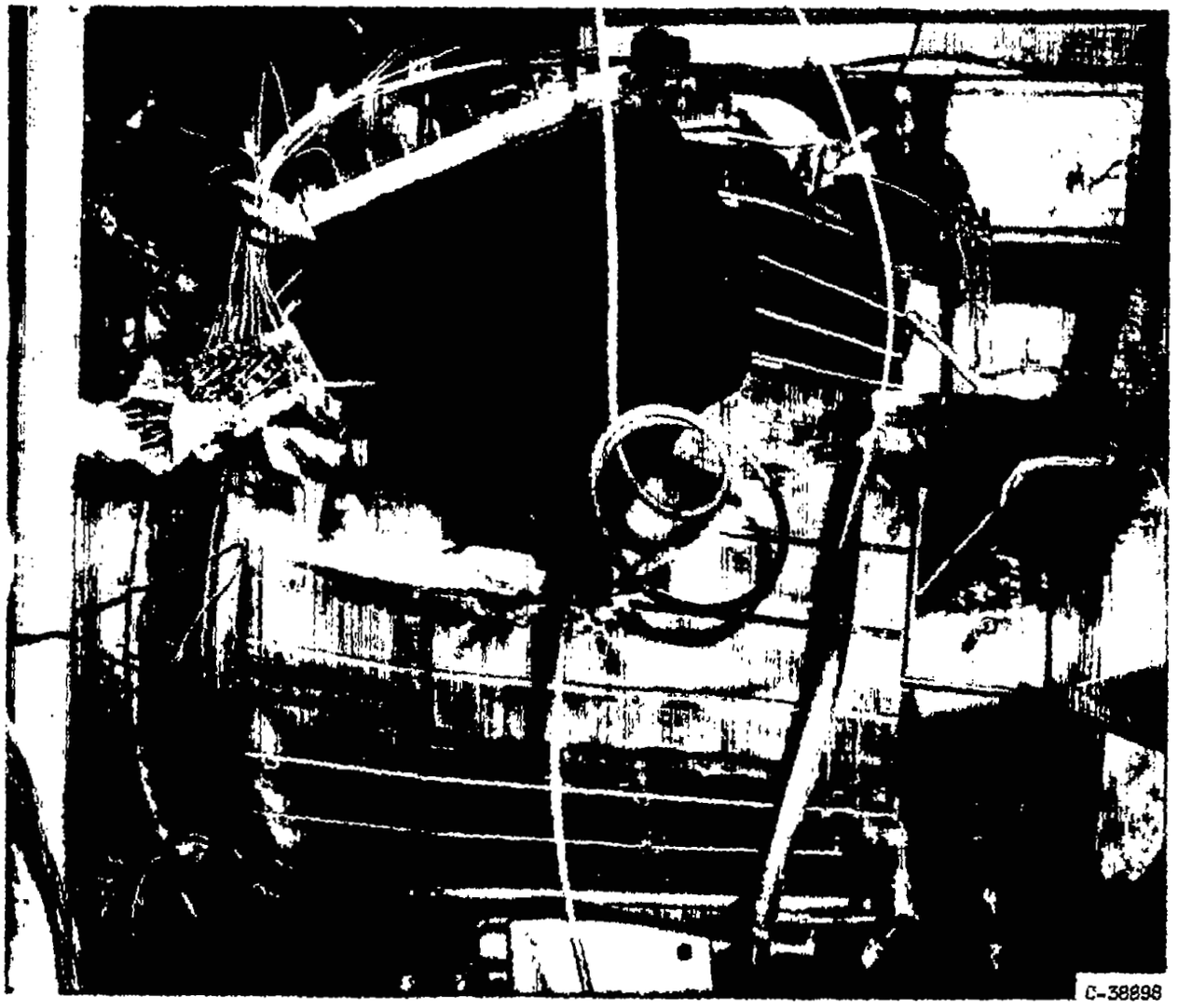

Figure 229. - Burner damaged by screech.

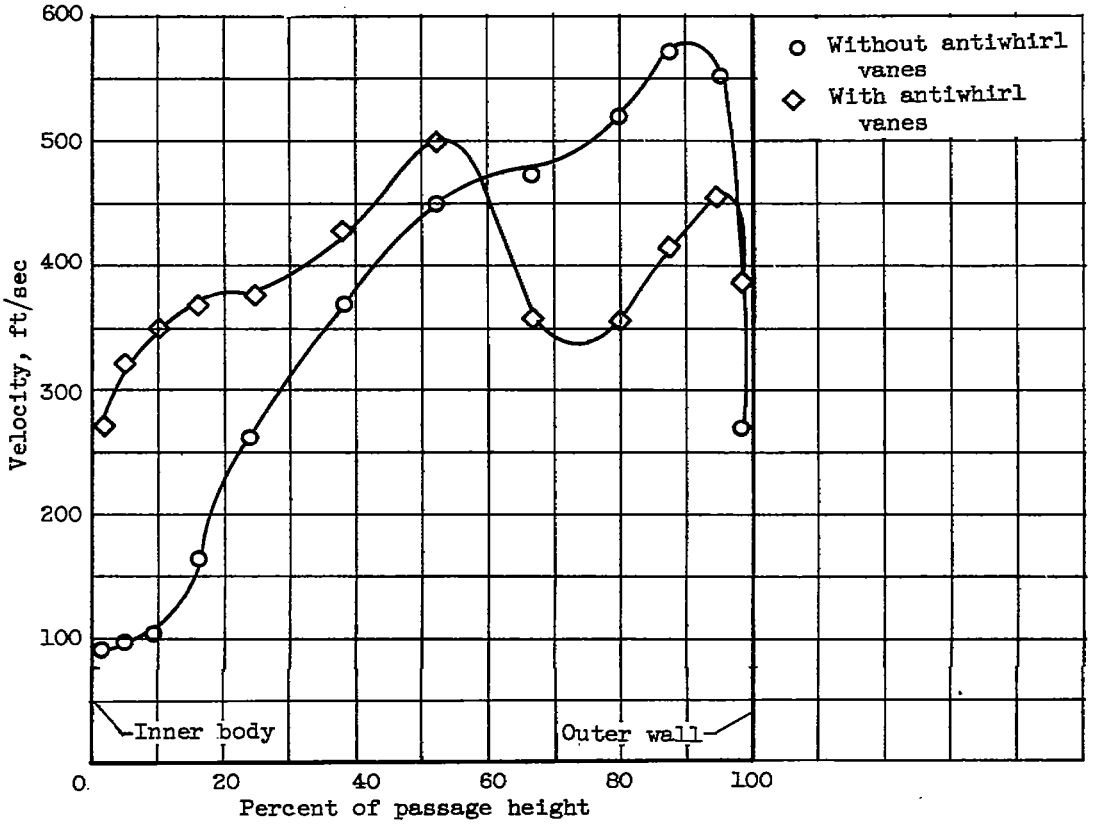

(a) Diffuser-exit velocity profile.

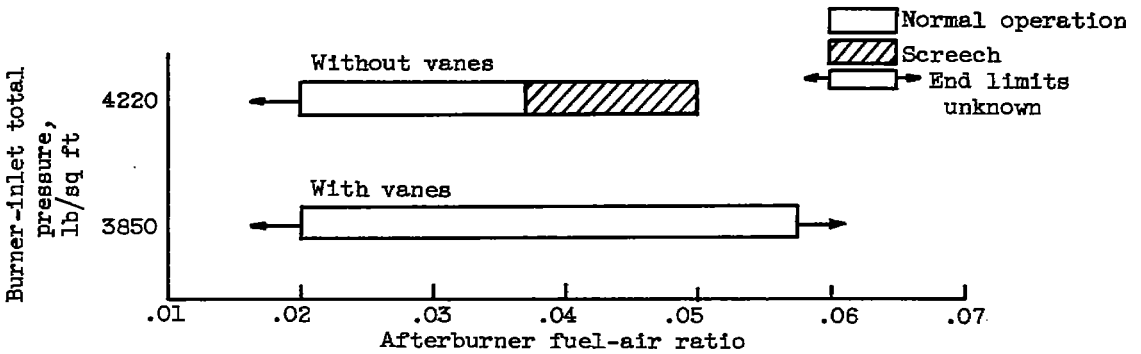

(b) Screech limits.

Figure 230. - Effect of radial distribution of velocity at afterburner inlet on screech limits.

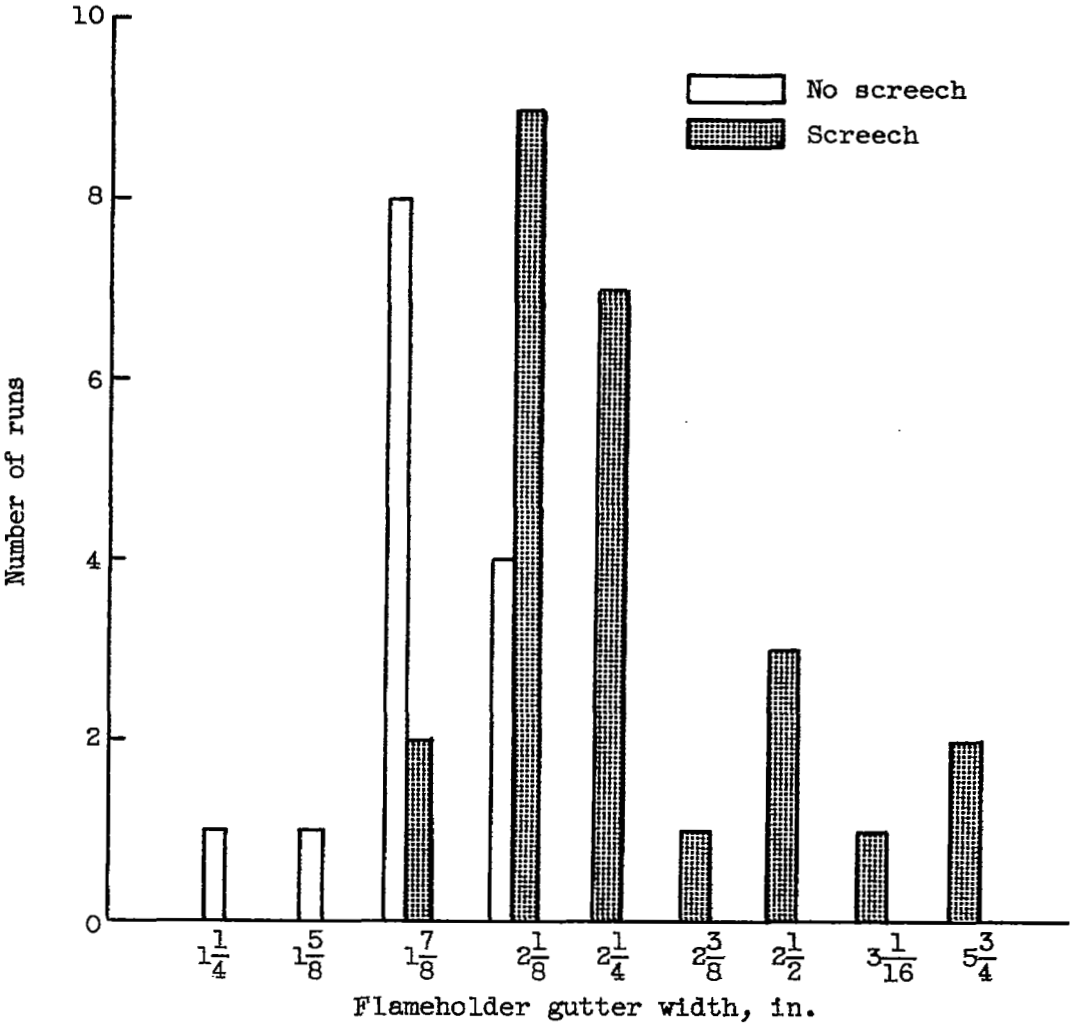

Figure 231. - Influence of flameholder gutter width on occurrence of screech. Burner-inlet total pressure, 3850 to 4220 pounds per square foot absolute; flameholder blockage, 32 to 40 percent of flow area.

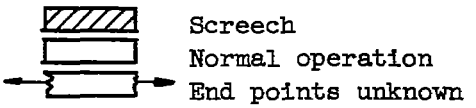

3925

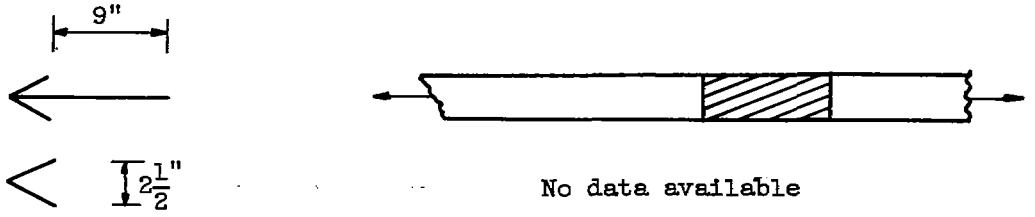

(a) Burner-inlet pressure, 1080 pounds per square foot.

(b) Burner-inlet pressure, 990 pounds per square foot.

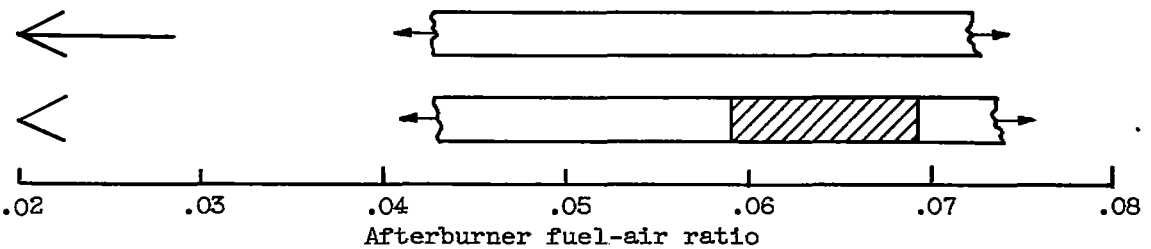

(c) Burner-inlet pressure, 870 pounds per square foot.

Figure 232. - Effect of flameholder splitter on screech limits.

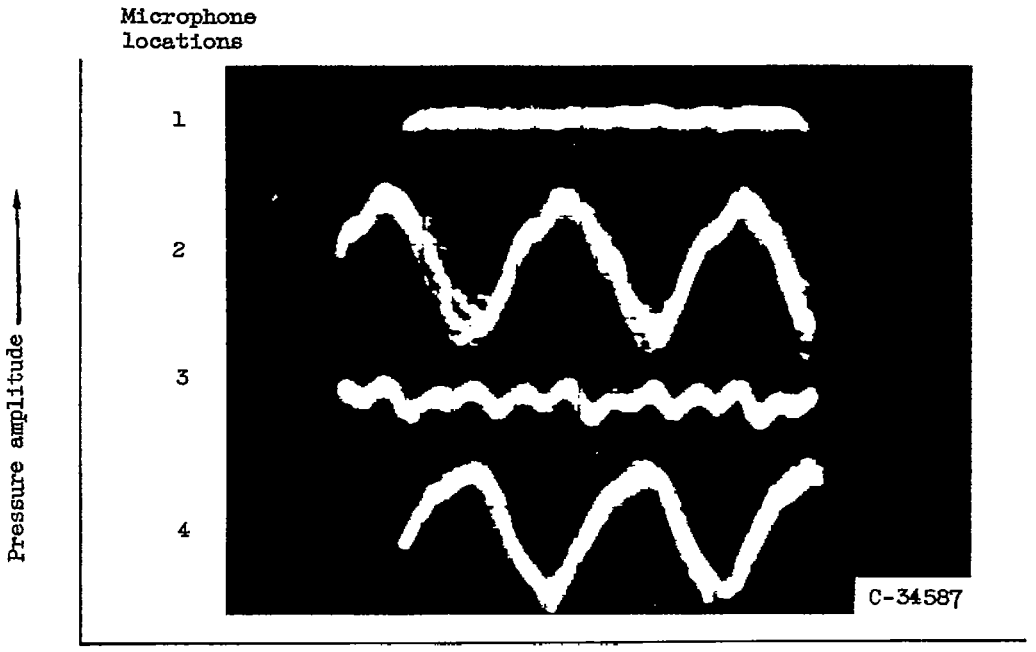

Figure 233. - Phase relations of screech oscillations in 26-inch-diameter afterburner with diametrical V-gutter flameholder. Microphones equally spaced; location of microphone taps, 1.0 inch downstream of flameholder; flameholder width, 8 inches; screech frequency, 650 cycles per second.

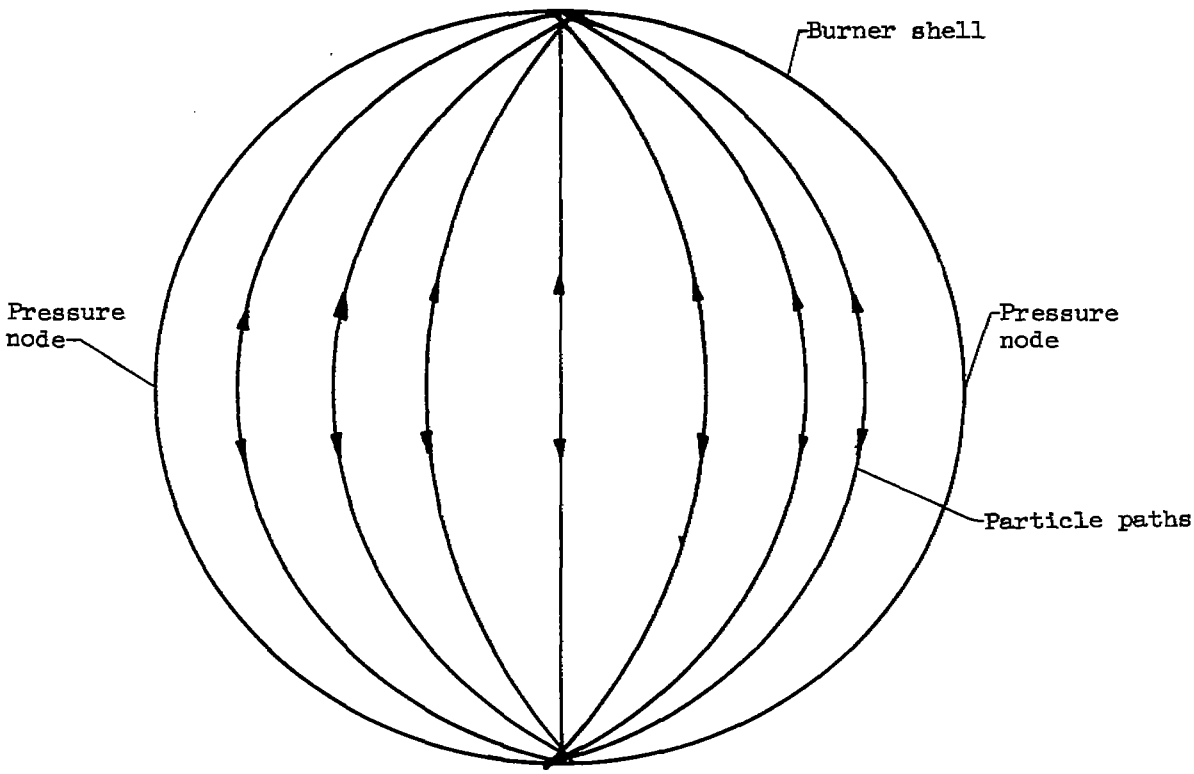

Figure 234. - Idealized cross section of afterburner, showing loci of wave-front paths for first transverse mode of oscillation.

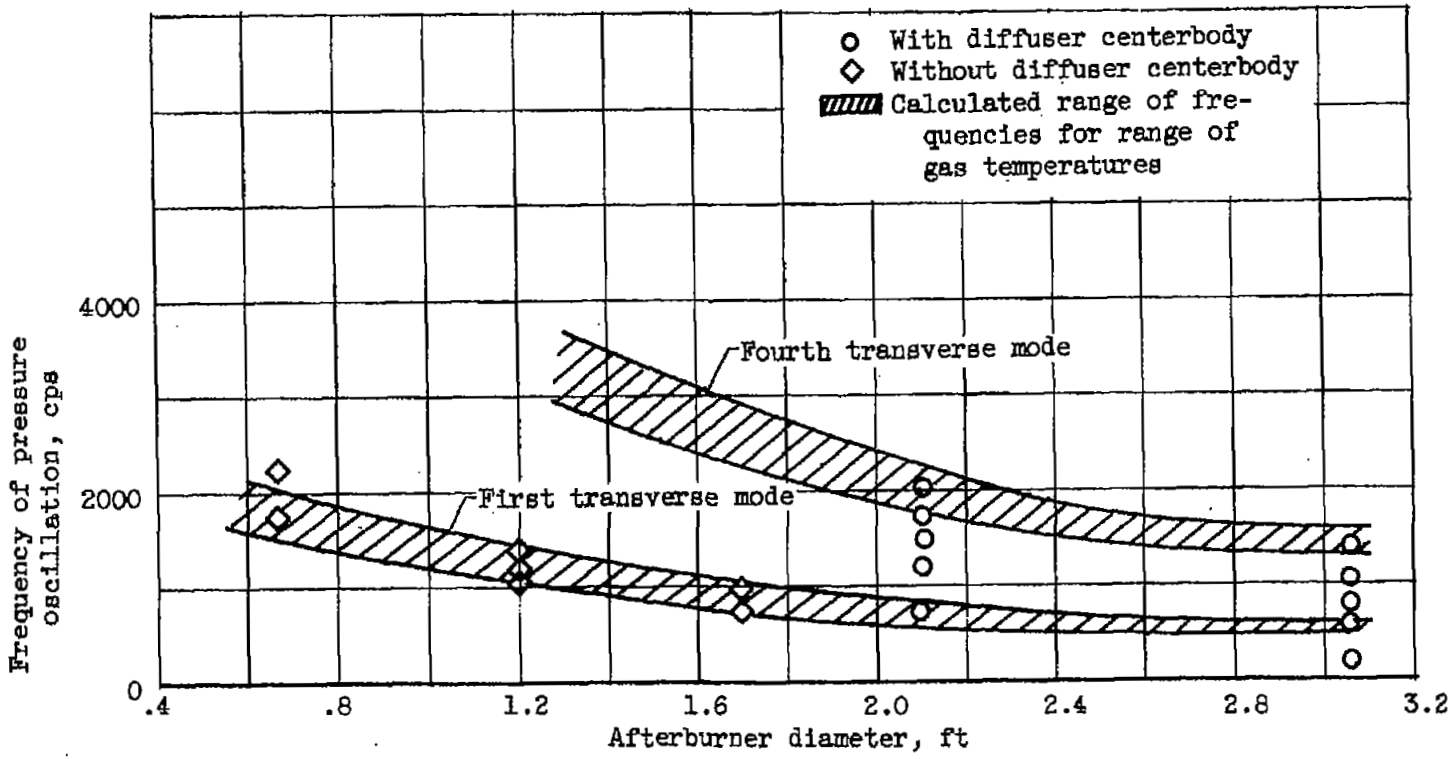

Figure 235. - Screech frequencies of afterburners of various diameters.

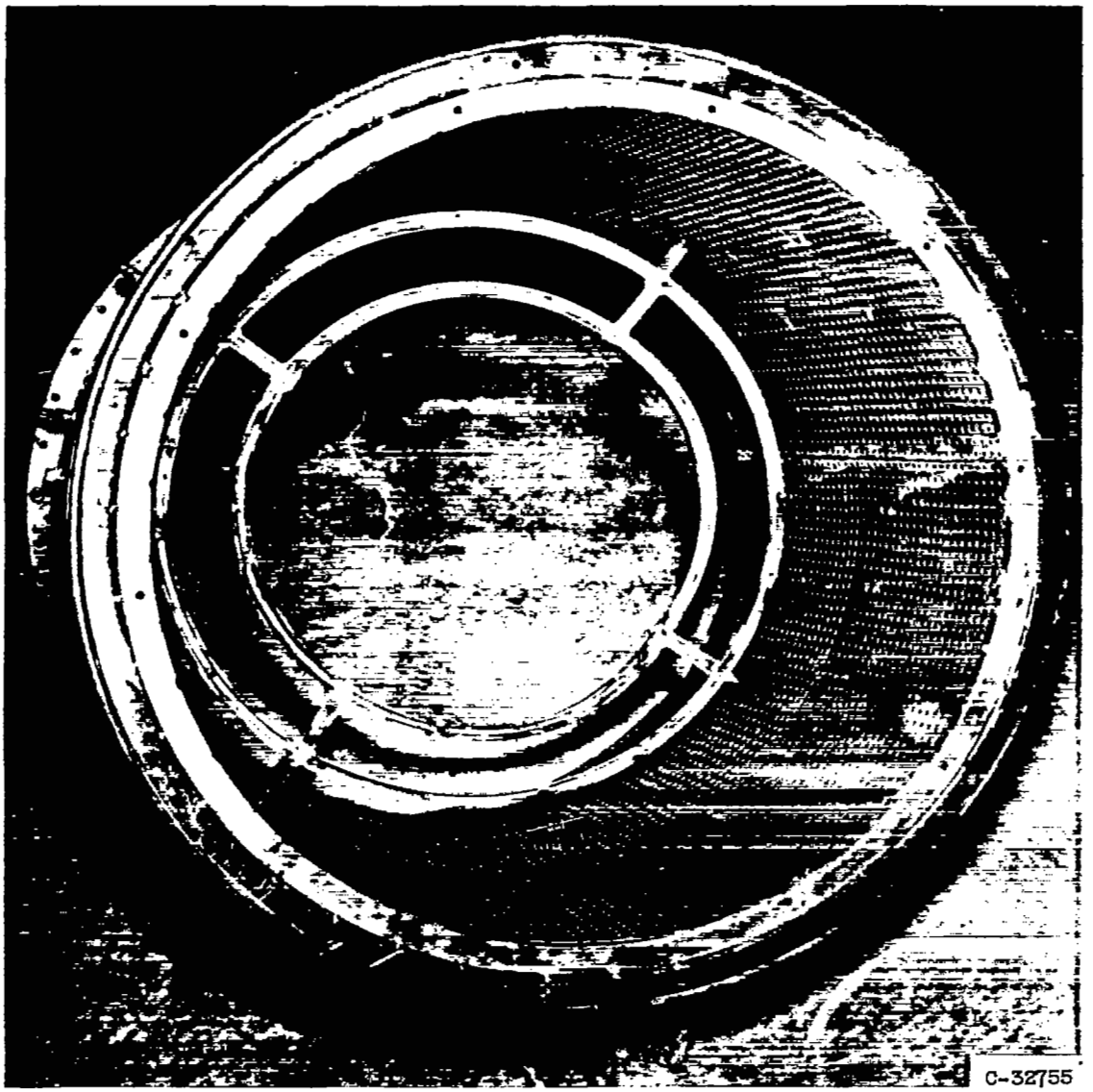

Figure 236. - Perforated liner installed in 32-inch-diameter afterburner for suppression of screech.

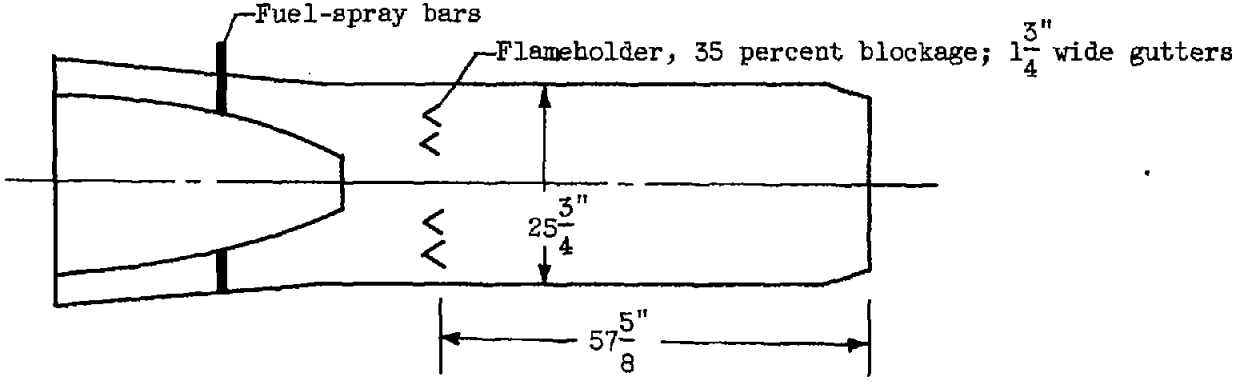

Figure 237. - Afterburner used with water-alcohol injection. Inlet velocity, 350 feet per second.

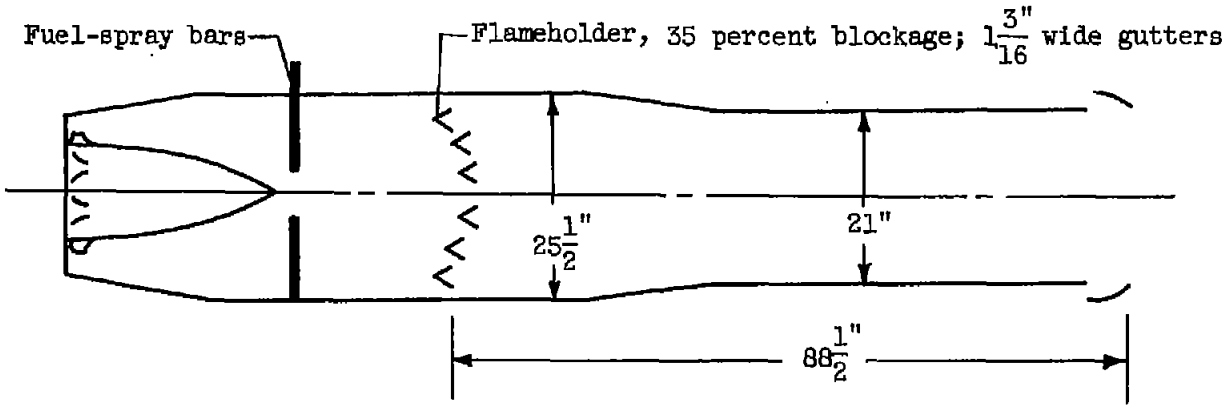

Figure 238. - Afterburner used with ammonia injection. Inlet velocity, 391 feet per second.

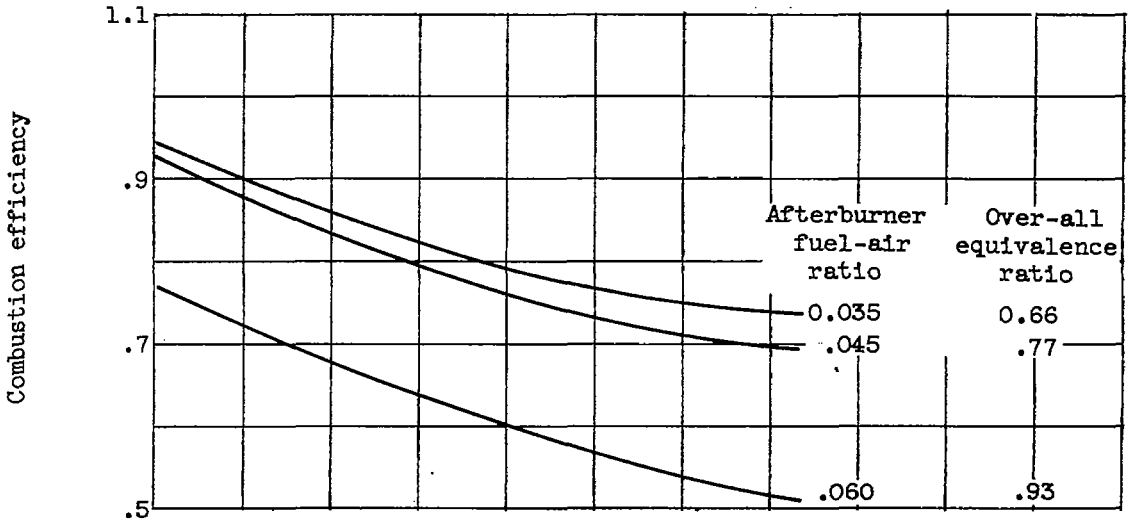

(a) Combustion efficiency.

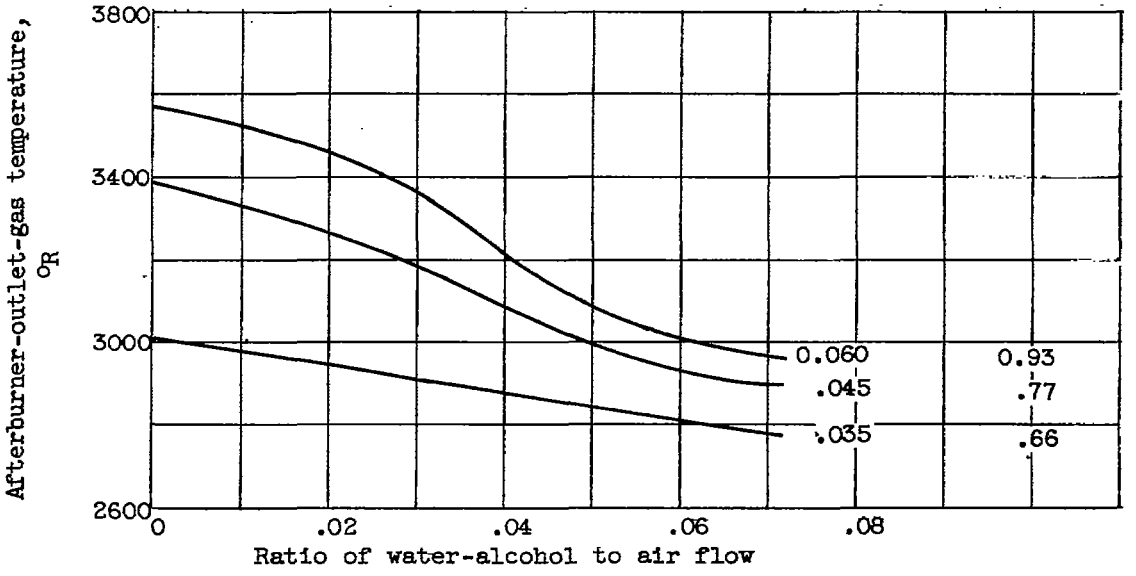

(b) Afterburner-outlet-gas temperature.

Figure 239. - Effect of water-alcohol injection on afterburner performance. Afterburner-inlet pressure, approximately 3800 pounds per square foot absolute.

[redacted]

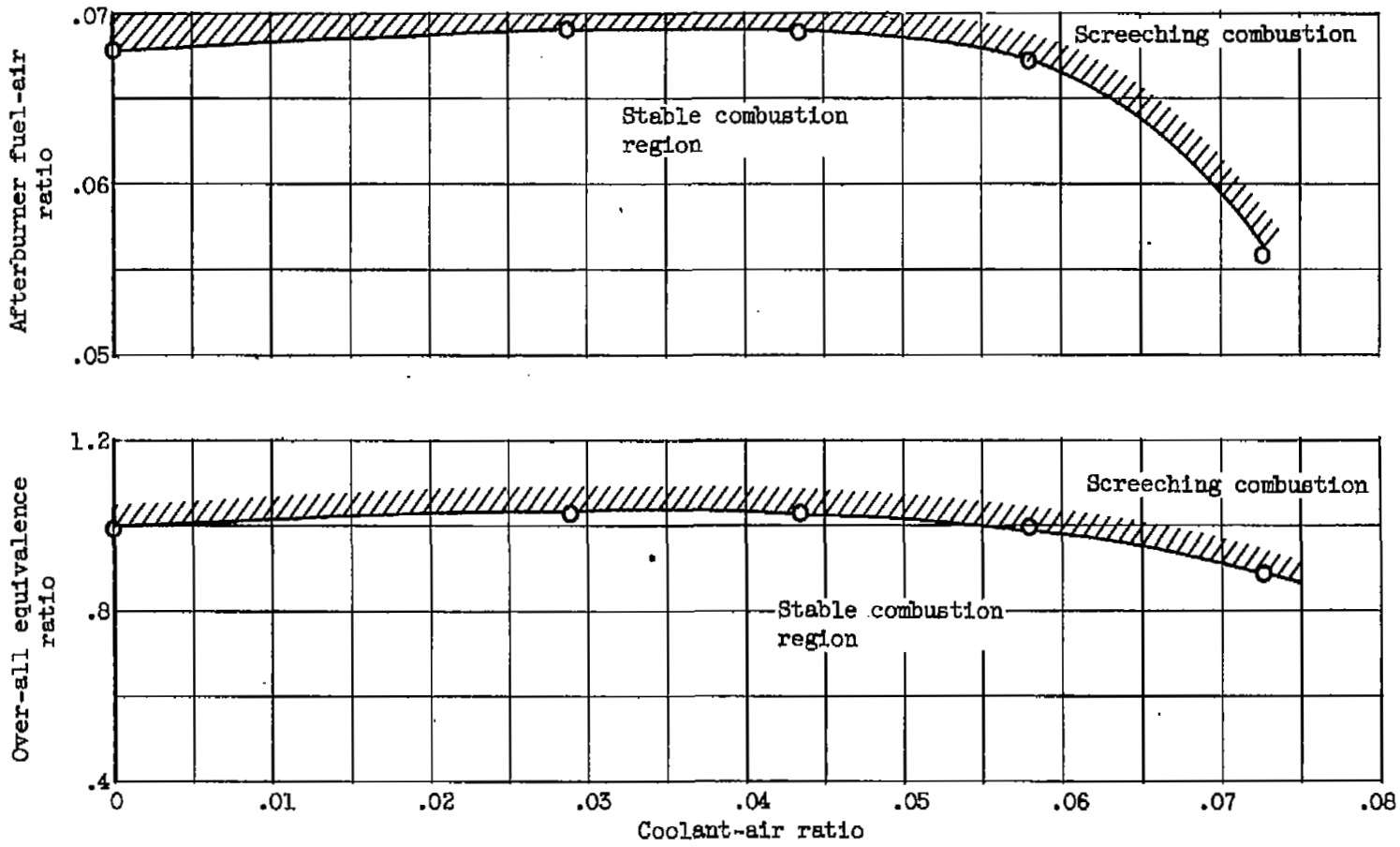

Figure 240. - Afterburner combustion stability limits with water-alcohol injection in compressor.

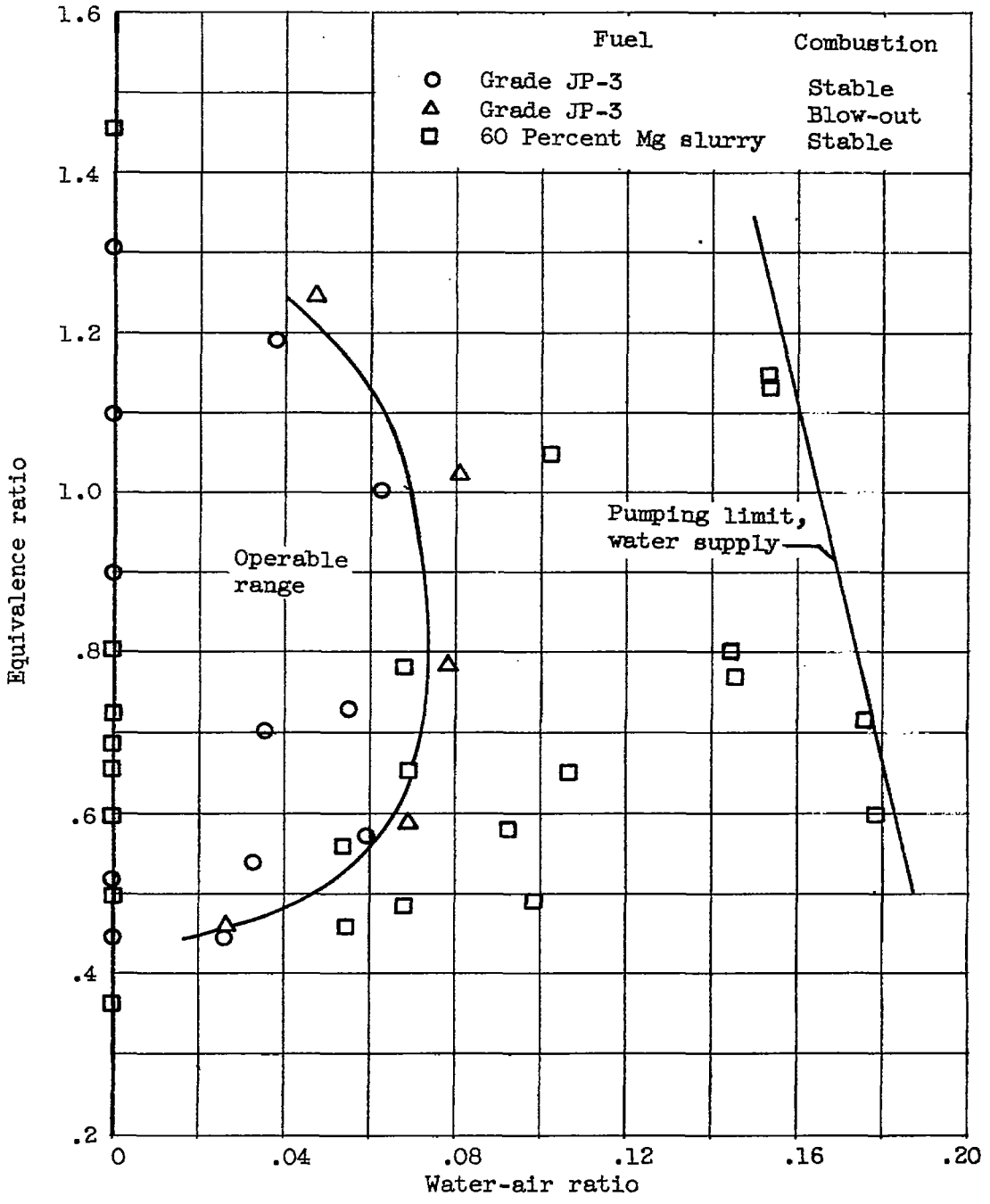

Figure 241. - Blow-out limits for JP-3 fuel and 60-percent magnesium slurry fuel in 6-inch burner. Burner-inlet velocity, 300 to 450 feet per second; burner-inlet pressure, 1100 to 1700 pounds per square foot absolute.

[redacted]

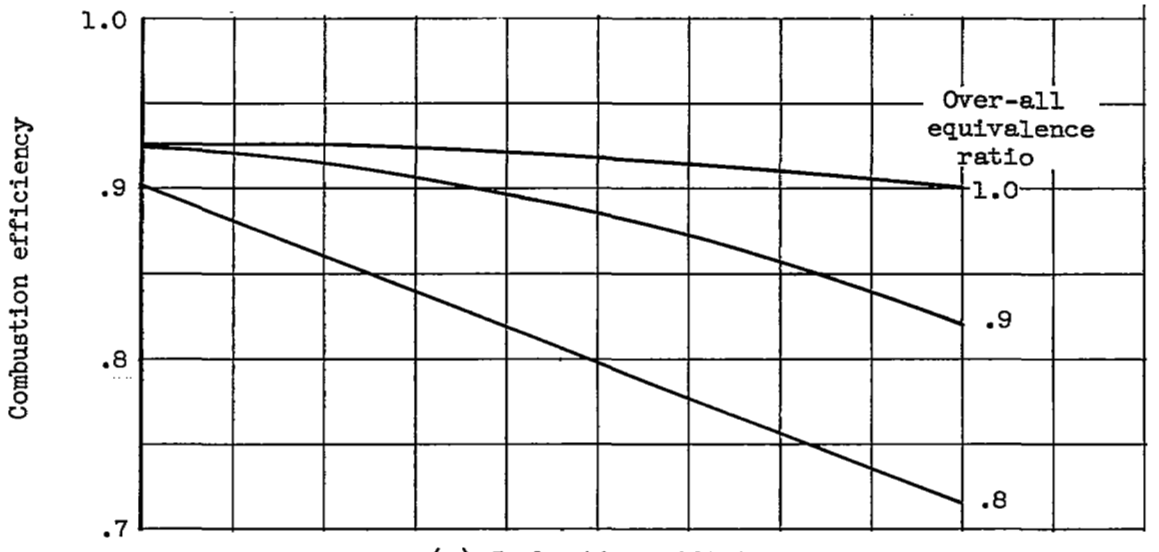

(a) Combustion efficiency.

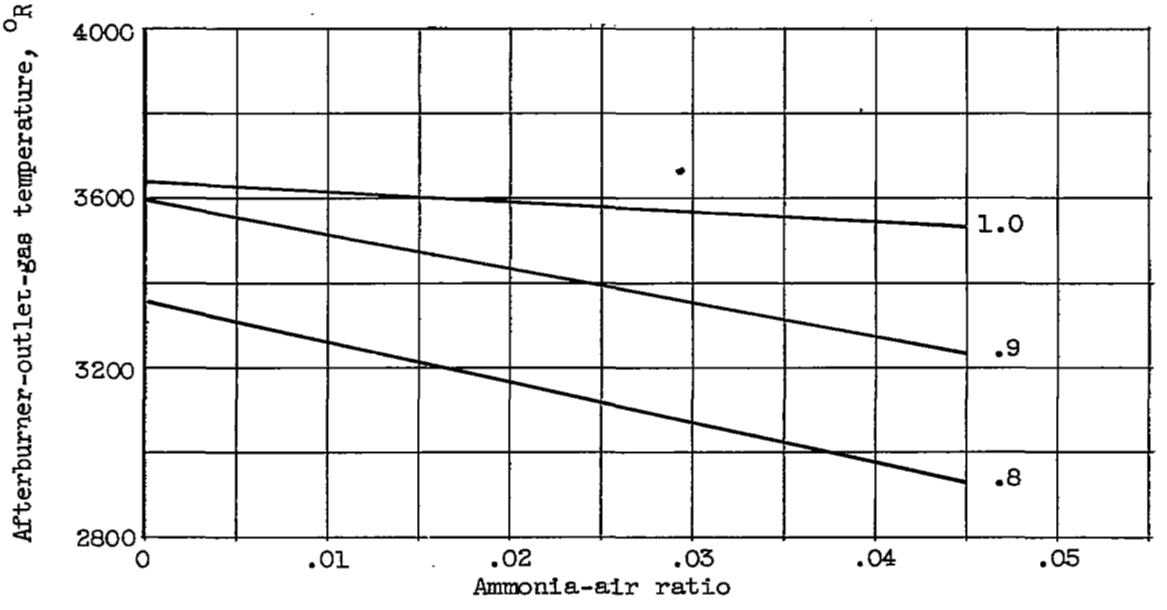

(b) Afterburner-outlet-gas temperature.

Figure 242. - Effect of ammonia injection on afterburner performance.. Afterburner-inlet pressure, 1780 pounds per square foot absolute.

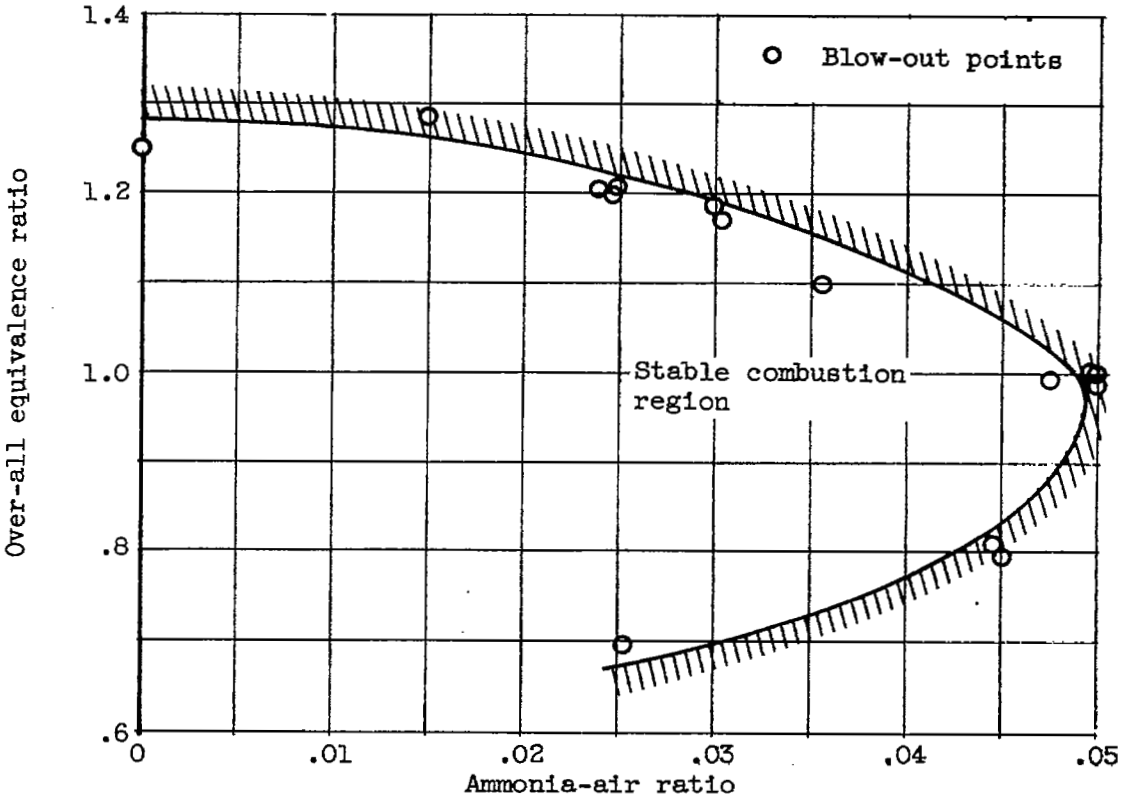

Figure 243. - Effect of ammonia-air ratio on blow-out limits. Afterburner-inlet pressure, 1780 pounds per square foot absolute.

UNCLASSIFIED

UNCLASSIFIED